DOCTOR OF PHILOSOPHY

Purification of protein phosphatases and 14-3-3-binding proteins and their regulation by the cAMP–PKA pathway

Reetoo, Namrata

Award date:
2012

DOCTOR OF PHILOSOPHY

Purification of protein phosphatases and 14-3-3-binding proteins and their regulation by the cAMP–PKA pathway

Namrata Reetoo

2013

University of Dundee

Purification of protein phosphatases and 14-3-3-binding proteins and their regulation by the cAMP–PKA pathway

by

Namrata Reetoo

A thesis submitted for the degree of
Doctor of Philosophy,
College of Life Sciences,
University of Dundee, Sept 2012.

List of Figures and Tables

Chapter One

Chapter Two

Chapter Three

Chapter Four

Acknowledgements

First, I would like to thank my supervisor Professor Carol MacKintosh for the opportunity to complete this project under her supervision. It has been great working under Carol who is always ready to support and hand out great advice, directions and nudges as and when required. Thanks also to Dr Gordon Simpson for his guidance during the first few months of the project. Huge thanks to Bob MacKintosh for proofreading my thesis.

I would like to thank Rachel Toth for excellent cloning support; the entire mass spectrometry team for analysing my hundreds of samples, especially Bob Gourlay, David Campbell, Sanjay Kothiya, Joby Varghese, Nick Morrice and Matthias Trost; Kirsten McLeod and Janis Kirsten for always catering to my last-minute requests for cells and incubators and the entire team of the Division of Signal Transduction Therapy (DSTT). Special thanks also to support staff for ensuring things run smoothly, so thank you Allison, Rachel and Maisie. A big thanks to Judith for keeping the paperwork in order and for being a great lunchtime buddy. Thank you to my financial sponsors: the Dorothy Hodgkin foundation, the James Hutton Institute and the Medical Research Council. A big thank you to all the companies who support the DSTT at the University of Dundee, namely AstraZeneca, Boehringer Ingelheim, GlaxoSmithKline, Merck Serono and Pfizer.

It would not have been such a memorable journey without the CMacKers so a huge thank you to all the people who have been exceptional throughout my PhD: Silvia Synowsky 'Königin de mass spec' but mainly just for being you; my great bay buddies Catherine Johnson-cheers for 'riding shotgun' on all my crazy plans, Sandra Crowther for all the great laughs, and Gerta Hoxhaj for helpful discussions. My eternal appreciation to our genius of a bioinformatician, Michele Tinti for all the help analysing the mountains of data, but more importantly, for the 'Baci'. Huge thanks to Margaret Stafford, Kumara Dissanayake and Olof Olsson for keeping things cheery with great jokes.

I would also like to thank Prem for his editing and unwavering support for the past decade; Monica, Ansari, Snehal, Jaydeep, Priti, Ashutosh and Hardeep: it's been a great journey, thank you for everything.

Finally I would like to thank my parents Unoop and Mala, my brother Abhijeeth and the other 100-odd Reetoos 'ek lalianne' for all their love and support across the seas.

Declarations

I hereby declare that the following thesis is based on the results of investigations conducted by myself, and that this thesis is of my own composition. Work other than my own is clearly indicated in the text by reference to the researchers or their publications. This dissertation has not in whole, or in part, been previously presented for a higher degree.

Namrata Reetoo

I certify that Namrata Reetoo has spent the equivalent of a least nine terms in research work in the MRC Protein Phosphorylation Unit, College of Life Sciences, University of Dundee, and that he has fulfilled the conditions of the Ordinance General No. 14 of the University of Dundee and is qualified to submit the accompanying thesis in application for the degree of Doctor of Philosophy.

Carol MacKintosh

Abstract

Reversible protein phosphorylation is a highly conserved mechanism that regulates the majority of proteins in a eukaryotic cell. Protein phosphorylation has been implicated in various cellular processes including glycogen metabolism, cell cycle control, RNA splicing, DNA synthesis, muscle contraction and mitosis. Protein kinases and phosphatases regulate the phosphorylation status of proteins in response to intra- and extracellular stimuli such as hormones and growth factors.

In **chapter 3**, I explore the regulation of protein phosphatases when the cAMP–PKA signalling pathway is activated and study the isoform specificity of PP1. Most protein phosphatases of the PPP family do not exist as free catalytic subunits: instead, they interact with regulatory subunits, which specify, target and/or inhibit their activities. Protein phosphatases of the PPP family such as PP1 and PP2, act specifically on serine/threonine phosphorylations; our understanding of phosphatase regulation stems from the regulation of members of the PPP family upon activation of the cAMP signalling pathway through protein kinase A. We wanted to find out whether there were more proteins that would regulate phosphatase activity when the cAMP–PKA pathway is activated and so started by doing a microcystin-affinity purification. Microcystin is a potent inhibitor of most PPP phosphatases and has been adapted to purify protein phosphatases from cellular extracts. I used the cAMP agonist forskolin to trigger activation of the cAMP–PKA pathway and used the H-89 inhibitor to block PKA activity. Although several protein phosphatases were identified along with their regulatory subunits, I could not find any striking enrichment of proteins upon activation or inhibition of the cAMP–PKA signalling pathway.

I also purified protein phosphatase 1 complexes from a cell line stably expressing GFP-TAP- PP1β with the aim of identifying PP1-regulatory subunits which would indicate potential PKA-mediated regulatory events. Again, cells were stimulated with forskolin and H-89 to monitor changes in the cAMP–PKA signalling pathway. Many known PP1 interacting proteins were identified including MYPT1, NIPP1, Inhibitor-2 and Staufen. Interestingly, three glycogen-related proteins, namely R6, glycogenin and glycogen synthase, were found to be highly enriched upon forskolin treatment which included prior inhibition of the pathway with H-89. R6 is a glycogen-targeting subunit of PP1 while glycogenin acts as the primer during glycogen synthesis; these glycogen moieties are then elongated by glycogen synthase. We think the enrichment of glycogen synthase and glycogenin from PP1 immunoprecipitates treated

with H-89 and forskolin could be linked to increased amounts of the R6-glycogen targeting subunit under the same conditions. Further experiments are required to check the correlation between R6 and the enzymes of glycogen synthesis.

PP1 isoforms alpha, beta and gamma are 97% identical in their catalytic residues, raising an important question of how these isoforms exert specificity in their substrates. Isoform specificity has been implicated in a number of regulatory processes including the selective nuclear targeting of the PP1γ subunit by Repo-Man and the preferential association of MYPT1 with PP1β to control muscle contraction. With such a high degree of similarity among PP1 isoforms, I wanted to evaluate whether the three isoforms varied much in their isoform specificity or whether they could be redundant in their substrates. For this, I stably expressed the three isoforms with an N-terminal GFP-TAP tag and analysed the immunoprecipitated protein complexes for each isoform. We found that there was no significant pattern of enrichment for any protein that could be used to specify isoform preference. Nonetheless, we did find higher amounts of MYPT1 with the beta isoform compared to alpha and gamma, in agreement with the reports of preferential PP1 beta binding to the ankyrin repeats of MYPT1. Overall though, these studies suggest that isoform specificity of the PP1 catalytic subunits may not be clear cut; in fact, most studies reporting PP1 isoform selectivity use bacterially-expressed PP1 proteins which have been shown to exhibit different properties to the native enzymes.

Protein phosphorylation creates binding sites for proteins such as 14-3-3s, which have been shown to dock onto dually-phosphorylated serine/threonine residues on target proteins. In **chapter 4**, I looked at the regulation of 14-3-3-binding proteins when the cAMP–PKA signalling pathway was activated. Again, I used forskolin as a cAMP agonist and H-89 as the non-specific PKA inhibitor to monitor changes in proteins involved in 14-3-3-binding in this pathway. 14-3-3s are involved in regulating various cellular proteins involved in insulin signalling, transcription, translation, glycogen metabolism, autophagy, vesicle and protein trafficking among others. Previous experiments in our laboratory explored the binding of 14-3-3s to its targets upon stimulation with hormones and growth factors such as insulin, IGF-1 and EGF, to monitor how changes in these pathways altered proteins involved in survival and growth promoting pathways. Understanding how and when 14-3-3s impact on these signalling targets enables us to gain regulatory insights into many areas of 14-3-3 biology. Since many proteins had already been observed to bind 14-3-3s upon forskolin

stimulation, I performed a large-scale 14-3-3-affinity pull-down to explore proteins in the cAMP–PKA proliferation-promoting pathway. Interestingly, many forskolin/H-89-regulated proteins were identified and I went on to validate a few of these candidate proteins as 14-3-3-binding targets, including the DENND4 family, EML3 and Atg9. The DENND4 proteins are guanine nucleotide exchange factors for Rab proteins, while Atg9 is a component of the autophagosome. Therefore, my findings indicate novel roles for 14-3-3s in regulation of intracellular membrane dynamics. My studies indicate that there are still many targets of 14-3-3s to be characterised and I hope that the data presented in my thesis will be extended in future and contribute towards our understanding of protein phosphorylation and14-3-3 biology.

Abbreviations

µ	micro
A	absorbance
AANAT	serotonin N-acetyltransferase
AC	adenylyl cyclase
AGC	cAMP-dependent protein kinase/protein kinase G/protein kinase C extended family
AKAP	A-kinase anchoring protein
Akt	v-akt murine thymoma viral oncogene homologue 1 (also known as PKB)
AMP	adenosine 5'-monophosphate
AMPK	adenosine 5'-monophosphate-activated protein kinase
aPK	atypical protein kinase superfamily
APS	SH2B adapter protein 2
AS160	Akt substrate of 160 kDa
A. thaliana	*Arabidopsis thaliana*
ATP	adenosine 5'-triphosphate
BAD	Bcl2 antagonist of cell death
BLAST	Basic Local Alignment Search Tool
BMH1 and BMH2	brain neuromodulin homologues 1 and 2 (*S. cerevisiae* 14-3-3s)
BRCA1	Breast cancer type 1 susceptibility protein
BRCT	domain named after the C-terminal domain of a breast cancer susceptibility protein
BSA	bovine serum albumin
CAMK	calcium/calmodulin dependent protein kinase
cAMP	cyclic adenosine 5'-monophosphate
Cdc25	Dual specificity phosphatase Cdc25
CDC25C	M-phase inducer phosphatase 3
CDKs	cyclin-dependent kinases
cDNA	complementary deoxyribonucleic acid
C.elegans	*Caenorhabditis elegans*
CMGC	CDK, MAP kinase, glycogen synthase kinase, and CDK-like
CREB	Cyclic AMP-responsive element-binding protein
C-terminus	carboxyl terminus
DENND	Differentially expressed in normal and neoplastic cells domain
DIG	digoxygenin-O-methylcarbonyl-ε-aminocaproic acid-N-hydroxysuccinimide
DIG-NHS	DIG-O-methylcarbonyl-ε-aminocaproic acid-N-hydroxysuccinimide ester
D. melanogaster	*Drosophila melanogaster*
DMEM	Dulbecco's Modified Eagle's Medium
DMSO	dimethyl sulphoxide
DNA	deoxyribonucleic acid
DSTT	Division of Signal Transduction Therapy
DTT	dithiothreitol
DUSP	dual specificity protein phosphatase
E. coli	*Escherichia coli*
ECL	enhanced chemiluminescence

EDTA	ethylenediamine tetracetic acid
EGTA	ethyleneglycol bis (2-aminoethylether)-N, N'-tetraacetic acid
EML3	echinoderm microtubule-associated protein-like 3
ER	endoplasmic reticulum
ERK	extracellular responsive kinase
EST	expressed sequence tag
ExoS	exoenzyme S
FAM122	protein family FAM122
FHA	forkhead-associated
FOXO1	forkhead transcription factor 1
FPA	flowering time control protein FPA
GADD34	Protein phosphatase 1 regulatory subunit 15A
GAP	GTPase activating protein
GEF	guanine exchange factor
GFP	green fluorescent protein
GSK3	glycogen synthase kinase 3
GST	glutathione-S-transferase
HA	haemagglutinin
HEK	human embryonic kidney
Hepes	N-[2-hydroxyethyl]piperazine-N'-[2-ethanesulphonic acid]
H.sapiens	*Homo sapiens*
HPLC	high performance liquid chromatography
HRP	horseradish peroxidase
I-1	inhibitor-1
I-2	inhibitor-2
IGF1	insulin-like growth factor 1
IgG	immunoglobulin G
IRLB	C-myc promoter-binding protein (DENND4A)
ISRE	interferon-stimulated response element
JNK	Mitogen-activated protein kinase
KLC	kinesin light chain
LB	Luria-Bertani medium
LCP1	plastin-2
LDS	lithium dodecyl sulphate
LPS	bacterial lipopolysaccharide
MABP	MVB12-associated β-prism
MALDI	matrix-assisted laser desorption ionisation
MAPKs	mitogen-activated protein kinases
MC-LR	microcystin with leucine and arginine in the variable positions
Mg-ATP	magnesium adenosine 5'-triphosphate complex
MRC PPU	Medical Research Council Protein Phosphorylation Unit
mRNA	messenger ribonucleic acid
MS	mass spectrometry
mTOR	mammalian target of rapamycin
MYPT1	myosin phosphatase-targeting subunit 1
NLS	nuclear localization sequence
NOM1	nucleolar MIF4G domain-containing protein 1
N-terminus	amino terminus
O. sativa indica	*Oryza sativa indica*
PAS	phospho-Akt substrate

p70 S6K	p70 ribosomal protein S6 kinase
PAGE	polyacrylamide gel electrophoresis
PANK2	pantothenate kinase 2, mitochondrial
PBS	phosphate-buffered saline
PCR	polymerase chain reaction
PDK1	3'-phosphoinositide-dependent protein kinase 1
PI 3-kinase	phosphatidylinositol 3-kinase
PKA	protein kinase A
PKB	protein kinase B (also known as Akt)
PKC	protein kinase C
PKD	protein kinase D
PKG	protein kinase G
PMSF	phenylmethanesulphonylfluoride
pNUTS	serine/threonine-protein phosphatase 1 regulatory subunit 10
PP	protein phosphatase
PPKL	PP1 and kelch-like phosphatases
PPP	phosphor-protein phosphatase
PRAS40	proline rich Akt substrate of 40 kDa
pSer	phosphorylated serine residue
PtdIns	phosphatidylinositol
PTEN	phosphatase and tensin homologue deleted on chromosome 10
pThr	phosphorylated threonine residue
RBM15	RNA-binding motif 15
RTK	receptor tyrosine kinase
SAC	soluble adenylyl cyclase
S.cerevisiae	*Saccharomyces cerevisiae*
SDS	sodium dodecyl sulphate
SH2	src homology 2 domain
SILAC	stable isotope labelling with amino acids in cell culture
siRNA	small interfering RNA
SPEN	split-end
TAE	Tris-acetate, EDTA
TAP	tandem affinity purification
TAK1	transforming growth factor beta-activated kinase 1
TBC domain	Tre-21/Bub21/Cdc 16 domain
TBC1D4	TBC1 domain family member 4
TBS	Tris-buffered saline
TBS-T	Tris-buffered saline-Tween
TE	Tris, EDTA
TFA	trifluoroacetic acid
TGN	trans Golgi network
TLC	thin layer chromatography
tmAC	transmembrane adenylyl cyclase
TOF	time-of-flight
Tris	Tris(hydroxymethyl)methylamine
TSC	tuberous sclerosis complex
Tween	polyethylene glycol sorbitan monolaurate
U	unit
ULK1	Unc51-like kinase 1
VASP	vasodilator-stimulated phosphoprotein
Vol	volume

Vps34	phosphatidylinositol 3-kinase catalytic subunit type 3
w/v	weight to volume
WD40-repeat	tryptophan/ aspartic acid repeat
Y2H	yeast 2-hybrid
ZNRF2	E3 ubiquitin-protein ligase ZNRF2

	Amino acid code	
Amino acid or residue	**Three letter symbol**	**One letter symbol**
Alanine	Ala	A
Arginine	Arg	R
Asparagine	Asn	N
Aspartate	Asp	D
Cysteine	Cys	C
Glutamate	Glu	E
Glutamine	Gln	Q
Glycine	Gly	G
Histidine	His	H
Isoleucine	Ile	I
Leucine	Leu	L
Lysine	Lys	K
Methionine	Met	M
Phenylalanine	Phe	F
Proline	Pro	P
Serine	Ser	S
Threonine	Thr	T
Tryptophan	Trp	W
Tyrosine	Tyr	Y
Valine	Val	V

Other amino acid residue symbols

Aliphatic residue (such as L, M or F)	ϕ
Unknown or any residue	X

Chapter One

Introduction

1.1 Reversible protein phosphorylation in eukaryotes

Cells respond to extracellular stimuli via signalling pathways that regulate enzyme activities and direct rearrangements of multicomponent complexes. Protein phosphorylation is one of the major regulatory mechanisms that enact these changes. The regulatory mechanism of protein phosphorylation was first identified in 1955 by Fischer and Krebs who were studying the interconversion of glycogen phosphorylase between its low and high activity states. Since then, this reversible protein modification has been implicated in the regulation of numerous cellular events such as glucose uptake and metabolism, muscle contraction, RNA processing, cell cycle progression, cell proliferation and differentiation, among others. Correspondingly, deregulated phosphorylation underlies a number of diseases such as various types of cancers, diabetes and neurological disorders.

The reversible phosphorylation status of proteins is directed by the actions of kinases and phosphatases on three main residues: serine, threonine and tyrosine. Protein kinases catalyse the addition of the phosphate moiety to a protein while phosphatases hydrolyse the phosphoamino acid esters to release phosphate. Complicated cascades of signalling networks direct the specificity and subcellular localisation of kinases and phosphatases to effect different cellular outcomes in response to stimuli.

Kinases and phosphatases make up about 2 to 4% of a typical eukaryotic genome (Manning et al., 2002a; Moorhead et al., 2009). In humans, there are about 518 kinases compared with 150 phosphatases, while plants have double the number of kinases at 1055 to 127 plant protein phosphatases (Kerk et al., 2008; Moorhead et al., 2009). These ratios raise the interesting question of how the smaller number of phosphatases regulates the dephosphorylation of the many substrates generated by such a large number of kinases. While kinases have generally evolved to recognise amino acid sequences flanking the phosphorylated residue, protein phosphatases are aided in their substrate recognition and action by targeting proteins. These proteins target the phosphatases to different cellular locations, thereby bringing them closer to their substrates where they can then exert their dephosphorylating action. For example, the G_M subunit of PP1 is responsible for targeting PP1 to glycogen in skeletal muscles where PP1 can then dephosphorylate and inactivate phosphorylase kinase and glycogen phosphorylase; and dephosphorylate and activate glycogen synthase, thereby modulating glycogen metabolism in these cells (Cohen, 1985;

Cohen, 1988). As well as targeting PP1, G_M also mediates its regulation by protein kinases A and C, contributing to the regulation of glycogen metabolism by these kinases. The targeting subunits also influence substrate specificity by providing additional substrate binding surfaces, blocking substrate-binding channels and/or altering the conformation of the catalytic subunit (Bollen et al 2010). In these ways, the substrate repertoire of the smaller number of phosphatases, compared with kinases, can be increased by the regulatory proteins that allow for differential regulation of the same protein phosphatase catalytic subunit in different physiological contexts.

1.2 Protein kinases

Eukaryotic Protein Kinases (ePK) make up one of the largest superfamilies, containing 1 to 2% of human genes, sub-divided into eight families based on sequence similarity in the catalytic domains, the presence of accessory domains and by comparison of their modes of action (Hanks et al., 1995; Manning et al., 2002a) (**Figure 1.1**). These are the AGC (including protein kinases A, G and C), CAMK (calmodulin regulated kinases), CK1 family (casein kinase 1 and closely related kinases), the CMGC kinases (including the mitogen-activated protein kinases, glycogen synthase kinase and cyclin-dependent kinases), RGC family (receptor guanylate cyclases), STE kinases (including kinases functioning in MAP kinase cascades, the TK family (tyrosine kinases) and lastly, the TKL (tyrosine-like kinases, which are in fact serine/threonine kinases) (Manning et al., 2002a; Manning et al., 2002b; Miranda-Saavedra and Barton, 2007). The majority of the ePK family remained conserved throughout evolution from yeast to man (~51 subfamilies). A comparatively larger number of kinase subfamilies are shared among worms, flies and humans (~93), implying that most of these kinase subfamilies would have evolved after the divergence from the common ancestor with yeast (Manning et al., 2002a).

In addition to ePKs, there are also the atypical Protein Kinases (aPKs), which lack sequence similarity with the ePKs, although some aPKs share structural similarity to the ePK catalytic domains (Hanks et al., 1995). Strong experimental evidence of protein kinase activity has been shown for the aPK enzymes of the Alpha, RIO, PIKK and PHDK families (Miranda-Saavedra and Barton, 2007).

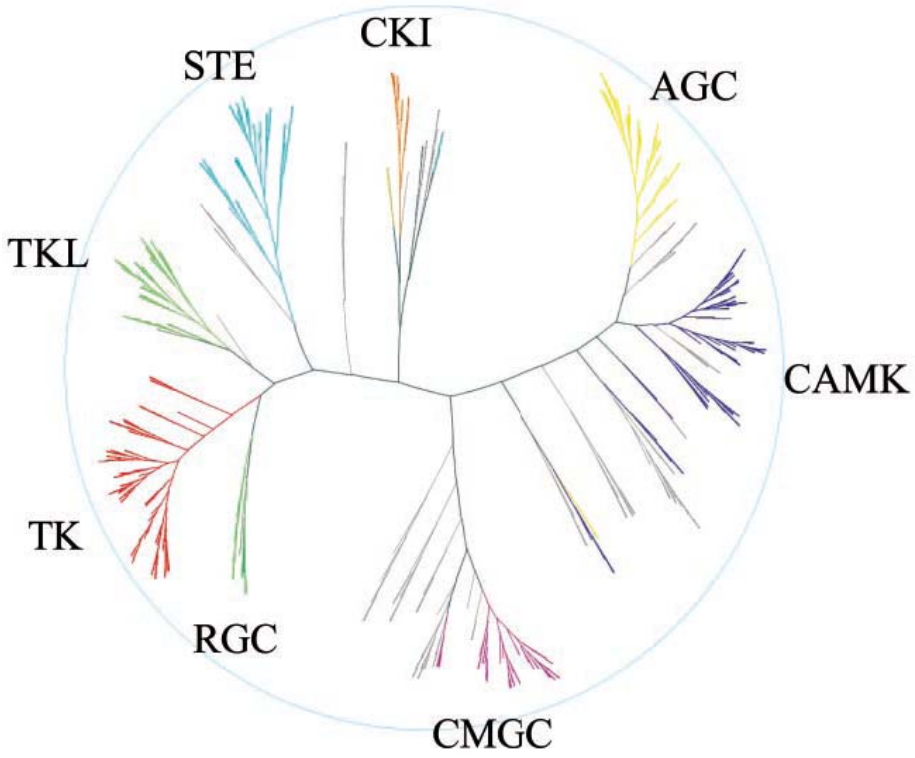

Figure 1.1: **The eight ePK subfamilies of kinases classified according to their kinase domain similarity and modes of action** (adapted from Manning et al., 2005b)

Miranda-Saavedra and Barton (2007) analysed 21 eukaryotic genomes and found that five ePK protein kinase families (AGC, CAMK, CK1, CMGC and STE) and two aPK protein kinase families (PIKK and RIO) were common to all of these genomes. Interestingly, they also found that while plants (namely *Arabidopsis* and rice) had almost double the number of kinases compared to human (see Table 1), there were markedly fewer TK-subfamily members in plants (7 in plants compared to 90 in humans) and many more TKL enzymes (1010 in plants compared to 55 in humans). Furthermore, plants had no RGC kinases at all, whereas humans expressed 5 compared to 28 such kinases in the worm *C. elegans*. As shown in **Table 1.1**, most of the other kinase families had more members in *Arabidopsis* compared to humans, especially in the CAMK, CMGC, STE and CK1 kinase families (Miranda-Saavedra and Barton, 2007).

Table 1.1
The protein kinase complement of eukaryotic organisms with the 8 ePK families and aPKs found in each organism

Taxonomy and species	AGC	CAMK	CK1	CMGC	RGC	STE	TK	TKL	Total ePKs	Total aPKs
Fungi										
S. cerevisiae	22	44	4	29	0	16	0	0	115	9
Plants										
A. thaliana	67	158	28	149	0	104	2	776	1284	17
O. sativa indica	54	93	15	97	0	55	6	1010	1330	8
Animals										
C. elegans	35	65	92	56	28	36	94	20	426	10
D. melanogaster	42	45	10	39	6	24	33	23	222	9
H. sapiens	84	98	12	70	5	61	93	55	478	40

(Compiled from: Manning et al., 2002b and Miranda-Saavedra and Barton, 2007*)*

1.2.1 The human kinome

The human kinome (**Figure 1.2**) contains 478 kinases from seven main ePKs families (the AGC, CAMK, CK1, CMGC, STE, TK and TKL families) and 40 kinases from the aPKs families. Of these, Manning et al. (2002b) reported that 244 kinases mapped to diseased loci or cancer-linked regions on chromosomes. This finding stresses the importance of understanding the different kinases and their regulation.

Though some protein kinases also have docking sites distinct from their active sites, the substrate specificity of the different kinases in the kinome is conferred through the residues of the target protein lying in the catalytic groove of the kinase. For example, the CMGC kinase Erk1 and the closely related Erk2 share the substrate recognition consensus motif X-P-X-pS/T-P-X (with pS/T being phosphorylated by the Erk isoforms) (Davis, 1993; Ubersax and Ferrell Jr., 2007; Roskoski Jr., 2012). CK1, on the other hand, phosphorylates targets to create phosphorylated pS-x-x-S motifs (Ubersax and Ferrell Jr., 2007). Kinases control most cellular functions in the cell by regulating the phosphorylation status of proteins and are hence required to be highly specific in their functions.

1.2.2 AGC and CAMK subfamilies and their specificities

The AGC and CAMK subfamilies are basophilic kinases, which are of particular interest to our group as most of the 14-3-3-interacting proteins that we have identified are phosphorylated by these enzymes. In contrast to many members of the CMGC family that require a proline at the +1 position relative to the phosphorylatable Ser/Thr residue, Zhu et al., (2005a) reported that proline at +1 cannot form a critical amide linkage with the carbonyl group in the catalytic cleft of AGC/CAMK kinases, which thereby hinders their interactions with such substrates (Zhu et al., 2005a).

Another feature of the substrate specificity of most AGC/CAMK family members is the requirement for an arginine residue at the -3 position. Interestingly, Zhu et al. (2005b) also reported that some of these kinases also displayed preference for arginine residues between -2 and -5 positions in their substrates. For example, PKA was the first shown to display preference for substrates having an Arg at the -3 and -2 positions (Kemp et al., 1975; Kemp et al., 1977).

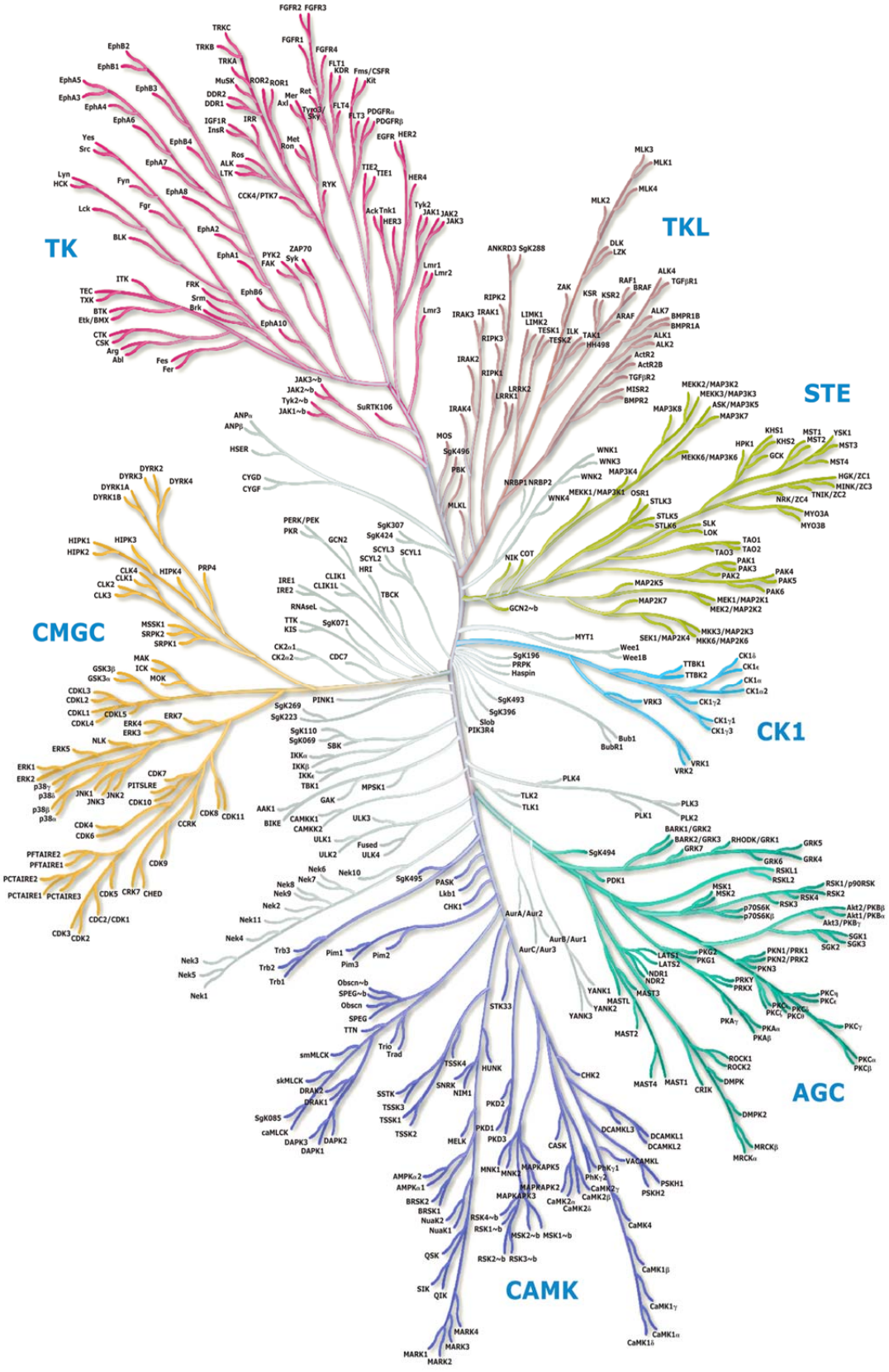

Figure 1.2: The human kinome (source: Manning et al., 2002b)

1.2.3 cAMP signalling and PKA regulation

Cyclic adenosine monophosphate (also known as cAMP or 3',5'-cyclic adenosine monophosphate) was the first intracellular second messenger to be identified. Sutherland and his co-worker Rall discovered the molecule in 1958 while working on the effects of hormonal changes in glucose metabolism following stimulation with adrenaline (Sutherland and Rall, 1958a; Sutherland and Rall, 1958b). While cAMP is in all mammalian tissues, its presence and whether cAMP acts as a second messenger molecule in plants is controversial (Gehring, 2010). cAMP gradients and localised cAMP pools in the cells are established by the opposing actions of adenylyl cyclases (ACs) that catalyse the formation of cAMP from ATP, and phosphodiesterases (PDEs) that hydrolyse cAMP. cAMP signalling is closely coupled with PKA signalling as this protein kinase is the major downstream effector of cAMP. Signalling through cAMP is also mediated by cyclic nucleotide gated (CNG) cation channels and guanine nucleotide exchange factors (GEFs) (discussed in **section 1.2.3.4**).

1.2.3.1 Protein Kinase A

Protein kinase A from the AGC kinase subfamily was the first kinase to have its crystal structure solved (**Figure 1.3**), the first protein reported to be myristylated and also the first kinase for which arginine residues at the -3 and -2 positions in its substrates were shown to be crucial (Kemp et al., 1975; Kemp et al., 1977; Carr et al., 1982; Knighton et al., 1991a; Knighton et al., 1991b).

PKA exists in an inactive heterotetramer comprising two regulatory and two catalytic subunits. The regulatory subunits act as inhibitors, which restrict the indiscriminate action of PKA on its targets. There are three PKA catalytic subunits expressed from three genes, namely Cα, Cβ and Cγ. The C-subunits consist of the catalytic cores, and also N- and C-terminal tails that are thought to mediate protein-protein interactions (Taylor et al., 2005). PKA activation involves its autophosphorylation at Thr197 in the activation loop, which induces conformational changes to bring the catalytic core residues into proximity, thereby converting the enzyme from an inactive to an active state (Steichen et al., 2010). Lys72 is one of the important residues, with equivalents in all protein kinases, and it interacts with the phosphate groups of ATP and also helps maintain the active conformation of the enzyme (Iyer et al., 2005; Taylor et al., 2005). It has also been shown that mutation of Lys72 to histidine suppresses the catalytic activity of PKA and restricts binding to

the R subunits; however, the phosphorylation of Thr197 by a heterologous kinase such as PDK1 is able to restore the interactions between the C subunit and the R subunits (Iyer et al., 2005).

There are two types of regulatory subunits: RI (α and β) and RII (α and β). The R subunits have N-terminal dimerization/docking (D/D) domains and two C-terminal cAMP-binding domains (Taylor et al., 2004). However, despite this conserved domain organisation, the R subunits are functionally non-redundant. They form homo- or heterodimers, which bind to the catalytic subunits of PKA, thereby generating different combinations with the three types of catalytic subunits, which in turn differentially influences substrate specificity in different cells and tissues (Tasken and Aandahl, 2004). These regulatory subunits also have an A-kinase anchoring protein (AKAP)-binding region, which allows them to further restrict the spatial action of PKA (discussed in **section 1.2.3.3**). PKA recognises and phosphorylates substrates with a consensus sequence 'RRXS'. Other consensus sequences for this kinase have also been reported: RRXT, RKXS/T, KKXS/T, KRXS/T, RXXS and RXS (listed in decreasing order of PKA affinity) (Shabb, 2001).

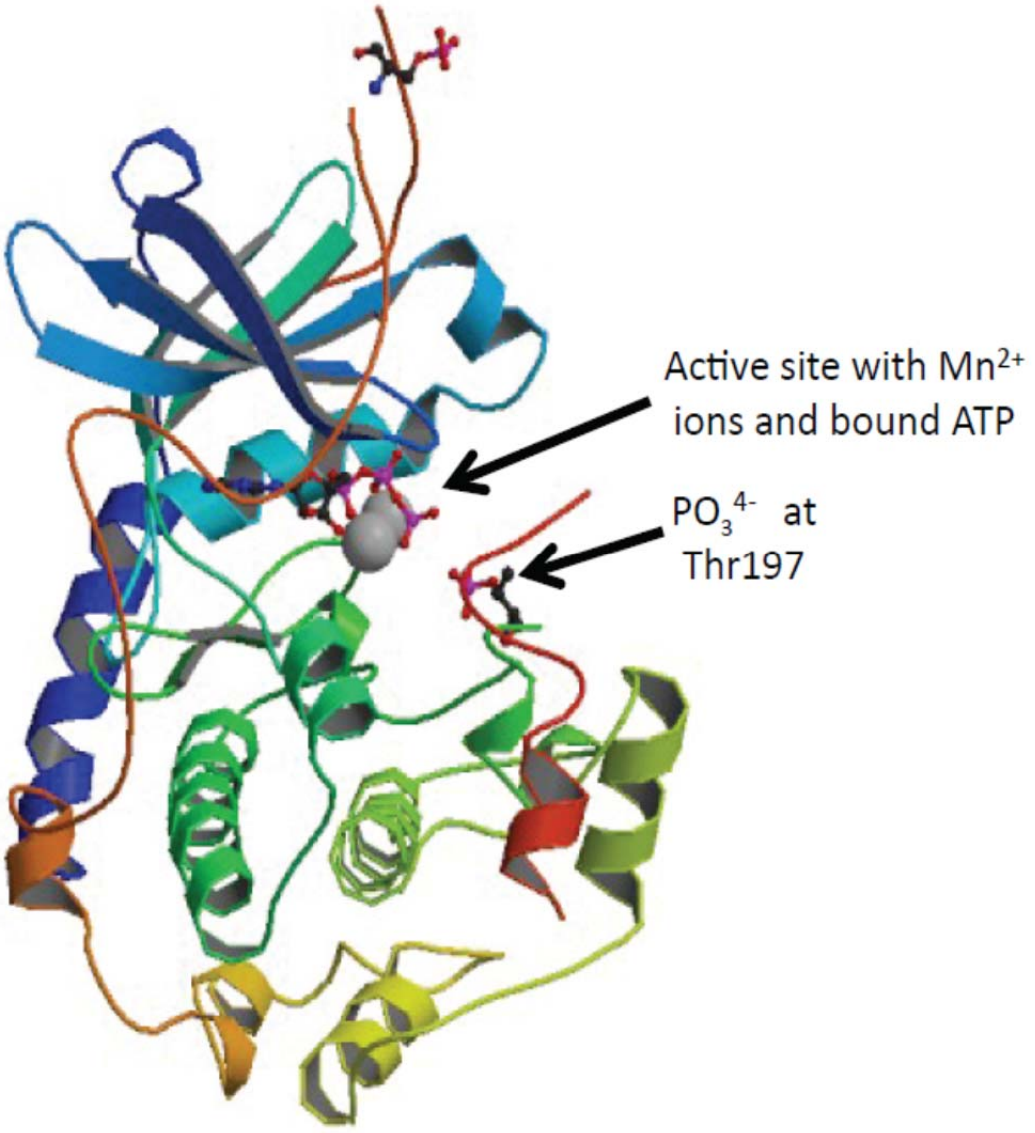

Figure 1.3: Crystal structure of the catalytic subunit of PKA
The catalytic subunit of PKA is bound to ATP (red/pink balls and sticks, center) and Mn^{2+} ions (grey balls) in the active site (Structure 1ATP from www.rcsb.org). The phosphate group important for activation of PKA on Thr197 is adjacent to the active site (ball and stick model, centre right) (Zheng et al., 1993).

1.2.3.2 Adenylyl cyclase and PKA-dependent cAMP signalling

Adenylyl cyclase, also known as adenylate cyclase and adenyl cyclase, was first identified as a transmembrane protein, which traverses the plasma membrane twelve times. Ten isoforms of AC have been reported in mammals, namely AC1-AC10. AC1-AC9 are transmembrane cyclases (tmAC) while AC10 is soluble (sAC) (Kamenetsky et al., 2006). The tmACs are activated by G-proteins and forskolin, with the exception of AC9. In contrast, sAC is activated by bicarbonate and calcium ions and exhibits distinct catalytic and regulatory functions compared to its transmembrane counterparts (Kamenetsky et al., 2006). Structurally, tmACs have a variable N-terminal region, followed by transmembrane spanning helices (TM1), catalytic domain C1, a further six transmembrane helices (TM2) and the second catalytic region C2 (Kamenetsky et al., 2006). The N-terminal domain and the catalytic regions protrude on the cytosolic side of the plasma membrane. Upon activation of the enzyme, the C1 and C2 catalytic regions come into close proximity and form the active site (**Figure 1.4**). This site is also the binding region for the plant diterpene forskolin, which is an AC agonist.

Activation of the G protein coupled receptors (GPCRs) by ligands such as adrenaline and glucagon activates heterotrimeric G proteins bound to the receptors. The G proteins consist of three subunits: Gα, Gβ and Gγ. Gβγ stay bound to each other, and in some cases also to the membrane, after activation of the receptor. Gα can be further sub-divided into four classes: $G\alpha_s$, $G\alpha_i$, $G\alpha_q$ and $G\alpha_{12/13}$. $G\alpha_q$ binds to and activates members of the phospholipase C isoform β family while $G\alpha_{12/13}$ activates the RGS domain-containing Rho guanine exchange factors (Hewavitharana and Wededaertner, 2012). On the other hand, $G\alpha_s$ activates, whereas $G\alpha_i$ inhibits adenylyl cyclase. The activated GPCR receptor acts as a guanine exchange factor that converts $G\alpha_s$–GDP to $G\alpha_s$–GTP. This $G\alpha_s$–GTP complex activates adenylyl cyclase to catalyse the conversion of ATP to cAMP, which in turn binds to the regulatory subunits of PKA. When two cAMP molecules bind cooperatively to each R subunit, the catalytic subunit of PKA is released to transmit the signal by phosphorylating its downstream targets (**Figure 1.4**).

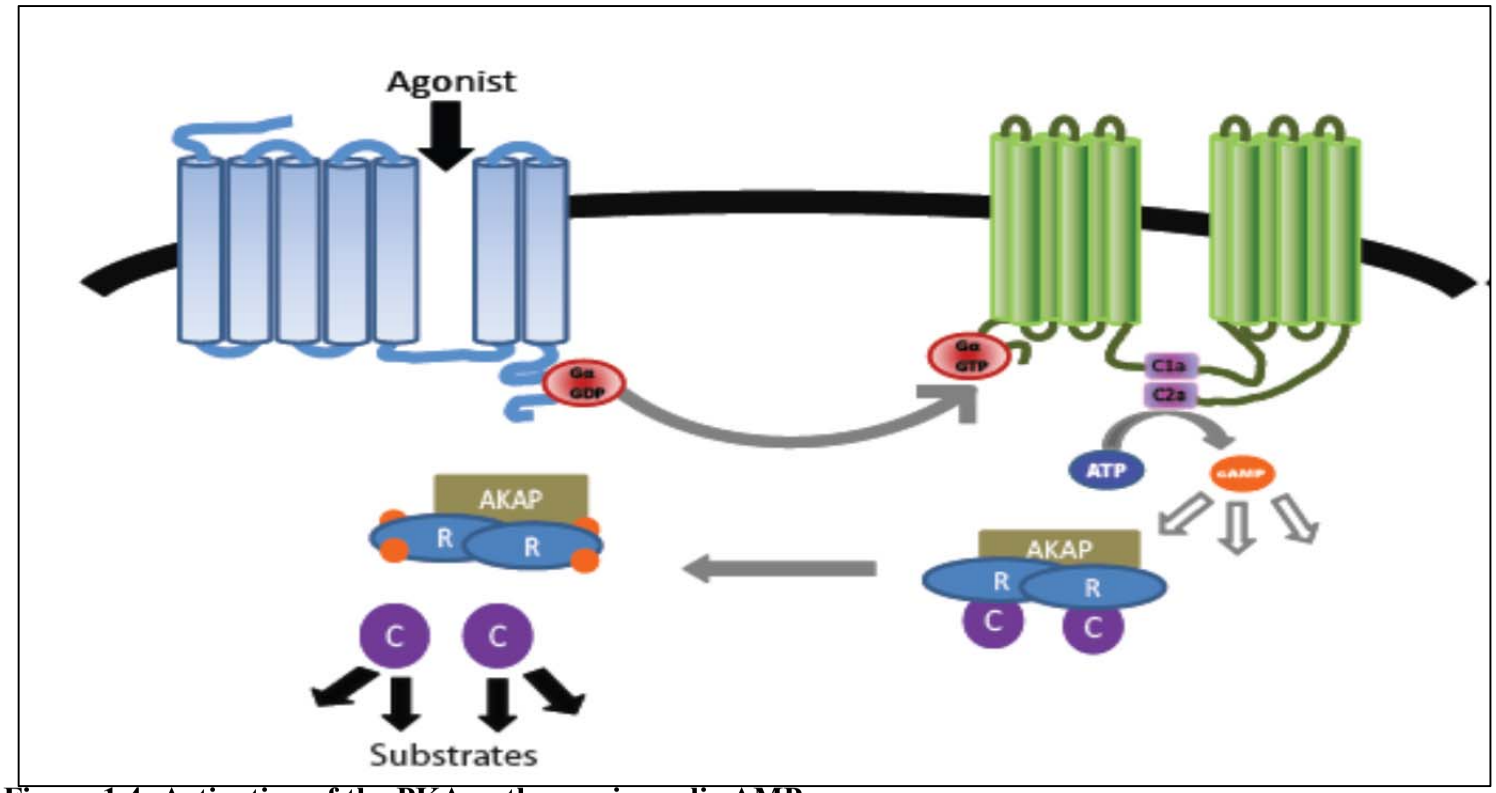

Figure 1.4: Activation of the PKA pathway via cyclic AMP

The G-protein coupled receptor (GPCR, *blue*) is activated upon ligand binding. Once the agonist binds to the GPCR, the latter acts as a GEF for $G\alpha_s$. $G\alpha_s$–GTP (*red*) is released from the receptor and travels along the membrane until it encounters AC (*green*). Once bound, $G\alpha_s$–GTP activates AC which catalyses the conversion of ATP into cAMP (*orange*) and PPi. Four cAMP molecules bind cooperatively to the R subunits of PKA, triggering the release of the catalytic subunit (C, *purple*). The free C subunit then phosphorylates its downstream targets.

1.2.3.3 Regulation of PKA activity: A-Kinase Anchoring proteins (AKAPs)

The AKAPs endow PKA with specificity by acting as scaffolds that restrict its actions by targeting the enzyme to different substrates and cellular locations, and regulating the timing of its action. For example, AKAP79 directs the activity of PKA towards plasma membrane ion channels in response to activation of glutamate receptors in brain and β_2-adrenergic receptors in cardiac cells (Tasken and Aandahl, 2004). Further specificity is introduced by the association of AKAPs with different isoforms of adenylyl cyclases in different tissues (Edwards et al., 2011). As mentioned in **section 1.2.3.2**, AC has nine transmembrane isoforms that are mainly activated by G-proteins. Some of these AC isoforms have also been described to associate with AKAPs at particular cellular locations, where they enhance the specificity of PKA regulation. This in turn is proposed to create a PKA signalosome where all the components of the system (AC, AKAP, PKA and PDEs) are in close proximity to effect localised changes, which can also be regulated (**Figure 1.4**). For example, in rat brain extracts, AKAP79 has been shown to associate with AC5/6, where bound PKA phosphorylates and inhibits AC5/6 activity and also desensitises the bound β_2-adrenergic receptor (β_2-AR) through phosphorylation (Bauman et al., 2006; Dessauer, 2009).

To ensure timely control of PKA, it is critical to have an efficient system to clear cAMP. PKA can phosphorylate many proteins and unregulated PKA would be disastrous to the cell. There is growing evidence that phosphodiesterases associate with AKAPs. For example, the cardiac splice variant of muscle AKAP (mAKAPβ) is attached to the nuclear envelope where it interacts with PKA, PDE4D3 and AC5. In this system, when β_2-AR-stimulated AC5 activates PKA, a feedback loop is also triggered whereby PKA phosphorylates and inhibits AC5 and at the same time activates PDE4D3, which lowers cAMP levels (Dessauer, 2009). In summary, by having the components and substrates for PKA activity and inhibition in close proximity, the actions of PKA can be tightly regulated spatially and temporally.

1.2.3.4 PKA-independent cAMP signalling

In addition to the well-established role of PKA in mediating responses to cAMP, other PKA-independent cAMP signalling networks have also been described. These include signalling through cyclic nucleotide-gated (CNG) channels and GEFs. CNG channels, such as the olfactory receptor, respond upon binding of cAMP and cGMP to control membrane potential and intracellular calcium levels

(Nakamura and Gold, 1987; Tasken and Aandahl, 2004). GEFs activate Ras-related proteins by stimulating their release of GDP and enhancing their binding of GTP (Bourne et al., 1990; Bourne et al., 1991). Two Rap-specific GEFs, namely Epac 1 and 2 (Exchange protein activated by cAMP) have one and two cAMP-binding sites respectively, and are directly regulated by cAMP (De Rooij et al., 1998; Kawasaki et al., 1998; De Rooij et al., 2000). cAMP binding to these Epacs results in conformational changes that activate their GEF domain (Rehmann et al., 2003).

1.3 Protein phosphatases

The function and regulation of protein phosphatases (PPs) are relatively less defined compared to protein kinases. There are far fewer protein phosphatases (150 in humans and 127 in Arabidopsis) compared to protein kinases (518 in humans and 1055 in *Arabidopsis*) (Kerk et al., 2008; Moorhead et al., 2009). How do such a comparatively small number of molecules control such a wide array of functions? Inside cells, protein phosphatases interact with many regulatory subunits, which define their function, substrate specificity and cellular localisation. In this way, relatively few catalytic subunits are directed to selectively control distinct processes inside a cell.

1.3.1 Protein phosphatase gene families and their specificities

Nine phosphorylated amino acids residues that have been reported to undergo dephosphorylation catalysed by PPs: serine, threonine, tyrosine, arginine, histidine, cysteine, lysine, glutamate and aspartate (Hunter, 2004), though phosphorylations of serine, threonine and tyrosine residues predominate in eukaryotic cells (Moorhead et al., 2009). Protein phosphatases can be divided into four main families (a) protein tyrosine phosphatases (PTP) (b) phospho-protein phosphatase (PPP), (c) metallo-dependent protein phosphatases (PPM) and (d) aspartate-dependent protein phosphatases (Moorhead et al., 2009). A summary of the catalytic site residues and signatures of the four protein phosphatase families are listed in **Table 1.2**.

As the name suggests, the PTP family mainly catalyses dephosphorylation of tyrosine residues on proteins but certain of these enzymes can also dephosphorylate non-protein targets such as mRNA (Kenelly, 2003), glycogen (Cohen, 2002) and phosphoinositides (Tonks, 2006). PTP family members, such as PTEN, DUSPs, Cdc25, are defined by the P loop in their active sites, which contain a CX_5R motif in

which phosphate from the substrate is temporarily transferred to the Cys residue during the dephosphorylation reaction (Tonks, 2006). The PPM family on the other hand dephosphorylate serine and threonine residues in a metal ion-dependent manner, more specifically, using Mn^{2+} or Mg^{2+}. In contrast to the PPP family members, the PPM family, which include PP2C and pyruvate dehydrogenase phosphatase, do not have regulatory subunits and are also resistant to the common PPP inhibitors such as okadaic acid and microcystin (Moorhead et al., 2009). Instead of separate regulatory proteins, the PPM family members have evolved with additional domains that confer specificity to these phosphatases.

The PPP family is defined structurally by the three signature motifs GDxHG, GDxVDRG and GNHE. This family comprises PP1, PP2, PP3 (also called PP2B), PP4, PP5, PP6, PP7 and PP1-like enzymes PPKL (PP1 and kelch-like) phosphatases. These enzymes are highly conserved across species, with the catalytic domain of mammalian PP1 sharing at least 76% similarity to plant and fungal PP1 (Moorhead et al., 2009). Members of this family are potently inhibited by a chemically-diverse group of natural toxins including microcystin and okadaic acid (Takai et al., 1987; Bialojan et al., 1988; Bialojan and Takai, 1988; MacKintosh et al., 1994). PPP enzymes have metal ions in their active sites that take part in nucleophilic attack on the phosphate attached to the substrate. Members of this family have a core catalytic centre and have evolved to bind to regulatory subunits, which specify their function, localisation and substrate specificity.

The eukaryotic aspartate-dependent protein phosphatases were discovered recently and relatively little is known about them. Their name comes from the use of an aspartate residue in their signature motif (DXDXT/V) to carry out their catalytic functions. Their specificity appears to be brought about by other domains, such as the BRCT domain, on the same polypeptides as their catalytic core, rather than by binding of separate regulatory subunits (Moorhead et al., 2009).

Table 1.2: Catalytic site signatures and components of the protein phosphatase families

Family	Active site signature	Active site components
PPP	-GDxHG(X)$_{\sim 23}$GDxVDRG(x)$_{\sim 25}$GHNE-	Two metal ions (Mn^{2+} and Fe^{2+} or $Fe^{2+}/Fe^{3+}$and Zn^{2+} for PP2B)
PPM	-(E/Q)D(x)$_n$DGH(A/G)(x)$_n$D(N/D)-B2-	Two metal ions (Mn^{2+} or Mg^{2+})
PTP	-Cx$_5$R-	-
Aspartate-dependent phosphatases	-DxDx(T/V)L-	Aspartic acid

1.3.2 The PPP family of protein phosphatases and their regulatory subunits

The members of the PPP family are distinct from other phosphatases in that they employ a variety of regulatory subunits to modulate their activity, specificity and localisation amongst other functions. The interaction between the catalytic subunit of a protein phosphatase and at least one of these regulatory subunits results in the formation of holoenzyme complexes which partake in a wide array of functions: control of cell cycle progression and regulation, protein synthesis, apoptosis, glycogen metabolism, muscle relaxation and contraction, and RNA processing among others. PP1 and PP2A are two of the most conserved enzymes known, with related enzymes also in prokaryotes (Moorhead et al., 2009). The 13 members of the PPP family can be broadly clustered based on the similarities of the amino acids in their catalytic domain: PP1, PP2A, PP2B, PP4, PP5, PP6 and PP7 in humans. Contrastingly, plants have a few different members compared to humans: they do not have any PP2B but have three distinct families including the PPKL family (Moorhead et al., 2009). Twelve PPP members are known in *S. cerevisiae*, while *Drosophila* has nineteen family members and *Arabidopsis* 26. A phylogenetic tree analysis of the catalytic domains of the PPP members in humans and *Arabidopsis* is shown in **Figure 1.5**. So far, there have been no reports indicating the existence of the free catalytic subunits of PP1, PP2A, PP2B, PP4 and PP6, implying that they are driven to function, and towards specificity, through the interaction with their respective regulatory subunits.

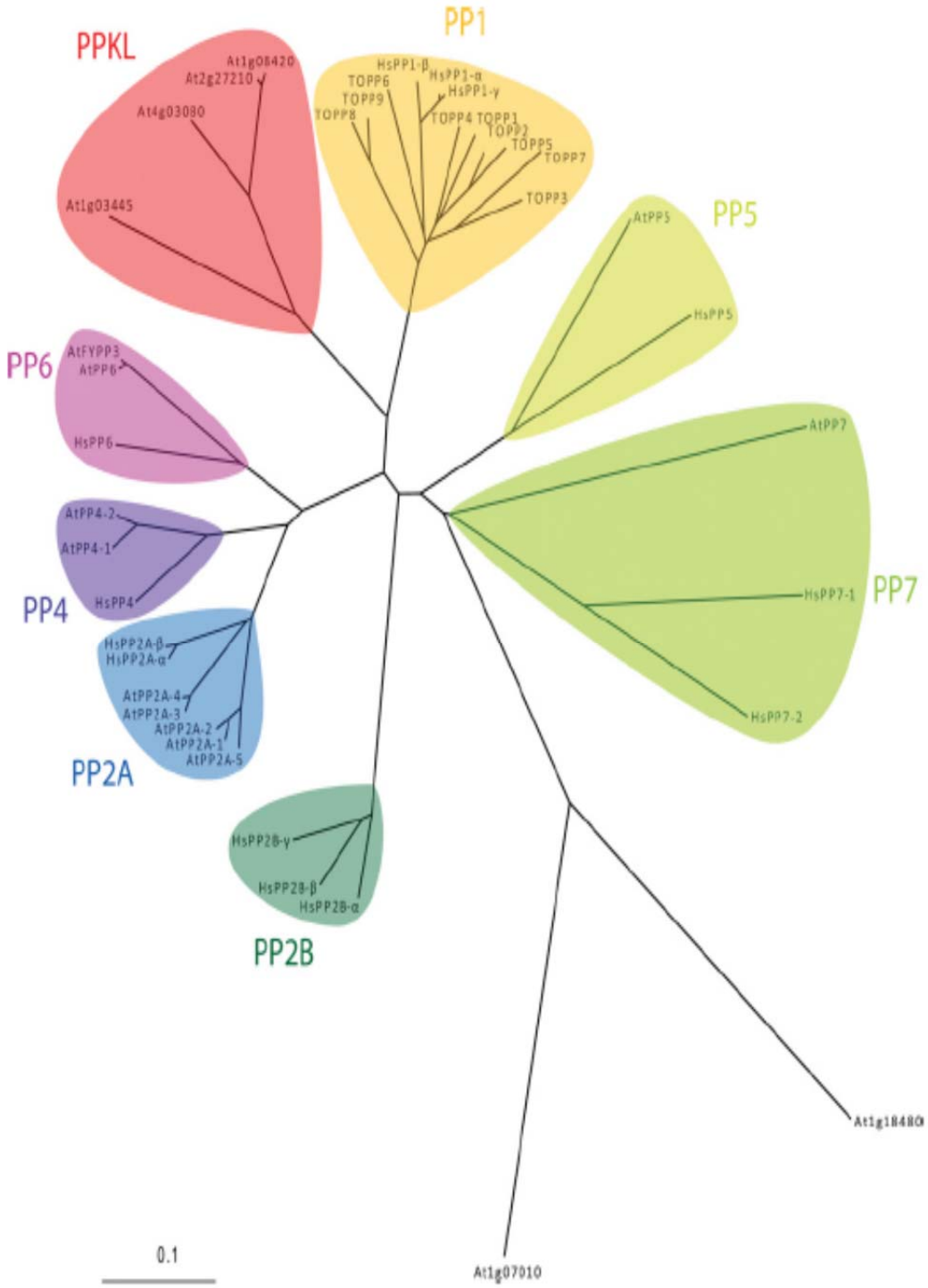

Figure 1.5: Phylogenetic tree analysis of the PPP family members in *Homo sapiens* and *Arabidopsis*

The PPP members are clustered according to the amino acid similarity in their catalytic domains. (TOPP: Type One Protein Phosphatase is the name given to PP1 in plants) (Source: Moorhead et al., 2009).

PP1, one of the most studied members of this family, was discovered to dock onto its regulatory subunits via the RVXF motif present on these subunits. Subsequently however, proteins that lacked the precise RVXF motif were found to bind to PP1. Then, bioinformatical analyses helped redefine the RVXF motif to the more degenerate [RK][VI]$_{012}$[X][FW] (Egloff et al., 1997). Also, two additional signature motifs have recently been described: [GS]IL[RK] and MyPhoNE (Hendrickx et al., 2009).

The PP1 catalytic isoforms in humans are expressed from three genes: PP1cα, PP1cβ and PP1cγ. PP1cγ also has two splice variants: PP1cγ1 and PP1cγ2. Although multiple isoforms have been reported in most mammals, *S. cerevisiae* has a single PP1c-encoding gene, *Glc7*, whose deletion is lethal. PP1 isoforms in plants are called TOPPs (Type One Protein Phosphatase). In humans, each PP1 isoform is fairly specific in their functions and the regulatory subunits to which they bind. For example, only PP1cβ binds to the muscle glycogen targeting subunit (G_M) and the myosin phosphatase-targeting subunit 1 (MYPT1) (Moorhead et al., 1998; Toole and Cohen, 2007; Zagorska et al., 2010).

Structural analyses of PP1 have shown that the enzyme has three binding grooves that are defined by their chemical (a hydrophobic cleft and an acidic groove) and structural (a C-terminal groove) properties respectively (**Figure 1.6a**). These three binding grooves form a Y-intersection, which radiates from the catalytic site. The active site contains two metal ions, which react with hydrated water molecules to initiate the nucleophilic attack during a dephosphorylation reaction. The β12-β13 loop, shown in green in **Figure 1.6b**, protrudes over the active site of PP1. This loop is important during substrate and inhibitor binding to PP1. For example, binding of microcystin to the PP1 active site has been shown to pull the loop inwards, thereby locking the PP1-microcystin complex tightly together. In contrast, regulatory subunits are thought to alter substrate selectivity of the enzyme, at least in part by altering the position of the β12-β13 loop. The three human PP1 isoforms are around 89% identical in their amino acid sequences and share more than 97% homology in their catalytic site residues (Barker et al., 1994; Zhang et al., 1997; Andreassen et al., 1998; Trinkle-Mulcahy et al., 2001). Despite this high similarity, it is thought that variations in the amino and carboxy termini of the PP1 isoforms mediate selective binding to their regulatory proteins. For instance, in

humans, MYPT1 has been shown to interact selectively with the C-terminal domain of PP1β through its eight tandem ankyrin repeat domains (Terrak et al., 2004).

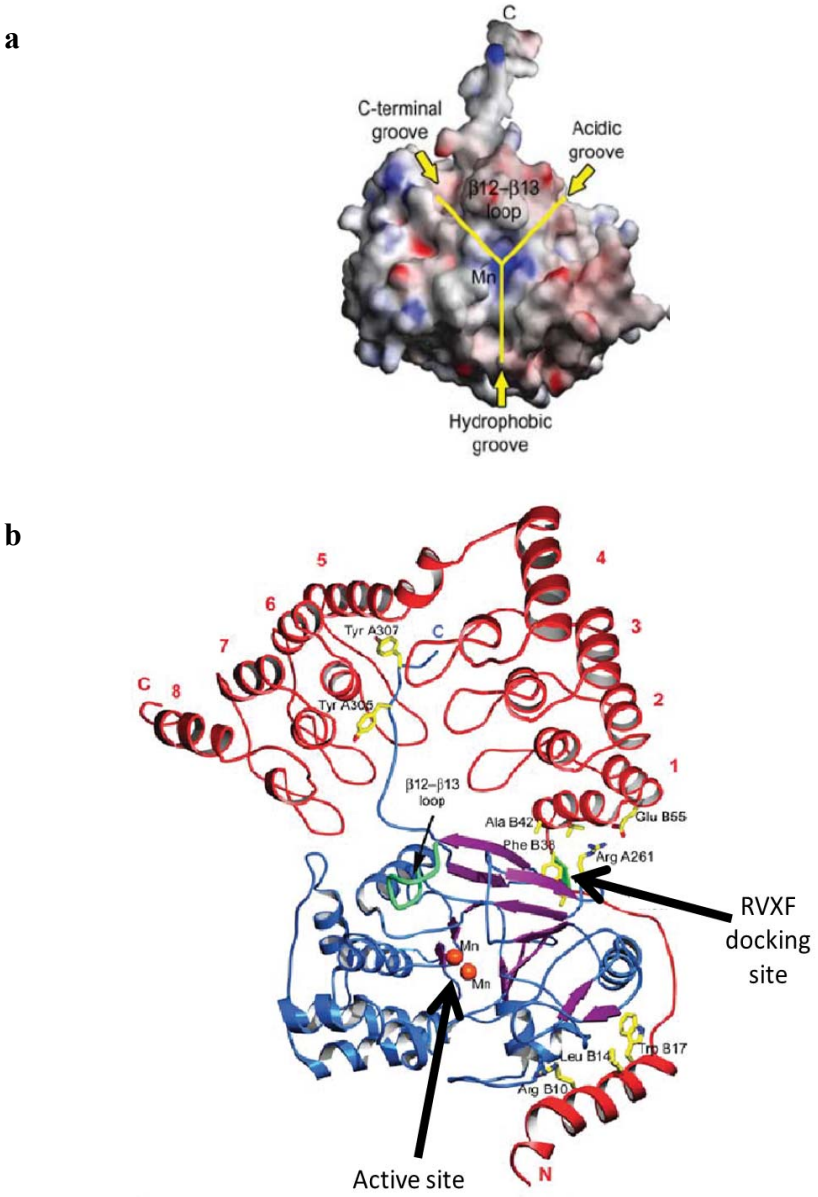

Figure 1.6: The structure of PP1c, showing the catalytic site and different binding grooves

(a) The active site contains two metal (Mn) atoms at its core. The substrate and inhibitor binding grooves (hydrophobic, acidic and C-terminal) form a Y-intersect over the active site. The site of interaction with the RVXF motifs present in the regulatory subunits is on the back end of the active site of the enzyme and cannot be seen in this view. (b) In this model, PP1c (blue ribbons) is complexed to MYPT1 (red ribbons). The β12-β13 loop, which overhangs the active site is shown in light green while the RVXF-interacting region in darker green, indicated by the arrow on the right side of the structure (source: Terrak et al., 2004).

The regulatory subunits of PP1 are important in specifying its activities. For example, the G_M subunit of PP1 targets the enzyme to regulate enzymes on glycogen-protein particles in skeletal muscles (Strälfors et al., 1985; Tang et al., 1991). MYPT1, on the other hand, targets PP1 to myosin light chains to regulate smooth muscle contraction and a more recent role of the MYPT-PP1 complex has been described in cell adhesion (Alessi et al., 1992; Chen et al., 1994; Shimizu et al., 1994; Shirazi et al., 1994; Zagorska et al., 2010). PNUTS/p99 is another targeting subunit of PP1, which directs its phosphatase activity towards the transcription factor LCP1, the telomeric protein TRF2 and the γ-aminobutyric acid receptor (Rose et al., 2008; Kim et al., 2009; Lee et al., 2009). Some PP1-targetting proteins also direct the localisation of PP1 in the cell (**Table 1.3**). These binding subunits bring PP1 into closer proximity to its substrates by increasing the local pool of PP1. In addition to targeting PP1 to its substrates, some PP1-binding proteins can themselves be PP1 substrates. For instance, BRCA1 and CDC25C are activated when they are dephosphorylated by PP1. Furthermore, indiscriminate dephosphorylation by PP1 is prevented by proteins such as I-1. When phosphorylated by PKA, I-1 sequesters and inhibits PP1 upon the release of the latter from its associated subunits. In contrast, Inhibitor-2 (I-2) must be unphosphorylated to form an inactive complex with PP1 that was first identified as the Mg.ATP-dependent PP1 (Goris et al., 1979). This name comes from the fact that when I-2 is phosphorylated on Thr72 by glycogen synthase kinase 3 (GSK) in the presence of magnesium ions and ATP, the PP1 catalytic subunit is released and can bind its targeting subunits (Goris et al., 1979; Hemmings et al., 1981; Hemmings et al., 1982; Ballou et al., 1983; Cohen, 1989). PP1 has also been known to bind to an inhibitor/targeting subunit and a substrate at one time. For example, I-2 has been shown to bind to a PP1-neurabin I holoenzyme complex (Terry-Lorenzo et al., 2002) while I-1 has been shown bound to a PP1-GADD34 complex (Connor et al., 2001).

Table 1.3: Regulatory subunits targeting PP1 to different subcellular localisations

Targeting subunit	Cellular localisation	References
G_M	Glycogen particles in skeletal muscles and heart	Strälfors et al., 1985; Tang et al., 1991
G_L	Glycogen particles in liver	Moorhead et al., 1995; Doherty et al., 1995
MYPT1	Myosin smooth muscle	Alessi et al., 1992; Chen et al., 1994; Shimizu et al., 1994; Shirazi et al., 1994; Zagorska et al., 2010
MYPT2	Skeletal muscle	Fujioka et al., 1998; Damer et al., 1998; Moorhead et al., 1998
GADD34	Endoplasmic reticulum	Novoa et al., 2001; Connor et al., 2001
URI	Mitochondria	Djouder et al., 2003; Theurillat et al., 2011
NOM1	Nucleoli	Gunawardena et al., 2008
RepoMan	Chromatin	Trinkle-Mulcahy et al., 2006
PNUTS/p99	Nucleus	Kreivi et al., 1997; Allen et al., 1998; Kim et al., 2004
RRP1B	Nucleoli	Chamousset et al., 2010

PP2/PP2A is distinct from PP1 in terms of binding to its regulatory subunits. The holoenzyme of PP2A consists of a catalytic core and a 65 kDa subunit termed the A subunit or PR65 subunit. A third variable subunit, called the B subunit completes the PP2A complex (Janssens and Gorris, 2001; Li and Virshup, 2002). There are at least 18 B subunits encoded by 14 genes in humans. In addition, there are two catalytic and two A subunits, which together with the B subunit, raise the potential number of different trimeric PP2A complexes to over 70. The subcellular localisations of these subunits vary, which could contribute to cell-type specific functions for these multiple holoenzymes.

PP2A is more potently inhibited by okadaic acid compared to PP1. The differences in these affinities have been exploited to distinguish between these two phosphatases during purification processes. Similarly, microcystin is a more potent inhibitor of PP2A than it is of PP1 (MacKintosh et al., 1990). PP2A is involved in the regulation of a number of processes including, but not limited to, DNA and protein synthesis, cell cycle progression, apoptosis, metabolism and stress responses. PP2A has also been shown to act as a tumour suppressor by dephosphorylating c-Myc, which leads to proteolytic degradation of the oncogenic c-Myc protein (Mumby, 2007).

PP3/PP2B is differentiated by the other phosphatases through its dependence on Ca^{2+} and resistance to most PPP inhibitors including okadaic acid and microcystin (Armstrong, 1989; MacKintosh et al., 1990). Also known as calcineurin, the catalytic core of PP2B binds to its regulatory subunit, which confers the Ca^{2+} dependence to the enzyme. This results in further interaction with calmodulin, enabling the holoenzyme to regulate the calcium/ calmodulin reflux changes in the cell (Klee et al., 1998). PP2B is abundant in the brain where it regulates, through dephosphorylation, dopamine, DARPP32, G-protein coupled receptors (AMPA) and the ligand gated ion channels (NMDA). PP2B is inhibited by the immunosuppressant drugs cyclosporine and FK506, when the latter are bound to immunophilin proteins, cyclophilin A and FK506-binding protein (Hardie, 2003). Unfortunately, in the kidneys, PP2B activates the sodium/potassium ATPase ion transporter, which means that these drugs cause nephrotoxicity in organ transplant patients (Naessens et al., 2009).

Like PP2A, PP4 forms both dimeric and trimeric holoenzyme complexes, although it has only three variable subunits, namely R3A, R3B and Gemin. The PP4

trimers comprise the catalytic core, one of the variable subunits and its R2 subunit. Dimeric structures are complexes of the catalytic subunit with its R1 subunit (Cohen et al., 2005). The functions of PP4 in the cell range from cellular signalling to spliceosome assembly and chromatin remodelling (Cohen et al., 2005).

There is no evidence to suggest the presence of regulatory subunits for PP5. Instead, this enzyme is thought to interact with its substrates via the three tetratricopeptide repeats (TPR) in its amino terminal domain (Chinkers, 2001; Yang et al., 2005). PP5 has been shown to be involved in a number of cellular processes including transcription, apoptosis, DNA damage and stress responses, cell cycle arrest and regulation of signal transduction pathways.

PP6, like PP4, forms dimeric and trimeric complexes (Stefansson et al., 2008). PP6 has been shown to stabilise cyclin D1 during G1/S cell cycle progression in human cells (Stefansson and Brautigan, 2007). It is also involved in the regulation of TAK1-mediated stress response pathways (Kajino et al., 2006).

PP7 is similar to PP2B in that it also depends on Ca^{2+} for its activity. A calmodulin-binding motif (distinct from the PP2B motif) in the amino terminal of PP7 mediates its interaction with calmodulin, while the EF hand-like sequences in the carboxy terminal of PP7 confer Ca^{2+} sensitivity (Andreeva and Kutuzov, 1999; Kutuzov et al., 2002). The functions of PP7 of mammals remain elusive (Andreeva and Kutuzov, 1999). The *Drosophila* PP7 homologue, rdgC, is involved in light sensing responses by dephosphorylating rhodopsin, resulting in its uncoupling from its G-protein receptor. However, mice deficient in PP7 exhibit normal rhodopsin phosphorylation and light responses, suggesting that the functions of PP7 might differ in mammals and flies (Ramulu et al., 2001).

1.3.3 Use of toxins to inhibit and purify protein phosphatases

To investigate the structures and functions of phosphatases, small-molecule inhibitors became in demand. When a phosphatase is inhibited, the levels of phosphorylated proteins in that particular cell increases, provided the relevant protein kinases are at least slightly active. The resulting cellular effects can give clues about how processes are affected by phosphorylation. Several natural protein phosphatase inhibitors have been discovered, namely microcystin-LR, okadaic acid, calyculin A, cantharidin, foestricin, tautomycin and nodularin. With the exception of cantharidin, these toxins mostly bind phosphatases at subnanomolar and nanomolar ranges (MacKintosh and Diplexcito, 2003). The first phosphatase inhibitor used,

okadaic acid, is a polyether fatty acid produced by marine microalgae (Dawson and Holmes, 1999). Although okadaic inhibits most PPP members, its potency is highest against PP2A and PP4, followed by PP1; PP5 is also inhibited by okadaic acid (reviewed in Cohen, 2010). Microcystin is a potent inhibitor of a wider range of PPPs: PP1, PP2A, PP4, PP5 and PP6 (reviewed in Cohen, 2010). Interestingly, none of these toxins are effective towards PP2B.

The microcystin (MC) cyclic peptides are potent hepatotoxins produced by cyanobacteria in fresh waters. Over 80 variants of MC have been identified, including amino acid variations and modifications (Feurstein et al., 2009), with the most common being MC-LR, MC-RR and MC-YR (L-Leucine, R-Arginine and Y-Tyrosine in the variable positions) (Puerto et al., 2009). The general structure of a microcystin, depicted in **Figure 1.7**, is cyclo-(D-Ala-X2-D-MeAsp3-Z4-Adda5-D-Glu6-Mdha7), where X and Z are variable amino acids such as L, R or Y, D-MeAsp represents D-erythro-β-methylaspartic acid, Mdha is N-methyldehydroalanine and Adda is the unusual amino acid (2S, 3S, 8S, 9S)-3-amino-9-methoxy-2,6,8-trimethyl-10-phenyldeca-4,6,dienoic acid (van Appledoorn et al., 2007). This Adda amino acid is critical for the toxicity of MC, and its oxidisation and isomerisation have been reported to reduce the potency of MC as a toxin (Tsuji et al., 1994; Song et al., 2006). While MCs have also been reported to either increase or decrease the activities of other proteins *in vivo*, these effects are probably mediated via inhibition of PPP enzymes. For example, MC has been shown to decrease the activity of DNA-PK during DNA repair in cell extracts (Ariza et al., 1996; Douglas et al., 2001). MC increases the gene and protein expression of p53, which is a well-known tumour suppressor, *in vivo*, in liver tissues, primary hepatocytes and HepG2 cell lines (Fu et al., 2005; Xing et al., 2008; Zegura et al., 2008). Furthermore, exposing liver tissues to MC *in vivo* has also been shown to increase the protein expression of Bax and JNK, thereby affecting apoptosis and MAPK signalling respectively (Weng et al., 2007; Wei et al., 2008).

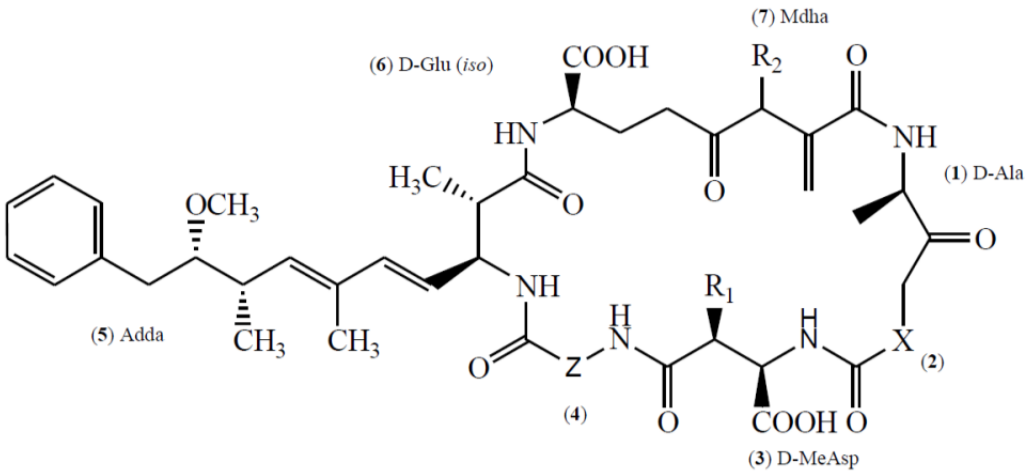

Figure 1.7: General structure of microcystin
Microcystin, a potent inhibitor of PPP family members (except PP3), is a cyclic peptide with the unusual ADDA moiety. (1) D-Ala is D-alanine; (2) X and (4) Z represent the L-amino acid variations for the many microcystin variants; (3) D-MeAsp is D-erythro-β-methylaspartic acid; (5) Adda is the unusual amino acid (2S,3S,8S,9S)-3-amino-9-methoxy-2,6,8-trimethyl-10-phenyldeca-4,6-dienoic acid; (6) Mdha is N-methyldehydroalanine (Source: Campos and Vasconcelos, 2010).

Microcystin and okadaic acid have similar 3-dimensional tadpole shapes and both interact with PP1 in a similar ways, at three points within the active site: the hydrophobic groove, the C-terminal groove and the β12-β13 loop above the catalytic site (**Figure 1.6**). Upon binding, MC-LR interacts with the two hydrated catalytic metal ions of the substrate-binding pocket of the phosphatase. The long hydrophobic tail comprising the Adda residue lies within the hydrophobic groove of PP1, which projects from the active site. The third point of contact is the β12-β13 loop, which overhangs the active site. MC-LR binding pulls this loop into the catalytic groove through a covalent bond formed between the dehydroalanine of MC-LR and Cys273 in the β12-β13 loop (MacKintosh et al., 1995). Mutating the adjacent Tyr272 in recombinantly expressed PP1 enzymes from *E.coli* decreases the sensitivity of PP1 to MC-LR, without affecting the enzymatic activity of PP1 per se (Zhang et al., 1996; Connor et al., 1998; Watanabe et al., 2001). However, PP1 purified from insect Sf9 cells showed decreased phosphatase activity when Tyr272 was mutated (Watanabe et al., 2001).

To study the properties of PPs, their purification from cell extracts was of essence, inspiring the design of microcystin affinity chromatography. Because the covalent bond between the dehydroalanine of MC-LR and Cys273 of PP1 is not essential for inhibition, the dedydroalanine could be adopted for immobilising the

toxin. Using Michael chemistry, the dehydroalanine residue can be reacted with small reactive thiols that also carry an amine group. The amine is in turn linked to N-hydroxy-succinamide activated Sepharose, biotins and other such compounds (Moorhead et al., 1994; Campos et al., 1996). The resulting microcystin-Sepharose beads allow the affinity purification of phosphatases and their regulatory subunits from cell extracts. In the case of PP1, the regulatory subunits can be displaced from the phosphatases bound to MC-LR on the column by competitive elution with a synthetic peptide containing the RVXF motif (Moorhead et al., 2008). The phosphatase catalytic subunits can be released using a chaotropic salt such as sodium thiocyanate in the case of PP1, while denaturing buffers are required to release PP2A from the microcystin columns (Moorhead et al., 1994).

1.3.4 Outstanding questions about the acute regulation of protein phosphatases

Protein phosphatases of the PPP family are involved in many signalling pathways. For example, PP2A has been heavily implicated in the regulation of the insulin- and Erk-signalling pathways by dephosphorylating and inactivating key kinases involved in these pathways (Millward et al., 1999). For instance, PP2A has been shown to dephosphorylate Akt *in vitro*, and this dephosphorylation is prevented upon okadaic acid treatment (Andjelkovic et al., 1996). Moreover, the p70S6K has also been shown to be dephosphorylated in vivo by PP2A and also stably associates with this phosphatase *in vivo* (Ballou et al., 1988; Westphal et al., 1999). PP2A has also been shown to dephosphorylate PKCα and Erk, thereby inactivating them (Hansra et al., 1996; Alessi et al., 1999; Gomez and Cohen, 1991; Anderson et al., 1990). However, little is known about the acute regulation of the PPPs by external stimuli.

In skeletal muscle, protein phosphatase 1 was reported in the mid to late 1980s to be regulated in vitro by cAMP-dependent protein kinase (PKA) (Caudwell et al., 1986) and in vivo by the hormone adrenaline (mediated by PKA) (MacKintosh et al., 1988). This regulation of PP1 was via its glycogen-binding G_M subunit. Upon phosphorylation of G_M by PKA, PP1 is released from the glycogen granules into the cytosol where it is sequestered by I-1 (Strålfors et al., 1985; MacKintosh et al., 1988). In common with many other targeting subunits of PP1, the G_M subunit has the degenerate RVXF motif that binds to the hydrophobic cleft of PP1 distal from the active site (Caudwell et al., 1986; Dent et al., 1990; Egloff et al., 1997; Wakula et al., 2003). This serine (SRRV**S**^{67}FAD) within the PP1-binding site

of G_M was identified to be one of the two sites whose phosphorylation by PKA disrupts the PP1.G_M complex in response to adrenaline (MacKintosh et al., 1988 Dent et al., 1990). The other PKA-phosphorylated site, Ser48 (PSRRG**S**^{48}GSSED), was shown to be important for the dissociation of PP1 from the G_M subunit, thereby enhancing the phosphorylation, and inhibition of glycogen synthase by PKA; this site has also been shown to be phosphorylated by p90RSK (Hiraga and Cohen, 1986; MacKintosh et al., 1988; Dent et al., 1990; Lavoinne et al., 1991). This remains until now the most lucid example of PP1 regulation through cAMP–PKA signalling by an external stimulus, in this case adrenaline.

PP1 is also regulated by I-1 and the related DARPP32 (Dopamine- and cAMP-regulated phosphoprotein of apparent Mr 32,000) in the brain via cAMP–PKA signalling (Aitken et al., 1982; Endo et al., 1996). Similar to I-1, DARPP32 inhibits PP1 in neurons upon phosphorylation of its Thr34 by PKA. At basal levels, DARPP32 is phosphorylated by Cdk5 at Thr75, which blocks the PKA-mediated phosphorylation of DARPP32 at Thr34 (Bibb et al., 1999). Interestingly, upon forskolin stimulation in neurons, PKA phosphorylates the B56δ subunit of the PP2A complex, which in turn dephosphorylates Thr75 of DARPP32, thereby enhancing parallel phosphorylation of Thr34 by PKA (Ahn et al., 2007). This coordinated regulation of PP1, involving PP2A and DARPP32 is interesting, and raises questions about whether there are other regulatory/inhibitory proteins that work in synchronised systems to regulate these dephosphorylating enzymes.

Other than these examples, very little is known about how protein phosphatases are regulated. Since most of these proteins seem to regulate PPs upon PKA activation, it would seem logical that there would be other proteins regulating under similar conditions. Following this thought, we were interested to investigate whether there were other proteins we could find which might be possibly involved in the acute regulation of protein phosphatase 1 in particular (see **Chapter three**).

1.4 Protein phosphorylation can create sites for binding to specific domains and proteins

The phosphorylation of proteins on serine, threonine and tyrosine residues can result in conformation changes that, for example, activate or inhibit the target protein. However, some phosphorylations have no direct effect on the isolated target, but rather inhibit or promote its interaction with other proteins. For example,

the PTB (phosphotyrosine binding) and SH2 (Src-2 homology) domain-containing proteins are known to bind phosphorylated tyrosine residues: the SH2-domain of APS binds to two phosphotyrosine residues in the activation loop of the insulin receptor kinase (Seet et al., 2006). Domains such as WW, WD40, FHA and BRCT can also mediate binding to their targets via phosphorylated serine/threonine residues (Seet et al., 2006). 14-3-3s are one such group of proteins that mainly bind to phosphorylated serine/threonine residues on their targets. However, in contrast to the other domains mentioned, which are domains within larger proteins, the 14-3-3s are 'stand-alone' dimers.

1.5 14-3-3 proteins

14-3-3s are becoming increasingly important in understanding signalling pathways and their regulation. 14-3-3 proteins were first identified from bovine brain extracts by Moore and Perez in 1967. The importance of 14-3-3s was first understood when they were shown to bind, and activate, phosphorylated tryptophan and tyrosine hydroxylases (Ichimura et al., 1987; Furukawa et al., 1993). The rather unusual name of this family is derived from their elution and migration pattern: the protein was found in the 14th fraction on DEAE-cellulose chromatography and in spot cluster 3.3 upon starch gel separation of a brain extract (Moore and Perez, 1967). 14-3-3s consist of a group of acidic proteins ranging from 28-30 kDa, which exist as dimers; they are highly conserved both within and across eukaryotic species (Aitken, 2006). Although 14-3-3s are quite varied in terms of cellular distributions, they are in particularly high abundance in the brain (~1% of total soluble brain protein) (Boston et al., 1982) and the implications of this are only now being understood. For instance, mutations in 14-3-3-binding (phospho)proteins such as Ndl1 and the Reep family are implicated in brain disorders (Burdick et al., 2008; Argasinska et al., 2009; Nicodemus et al., 2010; Park et al., 2010; McCorquodale III et al., 2011). Understanding the binding of 14-3-3s to their targets and elucidating the outcomes of such interactions is a priority, considering the vast number of disorders that involve 14-3-3s and their binding partners (Tinti et al., 2012).

1.5.1 Isoforms and structure of 14-3-3 proteins

In most eukaryotic species studied, 14-3-3s have been observed to have multiple isoforms: *Arabidopsis* is reported to have at least 12 isoforms; humans have 7 while yeast has two isoforms, BMH1 and BMH2. The 14-3-3 family in humans

are encoded by seven genes, giving rise to nine isoforms: α/β, γ, ζ/δ, ε, η, θ and σ (where α and δ are the phosphoforms of β and ζ respectively) (Aitken 2006; Aitken, 2011). A tenth isoform has recently been reported as the splice variant of 14-3-3 ε, known as 14-3-3 epsilon sv (Aitken 2011). In humans, 14-3-3ε was reported to be the oldest member (meaning most similar to the 14-3-3 isoforms from yeast and plants) while 14-3-3σ was thought to be the last evolved member (Rosenquist et al., 2000). However, the evolution of the 14-3-3 proteins should, perhaps, be revisited in view of recent discoveries about how their interacting phosphoproteins evolved at the evolutionary transition from invertebrates to vertebrate animals (Tinti et al., 2012). These evolutionary studies were ongoing during the latter part of my PhD studies and are discussed further in **Chapter 5**.

The high degree of conservation of 14-3-3 isotypes within and across eukaryotic species suggests that these proteins have evolved from early eukaryotes and play important roles in cells. Indeed, knocking out both 14-3-3 isoforms in *S. cerevisiae* was shown to be lethal; complementation with plant isoforms of 14-3-3 was able to rescue the phenotype (Gelperin et al., 1995). Thus far, no 14-3-3 or 14-3-3-like proteins have been found in prokaryotes (Bridges and Moorhead, 2005). 14-3-3 isoforms have been found to preferentially exist as dimers (homodimers and heterodimers) as monomeric 14-3-3 isoforms are thermodynamically unstable (Aitken, 2006). Since 14-3-3s are quite widely distributed in cells and differ in cell types, the occurrence of a particular heterodimer would then depend on the isoform distribution in that cell. For example, while most 14-3-3 isoforms are widely expressed, 14-3-3θ is predominant in T cells while epithelial cells express 14-3-3σ (Aitken, 2006). These cell types would then mainly have homodimers of the respective isoforms. Moreover, 14-3-3σ is evolutionarily distant from the other isoforms: it preferentially homodimerises and displays a unique binding affinity for its target protein (Wilker et al., 2005; Bridges and Moorhead, 2005).

Crystal structures have shown 14-3-3s to be highly helical: each monomer consists of nine antiparallel α-helices, forming a cup shaped dimer with a central amphipathic groove. This groove forms the interaction site with the target protein and consists of the most highly conserved residues in all the 14-3-3 isoforms in eukaryotes. The four residues Lys49, Arg56, Arg127 and Tyr128, which are involved in binding the phosphate group of the target protein lie in this region and are fully conserved across all species (residues labelled according to their positions

in 14-3-3ζ) (Yaffe et al., 1997; Petosa et al., 1998; Rittinger et al., 1999; Obsil et al., 2001; Wurtele et al., 2003). The N- and C-termini are less conserved and may be useful to ensure specificity of interactions with their target proteins. The amino terminal is responsible for the dimerization of the protein, while the carboxy tail of the protein is able to change its conformation upon getting phosphorylated, and upon a ligand binding into the groove. The overall structure of the 14-3-3 dimer is otherwise reported to be very rigid, acting as a backbone for binding its targets, which are able to modify their conformations to fit into the dimer (**Figure 1.8**). Each monomer of the 14-3-3 is able to bind a phosphate moiety from a single or two phosphorylated proteins; these phosphate groups have been observed to be approximately 34 Ångströms apart when bound to the 14-3-3-dimer.

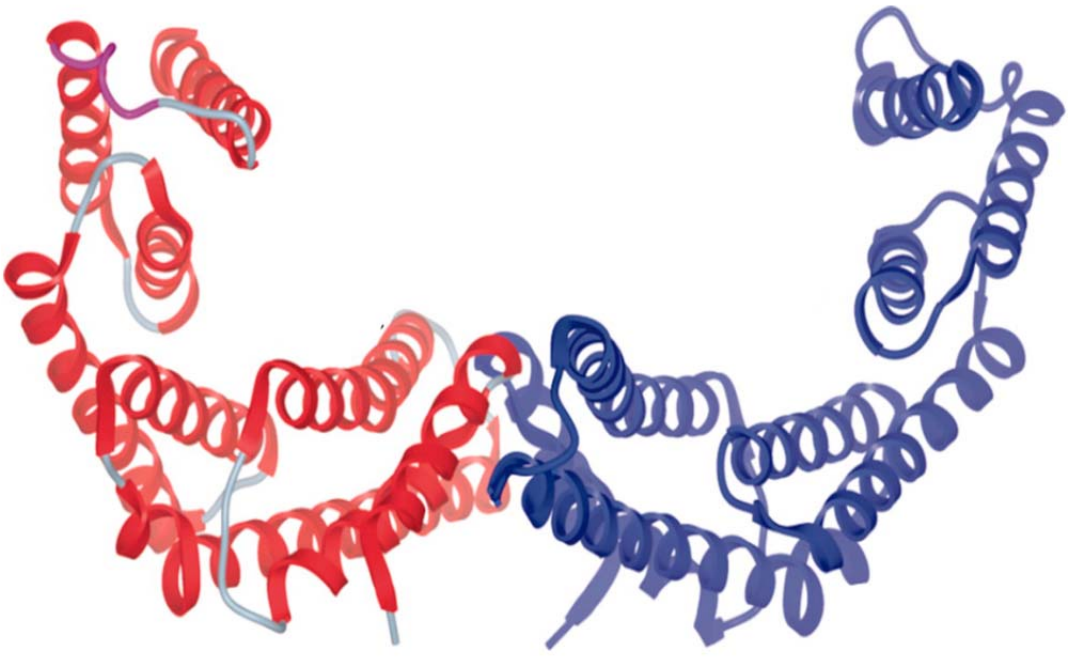

Figure 1.8: Structural representation of a 14-3-3β homodimer
One 14-3-3β monomer is in blue and the other in red (source: Yang et al., 2006).

1.5.2 Specificity and regulation of 14-3-3s

14-3-3s are involved in a wide array of functions in the cell, including cell cycle control, DNA and RNA binding, protein synthesis, apoptosis, cell signalling, and metabolism. It follows that there must be some kind of regulation and specificity in place to ensure that only the required 14-3-3 and target(s) are activated under a given stimulus. This specificity is brought about at different levels in 14-3-3-

signalling. These adapter molecules have been shown to bind phosphorylated targets: the target must have undergone a previous phosphorylation event by an upstream kinase to enable its interaction with 14-3-3s. This already confers some specificity as only a kinase activated by a particular signalling pathway would be able to phosphorylate its target, which would consequently bind to a 14-3-3 dimer. Members of the CAMK and AGC families are the major kinases known to phosphorylate 14-3-3-binding proteins. It is also inferred that the amount and distribution of 14-3-3s in the cell will greatly influence the type of interaction. The different heterodimers that are present would also reflect on the type of interactions occurring upon activation of a particular signalling pathway. 14-3-3 isoforms may bind to certain phosphorylated binding partners with stronger affinities than others. Thus 14-3-3s could be described as signal integrators, which amplify stronger signals in the cell while filtering out weaker interactions, to generate a meaningful physiological outcome, such as apoptosis.

Another level of specificity in the mode of action of 14-3-3s is conferred by their strong specificity for the residues flanking the phosphorylated sites. Phosphopeptide library and literature searches identified two major consensus motifs in the binding targets: mode I RSX(pS)XP and mode II RX(F/Y)X(pS)XP (Yaffe et al., 1997). Interestingly, proline at the +2 occurs in approximately only 50% of 14-3-3-binding phosphoproteins identified so far (Johnson et al., 2010). A proline at this position induces a twist by directing the residues lying at the carboxy-end of the phosphorylated sites outwards from the amphipathic groove. Yaffe et al (1997) observed that the binding affinity of a doubly phosphorylated peptide is 30-fold higher compared with a singly phosphorylated peptide, implying that binding of the target to a 14-3-3 dimer can be cooperative. This becomes important in a physiological context where a protein that displays two weak 14-3-3-binding sites in tandem can bind with a stronger affinity. A third consensus motif located at the extreme carboxy termini of proteins, (pS/T)X_{1-2} (mode III) has also been reported in the literature, although its occurrence is less frequent in the known 14-3-3-binding targets. In mammalian cells, few proteins have been reported to bind 14-3-3s through mode III, but the evidence is not very strong. The plant proton ATPase protein located at the plasma membrane is the best understood example of a mode III 14-3-3-binding target. In this case, three 14-3-3 dimers bind six adjacent phosphorylated ATPase proton pumps at the carboxy terminus, thereby stabilising

the oligomerisation of the proton pump to enable its function at the cell surface level (Ottmann et al., 2007).

Most of the interactions of 14-3-3s are described to be phosphorylation-dependent. However, there are a few reported cases of phosphorylation-independent 14-3-3-binding proteins. For example, the Exoenzyme S (ExoS) ADP-ribosyltransferase toxin of *Pseudomonas aeruginosa* requires 14-3-3-binding to activate its ADP-ribosyltransferase activity (Ottmann et al., 2007b). However, there are no known 14-3-3s in prokaryotes and since this interaction only occurs in infected host cells, this represents a case of opportunistic pathological interaction, as opposed to a true physiological interaction. The synthetic R18 peptide (PHCVPRDLSWLDLEANMCLP), used to bind 14-3-3s in competition with its phosphoprotein targets, is another example of phosphorylation-independent 14-3-3-binding: this peptide binds with high affinity to the amphipathic groove of 14-3-3s, in a similar fashion to phosphorylated targets (Wang et al., 1999; Jin et al., 2004).

It should be noted that 14-3-3s are themselves also subjected to phosphorylation as a regulatory mechanism, although the physiological relevance of this is still not very well understood. Phosphorylation of Ser58 on 14-3-3ζ has been shown to promote the formation of 14-3-3ζ monomers as opposed to the naturally occurring dimers, which would clearly affect the interaction of dimers involving 14-3-3ζ and their interacting partners (Powell et al., 2002; Woodcock et al., 2003). Another site, Ser233, in this isoform has been reported to negatively regulate interactions between 14-3-3 and its binding proteins by sitting in the phosphopeptide binding region of the 14-3-3 dimer, thereby competing with actual binding partners (Dubois et al., 1997; Aitken et al., 2002; Dumaz et al., 2003; Obsilova et al., 2004). Additionally, phosphorylation of Ser184 has been shown to decrease the interaction between 14-3-3 and its targets (Tsuruta et al., 2004; Yoshida et al., 2005). However, none of these sites are conserved in the human 14-3-3 isoforms, suggesting that these regulatory mechanisms may be applicable only under certain conditions, and only for certain isoforms, stressing the importance of phosphorylation in the heterodimerisation of the 14-3-3 proteins, and consequent binding to their targets.

1.5.3 14-3-3 phosphoproteomics show a link between AGC and CAMK kinases and 14-3-3-binding proteins

Many phosphorylated proteins bind to the 14-3-3s. Generally, a 14-3-3 dimer engages with a pair of tandem phosphorylated sites within disordered regions and/or

straddling either side of a functional domain (Johnson et al., 2010). Analyses of the 14-3-3-binding sites show that they fall into distinct subtypes that overlap with the specificities of basophilic protein kinases in the CAMK and AGC families, including PIMs, PKA, PKCs, PKB, p90RSK and AMPK (Johnson et al., 2010). Previously, members of the group have exploited the specificities of 14-3-3s to identify many new downstream targets of the CAMK and AGC kinases and their associated pathways: the PI 3-kinase–PKB, the (PKC)–Erk–p90RSK and AMPK pathways (Pozuelo Rubio et al., 2004; Dubois et al., 2009; Olsson, Synowsky and MacKintosh, unpublished results).

1.5.4 Initial focus of 14-3-3-binding phosphoproteome centred on the PI 3-kinase–PKB pathway

Proteomics coupled with the dimethyl labeling method (Boersema et al., 2008) were used to study the quantitative changes in the sets of proteins that are phosphorylated when the insulin–PI 3-kinase–PKB signaling pathways are activated in cells (Dubois et al., 2009). 14-3-3 affinity capture and release methods have been successfully developed to purify 14-3-3-binding proteins from lysates of differentially treated cells with agonists and/or inhibitors. Phosphoproteins that bind specifically to 14-3-3-Sepharose are competitively eluted using a synthetic phosphopeptide. The proteins thus captured are separated on a one-dimensional SDS-PAGE gel and the resulting bands are digested with trypsin. Thereafter, the tryptic digests are reacted with different isotopic combinations of formaldehyde and sodium cyanoborohydride (**Figure 1.9**), with the aim of dimethylating every primary amine. The different combinations of stable isotope labelling generate three stably ‘labelled’ sets of peptides: ‘light’, ‘intermediate’ and ‘heavy’, which each differ by 4 mass units for each amine group modified. The peptides are then identified using mass spectrometry and quantified to determine the ratios for each of the labelled peptides in the three conditions, thereby enabling the distinction between proteins whose peptides are highly enriched in one set of treatment, for example insulin-stimulated compared with inhibitor-treated cells or unstimulated cells. This method was successfully used to identify novel targets of the insulin–PI 3-kinase–PKB signalling pathway in cultured human cells (Dubois et al., 2009). In addition to known targets of PKB-phosphorylated 14-3-3-binding proteins including, PRAS40, TBC1D1 and FOXO1, further novel targets were also validated as insulin-regulated proteins in this study. For example, one of the novel targets, the E3 ubiquitin ligase

ZNRF2, was later discovered to mediate the regulation of ion pumps in response to multiple stimuli including insulin and IGF1 (Hoxhaj et al., 2012).

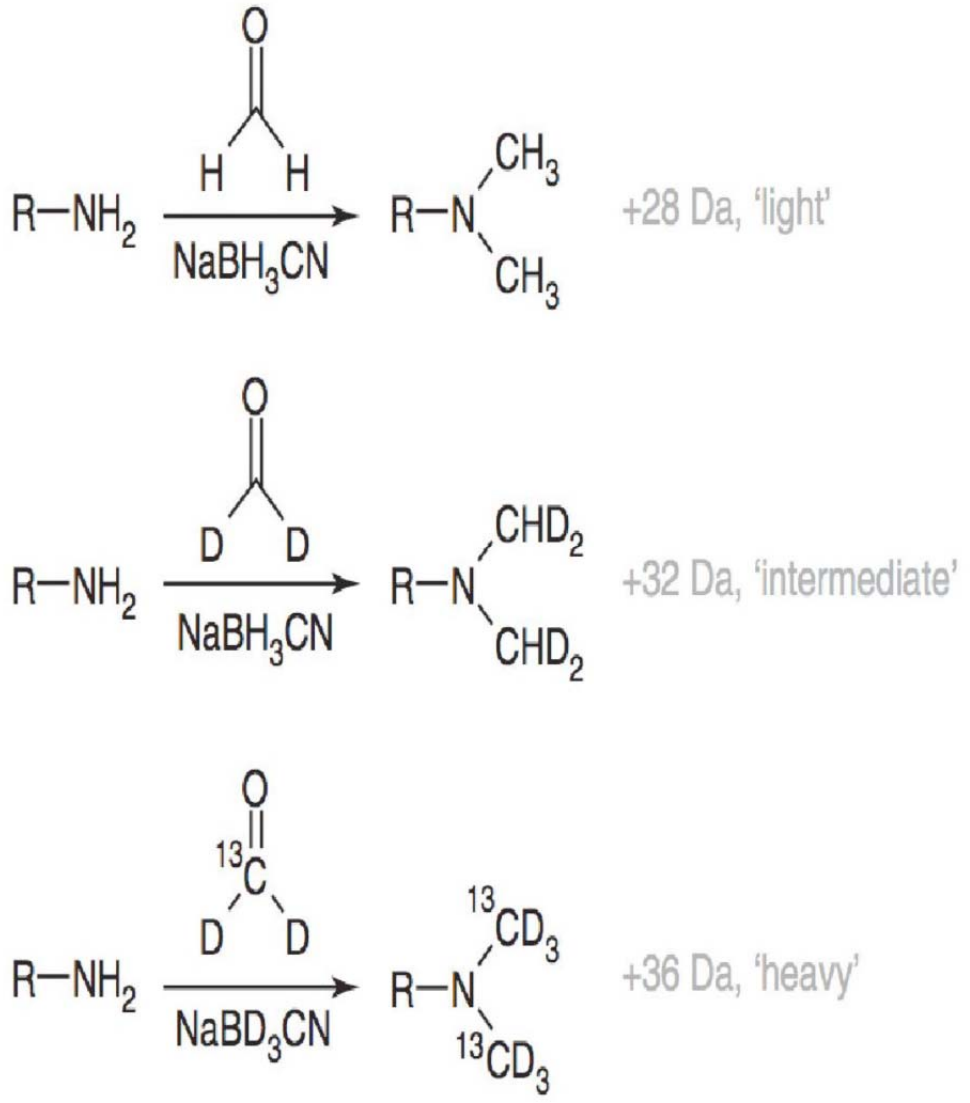

Figure 1.9: The dimethyl labelling method using stable isotopes
Different combinations of labelled isotopes of hydrogen and carbon atoms in formaldehyde and sodium cyanoborohydride are used to generate differentially 'labelled' amines in peptides (Source: Boersema et al., 2008).

1.5.5 PKB targets display differing responses to other stimuli, including cAMP elevating agents

In our studies, it soon became clear that few proteins are selectively induced to bind 14-3-3s by insulin–PI 3-kinase only. One exception is coiled-coil domain 6 (CCDC6) (Dubois et al., 2009), which was recently implicated in regulation of genome stability and S-phase of the cell cycle (Thanasopoulou et al., 2012). Binding

of CCDC6 to 14-3-3s needs phosphorylation of Ser240 by PKB, and this site is not a good substrate for any other kinases tested (MacKintosh group, unpublished results).

In contrast, other proteins that were first identified to bind to 14-3-3s downstream of insulin–PI 3-kinase signalling were subsequently also discovered to bind to 14-3-3s when other signalling pathways were activated. In other words, many proteins are convergence points whose 14-3-3 binding is promoted by multiple kinases.

One finding is that several proteins that bind to 14-3-3s in response to PKB activation also bind to 14-3-3s in response to cAMP-elevating agents, such as the adenylate cyclase activator forskolin, probably due to phosphorylation by PKA. These include the E3 ubiquitin ligases BRCA1 and ZNRF2, and PANK2 in the coenzyme A synthesis pathway (MacKintosh group, unpublished results). However, it seems surprising to find that the PI 3-kinase–PKB pathways and cAMP–PKA pathways have so many substrates in common because in many different physiological contexts these two signalling pathways have opposite outcomes, for instance, insulin stimulates glycogen synthesis in skeletal muscle, whereas adrenaline activates PKA that stimulates glycogen breakdown to provide energy for muscle action (discussed further in **section 1.5.5.1**).

1.5.5.1 Physiological opposing regulation of cellular processes by PKA and PKB

Under most conditions, PKA and PKB have distinct activating and signalling mechanisms. PKA signalling mainly occurs through ligand binding at the G-protein coupled receptors (GPCRs) in the plasma membrane, whereas PKB can be activated through ligand binding at receptor tyrosine kinases (RTKs) such as insulin receptor (IR), platelet-derived growth factor receptor (PDGF-R), epidermal growth factor (EGF), insulin-like growth factor (IGF1) and basic fibroblast growth factor (bFGF) (Hanada et al., 2004). In a number of cell types an increase in cellular cAMP levels is associated with cell differentiation and decreased proliferation, thereby antagonising the action of growth factors. On the other hand, PI 3-kinase–PKB signalling has generally been associated with the amplification of signals generated from growth factors and other stimuli to promote cell survival, growth and proliferation.

Upon ligand binding to any of the above-mentioned receptors involved in PKB signalling, phosphatidyl inositol-3-kinase (PI 3-kinase) is activated which in turn converts phosphatidyl inositol-3,4-phosphate (PIP_2) into phosphatidyl inositol-

3,4,5-triphosphate (PIP_3). PIP_3 next recruits PDK1 and PKB to the membrane, enabling PDK1 in turn to phosphorylate PKB at Thr308. The second site, Ser473, required for PKB activation, is phosphorylated by the upstream kinase mTORC2. Once both these sites are activated, PKB is released from the membrane and in turn propagates the signal to its downstream targets, which include GSK3, BAD, FOXO1 and AS160 among others (Burgering and Coffer, 1995; del Peso et al., 1997; Datta et al., 1997; Rena et al., 1999; Sano et al., 2003; Geraghty et al., 2007).

One of the first-described opposing physiological actions of PKB and PKA was the synthesis (PKB) and breakdown (PKA) of glycogen in animal tissues. In skeletal muscles, stimulation of the beta-adrenergic GPCR by adrenaline, results in PKA activation. In turn, PKA activates phosphorylase kinase, which phosphorylates glycogen phosphorylase, with the end result being glycogen breakdown. In contrast, when the PI 3-kinase pathway is triggered by insulin, PKB is activated. This activation results in glucose uptake by cells due to downstream phosphorylation and inhibition of GSK3 and simultaneous activation of glycogen synthase, resulting in a net increase in glycogen synthesis.

In another example, Monfar and colleagues reported that Interleukin-2 (IL-2) could activate p70S6K through PI 3-kinase to promote the transition from G_1-S in T cells. Interestingly, they went on to show that elevated cAMP levels in these cells could block this activation, thus inhibiting the G_1-S transition in T cells (Monfar et al., 1995). These studies indicate effects of PKB and PKA that are mutually antagonistic in controlling glucose homeostasis and T cell proliferation.

In addition to the above-mentioned examples of crosstalk between PKA and PKB, a number of other proteins have also been observed to have consensus phosphorylation sites for both of these AGC kinases, e.g. GSK3, CREB and ZNRF2. However, not all physiological contexts involving these two AGC kinases are clearly defined. Also, it seems to be commonly stated in the literature that activation of PKA also has a contributory effect activating PKB and/or enhancing the effect of PKB in particular physiological circumstances. Examples detailing some of the proposed scenarios are outlined below.

1.5.5.1.1 cAMP–PKA pathway antagonises the PI 3-kinase–PKB signalling pathway

When PKB phosphorylates and inhibits GSK3, this relieves the inhibitory phosphorylation of GSK3 on glycogen synthase, with the result that glycogen

synthesis is activated. It has also been shown that in rat hepatocytes, acute activation of PKB leads to inactivation of glycogen phosphorylase in a mechanism independent of the phosphorylation and inhibition of GSK3 (Aiston et al., 2006). This precise regulation of glycogen metabolism is crucial in maintaining glucose homeostasis in cells following a meal and during and after periods of strenuous exercise. In brown adipocytes, stimulation of the β_3-adrenergic receptors was found to counteract the insulin signalling pathway by inhibiting glucose uptake in these cells (Klein et al., 1999). In these adipocytes, treatment with insulin alone triggered activation of the PI 3-kinase–PKB signalling pathway leading to glucose uptake from the blood. On the other hand, pre-treating with a β_3-adrenergic agonist (CL316243) prior to insulin stimulation in these cells led to a significant decrease in PI 3-kinase activity and PKB activation. Although the precise mechanism remains unclear, the β_3-adrenergic agonist, and other cAMP analogues tested in these brown adipocytes cells, mediated the activation of PKA, which in turn was reported to inhibit PKB phosphorylation. Importantly, non-specific PKA inhibitors such as H-89 and PKC inhibitors reversed the effect observed upon pre-treatment with β_3-adrenergic agonists, suggesting crosstalks in these cells not only between PKA and PKB signalling, but also with some components of the PKC pathway. This might be a representative of glucose metabolism in brown adipocytes and might be important in understanding insulin resistance in states of adrenergic overactivity (Klein et al., 1999). However, better reagents are needed to dissect these events properly.

The PI 3-kinase signalling pathway has been implicated in promoting cellular proliferation by mediating the transmission of signals derived from growth factors and other mitogenic agents in cells. Lymphoid T cells have been reported to activate the PI 3-kinase signalling pathway via IL-2. This activation leads to the phosphorylation of p70S6 kinase, which through a series of downstream phosphorylation events promotes the transition of these T cells from the G_1 phase to the S phase. Elevating cAMP levels in these cells were shown to be inhibitory towards the activation of both PI 3-kinase and towards the phosphorylation of p70S6 kinase. PDK1 is the upstream kinase required for phosphorylation and activation of PKB. Upon ligand binding on the receptor tyrosine kinase (RTK), a series of auto-phosphorylation of the RTK leads to the phosphorylation of PI 3-kinase and generation of PIP_3 from PIP_2. PIP_3 in turn recruits both PDK1 and PKB to the plasma membrane to aid phosphorylation of PKB by PDK1 at Thr308. A second

phosphorylation site, Ser473, is also required for complete PKB activation and this phosphorylation is mediated by mTORC2 in response to growth factors, though other kinases including DNA-PK can also phosphorylate this site in response to DNA-damage (Bozulic et al., 2008). An elevation of cAMP in the cells has been reported to account for the reduced and/or loss of PKB activity. The high cAMP levels (a) reduces the lipid kinase activity of PI 3-kinase, thereby reducing its ability to phosphorylate PIP_2 into PIP_3, and (b) decrease the translocation of PDK1 from the cytosol to the plasma membrane which is required for PKB phosphorylation, with no loss of PDK1 activity as such (Kim et al., 2001).

The fasting hormone glucagon which signals through cyclic AMP is also well known to antagonise the actions of insulin in the liver to regulate gluconeogenesis. Glucose levels in the blood is maintained within a narrow range by a fine balance between glycogen synthesis, glycolysis and gluconeogenesis. Gluconeogenesis occurs primarily in the liver to generate glucose from new sources, including fatty acids, arginine and methionine and occurs during prolonged periods of fasting when blood glucose levels are low and the process is triggered by glucagon. Glucagon regulates the transcription of gluconeogenic genes such as phosphoenolpyruvate carboxykinase (PEPCK) and glucose-6-phosphatase (G6Pase). These genes are activated by FOXO transcription factors such as FoxO1, which are in turn activated by glucagon via cAMP—PKA signalling. Contrastingly, insulin-dependent PKB phosphorylation of Foxo1a has been shown to lead to its exclusion from the nucleus and 14-3-3-binding, which in turn affects its transcriptional activities (Rena et al., 1999; Rena et al., 2001; Rena et al., 2002). Furthermore, glycogen synthase kinase-3 (GSK3) has also been shown to regulate blood glucose levels by modulating the activities of G6Pase and PEPCK in the liver (Lochhead et al., 2001, Lipina et al., 2005). PKB phosphorylation of GSK3 inhibits its activity and this is promoted by insulin signalling (Sutherland et al., 1998; Cross et al., 1995).

Another example where insulin and cAMP agonists display opposing physiological effects concern leptin and resistin regulation in adipocytes. Leptin and resistin are two adipokines, which are important for regulation of energy homeostasis in the adipose tissues and have been implicated in metabolic disorders. Although both adipokines share some similarities in terms of inhibiting adipocyte differentiation and adipose development, they also play important opposing

physiological roles. Leptin increases insulin sensitivity and reduces gluconeogenesis. Resistin, on the other hand, suppresses insulin sensitivity and promotes gluconeogenesis (Rosetti et al., 1997; Ogawa et al., 1999; Steppan et al., 2001; Chepurny et al., 2010). Accordingly, insulin signalling increases the leptin-vesicle trafficking and promotes leptin secretion from these vesicles; insulin signalling also suppresses resistin-vesicle trafficking and secretion (Ye et al., 2010). cAMP–PKA signalling agonists such as forskolin, on the other hand, were reported to promote resistin-vesicle trafficking and secretion, while suppressing leptin trafficking and secretion in these adipocyte tissues (Ye et al., 2010).

1.5.5.1.2 Does cAMP activate Erk via PKA, or not, in melanocytes?

One caution about the above-mentioned interactions between cAMP–PKA signalling and the PI 3-kinase–PKB pathway is that mechanisms to explain the observed phenomena are lacking, and some of the data rely on non-specific inhibitors such as H-89. Further caution also comes from studies of the effects of the alpha-melanocyte stimulating hormone (αMSH) on melanocytes.

Several papers reported crosstalks between the cAMP–PKA and the Erk signalling pathways. Melanocortins such as αMSH have long been associated with activation of the cAMP cascade leading to melanogenic differentiation (Buscà and Ballotti, 2000; Buscà et al., 2000). For instance, it was reported that activation of the Melanocortin 1 receptor (MC1R) by α-MSH occurs through a cAMP-dependent pathway, which activates Erk1/2 in rat melanoma cells (Englaro et al., 1995; Buscà et al., 2000). Furthermore, cAMP was said to activate Erk in cystic epithelial cells from polycystic kidneys through the sequential phosphorylation of PKA, B-Raf and Erk, leading to the proliferation of autosomal dominant polycystic kidney disease (ADPKD) epithelial cells; this is however not observed in normal kidney cortex cells (Yamaguchi et al., 2003). The activation of Erk from cAMP via PKA has been proposed to be mediated by B-Raf; consequently, activation of B-Raf, but not C-Raf, by PKA enables B-Raf to signal to MEK, which in turn activates Erk leading to cellular proliferation (Stork and Schmitt, 2002; Yamaguchi et al., 2003). In contrast, PKA phosphorylation of C-Raf/Raf-1 leads to 14-3-3 binding, which prevents interaction with Ras, and hence prevents its activation (Dumaz and Marais 2003). Therefore, the role of PKA in regulating Raf isoforms as a whole is not clear.

Moreover, rather than cAMP–PKA signalling causing activation of Erk as has been reported in rat melanocytes (Englaro et al., 1995; Buscà et al., 2000;Amsen

et al., 2006), recent research in human melanocytes points to a cAMP–PKA-independent mechanism of Erk activation by αMSH. Rather, Erk activation by αMSH in normal human melanocytes and melanoma cells was discovered to involve transactivation of the cKIT tyrosine kinase receptor, most likely via Src (Herraiz et al., 2011). The potent cAMP-agonist forskolin has never been successfully shown to activate Erk in normal human melanocytes (Tada et al., 2002). Furthermore, a naturally-occurring E92K mutation in the MC1R receptor results in an increased constitutive activity for MC1R; the E92K mutation also abolishes the ability of the receptor to be stimulated by αMSH (Lu et al., 1998; Ling et al., 2003). Interestingly, cells with this mutation have been shown to have elevated cAMP, but not Erk activation, consistent with stimulation and activation of Erk by αMSH occuring independently of cAMP (Benned-Jensen et al., 2011). From these studies, it is apparent that crosstalks between signalling pathways are commonly misunderstood, and suggest that detailed analyses are required to delineate potential ambiguities between signalling pathways.

1.5.6 Outstanding questions about the acute regulation of 14-3-3s with their targets involving PKA

There is considerable information currently available on the acute regulation of phosphorylation and 14-3-3 binding to many target proteins upon activation of the insulin–PI 3-kinase–PKB signalling pathway. It would be interesting however, to define the 14-3-3-binding phosphoproteome involving PKA activation in cells. As discussed in **section 1.2.3**, PKA plays a major role in regulating a number of functions in the cell, including glycogen breakdown in hepatocytes and skeletal muscles, lipolysis in adipocytes and vasodilation. Numerous reports show that some 14-3-3-binding proteins seem to have preferential regulation under cAMP–PKA activation. It is also clear that another subset of 14-3-3-binding proteins may be phosphorylated by both PKA and PKB, presumably under differing physiological conditions/ stimulus to generate different outcomes. As discussed in **section 1.4.5.1**, PKA and PKB engage in crosstalk during their respective signalling activities at different levels, depending on the cell type and stimulus triggering the pathway. However, there is much in the literature that is contradictory. The field seems to be divided between those who argue for a crosstalk and those against a crosstalk between PKA and PKB. In order then to delineate the ambiguity, it would be helpful to perform a proteomics screen to identify proteins whose binding to 14-3-3 is

promoted via PKA-phosphorylated sites, but not via PKB, and vice versa. Such downstream target sites would be very useful for helping to delineate the intracellular processes regulated by each pathway, and help to disentangle some of the confusion about levels of crosstalk between the two pathways. One starting point could be 14-3-3-affinity capture of proteins from cells stimulated with cAMP-elevating agents, similar to the work undertaken previously to identify PKB-phosphorylated 14-3-3-binding proteins (Dubois et al., 2009).

1.6 Technical rationale and aims of this thesis

The few cases where PP enzymes have been linked to specific signalling pathways mainly involve the phosphorylation of their regulatory, and inhibitor, subunits via the cAMP–PKA pathway. So, we set out to try and identify how cAMP-elevating agents regulate the PPP family of protein serine/threonine phosphatases. This involved trialling a new approach to monitor how protein serine/threonine phosphatases of the PPP family are regulated in response to extracellular stimuli, such as the cAMP-elevating agent forskolin (**Chapter three**). Our group has exploited the specificity of 14-3-3s to identify many new downstream targets of the PI 3-kinase–PKB, PKC–Erk–p90RSK and AMPK pathways. PI 3-kinase–PKB and PKC–Erk–p90RSK are activated by insulin and growth factors, while AMPK is activated in cellular responses to energy stress. Identifying the substrates of these pathways, and the interplay between them, is particularly important because PI 3-kinase–PKB and PKC–Erk–p90RSK are deregulated in diabetes and cancers, while activating AMPK by exercise and drugs seems to have beneficial effects in these diseases. 14-3-3-binding sites fall into distinct subtypes that overlap with the specificities of basophilic protein kinases in the CAMK and AGC families, including PIMs, PKA, PKCs, PKB, p90RSK and AMPK (Johnson et al., 2010). Since there was little knowledge about the acute regulation of 14-3-3s upon PKA activation, we decided to investigate the sets of proteins that bind to 14-3-3s when intracellular cAMP levels are elevated (**Chapter four).** Several candidate proteins were identified in this screen and I started characterising a few of these as potential 14-3-3-binding targets: the DENND4 family (**section 4.2**), EML3 (**section 4.3**) and ATG9A (**section 4.4**). Initial studies suggest that the DENND4 family might possibly be one of the newly described 2-R ohnologue families of proteins, which bind 14-3-3s (Tinti et al., 2012). Preliminary studies with ATG9 also hint at a

potential new role of 14-3-3s in autophagy. Since many reports suggested crosstalks between PKA and PKB, I also wanted to compare the PKA data obtained with existing data on the proteins that bind to 14-3-3s when the PI 3-kinase–PKB pathway is activated.

Chapter two

Materials and Methods

2.1 Materials

2.1.1 General materials and equipment

Digoxygenin-O-methylcarbonyl-ε-aminocaproic-acid-N-hydroxysuccinimide (DIG) ester, anti-DIG HRP secondary antibody and 'complete' protease inhibitor cocktail tablets were from Boehringer Ingelheim/Roche (Lewes, UK). Coomassie protein assay reagent (Bradford reagent) was from Pierce (Chester, UK). Ponceau S, dimethyl sulphoxide (DMSO), cell culture trypsin solution and bovine serum albumin (BSA) were from Sigma-Aldrich (Poole, UK). Glutathione-Sepharose, protein G-Sepharose, enhanced chemilluminescence (ECL) immunoblotting kit were from Amersham International (Bucks, UK). Ni-NTA agarose and HiSpeed Plasmid Maxi Kit were from Qiagen (West Sussex, UK). Microcystin-LR was purchased from Dr Linda Lawton, Robert Gordon University, and Aberdeen, UK. Dialysis tubing (12-14 kDa molecular mass cut-off) was from Medicell International (London, UK). Pre-cast NuPAGE Bis-Tris and Tris-Acetate gels, NuPAGE MOPS and Tris-Acetate running buffers, Novex X-cell II electrophoresis tanks and X-cell II blot modules were from Invitrogen (Groningen, Netherlands). Vivaspin centrifugal concentration/filtration devices were from Vivascience (Lincoln, UK). Econopac column holders were from BioRad (Hemel Hempstead, UK). Centrifuges and rotors were from Beckman Instruments Inc. (Palo Alto, CA, USA). Leec CO_2 incubators were from Mackay and Lynn (Dundee, UK). Bradford reagent was from Pierce (Chester, UK). X-ray film was from Konica (Tokyo, Japan) and autoradiography cassettes, photographic fixative, and photographic developer solution from Kodak (Rochester, NY, USA). The Odyssey™ Infrared scanner was from Li-Cor Biosciences UK Ltd. The pH meters and electrodes were from Horiba (Kyoto, Japan). Plastic cell culture dishes were from Nunclon (Denmark) and cell scrapers from Costar (Cambridge, MA, USA). Dulbecco's Modified Eagle's Medium (DMEM), antibiotic/antimycotic solution, foetal bovine serum (FBS) and trypsin/EDTA (ethylenediaminetetraacetic acid) were from Invitrogen/Life Technologies (Paisley, UK). Skimmed milk powder (Marvel) was from Premier Beverages (Stafford, UK). Cellulose filters (0.22 μm) and nitrocellulose membranes were from Millipore Ltd. (Norwich, UK). HEK293 and HEK293 Flp-In T-REx cell lines were from the European Collection of Cell Cultures (http://www.ecacc.org.uk/) and were maintained by Kirsten McLeod and Janis Stark. Forskolin at >98 % purity was obtained from Sigma Aldrich. H-89, A23187 and Calyculin A were from Cell

Signaling (MA, USA). Other chemicals and reagents were from Sigma or Merck/BDH.

2.1.2 Synthetic peptides

Peptides were synthesised by Graham Bloomberg (University of Bristol) using N-9-fluorenylmethoxycarbonyl chemistry on an Applied Biosystems 430A peptide synthesizer and reagents supplied by the manufacturers. Phosphoserine residues were incorporated using FMOC (9-Fluorenylmethyloxycarbonyl)-phosphoserine (Novobiochem). Peptides were purified by reverse phase HPLC (High-performance liquid chromatography), their structures were verified by mass spectrometry, and peptide concentrations were determined by amino acid analysis.

2.1.3 Antibodies and antisera

The primary antibodies used for immunoblotting and immunopreciptation are listed in **Table 2.1**. Horseradish peroxidase-conjugated secondary antibodies, rabbit anti-sheep IgG was from Pierce, donkey anti-rabbit IgG, HRP anti-mouse IgG and donkey anti-goat IgG were from Promega (Tattenhall, Cheshire, UK). Alexafluor secondary antibodies for the Odyssey were from Rockland and Pierce. Some antibodies were raised against peptides and purified by staff in the Division of Signal Transduction Therapy, University of Dundee (DSTT) (see **Table 2.1**). The peptides were conjugated to bovine serum albumin and keyhole limpet haemocyanin, mixed and injected into sheep at Diagnostics Scotland (Penicuik, UK). The antibodies were affinity-purified by DSTT staff first by binding to the peptides coupled to NHS-activated CH-Sepharose (for coupling via lysine) or Iodoacetyl-activated UltraLink Support (for coupling via cysteine). Anti-TOPP antibodies were kindly provided by Dr Greg Moorhead (University of Alberta, Canada).

Table 2.1 Antibodies used in this thesis

Antibody	Immunogen	Host	Source	Usage
GFP	Full length GFP	Rabbit	Santa Cruz	1/1000
14-3-3(K-19)	Amino-terminus of human 14-3-3 β	Rabbit	Santa Cruz	1/1000
HA	YPYDVPDYA (influenza haemaglutinin-HA epitope)	Mouse	DSTT (12CA5)	0.1 μg/ml
AMPK (pThr172)	Phospho-AMPK alpha (pThr172)	Rabbit	Cell Signaling	1/1000
ERK	Total ERK	Rabbit	Cell Signaling	1/1000
ERK (pT202/ pY204)	Phospho-p44/42 MAPK (pThr202/ pY204)	Rabbit	Cell Signaling	1/1000
PKB	Total PKBα	Rabbit	Cell Signaling	1/1000
PKB (S473)	Phosphopeptide containing phosphorylated S473 of PKB	Rabbit	Cell Signaling	1/1000
VASP	Total VASP	Mouse	Abcam	1/10000
VASP (pS157)	VASP phosphopeptide containing phosphorylated S157	Mouse	Abcam	1/5000
ATG9	Total ATG9	Rabbit	Abcam	1/1000
DENND4A	Recognises internal region of DENND4A	Goat	Santa Cruz	1/5000
DENND4C	Recognises an internal region of DENND4C	Goat	Santa Cruz	1/5000
RBM15	Recognises an internal region of RBM15	Rabbit	Santa Cruz	1/1000
FPA	Raised against residues 441-901 of FPA	Rabbit	Dr G. Simpson	1/1000

2.2 Methods

2.2.1 General methods

2.2.1.1 Buffers and solutions

The lysis buffer contained Triton X-100 to solubilise the membranes, PMSF (phenylmethanesulphonyl fluoride) and benzamidine to inhibit serine and trypsin-like serine proteases, respectively. EDTA was added to chelate Mg^{2+} ions which are essential cofactors required by protein kinases. The reducing agent, β-mercaptoethanol was also added to the buffer to mimic the reducing cytosolic environment of the cell. Sodium fluoride, sodium β-glycerophosphate, sodium pyrophosphate and microcystin-LR were included to inhibit serine/threonine protein phosphatases. Sodium orthovanadate (Na_3VO_4) was used to inhibit protein tyrosine phosphatases. These ensured that the phosphorylation status of proteins in the extracts was fixed at the levels present *in vivo* at the time of lysis. The mammalian cell lysis buffer also contained a cocktail of inhibitors of metallo, aspartyl, cysteinyl, and seryl proteinases. A 200 mM solution of Na_3VO_4 was prepared by several successive rounds of boiling, cooling to room temperature on ice and adjusting to pH 10. This procedure was repeated until the pH remained stable at 10 after boiling and the solution became colourless. This procedure ensures that the majority of the Na_3VO_4 is in the depolymerised state that most favours tyrosine phosphatase inhibition. The solution was stored at 4^{o}C. The pH of Tris buffers changes significantly with temperature and so in this thesis, the temperature will be stated. Other commonly-used buffers during this thesis are listed in **Table 2.2**.

Table 2.2 Buffers used frequently used in this thesis

Mammalian cell lysis buffer	50 mM Tris-HCl pH 7.5 (4°C), 1 mM EDTA, 1 mM EGTA, 0.1% (v/v) Triton X-100, 1 mM sodium orthovanadate, 50 mM sodium fluoride, 5 mM sodium pyrophosphate, 0.27 M sucrose. Added fresh prior to use: 0.1 % (v/v) 2-mercaptoethanol, 1 mM benzamidine, 1 mM PMSF and 1 tablet/50 ml Complete protease inhibitor cocktail. Note: 1 μM microcystin-LR was added fresh prior to use to the above lysis buffer for all experiments in Chapter 4.
Dulbecco's PBS (Phosphate buffered saline, Gibco/ BioWhittaker)	137 mM NaCl, 2.7 mM KCl, 4.3 mM Na_2HPO_4, 1.4 mM KH_2PO_4
TBS (Tris-buffered saline)	50 mM Tris-HCl pH 7.5 (room temp.), 500 mM NaCl
TBST (Tris-buffered saline-Tween)	50 mM Tris-HCl pH 7.5 (room temp.), 500 mM NaCl, 0.1% (v/v) Tween-20.
High salt wash buffer	0.5 M NaCl, 50 mM Tris-HCl pH 7.5 (room temp.)
Low salt wash buffer	50 mM Tris-HCl pH 7.5 (room temp.), 1 mM EDTA, 0.1% 2-mercaptoethanol

2.2.2 Mammalian cell culture

2.2.2.1 Maintenance of cells

Human Embryonic Kidney (HEK) 293 cells were maintained in Dulbecco's Modified Eagle Medium (DMEM) supplemented with 10% (v/v) FBS (foetal bovine serum) (complete DMEM). Flp-In TREx cells stably expressing proteins of interest were cultured in DMEM supplemented with 10% FBS, hygromycin (100 μg/ml) and blasticidin (up to a final concentration of 15 μg/ml) (complete DMEM + H + B). The cells were grown at 37°C in a 95% air/5% CO_2 water-saturated incubator. Cells were rinsed with warm PBS, trypsinised into fresh medium and allowed to reach confluence prior to splitting or cell treatment.

2.2.2.2 Transfection of cells using PEI

Cells growing in DMEM supplemented with 10% FBS were seeded at 10 to 20% confluency in 10 cm-diameter dishes with 10 ml of media. After 8 to 24 h, cells were transfected with 30 μg polyethylenimine (PEI) and 10 μg of DNA. This mix was made up to 1 ml using DMEM, vortexed for 10 sec and allowed to stand at room temperature for 20 min. After this incubation period, the transfection mix was added slowly to the cells by dropping gently and evenly into the media, and dishes returned to the 37^{o}C incubator for 16 to 24 h.

2.2.2.3 Generation of Flp-In T-REx stable cell lines

Flp-In T-REx system (Invitrogen) was used for the generation of stable cell lines enabling tetracycline-inducible expression of GFP-TAP-tagged proteins. Flp-In T-REx 293 host cells contain an integrated FRT recombination sequence and stably express the Tet repressor. These cells were co–transfected with the pOG44 plasmid (which constitutively expresses the Flp recombinase) and with pcDNA5/FRT/TO vector containing a hygromycin resistance gene for selection and the gene of interest under the control of a tetracycline-regulated promoter. The result of co-transfection is a homologous recombination event between the FRT sites such that the FRT site on pcDNA5/FRT/TO construct is inserted into the FRT site integrated into the genome. The stable Flp-In T-REx cell lines were selected for hygromycin (gene of interest selection marker) and blasticidin (Flp-In T-REx host cell line selection marker) resistance. When the pcDNA5/FRT/TO vector is integrated into the genome at the FRT site, expression of the recombinant protein of interest can be induced by the addition of tetracycline. HEK293 Flp-In T-REx host cells were split in to T75 flasks and transfected at approximately 40% confluency with 10 μg DNA (1 μg pcDNA5/FRT/TO plasmid to express GFP-tagged protein of interest and 9 μg pOG44 plasmid). The cells were selected for hygromycin and blasticidin resistance three days after transfection by adding new medium that contains hygromycin (100 μg/ml) and blasticidin (7.5 μg/ml). After 2 weeks of selection the colonies were dissociated with trypsin and expanded. Expression of the protein was verified by inducing the cells with tetracycline at least 24 h before lysis and performing SDS-PAGE and Western blotting on the lysates.

2.2.2.4 Stimulation of cells

Cells were serum starved with DMEM for 6 to 12 h prior to stimulation. Cells were treated with activators for the indicated time in the figure legends; where indicated, cells were pre-treated with inhibitors prior to addition of the agonists.

2.2.2.5 Mammalian cell lysis

When cells reached about 90% confluence, they were lysed. The dishes were placed on ice, the medium aspirated and the cells were washed in ice-cold PBS. Lysis buffer was added (300 µm per 10 cm-diameter dish; 500 µl per 15 cm dish) and cells harvested by scraping. The lysates were transferred to labelled, pre-cooled Eppendorf tubes and kept on ice for 15 min. Lysates were spun at 13000 rpm for 20 min at 4^0C and supernatants transferred to fresh tubes, snap frozen in liquid nitrogen and stored at -80^{o}C.

2.2.3 Determination of protein concentration

The protein content of cell lysates was determined by using a Coomassie Protein Assay Reagent (Pierce, Rockford, IL, USA), based on the method of Bradford (1976). A standard curve was made using the microplate procedure in the manufacturer's protocol. Stock dilutions of BSA (5 µl of 25 to 2000 µg/ml) in water were added to 200 µl of Bradford reagent in a 96 well plate, using 5 µl of water in 200 µl of Bradford reagent as a blank. After mixing on a plate shaker for 1 min, the samples were stood at room temperature for 10 min. The absorbance at 595 nm was measured using a 96 well plate reader and plotted against the concentration of BSA in the sample. A new standard curve was prepared for each sample analysis. To determine the protein concentration of clarified lysates or purified proteins, a 1/10 dilution of the sample in water was prepared, and 5 µl added to 200 µl of Bradford reagent. The absorbance of the samples was measured as above. Protein concentration was extrapolated from the best-fit line of the standard curve.

2.2.4 Immunoprecipitation

2.2.4.1 Immunoprecipitation using non-covalently coupled antibodies

Lysates were pre-cleared prior to immunoprecipitation by incubating with PBS-washed protein G-Sepharose for 30 min at 4^{o}C on an IP shaker. The supernatants of these lysates were recovered by spinning in a refrigerated bench top

centrifuge at 5000 rpm for 1 min. The pre-cleared lysates were then transferred to fresh tubes containing the appropriate antibody-coupled protein G-Sepharose beads and incubated for 1 to 2 h at 4°C. After this period, the tubes were centrifuged at 5000 rpm at 4°C and the supernatant discarded. The proteins bound to the beads were washed twice in a high salt buffer followed by two no salt buffer washes. The beads were spun down briefly between washes at 5000 rpm at 4°C and each wash discarded. Proteins bound to the beads were eluted by heating in 2 x SDS sample buffer at 70°C for 10 min. The beads were spun down at 13000 rpm for 5 min to recover the denatured proteins (in the supernatant). The supernatant was stored at -20°C or loaded onto gels for SDS-PAGE.

2.2.4.2 GFP-Trap® pull downs

Lysates were pre-cleared as described in section **2.2.4.1**. GFP-Trap® beads bind the proteins with high capacity and so, a little amount of the beads (~5 µl) is usually sufficient for 2-5 mg pull downs. The GFP-Trap® beads were mixed in a ratio of 1:5 with Sepharose-6B to increase the volume for easier handling. The pre-cleared lysates (2-5 mg) were incubated with 20 µl of the GFP-Trap®/Sepharose-6B mix for 1 h at 4°C on an IP shaker. The beads were recovered by spinning at 5000 rpm for 1 min in a refrigerated centrifuge at 4°C. The supernatant was discarded and the pellet washed twice in high salt buffer, followed by two no-salt buffer washes, spinning the tubes at 5000 rpm for 30 s between the washes and discarding the used wash buffer. The proteins were denatured by heating in 2 x SDS sample buffer at 70°C for 10 min, centrifuged briefly and loaded onto SDS-PAGE gels or stored at -20°C until loading.

2.2.5 Dialysis tubing preparation

Dialysis tubing (cut-off mass 12-14 kDa) was boiled in a solution of 10 mM EDTA and 100 mM sodium acetate and then washed extensively with distilled water prior to use.

2.2.6 Preparation of self-cast ATTO gels

Self-cast gels were prepared by making a separating gel containing 375 mM Tris- HCl, 0.1% SDS, 0.05% APS and 0.05% TEMED at pH 8.6 and adjusting the

amount of acrylamide to 8, 10 or 12%. The stacking gel was made with 125 mM Tris-HCl, 0.1% SDS, 5% acrylamide, 0.1% APS and 0.1% TEMED at pH 6.8.

2.2.7 Protein separation using SDS-PAGE

Sodium dodecyl sulphate polyacrylamide gel electrophoresis (SDS-PAGE) separates proteins in a complex mixture by allowing the migration of proteins relative to their size, which is proportional to molecular weight because the SDS imparts a constant distribution of negative charge around the linearized proteins. Smaller proteins move faster through the gel than larger proteins. The protein mix in cell lysates and immunoprecipitates are first denatured by heating with 2 x SDS sample buffer at 70^{o}C for 10 min, in the presence of 1% DTT. The Precision Plus markers from Bio-Rad with molecular markers at 250, 150, 100, 75, 50, 37, 25, 20, 15 and 10 kDa were used as standards. The marker and samples were loaded onto either self-cast gels (10% polyacrylamide Tris-glycine gels) and run in Atto tanks with Tris-glycine SDS running buffer for ~100 min at 150 V, or onto Novex pre-cast gels (4-12% polyacrylamide Bis-Tris gels) and run with MOPS running buffer in an Xcell SureLock^{TM} Mini-Cell tank for 1 h at 200 V.

2.2.8 Coomassie Blue staining of gels for visualisation and mass spectrometry

The Colloidal Blue staining kit (Invitrogen) was used to stain protein gels for visualisation of the bands and general mass spectrometry. Gels were first fixed in 40% (v/v) Milli Q water, 10% (v/v) acetic acid and 50% (v/v) methanol for 10 min by shaking gently on a rocking platform. The gel was then rinsed in Milli Q water and incubated for 10 min with the staining solution mix: 55% (v/v) Milli Q water, 20% (v/v) methanol and 20% (v/v) stainer A. After 10 min, 5% (v/v) stainer B solution was added to the previous solution on the gel and left to stain for 3 to 12 h at room temperature. The background staining was removed by several washes in Milli Q water for at least 3 h.

2.2.9 Transfer of proteins from gels to nitrocellulose membranes

Gels were transferred onto nitrocellulose membranes for Western blotting using the Novex X-cell transfer modules from Invitrogen, according to the marnufacturer's protocol. Sponges, nitrocellulose membranes and Whatmann 3MM filter papers were pre-soaked in transfer buffer. A sponge was placed on the cathode

of the transfer cassette and the gel-membrane sandwich was built in the following way. A piece of wet Whatmann 3MM paper was placed on the sponge, followed by the gel (with wells and dye front removed), topped with the nitrocellulose membrane and then another piece of filter paper. The cassette was filled with sponges and placed in a Novex tank for transfer. The transfer cassette was filled with transfer buffer while the cooling chambers were filled with water. The gel was transferred for 2 to 3 h at 30 V, depending on the molecular weight of the protein.

2.2.10 Western Blotting and enhanced chemilluminescence or Odyssey detection

After the transfer, the nitrocellulose membranes were blocked in TBS containing 0.1% (w/v) Tween-20 (TBST) and 5% dried skimmed milk powder for 1 h at room temperature or at 4^{o}C overnight. The membrane was rinsed twice in TBST before incubating with the primary antibody at 4^{o}C overnight. The membrane was washed by fast shaking at least four times with TBST, each wash for approximately 10 min. The membrane was next incubated with the secondary antibody for 1 h at room temperature. The primary and secondary antibodies were diluted in TBST containing either 5% (w/v) milk powder or 5% BSA. The membrane was then washed as before and the antibody detected using the enhanced chemilluminescence (ECL) system. The blot was exposed to X-Ray film which was developed and fixed in an automatic processor. In some cases, the antibodies were stripped from the membrane by stripping the membrane in the '10 x strong Re-Blot' stripping solution (Millipore). The stock stripping solution was diluted 1 in 10 in Milli Q water and 5 ml of this diluted solution was enough for a blot. The blot was incubated with the stripping solution for 15 min at room temperature, washed briefly with TBST, and then blocked as described before with TBST-milk or TBST-BSA. The blot was then incubated with another primary antibody and the process repeated. Western blotting signals were also sometimes visualised using the Odyssey^{TM} Infrared Imaging System instead of the ECL. The procedure was the same until the addition of the secondary antibody. The blot was incubated for 1 h at room temperature with secondary antibodies labelled with either IRD800 (Rockland) or Alexa680 (Molecular Probes) dyes. The membrane was washed and the signal captured with an Odyssey Infrared Imaging system.

2.2.11 In vitro dephosphorylation of immunoprecipitated proteins with lambda phosphatase

GFP-pull downs of the protein were performed in triplicate and washed as described in section **2.2.4.2**. The immunoprecipitated protein (~3 mg cell lysate) was subjected to in vitro dephosphorylation using lambda phosphatase purified by the DSTT. Reactions were performed in a final volume of 100 µl no salt buffer (50 mM Tris-HCl pH 7.5 (room temperature) and 0.1% β-mercaptoethanol) containing 50 mU/ml lambda phosphatase with $MnCl_2$ and 1mM EDTA as indicated in the figure legends. The reactions were performed at 30^{o}C for 30 min by shaking in a Thermomixer. The reactions were stopped by adding 2 x SDS-sample buffer. When EDTA was used, the $MnCl_2$ and EDTA were mixed first to allow chelation prior to addition of the phosphatase to the tubes.

2.2.12 General molecular biology

2.2.12.1 Competent cell preparation and plasmid transformation of *Escherichia coli*

In general, the DH5α or the XL1-Blue strain of *Escherichia coli* (*E. coli*) was used to amplify for DNA plasmid whereas the BL21 strain was used to express recombinant proteins, except that the DH5α strain was used to express 6-His-tagged BMH1 and BMH2 proteins (the two 14-3-3 isoforms from *Saccharomyces cerevisiae*). The bacterial cells to be made competent for transformation were collected from a culture by centrifugation at 8000 rpm for 2 min in a Biofuge. The DH5α pellet was resuspended in 20 ml of cold, sterile 0.1 M $CaCl_2$ solution, and incubated on ice for 30 min. The cells were sedimented and resuspended again in 4 ml of cold, sterile 0.1 M $CaCl_2$ solution. This cell suspension was stored at 4^{o}C for up to 2 weeks or at –80^{o}C, and used as a source of competent cells for transformation. A 50 µl aliquot of chemically competent *E. coli* (usually DH5α strain) was removed from -80^{o}C and thawed on ice. Plasmid DNA (typically 2 µg) was added to the bacteria and the tube flicked gently to mix. The DNA and bacteria mix were kept on ice for 30 min. The tube was transferred to a 42^{o}C water bath for 1 min. The 'heat-shocked' cells were returned to ice for 5 min, at which point 500 µl of LB broth was added and the cells allowed recovering at 37^{o}C for at least 30 min. The cell suspension was centrifuged at 13000 rpm for 1 min in a benchtop microfuge. The supernatant was discarded and the pellet resuspended in 250 µl of

LB broth. Aliquots (50 µl) were spread onto agar plate containing 50 µg/ml of the relevant antibiotic (typically Ampicillin) and the cells were grown overnight at 37^{o}C. Single colonies were picked and transferred to 5 ml LB broth with the appropriate selection antibiotic and grown overnight at 37^{o}C in a shaking incubator.

2.2.12.2 DNA sequencing

DNA sequencing was performed by the Sequencing Service (http://www.dnaseq.co.uk/; College of Life Services, University of Dundee) on Applied Biosystems automated DNA sequencers. The sequencer results were viewed using the Editview software package and DNA alignments and other comparisons were made using the DNA Strider package.

2.2.12.3 Plasmid constructs

The following expression plasmids were used in this thesis. All the subcloning and PCR involved in their generation were carried out by Dr Rachel Toth in the DSTT (**Table 2.3**). The mammalian vector pCMV5 allows expression of proteins with an N-terminal HA-tag under control of the cytomegalovirus promoter. The pcDNA5 FRT/TO vector backbone was purchased from Invitrogen and modified by Dr Rachel Toth to express proteins with an N-terminal green fluorescent protein (GFP) or GFP-TAP (tandem affinity purification) tag under a tetracycline inducible promoter.

Table 2.3. Plasmids used in this thesis	
pcDNA3.1 ATG9-CRL	DU36917
pcDNA5 FRT/TO GFP ATG9	DU36887
pcDNA5 FRT/TO GFP DENND4B	DU36735
pcDNA5 FRT/TO GFP DENND4B P1078-end	DU40009
pcDNA5 FRT/TO GFP DENND4B M1-P1078	DU40052
pcDNA5 FRT/TO GFP DENND4B M1-Q899	DU40051
pcDNA5 FRT/TO GFP DENND4B M1-Q899 S343A	DU40007
pcDNA5 FRT/TO GFP DENND4B M1-Q899 S343A S732A	DU40024
pcDNA5 FRT/TO GFP DENND4B Q900-P1078	DU40008
pcDNA5 FRT/TO GFP DENND4B S343A	DU36830
pcDNA5 FRT/TO GFP DENND4B S732A	DU36831
pcDNA5 FRT/TO GFP DENND4B S961A	DU36832
pcDNA5 FRT/TO GFP-DENND4B M1-P1078 S343A	DU40026
pcDNA5 FRT/TO GFP-DENND4B M1-P1078 S343A S732A S961A	DU40025
pcDNA5 FRT/TO GFP-DENND4B S343A S732A	DU36993
pcDNA5 FRT/TO GFP-DENND4B S343A S732A S961A	DU36994
pcDNA5 FRT/TO GFP DENND4C 1017-1316	DU36836

pcDNA5 FRT/TO GFP DENND4C 1017-1316 S1042A	DU36850
pcDNA5 FRT/TO GFP DENND4C 1017-end S1042A	DU36833
pcDNA5 FRT/TO GFP DENND4C 1017-end S1404A	DU36834
pcDNA5 FRT/TO GFP DENND4C 1017-end S1426A	DU36835
pcDNA5 FRT/TO GFP DENND4C 1017-end S1608A	DU36846
pcDNA5 FRT/TO GFP DENND4C M1017-end	DU36745
pcDNA5 FRT/TO GFP DENND4C T1316-end	DU36827
pcDNA5 FRT/TO GFP DENND4C T1316-end S1404A	DU36851
pcDNA5 FRT/TO GFP DENND4C T1316-end S1426A	DU36852
pcDNA5 FRT/TO GFP DENND4C T1316-end S1608A	DU36881
pcDNA5 FRT/TO GFP FPA	DU16955
pcDNA5 FRT/TO GFP FPA F163A	DU16927
pcDNA5 FRT/TO GFP FPA V161A	DU16926
pcDNA5 FRT/TO GFP FPA V161A/F163A	DU16928
pcDNA5 FRT/TO GFP IRLB	DU36829
pcDNA5 FRT/TO GFP IRLB S1151A	DU36886
pcDNA5 FRT/TO GFP IRLB S1251A	DU36865
pcDNA5 FRT/TO GFP IRLB S1589A	DU36946
pcDNA5 FRT/TO GFP IRLB S1609A	DU36866
pcDNA5 FRT/TO GFP IRLB S1798A	DU36879
pcDNA5 FRT/TO GFP IRLB S338A	DU36868
pcDNA5 FRT/TO GFP IRLB S755A	DU36869
pcDNA5 FRT/TO GFP DENND4A	DU36708
pcDNA5 FRT/TO GFPTAP PP1 alpha	DU31245
pACT2.6 PP1 alpha	DU31264
pAS2.6 PP1 alpha	DU31246
pcDNA5 FRT/TO GFPTAP PP1 beta	DU31213
pACT2.6 PP1 beta	DU31254
pAS2.6 PP1 beta	DU31212
pcDNA5 FRT/TO GFPTAP PP1 gamma	DU31199
pACT2.6 PP1 gamma	DU31187
pAS2.6 PP1 gamma	DU31181
pcDNA5 FRT/TO GFP RBM15	DU16753
pcDNA5 FRT/TO GFP RBM15 F526A	DU16755
pcDNA5 FRT/TO GFP RBM15 L300-T600	DU31344
pcDNA5 FRT/TO GFP RBM15 M1-K720	DU31339
pcDNA5 FRT/TO GFP RBM15 M1-L300	DU31337
pcDNA5 FRT/TO GFP RBM15 M1-T600	DU31338
pcDNA5 FRT/TO GFP RBM15 S294A	DU31313
pcDNA5 FRT/TO GFP RBM15 S700A	DU31312
pcDNA5 FRT/TO GFP RBM15 T568A	DU31311
pcDNA5 FRT/TO GFP RBM15 T600-A900	DU31345

pcDNA5 FRT/TO GFP RBM15 V524A	DU16754
pcDNA5 FRT/TO GFP RBM15 V524A F526A	DU16756
pcDNA5 FRT/TO GFPTAP RBM15	DU16757
pcDNA5 FRT/TO GFPTAP RBM15	DU31117
pcDNA5 FRT/TO GFPTAP RBM15 F526A	DU16759
pcDNA5 FRT/TO GFPTAP RBM15 S294A	DU31315
pcDNA5 FRT/TO GFPTAP RBM15 S700A	DU31314
pcDNA5 FRT/TO GFPTAP RBM15 T568A	DU31316
pcDNA5 FRT/TO GFPTAP RBM15 V524A	DU16758
pcDNA5 FRT/TO GFPTAP RBM15 V524A F526A	DU16760
pCMV5.HA RBM15	DU16553
pCMV5.HA RBM15 F526A	DU16555
pCMV5.HA RBM15 V524A	DU16554
pCMV5.HA RBM15 V524A/F526A	DU16556
pACT2.6 RBM15	DU31183
pAS2.6 RBM15	DU31163
pcDNA5 FRT/TO GFP RBM15B	DU16795
pcDNA5 FRT/TO GFP RBM15B F489A	DU16837
pcDNA5 FRT/TO GFP RBM15B V487A	DU16828
pcDNA5 FRT/TO GFP RBM15B V487A F489A	DU16840
pcDNA5 FRT/TO GFPTAP RBM15B	DU31127
pcDNA5 FRT/TO GFPTAP RBM15B F489A	DU31203
pcDNA5 FRT/TO GFPTAP RBM15B V487A	DU31202
pcDNA5 FRT/TO GFPTAP RBM15B V487A F489A	DU31204
pCMV5.HA RBM15B	DU16557
pCMV5.HA RBM15B F489A	DU16563
pCMV5.HA RBM15B V487A	DU16562
pCMV5.HA RBM15B V487A/F489A	DU16564
pACT2.6 RBM15B	DU31188

2.2.12.4 Purification of plasmid DNA

Plasmid minipreps were performed by staff in the DSTT. To prepare microgram quantities of plasmid DNA, an individual colony of plasmid-transformed bacteria was transferred into ~5 ml of LB broth containing 100 μg/ml ampicillin and grown overnight (approximately 16 h) at 37^{o}C in a shaking incubator. The culture was then spun at 3000 rpm for 15 min in a Beckman Allegra benchtop centrifuge. The DNA was purified from the bacterial pellet using the Qiagen Mini-Prep system, by the College of Life Sciences Sequencing service (University of Dundee) using an automated Qiagen 9600 Bio-robot.

To prepare milligram quantities of DNA, an individual colony of plasmid transformed bacteria was transferred into 5 ml of LB broth, containing 100 μg/ml ampicillin or 50 μg/ml kanamycin and grown at 37°C for 6 to 8 h in a shaking incubator. The 5 ml culture was used to seed 500 ml LB broth (also containing the relevant antibiotic), which was grown overnight at 37°C in a shaking incubator. The following day, the culture was centrifuged at 3000 rpm in a Beckman J6 rotor for 15 min at 4°C to pellet the bacteria. The DNA was purified from the bacterial pellet using the Qiagen Mega-Prep kit, according to the manufacturer's instructions. The resulting DNA was solubilised in Milli Q water and stored at -20°C.

2.2.12.5 Determination of DNA concentration

The absorbance of DNA in aqueous solutions was measured in a NanoDrop (ThermoFisher) at 260 nm. Briefly, 2 μl of water was used to blank the machine, and 2 μl of each DNA sample was placed on the nanodrop counter according to the manufacturer's instructions. The counter was wiped clean in between each sample measurement. The purity of the sample was calculated by looking at the ratio of the absorbance at 260 nm and 280 nm. A ratio of 1.6 or greater was indicative of a highly purified sample of DNA.

2.2.13 14-3-3-affinity chromatography and 14-3-3-overlays

2.2.13.1 Expression of the *Saccharomyces cerevisiae* 14-3-3 isoforms Bmh1 and Bmh2

Two 2 L flasks each containing 500 ml LB-Amp medium (LB broth plus 100 μg/ml ampicillin) were inoculated with *E. coli* DH5α cells expressing the Bmh1 or Bmh2 14-3-3 isoforms from *S. cerevisiae*, each with an N-terminal 6-His-tag (a gift from Dr Marie Scarabel and Professor Alistair Aitken, University of Edinburgh). Starter cultures were grown overnight at 37°C, with shaking at 250 rpm, and used to inoculate 25 L LB-Amp in a fermenter with 1 ml antifoam. The culture was grown aerobically with stirring at 37°C until mid-log phase (optical density at 600 nm = 0.6 to 0.7). Expression of the 14-3-3 constructs was induced by adding 0.5 mM IPTG for 3 h. The bacteria were harvested by centrifugation for 20 min at 4200 rpm (or ~2100 x g using a Beckman J6-MI rotor), snap-frozen and stored at -80°C.

2.2.13.2 Purification of 6-His-tagged Bmh1 and Bmh2 from *Escherichia coli*

Recombinant 6-His-tagged *S. cerevisiae* 14-3-3 isoforms, Bmh1 and Bmh2 were supplied by Dr Jean Harthill in this laboratory or prepared using the following method by members of the DSTT. The frozen bacterial pellet from a 500 ml culture was thawed on ice in bacterial lysis buffer (50 mM Tris-HCl pH 7.5 (4^{o}C), 150 mM NaCl, 1 mM EDTA, 1 mM EGTA, 0.1% (v/v) Triton-X100, 0.07% (v/v) 2-mercaptoethanol, 1 mM benzamidine, 0.2 mM PMSF) and vortexed vigorously. The cells were lysed using a French press. The lysate was centrifuged at 15000 rpm for 30 min at 4^{o}C in a Beckman JLA 16.25 rotor. The supernatant was removed and incubated for 45 min at 4^{o}C with 2.4 ml pre-equilibrated nickel-NTA agarose (washed several times in equilibration buffer consisting of 50 mM Tris-HCl pH 7.5 (room temp), 0.5 M NaCl and 1 mM PMSF). The agarose was centrifuged at 3000 rpm for 10 min at 4^{o}C in a Beckman J6 rotor and the supernatant discarded. The pellet was resuspended in high salt wash buffer (50 mM Tris-HCl pH 7.5 (room temp), 0.5 M NaCl and 10 mM imidazole), poured into a Bio-Rad disposable Econopac column, and the column washed with at least 20 column volumes of high salt buffer, followed by 20 column volumes of low salt buffer (50 mM Tris-HCl pH 7.5 (room temp), 150 mM NaCl and 10 mM imidazole). When protein could no longer be detected in the eluate, protein bound to the resin was eluted with 50 mM nickel (II) sulphate in equilibration buffer. Twelve fractions of 1 ml were collected. The protein concentration of each fraction was measured and peak fractions were pooled, dialysed overnight at 4^{o}C in 15 ml Slide-a-Lyser cassette, against 25 mM HEPES pH 7.5, 1mM DTT, 50% glycerol and stored at -20^{o}C. An aliquot of the dialysed sample was subjected to SDS-PAGE, and the gel stained with colloidal Coomassie blue or immunoblotted to allow the purity and amount of protein to be checked.

2.2.13.3 Coupling Bmh1 and Bmh2 to activated CH-Sepharose 4B

Activated CH Sepharose 4B is actually NHS-activated Sepharose, which forms covalent bonds with lysine residues and other primary amine groups. Dry matrix (2 g, which swells to 6 ml) was poured onto the glass sinter of a filtering system and swelled in 500 ml of cold 1 mM HCl (43 µl concentrated HCl/500 ml). The solution was removed by vacuum suction, being careful not to let the matrix dry out. The matrix was washed with 200 to 300 ml coupling buffer (200 ml of 0.1 M

$NaHCO_3$, 0.5 M NaCl pH 8.0), and the appropriate amount (2 mg/ml) of 14-3-3 ligand was added and left to crosslink for 2 h at room temperature, or 4 h at 4°C. The matrix was centrifuged at 3000 rpm at 4°C for 5 min and the supernatant was removed. A 5 µl sample of the supernatant was used for a Bradford assay to assess the efficiency of protein coupling to the matrix. Any remaining reactive groups of the matrix were blocked in 0.1 M Tris-HCl pH 8.0 at room temperature for 1 h. The matrix was washed by pouring onto a glass sinter, which was drained to dampness under vacuum suction and washed alternately with 0.05 M Tris-HCl pH 8.0 (room temp), 0.5 M NaCl followed by 0.05 M sodium acetate, 0.5 M NaCl pH 4.0 for a total of 5 x 50 ml washes for each buffer. The 14-3-3 Sepharose was stored in 50 mM Tris-HCl pH 7.5 (room temp) and 0.05 % sodium azide at 4°C until use.

2.2.13.4 14-3-3-Sepharose affinity chromatography and purification

Cells were cultured, stimulated and lysed as indicated previously in section **2.2.2**. The broken cells were centrifuged at 15000 g for 30 min and the supernatant collected. The clarified solution was mixed end-over-end for 2 h at 4°C with 10 ml 14-3-3-Sepharose (for 100 dishes of cells). The mixture was poured onto an Econopac column, the flow through collected, and the column washed with 500 ml of 50 mM Tris-HCl pH 7.5, 500 mM NaCl, 1 mM DTT (buffer A). Proteins bound to the phosphopeptide binding site of 14-3-3s were eluted with 12 ml of 2 mM ARAApSAPA phosphopeptide in buffer A. Two elutions with the competitive phosphopeptide were performed. These eluates were pooled and concentrated in Vivaspin columns.

2.2.13.5 Preparation of the DIG-labelled 14-3-3 probe for 14-3-3-overlays

14-3-3 protein (50 µg each of the 6-His-tagged Bmh1 and Bmh2 isoforms) as incubated for 2 h at room temperature with 8 µg digoxygenin-O-methylcarbonyl-ε-aminocaproic acid-N-hydroxysuccinimide (DIG-NHS) ester, added from a 2 mg/ml stock solution in dimethyl sulphoxide, and 400 µl PBS, pH 8.5, with occasional mixing. The mixture was dialysed extensively in PBS pH 7.2 at 4°C to remove unreacted DIG ester, then aliquoted and stored at -20°C. For the 14-3-3 probe, aliquots of DIG-14-3-3 were diluted to a final protein concentration of 1 µg/ml in 25 mM Tris-HCl pH 7.5 (room temp), 500 mM NaCl, 1% non-fat milk powder. The resulting DIG-14-3-3 probe was stored at 4°C with 0.05% sodium azide. It was found that the probe could be reused many times.

2.2.13.6 DIG-14-3-3 overlay

To identify proteins that can bind directly to 14-3-3, a Far-Western overlay procedure was used. Proteins were separated by SDS-PAGE and transferred to nitrocellulose. The membrane was blocked with 5% non-fat milk in TBST as for Western blotting, then incubated with DIG-labelled 14-3-3 probe overnight at 4°C. The membrane was washed 6 x 10 min in TBST. HRP-conjugated anti-DIG antibody, diluted 1:2500 in TBST containing 1% non-fat milk powder, was applied for 1 h. The membrane was washed in TBST as before, and the overlay was developed with ECL reagent as described in the manufacturer's instructions.

2.2.14 Purification of protein phosphatases

2.2.14.1 Preparation of Microcystin-Sepharose beads

The aminoethanethiol-MC-LR-Sepharose beads were prepared by Carol MacKintosh and the DSTT staff using the following protocol. DMSO, aminoethanethiol and 5 M NaOH were purged separately with nitrogen gas. 1 vol. MC-LR (1-5 mg/ml in methanol) was then added to a solution comprising 1.5 vol. water, 2 vol. DMSO, 0.67 vol. 5 N NaOH and 1 vol. aminoethanethiol hydrochloride (1 g/ml). After incubation for 30 min at 50°C under N_2 gas, the solution was cooled, mixed with an equal volume of glacial acetic acid, then diluted 5-fold with 0.1% (v/v) TFA and the pH reduced to 1.5 by dropwise addition of 100% (v/v) TFA. The sample was applied to a Waters C18 Sep-Pak cartridge equilibrated in HPLC grade methanol and washed with 0.1% (v/v) TFA in 10% (v/v) acetonitrile. The aminoethanethiol-MC-LR was eluted from the cartridge with 0.1% (v/v) TFA/100% (v/v) acetonitrile, dried by rotary evaporation and dissolved in 0.02 ml of methanol. Chromatography of an aliquot on a Vydac C18 column developed with a gradient of water/acetonitrile in 0.1% TFA showed that >95% of the MC-LR had been converted to the aminoethanethiol derivative which was eluted at 33.7% acetonitrile, compared with 35.6% acetonitrile for unmodified MC-LR. Aminoethanethiol-MC-LR (1 mg) was reacted for 4 h at room temperature with 6 ml of swollen N-hydroxysuccinimide-activated CH-Sepharose 4B in 50 mM sodium bicarbonate, pH 8.0 with end-end rotation. The columns were washed alternately with 100 ml each of 50 mM sodium acetate pH 4.0 plus 0.5 M NaCl, and 50 mM Tris-HCl pH 8.0 plus 0.5 M NaCl (five times with each buffer). The beads were

finally washed and stored in 50 mM Tris-HCl pH 7.5 with a pinch (0.02%) of sodium azide.

2.2.14.2 Microcystin-affinity chromatography for the purification of protein phosphatases from cauliflower

The following protocol was carried out at 4°C. The outer florets of a cauliflower were shaved off and homogenised in a blender in two volumes of ice-cold buffer A (50 mM triethanolamine-HCl pH 7.5, 0.1 mM EGTA, 5% (v/v) glycerol, 0.1% (v/v) 2-mercaptoethanol, 1 mM benzamidine and 1 mM PMSF. The homogenate was clarified by centrifugation at 7000 rpm for 20 min and filtered through two layers of miracloth. The supernatant was then fractionated from 0-17 % poly(ethylene glycol) (PEG) by addition of 50% PEG6000 in buffer A. The sample was gently stirred for 30 min before centrifuging at 7000 rpm for 20 min. The pellet was resuspended to a total volume to 200 ml with buffer A and centrifuged again at 7000 rpm for 20 min. The supernatant was mixed end-over-end with 1 ml MC-Sepharose for 1 h. The mix was then poured onto Econopac columns and the flow through collected, ensuring the column did not run dry throughout the rest of the procedure. The column was washed with 100 ml of buffer A plus 300 mM NaCl, followed by another 100 ml wash with buffer A containing 500 mM KCl. The flow-throughs were collected and Bradford assays of the wash fractions, confirmed that the last wash contained less than 0.005 mg/ml protein. Two elutions with the RVDF competitive peptide (that binds to PP1 catalytic subunit in competition with regulatory subunits) in buffer A were performed, one at 0.5 mM followed by a 2 mM elution, with the peptide being mixed end-over-end for 30 min at each concentration, and eluates were pooled for concentration in Vivaspin columns. The protein phosphatases that remained bound to the beads were then eluted by mixing end-over-end with ~3 ml buffer A containing 3 M NaSCN. This step was repeated and the two fractions pooled and dialysed extensively with buffer A, with at least two changes of the dialysis buffer. The sample was then concentrated in Vivaspin columns and analysed using SDS-PAGE.

2.2.14.3 Microcystin-affinity chromatography for the purification of protein phosphatases from HEK293 cells

The following protocol was mostly carried out at 4ºC. HEK293 cells were harvested in ice-cold lysis buffer and the lysates centrifuged at 13000 rpm for 15 min. The supernatant was mixed end-over-end with 1 ml MC-Sepharose for 1 h. The mix was then poured onto Econopac columns and the flow through collected, ensuring the column did not run dry throughout the rest of the procedure. The column was washed with 250 ml of buffer A plus 300 mM NaCl. Two 1 ml elutions with the RVDF competitive peptide in buffer A were performed, one at 0.5 mM followed by a 2 mM elution, with the peptide being mixed end-over-end for 30 minutes at each concentration. The column was washed with 5 ml of buffer A containing 300 mM NaCl and this wash and the peptide elutions were pooled for concentration in Vivaspin columns. The protein phosphatases bound to the beads were then eluted by mixing end-over-end with ~3 ml buffer A containing 3 M NaSCN. This step was repeated and the two fractions pooled and dialysed extensively with buffer A, with at least two changes of the dialysis buffer. The sample was then concentrated in Vivaspin columns and analysed using SDS-PAGE.

2.2.14.4 GFP-Trap® pull downs for the purification of protein phosphatase 1 complexes from cells stably expressing the three human isoforms of PP1

Flp-In T-REx cells stably expressing the 3 isoforms of PP1, namely PP1α, PP1β and PP1γ were grown, tet-induced and lysed as described in sections **2.2.2.1**, **2.2.2.3** and **2.2.2.5**. Since these proteins were GFP-tagged, they were immunoprecipitated using GFP-Trap® beads as described in section **2.2.4.2**.

2.2.15 Protein chemistry for the analysis of peptides and phosphopeptides

2.2.15.1 Proteolytic digestion of proteins 'in gel'

Proteins were reduced and alkylated in the lysates by adding 10 mM DTT in 0.1 M ammonium bicarbonate for 45 min at 65°C followed by 50 mM iodoacetamide in 0.1 M ammonium bicarbonate for 20 min at room temperature. The gels were stained with colloidal Coomassie blue. Protein bands were excised with a razor blade and cut into small pieces (~1 mm^3) and placed in 1.5 ml

Eppendorf tube. The gel pieces were rinsed in turn sequentially for 15 min on a vibrating platform with 1 ml of the following: water, a 1:1 mixture of water and acetonitrile, 0.1 M ammonium bicarbonate, a 1:1 mixture of 0.2 M ammonium bicarbonate and acetonitrile. Gel pieces were shrunk in acetonitrile and dried by rotary evaporation, then incubated with 5 μg/ml trypsin in 25 mM triethylammonium bicarbonate for 16 h. An equal volume of acetonitrile was added and the mixture incubated on a shaking platform for 15 min. The supernatant was removed and dried by Speed-Vac and the gel pieces were further washed with 100 μl 50% acetonitrile/2.5% formic acid for 10 min. This supernatant was added to the first extract and dried.

2.2.15.2 N-dimethylation reaction for protein quantification

After the overnight trypsin digestion as described in section **2.2.15.1**, the peptides were transferred to fresh tubes. Up to 100 μl of 100 mM TEAB buffer was added to the gel pieces, which were shaken for a further 15 min, and the supernatant was combined with the first extract. One third of the combined sample was used for N-dimethyl labelling in the following way. All of the dimethyl labelling procedure and analysis (Chapter 3) were performed with the help of Dr Silvia Synowsky (College of Life Sciences, University of Dundee), using the procedure described by Boersema et al. (2008). Briefly, 4 μl of 4% formaldehyde (CH_2O) ('light') or 4% deuterated-formaldehyde (CD_2O) ('intermediate') or 4% ^{13}C-labelled deuterated formaldehyde ($^{13}CD_2O$)('heavy') was added to the respective peptides. Then, 4 μl of 600 mM $NaBH_3CN$ (light and intermediate) or 4 μl of 600 mM $NaBD_3CN$ (heavy) were added, respectively. The mixtures were incubated for 1 h at room temperature on a shaking platform. The reaction was quenched with 16 μl of 1% ammonia. Finally, 8 μl formic acid was added and desalted using C18 ZipTip (Millipore), filled with extra Reprosil (5 μm, Dr. Maisch GmbH, Germany) beads. Prior to mass spectrometric analyses the three differentially-labelled samples were pooled.

2.2.15.3 Mass spectrometry analysis for protein identification

All the mass spectrometric (MS) analyses reported in **Chapter 3** result section **3.4** were performed by Dr. David Campbell, Robert Gourlay and Sanjay Kothiya (College of Life Science, University of Dundee). Mass spectrometric analysis of proteins digested with proteases (as described in section **2.2.15.1**) was performed to identify proteins and phosphorylated residues in proteins. For protein fingerprinting, samples were analysed by Liquid Chromatography-Mass

Spectrometry (LC-MS) on a Thermo LTQ-Orbitrap system. The generated MS data was analysed through the Mascot search engine (www.matrixscience.com) against appropriate databases.

2.2.15.4 Phosphopeptide enrichment using titanium dioxide

The columns were made using C8-Empore Extraction Disks and adding TiO_2 beads previously resuspended in acetonitrile (ACN). The columns were first washed with acetonitrile and then equilibrated with 0.2% TFA. The peptide samples were adjusted to 70% ACN/ 3% TFA/ 250 mM lactic acid, loaded onto the columns and washed sequentially with 70% ACN/ 3% TFA/ 250 mM lactic acid, 70% ACN/ 3% TFA and 0.1% TFA. Peptides were eluted using 1% ammonium hydroxide into tubes containing 50% TFA (5% of the total volume) and loaded onto the Orbitrap for analysis.

2.2.15.5 LTQ-orbitrap analysis for protein quantification

All the mass spectrometric analyses in Chapter 3 and Chapter 4 were performed by Dr Silvia Synowsky (College of Life Sciences, University of Dundee). Samples were analyzed by nano-ESI-MS/MS on an LTQ-Orbitrap mass spectrometer coupled with a Proxeon Easy nLC HPLC system. HPLC separation was on a C18 reverse phase column (pepmap75µm ID, 15cm cat no 160321) with a linear gradient of buffer A (0.1% formic acid, 2% acetonitrile) from 5 to 40% buffer B (90% acetonitrile, 0.08% formic acid) over 80 min. The HPLC column was flushed with 80% buffer B for 10 min and re-equilibrated with 5% buffer B for 10 min. A Fourier Transform (FT) scan on mass range 300 to 1820 amu was acquired at a resolution of 60000 with an internal calibration by a single lockmass (445.120020) reference. Each FT scan led to 5 MS/MS (LTQ) with multistage activation (MSA) on the top five most intense detected ions. Raw data were converted to Mascot generic files using raw2msm software (gift from Matthias Mann) in order to search with an in house Mascot 2.2 server against the Swiss-Prot database. Mass tolerances were 10 ppm for precursor mass and 0.8 Da for fragment mass. Carbamidomethyl-cysteine was a fixed modification; dimethylated N-terminus and lysine for the three different conditions and oxidized methionine were variable modifications. The quantification of proteins was performed using a modified version of MSQuant, which allows for the quantification of triply-labelled peptides.

Chapter three

Identification and regulation of proteins that interact with protein phosphatases of the PPP family

3.1 Regulation of protein phosphatases

Many effects of protein phosphatases in cellular events have been identified by studies using genetic mutants, pharmacological inhibitors and biochemical studies (Dombradi et al., 1990; Alessi et al., 1992; Wek et al., 1992; Hubbard and Cohen, 1993; Ceulemans and Bollen, 1994; Depaoli-Roach et al., 1994; Stark et al., 1994; Luke et al., 1996; Smith and Walker, 1996; Baskin and Wilson, 1997; Helps et al., 1998; Evans et al., 1999; Lizotte et al., 1999; Evans and Hemmings, 2000). However, the number of protein phosphatases (150) compared to kinases (500) in humans is strikingly low, raising the question of how such a small number of phosphatases counterbalance the effects of the larger number of kinases (Moorhead et al., 2009). The emerging answer is that the actions of phosphatases are largely dependent on their regulatory subunits, which specify their function(s). Although the regulation of the PPs through their regulatory subunits are somewhat understood (**section 1.5.4**), there are relatively few cases where the mechanisms of regulation of the protein phosphatases in response to extracellular stimuli have been defined.

The studies in this Chapter stemmed from an investigation into whether three RNA-binding Spen (Split-end) proteins, namely *Arabidopsis* FPA, and human RBM15 and RBM15B, might be novel PP1 interacting proteins, and these experiments are described in the last sections of this Chapter. However, while the primary goal was to test for interactions of PP1 with FPA, RBM15 and RBM15B, we also extended the scope of the experiments by aiming to identify further protein phosphatase interacting proteins. In addition, the MacKintosh group has been using differential quantitative proteomics to identify proteins whose binding to 14-3-3 proteins is regulated by different extracellular stimuli and inhibitors of signalling pathways. We were therefore curious to know whether we could adopt analogous procedures to screen for cases where the interactions between regulatory proteins and protein phosphatase catalytic subunits are acutely regulated by extracellular stimuli.

3.1.1 Microcystin as a useful and potent inhibitor for purifying protein phosphatases from cellular extracts

Even though phosphatases were identified quite early, their structures and regulation were not well understood. The roles of phosphatases became clearer with the development of tools such as the microcystin-affinity chromatography. This method is based on the binding and inhibitory property of microcystin towards

several members of the serine/threonine protein phosphatase family, PPP, including PP1, PP2A, PP4, PP5 and PP6. Although other inhibitors are effective towards these phosphatases, the ability to couple a modified microcystin-LR to Sepharose provides an easy method of purifying phosphatases from cellular extracts. Briefly, the dehydroalanine residue of microcystin-LR is modified by reacting it via Michael addition to small reactive thiols, which carries an amine group that in turn is coupled to N-hydroxy-succinamide-activated Sepharose (**section 1.3.3**). While the dehydroalanine in the native toxin forms a covalent bond with a cysteine residue in the β12-13 loop of the protein phosphatases, this bond is not essential for tight binding of the toxin to the enzyme. This modification therefore allows the phosphatase catalytic subunits to bind non-convalently to the microcystin-Sepharose beads, and these interactions can be disrupted using a chaotropic salt such as sodium thiocyanate (Moorhead et al., 1994). This method enabled the purification of different plant and mammalian members of the PPP family of phosphatases and their different interacting proteins (Moorhead et al., 1994; Moorhead et al, 1995; Meek et al., 1999). In a further modified version of this technology, Moorhead et al (2008) added a further step using PP1-targetted peptides to elute the regulatory subunits specific to this phosphatase. A short synthetic peptide (GKK**RVRW**ADLE) containing a variation of the RVXF motif (known to direct the interaction between PP1 and its interacting proteins) can first be used to elute the binding partners off the column, followed by the chaotropic salt wash to elute the phosphatases.

3.1.2 Using the cAMP-agonist forskolin to find potential novel targets of protein phosphatases

Cases are known where protein phosphatase interactions with their regulatory subunits are regulated via PKA-phosphorylation. For example, the regulation of PP1 in skeletal muscles occurs through its glycogen-bound regulatory subunit, G_M. When the PP1.G_M subunit is phosphorylated by PKA at Ser67, PP1 is released into the cytosol from the glycogen granules (MacKintosh et al., 1988). This is because Ser67 is the residue X within the RVXF motif of the G_M subunit, which means that its phosphorylation directly disrupts the interaction (Hubbard and Cohen, 1989). A simultaneous phosphorylation of Inhibitor-1 by PKA at Thr34 sequesters the PP1 into an inactive cytosolic form, PP1-I (Stralfors et al., 1985). DARRP32, the brain homologue of I-1 is also known to exert an inhibitory regulation of PP1 in

brain cells upon activation by PKA (Desdouits et al., 1995; Endo et al., 1996; Huang et al., 1999).

Because of these precedents and because the group have an interest in PKA signalling (**sections 1.3.4** and **1.5.6**), testing the effects of modulating PKA activity on phosphatase–regulatory subunit interactions seemed a good place to start in trialling the use of microcystin affinity chromatography to search for further acutely-regulated interactions of protein phosphatases with their regulatory subunits. For this purpose, we used the adenylate cyclase agonist forskolin to activate the cAMP–PKA pathway in HEK293 cells, with the non-specific PKA inhibitor H-89 as the negative control. A further batch of cells was left unstimulated and used later for normalisation of the quantified data. Lysates of cells from these three conditions were passed through microcystin affinity columns (**section 3.1.1**) and bound proteins were eluted with a chaotropic salt, separated by SDS-PAGE and identified by mass spectrometry. The tryptic peptides were also labelled by reacting with borohydride and formaldehyde to dimethyl primary amines. The chemicals for each preparation contained different amounts of the stable isotopes ^{2}H and ^{13}C, which meant that the relative amounts of any given peptide in each of the three preparations could be determined by differential mass spectrometry (as described in **sections 2.2.15** and **3.1**; Boersema et al., 2008). These analyses allow the comparison on the enrichment of the different proteins under the various treatment conditions. I performed these experiments to test the effect(s) of cAMP–PKA activation on the acute regulation of interactions of proteins with protein phosphatases (PPP family) in general (**section 3.1.3**) and PP1β specifically (**section 3.1.4**). Furthermore, I wanted to explore the isoform specifities of protein phosphatase 1 and used HEK293 cells stably-expressing the three isoforms of PP1 to further analyse proteins that potentially displayed isoform preference for the PP1 catalytic subunits (**section 3.2**).

3.1.3 Results

Analysis of the mass spectrometry data from the MC-affinity chromatography eluates (**Figure 3.1**) identified a total of around 380 proteins (**Appendix I**) including expected protein phosphatases. The MC-Sepharose affinity chromatography purification of protein phosphatases and their respective regulatory subunits provide a closer look into the regulation of the endogenous proteins. The phosphorylation of the PKA substrate VASP (vasodilator-stimulated

phosphoprotein) at Ser157 was used as a control for the treatments with forskolin and H-89 (**Figure 3.2**). Several known regulatory subunits of protein phosphatases were isolated in this procedure, giving confidence in the methodology. Some of the protein phosphatases and their respective subunits identified in this screen were (the complete list can be found in **Appendix I**): PPP1C and its regulatory subunits NIPP1, p53BP2, MYPT1; PPP2C and its regulatory subunits PPP2R1A, PPP2R1B, PPP2R2A, PPP2R2D, PPP2R5D, PPP2R5E; PPP4C and its regulatory subunits PPP4R1, PPP4R2, SMEK1 and SMEK2, PPP4R4; PPP5C, PPP6C and its regulatory subunits SAPS1, SAPS2 and SAPS3, among others (Alessi et al., 1992; Helps et al., 1995; Van Eynde et al., 1995; Csortos et al., 1996; Zolnierowicz et al., 1996; Trinkle-Mulcahy et al., 1999; Cohen et al., 2005; Stefansson et al., 2008). However, we could not identify any protein which seemed to be highly enriched or decreased in amount in the preparation from forskolin-treated cells. Such changes would have indicated regulation of interactions of regulatory proteins with catalytic subunits of protein phosphatases that was mediated by cAMP-signalling, possibly via PKA. As can be seen from the correlation value (R^2) in **Figure 3.3**, the two different treatment conditions (forskolin only versus H-89 and forskolin, with both normalised to the serum starved condition) do not seem to have any major quantitative effect on the proteins that were affinity-purified from the microcystin-Sepharose column in this experiment.

Proteins identified in this screen (total of 384) were classified into two groups: cellular localisation (**Figure 3.4**) and functional classification (**Figure 3.5**) (based on associated gene ontology (GO) terms from the Swiss-Prot database). As described in **section 1.5.2**, although PP1 is widely distributed throughout the cell, it is targeted to different cellular structures by associating with its subunits. For example, G_M proteins target PP1 to glycogen particles in skeletal muscles, Repo-Man recruits PP1 onto mitotic chromatin, URI localises PP1 to the mitochondria, and GADD34 targets PP1 to the endoplasmic reticulum (Hubbard and Cohen, 1993; Connor et al., 2001; Novoa et al., 2001; Djouder et al., 2003; Trinkle-Mulcahy et al., 2006; Theurillat et al., 2011). The classification of the different proteins that were identified in this screen suggests that there are many more examples of protein phosphatase regulatory subunits yet to be characterised. The cellular distribution of protein phosphatases and their regulatory subunits identified in this screen are in agreement with previous studies on their localisation in the cell (Luke et al., 1996;

Janssens and Goris, 2001; Carnegie et al., 2003; Trinkle-Mulcahy et al., 2006a). Since most, if not all, of the protein phosphatases identified here have been implicated in DNA-damage repair pathways, transcription, mitosis and cell cycle progression, it is reassuring to find a high proportion of the proteins are linked to nuclear functions. In agreement with the effects of protein phosphatases on protein synthesis and intracellular trafficking (Peters et al, 1999; Janssens and Goris, 2001; Cohen, 2002; Cohen et al., 2005) a considerable fraction of the proteins identified here are also found on the ribosomes and cytoplasmic face of the endoplasmic reticulum. Similarly, the functional classification of the proteins (**Figure 3.5**) is in line with most of the functions with which microcystin-inhibited protein phosphatases have been associated. For example, some functions of these protein phosphatases include, but are not limited to: PP1 in glycogen metabolism, cell adhesion, cell cycle progression, spliceosome assembly and differentiation (Cohen, 2002); PP2A in cell cycle regulation, protein synthesis and apoptosis (Janssens and Goris, 2001); PP4 in protein synthesis, mitosis, cell cycle progression and DNA repair (Cohen et al., 2005); PP5 in the regulation of DNA-damage pathways and transcription (Ali et al., 2004; Ikeda et al., 2004); PP6 in mitosis and DNA-damage repair (Stefansson and Brautigan, 2007).

Overall therefore, several protein phosphatases and their respective regulatory subunits were identified using this technique. However, the list of proteins generated is not robust enough to confidently suggest proteins that might be cAMP-regulated in this screen. For instance, having at least two more biological replicates for this screen would induce more confidence in the prediction of cAMP—PKA-dependent regulation of protein phosphatases and their subunits. Furthermore, different PKA inhibitors could also be used to check whether these proteins are indeed PKA-regulated or rather due to the non-specific nature of H-89. Nonetheless, the data generated from this screen could be used as a rough guide for further experiments into the regulation of protein phosphatases regulated by the cAMP—PKA signalling pathway.

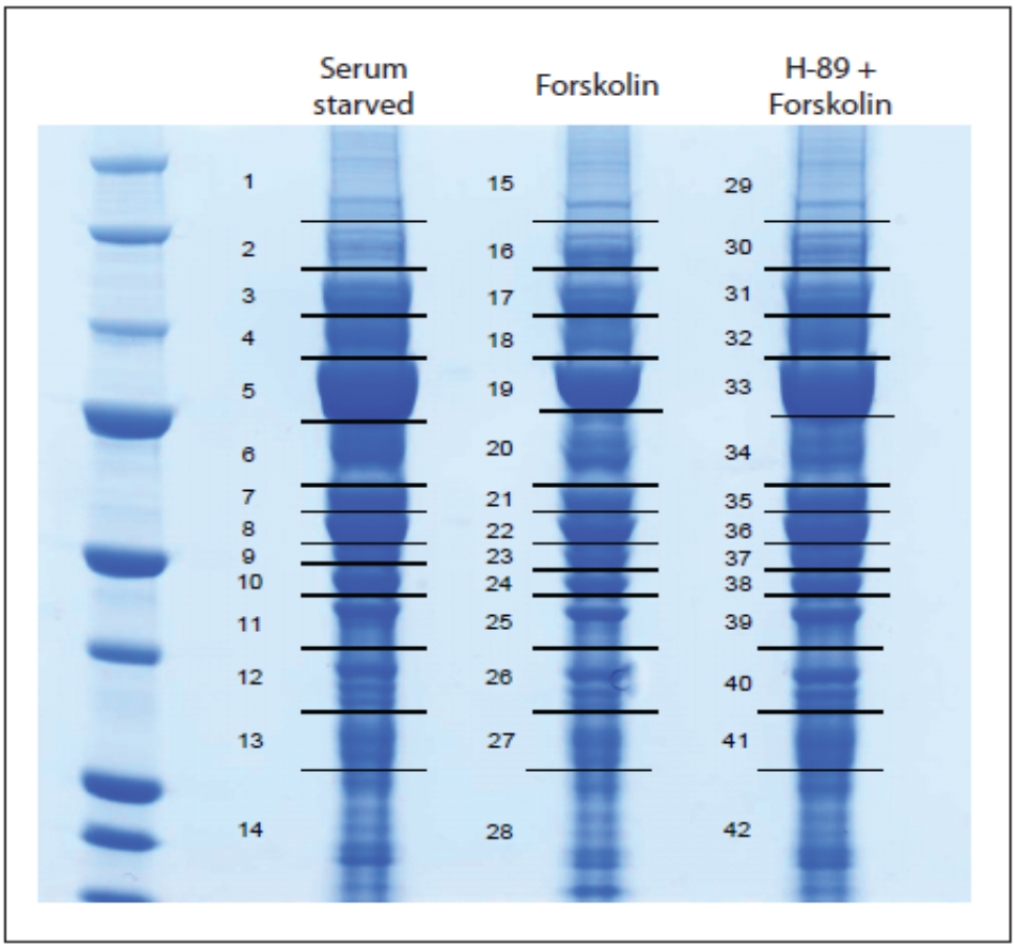

Figure 3.1: Coomassie-stained SDS-polyacrylamide gel of proteins that have been eluted from the microcystin-Sepharose columns
HEK293 cells were deprived of serum for 8 h. The serum-starved cells were kept in either serum-free medium, treated with forskolin (20 μM) for 30 min, or pre-treated with H-89 (30 μM) for 30 min before the addition of forskolin. Proteins in cell lysates were captured on microcystin-Sepharose and bound proteins phosphatases and their regulatory subunits were eluted with the chaotropic salt sodium thiocyanate. The column eluates (75% of each) were loaded onto each lane of an SDS-polyacrylamide gel, which was stained with colloidal Coomassie blue for protein visualisation. The lines and numbers represent the sections that were cut for further processing by the methods outlined in section **2.2.15**.

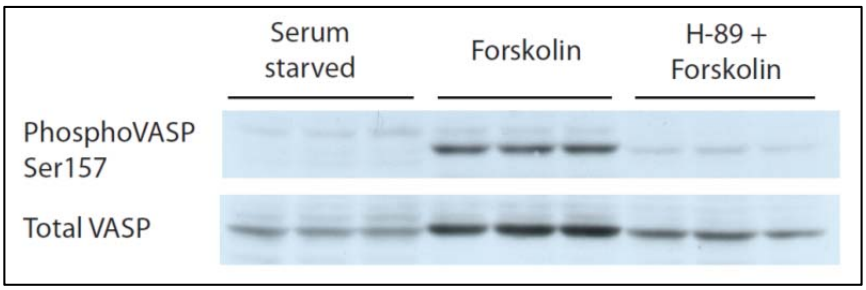

Figure 3.2: Western blots of phospho-VASP Ser157 and total VASP from the cell lysates used for the experiment in Figure 3.1
HEK293 cells were serum starved for 8 h. Serum starved cells were kept either in serum free medium, treated with forskolin (20 μM) for 30 min, or pre-treated with H-89 (30 μM) before adding forskolin (20 μM) for 30 min. Immnunoblots were performed with 40 μg of cell lysates run on SDS-PAGE and Western blotted with anti-phosphoSer157-VASP and anti-VASP.

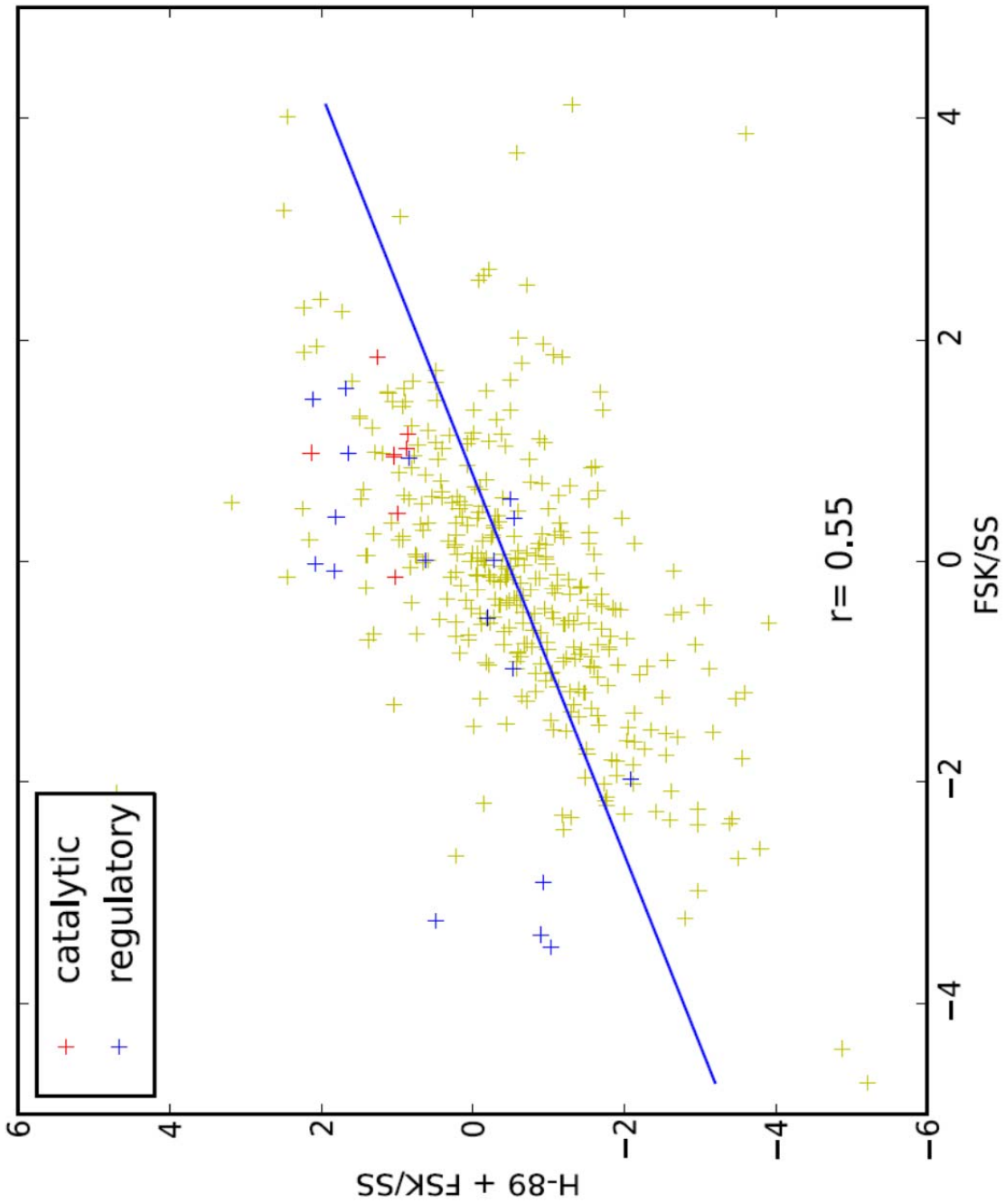

Figure 3.3: Comparison of the proteins that were affinity-purified on microcystin-Sepharose columns after treatment with forskolin (FSK) only or H-89 and forskolin

Proteins that were identified in the screen with at least two peptides were plotted on a scatter graph. The catalytic subunits of protein phosphatase 1, 2A, 4, 5 and 6 are in red while their known regulatory subunits are in blue. The quantification values in the two treatment conditions were normalised to the serum-starved (SS) condition. The correlation value (r) between the two treatments is shown on the graph.

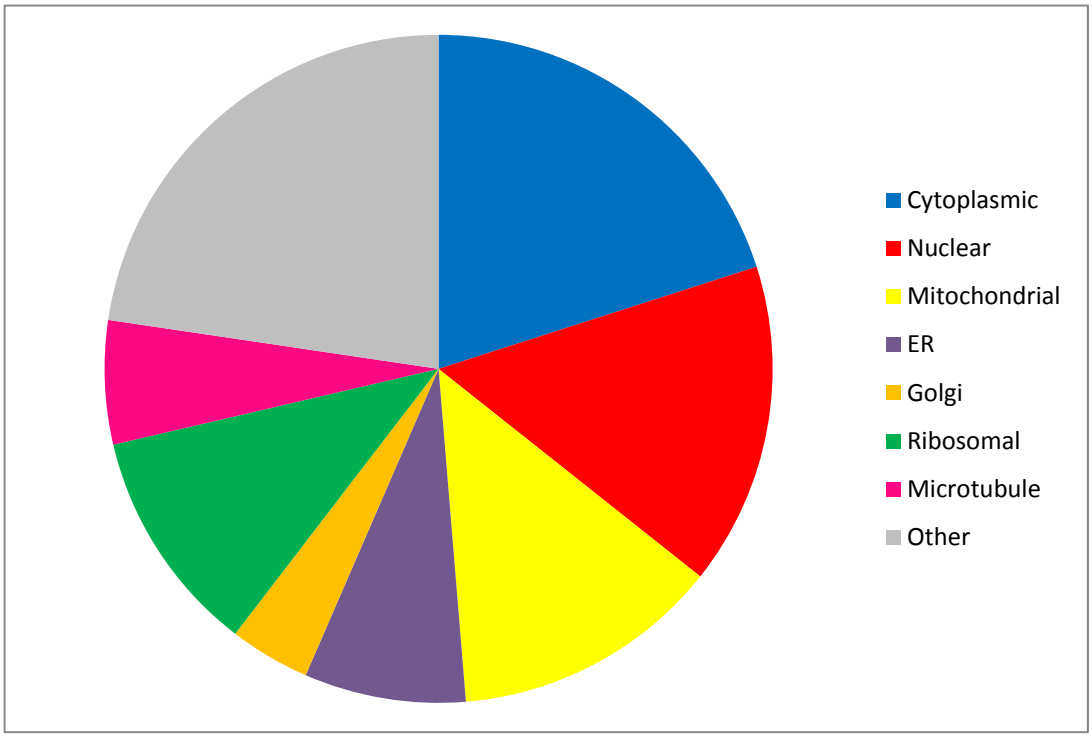

Figure 3.4: Subcellular distribution of the different proteins that were isolated with microcystin-Sepharose affinity chromatography
Protein phosphatases are found in the cytoplasm and nucleus, but can also be targeted to specific sub-cellular structures by association with regulatory subunits that contain motifs and domains for targeting to particular proteins and locations (section **1.5.2**). The 384 proteins identified in this screen have been categorized according to subcellular locations according to the Gene Ontology terms in the Swiss-Prot database, though these should be regarded as loose assignments because proteins can be found in more than one location.

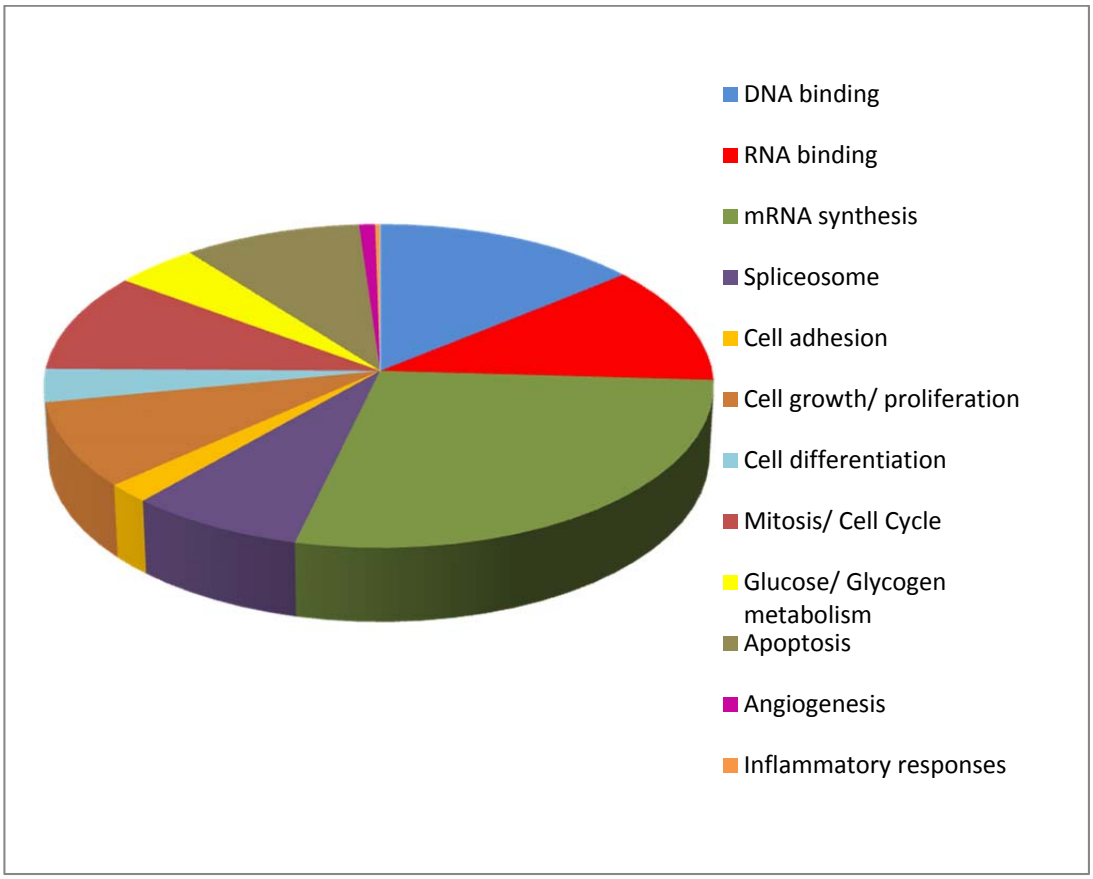

Figure 3.5: Functional distribution of the proteins that were affinity purified and identified from the microcystin-Sepharose affinity chromatography
Microcystin-Sepharose has been successfully used to enrich in protein phosphatases PP1, PP2A, PP4, PP5 and PP6. The protein hits identified in this screen (384 proteins) have been classified according to the different cellular processes that protein phosphatases and their regulatory subunits have been reported to be involved in according to the Gene Ontology terms in the Swiss-Prot database.

3.1.4 GFP-Trap pull-down to find potential PKA-mediated PP1 beta regulation events

In another approach to identify PP1-binding proteins that were potentially regulated by cAMP–PKA activation, we used HEK293 cells stably expressing PP1β with a GFP tag. These cells were expressed, treated with or without forskolin in the presence or absence of H-89 and purified on GFP-Trap® agarose beads. The proteins were run on an SDS-polyacryamide gel (**Figure 3.5**), digested with trypsin, differentially dimethyl-labelled with stable isotope and identified by mass spectrometry, as described in **section 2.2.15**. Control blots for cell lysates measured VASP phosphorylation at Ser157 to check PKA inhibition and activation following treatments with H-89 and forskolin respectively (**Figure 3.6**). Around 140 proteins (**Appendix II**) were identified in this screen and these have been classified based on their cellular localisations (**Figure 3.7**) and functions (**Figure 3.8**). A few known PP1 regulatory subunits were identified, including MYPT1, URI, Staufen, NIPP1, WDR82, Sds22, Mbs85, Inhibitor-2 and p53BP2 (Huang and Glinsmann, 1976; Allen et al., 1998; Alessi et al., 1992; Helps et al., 1995; Van Eynde et al., 1995; Kreivi et al., 1997; Trinkle-Mulcahy et al., 1999; Ceulemans et al., 2002; Tan et al., 2002; Monshausen et al., 2003; Trinkle-Mulcahy et al., 2006; Djouder et al., 2007; Theurillat et al., 2011). Interestingly, a few of these were seen to be slightly more enriched in forskolin-treated cells, though not strikingly so (**Table 3.1**).

However, one group of glycogen-related proteins (**Figure 3.9**) were highly enriched in the preparation from cells stimulated with forskolin in the presence of H-89 (**Table 3.2**). These proteins comprised PPP1R6 (also known as R6), glycogenin and glycogen synthase. PPP1R6 is one of a family of glycogen-targeting subunits of PP1 (Armstrong et al., 1997). Although little is known about its function, R6 has been shown to co-purify with glycogen granules, has a wide tissue distribution, but it has no apparent consensus sequence for PKA phosphorylation (Armstrong et al., 1997). Glycogenin was first described as the 44 kDa subunit of glycogen synthase (Nimmo et al., 1976) and in 1985, was isolated as the covalently bound protein part of muscle glycogen (Rodriguez and Whelan, 1985). A decade later, glycogenin was reported as the 38 kDa subunit of glycogen synthase required to initiate glycogen synthesis (Pitcher et al., 1987). Glycogenin binds to a glucose residue via its Tyr194 which triggers its glucosyltransferase activity, thereby catalysing the transfer of glucose molecules from the donor UDP-glucose to itself until the nascent

oligosaccharide chain is approximately eight glucose units long (Lomako et al., 1988; Pitcher et al, 1988; Cao et al., 1993). Glycogen synthase elongates the glycogen moiety started by glycogenin by linking glucose molecules through the α1-4 and α1-6 linkages. It was also reported that the ability of glycogen synthase to glucosylate glycogenin depends on the correct glucosylation state of glycogenin (Skurat et al., 1993). Glycogen synthase is also activated through dephosphorylation by PP1 (Brady et al., 1997). This suggests a very intricate role of glycogenin and glycogen synthase in regulating blood glucose levels.

Taken together, the increased amount of glycogenin and glycogen synthase associated with PP1 with H-89 and forskolin treatment might be linked to the enrichment of the R6 glycogen-targeting subunit of PP1 under the same condition. The coordinated behaviour of the three proteins in this experiment might indicate a role for R6 in targeting PP1 to actively lower blood glucose levels by promoting glycogen synthase activation. The cAMP cascade normally inhibits glycogen synthesis in the liver when blood glucose levels are low; PKA phosphorylates and inactivates glycogen synthase, while simultaneously phosphorylating glycogen phosphorylase through phosphorylase kinase leading to glycogen catabolism (Soderling et al., 1970; Cohen et al., 1978). Forskolin triggers the cAMP cascade and H-89 is known to block this activation: the observations in this experiment suggest that the enrichment of glycogen synthase, glycogenin and R6 are independent of PKA activation. Further experiments are required to check the correlation between R6 and the enzymes of glycogen synthesis and to delineate the reason underlying these observations.

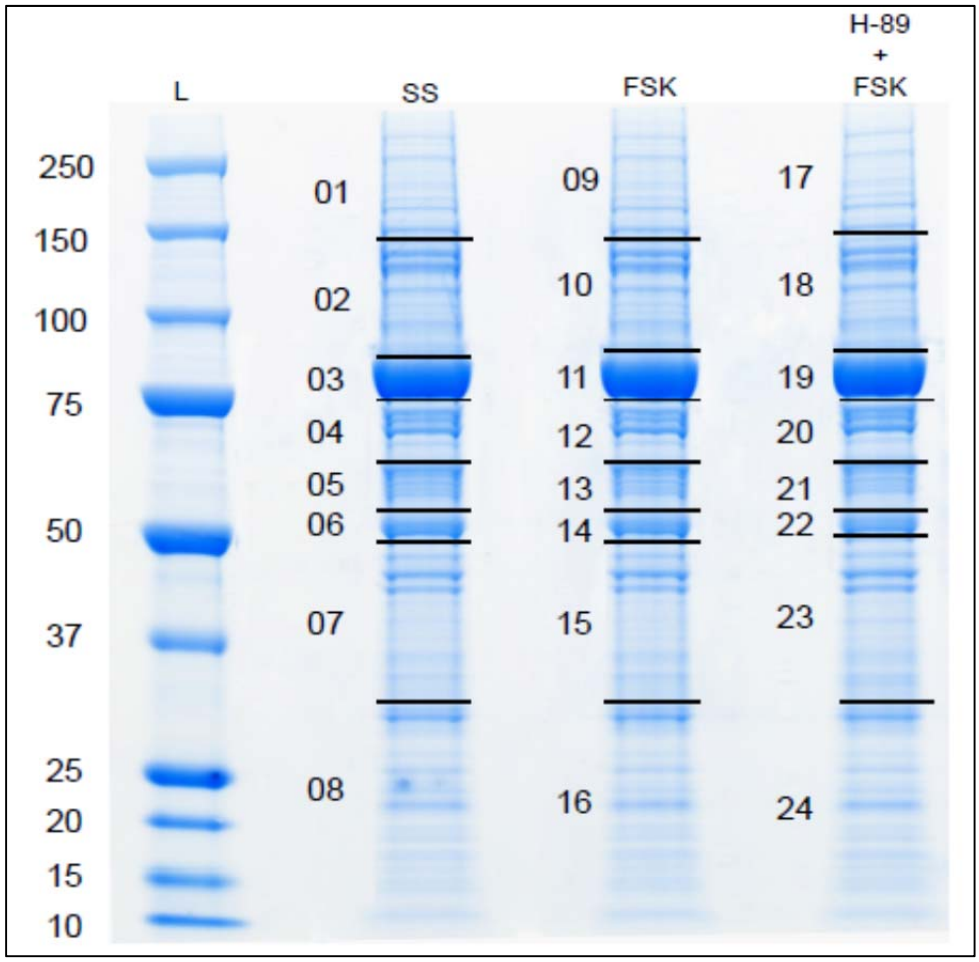

Figure 3.6: Coomassie-stained SDS-polyacrylamide gel of proteins that were captured with GFP-Trap® from lysates of cells expressing GFP-PP1β
Flp-In T-REx 293 cells were stably transfected to express GFP-TAP-PP1β in a tetracycline-inducible manner. Protein expression was induced with 1 mg/ml of tetracycline for 24 h. These cells were then serum starved for 8 h. Serum starved cells were either kept in serum free medium, treated with forskolin (20 μM) for 30 min, or pre-treated with H-89 (30 μM) for 30 min before the addition of forskolin. Proteins that co-immunoprecipitated with GFP-TAP-PP1β were captured on GFP-Trap® beads. Bound proteins were eluted by boiling the beads with 4 x SDS-loading buffer. Column eluates (75%) were loaded in each lane of an SDS-polyacrylamide gel that was then stained with colloidal Coomassie blue for protein visualization. The lines and numbers represent the sections that were cut for further processing by the methods outlined in **section 2.2.15**.

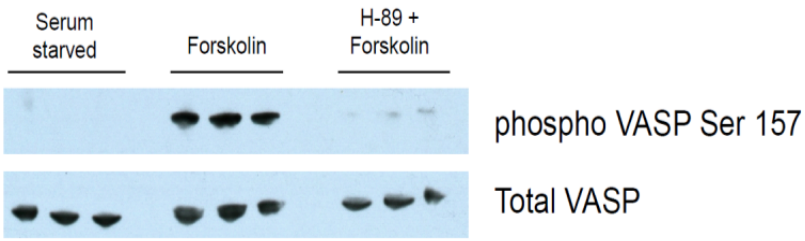

Figure 3.7: Western blots of phospho-Ser157-VASP and total VASP from the cell lysates used for the experiment in Figure 3.5

Flp-In T-REx 293 cells were stably transfected to express GFP-PP1β and induced to express the protein using 1 mg/ml tetracycline for 24 h. These cells were then serum starved for 8 h. Serum starved cells were either kept in serum free medium, treated with forskolin (20 μM) for 30 min, or pre-treated with H-89 (30 μM) for 30 min before the addition of forskolin. Immunoblottings were performed with 40 μg of cell lysates run on SDS-PAGE and Western blotted with anti-phospho- Ser157-VASP and anti-VASP.

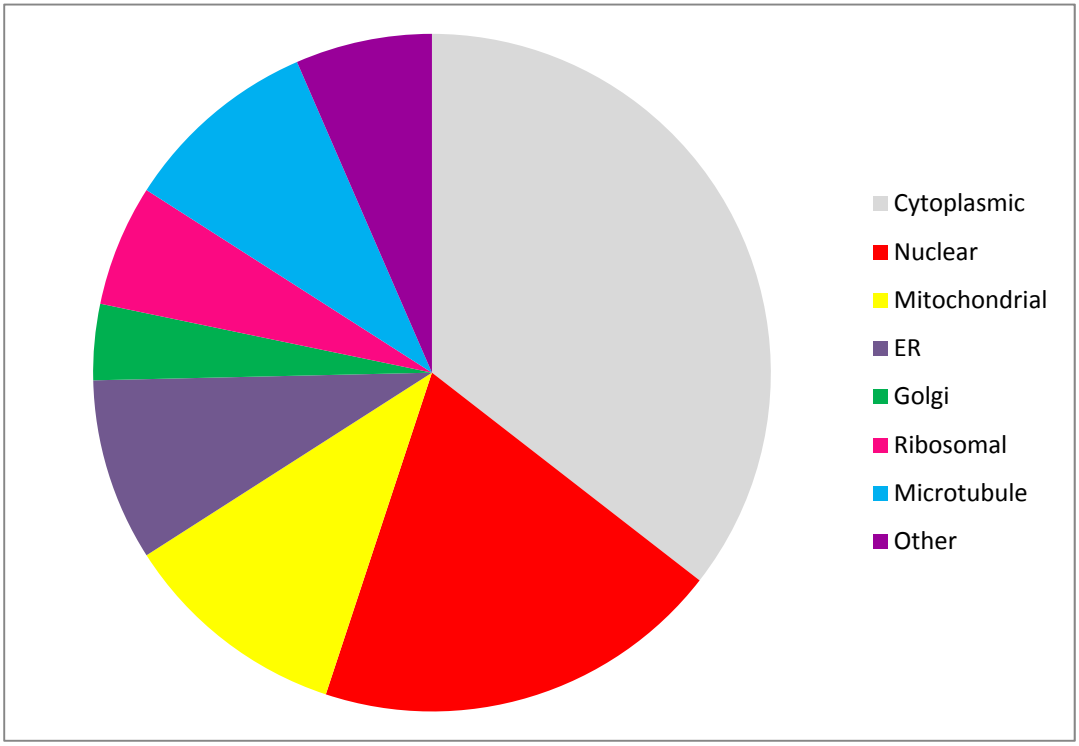

Figure 3.8: Subcellular distribution of the different PP1β-interacting proteins that were pulled down with the GFP-Trap® technology
Proteins (total 140) that were captured with PP1β on the GFP-Trap® beads have been grouped according to their cellular localisations. The relevant information was retrieved from the assigned GO terms for the relevant proteins from the Swiss-Prot database.

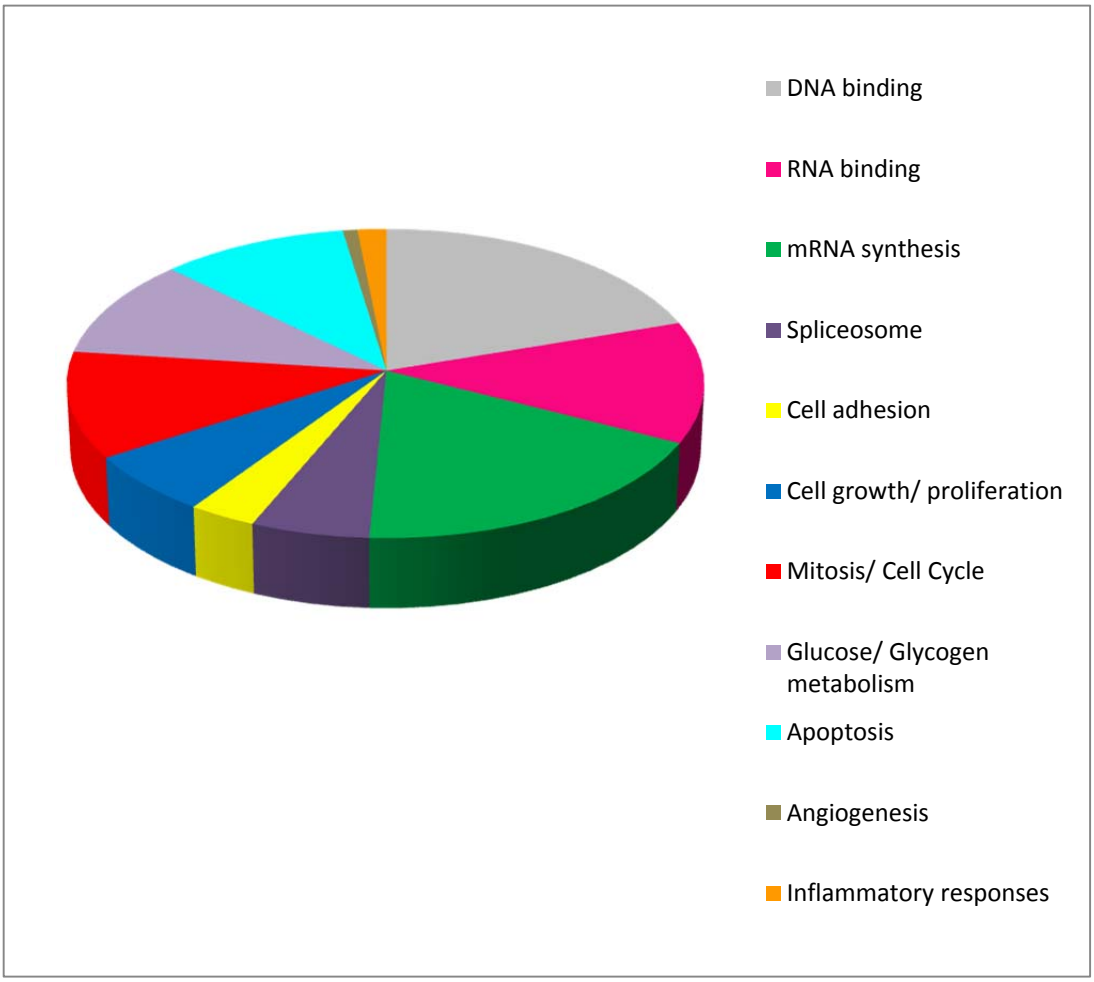

Figure 3.9: Functional classification of the different PP1β-interacting proteins identified in this screen

Proteins (total 140) that were captured with PP1β on the GFP-Trap® beads have been grouped according to their functional classifications based on the relevant information retrieved from the assigned GO terms in the Swiss-Prot database.

Table 3.1: Regulatory subunits of PP1 identified in this screen, with their enrichment values in the two treatment conditions normalised to the serum starved condition.

Swiss-prot ID	Swiss-prot description	Mass (kDa)	FSK/ serum-starved	H-89+FSK/ serum-starved	References
Q13625	Apoptosis-stimulating of p53 protein 2 TP53BP2	126.2	3.30	1.94	Helps et al., 1995
O95793	Double-stranded RNA-binding protein Staufen homolog 1 STAU1	63.4	1.16	1.87	Monshausen et al., 2003
Q12972	Nuclear inhibitor of protein phosphatase 1 PPP1R8	38.6	2.83	1.66	Van Eynde et al., 1995; Trinkle-Mulcahy et al., 1999
O60927	Protein phosphatase 1 regulatory subunit 11 PPP1R11	14.2	1.10	1.10	Zhang et al., 1998
O14974	Protein phosphatase 1 regulatory subunit 12A PPP1R12A	115.6	1.14	0.78	Alessi et al., 1992; Zagorska et al., 2010
O60237	Protein phosphatase 1 regulatory subunit 12B PPP1R12B	110.8	1.10	0.74	Moorhead et al., 1998
Q9BZL4	Protein phosphatase 1 regulatory subunit 12C PPP1R12C	85.3	1.16	1.16	Tan et al., 2002
Q86XI6	Protein phosphatase 1 regulatory subunit 3B PPP1R3B	33.1	2.28	2.46	Munro et al., 2002
Q15435	Protein phosphatase 1 regulatory subunit 7 PPP1R7	41.7	3.02	1.69	Ceulemans et al., 2002
Q01844	RNA-binding protein EWS EWSR1	68.7	1.08	1.00	Trinkle-Mulcahy et al., 2006
Q96QC0	Serine/threonine-protein phosphatase 1 regulatory subunit 10 PPP1R10	99.3	1.30	1.48	Kreivi et al., 1997; Allen et al., 1998
Q13263	Transcription intermediary factor 1-beta TRIM28	90.3	0.82	0.65	Li et al., 2010
Q6UXN9	WD repeat-containing protein 82 WDR82	35.5	6.19	3.98	Trinkle-Mulcahy et al., 2006
P49750	YLP motif-containing protein 1 YLPM1	220.1	1.21	1.10	Ulke-Lemee et al., 2007
O95685	Protein phosphatase 1 regulatory subunit 3D PPP1R3D	33.3	5.33	23.15	Armstrong et al., 1997

Table 3.2: Three proteins involved in glycogen metabolism that were highly enriched in the H-89 and forskolin treated cells.

Swiss-prot ID	Swiss-prot description	Mass (kDa)	Forskolin/ serum-starved	H-89 + FSK/ serum-starved
P13807	Glycogen [starch] synthase, muscle GYS1	84.531	2.361	18.633
P46976	Glycogenin-1 GYG1	39.701	2.674	15.442
O95685	Protein phosphatase 1 regulatory subunit 3D PPP1R3D	33.28	5.325	23.153

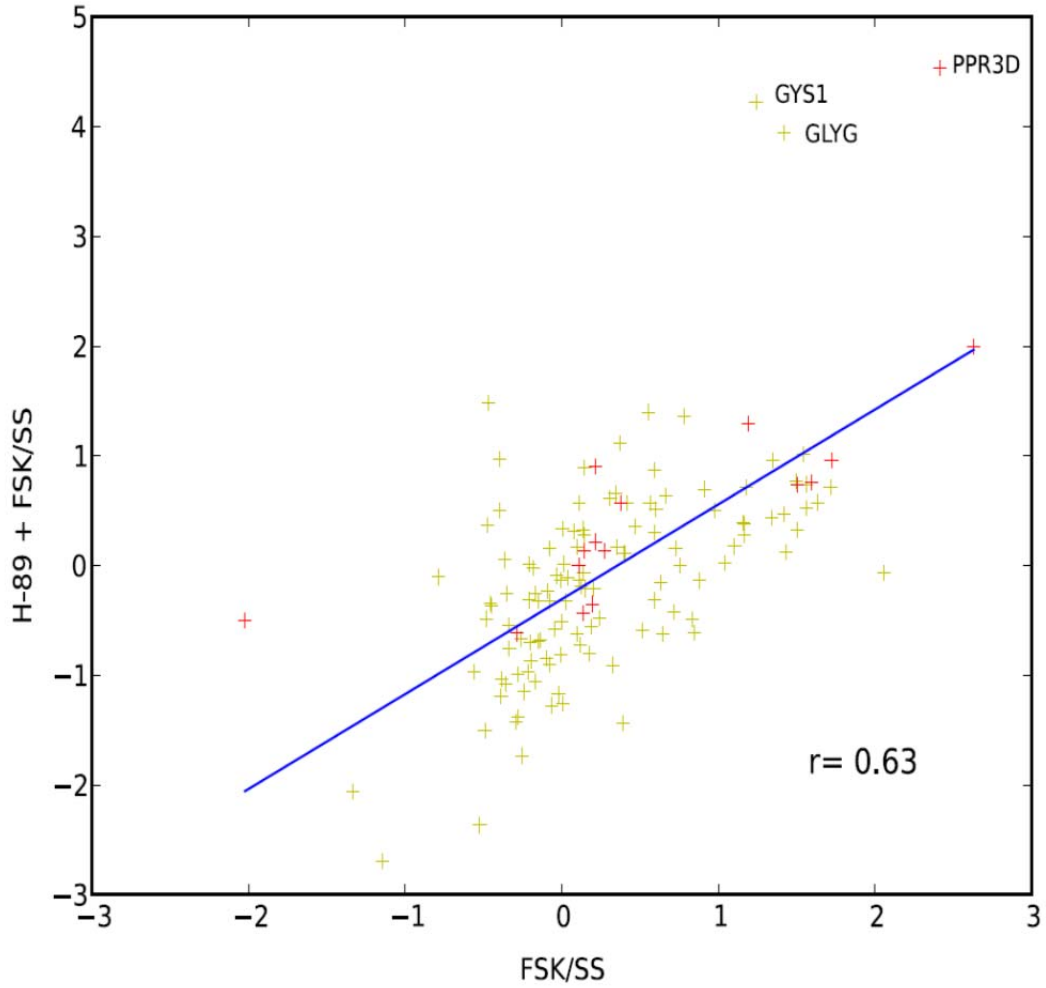

Figure 3.10: Comparison of the effects of forskolin (FSK) versus H-89 followed by forskolin treatments on PP1-beta expressing stable cell lines.
Proteins that were identified in the screen with at least two peptides were plotted on a scatter graph. The known regulatory subunits of protein phosphatase 1 are in red. The quantification values in the two treatment conditions were normalised to the serum-starved condition. The correlation value (r) between the two treatments is shown on the graph.

3.2 Comparison of the isoform specificity of PP1-binding proteins using GFP-Trap® capture of GFP-TAP-tagged proteins

Protein phosphatase 1, one of the most conserved eukaryotic proteins, is a serine/threonine protein phosphatase which has been implicated in a number of cellular processes, e.g., glycogen targeting to muscles, smooth muscle contraction, splicing, apoptosis etc. In humans, PP1 has three major catalytic isoforms-alpha, beta/delta and gamma, which are more than 89% identical to each other in their amino acid sequences. The major differences among these isoforms occur at their variable amino and carboxy terminals. The catalytic forms of PP1 do not exist freely in cells; rather, they associate with regulatory subunits which either inhibit, target or modulate the activity of PP1. Most of these regulatory subunits have been observed to bind non-specifically to all three isoforms of PP1, generally through a degenerate RVXF motif (**section 1.5.2**). However, some regulatory subunits are more selective: MYPT1 binds preferentially to PP1β while Repo-Man selectively recruits PP1γ (Alessi et al., 1992; Trinkle-Mulcahy et al., 2006; Zagorska et al., 2010). With the high degree of similarity (almost 90% amino acid sequence similarity) among the three PP1 isoforms, it seems reasonable to assume that a large proportion of these regulatory subunits would be shared among the catalytic subunits. Interestingly though, the different cellular expression patterns of these isoforms imply a higher degree of specificity than would have been originally thought. For instance, PP1α and PP1β have a rather diffused localisation throughout the cell whereas PP1γ has been observed to be concentrated in the nucleoli (Andreassen et al., 1998; Trinkle-Mulcahy et al., 2001; Trinkle-Mulcahy et al., 2006). Subcellular fractionation studies of the brain have revealed distinct associations of PP1β with microtubules, whereas PP1γ associates more with the actin cytoskeleton (Strack et al., 1999). Furthermore, some interacting proteins also target PP1c to different cellular structures, for example, MYPT1 targets PP1β to myosin chains in smooth muscles, p99/PNUTS targets PP1α to the nucleus, while the G_M targets PP1 to glycogen particles in skeletal muscles (Alessi et al., 1992; Hubbard and Cohen, 1993; Allen et al., 1998).

We generated stable cell lines expressing the three PP1 catalytic subunits tagged to GFP-TAP. The proteins were expressed, immunoprecipitated using the GFP-Trap® beads and the protein partners analysed and quantified by mass spectrometry (**section 2.2.15**). As can be seen from **Figure 3.10**, all three catalytic

PP1 isoforms were successfully expressed and identified as the major bands in the respective lanes. Many of the known regulatory subunits of PP1 were identified, giving confidence in the screen. The co-immunoprecipitated proteins (**Appendix III**) were quantified and the values converted to log 2 and used as a measure of enrichment for each protein with that particular PP1 isoform. The identified proteins have been recorded on a graph on **Figure 3.11,** which shows the different log 2 ratios for each protein when comparing gamma to alpha. A more exhaustive comparison of the three isoforms has been included in **Appendix IV**. We could not find any pattern which would indicate a preference for any of the PP1 isoform relative to the other two in this screen.

Using the dimethyl labelling approach meant that only two sets of pull-downs could be compared side-by-side and so all the data were normalised to the values in the PP1α preparation for the following part of the analysis. Since not much has been published in terms of isoform selectivity for PP1, we could not verify all of the data. Nonetheless, some of the data obtained were in agreement with the information that was available (**Table 3.3**). For instance, MYPT had a higher enrichment value with PP1β (8.7) compared to PP1γ (1.7), suggesting that MYPT1 might have a higher affinity for PP1β compared to PP1γ, as previously described by Zagorska and colleagues (2010). In addition, NIPP1 was preferentially isolated with PP1β (46.6) compared to PP1γ (6.9). Known regulatory subunits of PP1 that were identified in this screen are listed in **Table 3.3** along with the different enrichment values for the specific isoforms. Some regulatory subunits such as Tra2-beta and SDS22 did not show any isoform specificity under these conditions. Although Repo-Man has been widely cited as preferentially binding to PP1γ, overexpression of Repo-Man has also led to binding to PP1α (Trinkle-Mulcahy et al., 2006). This suggests that although the regulatory subunits exhibit some degree of specificity for isoform selectivity, there can still be some degree of overlap. The data from this experiment suggests that the isoform preferences of the regulatory subunits of PP1 are not as striking as initially thought. Previous experiments using bacterially-expressed protein phosphatases could have been affected by the fact that the bacterially-expressed protein, albeit active, does not appear to fold up correctly and have different properties from the native enzymes isolated from eukaryotic cells and tissues (MacKintosh et al., 1996). This would likely contribute to bias in readouts,

similar to the data shown about overexpression of the targeting subunits leading to isoform bias (Trinkle-Mulcahy et al., 1999; Trinkle-Mulcahy et al., 2006).

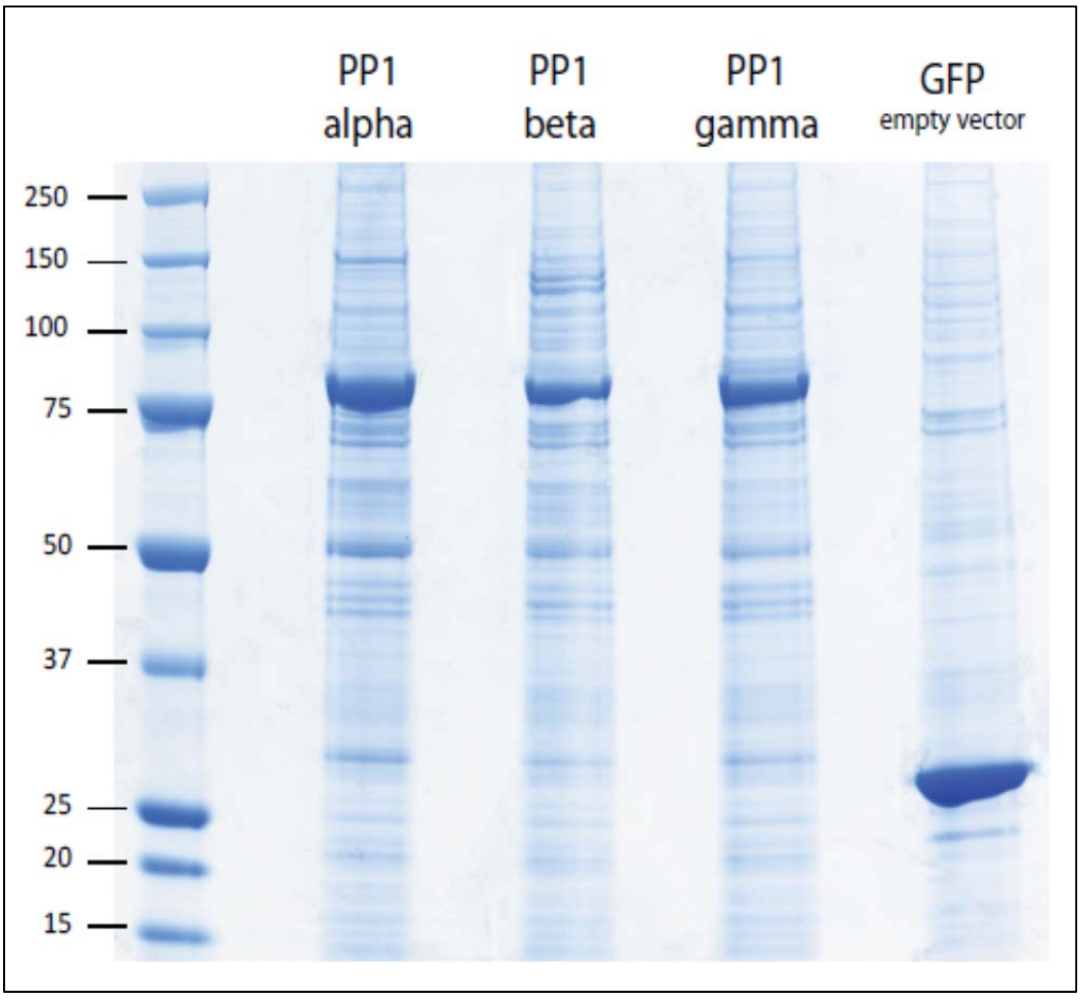

Figure 3.12: Coomassie-stained SDS-polyacrylamide gel of PPP1C isoforms alpha, beta and gamma and their respective interacting proteins that have been eluted from GFP-Trap® immunoprecipitates
Stably transfected Flp-In T-REx 293 cells were treated with tetracycline for 24 h to stably express the GFP-TAP-tagged versions of the three catalytic isoforms of PP1, namely PP1α, PP1β and PP1γ. Proteins that co-immunoprecipitated with the three catalytic PP1 isoforms were captured on GFP-Trap® beads. Bound proteins were eluted by boiling the beads with 4 x SDS-loading buffer. Column eluates (75%) were loaded onto each lane of an SDS-polyacrylamide gel that was then stained with colloidal Coomassie blue for protein visualisation. Each lane was then cut into eight gel pieces, digested with trypsin, labelled with the dimethyl approach as outlined in section **2.2.15** and analysed by mass spectrometry.

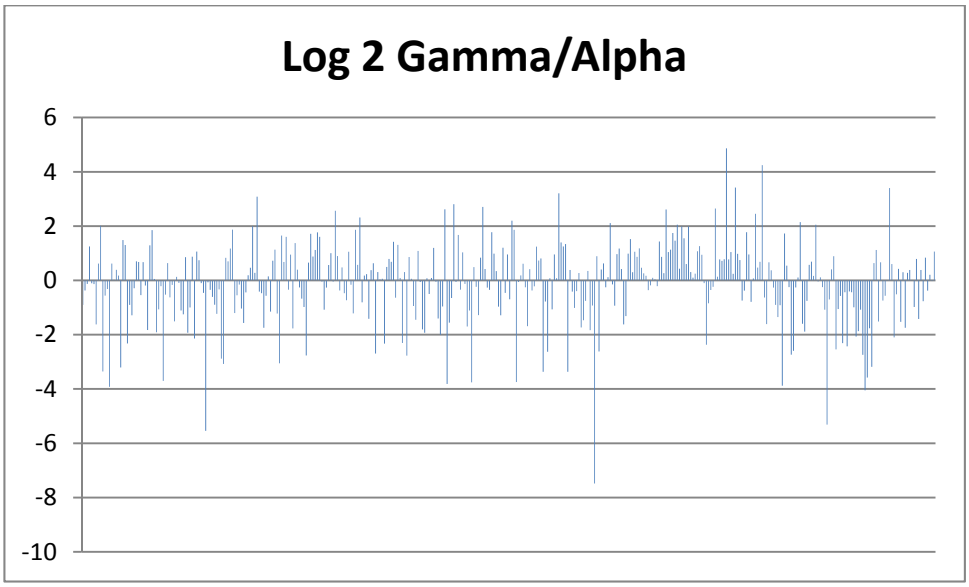

Figure 3.12: Ratio of PP1-interacting proteins from PP1γ and PP1α
Enrichment values from PP1α and PP1γ were converted to log 2 values and plotted as a ratio of their abundance in the preparations, with PP1γ:PP1α respectively.

Table 3.3: Known regulatory subunits of protein phosphatase 1 with their enrichment values in terms of the relative amounts of proteins isolated with the different catalytic subunits of PP1. Known isoform preferences for the respective regulatory subunits are also indicated.

Uniprot ID	Protein ID	Mass (kDa)	Mascot score	Enrichment value in		Previously reported preferences	References
				PP1β/α	PP1γ/α		
Q12972	NIPP1	38.6	434	46.62	6.96	Isoform preference- **alpha** (Trinkle-Mulcahy et al., 2006)	Van Eynde et al., 1995; Trinkle-Mulcahy et al., 1999
Q96QC0	p99/PNUTS	99.3	1093	42.87	41.37	Isoform preference-**alpha** (Trinkle-Mulcahy et al., 2006)	Kreivi et al., 1997; Allen et al., 1998
O14974	MYPT1	115.6	894	8.71	1.73	Isoform preference-**beta** (Zagorska et al., 2010)	Alessi et al., 1992; Zagorska et al., 2010
Q15435	Sds22	41.7	1271	6.35	5.34	Interaction has been studied with all three isoforms but no preference has been found (Ceulemans et al., 2002)	Ceulemans et al., 2002
Q13625	p53BP2	126.2	1112	5.63	51.08	The original study for PP1 binding with gamma (Helps et al., 1995) but preference with isoform **alpha** reported by Trinkle-Mulcahy et al. (2006)	Helps et al., 1995
Q01844	EWS	68.7	159	4.06	5.34	Preference for isoform **alpha** (Trinkle-Mulcahy et al., 2006)	Trinkle-Mulcahy et al., 2006
P62995	Tra2beta	33.8	164	2.40	2.32	PP1 binding reported with isoform gamma	Novoyatleva et al., 2008
P49750	ZAP3	220.1	467	1.67	6.84	The original interaction with PP1 was described with PP1alpha (Ulke-Lemee et al., 2007) but no isoform preference has been reported (Trinkle-Mulcahy et al., 2006)	Ulke-Lemee et al., 2007
Q6UXN9	WDR82	35.5	514	1.36	11.78	No isoform preference has been reported (Trinkle-Mulcahy et al., 2006)	Trinkle-Mulcahy et al., 2006
O95793	Staufen	63.4	276	0.67	2.12	Interacts with all three isoforms and no isoform preference has been reported (Monshausen et al., 2003)	Monshausen et al., 2003
O94763	URI	60.3	522	0.52	3.62	Interaction has been studied with the gamma isoform (Djouder et al., 2007; Theurillat et al., 2011) but no preference has been reported	**Djouder et al., 2007; Theurillat et al., 2011**
Q9BZL4	MBS85	85.3	1480	19.69	1.20	Only associates with the **gamma** isoform (Tan et al., 2002)	Tan et al., 2002

3.2.1 Bioinformatic analysis of novel PP1-binding motifs

Most PP1-interactors were previously defined by their ubiquitous [RK][VI]$_{012}$[X][FW] (commonly referred to as the RVXF signature) motif, through which interaction with PP1 was mediated. It is now becoming increasingly clear that other motifs exist which are also able to mediate interaction with PP1. For example, the recently described MyPhoNE and [GS]IL[RK] (commonly referred to as SILK) motifs, although not very common, are also able to mediate interaction with PP1 to effect a specific cellular function (Hendrickx et al., 2009; Roy and Cyert, 2009). Inhibitor-1, although not identified in this screen, was one of the first PP1-regulatory subunits reported to interact and inhibit PP1 through its SILK motif (Huang et al., 1999; Wakula et al., 2003). The SILK motif can functionally replace the RVXF motif as demonstrated with NIPP1 (Wakula et al., 2003). MYPT1 has a MyPhone motif which mediates its interaction with PP1beta to effect muscular contractions and cell adhesion (Zagorska et al., 2010). In order to analyse whether other proteins have these two new motifs, a bioinformatics approach was undertaken. Protein interactors of three different isoforms of PP1 that were identified in the GFP-Trap immunoprecipitates were analysed and classified into three broad groups: RVXF, SILK and MyPhoNE. Of the 234 proteins isolated, 15 were found to have the SILK/GILK motif and 4 proteins had the MyPhoNE motif (**Table 3.4**). Of the 15 SILK/GILK motif-containing proteins identified here, 2 have been cited in other studies to putatively interact with PP1, namely NUP153 and RMP (Djouder et al., 2007; Moorhead et al., 2009). Three out of the four proteins containing the MyPhoNE motif belong to the MYPT family: PPP1R12A, PPP1R12B and PPP1R12C. The only other protein seen in this experiment that has such a motif is SH2D4A, which is a cytoplasmic protein involved in the development of T-cells and also in the inhibition of oestrogen-induced cellular proliferation (Lapinski et al., 2008; Li et al., 2009).

Table 3.4: PP1-binding proteins displaying the SILK and MyPhoNE motifs identified in HEK293 cells stably expressing GFP-TAP-PP1

Accession #	Description	Motif	References
SILK/GILK			
P49790	Nuclear pore complex protein Nup153 NUP153	$^{246-250}$ SILK	Moorhead et al., 2009
P07814	Bifunctional aminoacyl-tRNA synthetase EPRS	$^{52-56}$ SILR	-
Q14160	Protein LAP4 SCRIB	$^{268-272}$ SILK	-
P49327	Fatty acid synthase FASN	$^{518-522}$ SILR	-
O94763	Unconventional prefoldin RPB5 interactor RMP	$^{407-411}$ SILK	Djouder et al., 2007
P50991	T-complex protein 1 subunit delta CCT4	$^{302-306}$ SILR, $^{527-531}$ SILK	-
P06733	Alpha-enolase ENO1	$^{1-5}$ SILK	-
P12004	Proliferating cell nuclear antigen PCNA	$^{9-13}$ SILK	-
Q00610	Clathrin heavy chain 1 CLTC	$^{389-393}$ GILR	-
O94822	RING finger protein 160 RNF160	$^{1187-1191}$ GILK	-
Q9P2J5	Leucyl-tRNA synthetase, cytoplasmic LARS	$^{762-766}$ GILR	-
P11021	78 kDa glucose-regulated protein HSPA5	$^{506-510}$ GILR	-
P49411	Elongation factor Tu, mitochondrial TUFM	$^{281-285}$ GILK	-
Q06830	Peroxiredoxin-1 PRDX1	$^{136-140}$ GILR	-
Q6NXS1	Putative protein phosphatase inhibitor 2-like protein 3 PPP1R2P3	$^{12-16}$ GILK	-
MyPhoNE			
O14974	Protein phosphatase 1 regulatory subunit 12A PPP1R12A	$^{9-17}$ RNEQLKRW	Alessi et al., 1992
O60237	Protein phosphatase 1 regulatory subunit 12B PPP1R12B	$^{18-26}$ RAEQLRRW	Fujioka et al., 1998
Q9BZL4	Protein phosphatase 1 regulatory subunit 12C PPP1R12C	$^{21-29}$ RREQLRQW	Tan et al., 2001
Q9H788	SH2 domain-containing protein 4A SH2D4A	$^{31-39}$ REEQIRRW	Hendrickx et al., 2009; Roy and Cyert, 2009

The numbers in superscript next to the motif sequences denote the positions of those amino acids in the protein sequences. The proteins whose interaction with PP1 have been tested and validated are given in the papers cited.

3.3 Do the RVDF-containing SPEN proteins FPA and RBM15 interact with Protein Phosphatase 1?

The RVXF motif has long been recognised as the major motif-determinant for specifying PP1 interaction with its targeting subunits. This motif was first identified in studies of the myosin-targeting subunit M_{110} and the glycogen-targeting subunits G_M and G_L of PP1. Thereafter, it was found to mediate the interaction with a number of PP1-targeting subunits, such as PNUTS/p99, NIPP1, I-1 and p53BP2 among others. In 2008, Novoyatleva et al. described the novel interaction between PP1 and the splicing factor transformer-2 beta-1 (Tra2-beta-1). This proved interesting as this interaction was mediated through the RVDF motif of Tra2-beta-1; furthermore, this motif was present in the beta-4 strand of the RNA-recognition motif (RRM) domain of the protein (Novoyatleva et al., 2008). The authors proposed a novel functional role of PP1 in alternative splicing events by PP1 binding to splicing factors such as Tra2-beta-1, SF2/ASF and SRp30c. Tra2-beta-1 is a serine arginine (SR)-like protein involved in regulating splice site selection on RNA substrates; it has an RRM domain flanked by an SR-rich domain on either side. Eight other SR proteins including SF2/ASF also have the RVDF motif in the beta-4 strand of their respective RRMs which may be used to bind PP1, suggesting a new role for RRMs as binding partners of PP1 (Novoyatleva et al., 2008).

Bioinformatical analysis of FPA, a protein being studied in the laboratory of Dr Gordon Simpson, showed that FPA also had an RVDF motif in its beta 4 strand of its third RRM domain. FPA is a Spen (Split-end) protein involved in flowering control and more recently shown to be involved in mediating polyadenylation events in *Arabidopsis* (Hornyik et al., 2010). Spen proteins were first identified in *Drosophila* where mutations of the protein led to lethal developmental defects in the embryo and they have now been implicated in cell-fate determination and transcriptional repression (Ariyoshi and Schwabe, 2003). A reciprocal *BLAST* search of FPA against the human database suggested two other Spen proteins, RBM15 and RBM15B, as the human homologues of FPA. Analyses of the sequences of these human proteins showed that they also have an RVDF motif within their respective RRM domains. We thus set out to verify whether these three Spen proteins, FPA, RBM15 and RBM15B, could be novel PP1 interacting proteins (**sections 3.2.4.1** and **3.2.4.2** respectively).

3.3.1 Is FPA a novel PP1-interacting protein in *Arabidopsis thaliana*?

Different pathways control the floral transition in plants including the autonomous pathway (AP), the photoperiod pathway (PP) and the gibberillic acid pathway (GA). Genes in the PP and GA pathways act mainly by promoting the upregulation of the floral meristem idendity (FMI) genes. FPA is a gene in the autonomous pathway which affects flowering independent of day-length (Lorkovic and Barta, 2002). FPA has been shown to control the expression of Flowering Locus C (FLC); FLC in turn regulated FMI genes. The FMI in turn controls the switch from the vegetative state to the reproductive state in a plant (Simpson et al., 1999). *fpa* mutants exhibit late-flowering phenotypes due to mis-regulation of FLC, whereas double mutant *fpa flc* plants flowered as early as single *flc*-3 mutants, which indicates that a functional FLC gene is required to repress flowering (Veley and Michaels, 2008). While FLC is not very conserved, FPA is highly conserved amongst plant species, suggesting that FPA plays a significant role in plants other than just controlling flower development, consistent with its expression in other plant tissues (Schomburg et al., 2010). FPA also has the highest expression in young and actively growing tissues (Schomburg et al., 2001). Subsequently, FPA has been implicated in RNA-mediated chromatin silencing (Baurle et al. 2007) and reported to regulate 3'end formation through alternative polyadenylation (Hornyik et al., 2010). The initial studies on FPA localisation using the GUS promoter fused to the FPA gene showed that this protein was expressed throughout the life cycle of the plant, with the highest expression being in young developing tissues. This indicated that expression of FPA is not triggered or restricted by floral induction but suggested that FPA may be involved in more fundamental aspects of plant development, hence its high expression in developing tissues. Characteristic of the SPEN family, FPA has three RNA-Recognition motifs (RRMs) in the N-terminal region, which are involved in RNA-binding, and a SPEN Paralogue and Orthologue C-terminal (SPOC) domain (**Figure 3.12**), which is used for protein-protein interactions (Schomburg et al., 2001). FPA has the RVDF motif in its third RRM; the RVDF motif has been found in most regulatory subunits of PP1. We therefore set out to investigate whether FPA interacts with PP1 through its RVDF motif.

Working with *Arabidopsis* confers many advantages, but one of the many limitations of this model organism is its tiny size, which restricts the amount of starting material for any experiment. To circumvent this, we decided to use

cauliflower as a source material to work with FPA for this purpose. *Arabidopsis* and cauliflower are closely related to each other in the Brassicacae (mustard plants). The endogenous levels of FPA in *Arabidopsis* (Col-0) are relatively low as can be seen by the Western blot detection (**Figure 3.13**). The *fpa-7* mutant does not show any signal as expected, indicating that the antibody is highly specific to the protein. Moreover, the results showed that the purified FPA antibody is able to recognise the FPA protein expressed in cauliflower (**Figure 3.14**) and can hence be used to detect this protein during its purification from cauliflower. Total cell extract from cauliflower inflorescence was used as a starting material to extract FPA-interacting partners. The cauliflower extracts were subjected to the microcystin-Sepharose affinity chromatography, to enrich for protein phosphatases, including PP1 (**section 1.3.3**). We used the synthetic peptides described by Moorhead et al. (2009) to specifically elute PP1-binding proteins displaying the RVXF motif. The anti-FPA antibody was used to track the FPA protein through the procedure; anti-TOPP1 antibody was also used to blot for the PP1 protein (the plant PP1 catalytic subunits are named TOPPs for Type One Protein Phosphatases). Although FPA could be tracked through all steps prior to the elution, there was relatively less FPA in these fractions, which were loaded onto the microcystin column, compared to a parallel preparation that started with a urea extraction (**Figure 3.14**). The results indicate that the FPA did not solubilise properly under the extraction conditions used in this procedure. Lanes 1-6 are the sequential samples during the homogenisation steps: lane 1 has the whole tissue extract, lane 2 is the first pellet after filtering the homogenate through miracloth, lane 3 is the corresponding supernatant (SP), lane 4 is the supernatant after the centrifugation of the supernatant from lane 3, lane 5 is the corresponding pellet, lane 6 is the supernatant after filtering the supernatant from lane 4 through miracloth. Lane 7 is the fraction that was incubated with microcystin-Sepharose and lane 8 is the flow through, which runs through the column after this incubation but prior to any washing. The washes of the column after step 8 did not show any bands except in lane 9. Lane 9, on the other hand, is the sample collected at the washes after the peptide elution steps. The samples after elution with the peptides did not appear to have any FPA on the blot either (data not shown). The sample in lane 9 was the last step where the FPA protein was detected, suggesting that a small fraction of FPA might have been on the column and was eluted by the peptide washes. In contrast, TOPP1 was detected only in lane 5 (lower band ~35

kDa) and lane 8 (upper band ~37 kDa). This meant that the protein in the 35 kDa band was not in the soluble fraction and was pelleted during the centrifugation step. The ~37 kDa forms of TOPP1 though, were detected up to lane 8, which is the eluate after incubation with the microcystin-Sepharose beads. This suggests that the TOPP1 isoform of 37 kDa did not bind to the microcystin-Sepharose beads as expected. Neither protein was detected in the subsequent steps whereby the proteins were displaced by the synthetic peptide until the wash following peptide elution. The FPA and TOPP1 proteins were not detected in the control column either, suggesting that most of the proteins could have been degraded during the process and this might explain why there was no indication of the proteins on either column following the incubation with microcystin-Sepharose beads. However, FPA was readily detected in urea extracts of cauliflower, showing that the protein was present in this tissue. However, urea cannot be used in experiments that aim to maintain protein:protein interactions. These results suggest that FPA was not solubilised properly under the native extraction conditions used, and for this technical reason it was not possible to determine whether or not the protein could be co-immunoprecipitated with PP1.

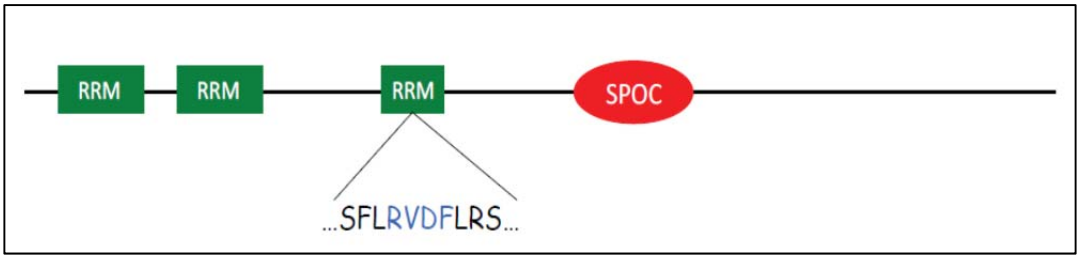

Figure 3.13: Structural representation of the protein FPA
FPA is a Spen protein containing three RNA-recognition motifs (RRM) and a Spen Paralogue and Orthologue C-terminal (SPOC) domain. FPA also has an RVDF motif in its third RRM domain.

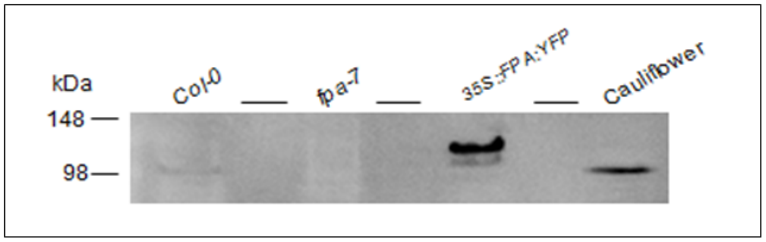

Figure 3.14: Detection of FPA protein in *Arabidopsis* and cauliflower using the anti-FPA antibody
A wild type plant (Col-0), a *fpa*-7 mutant, a plant over-expressing *FPA* tagged to the YFP protein (35S::FPA:YFP) and cauliflower.

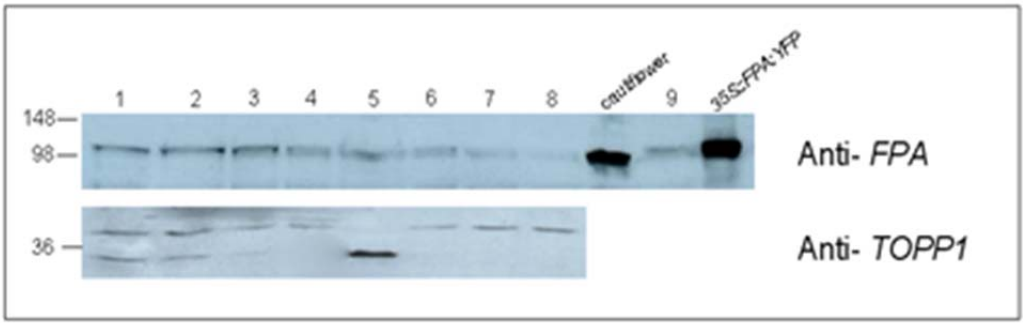

Figure 3.15: **Purification of FPA and TOPP1 from cauliflower extract**
Lanes 1-9 show the different steps during the purification. The lane labelled 'cauliflower' represents a urea extract of cauliflower and 35S::FPA:YFP is the over-expressed FPA protein from *Arabidopsis* protein: both were loaded as positive controls. These samples represent the steps where a positive signal was observed for the respective proteins blotted for. The same lysates for each step were used to blot for the FPA and TOPP1 proteins using anti-FPA and anti-TOPP1 respectively. Lanes 1-6 are samples taken during the homogenisation steps; lane 7 is the sample prior to loading onto the microcystin-Sepharose beads; lane 8 is the eluate after incubation with microcystin-Sepharose beads; lane 9 is the sample after the peptide elution from microcystin-Sepharose beads.

3.3.2 Do RBM15 and RBM15B interact with PP1 via their RVDF motifs?

RBM15 (RNA-binding protein motif 15, also known as OTT1-One twenty two protein 1), and RBM15B (RNA-binding protein motif 15B also known as OTT3-One twenty two protein 3) are Spen (Split End) proteins, which have been widely implicated in development (Mercher et al., 2001; Ariyoshi and Schwabe, 2003). RBM15 was initially characterised as the genetic aberration involved in infant acute megakaryocytic leukaemia, where it was described as being possibly involved in chromatin modulation through its translocation fusion to the Megakaryocytic Acute Leukemia (MAL) gene (Li et al., 2001; Mercher et al., 2001). Both RBM15 and RBM15B have three RRM domains and a SPOC (Spen Paralogue and Orthologue C-terminal domain) (**Figure 3.15**). RBM15 and RBM15B interestingly have this consensus RVDF motif in their RRM domains. Given the structural relationship between FPA, RBM15 and RBM15B we were interested to know whether RBM15 and RBM15B are able to bind to PP1 through this motif. For simplicity, only the RBM15 results will be shown and discussed here; both RBM15 and RBM15B gave similar results in these experiments. To test the potential RBM15-PP1 interaction, we used HEK293 cells transiently and stably expressing GFP-tagged RBM15. In both cases, the cells were lysed, GFP proteins immunoprecipitated using the GFP-Trap beads, separated on SDS-polyacrylamide gels, digested with trypsin and the peptides analysed by mass spectrometry.

Analysis of the mass spectrometry data from the peptides showed that RBM15 was successfully expressed and purified from the cells as the major band on the gel (**Figure 3.16**). Moreover, NXF1 was also pulled down in this experiment, albeit with a low Mascot score. NXF1 is a nuclear export factor protein reported in a study of the NXF1 export pathway to interact with RBM15 to promote RTE-containing retrotransposon mRNA transcripts out of the nucleus (Lindtner et al., 2006). On the other hand, PP1 was co-immunoprecipitated with a very low Mascot score, and not any more enriched than in the GFP control where it was also identified as a low-scoring protein. This suggests that trace amounts of PP1 were being isolated via the GFP-tag in the GFP-RBM15 expressing cells. However, reciprocal GFP-PP1 pull-down experiments did not identify RBM15 as a PP1 interactor (**Appendices II and III**). Interestingly, the protein identified by Novoyatleva et al (2008), Tra2-beta-1 was identified in the PP1-GFP

immunoprecipitates (**Figure 3.17)**. These experiments suggest that PP1 and RBM15 (RBM15B) do not interact with each other, at least under the experimental conditions used here. Nonetheless, it could be possible that RBM15 and PP1 interact transiently and/or under different conditions, which have not been explored in this thesis.

Figure 3.16: Structural representation of RBM15 and RBM15B
RBM15 and RBM15B are members of the Spen family of proteins in humans. Both RBM15 and RBM15B have three RRM domains and a SPOC domain, characteristic of Spen proteins. RBM15 has the RVDF motif in its third RRM domain, while RBM15B has the RVDF motif in its second RRM domain.

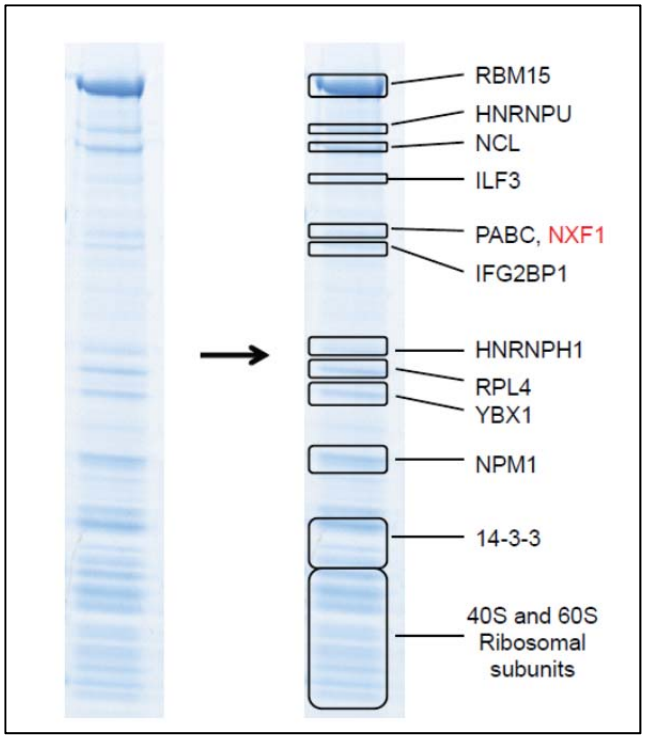

Figure 3.17: Coomassie-stained SDS polyacrylamide gel of GFP-RBM15 immunoprecipitated using GFP-Trap® from lysates of transfected HEK293 cells, and the identified proteins
Proteins were isolated from GFP-RBM15-expressing HEK293 cells using the GFP-Trap technology to identify the protein interacting partners of RBM15. RBM15 was identified as the major protein band on the gel, as were a number of RNA-binding proteins. A known interactor of RBM15, namely NXF1, was also identified.

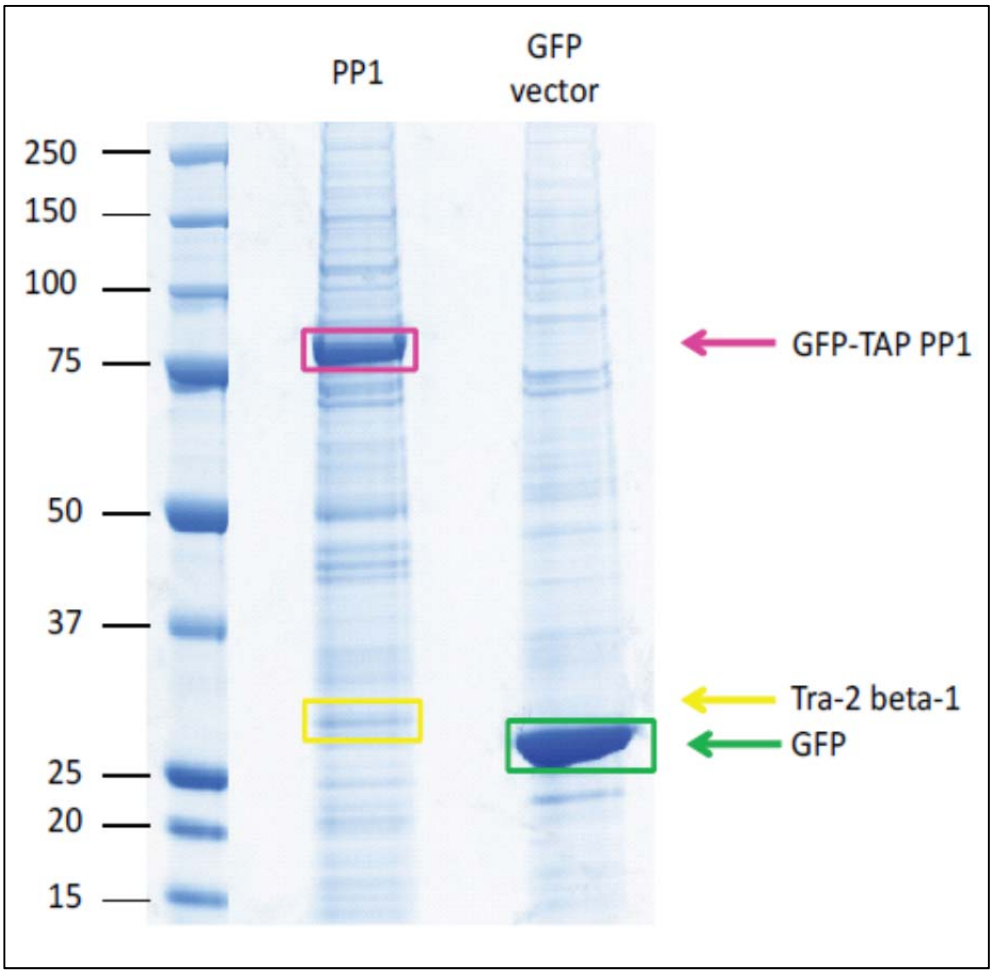

Figure 3.18: Coomassie-stained SDS polyacrylamide gel of GFP-PP1
Proteins were isolated from HEK293 cells stably expressing GFP-PP1 using the GFP-Trap® technology and run on an SDS-PAGE gel. Peptides were extracted from the gel by trypsin digestion and identified using mass spectrometry to identify the protein interacting partners of PP1. Tra-2 beta-1 was identified as a PP1-interactor but not RBM15.

3.3 Discussion

For many years, the importance of protein phosphatases has been highlighted for their roles in regulating cellular events, including DNA synthesis, mitosis, cell cycle control, glycogen metabolism, muscle contraction and regulation of RNA splicing. Regulation of protein phosphatases is thus critical to maintain the balance in the cellular processes controlled by these enzymes. Most of the protein phosphatases are controlled through interactions with their regulatory subunits, which either target them to their substrates and/or different cellular localisations, or inhibit their activities. The usage of naturally-occurring toxins such as microcystin and okadaic acid for the study of protein phosphatases has proven beneficial as it helped identify their regulatory subunits. As described in **section 3.1.1**, modifying microcystin-LR and coupling it to Sepharose beads has been successfully employed to study protein phosphatases at endogenous levels. Most of the knowledge about the acute regulation of serine/threonine protein phosphatases involves regulation through the cAMP-dependent protein kinase. Using forskolin as a cAMP-elevating agent (**section 3.1.2**), we tried to identify novel targets of protein phosphatases that might be PKA-regulated. The dimethyl labelling approach (Boersema et al., 2008) allows the quantification of peptides; although around 99% of the peptides are labelled, the quantification values only provide an indication on the enrichment ratios of the different peptides, and are not absolute values. For instance, the treatment with forskolin on the lysates in **section 3.2** shows no enrichment when compared to the lysates pre-treated with H-89 prior to the addition of forskolin (**Figure 3.3**). No proteins were found to have a high enrichment ratio, which does not necessarily indicate that none of these proteins are actually PKA-regulated, since these values mostly represent enrichment fractions, and not absolute expression values. Other labelling methods such as SILAC (stable isotope labelling by amino acids in cell culture) have been shown to more accurately represent expression values of proteins through their quantitative analysis. The dimethyl labelling method used here was a cheaper and easier alternative to SILAC, and nonetheless provided a good indication on the differential enrichment of PP-interacting proteins. Furthermore, if more positive results had been obtained with the plant studies, the differential dimethyl labelling procedures could have been useful for determining how interactions of the plant protein(s) with PP1 are regulated under different

conditions. SILAC is not possible with plants, though it is being adapted for work with plant cell cultures (Gruhler et al., 2005; Schütz et al., 2011).

The catalytic and regulatory subunits of several PPs (**section 3.1.3**) were successfully identified, adding confidence to the microcystin-Sepharose methodology. A similar approach was undertaken to identify regulatory subunits that bound PP1β upon forskolin treatment (**section 3.1.4**). Regulatory subunits of PP1 were identified in this screen and these comprised the highest scoring peptides during the mass spectrometry identifications. Interestingly, a subset of proteins was seen to be enriched in the cells treated with H-89 and forskolin. These differentially enriched proteins, namely R6, glycogenin and glycogen synthase, are all involved in glycogen metabolism. Forskolin acts as a cAMP-agonist to activate PKA; elevated cAMP levels are usually associated with glycogen breakdown in skeletal muscle cells. Although H-89 has been shown to antagonise the action of forskolin, it is nonetheless a non-specific PKA inhibitor. It might be possible that treatment with H-89 and forskolin in these cells result in additional inhibition/activation of undefined targets, which are in turn responsible for the enrichment of these regulatory proteins of glycogen metabolism. Further experiments are needed to define the roles of these proteins in cells treated with H-89 and forskolin.

Protein phosphatase 1 is one of the most conserved eukaryotic proteins. In humans, there are three catalytic subunits of PP1 expressed from three genes: alpha, beta/delta and gamma. The beta and delta isoforms are alternative splicing products of the same PP1 gene. The three PP1 isoforms are more than 89% identical in amino acid sequence and only vary at their carboxy and amino-terminals (Barker et al., 1994; Andreassen et al., 1998; Trinkle-Mulcahy et al., 2001). The catalytic residues of the PP1 isoforms share at least 97% homology and have been shown to perform similar activities *in vitro* (Zhang et al., 1997). The regulatory subunits have mostly been defined by the RVXF motif, which mediates binding to PP1. Most of the regulatory subunits of PP1 are known to bind non-specifically to all three isoforms, which is expected with such a high degree of identity. Additional interactions with the terminal domains of the different PP1 isoforms provide specificity in terms of isoform preference. For example, MYPT1 has been shown to bind preferentially to the C-terminus of the beta isoform through its eight ankyrin repeats (Terrak et al., 2004). **Section 3.2** describes how ectopic expression of the three forms of PP1 was used to identify proteins that display differential enrichments in terms of their

binding to each isoform, as a potential measure of isoform preference. These data provide an indication on the preference of the different regulatory subunits of PP1 for the different isoforms. However, we found no evidence to suggest a specific preference of a particular PP1 isoform for any given protein. Most of the evidence of isoform preference for PP1 isoforms stem from their differential cellular localisations, which indicate binding to proteins found in those particular organelles. However, Trinkle-Mulcahy and colleagues (1999) showed how overexpression of targeting subunits leads to the re-distribution of PP1 isoforms in the cell (Trinkle-Mulcahy et al., 1999). Since most of the reports on isoform preference could possibly be biased in terms of PP1-interacting protein overexpression, it is likely that the isoform preference observed in these conditions are simply reflective of an artefact generated through the overexpression of a particular protein in the cell. Nonetheless, a handful of proteins could very well bind specifically to one particular isoform, especially if the interaction between PP1 and its subunit occurs at the C- or N-terminal of PP1. For instance, the binding of MYPT1 to PP1 has been well-characterised and shows how the interaction of MYPT1, through its eight tandem ankyrin repeat domains, occurs with the C-terminal domain of PP1β (Terrak et al., 2004). Although isoform preference is possible, it is most likely restricted to only a handful of PP1-interacting proteins. Consequently, it is becoming increasingly clear that the RVXF motif which was long thought to be the major mediator of PP1-interaction with its subunits is not the only PP1-binding motif. Two novel motifs mediating PP1-binding were recently reported: the SILK and MyPhoNE motifs (Hendrickx et al., 2009; Roy and Cyert, 2009). A motif-based bioinformatics analysis of the different proteins identified in this screen showed that 15 proteins, including previously reported PP1-interactors, NUP153 and RMP, as having the SILK motif while 4 proteins including MYPT1 and MBS85 had the MyPhoNE motif (Alessi et al., 1992; Tan et al., 2002; Trinkle-Mulcahy et al., 2006; Djouder et al., 2007; Zagorska et al., 2010; Theurillat et al., 2011). Further biochemical and mutational analyses are required to verify whether these motifs are required to mediate PP1 binding and modulate the actions of PP1.

A report suggested binding of PP1 to the RRM domains of splicing factors such as tra-2 beta and ASF/SF2 as a novel function of the PP1 in splicing-mediated events (Novoyatleva et al., 2008). Tra-2 beta was found to have the RVDF motif in the fourth beta sheet of its RRM domain, only one of eight such human proteins

(Novoyatleva et al., 2008). The Spen proteins FPA, RBM15 and RBM15B were also found to have the RVDF motifs in their RRM domains. As described in **section 3.3.1**, the extraction conditions of FPA were not optimal to test a potential PP1-FPA interaction. In **section 3.3.2**, it was shown that PP1 did not bind to the human Spen proteins RBM15 and RBM15B, at least not under the experimental conditions used. Although the RVXF motif is present in most PP1-interacting proteins, this motif is also present in about a quarter of all eukaryotic proteins (Ceulemans and Bollen, 2006). Only a small proportion of these are actual PP1-interacting proteins, suggesting that the presence of an RVXF motif by itself is not sufficient to classify a protein as a putative PP1 interactor, as demonstrated by FPA and RBM15. More recently, the RVXF motif has been suggested to act more as a 'specifying' sequence that mediates PP1 interaction with other motifs and/or promoting secondary interactions (Bollen, 2001; Hurley et al., 2007; Carmody et al., 2008). In other words, the RVXF motif brings PP1 and its interactor in close enough proximity to enable other interactions to occur via different motifs, e.g. the [S/G]IL[K/L] motif. The occurrence of the RVXF motif in such a high number of proteins in the genome suggests that there should be additional regulatory mechanisms that would mediate binding of RVXF-containing proteins with PP1. The studies here suggest that many more PP1-interactors exist than previously thought. As more sensitive techniques become available, it would become easier to fully understand the plethora of PP1-binding proteins.

Chapter four

Regulation of the 14-3-3-phosphoproteome upon activation of the cAMP—PKA signalling pathway

4.1 Introduction

Many phosphorylated proteins bind to the family of phosphoprotein-binding proteins, 14-3-3s. 14-3-3s are dimers that engage with a pair of tandem phosphorylated sites within disordered regions and/or that straddle a functional domain (Johnson et al., 2010). Binding of a 14-3-3 dimer can force a conformational change in a target, or can mask a binding site, for example a DNA-binding domain or nuclear localisation sequence. In these ways, 14-3-3s can change the activity, localisation and interactions of target proteins (Aitken, 2006).

The two consensus motifs of 14-3-3-binding sites overlap with the specificities of basophilic protein kinases in the CAMK and AGC families (**section 1.2.2**), including PIMs, PKA, PKCs, PKB, p90RSK and AMPK (Johnson et al., 2010). Our group has therefore exploited the specificity of 14-3-3s to identify many new downstream targets of the PI 3-kinase–PKB, (PKC)–Erk–p90RSK and AMPK pathways. PI 3-kinase–PKB and (PKC)–Erk–p90RSK are activated by insulin and growth factors, while AMPK is activated in cellular responses to energy stress. Defining the substrates of these pathways, and the interplay between them, is particularly important because PI 3-kinase–PKB and PKC–Erk–p90RSK are deregulated in diabetes and cancers, while activating AMPK by exercise and drugs seems to have beneficial effects in these diseases. The cAMP–PKA signalling has on the other hand been implicated in HIV-associated immunosuppression, lupus erythemathosus, neurological disorders, asthma and airway diseases (Kammer et al., 1994; Aandahl et al., 1998; Billington and Hall, 2012). Our group has noticed that several proteins that were first identified for the binding to 14-3-3s in response to insulin also have their binding to 14-3-3 stimulated by the adenylate cyclase activator forskolin (unpublished). Based on this background, it would be useful and interesting to more fully define the sets of proteins that bind to 14-3-3 when intracellular cAMP levels are elevated, and compare them with existing data on the sets of proteins that bind to 14-3-3s when the PI 3-kinase–PKB pathway is activated. We therefore set out to identify those proteins that are uniquely targeted for 14-3-3 binding by the cAMP–PKA pathway, and also proteins that bind to 14-3-3s in response to both pathways.

The approach we took was 14-3-3 affinity purification of proteins from lysates of cells. Peptides from the captured proteins were then modified using the dimethyl isotope labelling method developed by Hsu et al (2003) and Boersema and

colleagues (2008). The labelling with this approach introduces a dimethyl group onto lysine residues on parallel sets of peptides, but with a 4 Dalton difference between samples due to different amounts of deuterium and C13 in the chemicals (light: +0 Da, intermediate: +4 Da; heavy: +8 Da); these modifications provide an indication as to the abundance of the different peptides in each preparation (**Figure 1.9**). This method was used successfully in the MacKintosh laboratory to identify novel targets of the insulin–PI 3-kinase–PKB signalling pathway in cultured human cells (Dubois et al., 2009). Since then, a number of such screens have been performed in the group in studies of the PI 3-kinase–PKB signalling pathways and ERK–p90RSK signalling pathways (**section 1.4.3**). Each round of high-throughput mass spectrometry was followed by biochemical validation experiments that were then used to build up a core list of 'gold standards' to feed into further experiments.

The sequencing of the amphioxus genome has helped considerably towards our understanding of 14-3-3 biology in humans and other vertebrate animals. Over 500 million years ago, the vertebrate genome arose from two rounds of whole genome duplications (2R-WGD). While most of the resulting protein duplicates (termed 2R-ohnologues) were lost before the modern-day vertebrate species evolve, several hundred 2R-ohnologue protein families have been retained (Huminiecki et al., 2010; Makino et al., 2010) and these have been discovered to be highly enriched in 14-3-3-binding proteins (Tinti et al., 2012). In contrast, amphioxus is the basal-most chordate, and is an invertebrate. Sequencing of the amphioxus genome has shown that its ancestors did not go through the 2R-WGD, which means that the amphioxus has one 'ancestral' protein for every human 2R-ohnologue family (Putnam et al., 2008; Tinti et al., 2012). Amphioxus is therefore a useful 'proxy' for our pre-2R-WGD ancestor.

As described in **Chapter 1**, forskolin is a cAMP-elevating agent, which hence activates protein kinase A (PKA). The major PKA consensus is R-R-X-pS (see **section 1.2.3.1**) and this sequence overlaps with the optimal consensus sequences for 14-3-3 binding, which are mode I R-X-X-pS/pT-X-P and mode II R-X-X-X-pS/pT-X-P. To identify PKA-regulated 14-3-3-binding proteins more systematically, we used 14-3-3 affinity capture and release to isolate proteins from lysates of cells stimulated with forskolin, in the absence or presence of the non-specific PKA-inhibitor H-89. Competition with a synthetic peptide (ARAApSAPA) was used to eluate those proteins that had been captured specifically within the

central binding groove of the immobilised 14-3-3s. Half of each eluate was used to measure quantitative differences by differential isotope dimethyl labelling of tryptic digests and mass spectrometry (Boersema et al., 2008) while the rest was used for phosphopeptide enrichment and identification. The results, and further developments, are given in the following sections.

4.2 Results

Large 14-3-3-phosphoproteomics screens are becoming increasingly valuable in uncovering the roles of these versatile signalling proteins; such screens provide a wealth of information on the different possible protein partners of 14-3-3s. However, no one screen is exhaustive since the mass spectrometric analyses of the proteins captured in each round of purification are stochastic, resulting in a 'patchy' picture of incomplete datasets for each round of analyses. Hence, more-and-more proteins are routinely uncovered in further rounds of purification, and improvements also come from newer and more sensitive mass spectrometry techniques being employed. Here, we used 14-3-3-affinity chromatography to identify those proteins that bind to the 14-3-3 proteins when the cAMP–PKA signalling pathway is activated. Cells were serum starved for 10 h to return the activation status of various signalling pathways to basal levels, and used as the baseline to obtain enrichment values for the following treatment conditions. The second condition used forskolin as the cAMP-elevatgent, while the non-specific PKA inhibitor H-89 was used in combination with forskolin as the third treatment. Cells were lysed and loaded onto 14-3-3-affinity Sepharose columns; 14-3-3-binding proteins were eluted from the columns by competitive elution using the ARAApSAPA synthetic peptide. The proteins in the eluate were pre-fractionated by running an SDS-polyacrylamide gel in order to reduce the complexity in each of the protein mixtures used for subsequent analyses (**Figure 4.1**). Cell lysates were also immunoblotted for the phosphorylation of the PKA substrate VASP (vasodilator-stimulated phosphoprotein) at Ser157 as a control for the efficacy of the forskolin and H-89 (**Figure 4.2**). The protein bands in the three treatment lanes were excised as labelled on **Figure 4.1**, reduced, alkylated and digested with trypsin. Half of the resulting peptides were labelled using the dimethyl labelling approach as described previously in **Chapter 1** (**Figure 1.9**) and **section 4.1** (Boersema et al., 2008). The other half set of peptides was used to enrich in phosphopeptides. Around 300 proteins were identified in the screen (**Appendix IV**), with several of these being 'gold standards' seen in previous 14-3-3-affinity capture experiments (**Figure 4.3**). These 'gold standards' are proteins which have been characterised as genuine 14-3-3-binding proteins and for which 14-3-3-binding phosphosites have been identified through biochemical experiments (173 gold standards sofar) (Johnson et al., 2011). I then used commercially-available antibodies to follow the purification of a few proteins that were identified in this

screen as potential 14-3-3-binding proteins (**Figure 4.4**). I chose to further test the three members of the DENND4 family of proteins (**section 4.2.1**), EML3 (**section 4.2.2**) and ATG9a (**section 4.2.3**) as potential 14-3-3-binding candidates.

As the first step towards pinpointing 14-3-3-binding sites for the 14-3-3-captured proteins, the unused half of the tryptic digests for the forskolin-treated samples generated from the preparations in **Figure 4.1** were used to enrich for phosphopeptides. Columns made with C-8-Empore extraction disks and titanium dioxide beads were pre-washed with acetonitrile (ACN) and equilibrated in 0.2% trifluoroacetic acid (TFA). The tryptic peptides were adjusted to 70% ACN/ 3% TFA/ 250 mM lactic acid and loaded onto the columns. Three sequential washes were performed with 70% ACN/ 3% TFA/ 250 mM lactic acid, 70% ACN/ 3% TFA and 0.1% TFA respectively to remove unbound peptides and other contaminants. Bound phosphopeptides were eluted with a base (1% ammonium hydroxide) into tubes containing 50% TFA (5% of the total volume) and loaded onto the Orbitrap for analysis. The results were exciting as a number of 14-3-3-phosphopeptides were enriched and identified in these preparations (**Appendix VI**), including 14-3-3-binding sites of AS160 (Ser 341), AKTS1 (Ser 183, Ser 246), KLC2 (Ser 582), NED4L (Ser 448), REEP3/4 (Ser 152), YAP1 (Ser 127) and ZNRF2 (Ser 19, Ser 82).

The other phosphosites identified were examined using bioinformatic analyses to search for further potential 14-3-3-binding sites:

Sequence alignments of human and amphioxus proteins indicate that at least some of the 14-3-3-binding sites in human 2R-ohnologues are conserved in amphioxus, and were therefore derived from the 14-3-3-binding sites in the pre-2R-WGD ancestor. We therefore carried out bioinfomatical comparisons of the phosphopeptide sequences which were identified experimentally, by matching them to the corresponding amphioxus protein sequences to predict the most likely 14-3-3-binding sites (**Appendix IV**). The data will be a useful resource for future validation experiments: For example, to test whether mutagenesis of the pinpointed residues causes proteins to lose their binding to 14-3-3s. Additionally, I have manually tried to assign potential binding phosphosites based on the known 14-3-3-binding consensus motifs mode I RSX(pS)XP and mode II RX(F/Y)X(pS)XP (**Appendix IV**).

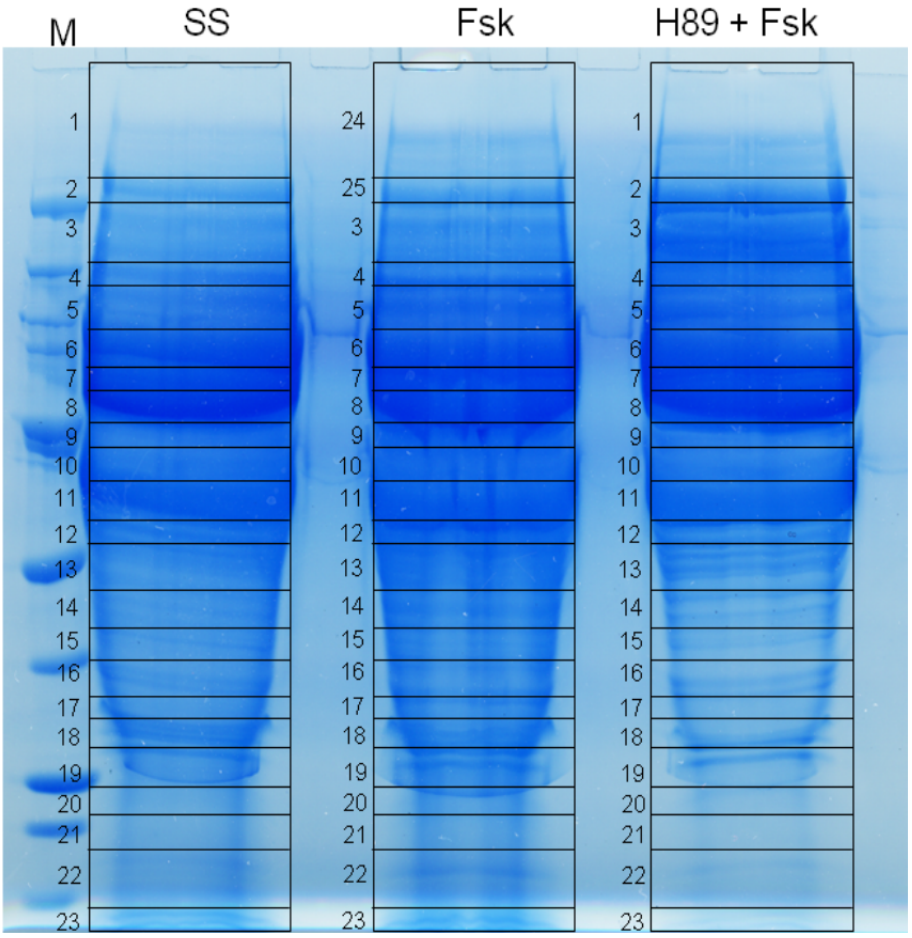

Figure 4.1: Coomassie-stained SDS-polyacrylamide gel of proteins that have been eluted from the 14-3-3-affinity Sepharose columns

HEK293 cells were serum starved for 8 h. Serum starved cells were kept in either serum free medium, treated with forskolin (20 μM) for 30 min, or pre-treated with H-89 (30 μM) for 30 min before the addition of forskolin. Proteins in cell lysates were captured on 14-3-3-Sepharose affinity columns and specifically-bound proteins were eluted by competition with the ARAApSAPA 14-3-3-binding phosphopeptide to displace the proteins that bind to 14-3-3. The column eluates (75% of each) were loaded onto each lane of an SDS-polyacrylamide gel, which was stained with colloidal Coomassie blue for protein visualization. The lines and numbers represent the sections that were cut for further processing by the methods outlined in section **2.2.15**.

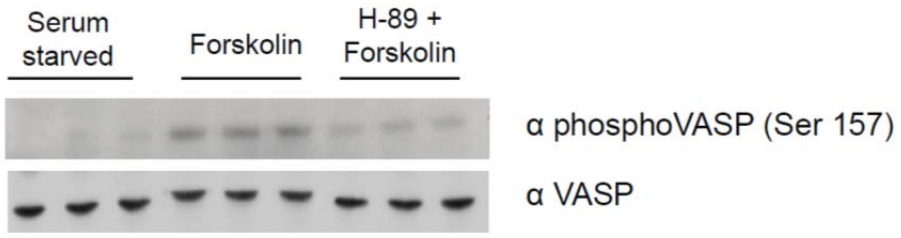

Figure 4.2: Western blots of phospho-Ser157-VASP and total VASP from the cell lysates used for the experiment in Figure 4.1
HEK293 cells were serum starved for 8 h. Serum starved cells were kept either in serum free medium, treated with forskolin (20 μM) for 30 min, or pre-treated with H-89 (30 μM) before adding forskolin (20 μM) for 30 min. Immunoblots were performed with 40 μg of cell lysates run on SDS-PAGE and Western blotted with anti-phosphoSer157-VASP and anti-VASP.

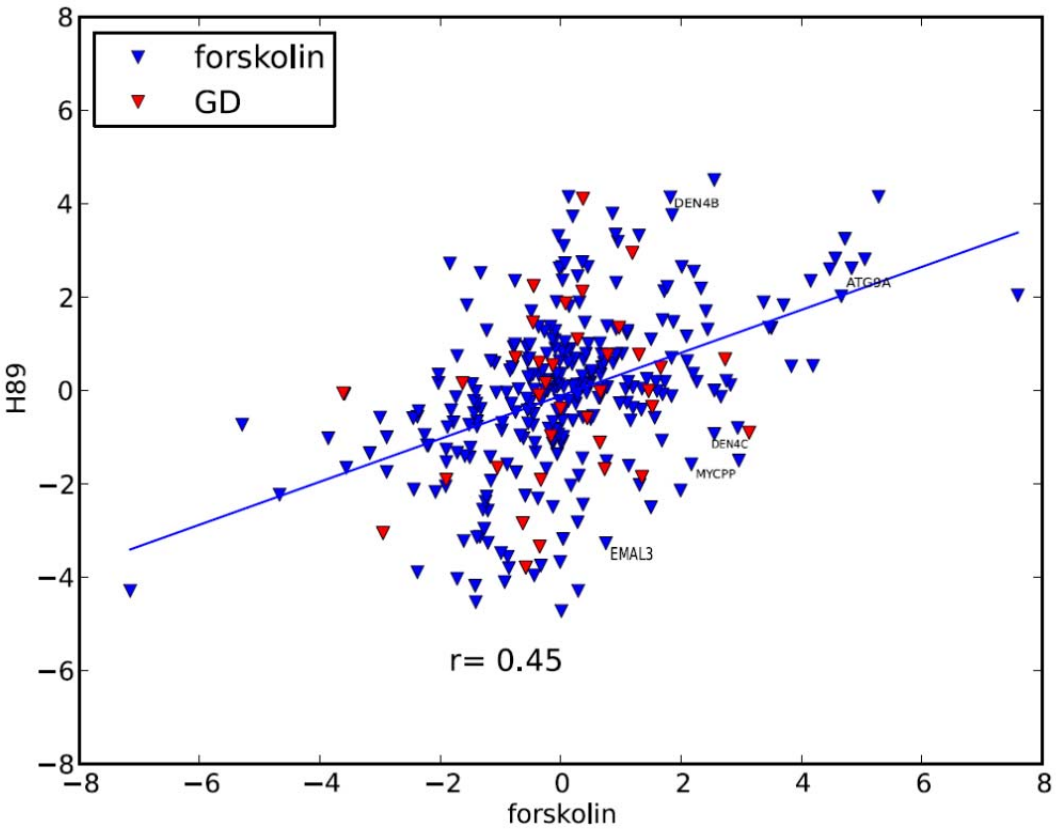

Figure 4.3: Proteins identified in the cAMP–PKA-activated 14-3-3-phosphoproteomic screen

The proteins which were isolated using 14-3-3-affinity chromatography from lysates of cells stimulated with forskolin in the presence or absence of H-89 are plotted on a scatter graph. All proteins were normalised to their counterparts in the serum-starved conditions to obtain a ratio of those proteins which were enriched in the treatment (in this case forskolin only or H-89 and forskolin) conditions. Proteins with at least two unique peptides were then selected from the list. All the proteins identified in this screen are represented by a triangle; red triangles represent those proteins that are also in the 'gold standard' list.

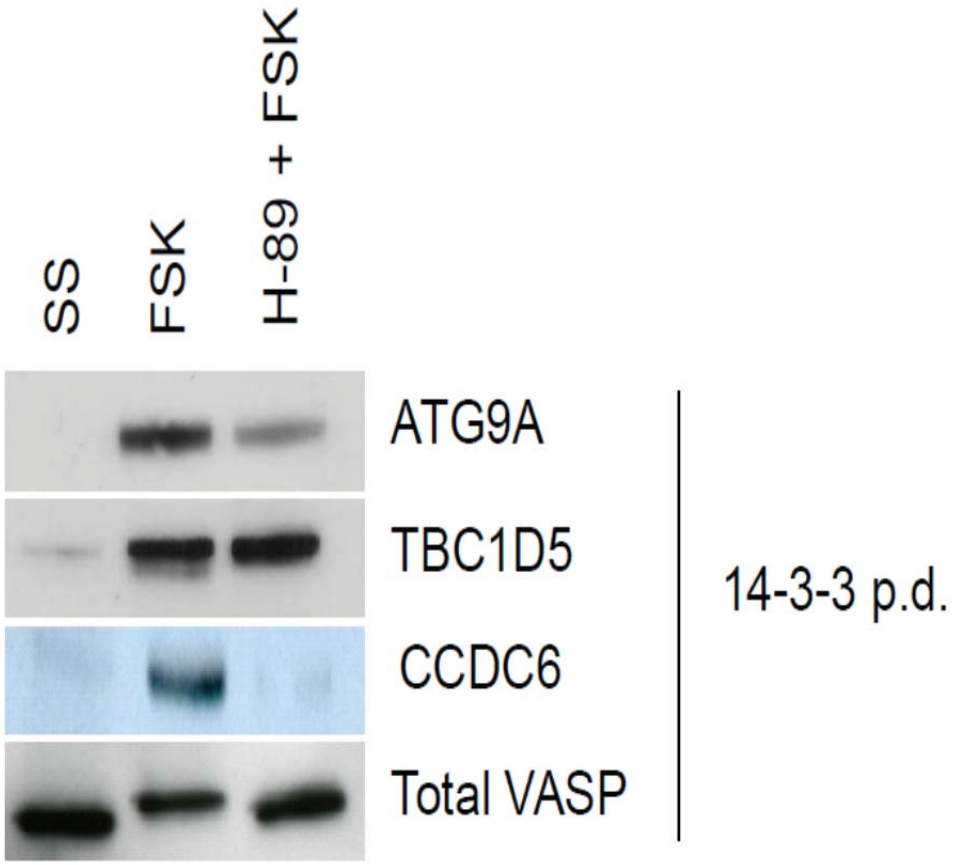

Figure 4.4: Western blots of proteins that have been eluted from the 14-3-3-Sepharose column
HEK293 cells were serum starved for 10 h. Serum starved cells were kept in serum free medium, treated with forskolin (20 µM) for 30 min, or pretreated with H-89 (30 µM) for 30 min before the addition of forskolin (20 µM). Proteins from the lysates (40 µg) were isolated by binding to 14-3-3-Sepharose (14-3-3 pulldowns (p.d.)). Western blots of the 14-3-3 pulldowns were performed using antibodies against the proteins indicated: ATG9A, TBC1D5, CCDC6 and VASP.

4.2.1 DENND4 proteins as 14-3-3-binding proteins

The DENND4 proteins DENND4A (also known as IRLB), DENND4B and DENND4C are members of the DENND (DENN domain) family of proteins. DENN-domain (Differentially Expressed in Normal and Neoplastic cells) containing proteins were first described as Rab GEFs (Guanine Exchange Factors) by the purification of Rab3 from bovine brain (Wada et al., 1997). DENND proteins are evolutionarily conserved and are found in most eukaryotes, including *Caenorhabditis elegans*, *Arabidopsis thaliana*, *Drosophila, Homo sapiens* and *Schizosaccharomyces pombe*. There are eight DENND families in humans encoded by eighteen genes (**Figure 4.5**); the families are grouped according to their sequence homology and domain organisation. These are DENND1A-1C, DENND2A-2D, DENND3, DENND4A-4C, DENND5A/5B, DENND6A/6B, MTMR5/13 and DENN/MADD (Marat et al., 2011). The DENN domain comprises a central DENN region flanked by an upstream (uDENN) and downstream (dDENN) DENN module; all of the DENND human proteins have the DENN domains at their amino terminal, with the exception of the DENND2 family, where the DENN region is at the carboxy end (Marat et al., 2011). Other than their DENN domain similarity, the DENND proteins do not share any common features. Although the DENND proteins were identified long ago and thought to be GEFs, their functional roles were not appreciated until recently. Seventeen of the DENND proteins were found to be specific GEFs for 10 Rab proteins (Yoshimura et al., 2010). Rab proteins are small GTPases, which cycle between a GDP-bound (inactive) and GTP-bound (active) state; active Rabs are involved in membrane trafficking (Marat et al., 2011). GEFs function by promoting GDP release and loading of GTP to the Rab protein thereby activating the Rabs (Pfeffer and Aivazian, 2004). On the other hand, GAPs (GTPase-activating proteins) promote GTP hydrolysis from the Rab proteins, thereby balancing the GDP-GTP cycle for the activation/inactivation of Rabs. Understanding the biological implications of DENND proteins are likely to provide insights into vesicle trafficking pathways and related human diseases.

We came across DENND4 proteins during our 14-3-3-proteomics screen aimed at finding proteins which are highly enriched upon activation of the cAMP–PKA pathway. Interestingly, all three DENND4 proteins were identified during this screen and we wanted to understand how this DENND family might interact with 14-3-3s. DENND4 proteins comprise three members: DENND4A (also known as

IRLB), DENND4B and DENND4C. IRLB was the first DENND4 protein to be studied and it has been shown to interact with the ISRE in the promoter region of human Myc (Postel et al., 1996; Semova et al., 2003). However, although DENND4A and DENND4C each have a nuclear localisation signal, it remains unclear if they localise to the nucleus (Yoshimura et al., 2010; Marat et al., 2011). Additionally, DENND4 proteins have a MABP domain, which is thought to mediate membrane-specific interactions (de Souza and Aravind, 2010). DENND4 proteins have recently been shown to be involved in apical and basolateral sorting by interacting with Rab10 to control polarised trafficking (Yoshimura et al., 2010). Furthermore, DENND4C interaction with Rab10 has also been shown to promote GLUT4 trafficking by increasing GTP-binding to Rab10 in adipocytes (Sano et al., 2011). Interestingly, GLUT4 trafficking also involves another pair of 14-3-3-binding proteins, TBC1D1 and TBC1D4/AS160, which functions as Rab GTPase activating proteins (GAPs) for Rab10, and which have been the subject of a major project in our laboratory. Upon insulin stimulation, PKB has been shown to phosphorylate TBC1D4, which alleviates its Rab GAP activity on Rab10, thereby promoting GLUT4 translocation to the plasma membrane; this phosphorylated TBC1D4 is also sequestered by 14-3-3 proteins (Sakamoto and Holman, 2008; Chen et al., 2008 Sano et al., 2011). In contrast, one of the 14-3-3 binding sites for TBC1D1 is phosphorylated by non-insulin-activated kinases including AMPK. It is therefore inferred that TBC1D4 and TBC1D1 mediate GLUT4 trafficking, and hence glucose homeostasis, in response to different stimuli (Chen et al., 2011).

Since the full scale of 14-3-3 involvement in cellular trafficking is still at an early stage, it is exciting to find another family of protein, namely DENND4, involved in controlling GLUT4 trafficking being potentially able to interact with these adaptor-regulator 14-3-3s. Understanding the intricacies of these interactions might be potentially useful in controlling diabetes and other related diseases. We thus set out to understand more about the DENND4–14-3-3 interaction.

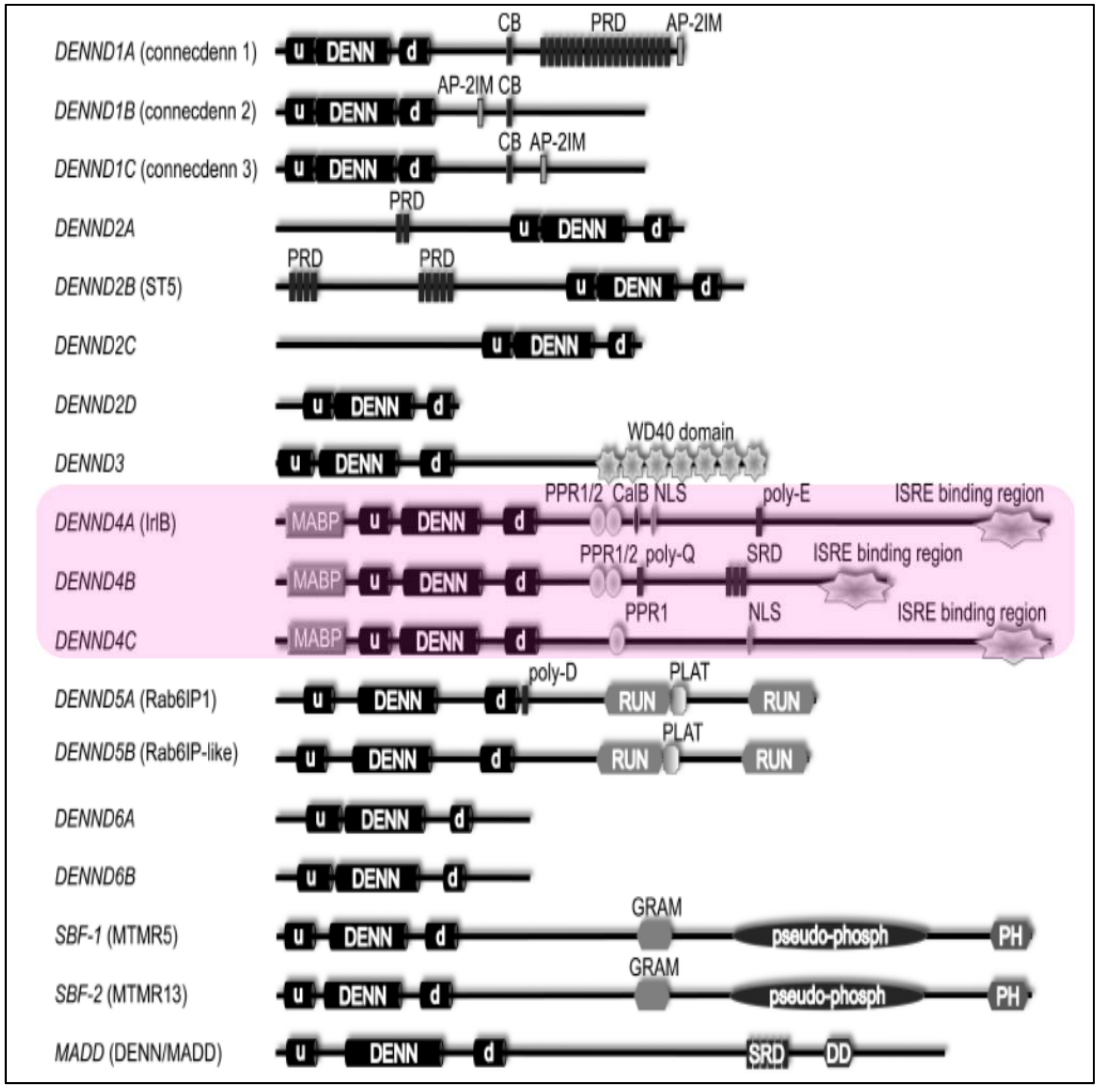

Figure 4.5: Representation of the domains in the DENND proteins found in humans.

The eighteen DENN domain proteins in the human genome, with the three DENND4 proteins highlighted in pink. The gene names are aligned on the left and the protein name (if different) are in parentheses. The different domains in these proteins are: u, uDENN module; d, dDENN; MABP, MVB12-associated β-prism; CB, clathrin-binding motif; SRD, serine-rich domain; PRD, proline-rich domain; NLS, nuclear localisation sequence; poly-E, polyglutamic acid domain; poly-Q, polyglutamine domain; poly-D, polyaspartic acid domain; CalB, calmodulin-binding domain; ISRE, interferon-stimulated response element; AP-2IM, AP-2 interaction motif; DD, death domain; PPR, pentatricopeptide repeat; PLAT, polycycstin-1/lipoxygenase/α-toxin domain; GRAM, glucosyltransferase/Rab-like GTPase activator/myotubularin domain; pseudo-phosph, pseudo-phosphatase domain (Source: Marat, Dokainish and McPherson, 2011).

4.2.1.1 DENND4 proteins share a high sequence similarity

DENND4 proteins share a high sequence homology with each other, which could explain in part the redundant functions they all exert on Rab10, both as the Rab GEF in GLUT4 trafficking and in the basolateral and apical sorting in polarised membrane trafficking (Yoshimura et al., 2010; Sano et al., 2011). Knocking down DENND4C did not completely abolish the Rab GEF on Rab10; similarly, cells with knockdown of DENND4A or DENND4B still showed RabGEF activity on Rab10, suggesting that the other DENND4 proteins are able to compensate for the silenced protein (Sano et al., 2011).

This family of proteins is potentially a member of the 2R-ohnologue families, where the different members of a protein family have evolved by the two rounds of whole genome duplication that occurred at the evolutionary origins of the vertebrates (Manning and Scheeff, 2010; Huminiecki and Heldin, 2010; Makino and McLysaght, 2010, Tinti et al., 2012). Accordingly, in humans, DENND4A and DENND4C share a higher sequence similarity with each other rather than with DENND4B suggesting that DENND4A and DENND4C might share a more recent common ancestor compared to DENND4B, as seen from the phylogenetic tree analysis (**Figure 4.6**). The uDENN, core DENN and dDENN domains of the three proteins are shown in **Figure 4.7**.

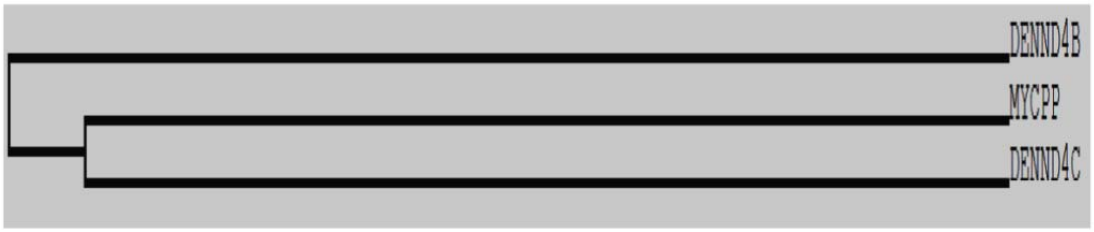

Figure 4.6: Phylogenetic tree analysis of the DENND4 proteins in humans.
The amino acids sequences of the three DENND4 proteins, namely DENND4A (MYCPP), DENND4B and DENND4C were retrieved from the UniProt database and aligned using the UniProt alignment tool, which also generated the phylogenetic tree (shown here) for these sequences.

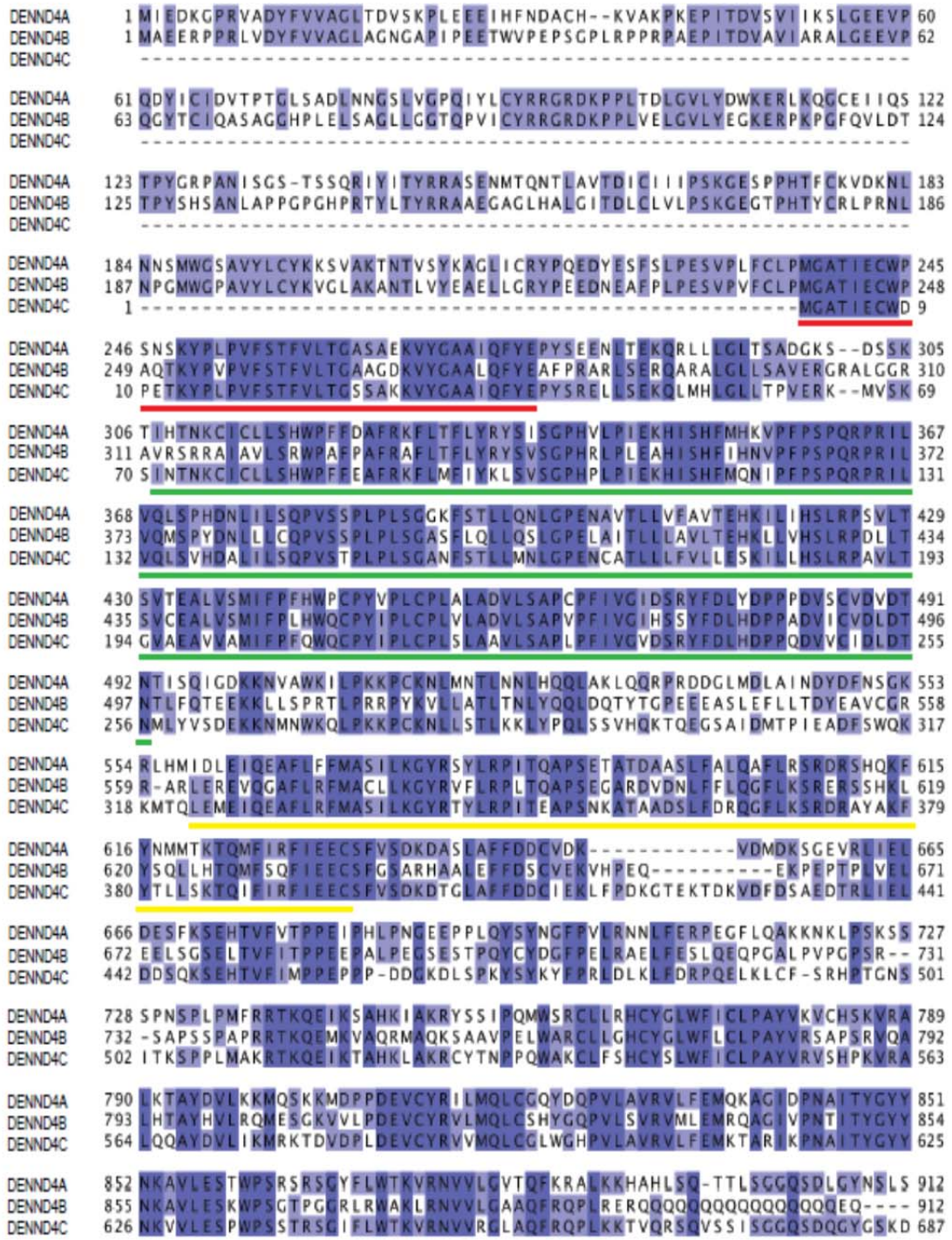

Figure 4.7: Alignment of the DENN domain of the three DENND4 proteins
The protein sequences of the DENN domains of DENND4A, DENND4B and DENND4C were retrieved from the UniProt database and aligned using JalView. The three underlined regions are the upper DENN (*red*), the core DENN (*green*) and the downstream DENN (*yellow*) domains respectively. The domains are underlined with respect to the domain numbering in DENND4C. The highly conserved residues are shaded in blue while the lesser-conserved residues among the three proteins are in lavender.

4.2.1.2 DENND4 family members bind 14-3-3 in a phosphorylation dependent manner

All three DENND4 family members were identified in the 14-3-3-phosphoproteomic screen (**Appendix V**); this was interesting as a previous insulin–PI 3-kinase screen in the lab had only identified DENND4A as a putative 14-3-3 binding protein (Dubois et al., 2009). Since most 14-3-3-binding proteins have been shown to bind in a phosphorylation-dependent manner, we tested the binding of the DENND4 proteins under different states of phosphorylation. The DENND4 proteins were expressed as GFP fusions, with the tag at the N-terminus. While full-length constructs were obtained for DENND4A and DENND4B, it was rather difficult to clone DENND4C in its entirety and the work describe hereafter has been performed with a construct expressing residues 1017-1673 of DENND4C. The GFP-tag allowed for a clean immunoprecipitation (pull down) using the GFP-Trap® agarose beads, which bind to GFP with a high capacity and high affinity. HEK293 cells were transiently transfected to express GFP-DENND4A, GFP-DENND4B, and GFP-DENND4C(1017-1673), and grown in DMEM containing 10% serum for 24 h before lysis. For each construct, three sets of pull-downs were done in parallel using 3 mg of cell lysates each; one pull-down per condition was used in the subsequent dephosphorylation assay. The lysates were pre-cleared with protein G-Sepharose and the supernatant incubated with the GFP-Trap® beads for 1 h. After washing, the immunoprecipitated proteins were incubated in the absence or presence of purified lambda phosphatase and its co-factor manganese chloride to dephosphorylate samples in vitro. A control reaction where lambda phosphatase activity had been inhibited by prior incubation of the manganese chloride with EDTA was also performed. Proteins were denatured and separated by SDS-PAGE, transferred to nitrocellulose and analysed by 14-3-3 Far Western overlay analysis. GFP-DENND4A, GFP-DENND4B and GFP-DENND4C immunoprecipitated from cells bound directly to 14-3-3s in the overlay, but binding was abolished in the sample dephosphorylated with lambda phosphatase, indicating that 14-3-3s can only interact with the phosphorylated DENND4 proteins (**Figure 4.8**).

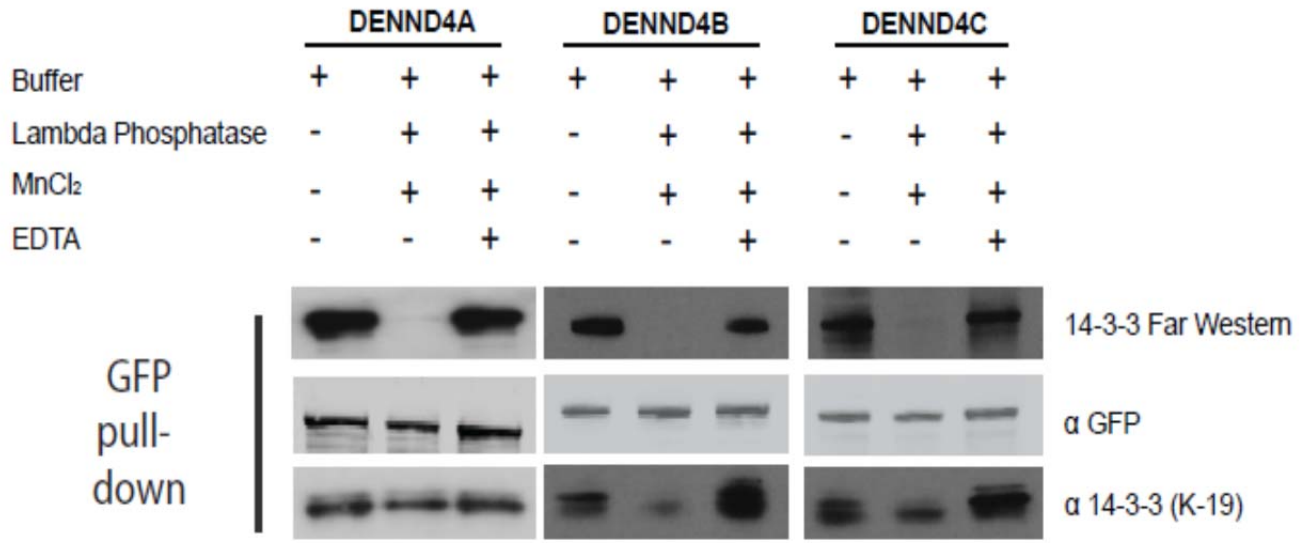

Figure 4.8: Phosphorylation-dependent binding of DENND4A, DENND4B and DENND4C to 14-3-3s

Plasmids to express the GFP-tagged DENND4A, DENND4B and DENND4C were transfected into HEK293 cells. After 20 h, cells were lysed and proteins were pulled down using the GFP-Trap® beads from 3 mg of clarified cell lysate. The immunoprecipitates were treated with buffer only or with 50 mU/ml lambda phosphatase in the presence of its cofactor manganese chloride for 30 min at 30°C as indicated. A negative control for the lambda phosphatase was done by chelating the manganese chloride to EDTA prior to incubation with the phosphatase. All immunoprecipitated proteins were separated by SDS-PAGE, transferred to nitrocellulose and probed for binding to 14-3-3s, with an anti-GFP immunoblot as loading control.

4.2.1.3 Generation of stable cell lines expressing the GFP-tagged DENND4 proteins

Perhaps because the DENND4 proteins are relatively large (ranging from 163 to 216 kDa), they were difficult to express at optimum level between replicate experiments using transient transfection methods. We therefore decided to generate stable cell lines expressing the GFP-tagged DENND4 proteins using the Flp-In TRex system. This system confers the advantage of expressing the tagged protein at close to endogenous levels under the control of a tetracycline inducible promoter.

4.2.1.4 GFP-DENND4A binds 14-3-3s mainly upon phorbol ester (PMA) stimulation, suggesting it could be phosphorylated by kinases in the PKC pathway

Most known 14-3-3-binding motifs have basic residues at the -3 to the -5 position relative to the phosphorylated site. Basophilic kinases of the AGC and CAMK families have been shown to prefer these consensus motifs and preferentially phosphorylate the majority of 14-3-3-binding proteins. To delineate which kinase and/or signalling pathway might be involved in phosphorylating these proteins, a panel of extracellular stimuli has been developed in the group. In this panel, various combinations of agonists and inhibitor are used in order to activate or inhibit certain pathways, which have been observed to be most involved in signalling to promote phosphorylations of proteins that consequently bind to 14-3-3. Cells transiently expressing GFP-DENND4A were serum starved for 6 h and treated as follows: IGF1 treatment leading to activation of the PI 3-kinase signalling cascade and PKB; IGF1 after prior inhibition with the PI 3-kinase and mTOR inhibitor PI-103; EGF to activate the classical MAPK/Erk cascade; phorbol ester (PMA) to activate the Erk cascade, the stress activated protein kinase p38 and some PKCs; PMA after prior inhibition of p90 RSK isoforms using BI-D1870; the adenylate cyclase activator forskolin; forskolin after prior inhibition of PKA using the nonspecific inhibitor H-89; the calcium ionophore A23187; A769662 as an activator of AMPK; and the protein phosphatase inhibitor calyculin A. The proteins from the lysates of cells exposed to these different treatments were pulled down using the GFP-Trap® agarose beads and analysed by the Far Western 14-3-3 overlay assay. The phorbol ester PMA appears to be the major agonist to phosphorylate DENND4A which leads to its binding with 14-3-3s; interestingly, the p90RSK inhibitor BI-D1870 seems to reduce the phosphorylation (**Figure 4.9**).

There is also slight binding of DENND4A to 14-3-3s in response to the growth factor EGF, the calcium ionophore A23187, as well as forskolin (most likely through PKA).

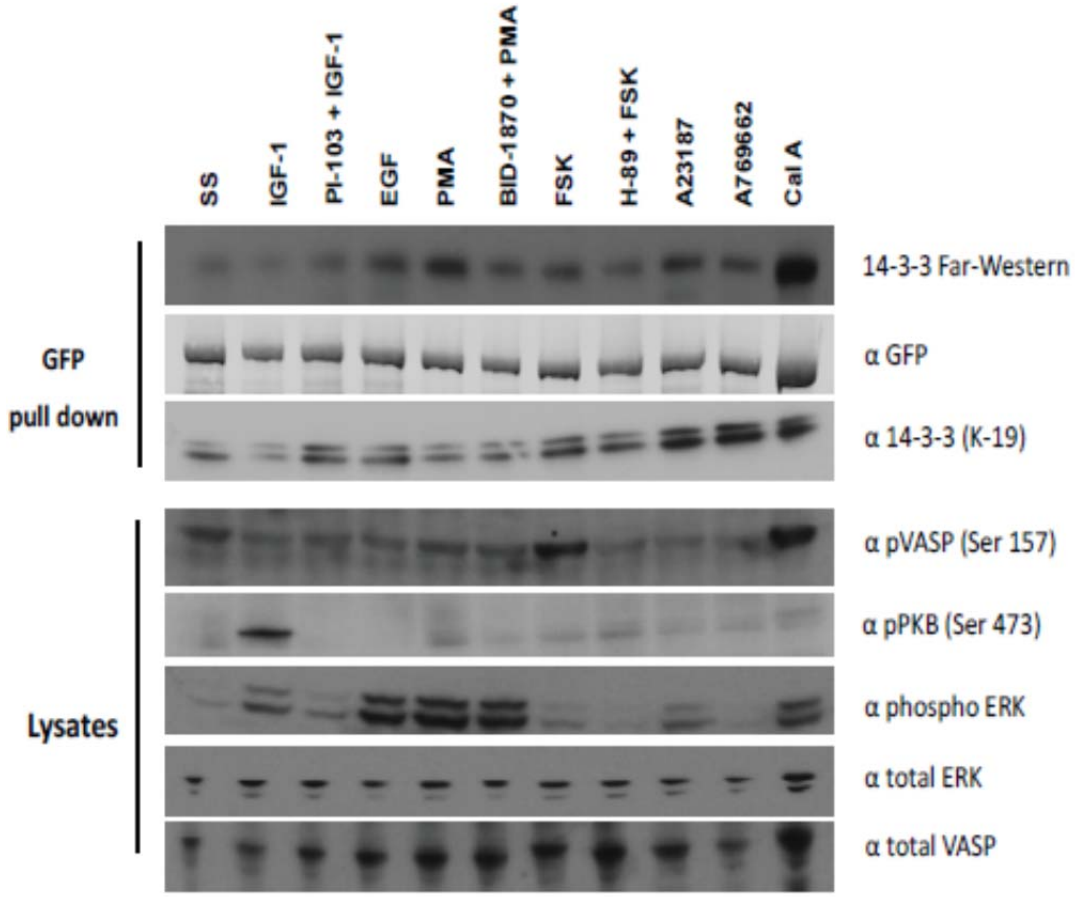

Figure 4.9: 14-3-3 binding of GFP-DENND4A in response to various kinase inhibitors and agonists
Cells stably expressing GFP-DENND4A were induced with tetracycline for 24 hours. These cells were serum-starved for 6 h and pre-treated with the indicated kinase inhibitors before stimulation (30 min with 1 μM PI-103, 10 μM BI-D1870, 30 μM H-89). Stimulations were: 50 ng/ml IGF1 for 20 min; 100 ng/ml EGF for 15 min; 100 ng/ml PMA for 30 min; 20 μM forskolin for 30 min; 10 μM A23187 for 20 min; 50 μM A769662 for 1 h; 50 nM calyculin A for 5 min. GFP-DENND4A was isolated from 2.5 mg lysate on GFP-Trap. Samples were separated by SDS-PAGE, transferred to nitrocellulose and probed with the indicated antibodies. Growth factor stimulated phosphorylation of PKB and Erk1/2, and phosphorylation of VASP by forskolin was tested by immunoblotting lysates (40 μg) with the indicated antibodies. SS-serum-starved, FSK-forskolin, Cal A-calyculin A.

4.2.1.5 GFP-DENND4B binds 14-3-3s under all cellular conditions tested

Similarly, lysates of cells transiently expressing GFP-DENND4B were screened for binding of the protein to 14-3-3 after using the same panel of activators and inhibitors to identify the kinases likely to phosphorylate the protein. Under all conditions tested, DENND4B was seen to bind to 14-3-3s in the overlay assays (**Figure 4.10**). However, endogenous 14-3-3s were observed to co-immunoprecipitate with DENND4B upon treatment with the PMA plus or minus the p90RSk inhibitor BI-D1870, the calcium ionophore A23187 and the phosphatase inhibitor calyculin A. This suggests that kinases activated in these pathways could be phosphorylating serine and/or threonine residues in DENND4B that could potentially mediate 14-3-3-binding. One possibility is that one 14-3-3-binding site on DENND4B is phosphorylated under all the conditions tested, and the other phosphorylated by kinases that are activated in response to PMA and A23187. To identify the kinases responsible for 14-3-3 binding, truncation mutants of DENND4B have been generated to pinpoint which part of the protein binds 14-3-3 as the next step towards understanding regulation of DENND4B by 14-3-3s (**section 4.2.1.8**).

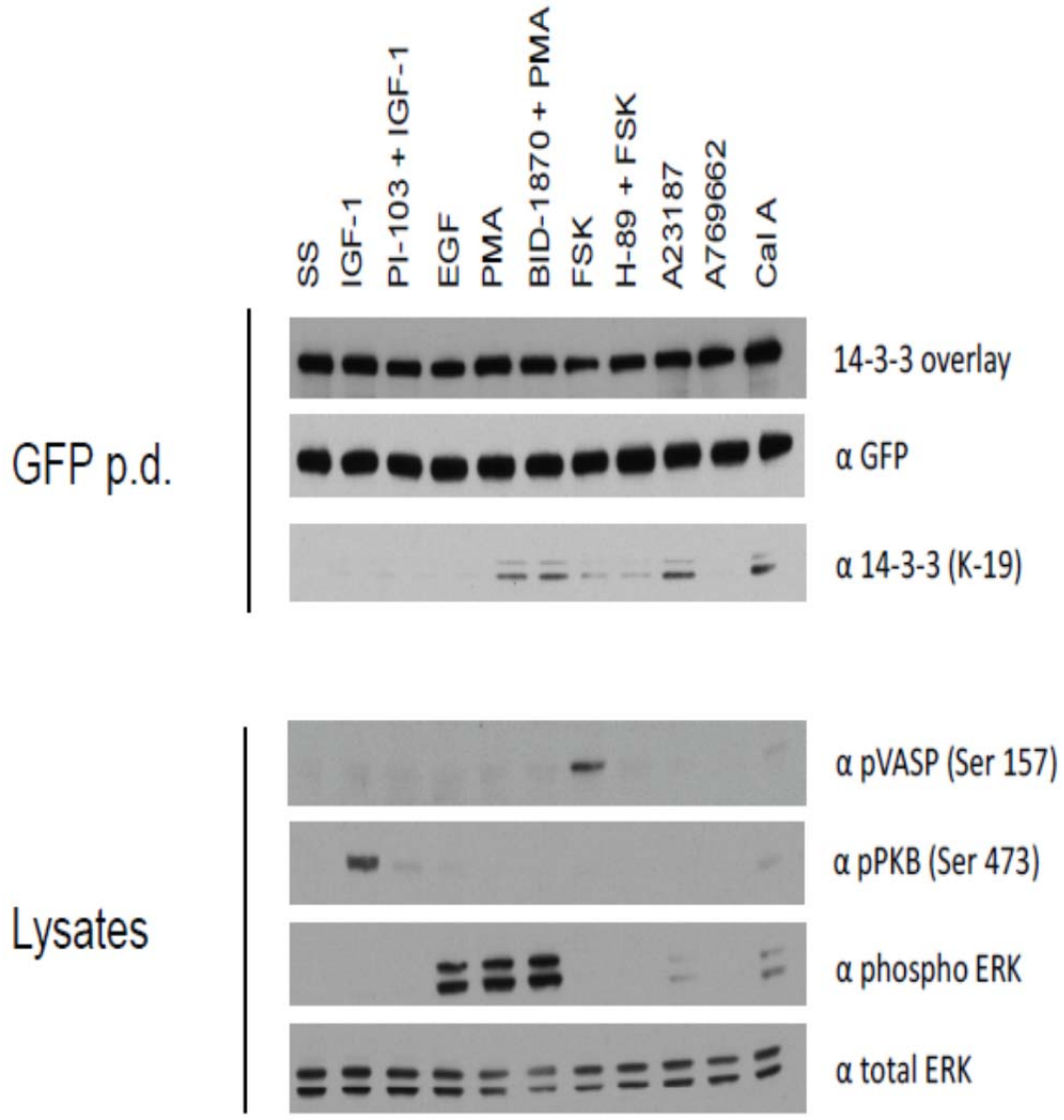

Figure 4.10: 14-3-3 binding of GFP-DENND4B in response to various inhibitors and agonists

HEK293 cells were transiently transfected to express GFP-DENND4B, and after 24 h cells were serum-starved for 6 h and pre-treated with the indicated kinase inhibitors before stimulation (30 min with 1 μM PI-103, 10 μM BI-D1870, 30 μM H-89). Stimulations were: 50 ng/ml IGF1 for 20 min; 100 ng/ml EGF for 15 min; 100 ng/ml PMA for 30 min; 20 μM forskolin for 30 min; 10 μM A23187 for 20 min; 50 μM A769662 for 1 h; 50 nM calyculin A for 5 min. GFP-DENND4B was isolated from 2.5 mg lysate on GFP-Trap. Samples were separated by SDS-PAGE, transferred to nitrocellulose and probed with the indicated antibodies. Growth factor stimulated phosphorylation of PKB and Erk1/2, and phosphorylation of VASP by forskolin was tested by immunoblotting lysates (40 μg) with the indicated antibodies. SS-serum-starved, Cal A-calyculin A.

4.2.1.6 GFP-DENND4C binds 14-3-3s pre-dominantly upon cAMP/PKA activation

Interestingly, treatment with forskolin was observed to increase DENND4C binding to 14-3-3s in the Far-Western 14-3-3 overlay assay (**Figure 4.11**). This binding was inhibited by the non-specific PKA inhibitor H-89, suggesting that PKA might phosphorylate one or more of the 14-3-3-binding phosphosites on DENND4C. Co-immunoprecipitation of endogenous 14-3-3s also coincided with forskolin treatment and was decreased upon inhibition of PKA by H-89. Interestingly, PMA also induced the co-immunoprecipitation of endogenous 14-3-3s with DENND4C although no overlay signal could be detected under this treatment. Further analyses are required to pinpoint the phosphosites in DENND4C which mediate its binding to 14-3-3s.

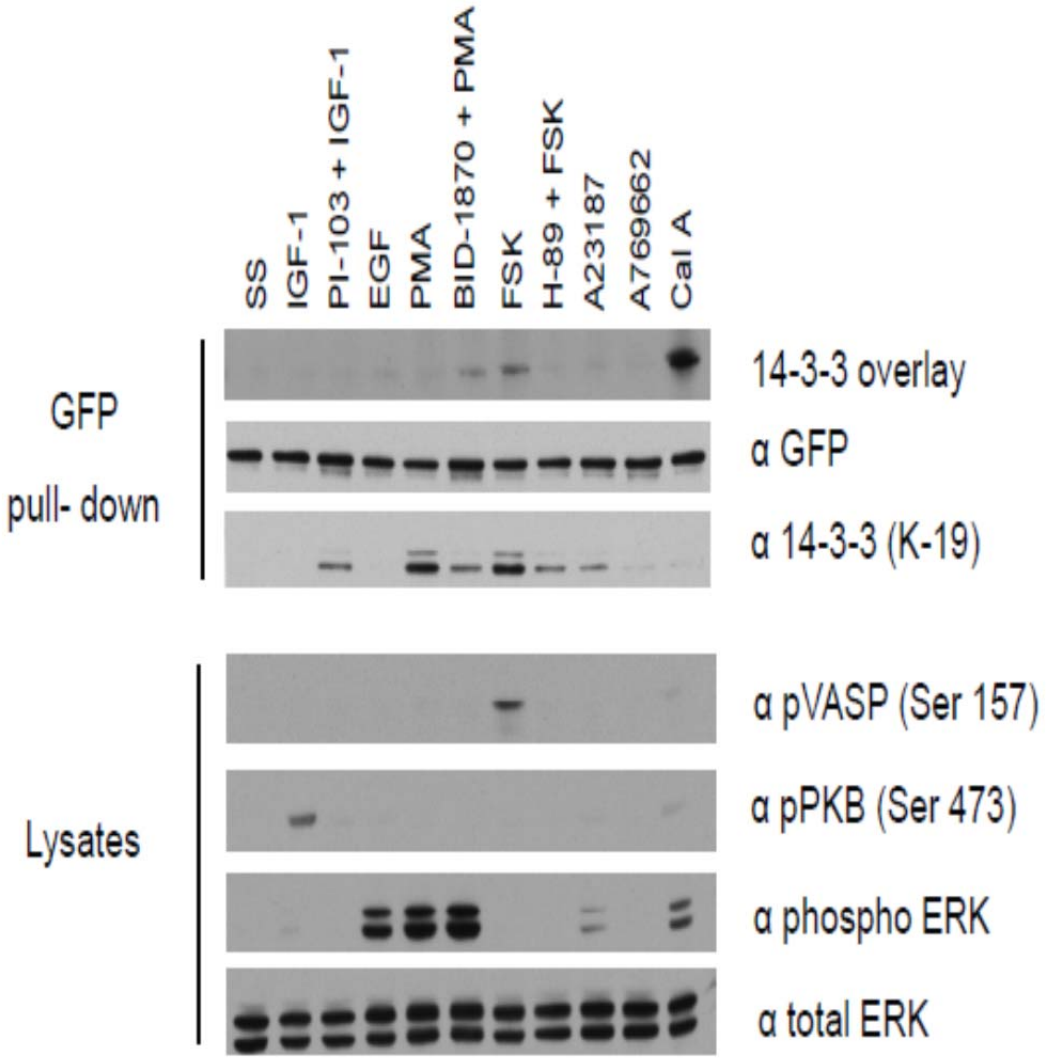

Figure 4.11: 14-3-3 binding of GFP-DENND4C in response to various stimuli and inhibitors

HEK293 cells were transiently transfected to express GFP-DENND4C, and after 24 h cells were serum-starved for 6 h and pre-treated with the indicated kinase inhibitors (30 min with 1 μM PI-103, 10 μM BI-D1870, 30 μM H-89) before stimulation with growth factors and protein kinase activators. Stimulations were: 50 ng/ml IGF1 for 20 min; 100 ng/ml EGF for 15 min; 100 ng/ml PMA for 30 min; 20 μM forskolin for 30 min; 10 μM A23187 for 20 min; 50 μM A769662 for 1 h; 50 nM calyculin A for 5 min. GFP-DENND4C was isolated from 2.5 mg lysate on GFP-Trap resin. Samples were separated by SDS-PAGE, transferred to nitrocellulose and probed with the indicated antibodies. Growth factor stimulated phosphorylation of PKB and Erk1/2, and phosphorylation of VASP by forskolin was tested by immunoblotting lysates (40 μg) with the indicated antibodies. SS-serum-starved, Cal A-calyculin A.

4.2.1.7 *In silico* analysis of putative 14-3-3-binding phosphorylation sites on the DENND4 proteins

14-3-3 proteins dock onto phosphorylated serine or threonine residues on their target proteins. We did an *in silico* analysis of the three amino acid sequences of the DENND4 proteins and tried to match sequences that were close to the two 14-3-3-binding motifs: RSX(pS)XP (mode I) and RX(F/Y)X(pS)XP (mode II) (Yaffe et al., 1997). Interestingly, DENND4A and DENND4C had multiple candidates as potential phosphorylation sites (7 and 4 respectively) while DENND4B had three. Since we did not have the full-length construct for DENND4C, we selected only those potential residues that were in the construct we obtained for residues 1017-1673. These potential 14-3-3-binding serine residues in the DENND4 proteins (**Table 4.1**) were mutated to non-phosphorylatable alanine residues to check their interaction with 14-3-3s.

Table 4.1: The potential 14-3-3-binding serine residues in the DENND4 proteins and their corresponding alanine mutants

IRLB (DENND4A)	S338	pcDNA5 FRT/TO GFP IRLB S338A	DU36868
	S755	pcDNA5 FRT/TO GFP IRLB S755A	DU36869
	S1151	pcDNA5 FRT/TO GFP IRLB S1151A	DU36886
	S1251	pcDNA5 FRT/TO GFP IRLB S1251A	DU36865
	S1589	pcDNA5 FRT/TO GFP IRLB S1589A	DU36946
	S1609	pcDNA5 FRT/TO GFP IRLB S1609A	DU36866
	S1798	pcDNA5 FRT/TO GFP IRLB S1798A	DU36879
DENND4B	S343	pcDNA5 FRT/TO GFP DENND4B S343A	DU36830
	S732	pcDNA5 FRT/TO GFP DENND4B S732A	DU36831
	S961	pcDNA5 FRT/TO GFP DENND4B S961A	DU36832
DENND4C	S1042	pcDNA5 FRT/TO GFP DENND4C 1017-end S1042A	DU36833
	S1404	pcDNA5 FRT/TO GFP DENND4C 1017-end S1404A	DU36834
	S1426	pcDNA5 FRT/TO GFP DENND4C 1017-end S1426A	DU36835
	S1608	pcDNA5 FRT/TO GFP DENND4C 1017-end S1608A	DU36846

4.2.1.8 Truncation mutants of DENND4B to determine 14-3-3-binding

From the 14-3-3-overlay kinase panel experiment (**Figure 4.10**), it was difficult to pinpoint the possible kinase(s) that could be phosphorylating DENND4B since the overlay signal was observed for all treatment conditions. We decided to use another approach to narrow down the part of the DENND4B protein responsible

for 14-3-3-binding. Using the GlobPlot analysis tool, we looked at the different regions in the predicted structure of DENND4B and truncated the protein into different fragments within disordered regions (**Figure 4.12**). These fragments will be tested for binding to 14-3-3.

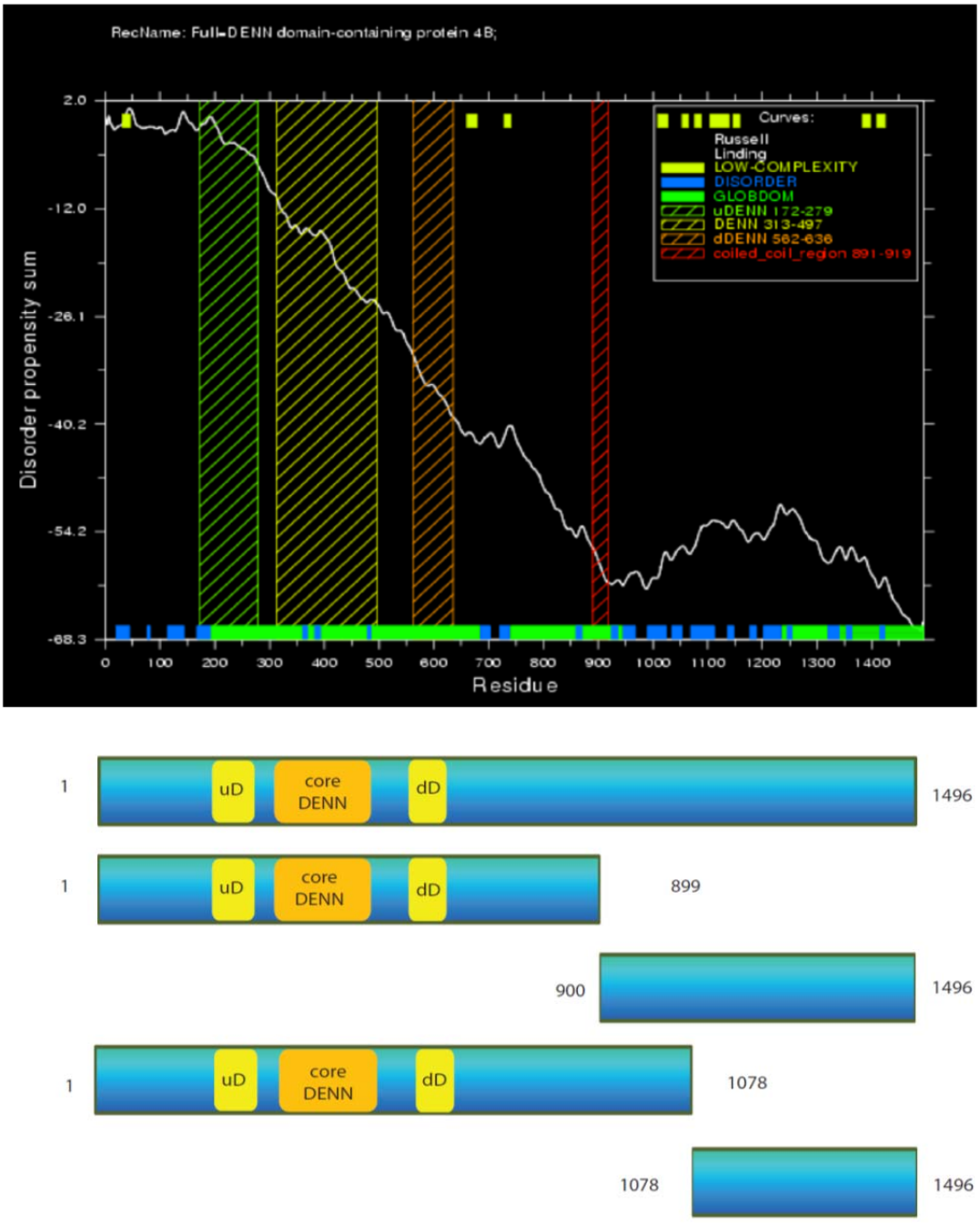

Figure 4.12: Globplot analysis and truncation mutants of DENND4B
The Globplot tool (http://www.globplot.embl.de) was used to analyse the DENND4B protein (O75064), which predicts disorder propensity upon Pfam domain predictions. Based on this information, truncation mutants of DENND4B were generated encompassing different combinations of the globular and DENN domains in DENND4B.

4.2.2 Characterisation of EML3 as a potential 14-3-3-binding protein

EML3, also known as ELP95 (Echinoderm-like protein 95) was also identified in the cAMP–PKA-stimulated 14-3-3-phosphoproteomic screen and we set out to characterise this protein and its binding to 14-3-3s. EML3 was first identified in this laboratory by Pozuelo-Rubio et al. (2004), and subsequently by Dubois et al. (2009) as part of 14-3-3 affinity capture screens. In 2008, Tegha-Dunghu and colleagues reported the co-localisation of EML3 with cytoplasmic microtubules during interphase and its association with spindle microtubules throughout mitosis (Tegha-Dunghu et al., 2008). Initial characterisation of EML3 as a 14-3-3 binding target was done by Drs Kathryn Geraghty and Kumara Dissanayake: they found that EML3 bound to 14-3-3s in a phosphorylation dependent manner. I started by stimulating cells expressing GFP-EML3 with the panel of inhibitors and agonists to try and identify the possible kinase(s) and/or pathway(s) involved in EML3 phosphorylation. The lysates from these treated cells were pre-cleared for an hour with protein G-Sepharose and then incubated with 14-3-3-Sepharose beads for 2 h at 4°C. The beads were washed prior to elution with 2 x SDS-sample buffer. Proteins were run on an SDS-PAGE gel and analysed for 14-3-3-binding. Interestingly, EML3 was found to bind 14-3-3s in response to stimulation with forskolin; consequently, treatment with the non-specific PKA inhibitor H-89 abolished 14-3-3-binding (**Figure 4.13**). To find potential protein partners of EML3, the protein was expressed with a GFP-tag, pulled down on GFP-Trap beads, separated by one-dimensional SDS-PAGE and analysed by mass spectrometry techniques. Mass spectrometric analysis of GFP-tagged EML3 identified it as part of a complex with two other proteins, p32, a nuclear-encoded mitochondrial protein, and RanBP5, a member of the importin beta family (**Figure 4.14;** Geraghty and MacKintosh, unpublished results). In order to ascertain the phosphorylation sites of EML3 which mediated its binding to 14-3-3s, its amino acid sequence was scanned for potential 14-3-3-binding motifs. Two 14-3-3 binding sites of EML3, namely Ser127 and Ser147, both located in the N-terminal region of the protein were chosen as the most likely candidates (Dissanayake and MacKintosh, unpublished results). The GFP-EML3 protein was expressed and affinity purified on 14-3-3-Sepahrose beads; the immunoprecipitates were then analysed for EML3 binding to 14-3-3s. Both single and double mutations of these serine residues to their non-phosphorylatable alanine counterparts disrupt binding to 14-3-3s, with Ser127 being

the pre-dominant site (**Figure 4.15**). Mutations of the 14-3-3 binding sites of EML3 did not affect its interaction with either p32 or RanBP5 (**Figure 4.15**). Next, truncation mutants of EML3 were generated to elucidate the region(s) of EML3 interacting with p32 and RanBP5 (**Figure 4.16**). Preliminary results suggest that both of these proteins bind EML3 at the C-terminal region involving the WD40 repeat motifs (**Figure 4.17**). So far, it seems that the interaction of EML3 with 14-3-3-s is independent of its interaction with RanBP5 and p32. Also, the results suggest that these interacting partners bind EML3 at different regions in the protein. Further experiments are required to understand the effect of 14-3-3-binding to EML3, and the effect of EML3 interactions with p32 and RanBP5.

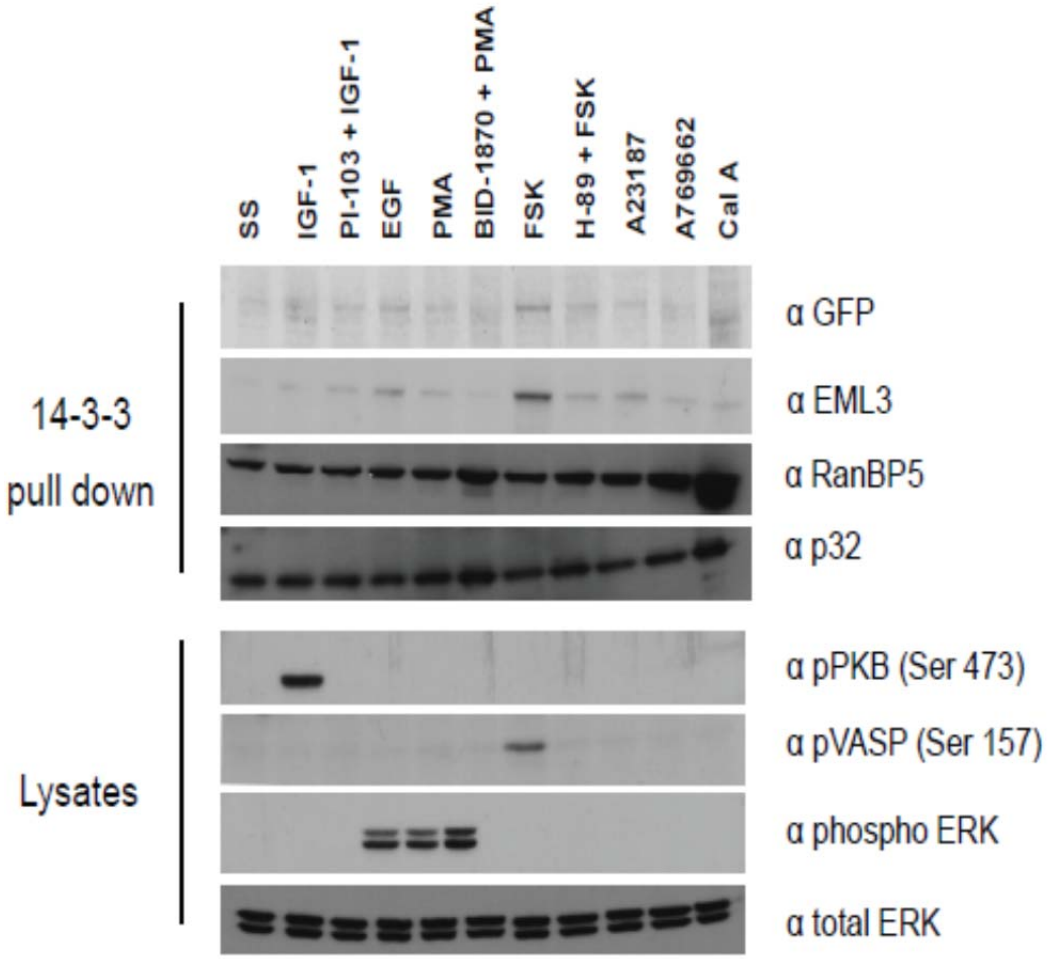

Figure 4.13: 14-3-3 binding of GFP-EML3 in response to various kinase inhibitors and agonists

HEK293 cells were transiently transfected to express GFP-EML3, and after 24 h cells were serum-starved for 6 h and pre-treated with the indicated kinase inhibitors before stimulation (30 min with 1 μM PI-103, 10 μM BI-D1870, 30 μM H-89). Stimulations were: 50 ng/ml IGF1 for 20 min; 100 ng/ml EGF for 15 min; 100 ng/ml PMA for 30 min; 20 μM forskolin for 30 min; 10 μM A23187 for 20 min; 50 μM A769662 for 1 h; 50 nM calyculin A for 5 min. GFP-EML3 was isolated from 2.5 mg lysate on 14-3-3-Sepharose. Samples were separated by SDS-PAGE, transferred to nitrocellulose and probed with the indicated antibodies. Growth factor stimulated phosphorylation of PKB and Erk1/2, and phosphorylation of VASP by forskolin was tested by immunoblotting lysates (40 μg) with the indicated antibodies. SS-serum-starved, FSK-forskolin, Cal A-calyculin A.

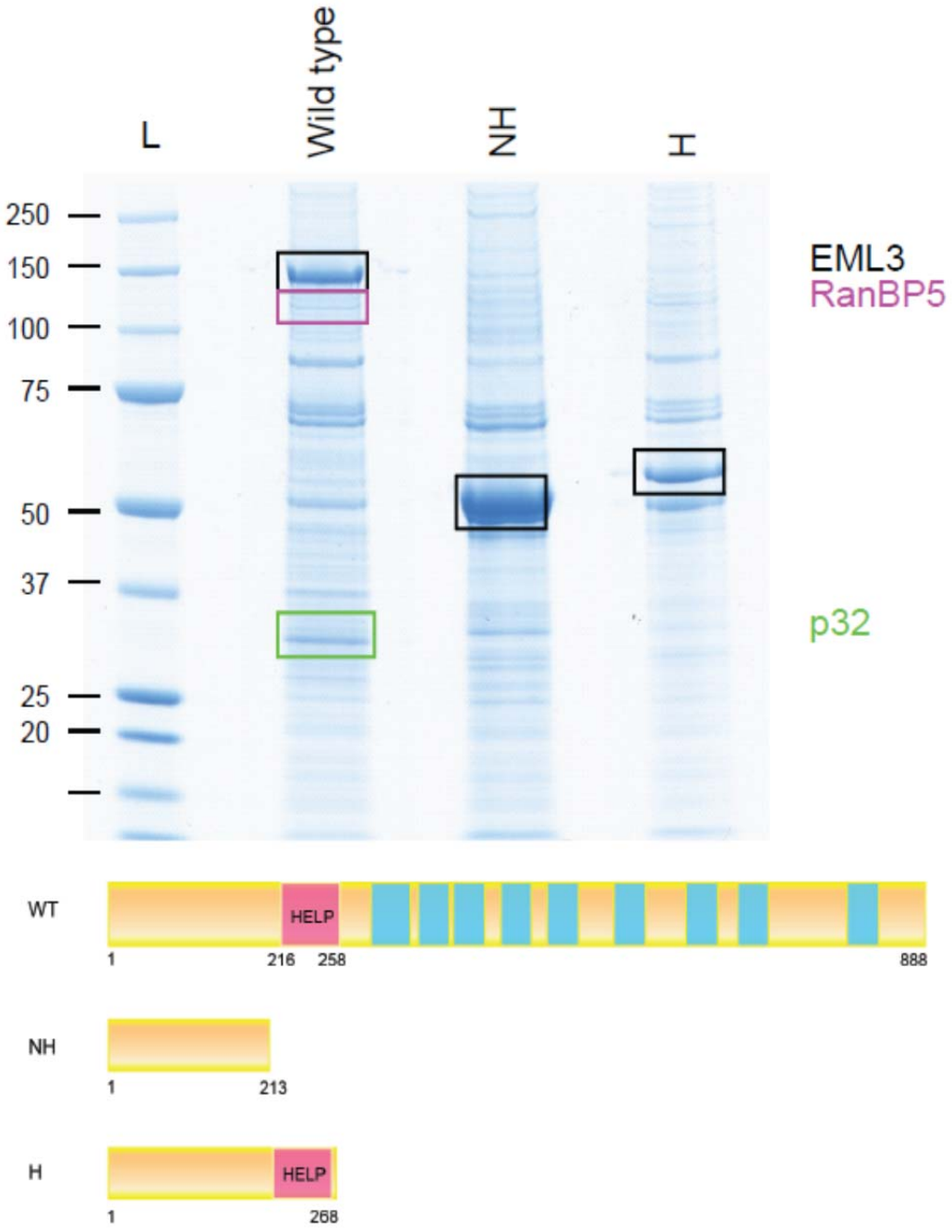

Figure 4.14: Coomassie-stained SDS-polyacrylamide gel of proteins that have been eluted from the GFP-EML3 pull down using GFP-Trap® beads
HEK293 cells were transiently transfected with forms of GFP-EML3 (wild type, mutants without and with the HELP domains (NH and H respectively). Proteins in cell lysates were captured on GFP-Trap beads and bound proteins were eluted by boiling in 2X sample buffer. The column eluates (75% of each) were loaded onto each lane of an SDS-polyacrylamide gel, which was stained with colloidal Coomassie blue for protein visualization. The boxes represent the sections that were cut for further processing by the methods outlined in section **2.2.15**.

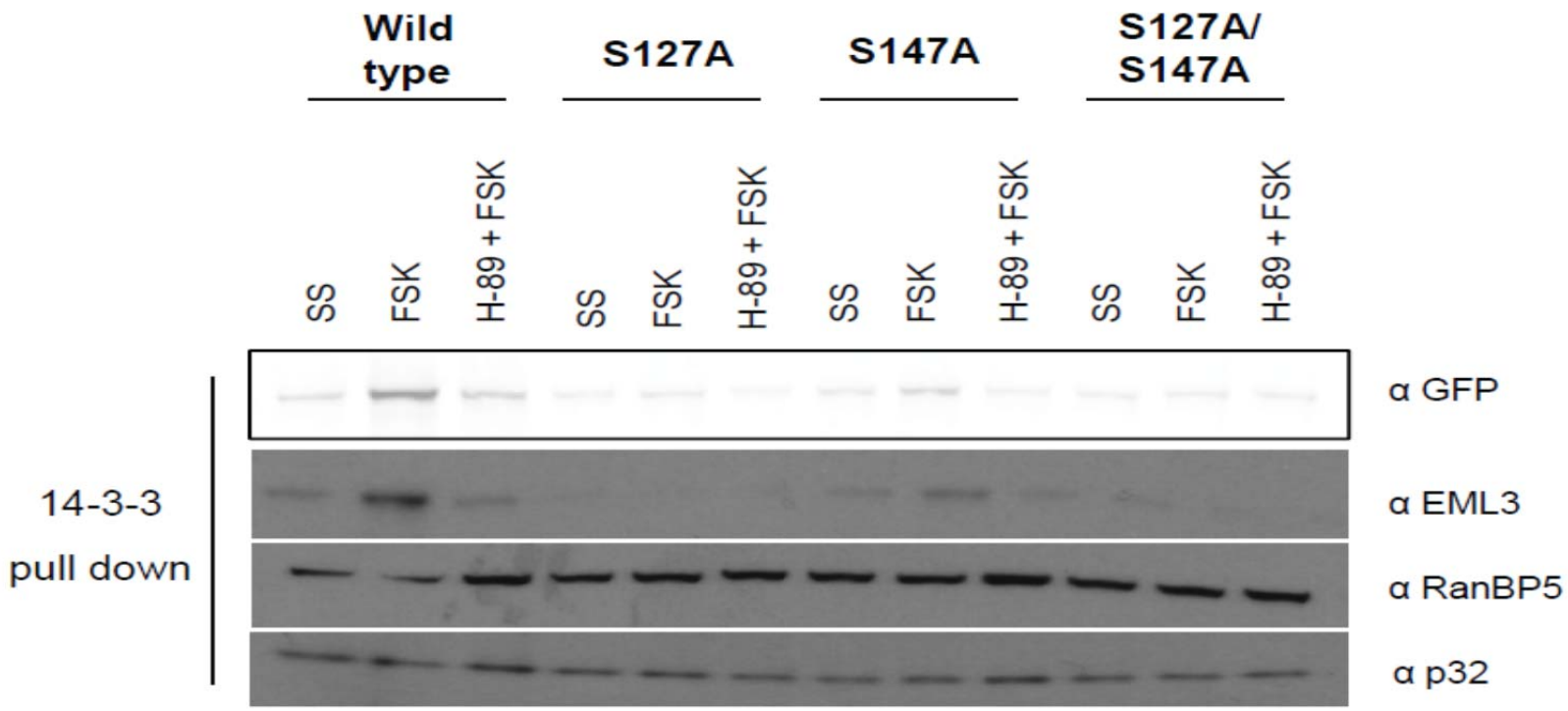

Figure 4.15: 14-3-3-binding phosphosites of EML3
HEK293 cells were transfected to transiently express EML3 wild-type, EML3 with either the S127A or the S147A mutation, or the double phosphomutant S127A/S147A. Cells were grown to 90% confluency before lysis. 3 mg of lysates for each sample were affinity purified on 14-3-3-Sepharose beads and eluted using 2 x sample buffer. Samples were separated by SDS-PAGE, transferred to nitrocellulose and probed with the indicated antibodies.

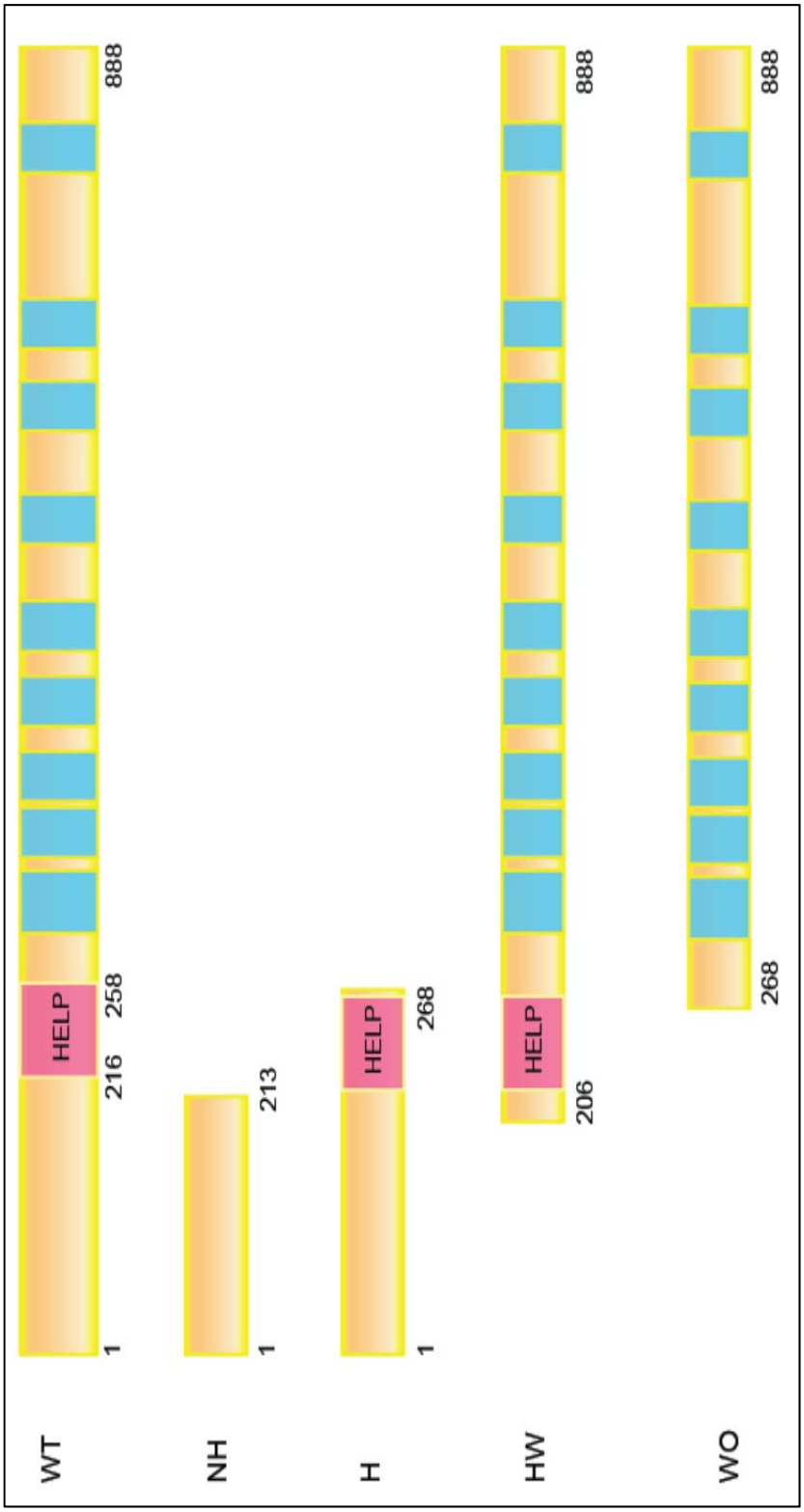

Figure 4.16: Truncation mutants of EML3
The amino acid sequence of EML3 was analysed through the GlobPlot analysis software to predict globular and disordered regions within the protein. Based on this analysis, truncation mutants of EML3 were generated for the amino acids indicated in the figure. WT-wild type, NH-No Help domain, H-Help domain only, HW-Help and WD40 repeats, WO-WD40 repeats only. The WD40 repeats are shaded cyan.

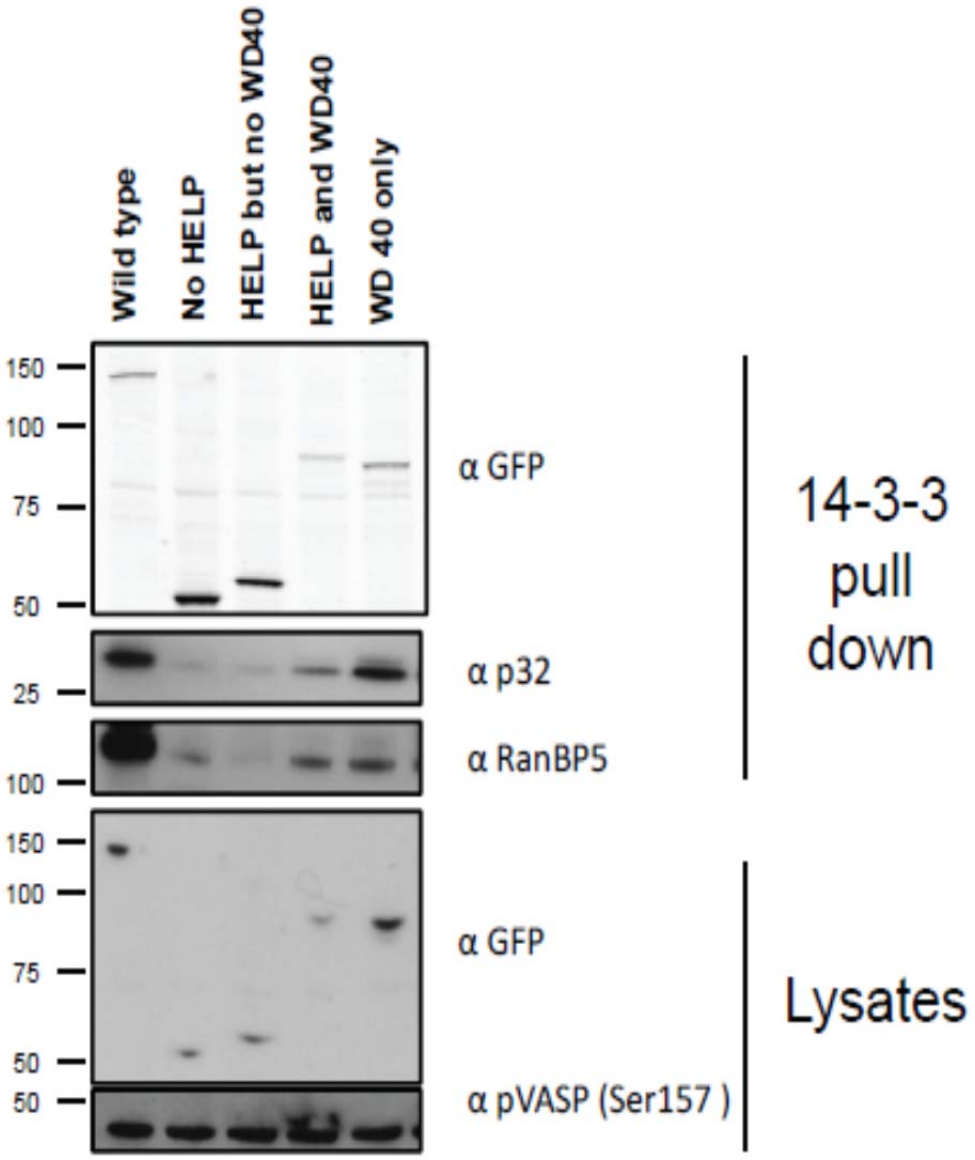

Figure 4.17: Truncation mutants of EML3 to study RanBP5 and p32 binding
HEK293 cells were transfected to transiently express EML3 wild-type and its truncated mutants as described in Figure 4.16. Cells were grown to 90% confluency before lysis. 3 mg of lysates for each sample were affinity purified on 14-3-3-Sepharose beads and eluted using 2 x sample buffer. Samples were separated by SDS-PAGE, transferred to nitrocellulose and probed with the indicated antibodies.

4.2.3 Is ATG9a a novel 14-3-3-interacting protein?

Interestingly, a key player in the initiation of autophagy in mammalian cells was identified in my 14-3-3 screen, namely ATG9a. This was exciting as it implicated 14-3-3s in a novel function previously undescribed for these signalling proteins, and which might relate to the membrane trafficking interests of the group. Furthermore, another autophagy-related protein, ULK1 (Unc-like kinase 1), has been very recently shown to interact with 14-3-3s upon phosphorylation by AMPK during stress responses (Mack et al., 2012). Although ATG9 itself has been studied for a few years, its interaction with 14-3-3s has not been previously reported.

Autophagy is one of two major protein-degradation pathways in the cell, which maintain cellular homeostasis between protein synthesis and protein degradation. It has been shown to occur at basal levels to maintain balanced protein levels and is upregulated during cellular stress and nutrient starvation (Webber and Tooze, 2010). While autophagy degrades long-lived proteins and organelles to generate amino acids during starvation and stress to maintain cellular energy levels, the ubiquitin-proteasome pathway has been implicated in the degradation of short-lived proteins (Webber and Tooze, 2010). It follows that deregulations in this pathway would have detrimental effects on the cell; consequently, defects in autophagy have been implicated in cancers, neurodegenerative diseases such as Parkinson's, Huntington's and Alzheimer's, and more recently in muscular atrophies (Mizushima, 2009; Sanchez et al., 2012).

Initiation of autophagy occurs through the formation of the autophagosome, which fuses with the lysosome, enabling the lysosomal hydrolases to degrade the sequestered proteins (Webber and Tooze, 2010). Proteins required for autophagy are named 'autophagy related proteins' (Atg) and yeast genetic screens have identified over 30 such proteins (Xie and Klionsky, 2007). Most of these Atg proteins have been found to transiently colocalise at the pre-autophagosomal structure (PAS) site, where they are recruited for autophagy (Suzuki et al., 2001; Kim et al., 2002). The core machinery for autophagy consists of a protein kinase complex (including Atg1 (ULK1) and other Atg proteins such as Atg13 and Atg17), a phosphatidylinositol 3-kinase complex (consisting of a class III PI 3-kinase Vps34, p150, Beclin1 and Atg14), two ubiquitin-like conjugation systems and Atg9 (Chan and Tooze, 2009; Simonsen and Tooze, 2009; Webber and Tooze, 2010).

Atg9 is highly conserved protein among eukaryotes and was first identified in yeast genetic screens from cells having autophagic defects (Webber and Tooze, 2010). Knockout of Atg9 plants have been shown to result in accelerated leaf senescence, while knocking down the protein in *Drosophila melanogaster* renders the fly more susceptible to infections by the vesicular stomatitis virus (VSV), and both the plant and fly phenotypes are directly linked to defects in autophagy (Liu et al., 2005; Shelly et al., 2009). Furthermore, deletion of the *C. elegans* orthologue of Atg9 reduces the life span of the worms (Toth et al., 2008). In yeast, Atg9 deficient cells are unable to form the autophagosome, resulting in a decreased total protein turnover and reduced survival rate during starvation (Lang et al., 2000; Noda et al., 2000). Atg9 thus plays a very important role in ensuring autophagy occurs to maintain cellular growth in various organisms.

Atg9 is a transmembrane protein with six membrane-spanning domains, with its amino- and carboxy-ends lying at the cytosolic face. There are two mammalian othologues of Atg9: Atg9a (referred to as Atg9 in this thesis) which is ubiquitously expressed and Atg9b whose expression is reportedly restricted to the placenta and pituitary gland (Yamada et al., 2005). Knockdown of Atg9 in HEK293 cells was shown to inhibit protein degradation and LC3 lipidation, implicating Atg9 in autophagy in mammalian cells (Yamada et al., 2005; Young et al., 2006). Additionally, Atg9 knockout mice have also been generated which indicate that Atg9 is required immediately after birth for survival (Saitoh et al., 2009). In nutrient rich conditions, Atg9 has been found to localise with the trans-Golgi network (TGN) and endosomal proteins. During starvation, Atg9 co-localises with markers of autophagy, including LC3 on pre-autophagosomes and both LC3 and Rab7 on degradative autophagosomes (Young et al., 2006). The trafficking of Atg9 from the TGN to the PAS has been shown to require ULK1 and Atg13, although no direct interaction has been shown to occur between ULK1 and Atg9 (Young et al., 2006; Chan et al., 2009). So far, the only known interactors of Atg9 are p38IP (p38 MAP kinase interacting protein, also known as FAM48) and the recently characterised myosin II which acts as a motor protein in the trafficking of Atg9 to the PAS during starvation (Tang et al., 2011).

I wanted to characterise the potential interaction of Atg9 with 14-3-3s and started by testing whether Atg9 also bound 14-3-3s in a phosphorylation-dependent manner. To test this, I stably expressed GFP-ATG9 in HEK293 cells and pulled-

down ATG9 using the GFP-Trap® beads. Prior to elution, the immunoprecipitates were subjected to dephosphorylation using lambda phosphatase as described in **section 2.2.11**. Samples were run on a gel and analysed using different antibodies which are routinely used to study 14-3-3 interactions. Interestingly, like most 14-3-3-binding proteins, Atg9 also bound 14-3-3s in a phosphorylation-dependent manner (**Figure 4.18**). Next, I wanted to identify the probable kinase(s) involved in Atg9 phosphorylation and used the standard panel of kinase inhibitors and agonists to screen for this. The phorbol ester PMA, which activate PKC and the cAMP agonist forskolin appeared to enhance Atg9 binding to 14-3-3s as seen from the Far Western overlay (**Figure 4.19**). These observations were confirmed using the 14-3-3 motif antibody which specifically recognises proteins displaying the 14-3-3-binding consensus motif (**Figure 4.19**). Intriguingly, the co-immunoprecipitation of endogenous 14-3-3s seemed to be in contrast to the above observations. It is possible that the endogenous 14-3-3s are interacting with another protein or proteins that interact with Atg9, and whose binding to 14-3-3s is differentially regulated compared with Atg9.

To further investigate the interaction of Atg9 with 14-3-3s, and any other proteins, I therefore used using mass spectrometry to identify proteins that were co-immunoprecipitated with stably expressed GFP-Atg9 from HEK293 cells using the GFP-Trap® beads. The immunoprecipitates were separated on an SDS-PAGE gel, stained with Coomassie Blue and the bands cut out and digested with trypsin (**Figure 4.20**). The peptides were then analysed using mass spectrometry and interestingly 14-3-3s were found to co-purify with Atg9 (**Figure 4.20**). Additionally, mTOR, a key regulator of autophagy was also found to co-purify with Atg9. The complete list of potential Atg9-interactors identified is listed in **Appendix VII**. Unfortunately, due to lack of time I could not pursue this further but it would be very interesting to further investigate these findings.

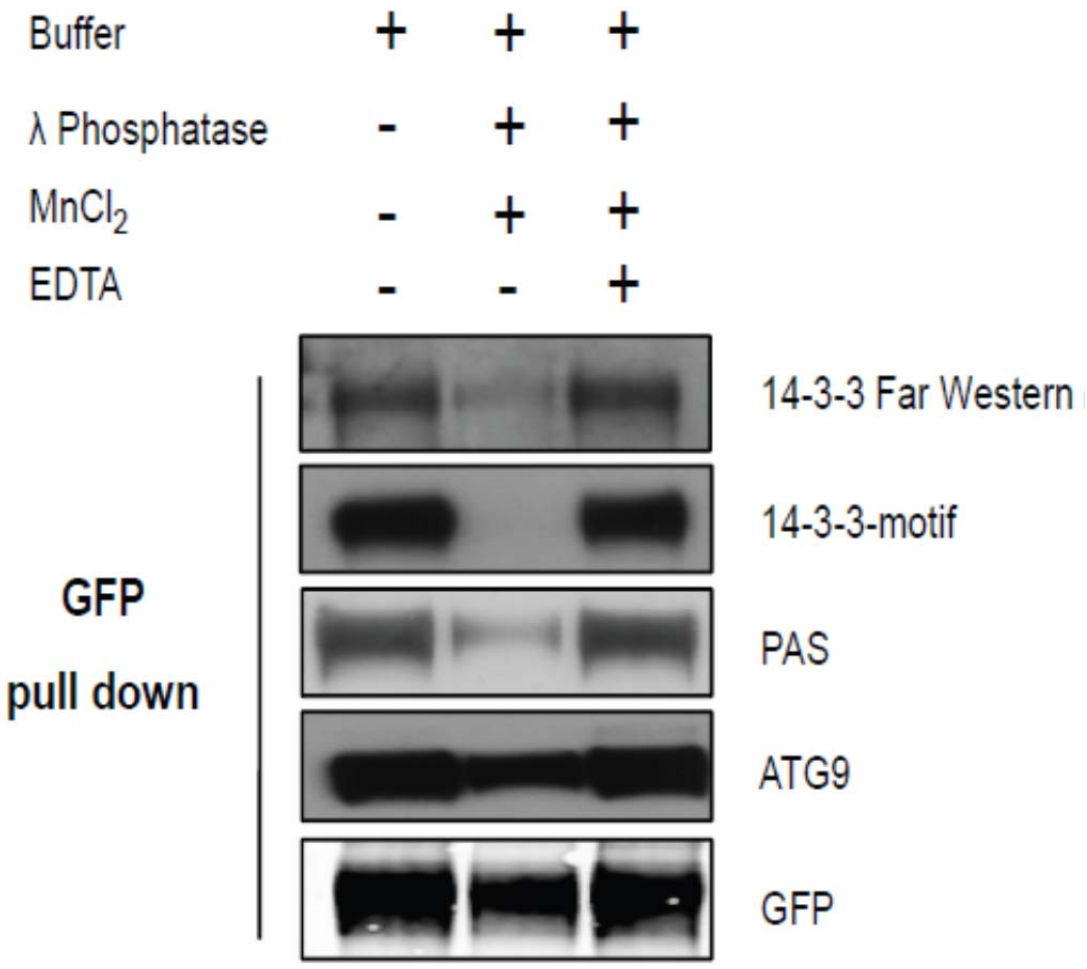

Figure 4.18: Phosphorylation-dependent binding of ATG9 to 14-3-3s
HEK293 stably expressing GFP-ATG9 under the tet inducible promoter were grown to 90% confluency and induced with tetracycline 24 h prior to lysis. Cells were lysed and proteins were pulled down using the GFP-Trap® beads from 3 mg of clarified cell lysate. The immunoprecipitates were treated with buffer only or with 50 mU/ml lambda phosphatase in the presence of its cofactor manganese chloride for 30 min at 30°C as indicated. A negative control for the lambda phosphatase was prepared by chelating the manganese chloride to EDTA prior to incubation with the phosphatase. The immunoprecipitated proteins were separated by SDS-PAGE, transferred to nitrocellulose and probed for binding to 14-3-3s using a 14-3-3 overlay assay (Far Western), a 14-3-3-binding motif recognising antibody and the phospho-AKT substrate(PAS) antibody. Antibodies recognising ATG9 and GFP were used as loading control.

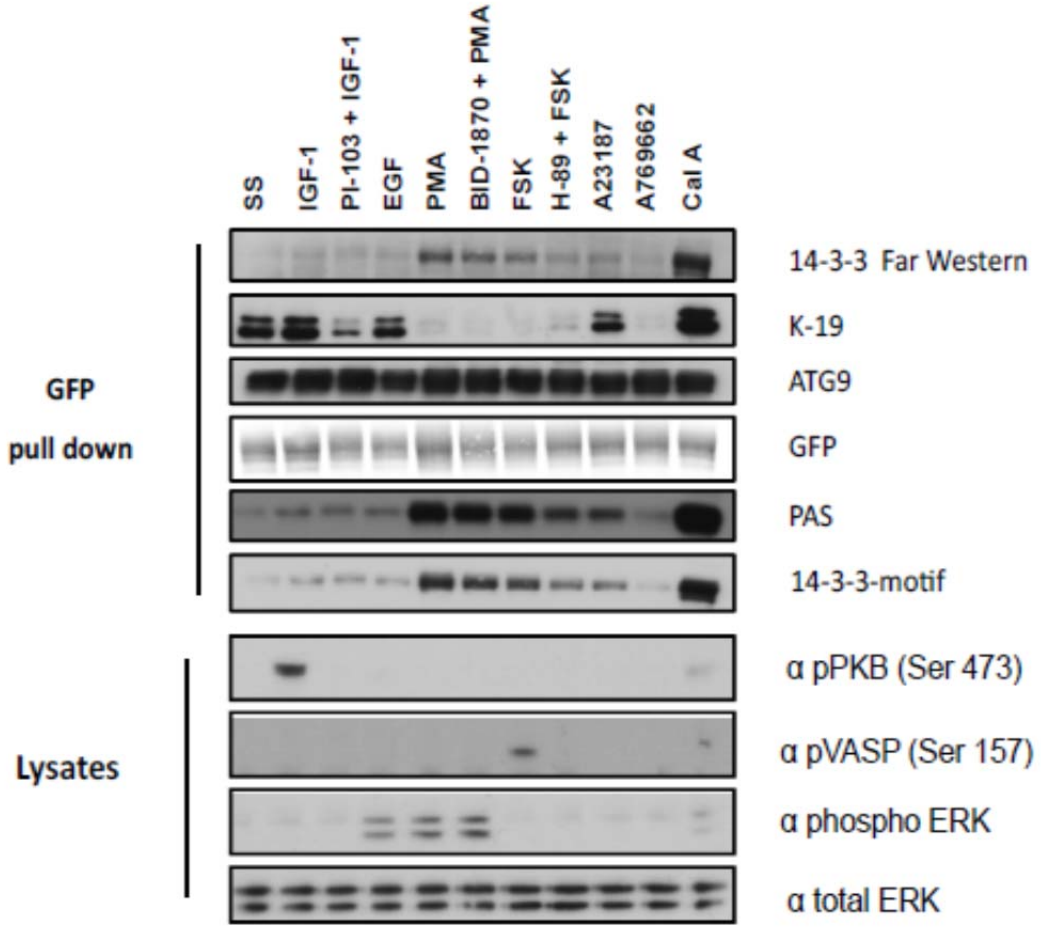

Figure 4.19: 14-3-3 binding of GFP-ATG9 in response to various kinase inhibitors and agonists

HEK293 cells were transiently transfected to express GFP-ATG9, and after 24 h cells were serum-starved for 6 h and pre-treated with the indicated kinase inhibitors before stimulation (30 min with 1 μM PI-103, 10 μM BI-D1870, 30 μM H-89). Stimulations were: 50 ng/ml IGF1 for 20 min; 100 ng/ml EGF for 15 min; 100 ng/ml PMA for 30 min; 20 μM forskolin for 30 min; 10 μM A23187 for 20 min; 50 μM A769662 for 1 h; 50 nM calyculin A for 5 min. GFP-ATG9 was isolated from 2.5 mg lysate on GFP-Trap. Samples were separated by SDS-PAGE, transferred to nitrocellulose and probed with the indicated antibodies. Growth factor stimulated phosphorylation of PKB and Erk1/2, and phosphorylation of VASP by forskolin was tested by immunoblotting lysates (40 μg) with the indicated antibodies. SS-serum-starved, FSK-forskolin, Cal A-calyculin A.

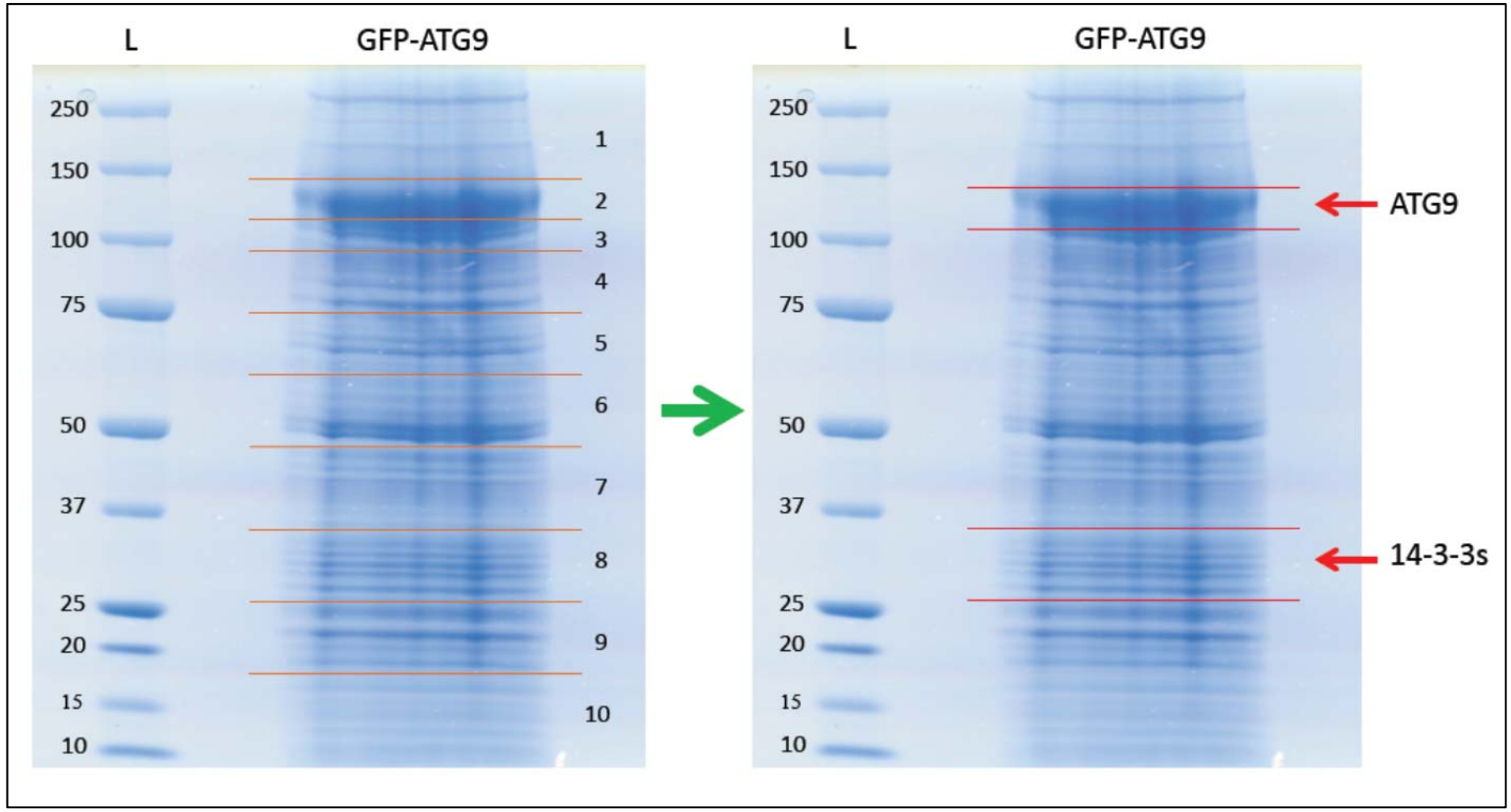

Figure 4.20: Coomassie-stained gel of GFP-ATG9
Cells stably expressing GFP-ATG9 were grown in serum to 90% confluency before lysis. Lysates were immunoprecipitated on GFP-Trap beads and the proteins eluted from the beads by boiling with 2 x sample buffer. The immunoprecipitates (75%) were separated by SDS-PAGE and stained with Coomassie Blue for visualisation (*left*). Bands were excised as labelled on the left gel, digested with trypsin and the peptides analysed by mass spectrometry.

4.3 Crosstalk between the cAMP–PKA and PI-3 kinase–PKB signalling pathways

Many 14-3-3-binding proteins have been found to be phosphorylated in response to different kinases. One finding is that several proteins that bind to 14-3-3s in response to PKB also bind to 14-3-3s in response to cAMP-elevating agents, such as the adenylate cyclase activator forskolin, probably due to phosphorylation by PKA.

Of the 310 proteins identified in this cAMP–PKA screen, 282 of these were found to be common with previous screens for IGF1–PKB signalling (**Figure 4.21**) (MacKintosh group, unpublished results). Because the quantitative data shows regulation in each screen under the different stimuli used, it does not necessarily mean that proteins identified in the PKA screen with high +/- forskolin ratios would necessarily have also have high +/- IGF1 ratios in the other screens. For instance, ZNRF2 (**Figure 4.22**) is slightly phosphorylated in response to IGF-1, but is more strongly regulated by other stimuli, and is also pulled down in IGF1/insulin screens done in the lab. Coiled-coil domain 6 (CCDC6) (Dubois et al., 2009), whose binding to 14-3-3s needs phosphorylation of Ser240 by PKB does not seem to be phosphorylated by any other kinases tested in vitro (**Figure 4.22**) (MacKintosh group, unpublished results). However, CCDC6, initially identified in the insulin–PKB 14-3-3 screen by Dubois et al (2009), was also identified in this cAMP–PKA screen. However, side-by-side comparison with IGF1 and forskolin (**Figure 4.22**) shows that the 14-3-3 binding signal for CCDC6 from IGF1-stimulated cells is markedly greater than that from forskolin-stimulated cells. These comparisons emphasise the importance of quantitative comparisons across the panel of stimuli and inhibitors to obtain the 'signalling signature' of each protein.

Although most signalling pathways are now well understood, the crosstalk occurring among them is not significantly appreciated. Additionally, as discussed previously, it seems surprising to find that the PI 3-kinase–PKB pathways and cAMP–PKA pathways have so many substrates in common because in many different physiological contexts, these two signalling pathways have opposite outcomes (**section 1.5.5.1**). A trial experiment with suspension HEK293 cells stimulated with forskolin showed an increased phosphorylation of PKB (Ser473) in these cells; it turned out that the media for suspension cells had minimal amounts of insulin, which in the presence of forskolin, seemed to enhance PKB phosphorylation

at Ser473. I decided to emulate this using monolayer HEK293 cells: cells were serum starved for 10 h and stimulated with different concentrations of insulin. Some of the cells were inhibited with PI-103 prior to insulin stimulation. When used in conjunction with PKA inhibiting or activating reagents, insulin was added to the cells 30 min before addition of either H-89 or forskolin. Interestingly, these results showed that insulin-dependent phosphorylation of PKB at Ser473 is enhanced when the cells are co-stimulated with forskolin (**Figure 4.23**). At lower concentration (5 nM), inhibiting PKA using H-89 prior to forskolin stimulation in insulin-activated cells seemed to reduce PKB phosphorylation; this inhibition did not occur at higher concentration of insulin (10 nM) (**Figure 4.23**). Conversely, inhibiting the PI 3-kinase pathway with PI-103 seemed to abolish phosphorylation of VASP at Ser157 when insulin (as low as 1 nM) was present in the culture medium (**Figure 4.23**).

It has been observed that inhibiting one pathway could lead to activation of another pathway. For example, inhibition of mTORC1 has been shown to activate the MAPK pathway in a PI 3-kinase-dependent manner in human cancer cells (Carracedo et al., 2008). Also, inhibition of MEK leads to increased PKB phosphorylation in EGFR-driven cancer cells (Faber et al., 2009; Hoeflich et al., 2009; Mirzoeva et al., 2009; Yoon et al., 2009; Turke et al., 2012). To test this in the context of PKA and PKB signalling, I inhibited serum-starved HEK293 cells with H-89 prior to addition of insulin, and looked at PKB phosphorylation (Ser473). Interestingly, H-89 seemed to enhance PKB phosphorylation when used in combination with insulin in this experiment (**Figure 4.24**). This result seemed in contrast to a previous report showing that H-89 was also able to inhibit PKB among other members of the AGC kinases, other than PKA (Bain et al., 2007). Furthermore, there was no difference to the phosphorylation of VASP at Ser157, which we currently use as a marker of PKA activation. These results suggest there might be more than a simple inhibition of PKA by H-89, and potentially there might exist crosstalks occurring between the cAMP–PKA and PI 3-kinase–PKB/Akt signalling pathways. Further experiments are required to understand the complexities in these two signalling pathways.

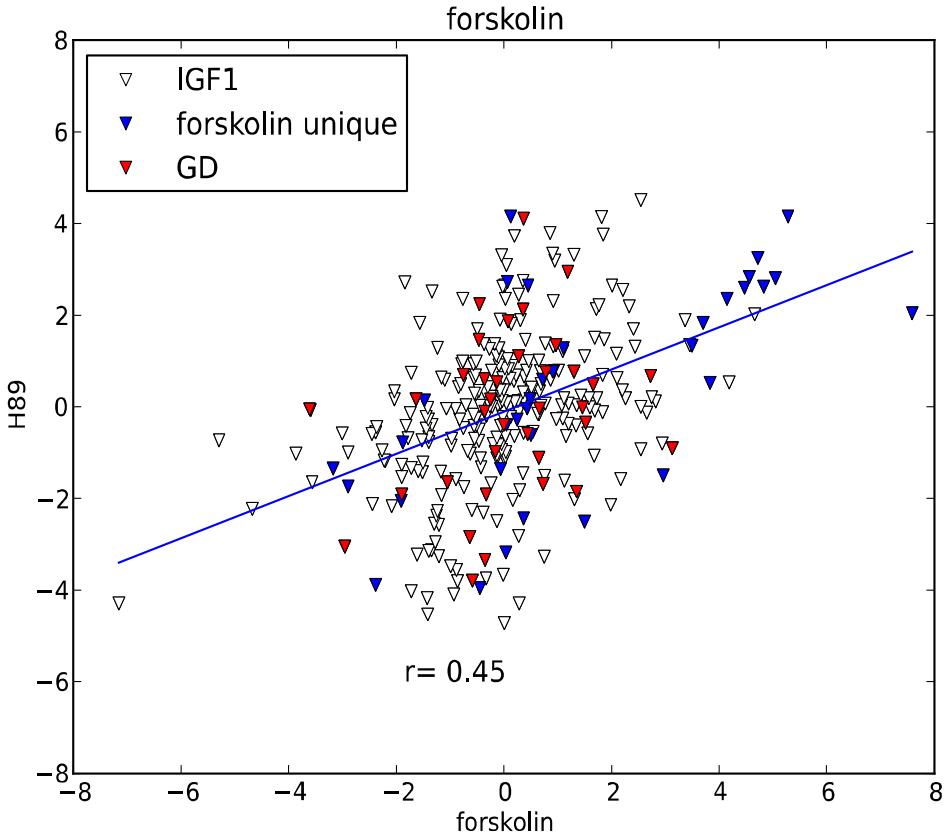

Figure 4.21: Comparison of the proteins identified in the cAMP–PKA-activated screen with overlapping members in the PI 3-kinase–PKB-activated 14-3-3-phosphoproteomic screens

The proteins which were pulled-down using 14-3-3-affinity chromatography from lysates of cells stimulated with forskolin in the presence or absence of H-89 are plotted on a scatter graph. All proteins were normalised to their counterparts in the serum-starved conditions to obtain a ratio of those proteins that were enriched in the treatment (in this case forskolin only or H-89 and forskolin) conditions. Proteins with at least two unique peptides were then selected from the list. All the proteins identified in this screen are represented by triangles; blue triangles represent proteins that were uniquely identified in this screen using inhibition with H-89 and forskolin as agonist; white triangles represent those proteins that are common with IGF1/insulin-stimulated screens; red triangles represent those proteins that are also in the 'gold standard' list. The correlation value, r, denotes the correlation between the two treatment conditions.

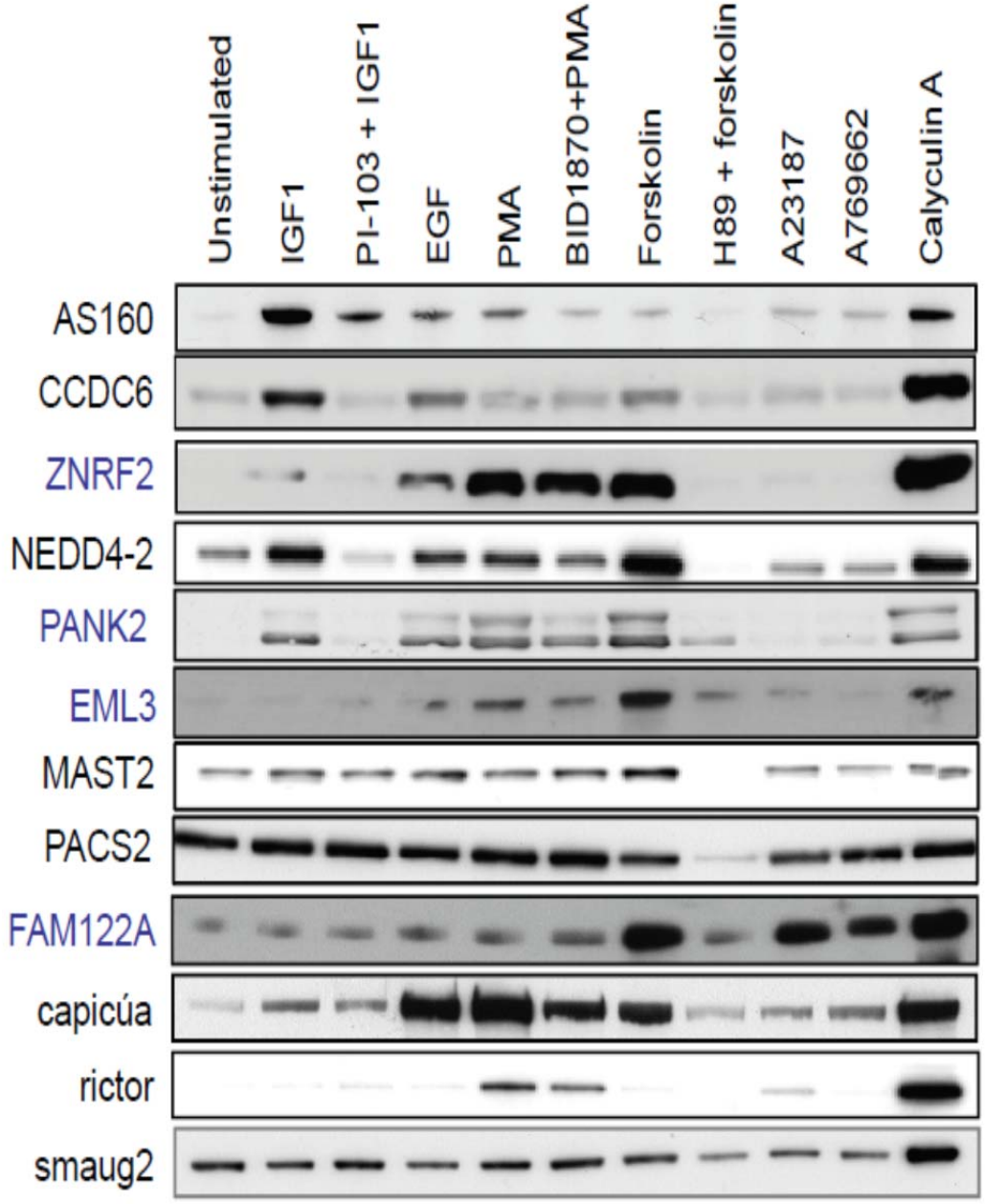

Figure 4.22: Signalling signatures of the 14-3-3-binding phosphoproteome
A panel of kinase inhibitors and agonists are routinely used to screen potential 14-3-3-binding candidates. Proteins were expressed as GFP-tagged forms, and cells treated as indicated, before GFP-Trap immunoprecipitation and 14-3-3 Far-Western overlay assays were performed. Many of the 14-3-3-binding proteins studied in the MacKintosh laboratory have been observed to bind to 14-3-3s in response to phosphorylation by more than one kinase. The data in this figure was contributed by various members of the group, and not shown are the loading controls for GFP, and also assays of lysates that showed the efficacy of the stimuli and inhibitors.

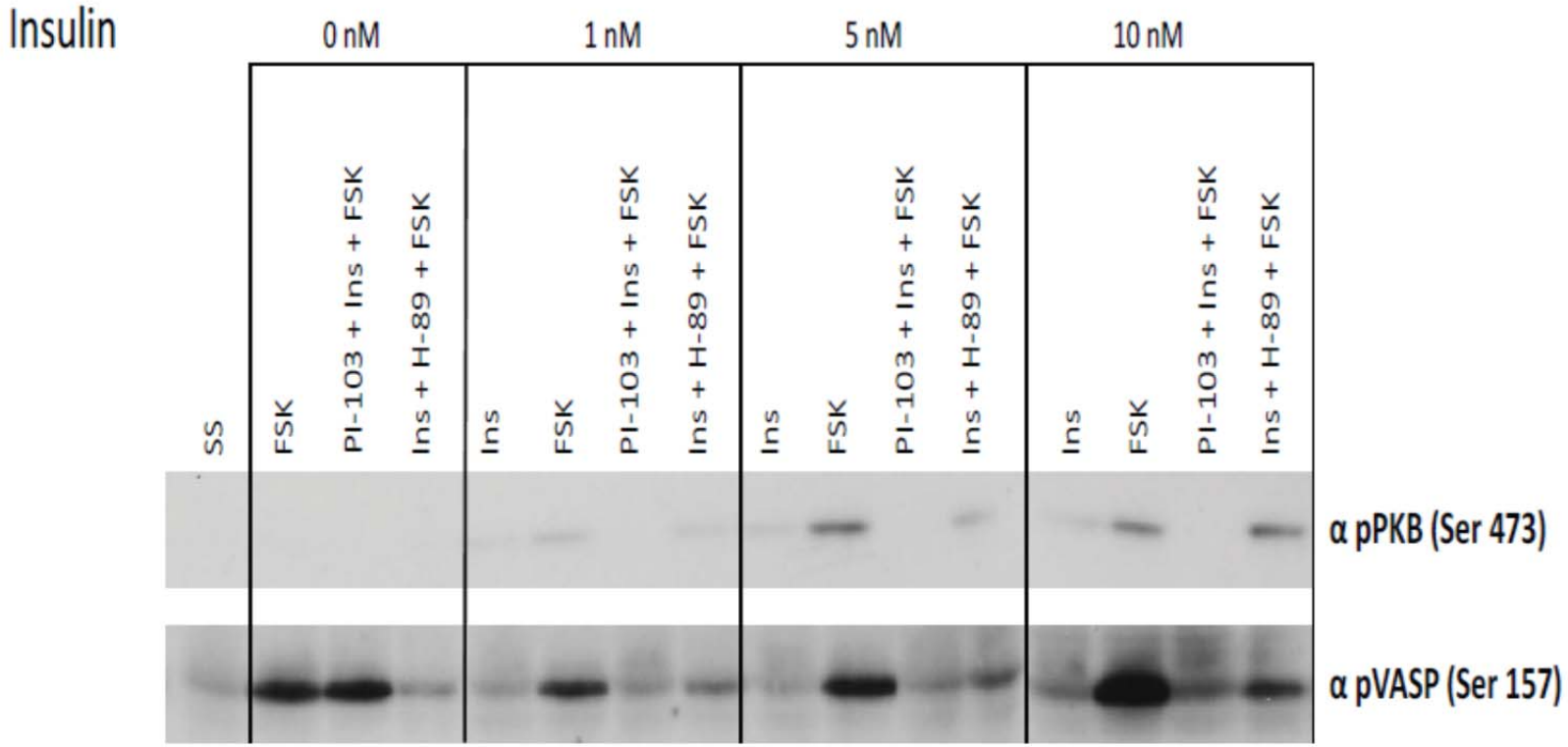

Figure 4.23: Increased phosphorylation of PKB (Ser473) upon co-stimulation with forskolin
HEK293 cells were serum starved (SS) for 10 h prior to inhibition with 30 min with 1 μM PI-103 or 30 μM H-89 for 30 min and/or stimulation with 20 μM forskolin (FSK) for 30 min as indicated. These were done in the absence or presence of different nanomolar concentrations of insulin. When more than one reagent was used, they were added sequentially as shown on the panel, with insulin being added after inhibition with PI-103. Antibodies against the phosphorylations of PKB (Ser473) and VASP (Ser157) were used to monitor activation of the PI 3-Kinase-Akt and cAMP-PKA pathways respectively.

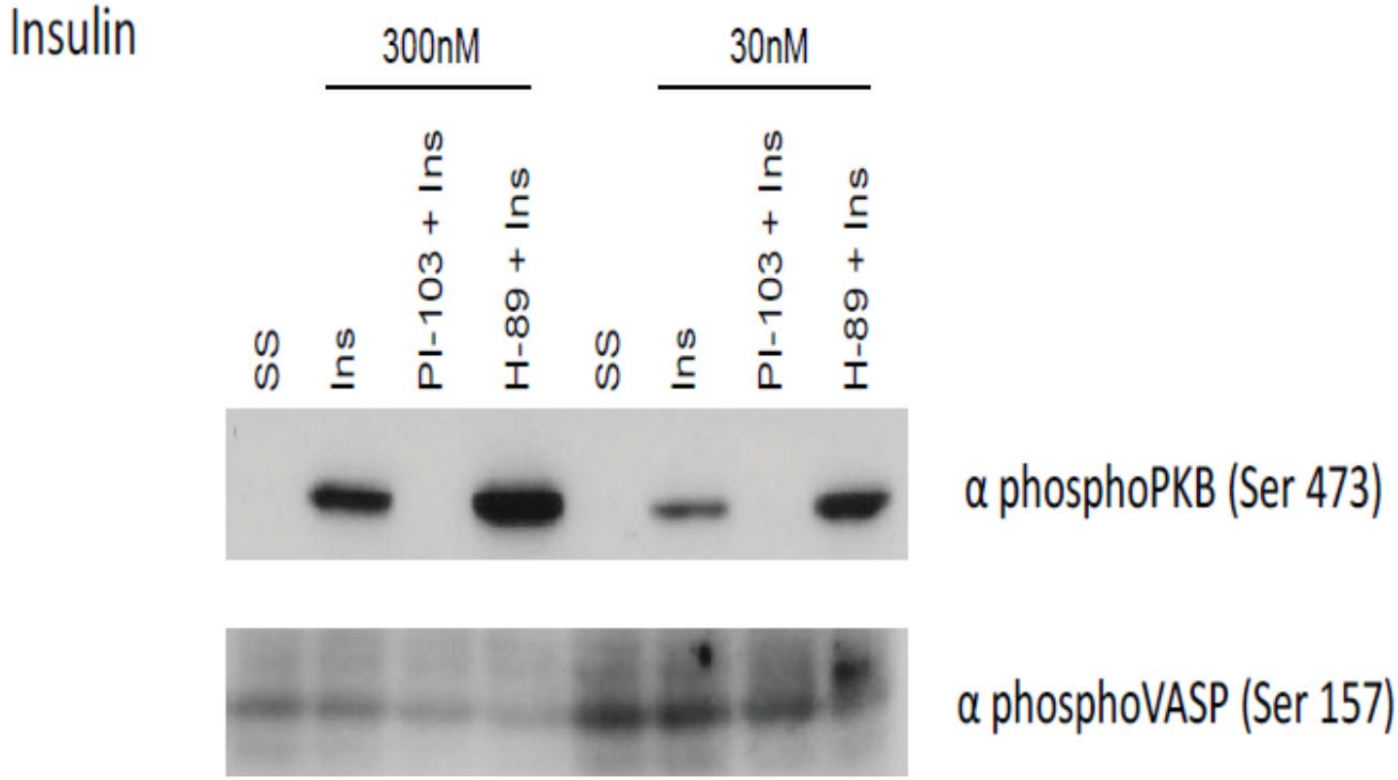

Figure 4.24: Increased phosphorylation of PKB at Ser473 in cells inhibited with H-89 and sequentially stimulated with insulin

HEK293 cells were serum starved (SS) for 10 h prior to inhibition with 30 min with 1 μM PI-103 or 30 μM H-89 for 30 min and/or stimulation with 30 or 300 nM insulin (Ins) for 15 min as indicated. When more than one reagent was used, they were added sequentially as shown on the panel.

4.4 Discussion

For a long time, the role of 14-3-3 binding to proteins was not very well understood; there are hundreds of 14-3-3-binding proteins in the cell and as such understanding the complete functional role of 14-3-3s is quite an overwhelming task. Generally, 14-3-3s interact with phosphorylated proteins, and these phosphorylations have been attributed to members of the AGC and CAMK kinase families. Defining the signalling pathways that create the 14-3-3-binding sites on target proteins thus becomes crucial for understanding the global regulation of 14-3-3s and their functions. Towards this aim, we used 14-3-3-affinity capture and release together with proteomics to explore the subset of proteins that interact with 14-3-3s upon activation of the cAMP–PKA signalling pathway. Around 300 proteins were identified; the majority of these were also identified in previous screens targeting the PI 3-kinase–PKB pathway. A minority of proteins only identified in this cAMP–PKA screen included a previously undescribed interaction between 14-3-3s and a main player in autophagy, ATG9.

In this screen, we used the dimethyl labelling approached to label peptides with different stable isotopes so as to be able to quantify peptide enrichments upon various treatments (Boersema et al., 2008). This technique confers several advantages as it is relatively easy to label the digested peptides and cheap compared to other labelling methods including SILAC. A major hurdle in using the dimethyl labelling is that the data are indicative of ratios and not absolute stoichiometry of the different proteins. For instance, a protein whose stoichiometry of phosphorylation changed from 0.1% to 2% in response to forskolin would have a +/- forskolin ratio of 20 (provided the peptides were sufficiently abundant and gave clear mass spectrometry signals), whereas another phosphorylation stoichiometry changed from 5% to 100% would also have a ratio score of 20 in this screen. However, the latter protein would be considered a more relevant target of the signalling pathway. For instance, PANK2 which has an enrichment value of 1.02 upon forskolin stimulation and 0.79 upon H-89 and forskolin treatment does not clearly define a change in treatment (these values are represented as treatment/serum starved ratios). However, a closer inspection of PANK2 shows a clear regulation upon forskolin treatment (**Figure 4.22**). A similar phenomenon is seen with EML3, where the enrichment values (a ratio of 0.75 with forskolin/serum starved compared to -3.27 H-89 and forskolin/serum starved stimulation) in the high-throughput screen do not provide a

clear picture as to the regulation of the protein as observed when EML3 is expressed and screened through the panel of kinase inhibitors and activators (**Figure 4.13**). The plot graph suggests there is some difference in the two treatments; however, the fact that most of the points still lie fairly close to the line suggest otherwise. Nevertheless, this can still be accounted for by the fact that the relative values denote enrichment, and not stoichiometry, as discussed above. For instance, we see no relative enrichment between the two treatments for the proteins FAM122A and PANK2 which, however, have been observed to bind 14-3-3s in response to forskolin and this binding is reduced upon pre-treatment with H-89 (**Figure 4.22**) (Stafford, Synowsky and MacKintosh, unpublished results). In retrospect, it may have been preferable to cut the SDS-gels into fewer sections before differential isotope dimethyl labelling, because proteins may be unequally distributed on either side of the cut point in the different lanes. Furthermore, in such a large pull-down, those proteins binding to 14-3-3s with higher affinity and/or higher abundance in the cell would also be more enriched in the eluates; consequently, these proteins would also be proportionately labelled and represented as a higher fraction. Nonetheless, these screens are still important as they paint a portrait of the different proteins involved in 14-3-3-binding and provide an insight into the 14-3-3-phosphoproteome upon stimulation with different inhibitors and agonists. The data obtained from such screens then provides enough information to look at individual proteins systematically, which then gives a clearer picture of their regulation by 14-3-3s.

The phosphopeptide enrichment, although informative proved to be limited in terms of phosphopeptide yield. Since we were trialling the technique, it was still successful in identifying some known 14-3-3-binding phosphosites from the forskolin-treated samples (**Appendix VI**). However, further analysis confirmed that the column:peptide ratio we used was not optimal, which resulted in those peptides in higher abundance and/or binding better to the columns being eluted and subsequently identified preferentially (data not shown). For instance, we see AS160 with five phosphopeptides identified, one of which is the 14-3-3-binding Ser341 residue, but the second 14-3-3-phosphosite on this protein, namely phosphoSer642, was not identified (Geraghty et al., 2007; **Appendix VI**). The results show that the technique could be very useful for identifying 14-3-3-phosphosites if the yield could be improved. For instance, the column:peptide ratio could be enhanced by loading more peptides onto the columns. Furthermore, since the titanium dioxide beads have

a high binding capacity, the volume of the beads in the column could be amended depending on the amount of peptides. Overall, such enrichments would help considerably in identifying those phosphosites involved in 14-3-3-binding that do not conform to the known mode I and mode II binding sites. The benefit of persisting with this approach is that it would generate a short list of 14-3-3-binding sites from multiple proteins in one go. In this way, a priority list of residues would be generated for further testing by the conventional techniques of testing how non-phosphorylatable alanine mutations affect binding of the phosphoprotein to 14-3-3s.

It is becoming increasingly clear that 14-3-3s are able to bind multiple members of a protein family and differentially regulate their functions in cells. One of the first examples we had in the laboratory was of TBC1D1 and AS160 (TBC1D4). Both of these closely-related proteins were shown to bind 14-3-3s in response to various stimuli and effect different cellular outcomes (Geraghty et al., 2007; Chen et al., 2011). Other families have since been studied and shown to bind 14-3-3s in the MacKintosh laboratory, including the REEP family (Reep1-4), the srGAPs, FAM122(A-C) and the RING-type E3 ubiquitin ligases ZNRF1 and ZNRF2 (Hoxhaj et al., 2012; Tinti et al., 2012; Olsson, Stafford and MacKintosh, unpublished results). Interestingly, another such family of proteins was captured by 14-3-3s in response to forskolin, namely the DENND4s. These are proteins containing the DENN domain and which have been shown to function as Rab GEFs. There are eight such DENN-domain protein families and they are highly conserved throughout eukaryotes. From my experiments, the DENND4 family members, namely DENND4A (IRLB), DENND4B and DENND4C all bind to 14-3-3s in a phosphorylation-dependent manner in response to various stimuli (**Figures 4.8-4.11**). This is very interesting as although they share a high degree of similarity, these proteins bind 14-3-3s in response to different stimuli: DENND4A binds 14-3-3s pre-dominantly upon stimulation with the phorbol ester PMA which activates the PKC–ERK–p90RSK pathway while DENND4C binds 14-3-3s upon forskolin stimulation which activates the cAMP–PKA pathway, and to a lesser extent upon PMA stimulation (**Figures 4.9** and **4.11**). This is reminiscent with our recently proposed 'lynchpin' hypothesis whereby in a 14-3-3-binding family, one 14-3-3-binding site is conserved, enabling the second site to evolve and be regulated by different kinases on the other family members; for example, here the DENND4 proteins binding 14-3-3s in response to PMA but also other kinase activators

(Dubois et al., 2009; Johnson et al., 2011; Tinti et al., 2012). In such cases then, even minor changes in the amino acid sequence of the protein would enable the protein to be phosphorylated in response to different kinases, allowing the protein to be differentially regulated in response to different stimuli. This in turn generates an overload of signalling inputs for a single protein, which can then be used to explain the evolution of different members of a protein family being regulated by different stimuli, as in the case of the DENND4 proteins. A recent paper from our laboratory studying another 14-3-3-binding family, the REEPs, proposed the 'MIMO' (multiple input multiple output) hypothesis to describe the evolution of different proteins in a family being regulated by different stimuli to bind 14-3-3s, resulting in different outcomes (Tinti et al., 2012).

The differential regulation of DENND4 binding to 14-3-3s suggests that these proteins have evolved to perform different functions as a response to 14-3-3-binding; nonetheless, due to their high similarity, these proteins could also perform redundant functions to compensate for each other. For instance, Sano et al (2011) reported that knockdown of DENND4C did not completely abolish its function as the Rab GEF for Rab10 in mediating GLUT4 trafficking since it is possible that DENND4A or DENND4B could compensate for the silencing of DENND4C. This is not very surprising since all three DENND4 proteins are highly similar in the amino terminal, including the DENN domain regions; they only differ at their carboxy ends. Indeed, DENND4A and DENND4B have also been reported to function as Rab GEF for Rab10 *in vitro* (Yoshimura et al., 2010). It would be very interesting to delve further into the interactions of these DENND4 proteins with 14-3-3s. DENND4C was recently reported to be the Rab GEF for Rab10, which is involved in GLUT4 trafficking. Interestingly, our laboratory showed how TBC1D1 and AS160 also controlled GLUT4 trafficking in response to various stimuli whose phosphorylation promoted 14-3-3-binding to TBC1D1 and AS160 (Chen et al., 2011; Ducommun et al., 2012). While AS160 has been shown to be the Rab GAP for Rab10, DENND4C was recently shown to be the Rab GEF for Rab10; this is indeed very interesting as both these proteins controlling Rab10 function bind 14-3-3s. It would be very exciting to see if DENND4C binding to 14-3-3s also masks its intricate Rab GEF activity, as is the case with AS160.

Another protein we found bound to 14-3-3s in response to elevated cAMP levels in the cells was EML3. This protein was initially identified in a previous 14-

3-3 screen in this laboratory back in 2006 by Kathryn Geraghty (Geraghty and MacKintosh, unpublished results). EML3 belongs to the EMAP (Echinoderm Microtubule Associated Protein) proteins, which were initially identified in sea urchins as the most abundant microtubule-binding proteins (Suprenant et al., 2000). EML3 has a HELP domain, common to all EMAP proteins, which has been shown to be required for direct microtubule-binding (Pollman et al., 2006). Consequently, EML3 has been shown to associate with cytoplasmic microtubules during all stages of the cell-cycle and constantly shuttles between the cytoplasm and the nuclei during interphase (Tegha-Dungu et al., 2008). Tegha-Dungu and colleagues (2008) went on to show how the presence of EML3 was critical for the correct alignment of chromosomes during metaphase (Tegha-Dungu et al., 2008). Furthermore, EML3 also has seven WD40 repeats in its C-terminal, which bind to p32 and RanBP5 (**Figure 4.17**).

p32 has been described as a 'moonlighting' protein of multiple functions localising to various cellular compartments, including the nucleus, mitochondria and cytoplasm. p32 was originally identified through its co-purification with the splicing factor SF-2 and has a mitochondrial localisation signal (Krainer et al., 1991; Muta et al., 1997). The various reports on p32 only intensified the curiosity on this protein since it has been shown to be involved in oxidative phosphorylation, translation of mitochondria-encoded proteins and replication of viruses including HIV (Muta et al., 1997; Jiang et al., 1999; Zheng et al., 2003; Fogal et al., 2010). Knocking down p32 in cancer cells promoted a shift from oxidative phosphorylation to glycolysis (Fogal et al., 2010). A potential role of p32 in the nucleo-cytoplasmic shuttling of proteins has also been proposed following observations that p32 binds to the adenovirus core protein V soon after viral infection with the result being both proteins then move into the nucleus with the help of dynein and microtubules (Matthews and Russell, 1998; Suomalainen et al., 1999; Leopold et al., 2000). In addition, the phosphorylation of p32 by Erk1 was shown to be required for the translocation of p32 into the nucleus (Majumdar et al., 2002).

RanBP5, on the other hand, is an importin-beta family member, which was shown to be involved in the nuclear import of ribosomal proteins (Jäkel and Görlich, 1998). This raises the possibility that EML3 may act together with RanBP5 in the nuclear trafficking of p32. Interestingly, EML3 binds to 14-3-3s at its N-terminal end through phosphorylated Ser127 and Ser147 residues (**Figure 4.15**). We still do

not know the effect of 14-3-3-binding to EML3; since these residues are not within the functional HELP domain, it would be hard to speculate as to whether 14-3-3-binding to EML3 might affect its association with microtubules. Deletion of the HELP domain and WD40 repeats showed that EML3 failed to colocalise with microtubules during interphase and mitosis; in contrast, a truncated version of EML3 with the WD40 repeats deleted still colocalised with microtubules at interphase but the protein failed to accumulate at the mitotic spindles (Tegha-Dungu et al., 2008). In addition, knocking down EML3 resulted in the inhibition of cellular proliferation with cells accumulating during metaphase, inferring a role for EML3 at the spindle assembly checkpoint (Tegha-Dungu et al., 2008). These raise interesting questions about the possible function(s) of EML3-binding to 14-3-3s, p32 and RanBP5. It would be interesting to further analyse these interactions and to check if binding to 14-3-3s somehow prevented EML3 from accumulating in interphase nuclei and/or with spindle microtubules during mitosis (Tegha-Dughu et al., 2008). On the other hand, I showed that p32 and RanBP5 binding to EML3 do not depend on its interaction with 14-3-3s (**Figure 4.15**). It would be very exciting to know whether, in contrast, p32 and RanBP5 somehow altered EML3 binding to 14-3-3s. Also, it would be interesting to know whether viral replication was affected by knocking down EML3 and/or RanBP5.

A novel role of 14-3-3s in autophagy is becoming apparent as these docking proteins are shown to bind ATG9 (**Figure 4.18**), ULK1, Beclin-1 and Vps34, which are all key players in autophagy (Wang et al., 2010; Woo et al., 2010; Bach et al., 2011; Pozuelo-Rubio, 2011; Mack et al., 2012). The Atg1 kinase homologues ULK1 and ULK2 have been implicated in starvation-induced autophagy in mammals (Kuruyanagi et al., 1998; Chan et al., 2007). ULK1 forms a stable complex with mAtg13 and FIP200, and this complex is thought to be important in the regulation of autophagy in an mTOR-dependent manner (Jung et al., 2009; Hosokawa et al., 2009). Phosphorylation of ULK1 by AMPK on Ser555 in vitro was shown to be critical for 14-3-3-binding (Bach et al., 2011); interestingly, a second site phosphorylated by PKB/Akt was also identified (Ser774) on ULK1 but whether this was the second site leading to 14-3-3-binding was not clear (Bach et al., 2011). Since mTORC1 has been shown to phosphorylate and inhibit ULK1-kinase activity, it has been proposed that activation of AMPK by AICAR blocks mTORC1 inhibition on ULK1, thereby enabling the initiation of autophagy (Ganley et al.,

2009; Jung et al., 2009; Hosokowa et al., 2009). Furthermore, AICAR-induced phosphorylation of Raptor has also been reported leading to 14-3-3-binding to Raptor and this in turn results in mTORC1 inhibition (Gwinn et al., 2008; Lee et al., 2010). Although the precise outcome of 14-3-3-binding to ULK1 has not yet been elucidated, the fact that 14-3-3s are involved at multiple steps in the autophagy process hints at an important role.

Another autophagic complex described to have a high binding to 14-3-3s involves the Beclin 1/hVps34 proteins. Beclin 1 was first identified as an interacting partner for the anti-apoptotic protein Bcl-2 and later shown to be a haploinsufficient tumour-suppressor gene with reduced expression in different cancers (Liang et al., 1998; Aita et al., 1999; Yue et al., 2003; Funderberk et al., 2010). It is the mammalian orthologue of yeast Atg6 and has been shown to positively regulate autophagy (Liang et al., 1999). Depletion of 14-3-3τ expression has been shown to result in reduced Beclin 1 expression, affecting autophagy induction during serum starvation and rapamycin treatment (Wang et al., 2010). However, although Beclin 1 expression was shown to be regulated by 14-3-3τ, no direct interaction between these two proteins was shown to occur; interestingly, Beclin 1 was also pulled down in my 14-3-3-screen (**Appendix V**) but a closer look at the amino acid sequence of the protein did not show any potential 14-3-3-binding sites. Interestingly however, Beclin 1 also forms a complex with hVps34, a vacuolar sorting protein involved in autophagosome formation (Zeng et al., 2006). Interestingly, 14-3-3ζ was shown to bind and inhibit hVps34 activity upon PMA stimulation, involving phosphorylation of Thr197 and Ser212 (Pozuelo-Rubio, 2011). This binding reduced the lipid kinase activity of hVps34, and this lipid kinase activity is essential during autophagy initiation. Remarkably, upon starvation, 14-3-3 ζ was shown to dissociate from hVps34, leading to activation of hVps34 and autophagy (Pozuelo-Rubio, 2011). These autophagic proteins are in agreement with the emerging idea that sets of 14-3-3-binding protein families have co-evolved in the vertebrates, which regulate related functions, in this case autophagy. Similarly, sets of 14-3-3-binding proteins have been discovered in cellular metabolism and neurological pathologies (Tinti et al., 2012).

Although it is clear from our experiments that Atg9 also binds to 14-3-3s, much work has to be done to elucidate the result of such binding. Since most 14-3-3-binding promotes survival pathways, it would be very exciting to see in what way

14-3-3-binding to Atg9 would affect autophagy. Furthermore, since 14-3-3s generally bind to their target through dually-phosphorylated serine and/or threonine residues, it would be crucial to find these binding sites. A manual analysis of the Atg9 amino acid sequence has suggested Ser761 as a potential 14-3-3-binding site but further analyses are required to test this. Data from the phosphopeptide enrichment analysis also has potential candidate sites (**Appendix VI**). Altogether, these results show promising new roles for 14-3-3s in the regulation of mammalian autophagy.

Many proteins were identified in the two screens performed to capture targets that bind to 14-3-3s downstream of PI 3-kinase–PKB and of cAMP–PKA signalling, respectively. However, determining the relative degree of regulation of any given protein by each pathway will require further biochemical analysis. One reason is that the MS data only report on ratios of protein abundances in two samples, not the absolute amounts. Therefore, if a stimulus increases the proportion of a protein binding to 14-3-3s from 1% to 5%, the ratio would be the same as for a protein that changed from 20% to 100% binding. Therefore, the MS experiments report on trends, but not stoichiometry. Additionally, a few proteins being studied in the MacKintosh laboratory are targeted by different kinases in different signalling pathways. Some proteins, e.g. PANK2, FAM122A, which are predominantly activated by forskolin (**Figure 4.22**) do not seem to have high ratios in this screen. This could simply be that although they are identified in the pull-down, the amount of the protein being pulled down is low relative to its 14-3-3-binding affinity.

Another possibility for such observations in this pull down is the number of proteins competitively binding to 14-3-3s: those that bind best are quantified with higher ratios. When the protein in question is GFP-tagged and pulled down, a clearer regulation is observed with respect to 14-3-3 binding. For example, immunoprecipitated GFP-tagged PANK2 and FAM122A (C MacKintosh group, unpublished data) can be seen to be predominantly phosphorylated by forskolin in **Figure 4.22** but the quantified data from the screen does not provide such a clear picture.

In addition, there could also potentially be an overlap between PKA and PKB consensus phosphorylation motifs with each other, in addition to 14-3-3-binding consensus motifs. For instance, the minimal motif required by PKA to phosphorylate its substrate is RRXS/T while PKB prefers the RXRXXS/T motif; 14-

3-3s on the other hand have two consensus motifs mode I RSX(pS)XP and mode II RX(F/Y)X(pS)XP (**Chapter 1**). As can be seen, it would be very easy for 14-3-3-binding protein to have a large overlap with PKB-phosphorylated substrates. This might in part explain why such a large proportion of proteins identified in the screen in this chapter have also been seen in previous IGF1/insulin–PI 3-kinase screens in the laboratory. Furthermore, since the consensus phosphorylation motif of PKA is so short, it also minimally overlaps with the PKB consensus motif, which means that motifs that satisfy the specificity requirements for both kinases are possible. For instance, ZNRF2 which was identified by Dubois et al. (2009), in an insulin-stimulated 14-3-3-screen, has been shown to be regulated not by the insulin–PI 3-kinase pathway but rather by the cAMP–PKA and PKC–Erk pathways (Hoxhaj et al., 2012). Hence, although these large proteomics screen are immensely valuable in generating a wealth of data, biochemical analysis of individual proteins are crucial as they provide a clearer picture of the regulation of the protein in question.

Furthermore, another possibility for the observation of multiple proteins being highly enriched upon combined H-89 and forskolin treatment may be suggestive of a cAMP-dependent but PKA-independent event. Using fluorescence-based reporters, Aye-Han and colleagues (2012) showed that treating cells with H-89 and forskolin inhibits PKA but still triggers activation of cAMP. Thus, while using H-89 in combination with forskolin inhibits PKA, cAMP-mediated PKA-independent events can still occur, through ERK, PKB or Epac for example (**Chapter 1**). Moreover, H-89 has also been shown to inhibit other kinases in the AGC family including PKB, AMPK, MSK1, S6K1, PKD1, RSK1 and RSK2 among others (Bain et al., 2007). Nonetheless, in most cases a clear signature of the protein is observed when comparing its 14-3-3-binding occurring upon FSK stimulation, and which is then subsequently lost upon pre-treatment with H-89.

Overall, my 14-3-3 screen generated a high number of potential 14-3-3-binding candidates. The most interesting targets now need to be biochemically validated as 14-3-3-interactors and the functionality of this binding must be determined, for example with the DENND4 proteins and ATG9.

Chapter five

General conclusions and future perspectives

5.1 General conclusions

The work presented in this thesis explored the regulation of two major classes of proteins which regulate serine/threonine-phosphorylated proteins, namely protein phosphatases of the PPP family and 14-3-3s, upon activation of the cAMP-PKA pathway. Reversible protein phosphorylation occurs in up to a third of all eukaryotic proteins (Bollen and Beullens, 2002). Remarkably, serine and threonine phosphorylations account for over 90% of all phosphorylated amino acids (Olsen et al., 2006). Protein phosphatases regulate proteins through dephosphorylation; on the other hand, phosphorylation of serine/threonine residues promote 14-3-3-binding to target proteins. Although not common, a few proteins are known to bind both protein phosphatases and 14-3-3s. For instance, MYPT1 was shown to be in a complex with PP1 and 14-3-3s in the regulation of cell adhesion (Zagorska et al., 2010). Also FAM122A, initially identified as a 14-3-3-binding protein in our laboratory has also been observed to interact with PP2A, and the phosphatase and 14-3-3s can exist together in a complex with FAM122A (Stafford, Murugesan and MacKintosh, unpublished results). Since we could not find any proteins whose interaction with protein phosphatases was clearly regulated by cAMP elevating agents from the phosphatase screens in **Chapter 3**, I decided to focus more on the 14-3-3-phosphoproteomics studies.

One of the major advantages of doing a high-throughput screen is the amount of information generated at one go; consequently it becomes a mammoth task to analyse all the individual proteins in such a screen. Nonetheless, these large-scale 14-3-3-binding proteomic studies suggest that the 14-3-3-phosphoproteome is much larger than what was originally thought and no one screen is near saturation since new binding candidates are constantly being reported. Based on the known 14-3-3-binding consensus motifs, members of the CAMK and AGC kinases are most likely to phosphorylate 14-3-3-binding targets; however, studying the full plethora of 14-3-3-binding proteins is somewhat restricted to those kinases for which there are good agonists available. In addition, most 14-3-3-binding proteins have two tandemly phosphorylated sites generated by one or more kinases; binding to 14-3-3s in most cases results in regulation of the protein. Since each kinase on one of the two sites can have a different outcome, this generates a very tight regulatory control of the protein upon 14-3-3-binding. Studies from our laboratory and others have been quite successful in identifying multiple proteins binding to 14-3-3s in response to

activation of different signalling pathways, including the IGF1/insulin–PI 3-kinase–PKB, PKC–Erk–p90RSK and cAMP–PKA pathways. Extensive bioinformatical analyses conducted in our laboratory has generated an 'overview' of the 14-3-3-interactome based on our own 14-3-3-screens and reported 14-3-3-interactions in the literature (Johnson et al., 2011; Tinti et al., 2012). Proteins that were biochemically validated, with their phosphosites elucidated were collected from the literature and labelled as 'golden standards' (Johnson et al., 2011). Furthermore, it had also been discovered that the lists of 14-3-3-binding phosphoproteins, both 'golden standards' and those identified in proteomics screens, are highly enriched in members of protein families of two to four members, whose origins were traced to the same point in evolution – two rounds of whole genome duplication at the origins of the vertebrates. Moreover, in several protein families, it was found most, if not all, members of a given protein family could bind to 14-3-3s. However, many of these protein members were also seen to be differentially regulated upon different stimuli, for example TBC1D1 and AS160, the REEP family and as shown in this thesis, the DENND4 family (Geraghty et al., 2007; Tinti et al., 2012). This is exciting because it means that the signal multiplexing properties of these families, with different family member being regulated by 14-3-3s in response to different signalling pathways, means that such signalling complexity may have been fundamental to the evolution of the vertebrate animals, including humans.

Recent papers on whole genome duplications in vertebrates coupled to the recent genomic sequencing of amphioxus have helped our understanding of this observation. Around 500 million years ago, the vertebrate genome arose from two rounds of whole genome duplications (2R-WGD), from which several 2R-ohnologue protein families then emerged (Huminiecki et al., 2010; Makino et al., 2010). 2R-ohnologues have been described as those protein-coding genes, which were duplicated during the 2R-WGD. Amphioxus (also known as *Branchiostoma* and lancelet) is an invertebrate that is the most basal, least-derived member of the chordates. The amphioxus genome has shown that its ancestors did not go through the 2R-WGD, which means that the amphioxus has one 'ancestral' protein for every human 2R-ohnologue family (Putnam et al., 2008; Tinti et al., 2012). Most of the 14-3-3-binding families in humans seem to have evolved from the 2R-WGD event. In these families, one or more members have a common 14-3-3-phosphosite, while the other site varies and could be regulated by different stimuli to effect different

functions, giving rise to the 'lynchpin' hypothesis (Tinti et al., 2012). The regulation of proteins in 2R-ohnologue families through multiple kinases generates a multiplex signalling system similar to the multiple input multiple output system (MIMO) (Tinti et al., 2012). 14-3-3-binding proteins are phosphorylated by kinases involved in different signalling pathways which regulate growth factor and developmental signalling, membrane trafficking and metabolism, deregulation of any component in these signalling pathways could result in diseases. A notable 91% association has been reported between 14-3-3-binding proteins (gold and silver standard proteins) and diseases including various cancers, diabetes and neurological disorders (Tinti et al., 2012). Understanding the intricate regulation of 14-3-3-binding proteins which are impaired in these signalling pathways leading to pathological conditions is thus very important.

5.2 Future perspectives:

Following up on proteins such as the DENND4s would be helpful towards understanding GLUT4 trafficking. Phosphorylation of AS160 by PKB at Ser341 and Thr642 upon insulin stimulation promotes 14-3-3 binding; this binding is thought to inhibit the RabGAP domain of AS160, so that it is no longer able to hydrolyse the GTP from Rab10 to control GLUT4 trafficking. The DENND4C protein has been reported to be a GEF that acts in GLUT4 trafficking (Sano et al., 2011). A key question arising from these studies is whether 14-3-3s somehow alter the GEF activity of the DENND4 proteins towards Rab10, to complement and coordinate with the regulation of AS160 and TBC1D1 by 14-3-3. For instance, does 14-3-3-binding to DENND4C mask the GEF (DENN) domain of the protein, such that it can no longer promote Rab10 activity? In order to further investigate this, it would be critical to first identify the sites of phosphorylation on DENND4C that mediate 14-3-3-binding. For example, since we now know DENND4C binding to 14-3-3s is promoted upon forskolin stimulation, PKA is the most likely kinase involved in phosphorylating this protein (**Figure 4.11**). In vitro assays could be performed to further test PKA as the upstream kinase for DENND4C phosphorylation. The regulation of Rab10 could potentially be another example of antagonising actions of PKA and PKB in the control of GLUT4 trafficking by promoting 14-3-3-binding to DENND4C and AS160 respectively. For instance, if PKA-induced 14-3-3-binding on DENND4C were to reduce/mask the GEF activity of DENND4C, this would

result in an overall decrease in GLUT4 trafficking by decreasing the GTP loading of the Rab proteins. On the other hand, if PKA-mediated 14-3-3 binding were to activate the GEF activity of DENND4C, this would amplify the effects of inhibiting AS160 and enhance the GTP loading of the Rab proteins. Measuring GLUT4 levels following forskolin stimulation in DENND4C-expressing cells should potentially provide clues as to whether 14-3-3-binding alters the RabGEF activity of DENND4C. However, this would have to be performed in cells such as adipocytes that use GLUT4 for glucose import.

The next experimental stage is prepared, as the potential 14-3-3-binding sites in our DENND4 constructs have been mutated to generate non-phosphorylatable alanine residues: biochemical analyses of these mutants should be fairly quick and provide clues into the probable 14-3-3-binding phosphosites of these DENND4 proteins. Phosphomapping analyses of the protein could also be explored to find phosphorylated amino acids on the protein. Following on then, it would be very interesting to see whether abolishing the 14-3-3-binding sites on DENND4C would restore GLUT4 trafficking, even after forskolin stimulation.

Another membrane trafficking protein that I identified and studied was Atg9. The increasing evidence of autophagy-deregulation in diseased states makes it imperative to fully understand the proteins regulating this process. In light of the recent evidence suggesting Atg9-containing vesicles form the autophagosome during autophagy initiation (Yamamoto et al., 2012), it would be exciting to understand how 14-3-3-binding to this autophagic protein might regulate its function. As a first step towards understanding 14-3-3-binding, it would be important to find the phosphosites of Atg9 which mediate 14-3-3-binding. As I mentioned in **Chapter 4**, a manual scan of the Atg9 amino acid sequence suggested Ser761 as a potential candidate for 14-3-3-binding. So far, I have been unable to find other possible candidate phosphosites, but doing an experimental phosphomapping analysis of Atg9 should help in identifying other phosphorylated residues. Furthermore, it would be interesting to explore the effects of 14-3-3-binding to Atg9 with respect to autophagy. For instance, would 14-3-3-binding enhance or reduce Atg9 function in the initiation of autophagy? Stimulating cells with forskolin upon amino acid starvation and immunoblotting for markers of autophagy Rab7 and LC-3 should provide insights into whether 14-3-3-binding alters Atg9 activity during autophagy. The known direct interactors of Atg9 thus far are quite restricted to

FAM48 and myosin II. A number of potential Atg9-interactors have been identified from my GFP-ATG9 gel using mass spectrometry data (**Appendix VII**). Validating some of these interactors would provide crucial understanding into autophagy. 14-3-3s and mTOR (mammalian target of rapamycin) are both implicated in autophagy through their interactions with other autophagic proteins such as Beclin-1, Vps34 and ULK1 (discussed in **Chapter 4**). Since mTOR has also been identified from the Coomassie gel of GFP-Atg9 pull down (**Figure 4.20**), it would be exciting to see whether mTOR is able to interact with Atg9 directly. mTOR has been implicated in the negative control of autophagy through its interactions with ULK1 and AMPK (Kim et al., 2011; Löffler et al., 2011). Notably, ULK1 has also been reported to bind 14-3-3s upon AMPK phosphorylation and although the immediate effect of this binding is still unknown, some AMPK-phosphorylation sites on ULK1 have recently been reported to be crucial in regulating Atg9 trafficking (Mack et al., 2012). Furthermore, Rab7, an early marker of autophagy was also co-immunoprecipitated with Atg9 along with a number of other Ras-related Rab proteins, although no previous interaction of Atg9 with Rab7 has been reported (**Appendix VII**). Proteins in nutrient sensing and membrane trafficking were identified in the Atg9 immunoprecipitates, together with 14-3-3s and knowing whether these proteins really interact with Atg9 would very exciting and further help our understanding of the regulation of autophagy.

Overall therefore, the data presented in my thesis has explored another pathway in 14-3-3-signalling, namely cAMP—PKA signalling, that involves several 14-3-3-binding proteins and many potential candidates have emerged. I have shown how binding of the DENND4 proteins to 14-3-3s are regulated by different kinases, in agreement with the 2R-ohnologue proteins, the ‘lynchpin’ and ‘MIMO’ hypotheses. In summary, my studies have opened new avenues of 14-3-3 research that will hopefully be further explored in our laboratory and others.

References:

Aandahl E.M., Aukrust P., Skålhegg B.S., Müller F., Frøland S.S., Hansson V. and Taskén K. (1998). Protein kinase A type I antagonist restores immune responses of T cells from HIV-infected patients. FASEB Journal, 12, 855-862.

Ahn J., McAvoy T., Rakhilin S.V., Nishi A., Greengard P. and Nairn A.C. (2007) Protein kinase A activates protein phosphatase 2A by phosphorylation of the B56δ subunit. Proceedings of the National Academy of Sciences USA, 104, 2979-2984.

Aiston S., Hampson L.J., Arden C., Iynedjian P.B. and Agius L. (2006) The role of protein kinase B/Akt in insulin-induced inactivation of phosphorylase in rat hepatocytes. Diabetologia, 49, 174-182.

Aita V.M. Liang X.H., Murty V.V., Pincus D.L., Yu W., Cayanis E., Kalachikov S., Gilliam T.C. and Levine B. (1999) Cloning and genomic organization of beclin 1, a candidate tumor suppressor gene on chromosome 17q21. Genomics, 59, 59-65.

Aitken A. (2002) Functional specificity in 14-3-3 isoform interactions through dimer formation and phosphorylation. Chromosome location of mammalian isoforms and variants. Plant Molecular Biology, 50, 993-1010.

Aitken A. (2006) 14-3-3 proteins: A historic overview. Seminars in Cancer Biology, 16, 162-172.

Aitken A. (2011) Post-translational modification of 14-3-3 isoforms and regulation of cellular function. Seminars in Cell and Developmental Biology, 22, 673-680.

Aitken A., Baxter H., Dubois T., Clokie S., Mackie S., Mitchell K., Peden A. and Zemlickova E. (2002) 14-3-3 proteins in cell regulation. Biochemical Society Transactions, 30, 351-421.

Aitken A., Bilham T. and Cohen P. (1982) Complete Primary structure of protein phosphatase inhibitor-1 from rabbit skeletal-muscle. European Journal of Biochemistry, 126, 235-246.

Allen P.B., Kwoni Y-G., NairnA.C. and Greengard P. (1998). Isolation and characterization of PNUTS, a putative Protein Phosphatase-1 nuclear targeting subunit. Journal of Biological Chemistry, 273, 4089-4095.

Alessi D.R., Gomez N., Moorhead G., Lewis T., Keyse S.M. and Cohen P. (1995) Inactivation of p42 MAP kinase by protein phosphatase 2A and a protein tyrosine phosphatase, but not CL100, in various cell lines. Current Biology, 5, 283-295.

Alessi D., MacDougall L.K., Sola M.M., Ikebe M. and Cohen P. (1992). The control of protein phosphatase-1 by targeting subunits: the major myosin phosphatase in avian smooth muscle is a novel form of protein phosphatase-1. European Journal of Biochemistry, 210, 1023-1035.

Ali A., Zhang J., Bao S., Liu I., Otterness D., Dean N.M., Abraham R.T. and Wang X.F. (2004). Requirement of protein phosphatase 5 in DNA-damage-induced ATM activation. Genes and Development, 18, 249-54.

Allen P.B., Kwon Y.G., Nairn A.C. and Greengard P. (1998). Isolation and characterization of PNUTS, a putative protein phosphatase 1 nuclear targeting subunit. Journal of Biological Chemistry, 273, 4089-4095.

Amsen E.M., Pham N., Pak Y. and Rotin D. (2006) The guanine nucleotide exchange factor CNrasGEF regulates melanogenesis and cell survival in melanoma cells. Journal of Biological Chemistry, 281, 121-128.

Anderson N.G., Maller J.L., Tonks N.K. and Sturgill T.W. (1990) Requirement for integration of signals from two distinct phosphorylation pathways for activation of MAP kinase. Nature, 343, 651-653.

Andjelković M., Jakubowicz T., Cron P., Ming X.F., Han J.W. and Hemmings B.A. (1996) Activation and phosphorylation of a pleckstrin homology domain containing protein kinase (RAC-PK/PKB) promoted by serum and protein phosphatase inhibitors. Proceedings of the National Academy of Sciences USA, 93, 5699-5704.

Andreassen P.R., Lacroix F.B., Villa-Moruzzi E. and Margolis R.L. (1998). Differential subcellular localization of protein phosphatase-1 α, γ1, and δ isoforms during both interphase and mitosis in mammalian cells. Journal of Cell Biology, 141, 1207-1215.

Andreeva A.V. and Kutuzov M.A. (1999) RdgC/PP5-related phosphatases: novel components in signal transduction. Cell Signalling, 11, 555-562.

Argasinska J., Rana A.A., Gilchrist M.J., Lachani K., Young A. and Smith J.C. (2009) Loss of REEP4 causes paralysis of the Xenopus embryo. International Journal of Developmental Biology, 53, 37-43.

Ariyoshi M and Schwabe J.W.R. (2003) A conserved structural reveals the essential transcriptional repression function of Spen proteins and their role in developmental signalling. Genes and Development, 17, 1909-1920.

Ariza R.R., Keyse S.M., Moggs J.G. and Wood R.D. (1996) Reversible protein phosphorylation modulates nucleotide excision repair of damaged DNA by human cell extracts. Nucleic Acid Research, 24, 433-440.

Armstrong C.G., Browne G.J., Cohen P. and Cohen P.T.W. (1997) PPP1R6, a novel member of the family of glycogen-targeting subunits of protein phosphatase 1. FEBS Letters, 418, 210-214.

Armstrong D.L. (1989) Calcium channel regulation by calcineurin, a Ca^{2+}-activated phosphatase in mammalian brain. Trends in Neuroscience, 12, 117-122.

Aye-Han N-N., Allen M.D., Ni Q. and Zhang J. (2012) Parallel tracking of cAMP and PKA signaling dynamics in living cells with FRET-based fluorescent biosensors. Molecular BioSystems, 8, 1435-1440.

Bach M., Larance M., James D.E. and Ramm G. (2011) The serine/threonine kinase ULK1 is a target of multiple phosphorylation events. Biochemical Journal, 440, 283-291.

Bain J., Plater L., Elliott M., Shpiro N., Hastie C.J., McLauchlan H., Klevernic I., Arthur J.S.C., Alessi D.R. and Cohen P. (2007) The selectivity of protein kinase inhibitors: a further update. Biochemical Journal, 408, 297-315.

Ballou L., Brautigan D.L. and Fischer E.H. (1983) Subunit structure and activation of inactive phosphorylase phosphatase. Biochemistry, 22, 3393-3399.

Ballou L.M., Jenö P. and Thomas G. (1988) Protein phosphatase 2A inactivates the mitogen-stimulated S6 kinase from Swiss mouse 3T3 cells. Journal of Biology Chemistry, 263, 1188-1194.

Barker H.M., Brewis N.D., Street A.J., Spurr N.K. and Cohen P.T.W. (1994) Three genes for protein phosphatase 1 map to different human chromosomes: sequence expression and gene localisation of protein serine/threonine phosphatase 1 β (PPP1Cβ) Biochimica et Biophysica Acta, 1220, 212–218.

Baskin T.I. and Wilson J.E. (1997) Inhibitors of protein kinases and phosphatases alter root morphology and disorganize cortical microtubules. Plant Physiology, 113, 493-502.

Bauman A.L., Soughayer J., Nguyen B.T., Willoughby D., Carnegie G.K., Wong W., Hoshi N., Langeberg L.K., Cooper D.M.F, Dessauer C.W. and Scott J.D. (2006) Dynamic regulation of cAMP synthesis through anchored PKA-adenylyl cyclase V/VI complexes. Molecular Cell, 23, 925-931.

Baurle I., Smith L., Baulcombe D.C. and Dean C. (2007) Widespread role for the flowering time regulators FCA and FPA in RNA-mediated chromatin silencing. Science, 308, 109-112.

Benned-Jensen T., Mokrosinski J. and Rosenkilde M.M. (2011) The E92K melanocortin 1 receptor mutant induces cAMP production and arrestin recruitment but not ERK activity indicating biased constitutive signaling. Plos One, 6, e24644.

Bialojan C. and Takai A. (1988) Inhibitory effect of a marine-sponge toxin, okadaic acid, on protein phosphatases: Specificity and kinetics. Biochemical Journal, 256, 283-290.

Bialojan C., Rüegg J.C. and Takai A. (1988) Effects of okadaic acid on isometric tension and myosin phosphorylation of chemically skinned guinea-pig taenia coli. Journal of Physiology, 398, 81-95.

Bibb J.A., Snyder G.L., Nishi A., Yan Z., Meijer L., Fienberg A.A., Tsai L.H., Kwon Y.T., Girault J.A., Czernik A.J., Huganir R.L., Hemmings, H.C. Jr, Nairn A.C. and Greengard P. (1999) Phosphorylation of DARPP-32 by Cdk5 modulates dopamine signalling in neurons. Nature, 402, 669-971.

Billington C.K. and Hall I.P. (2012) Novel cAMP signaling paradigms: therapeutic implications for airway disease. British Journal of Pharmacology, 166, 401-410

Boersema P.J., Aye T.T., van Veen T.A.B., Heck A.J.R. and Mohammed S. (2008) Triplex protein quantification based on stable isotope labelling by peptide dimethylation applied to cell and tissue lysates. Proteomics, 8, 4624-4632.

Bollen M. (2001). Combinatorial control of protein phosphatase-1. Trends in Biochemical Science, 26, 426-431.

Bollen M. and Beullens M. (2002) Signalling by protein phosphatases in the nucleus. Trends in Cell Biology, 12, 138-145.

Bollen M., Peti W., Ragusa M.J. and Beullens M. (2010) The extended PP1 toolkit: designed to create specificity. Trends in Biochemical Sciences, 35, 450-458.

Boston P.F., Jackson P. and Thompson R.J. (1982) Human 14-3-3 protein: Radioimmunoassay, tissue distribution and cerebrospinal fluid levels in patients with neurological disorders. Journal of Neurochemistry, 38, 1475-1482.

Bozulic L., Surucu B., Hynx D. and Hemmings B.A. (2008) PKBalpha/Akt1 acts downstream of DNA-PK in the DNA double-strand break response and promotes survival. Molecular Cell, 30, 203-213.

Brady M.J., Nairn A., and Saltiel A.R. (1997) The regulation of glycogen synthase by protein phosphatase 1 in 3T3–L1 adipocytes. Evidence for a potential role for DARPP-32 in insulin action. Journal of Biological Chemistry, 272, 29698–29703.

Bridges D. and Moorhead G.B.G. (2005) 14-3-3 proteins: A number of functions for a numbered protein. Science STKE, 296, re10.

Burdick K.E., Kamiya A., Hodgkinson C.A., Lencz T., DeRosse P., Ishizuka K., Elashvili S., Arai H., Goldman D., Sawa A. and Malhotra A.K. (2008) Elucidating the relationship between DISC1, NDEL1 and NDE1 and the risk for schizophrenia: evidence of epistasis and competitive binding. Human Molecular Genetics, 17, 2462-2473.

Burgering B. and Coffer P.J. (1995) Protein kinase B (c-Akt) in phosphatidylinositol-3-OH kinase signal transduction. Nature, 376, 599-602.

Buscà R. and Ballotti R. (2000) Cyclic AMP a key messenger in the regulation of skin pigmentation. Pigment Cell Research, 13, 60-69.

Buscà R., Abbe P., Mantoux F., Aberdam E., Peyssonnaux C., Eychène A., Ortonne J.P. and Ballotti R. (2000) Ras mediates the cAMP-dependent activation of extracellular signal-regulated kinases (ERKs) in melanocytes. EMBO Journal, 19, 2900-2910.

Campos A. and Vasconcelos V. (2010) Molecular mechanisms of microcystin toxicity in animal cells. International Journal of Molecular Sciences, 11, 268-287.

Cao Y., Mahrenholz A.M., De Paoli-Roach A.A and Roach P.J. (1993). Characterisation of rabbit skeletal muscle glycogenin. Tyrosine 194 is essential for function. Journal of Biological Chemistry, 268, 14687-14693.

Carmody L.C., Baucum A.J. 2nd, Bass M.A. and Colbran R.J. (2008) Selective targeting of the gamma1 isoform of protein phosphatase 1 to F-actin in intact cells requires multiple domains in spinophilin and neurabin. FASEB, 22, 1660-1671.

Carnegie G.K., Sleeman J.E., Morrice N., Hastie J.C., Peggie M.W., Philp A., Lamond A.I. and Cohen P.T.W. (2003) Protein phosphatase 4 interacts with the Survival of Motor Neurons complex and enhances the temporal localisation of snRNPs. Journal of Cell Signalling, 116, 1905-1913.

Carr S., Biemann K., Shoji S., Parmalee D.C. and Titani K. (1982) N-Tetradecanoyl is the NH2-terminal blocking group of the catalytic subunit of cAMP-dependent protein kinase from bovine cardiac muscle. Proceedings of the National Academy of Sciences USA, 79, 6128-6131.

Carracedo A., Ma L., Teruya-Feldstein J., Rojo F., Salmena L., Alimonti A., Egia A., Sasaki A.T., Thomas G., Kozma S.C., Papa A., Nardella C., Cantley L.C., Baselga J. and Pandolfi P.P. (2008) Inhibition of mTORC1 leads to MAPK pathway activation through a PI3K-dependent feedback loop in human cancer. Journal of Clinical Investigation, 118, 3065-3074.

Caudwell F. B., Hiraga A. and Cohen P. (1986) Amino acid sequence of a region on the glycogen-binding subunit of protein phosphatase-1 phosphorylated by cyclic AMP-dependent protein kinase. FEBS Letters, 194, 85-90.

Ceulemans H. and Bollen M. (2006) A tighter RVxF motif makes a finer sift. Chemical Biology, 13, 6-8.

Ceulemans H., Vulsteke V., De Maeyer M., Tatchell K., Stalmans W. and Bollen M. (2002) Binding of the concave surface of the Sds22 superhelix to the alpha 4/alpha 5/alpha 6-triangle of protein phosphatase-1. Journal of Biological Chemistry, 277, 47331-47337.

Chamousset D., De Wever V., Moorhead G.B., Chen Y., Boisvert F.M., Lamond A.I. and Trinkle-Mulcahy L. (2010) RRP1B targets PP1 to mammalian cell nucleoli and is associated with Pre-60S ribosomal subunits. Molecular Biology of the Cell, 21, 4212-4226.

Chan E.Y., Kir S. and Tooze S.A. (2007) siRNA screening of the kinome identifies ULK1 as a multidomain modulator of autophagy. Journal of Biological Chemistry, 282, 25464-25474.

Chen S., Murphy J., Toth R., Campbell D.G., Morrice N.A. and MacKintosh C. (2008) Complementary regulation of TBC1D1 and AS160 by growth factors, insulin and AMPK activators. Biochemical Journal, 409, 449-459.

Chinkers M. (2001) Protein phosphatase 5 in signal transduction. Trends in Endocrinology and Metabolism, 12, 28-32.

Cohen P. (1988) Protein phosphorylation and hormone action. Proceedings of the Royal Society of London, B234, 115-144.

Cohen P. (2002) The origins of protein phosphorylation. Nature Cell Biology, 4, E127-E130.

Cohen P. (1985) The role of protein phosphorylation in the hormonal control of enzyme activity. European Journal of Biochemistry, 151, 439-448.

Cohen P. (1989) The structure and regulation of protein phosphatases. Annual Reviews of Biochemistry, 58, 435-508.

Cohen P., Nimmo H.G. and Proud C.G. (1978) How does insulin stimulate glycogen synthesis? Biochemical Society Symposium, 43, 69-95.

Cohen P.T.W. (2002a) Protein phosphatase 1-targeted in many directions. Journal of Cell Science, 115, 241-256.

Cohen P.T.W. (2011) Sorting the protein phosphatases: okadaic acid led the way. Biochemical Journal, doi:10.1042/BJ20091054.

Cohen P.T.W., Philip A. and Vazquez-Martin C. (2005) Protein phosphatase 4-from obscurity to vital functions. FEBS Letters, 579, 3278-3286.

Connor J.H., Quan H.N., Ramaswamy N.T., Zhang L., Barik S., Zheng J., Cannon J.F., Lee E.Y. and Shenolikar S. (1998) Inhibitor-1 interaction domain that mediates the inhibition of protein phosphatase-1. Journal of Biological Chemistry, 273, 27716-27724.

Connor J.H., Weiser D.C., Li S., Hallenbeck J.M. and Shenolikar S. (2001) Growth arrest and DNA damage-inducible protein GADD34 assembles a novel signalling complex containing protein phosphatase-1 and inhibitor-1. Molecular and Cellular Biology, 21, 6841-6850.

Cross D.A.E., Alessi D.R., Cohen P., Andjelkovich M. and Hemmings B.A. (1995) Inhibition of GSK3 by insulin mediated by protein kinase B. Nature, 378, 785-789.

Csortos C., Zolnierowicz S., Bakó E., Durbin S.D. and DePaoli-Roach A.A. (1996). High complexity in the expression of the B' subunit of protein phosphatase 2A0. Evidence for the existence of at least seven novel isoforms. Journal of Biological Chemistry, 271, 2578-2588

Damer C.K., Partridge J., Pearson W.R. and Haystead T.A. (1998) Rapid identification of protein phosphatase 1-binding proteins by mixed peptide sequencing and data base searching. Characterization of a novel holoenzymic form of protein phosphatase 1. Journal of Biological Chemistry, 273, 24396-24405.

Datta S.R., Dudek H., Tao X., Masters S., Fu H., Gotoh Y., Greenberg M.E. (1997) Akt phosphorylation of BAD couples survival signals to the cell-intrinsic death machinery. Cell, 91, 231-241.

Davis RJ. (1993) The mitogen-activated protein kinase signal transduction pathway. Journal of Biological Chemistry, 268, 14553-14556.

Dawson J.F. and Holmes C.F. (1999) Molecular mechanisms underlying inhibition of protein phosphatases by marine toxins. Frontiers in Bioscience, 4, D646-D658.

De Rooij J., Rehmann H., Van Triest M., Cool R.H, Wittinghofer A. and Bos J.L. (2000) Mechanism of regulation of the Epac family of cAMP-dependent RapGEFs. Journal of Biological Chemistry, 275, 20829-20836.

De Rooij J., Zwartkruis F.J., Verheijen M.H., Cool R.H., Nijman S.M., Wittinghofer A. and Bos J.L. (1998) Epac is a Rap1 guanine-nucleotide-exchange factor directly activated by cyclic AMP. Nature, 396, 474-477.

del Peso L., Gonzalez-Garcia M., Page C., Herrera R. and Nunez G. (1997) Interleukin-3-induced phosphorylation of BAD through the protein kinase Akt. Science, 278, 687-689.

Dent P., Campbell D.G., Caudwell B. and Cohen P. (1990) Identification of three in vivo phosphorylation sites on the glycogen binding subunit of protein phosphatase 1 from rabbit skeletal muscle and their response to adrenalin. FEBS Letters, 259, 281-285.

Depaoli-Roach A.A., Park I.K., Cerovsky V., Csortos C., Durbin S.D., Kuntz M.J., Sitikov A., Tang P.M., Verin A. and Zolnierowicz S. (1994) Serine/threonine protein phosphatases in the control of cell function. Advances in Enzyme Regulation, 34, 199-224.

de Souza R.F. and Aravind L. (2010) UMA and MABP domains throw light on receptor endocytosis and selection of endosomal cargoes. Bioinformatics, 26, 1477-1480.

Desdouits F., Cheetham J. J., Huang H. B., Kwon Y. G., da Cruz e Silva E. F., Denefle P., Ehrlich M. E., Nairn A. C., Greengard P. and Girault J. A. (1995) Biochem. Biophys. Research Communications, 206, 652-658.

Dessauer C.W. (2009) Adenylyl cyclase-A-kinase anchoring protein complexes: The next dimension in cAMP signalling. Molecular Pharmacology, 76, 935-941.

Djouder N., Metzler S.C., Schmidt A., Wirbelauer C., Gstaiger M., Aebersold R., Hess D. and Krek W. (2007) S6K1-mediated disassembly of mitochondrial URI/PP1gamma complexes activates a negative feedback program that counters S6K1 survival signaling. Molecular Cell, 28, 28-40.

Doherty M.J., Moorhead G., Morrice N., Cohen P. and Cohen P.T. (1995) Amino acid sequence and expression of the hepatic glycogen-binding (GL)-subunit of protein phosphatase-1. FEBS Letters, 375, 294-298.

Dombradi V., Axton J.M., Barker H.M. and Cohen P.T.W. (1990) Protein phosphatase 1 activity in Drosophila mutants with abnormalities in mitosis and chromosome condensation. FEBS Letters, 275, 39-43.

Douglas P., Moorhead G.B., Ye R. and Lees-Miller S.P. (2001) Protein phosphatases regulate DNA-dependent protein kinase activity. Journal of Biological Chemistry, 276, 18992-18998.

Dubois F., Vandermoere F., Guernez A., Murphy J., Toth R., Chen S., Geraghty K.M., Morrice N. and MacKintosh C. (2009) Differential 14-3-3-affinity capture reveals new downstream targets of PI 3-kinase signalling. Molecular and Cellular Proteomics, 8, 2487-2499.

Dubois T., Rommel C., Howell S., Steinhussen U., Soneji Y., Morrice N., Moelling K. and Aitken A. (1997) 14-3-3 is phosphorylated by casein kinase I on residue 233: Phosphorylation at this site in vivo regulates Raf/14-3-3 interaction. Journal of Biological Chemistry, 272, 28882-28888.

Ducommun S., Wang H.Y., Sakamoto K., MacKintosh C. and Chen S. (2012) Thr649Ala-AS160 knock-in mutation does not impair contraction/AICAR-induced glucose transport in mouse muscle. American Journal Physiology. Endocrinology and Metabolism, 302, E1036-1043.

Dumaz N. and Marais R. (2003) Protein kinase A blocks Raf-1 activity by stimulating 14-3-3 binding and blocking Raf-1 interaction with Ras. Journal of Biological Chemistry, 278, 29819-29823.

Egloff M. P., Johnson D.F., Moorhead G., Cohen P.T., Cohen P. and Barford D. (1997) Structural basis for the recognition of regulatory subunits by the catalytic subunit of protein phosphatase 1. EMBO Journal, 16, 1876-1887.

Endo S., Zhou X., Connor J., Wang B. and Shenolikar S. (1996) Multiple structural elements define the specificity of recombinant human inhibitor-1 as a protein phosphatase-1 inhibitor. Biochemistry, 35, 5220-5228.

Englaro W., Rezzonico R., Durand-Clément M., Lallemand D., Ortonne J.P. and Ballotti R. (1995) Mitogen-activated protein kinase pathway and AP-1 are activated during cAMP-induced melanogenesis in B-16 melanoma cells. Journal of Biological Chemistry, 270, 24315-24320.

Evans D.R.H. and Hemmings B.A. (2000) Important role for phylogenetically invariant PP2Aca active site and C-terminal residues revealed by mutational analysis in Saccharomyces cerevisiae. Genetics, 156, 21-29.

Evans D.R.H., Myles T., Hofsteenge J. and Hemmings B.A. (1999) Functional expression of human PP2Ac in yeast permits the identification of novel C-terminal and dominant-negative mutant forms. Journal of Biological Chemistry, 274, 24038-24046.

Fabera A.C., Lib D., Songa Y., Liang M-C., Yeapa B.Y., Bronsone R.T., Lifshitsa E., Chen Z., Mairaf S-M., García-Echeverríaf C., Wong K-K. and Engelmana J.A. (2009) Differential induction of apoptosis in HER2 and EGFR addicted cancers following PI3K inhibition. PNAS, 106, 19503-19508.

Feurstein D., Holst K., Fischer A. and Dietrich D.R. (2009) Oatp-associated uptake and toxicity of microcystins in primary murine whole brain extract cells. Toxicology and Applied Pharmacology, 234, 247-255.

Fischer E.H. and Krebs E.G. (1955) Conversion of phosphorylase B to phosphorylase A in muscle extracts. Journal of Biological Chemistry, 216, 121-132.

Fu W.Y., Chen J.P., Wang X.M. and Xu L.H. (2005) Altered expression of p53, Bcl-2 and Bax induced by microcystin-LR in vivo and in vitro. Toxicon, 46, 171-177.

Fujioka M., Takahashi N., Odai H., Araki S., Ichikawa K., Feng J., Nakamura M., Kaibuchi K., Hartshorne D.J., Nakano T. and Ito M. (1998) A new isoform of human myosin phosphatase targeting/regulatory subunit (MYPT2): cDNA cloning, tissue expression, and chromosomal mapping. Genomics, 49, 59-68.

Funderburk S.F., Wang Q.J. and Yue Z. (2010) The Beclin 1-VPS34 complex-at the crossroads of autophagy and beyond. Trends in Cell Biology, 20, 355-362.

Furukawa Y., Ikuta N., Omata S., Yamauchi T., Isobe T. and Ichimura T. (1993) Demonstration of the phosphorylation-dependent interaction of tryptophan hydroxylase with the 14-3-3 protein. Biochemical and Biophysical Research Communications, 194, 144-149.

Ganley I.G., Lam du H., Wang J., Ding X., Chen S. and Jiang X. (2009) ULK1.ATG13.FIP200 complex mediates mTOR signaling and is essential for autophagy. Journal of Biological Chemistry, 284, 12297-12305.

Gehring C. (2010) Adenylyl cyclases and cAMP in plant signalling- past and present. Cell Communications and Signaling, 8, 15-19.

Geraghty K.M., Chen S., Harthill J.E., Ibrahim A.F., Toth R., Morrice N.A., Vandermoere F., Moorhead G.B., Hardie D.G. and MacKintosh C. (2007) Regulation of multisite phosphorylation and 14-3-3 binding of AS160 in response to IGF-1, EGF, PMA and AICAR. Biochemical Journal, 407, 231-241.

Gómez N. and Cohen P. (1991) Dissection of the protein kinase cascade by which nerve growth factor activates MAP kinases. Nature, 353, 170-173.

Goris J., Defreyn G. and Merlevede W. (1979) Resolution of the ATP-Mg-dependent phosphorylase phosphatase from liver into a two protein component system. FEBS Letters, 99, 279-282.

Grühler A., Schulze W.X., Matthiesen R., Mann M. and Jensen O.N. (2005) Stable isotope labeling of *Arabidopsis thaliana* cells and quantitative proteomics by mass spectrometry. Molecular and Cellular Proteomics, 4, 1697-1709.

Gunawardena S.R., Ruis B.L., Meyer J.A., Kapoor M. and Conklin K.F. (2008) NOM1 targets protein phosphatase I to the nucleolus. Journal of Biological Chemistry, 283, 398-404.

Gwinn D.D., Shackelford D.B., Egan D.F., Mihaylova M.M., Mery A., Vasquez D.S., Turk B.E. and Shaw R.J. (2008) AMPK phosphorylation of raptor mediates a metabolic checkpoint. Molecular Cell, 30, 214-226.

Hanada M., Feng J. and Hemmings B.A. (2004) Structure, regulation and function of PKB/AKT-a major therapeutic target. Biochimica et Biophysica Acta, 1697, 3-16.

Hanks S.K. and Hunter T. (1995) Protein kinases 6: The eukaryotic protein kinase superfamily: Kinase (catalytic) domain structure and classification. FASEB Journal, 9, 576-596.

Hardie D.G. (1999) Analysis of signal transduction pathways using protein-serine/threonine phosphatase inhibitors. In Protein Phosphorylation, A practical approach. Second Edition, Edited by Hardie G. pp 53-65.

Helps N.R., Barker H.M., Elledge S.J., and Cohen P.T. (1995) Protein phosphatase 1 interacts with p53BP2, a protein which binds to the tumour suppressor p53. FEBS Letters, 377, 295-300.

Helps N.R., Brewis N.D., Lineruth K., Davis T., Kaiser K. and Cohen P.T.W. (1998) Protein phosphatase 4 is an essential enzyme required for organisation of microtubules at centrosomes in Drosophila embryos. Journal of Cell Signalling, 111, 1331-1340.

Hemmings B.A, Resink T. and Cohen P. (1982) Reconstitution of a Mg-ATP-dependent protein phosphatase and its activation through a phosphorylation mechanism. FEBS Letters, 150, 319-324.

Hemmings B.A., Yellowlees D., Kernohan J.C. and Cohen P. (1981) Purification of glycogen synthase kinase-3 from rabbit skeletal muscle. European Journal of Biochemistry, 119, 443-451.

Hendrickx A., Beullens M., Ceulemans H., Abt T.D., Van Eynde A., Nicolaescu E., Lesage B. and Bollen M. (2009) Docking motif-guided mapping of the interactome of protein phosphatase-1. Chemistry and Biology, 16, 365-371.

Herraiz C., Journé F., Abdel-Malek Z., Ghanem G., Jiménez-Cervantes C. and Garcia-Borrón J.C. (2011) Signaling from the human melanocortin 1 receptor to ERK1 and ERK2 mitogen-activated protein kinases involves transactivation of cKIT. Molecular Endocrinology, 25, 138-156.

Hewavitharana T. and Wedegaertner P.B. (2012) Non-canonical signalling and localisations of heterotrimeric G proteins. Cellular Signalling, 24, 25-34.

Hiraga A. and Cohen P. (1986) Phosphorylation of the glycogen-binding subunit of protein phosphatase-1γ by cyclic-AMP-dependent protein-kinase promotes translocation of the phosphatase from glycogen to cytosol in rabbit skeletal muscle. European Journal of Biochemistry, 161, 763-769.

Hiriart E., Gruffat H., Buisson M., Mikaelian I., Keppler S., Meresse P., Mercher T., Bernard O.A., Sergeant A. and Manet E. (2005) Interaction of the Epstein-Barr virus mRNA export factor EB2 with human Spen proteins SHARP, OTT1, and a novel member of the family, OTT3, links Spen proteins with splicing regulation and mRNA export. Journal of Biological Chemistry 280, 36935-36945.

Hoeflich K.P., O'Brien C., Boyd Z., Cavet G., Guerrero S., Jung K., Januario T., Savage H., Punnoose E., Truong T., Zhou W., Berry L., Murray L., Amler L., Belvin M., Friedman L.S. and Lackner M.R. (2009) In vivo antitumor activity of MEK and phosphatidylinositol 3-kinase inhibitors in basal-like breast cancer models. Clinical Cancer Research, 15, 4649-4664.

Hornyik C., Terzi L.C. and Simpson G.G. (2010) The Spen family protein FPA controls alternative cleavage and polyadenylation of RNA. Developmental Cell, 18, 203-213.

Hosokawa N., Hara T., Kaizuka T., Kishi C., Takamura A., Miura Y., Iemura S., Natsume T., Takehana K., Yamada N., Guan J.L., Oshiro N. and Mizushima N. (2009) Nutrient-dependent mTORC1 association with the ULK1-Atg13-FIP200 complex required for autophagy. Molecular Biology of the Cell, 20, 1981-1991.

Hoxhaj G., Najafov A., Toth R., Campbell D.G., Prescott A.R. and MacKintosh C. (2012) ZNRF2 is released from membranes by growth factors and with ZNRF1 regulates the Na+/K+ATPase. Journal of Cell Science, (in press).

Hsu J.L., Huang S.Y., Chow N.H. and Chen S.H. (2003) Stable-isotope dimethyl labeling for quantitative proteomics. Analytical Chemistry, 75, 6843-6852.

Huang F.L. and Glinsmann W.H. (1976) Separation and characterization of two phosphorylase phosphatase inhibitors from rabbit skeletal muscle. European Journal of Biochemistry, 70, 419-426.

Huang H.B., Horiuchi A., Watanabe T., Shih S.R., Tsay H.J., Li H.C., Greengard P. and Nairn A.C. (1999) Characterization of the inhibition of protein phosphatase-1 by DARRP-32 and inhibitor-2. Journal of Biological Chemistry, 274, 7870-7878.

Hubbard M.J., and Cohen P. (1993) On target with a new mechanism for the regulation of protein phosphorylation. Trends in Biochemical Science, 18, 172-177.

Hubbard M.J. and Cohen P. (1989) Regulation of protein phosphatase 1-G from rabbit/skeletal muscle. Phosphorylation by cAMP-dependent protein kinase at site 2 releases catalytic subunit from the glycogen-bound holoenzyme. European Journal of Biochemistry, 186, 701-709.

Huminiecki L. and Heldin C.H. (2010) 2R and remodeling of vertebrate signal transduction engine. BMC Biology, 8, 146.

Hunter, T. (2004) Protein phosphorylation: What does the future hold? In: I.S. Ehud Keinan and M. Sela, eds., Life Sciences for the 21st Century (pp. 191-223). Hoboken, NJ: Wiley.

Hurley T.D., Yang J., Zhang L., Goodwin K.D., Zou Q., Cortese M., Dunker A.K. and DePaoli-Roach A.A. (2007) Structural basis for regulation of Protein Phosphatase 1 by Inhibitor-2. Journal of Biological Chemistry, 282, 28874-28883.

Ichimura T., Isobe T., Okuyuma T., Yamauchi T. and Fujisawa H. (1987) Brain 14-3-3 protein is an activator protein that activates tryptophan 5-monooxygenase and tyrosine 3-monooxygenase in the presence of Ca^{2+} calmodulin-dependent protein kinase II. FEBS Letters, 219, 79-82.

Ikeda K., Ogawa S., Tsukui T., Horie-Inoue K., Ouchi Y., Kato S., Muramatsu M. and Inoue S. (2004) Protein phosphatase 5 is a negative regulator of estrogen receptor-mediated transcription. Molecular Endocrinology, 18, 1131-1143.

Iyer G., Garrod S., Woods V.L. and Taylor S.S. (2005) Catalytic independent functions of a protein kinase as revealed by a kinase-dead mutant: study of the Lys72His mutant of cAMP-dependent kinase. Journal of Molecular Biology, 351, 1110-1122.

Jäkel S. and Görlich D. (1998) Importin β, transportin, RanBP5 and RanBP7 mediate nuclear import of ribosomal proteins in mammalian cells. EMBO Journal, 17, 4491-4502.

Janssens V. and Gorris J. (2001) Protein phosphatase 2A: a highly regulated family of serine/threonine phosphatases implicated in cell growth and signalling. Biochemical Journal, 353, 417-439.

Johnson C., Crowther S., Stafford M.J., Campbell D.G., Toth R. and MacKintosh C. (2010) Bioinformatic and experimental survey of 14-3-3-binding sites. Biochemical Journal, 427, 69-78.

Johnson D.F., Moorhead G., Caudwell F.B., Cohen P., Chen Y.H., Chen M.X. and Cohen P.T. (1996) Identification of protein-phosphatase-1-binding domains on the glycogen and myofibrillar targetting subunits. European Journal of Biochemistry, 239, 317-325.

Jost P., Fasshauer M., Kahn C.R., Benito M., Meyer M., Ott V., Lowell B.B., Klein H.H. and Klein J. (2002) Atypical β-adrenergic effect on insulin signalling and action in β3-adrenoreceptor-deficient brown adipocytes. American Journal of Physiology, Endocrinology and Metabolism, 283, 146-153.

Jung C.H., Jun C.B., Ro S.H., Kim Y.M., Otto N.M., Cao J., Kundu M. and Kim D.H. (2009) ULK-Atg13-FIP200 complexes mediate mTOR signaling to the autophagy machinery. Molecular Biology of the Cell, 20, 1992-2003.

Junttila M.R., Puustinen P., Niemela M., Ahola R., Arnold H., Bottzauw T., Alaaho R., Nielsen C., Ivaska J., Taya Y., Lu S.L., Lin S., Chan E.K., Wang X.J., Grenman R., Kast J., Kallunki T., Sears R., Kahari V.M. and Westermarck J. (2007) CIP2A inhibits PP2A in human malignancies. Cell, 130, 51-62.

Kajino T. Ren H., Iemura S., Natsume T., Stefansson B., Brautigan D.L., Matsumoto K. and Ninomiya-Tsuji J. (2006) Protein phosphatase 6 downregulates TAK1 kinase activation on the IL-1 signalling pathway. Journal of Biological Chemistry, 281, 39891-19896.

Kamenetsky M., Middelhaufe S., Bank E.M., Levin L.R., Buck J. and Steegborn C. (2006) Molecular details of cAMP generation in mammalian cells: A tale of two systems. Journal of Molecular Biology, 362, 623-639.

Kammer G.M., Khan I.U. and Malemud C. J. (1994) Deficient type I protein kinase A isozyme activity in systemic lupus erythematosus T lymphocytes. Journal of Clinical Investigation, 94, 422-430.

Kawasaki H., Springett G.M., Mochizuki N., Toki S., Nakaya M., Matsuda M., Housman D.E. and Graybiel A.M. (1998) A family of cAMP-binding proteins that directly activate Rap1. Science, 282, 2275-2279.

Kemp B.E., Bylund D.B., Huang T.S. and Krebs E.G. (1975) Substrate specificity of the cyclic AMP-dependent protein kinase. Proceedings of the National Academy of Sciences USA, 72, 3448-3452.

Kemp B.E., Graves D.J., Benjamini E. and Krebs E.G. (1977) Role of multiple basic residues in determining the substrate specificity of cyclic AMP-dependent protein kinase. Journal of Biological Chemistry, 252, 4888-4894.

Kennelly, P. J. (2003) Archaeal protein kinases and protein phosphatases: Insights from genomics and biochemistry. Biochemical Journal, 370, 373-389.

Kerk D., Templeton G. and Moorhead G.B.G. (2008) Evolutionary radiation pattern of novel protein phosphatases revealed by analysis of protein data from the

completely sequenced genomes of humans, green algae and higher plants. Plant Physiology, 146, 351-367.

Kim S., Jee K., Kim D., Koh H. and Chung J. (2001) Cyclic AMP inhibits Akt activity by blocking the membrane localisation of PDK1. Journal of Biological Chemistry, 276, 12864-12870.

Kim Y.M., Watanabe T., Allen P.B., Kim Y.M., Lee S.J., Greengard P., Nairn A.C. and Kwon Y.G. (2003) PNUTS, a protein phosphatase 1 (PP1) nuclear targeting subunit. Characterization of its PP1- and RNA-binding domains and regulation by phosphorylation. Journal of Biological Chemistry, 278, 13819-13828.

Klee C.B., Ren H. and Wang X. (1998) Regulation of the calmodulin-stimulated protein phosphatase calcineurin. Journal of Biological Chemistry, 273, 13367-13370.

Klein J., Fasshauer M., Ito M., Lowell B.B., Benito M. and Kahn C.R. (1999) β3-adrenergic stimulation differentially inhibits insulin signalling and decreases insulin-induced glucose uptake in brown adipocytes. Journal of Biological Chemistry, 274, 34795-34802.

Knighton D.R., Zheng J., Ten Eyck L.F., Ashford V.A., Xuong N.H., Taylor S.S. and Sowadski J.M. (1991b) Crystal structure of the catalytic subunit of cyclic adenosine monophosphate-dependent protein kinase. Science, 253, 407-414.

Knighton D.R., Zheng J., Ten Eyck L.F., Xuong N.H., Taylor S.S. and Sowadski J.M. (1991a) Structure of a peptide inhibitor bound to the catalytic subunit of cyclic adenosine monophosphate-dependent protein kinase. Science, 253, 414-420.

Kovacina K.S., Park G.Y., Bae S.S., Guzzetta A.W., Schaefer E., Birnbaum M.J. and Roth R.A. (2003) Identification of a proline-rich Akt substrate as a 14-3-3 binding partner. Journal of Biological Chemistry, 278, 10189-10194.

Krainer A.R., Mayeda A., Kozak D. and Binns G. (1991) Functional expression of cloned human splicing factor SF2: homology to RNA-binding proteins, U1 70K, and Drosophila splicing regulators. Cell, 66, 383-394.

Kreivi J.P., Trinkle-Mulcahy L., Lyon C.E., Morrice N.A., Cohen P. and Lamond A.I. (1997) Purification and characterisation of p99, a nuclear modulator of protein phosphatase 1 activity. FEBS Letters, 420, 57-62.

Kuroyanagi H., Yan J., Seki N., Yamanouchi Y., Suzuki Y., Takano T., Muramatsu M. and Shirasawa T. (1998) Human ULK1, a novel serine/threonine kinase related to UNC-51 kinase of *Caenorhabditis elegans*: cDNA cloning, expression, and chromosomal assignment. Genomics, 51, 76-85.

Kutuzov M.A., Solov'eva O.V., Andreeva A.V. and Bennett N. (2002) Protein Ser/Thr phosphatases PPEF interact with calmodulin. Biochemical and Biophysical Research Commununications, 293, 1047-1052.

Kwon G., Marshall C.A., Pappan K.L., Remedi M.S. and McDaniel M. (2004) Signaling elements involved in the metabolic regulation of mTOR by nutrients, incretins and growth factors in Islets. Diabetes, 53, 225-232.

Lavoinne A., Erikson E., Maller J.L., Price D.L., Avruch J. and Cohen P. (1991) Purification and characterisation of the insulin-stimulated protein kinase from rabbit

skeletal muscle: Close similarity to S6 kinase II. European Journal of Biochemistry, 199, 723-728.

Lee J.W., Park S., Takahashi Y. and Wang H-G. (2010) The association of AMPK with ULK1 regulates autophagy. PLoS One, 5, e15394.

Leopold P.L., Kreitzer G., Miyazawa N., Rempel S., Pfister K.K., Rodriguez-Boulan E. and Crystal R.G. (2000) Dynein- and microtubule-mediated translocation of adenovirus serotype 5 occurs after endosomal lysis. Human Gene Therapy, 11, 151-165.

Li X., Lin H.H., Chen H., Xu X., Shih H.M., Ann D.K. (2010) SUMOylation of the transcriptional co-repressor KAP1 is regulated by the serine and threonine phosphatase PP1. Science Signaling, 3, RA32-RA32.

Li X. and Virshup D. (2002) Two conserved domains in the regulatory B subunits mediate binding to the A subunit of protein phosphatase 2A. European Journal of Biochemistry, 269, 546-552.

Liang X.H., Kleeman L.K., Jiang H.H., Gordon G., Goldman J.E., Berry G., Herman B. and Levine B. (1998) Protection against fatal Sindbis virus encephalitis by beclin, a novel Bcl-2-interacting protein. Journal of Virology, 72, 8586-8596.

Lindtner S., Zolotukhin A.S., Uranishi H., Bear J., Kulkarni V., Smulevitch S., Samiotaki M., Panayotou G., Felber B.K. and Pavlakis G.N. (2006) RNA-binding Motif Protein 15 binds to the RNA transport element RTE and provides a direct link to the NXF1 export pathway. Journal of Biological Chemistry, 281, 36915-36928.

Ling M.K., Lagerstrom M.C., Fredriksson R., Okimoto R., Mundy N.I., Takeuchi S. and Schiöth H.B. (2003) Association of feather colour with constitutively active melanocortin 1 receptors in chicken. European Journal of Biochemistry, 270, 1441-1449.

Lipina C., Huang X., Finlay D., McManus E.J., Alessi D.R. and Sutherland C. (2005) Analysis of hepatic gene transcription in mice expressing insulin-insensitive GSK3. Biochemical Journal, 392, 633-639.

Liu J., Wu J., Oliver C., Shenolikar S. and Brautigan D.L. (2000) Mutations of the serine phosphorylated in the protein phosphatase-1-binding motif in the skeletal muscle glycogen-targeting subunit. Biochemical Journal, 346, 77-82.

Lizotte D.L., McManus D.D., Cohen H.R. and DeLong A. (1999) Functional expression of human and Arabidopsis protein phosphatase 2A in *Saccharomyces cerevisiae* and isolation of dominant-defective mutants. Gene, 234, 35-44.

Lochhead P.A., Coghlan M., Rice S.Q. and Sutherland C. (2001) Inhibition of GSK-3 selectively reduces glucose-6-phosphatase and phosphatase and phosphoenolypyruvate carboxykinase gene expression. Diabetes, 50, 937-946.

Lomako J., Lomako W.M. and Whelan W.J. (1988) A self-glucosylating protein is the primer for rabbit muscle glycogen biosynthesis. FASEB Journal, 2, 3097-3103.

Lorkovic Z. J. and Barta A. (2002) Genome Analysis: RNA recognition motif (RRM) and K homology (KH) domain RNA-binding proteins from the flowering plant Arabidopsis thaliana. Nucleic Acids Research, 30, 623-635.

Lu D., Vage D.I. and Cone R.D. (1998) A ligand-mimetic model for constitutive activation of the melanocortin-1 receptor. Molecular Endocrinology, 12, 592-604.

Luke M.M., Della Seta F., di Como C.J., Sugimoto H., Kobayashi R. and Arndt K.T. (1996) The SAPs, a new family of proteins, associate and function positively with the SIT4 phosphatase. Molecular and Cellular Biology, 16, 2744-2755.

Ma Z., Morris S.W., Valentine V., Martin L., Herbrick J-A., Cui X., Bouman D., Li Y., Mehta P.K., Nizetic D., Kaneko Y., Chan G.C.F., Chan L.C., Squire J., Scherer S.W. and Hitzler J.K. (2001) Fusion of two novel genes, RBM15 and MKL1, in the t(1;22)(p13;q13) of acute megakaryoblastic leukemia. Nature Genetics, 28, 220-221

Mack H.I., Zheng B., Asara J. and Thomas S.M. (2012) AMPK-dependent phosphorylation of ULK1 regulates ATG9 localization. Autophagy, 8, 1197-1214.

MacKintosh C. and Diplexcito J. (2003) Naturally occurring inhibitors of protein serine/threonine phosphatases, Chapter 102, pp 607-612 of Handbook of Cell Signaling. Edited by Bradshaw R.A. and Dennis E.A. for Academic Press, San Diego.

MacKintosh C., Beattie K.A., Klumpp S., Cohen P. and Codd G.A. (1990) Cyanobacterial microcystin-LR is a potent and specific inhibitor of protein phosphatases 1 and 2A from both mammals and higher plants. FEBS Letters, 264, 187-192.

MacKintosh C., Campbell D.G., Hiraga A. and Cohen P. (1988) Phosphorylation of the glycogen-binding subunit of protein phosphatase-1G in response to adrenalin. FEBS Letters, 234, 189-194.

MacKintosh C., Garton A.J., McDonnell A., Barford D., Cohen P.T., Tonks N.K. and Cohen P. (1996) Further evidence that inhibitor-2 acts like a chaperone to fold PP1 into its native conformation. FEBS Letters, 397, 235-238.

MacKintosh R.W., Dalby K.N., Campbell D.G., Cohen P.T., Cohen P. and MacKintosh C. (1995) The cyanobacterial toxin microcystin binds covalently to cysteine-273 on protein phosphatase 1. FEBS Letters, 371, 236-240.

Makino T. and McLysaght A. (2010) Ohnologs in the human genome are dosage balanced and frequently associated with disease. Proceedings of the National Academy of Sciences USA, 107, 9270-9274.

Majumdar, M., Meenakshi, J., Goswami, S. K. and Datta, K. (2002) Hyaluronan binding protein 1 (HABP1)/C1QBP/p32 is an endogenous substrate for MAP kinase and is translocated to the nucleus upon mitogenic stimulation. Biochemical and Biophysical Research Communications, 291, 829-837.

Manning G., Plowman G.D., Hunter T. and Sudarsanam S. (2002a) Evolution of protein kinase signalling from yeast to man. Trends in Biochemical Sciences, 27, 514-520.

Manning G., Whyte D.B., Martinez R., Hunter T. and Sudarsanam S. (2002b) The protein kinase complement of the human genome. Science, 298, 1912-1934.

Marat A.L., Dokainish H. and McPherson P.S. (2009). DENN Domain proteins: Regulators of Rab GTPases. Journal of Biological Chemistry, 286, 13791-13800.

McCorquodale III D.S., Ozomaro U., Huang J., Montenegro G., Kushman A., Citrigno L., Price J., Speziani F., Pericak-Vance M.A. and Züchner S. (2011) Mutation screening of *spastin*, *atlastin*, and *REEP1* in hereditary spastic paraplegia. Clinical Genetics, 79, 523-530.

Mercher T., Busson-Le Coniat M., Monni R., Mauchauffé M., Khac F.N., Gressin l., Mugneret F., Leblanc T., Dastugue N., Berger R. and Bernard O.A. (2001) Involvement of a human gene related to the Drosophila spen gene in the recurrent t(1;22) translocation of acute megakaryocytic leukemia. Proceedings of National Academy of Sciences USA, 98, 5776-5779.

Millward T.A., Zolnierowicz S. and Hemmings B.A. (1999) Regulation of protein kinase cascades by protein phosphatase 2A. Trends in Biochemical Sciences, 24, 186-191.

Miranda-Saavedra D. and Barton G. (2007) Classification and functional annotation of eukaryotic protein kinases. Proteins, 68, 893-914.

Mirzoeva O.K., Das D., Heiser L.M., Bhattacharya S., Siwak D., Gendelman R., Bayani N., Wang N.J., Neve R.M., Guan Y., Hu Z., Knight Z., Feiler H.S., Gascard P., Parvin B., Spellman P.T., Shokat K.M., Wyrobek A.J., Bissell M.J., McCormick F., Kuo W.L., Mills G.B., Gray J.W. and Korn W.M. (2009) Basal subtype and MAPK/ERK kinase (MEK)-phosphoinositide 3-kinase feedback signaling determine susceptibility of breast cancer cells to MEK inhibition. Cancer Research, 69, 565-572.

Monfar M., Lemon K.P., Grammer T.C., Cheatham L., Chung J., Vlahos C.J., and Blenis J. (1995) Activation of pp70/85 S6 kinases in Interleukin-2-responsive lymphoid cells is mediated by phosphatidylinositol 3-kinase and inhibited by cyclic AMP. Molecular and Cellular Biology, 15, 326-337.

Monshausen M., Rehbein M., Richter D. and Kindler S. (2002) The RNA-binding protein Staufen from rat brain interacts with protein phosphatase-1. Journal of Neurochemistry, 81, 557-564.

Moore B.E. and Perez V.J. (1967) Specific acidic proteins of the nervous system. In: F.D. Carlson, ed, Physiological and Biochemical Aspects of Nervous Integration (pp. 343-359). Englewood Cliffs, NJ: Prentice-Hall.

Moorhead G.B., De Wever V., Templeton G. and Kerk D. (2009) Evolution of protein phosphatases in plants and animals. Biochemical Journal, 417, 401-409.

Moorhead, G.B., Johnson, D., Morrice, N. and Cohen, P. (1998) The major myosin phosphatase in skeletal muscle is a complex between the β-isoform of protein phosphatase 1 and the MYPT2 gene product. FEBS Letters, 438, 141-144.

Moorhead G., MacKintosh C., Morrice N. and Cohen P. (1995) Purification of the hepatic glycogen-associated form of protein phosphatase-1 by microcystin-Sepharose affinity chromatography. FEBS Letters, 362, 101-105.

Moorhead G.B., Trinkle-Mulcahy L., Nimick M., De Weever V., Campbell D.G., Gourlay R., Lam Y.W. and Lamond A.I. (2008) Displacement affinity chromatography of protein phosphatase one (PP1) complexes. BMC Biochemistry, 9, 1-10.

Mumby M. (2007) PP2A: unveiling a reluctant tumour suppressor. Cell, 130, 21-24.

Munro S., Cuthbertson D.J., Cunningham J., Sales M., Cohen P.T.W. (2002) Human skeletal muscle expresses a glycogen-targeting subunit of PP1 that is identical to the insulin-sensitive glycogen-targeting subunit G(L) of liver. Diabetes, 51, 591-598.

Muta T., Kang D., Kitajima S., Fujiwara T. and Hamasaki N. (1997) P32 protein, a splicing factor 2-associated protein, is localized in mitochondrial matrix and is functionally important in maintaining oxidative phosphorylation. Journal of Biological Chemistry, 272, 24363-24370.

Naesens M., Kuypers D.R.J. and Sarwal M. (2009) Calcineurin inhibitor nephrotoxicity. Clinical Journal of the American Society of Nephrology, 4, 481-508.

Nakamura T. and Gold G.H. (1987) A cyclic nucleotide-gated conductance in olfactory receptor cilia. Nature, 325, 442-444.

Nascimento E.B., Snel M., Guigas B., van der Zon G.C., Kriek J., Maassen J.A., Jazet I.M., Diamant M. and Ouwens D.M. (2010) Phosphorylation of PRAS40 on Thr246 by PKB/AKT facilitates efficient phosphorylation of Ser183 by mTORC1. Cell Signaling, 22, 961-967.

Neukamm S.S., Toth R., Morrice N., Campbell D.G., MacKintosh C., Lehmann R., Haering H-U., Schleicher E.D. and Weigert C. (2012) Identification of the amino acids 300–600 of IRS-2 as 14-3-3 binding region with the importance of IGF-1/Insulin-regulated phosphorylation of Ser-573. PLoS ONE 7, e43296.

Nimmo H.G., Proud C.G. and Cohen P. (1976) The purification and properties of rabbit skeletal muscle glycogen synthase. European Journal of Biochemistry, 68, 21-30.

Novoa I., Zeng H., Harding H.P. and Ron D. (2001) Feedback inhibition of the unfolded protein response by GADD34-mediated dephosphorylation of eIF2alpha. Journal of Cell Biology, 153, 1011-1022.

Obsil T., Ghirlando R., Klein D.C., Ganguly S. and Dyda F. (2001) Crystal structure of the 14-3-3ζ:serotonin N-acetyltransferase complex: A role for scaffolding in enzyme regulation. Cell, 105, 257-267.

Obsilova V., Herman P., Vecer J., Sulc M., Teisinger J., and Obsil T. (2004) 14-3-3ζ C-terminal stretch changes its conformation upon ligand binding and phosphorylation at Thr232. Journal of Biological Chemistry, 279, 4531-4540.

Olsen J.V., Blagoev B., Gnad F., Macek B., Kumar C., Mortensen P. and Mann M. (2006) Global, *in vivo*, and site-specific phosphorylation dynamics in signaling networks. Cell 127, 635-648.

Ottmann C., Marco S., Jaspert N., Marcon C., Schauer N., Weyand M., Vandermeeren C., Duby G., Boutry M., Wittinghofer A., Rigaud J.L. and Oecking C. (2007) Structure of a 14-3-3 coordinated hexamer of the plant plasma membrane H+-ATPase by combining X-ray crystallography and electron cryomicroscopy. Molecular Cell, 25, 427-440.

Ottmann C., Yasmin L., Weyand M., Veesenmeyer J.L., Diaz M.H., Palmer R.H., Francis M.S., Hauser A.R., Wittinghofer A. and Hallberg B. (2007b) Phosphorylation-independent interaction between 14-3-3 and exoenzyme S: From structure to pathogenesis. EMBO Journal, 26, 902-913.

Park S.H., Zhu P.P., Parker R.L. and Blackstone C. (2010) Hereditary spastic paraplegia proteins REEP1, spastin, and atlastin-1 coordinate microtubule interactions with the tubular ER network. Journal of Clinical Investigation, 120, 1097-110.

Peters C., Andrews P.D., Stark M.J., Cesaro-Tadic S., Glatz A., Podtelejnikov A., Mann M. and Mayer A. (1999) Control of the terminal step of intracellular membrane fusion by protein phosphatase 1. Science, 285, 1084-1087.

Petosa C., Masters S.C., Bankston L.A., Pohl J., Wang B., Fu H. and Liddington R.C. (1998) 14-3-3ζ binds a phosphorylated Raf peptide and an unphosphorylated peptide via its conserved amphipathic groove. Journal of Biological Chemistry, 273, 16305-16310.

Pitcher J., Smythe C., Campbell D.G. and Cohen P. (1987) Identification of the 38-kDa subunit of rabbit skeletal muscle glycogen synthase as glycogenin. European Journal of Biochemistry, 169, 497-502.

Pitcher J., Smythe C. and Cohen P. (1988) Glycogenin is the priming glucosyltransferase required for the initiation of glycogen biogenesis in rabbit skeletal muscle. European Journal of Biochemistry, 176, 391-395.

Pollmann M., Parwaresch R., Adam-Klages S., Kruse M.L., Buck F. and Heidebrecht H.J. (2006) Human EML4, a novel member of the EMAP family, is essential for microtubule formation. Experimental Cell Research, 312, 3241-3251.

Postel E.H., Weiss V.H., Beneken J. and Kirtane A. (1996) Mutational analysis of NM23-H2/NDP kinase identifies the structural domains critical to recognition of a c-myc regulatory element. Proceedings of National Academy of Sciences USA, 93, 6892-6897.

Powell D.W., Rane M.J., Chen Q., Singh S. and McLeish K.R. (2002) Identification of 14-3-3ζ as a protein kinase B/Akt substrate. Journal of Biological Chemistry, 277, 21639-21642.

Pozuelo-Rubio M. (2011) Regulation of autophagic activity by 14-3-3ζ proteins associated with class III phosphatidylinositol-3-kinase. Cell Death and Differentiation, 18, 479-492.

Pozuelo Rubio M., Geraghty K.M., Wong B.H., Wood N.T., Campbell D.G., Morrice N. and MacKintosh C. (2004) 14-3-3-affinity purification of over 200 human phosphoproteins reveals new links to regulation of cellular metabolism, proliferation and trafficking. Biochemical Journal, 379, 395-408

Puerto M., Picardo S., Jos A., and Camean A.M. (2009) Comparison of the toxicity induced by microcystin-RR and microcystin-YR in differentiated and undifferentiated Caco-2 cells. Toxicon, 54, 161-169.

Putnam N.H., Butts T., Ferrier D.E., Furlong R.F., Hellsten U., Kawashima T., Robinson-Rechavi M., Shoguchi E., Terry A., Yu J.K., Benito-Gutiérrez E.L., Dubchak I., Garcia-Fernàndez J., Gibson-Brown J.J., Grigoriev I.V., Horton A.C., de Jong P.J., Jurka J., Kapitonov V.V., Kohara Y., Kuroki Y., Lindquist E., Lucas S., Osoegawa K., Pennacchio L.A., Salamov A.A., Satou Y., Sauka-Spengler T., Schmutz J., Shin-I T., Toyoda A., Bronner-Fraser M., Fujiyama A., Holland L.Z., Holland P.W., Satoh N. and Rokhsar D.S. (2008) The amphioxus genome and the evolution of the chordate karyotype. Nature, 453, 1064-1071.

Raffel G.D., Chu G.C., Jesneck J.L., Cullen D.E., Bronson R.T., Bernard O.A. and Gilliland D.G. (2009) Ott1 (Rbm15) is essential for placental vascular branching morphogenesis and embryonic development of the heart and spleen. Molecular and Cellular Biology, 29, 333-341.

Rall T.W. and Sutherland E.W. (1958) Formation of a cyclic adenine ribonucleotide by tissue particles. Journal of Biological Chemistry, 232, 1065-1076.

Ramulu P., Kennedy M., Xiong W.-H., Williams J., Cowan M., Blesh D., Yau K.-W., Hurley J. B. and Nathans J. (2001) Normal light response, photoreceptor integrity and rhodopsin dephosphorylation in mice lacking both protein phosphatases with EF hands (PPEF-1 and PPEF-2). Molecular and Cellular Biology, 21, 8605-8614.

Rehmann H., Prakash B., Wolf E., Rueppel A., De Rooij J., Bos J.L. and Wittinghofer A. (2003) Structure and regulation of the cAMP-binding domains of Epac2. Nature Structural Biology, 10, 26-32.

Rena G., Guo S., Cichy S.C., Unterman T.G. and Cohen P. (1999) Phosphorylation of the transcription factor forkhead family member FKHR by protein kinase B. Journal of Biological Chemistry, 274, 17179-17183.

Rena G., Prescott A.R., Guo S., Cohen P. and Unterman T.G. (2001) Roles of the forkhead in rhabdomyosarcoma (FKHR) phosphorylation sites in regulating 14-3-3 binding, transactivation and nuclear targetting. Biochemical Journal, 354, 605-612.

Rena G., Woods Y.L., Prescott A.R., Peggie M., Unterman T.G., Williams M.R. and Cohen P. (2002) Two novel phosphorylation sites on FKHR that are critical for its nuclear exclusion. EMBO Journal, 21, 2263-2271.

Rittinger K., Budman J., Xu J., Volinia S., Cantley L. C., Smerdon S. J., Gamblin S.J. and Yaffe M.B. (1999) Structural analysis of 14-3-3 phosphopeptide complexes identifies a dual role for the nuclear export signal of 14-3-3 in ligand binding. Molecular Cell, 4, 153-166.

Robens J.M., Lee Y.F., Ng E., Hall C. and Manser E. (2010) Regulation of IRSp53-dependent filopodial dynamics by antagonism between 14-3-3 binding and SH3-mediated localization. Molecular and Cellular Biology, 30, 829-844.

Rodriguez I.R. and Whelan M.J. (1985) A novel glycosyl-amino acid linkage: Rabbit-muscle glycogen is covalently linked to a protein via tyrosine. Biochemical and Biophysical Research Communications, 132, 829-836.

Rosenquist M., Sehnke P., Ferl R.J., Sommarin M. and Larsson C. (2000) Evolution of the 14-3-3 protein family: Does the large number of isoforms in multicellular organisms reflect functional specificity? Journal of Molecular Evolution, 51, 446-458.

Roskoski R. Jr. (2012) ERK1/2 MAP kinases: Structure, function, and regulation. Pharmacological Research, 66, 105-143.

Sakamoto K. and Holman G.D. (2008) Emerging role for AS160/TBC1D4 and TBC1D1 in the regulation of GLUT4 traffic. American Journal of Physiology, Endocrinology and Metabolism, 295, E29–E37.

Sanchez A.M.J., Candau R., Csibi A., Raibon A. and Bernardi H. (2012) The role of AMP-activated protein kinase in the coordination of skeletal muscle turnover and energy homeostasis. American Journal Physiology. Cell Physiology. (in press)

Sano H., Kane S., Sano E., Mîinea C.P., Asara J.M., Lane W.S., Garner C.W. and Lienhard G.E. (2003) Insulin-stimulated phosphorylation of a Rab GTPase-

activating protein regulates GLUT4 translocation. Journal of Biological Chemistry, 278, 14599-14602.

Schlegelmilch K., Mohseni M., Kirak O., Pruszak J., Rodriguez J.R., Zhou D., Kreger B.T., Vasioukhin V., Avruch J., Brummelkamp T.R. and Camargo F.D. (2011) Yap1 acts downstream of α-catenin to control epidermal proliferation. Cell, 144, 782-795.

Schomburg F.M., Patton D.A., Meinke D.W. and Amasino R.M. (2001) FPA, a gene involved in floral induction in Arabidopsis, encodes a protein containing RNA-recognition motifs. Plant Cell, 13, 1427-1436.

Schütz W., Hausmann N., Krug K., Hampp R. and Macek B. (2011) Extending SILAC to proteomics of plant cell lines. Plant Cell, 23, 1701-1705.

Semova N., Kapanadze B., Corcoran M., Kutsenko A., Baranova A. and Semov A. (2003) Molecular cloning, structural analysis, and expression of a human IRLB, MYC promoter-binding protein: new DENN domain-containing protein family emerges small star, filled. Genomics, 82, 343-354.

Shankar D.B., Cheng J.C., Sakamoto K.M. (2005) Role of cyclic AMP response element binding protein in human leukemias. Cancer, 104, 1819-1824.

Simpson G.G., Gendall A. R. and Dean C. (1999) When to switch to flowering. Annual Review of Cell Development Biology, 99, 519-550.

Shabb J.B. (2001) Physiological substrates of cAMP-dependent kinase. Chemical Reviews, 101, 2381-2411.

Skurat A., Cao Y. and Roach P.J. (1993) Glucose control of rabbit skeletal muscle glycogenin expressed in COS cells. Journal of Biological Chemistry, 288, 14701-14707.

Smith R.D. and Walker J.C. (1996) Plant protein phosphatases. Annual Review of Plant Physiology and Plant Molecular Biology, 47, 101-125.

Soderling T.R., Hickenbottom J.P., Reimann E.M., Hunkeler F.L., Walsh D.A. and Krebs E.G. (1970) Inactivation of glycogen synthetase and activation of phosphorylase kinase by muscle adenosine 3',5'-monophosphate-dependent protein kinases. Journal of Biological Chemistry, 245, 6317-6328.

Song W., de la Cruz A.A., Rein K. and O'Shea K.E. (2006) Ultrasonically induced degradation of microcystin-LR and -RR: Identification of products, effect of pH, formation and destruction of peroxides. Environmental Science and Technology, 40, 3941-3946.

Stark M.J., Black S., Sneddon A.A. and Andrews P.D. (1994) Genetic analyses of yeast protein serine/threonine phosphatases. FEMS Microbiology Letters, 117, 121-130.

Stefansson B. and Brautigan D. L. (2007) Protein phosphatase PP6 N terminal domain restricts G1 to S phase progression in human cancer cells. Cell Cycle, 6, 1386-1392.

Stefansson B., Ohama T., Daugherty A.R. and Brautigan D.L. (2008) Protein phosphatase 6 regulatory subunits composed of ankyrin repeat domains. Biochemistry, 47, 1442-1451.

Steichen J.M., Iyer G.H., Li S., Saldanha S.A., Deal M.S., Woods V.L. Jr and Taylor S.S. (2010) Global consequences of activation loop phosphorylation on protein kinase A. Journal of Biological Chemistry, 285, 3825-3832.

Stork P.J.S. and Schmitt J.M. (2002) Crosstalk between cAMP and MAP kinase signalling in the regulation of cell proliferation. Trends in Cell Biology, 12, 258-266.

Strack S., Kini S., Edner F.F., Wadzinski B.E. and Colbran R.J. (1999) Differential cellular and subcellular localization of protein phosphatase 1 isoforms in brain. Journal of Comparative Neurology, 413, 373-384.

Stralfors P., Hiraga A. and Cohen P. (1985) The protein phosphatases involved in cellular regulation. European Journal of Biochemistry, 149, 295-303.

Suomalainen M., Nakano M.Y., Keller S., Boucke K., Stidwill R.P. and Greber U.F. (1999) Microtubule-dependent plus- and minus end-directed motilities are competing processes for nuclear targeting of adenovirus. Journal of Cell Biology, 144, 657-672.

Suprenant K.A., Tuxhorn J.A., Daggett M.A., Ahrens D.P., Hostetler A., Palange J.M., VanWinkle C.E. and Livingston B.T. (2000) Conservation of the WD-repeat, microtubule-binding protein, EMAP, in sea urchins, humans, and the nematode C. elegans. Development Genes and Evolution, 210, 2-10.

Sutherland E.W. and Rall T.W. (1958) Fractionation and characterization of a cyclic adenine ribonucleotide formed by tissue particles. Journal of Biological Chemistry, 232, 1077-1092.

Syed N.A. and Khandelwal R.L. (2000) Reciprocal regulation of glycogen phosphorylase and glycogen synthase by insulin involving phosphatidylinositol-3 kinase and protein phosphatase-1 in HepG2 cells. Molecular and Cellular Biochemistry, 211, 123-136.

Tada A., Pereira E., Beitner-Johnson D., Kavanagh R. and Abdel-Malek Z.A. (2002) Mitogen- and ultraviolet-B-induced signaling pathways in normal human melanocytes. Journal of Investigative Dermatology, 118, 316-322.

Takai A., Bialojan C., Troschka M. and Rüegg J.C. (1987) Smooth muscle myosin phosphatase inhibition and force enhancement by black sponge toxin. FEBS Letters, 217, 81-84.

Tan I., Ng C.H., Lim L. and Leung T. (2001) Phosphorylation of a novel myosin binding subunit of protein phosphatase 1 reveals a conserved mechanism in the regulation of actin cytoskeleton. Journal of Biological Chemistry, 276, 21209-21216.

Tasken K. and Aandahl E.M. (2004) Localised effects of cAMP mediated by distinct routes of protein kinase A. Physiological Reviews, 84, 137-167.

Taylor S.S., Kim C., Vigil D., Haste N.M., Yang J., Wu J. and Anand G. (2005) Dynamics of signalling by PKA. Biochimica et Biophysica Acta, 1754, 25-37.

Tegha-Dunghu J., Neumann B., Reber S., Krause R., Erfle H., Walter T., Held M., Rogers P., Hupfeld K., Ruppert T., Ellenberg J. and Gruss O.J. (2008) EML3 is a nuclear microtubule-binding protein required for the correct alignment of chromosomes in metaphase. Journal of Cell Science, 121, 1718-1726.

Terrak M., Kerff F., Langsetmo K., Tao T. and Dominguez R. (2004) Structural basis of protein phosphatase-1 regulation. Nature, 429, 780-784.

Terry-Lorenzo R.T., Elliot E., Weiser D.C., Prickett T.D., Brautigan D.L. and Shenolikar S. (2002) Neurabins recruit protein phoaphatase-1 and inhibitor-2 to the actin cytoskeleton. Journal of Biological Chemistry, 277, 46535-46543.

Thanasopoulou A., Stravopodis D.J., Dimas K.S., Schwaller J. and Anastasiadou E. (2012) Loss of CCDC6 affects cell cycle through impaired intra-S-phase checkpoint control. PLoS One, 7, e31007.

Theurillat J.P., Metzler S.C., Henzi N., Djouder N., Helbling M., Zimmermann A.K., Jacob F., Soltermann A., Caduff R., Heinzelmann-Schwarz V., Moch H. and Krek W. (2011) URI is an oncogene amplified in ovarian cancer cells and is required for their survival. Cancer Cell, 19, 317-332.

Tinti M., Johnson C., Toth R., Ferrier D.E.K. and MacKintosh C. (2012) Evolution of signal multiplexing by 14-3-3-binding 2R-ohnologue protein families in the vertebrates. Open Biology, 2, 120103.

Tonks N.K. (2006) Protein tyrosine phosphatases: From genes, to function, to disease. Nature Reviews Molecular Cell Biology, 7, 833-846.

Toole, B. J. and Cohen, P. T. W. (2007) The skeletal muscle-specific glycogen targeted protein phosphatase 1 plays a major role in the regulation of glycogen metabolism by adrenaline in vivo. Cellular Signalling, 19, 1044-1055.

Trinkle-Mulcahy L., Ajuh P., Prescott A., Claverie-Martin F., Cohen S., Lamond A.I. and Cohen P. (1999) Nuclear organisation of NIPP1, a regulatory subunit of protein phosphatase 1 that associates with pre-mRNA splicing factors. Journal of Cell Science, 112, 157-168.

Trinkle-Mulcahy L., Andersen J., Lam Y.W., Moorhead G., Mann M. and Lamond A.I. (2006) Repo-Man recruits PP1γ to chromatin and is essential for cell viability. Journal of Cell Biology, 172, 679-692.

Trinkle-Mulcahy L., Chusainow J., Lam Y.W., Swift S. and Lamond A.I. (2006a) Edited by G. Moorhead. Visualization of intracellular PP1 targeting through transiently and stably expressed fluorescent protein fusions Methods in Molecular Biology (Protein phosphatase protocols), 365, 133-154.

Trinkle-Mulcahy L., Sleeman J.E. and Lamond A.I. (2001) Dynamic targeting of protein phosphatase 1 within the nuclei of living mammalian cells. Journal of Cell Science, 114, 4219-4228.

Tsuji K., Naito S., Kondo F., Ishikawa N., Watanabe M.F., Suzuki M. and Harada K-I. (1994) Stability of microcystins from cyanobacteria: Effect of light on decomposition and isomerization. Environmental Science and Technology, 28, 173-177.

Tsuruta F., Sunayama J., Mori Y., Hattori S., Shimizu S., Tsujimoto Y., Yoshioka K., Masuyama N. and Gotoh Y. (2004) JNK promotes Bax translocation to mitochondria through phosphorylation of 14-3-3 proteins. EMBO Journal, 23, 1889-1899.

Turke A.B., Song Y., Costa C., Cook R., Arteaga C.L., Asara J.M. and Engelman J.A. (2012) MEK Inhibition Leads to PI3K/AKT Activation by Relieving a Negative Feedback on ERBB Receptors. Cancer Research, 72, 3228-3237.

Ubersax J.A. and Ferrell J.E. Jr. (2007) Mechanisms of specificity in protein phosphorylation. Nature Reviews Molecular Cell Biology, 8, 530-541.

Ulke-Lemee A., Trinkle-Mulcahy L., Chaulk S., Bernstein N.K., Morrice N., Glover M., Lamond A.I. and Moorhead G.B.G. (2007) The nuclear PP1 interacting protein ZAP3 (ZAP) is a putative nucleoside kinase that complexes with SAM68, CIA, NF110/45, and HNRNP-G. Biochimica et Biophysica Acta, 1774, 1339-1350.

Van Eynde A., Wera S., Beullens M., Torrekens S., Van Leuven F., Stalmans W. and Bollen M. (1995) Molecular cloning of NIPP-1, a nuclear inhibitor of protein phosphatase-1, reveals homology with polypeptides involved in RNA processing. Journal of Biological Chemistry, 270, 28068-28074.

Veley K. M. and Michaels S. D. (2008) Functional redundancy and new roles for genes of the autonomous floral-promotion pathway. Plant Physiology, 147, 682-695.

Wakula P., Beullens M., Ceulemans H., Stalmans W. and Bollen M. (2003) Degeneracy and function of the ubiquitous RVXF motif that mediates binding to protein phosphatase-1. Journal of Biological Chemistry, 278, 18817-18823.

Wang B., Ling S. and Lin W-C. (2010) 14-3-3τ regulates Beclin 1 and is required for autophagy. PLoS One, 5, e10409.

Wang B., Ling S. and Lin W-C. (2010) 14-3-3τ regulates Beclin 1 and is required for autophagy. PLoS One, 5, e10409.

Wei Y., Weng D., Li F., Zou X., Young D.O., Ji J. and Shen P. (2008) Involvement of JNK regulation in oxidative stress-mediated murine liver injury by microcystin-LR. Apoptosis, 13, 1031-1042.

Wek R.C., Cannon J.F., Dever T.E. and Hinnebusch A.G. (1992) Truncated protein phosphatase GLC7 restores translational activation of GCN4 expression in yeast mutants defective for the eIF-2 alpha kinase GCN2. Molecular and Cellular Biology, 12, 5700-5710.

Weng D., Lu Y., Wei Y., Liu Y. and Shen P. (2007) The role of ROS in microcystin-LR-induced hepatocyte apoptosis and liver injury in mice. Toxicology, 232, 15-23.

Westphal R.S., Coffee R.L. Jr., Marotta A., Pelech S.L. and Wadzinski B.E. (1999) Identification of kinase-phosphatase signaling modules composed of p70 S6 kinase-protein phosphatase 2A (PP2A) and p21-activated kinase-PP2A. Journal of Biological Chemistry, 274, 687-692.

Wilker E.W., Grant R.A., Artim S.C. and Yaffe M.B. (2005) A structural basis for 14-3-3σ functional specificity. Journal of Biological Chemistry, 280, 18891-18898.

Woodcock J.M., Murphy J., Stomski F.C., Berndt M.C. and Lopez A.F. (2003) The dimeric versus monomeric status of 14-3-3ζ is controlled by phosphorylation of Ser58 at the dimer interface. Journal of Biological Chemistry, 278, 36323-36327.

Wurtele M., Jelich-Ottmann C., Wittinghofer A. and Oecking C. (2003) Structural view of a fungal toxin acting on a 14-3-3 regulatory complex. EMBO Journal, 22, 987-994.

Xing M.L., Wang X.F. and Xu L.H. (2008) Alteration of proteins expression in apoptotic FL cells induced by MC-LR. Environmental Toxicology, 23, 451-458.

Yaffe M.B., Rittinger K., Volinia S., Caron P.R., Aitken A., Leffers H., Gambin S.J., Smerdon S.J. and Cantley L.C. (1997) The structural basis for 14-3-3: Phosphopeptide binding specificity. Cell, 91, 961-971.

Yamaguchi T., Nagao S., Wallace D.P., Belibi F.A., Cowley Jr. B.D., Pelling J.C. and Grantham J.J. (2003) Cyclic AMP activates B-Raf and ERK in cyst epithelial cells from autosomal-dominant polycystic kidneys. Kidney International, 63, 1983-1994.

Yamamoto H., Kakuta S., Watanabe T.M., Kitamura A., Sekito T., Kondo-Kakuta C., Ichikawa R., Kinjo M. and Ohsumi Y. (2012) Atg9 vesicles are an important membrane source during early steps of autophagosome formation. Journal of Cell Biology, 198, 219-233.

Yang J., Roe S.M., Cliff M.J. Williams M.J., Ladbury M.A., Cohen P.T.W. and Barford D. (2005) Molecular basis for TPR domain-mediated regulation of protein phosphatase 5. EMBO Journal, 24, 1-10.

Yang X., Lee W.H., Sobott F., Papagrigoriou E., Robinson C.V., Grossmann J.G., Sundström M., Doyle D.A. and Elkins J.M. (2006) Structural basis for protein-protein interactions in the 14-3-3 protein family. Proceedings of the National Academy of Sciences USA, 103, 17237-17242.

Ye F., Than A., Zhao Y., Goh K.H. and Chen P. (2010) Vesicular storage, vesicle trafficking and secretion of leptin and resistin: the similarities, differences and interplays. Journal of Endocrinology, 206, 27-36.

Yoon Y.K., Kim H.P., Han S.W., Hur H.S., Oh do Y., Im S.A., Bang Y.J. and Kim T.Y. (2009) Combination of EGFR and MEK1/2 inhibitor shows synergistic effects by suppressing EGFR/HER3-dependent AKT activation in human gastric cancer cells. Molecular Cancer Therapeutics, 8, 2526-2536.

Yoshida K., Yamaguchi T., Natsume T., Kufe D. and Miki Y. (2005) JNK phosphorylation of 14-3-3 proteins regulates nuclear targeting of c-Abl in the apoptotic response to DNA damage. Nature Cell Biology, 7, 278-285.

Yue Z. Jin S., Yang C., Levine A.J. and Heintz N. (2003) Beclin 1, an autophagy gene essential for early embryonic development, is a haploinsufficient tumor suppressor. Proceedings of the National Academy of Sciences USA, 100, 15077-15082.

Zegura B., Zajc I., Lah T.T. and Filipic M. (2008) Patterns of microcystin-LR induced alteration of the expression of genes involved in response to DNA damage and apoptosis. Toxicon, 51, 615-623.

Zhang Z., Bai G., Shima M., Zhao S., Nagao M. and Lee E.Y.C. (1993) Expression and characterization of rat protein phosphatases -1α, -1γ1, -1γ2, and -1δ. Archives of Biochemistry and Biophysics, 303, 402-440.

Zhang L., Zhang Z., Long F. and Lee E.Y.C. (1996) Tyrosine-272 is involved in the inhibition of Protein Phosphatase-1 by multiple toxins. Biochemistry, 35, 1606-1611.

Zhao B., Wei X., Li W., Udan R.S., Yang Q., Kim J., Xie J., Ikenoue T., Yu J., Li L., Zheng P., Ye K., Chinnaiyan A., Halder G., Lai Z-C. and Guan K-L. (2007) Inactivation of YAP oncoprotein by the Hippo pathway is involved in cell contact inhibition and tissue growth control. Genes and Development, 21, 2747-2761.

Zheng J., Trafny E.A., Knighton D.R., Xuong N.H., Taylor S.S., Ten Eyck L.F. and Sowadski J.M. (1993) 2.2 A refined crystal structure of the catalytic subunit of cAMP-dependent protein kinase complexed with MnATP and a peptide inhibitor. Acta Crystallographica Section D, Biological Crystallography, 49, 362-365.

Zheng Y.H., Yu H.F. and Peterlin B.M. (2003) Human p32 protein relieves a post-transcriptional block to HIV replication in murine cells. Nature Cell Biology, 5, 611-618.

Zhu G., Fuji K., Belkina N., Liu Y., James M., Herrero J. and Shaw S. (2005a) Exceptional disfavour for proline at the P+1 position among AGC and CAMK kinases establishes reciprocal specificity between them and the proline-directed kinases. Journal of Biological Chemistry, 280, 10743-10748.

Zhu G., Fuji K., Liu Y., Codrea V., Herrero J. and Shaw S. (2005b) A single pair of acidic residues in the kinase major groove mediates strong substrate preference for P-2 or P-5 arginine in the AGC, CAMK and STE kinase families. Journal of Biological Chemistry, 280, 36372-36379.

Zolnierowicz S., Van Hoof C., Andjelković N., Cron P., Stevens I., Merlevede W., Goris J., Hemmings B.A. (1996) The variable subunit associated with protein phosphatase 2A0 defines a novel multimember family of regulatory subunits. Biochemical Journal, 317, 187-194.

Appendix I

Proteins that were purified by microcystin-Sepharose affinity chromatography from cell lysates of HEK293 cells stimulated with or without forskolin and in the presence or absence of H-89. Peptides were extracted from the SDS gel (**Figure 3.1**) and identified from the SwissProt database (accession number; description) and their Mascot score (score) determined. The number of unique peptides (pep) identified in each protein is also listed along with the gel band (band) in which they were identified. Peptides were quantitatively measured using the MS Quant software following the dimethyl labelling. The ratios of the different treatment conditions are listed in the table below (SS-serum starved, Fsk-forskolin, H-89+ Fsk-H-89 and forskolin).

Accession number	Mass [Da]	Pep	Score	Description	SS/SS	Fsk/SS	H-89+Fsk/SS	Band
sp|P26368|U2AF2_HUMAN	53809	3	142	Splicing factor U2AF 65 kDa subunit U2AF2	1	17.391	0.404	7
sp|P08670|VIME_HUMAN	53676	29	1466	Vimentin VIM	1	16.113	5.456	8
sp|Q99729|ROAA_HUMAN	36316	2	85	Heterogeneous nuclear ribonucleoprotein A/B HNRNPAB	1	14.535	0.082	11
sp|P51148|RAB5C_HUMAN	23696	3	215	Ras-related protein Rab-5C RAB5C	1	12.855	0.668	14
sp|P12236|ADT3_HUMAN	33073	8	512	ADP/ATP translocase 3 SLC25A6	1	8.982	5.654	13
sp|Q9Y277|VDAC3_HUMAN	30981	4	188	Voltage-dependent anion-selective channel protein 3 VDAC3	1	8.655	1.945	13
sp|P83916|CBX1_HUMAN	21519	2	88	Chromobox protein homolog 1 CBX1	1	6.227	0.861	13
sp|Q15233|NONO_HUMAN	54311	2	72	Non-POU domain-containing octamer-binding protein NONO	1	5.989	0.905	7
sp|P22087|FBRL_HUMAN	33877	3	103	rRNA 2'-O-methyltransferase fibrillarin FBL	1	5.816	0.949	12
sp|Q9Y5B9|SP16H_HUMAN	120409	17	793	FACT complex subunit SPT16 SUPT16H	1	5.623	0.612	2
sp|Q9NXA8|SIRT5_HUMAN	34543	6	360	NAD-dependent deacetylase sirtuin-5 SIRT5	1	5.135	4.024	13
sp|P07196|NFL_HUMAN	61536	25	1311	Neurofilament light polypeptide NEFL	1	4.868	4.707	6
sp|P36542|ATPG_HUMAN	33032	4	212	ATP synthase subunit gamma, mitochondrial ATP5C1	1	4.766	3.32	13
sp|P06899|H2B1J_HUMAN	13896	2	68	Histone H2B type 1-J HIST1H2BJ	1	4.056	0.658	14
sp|P50991|TCPD_HUMAN	58401	3	193	T-complex protein 1 subunit delta CCT4	1	3.898	0.527	7
sp|P10412|H14_HUMAN	21852	2	120	Histone H1.4 HIST1H1E	1	3.833	4.164	13
sp|Q13409|DC1I2_HUMAN	71811	5	325	Cytoplasmic dynein 1 intermediate chain 2 DYNC1I2	1	3.694	4.668	6
sp|Q16629|SFRS7_HUMAN	27578	3	110	Splicing factor, arginine/serine-rich 7 SFRS7	1	3.628	0.476	12
sp|Q6NUP7|PP4R4_HUMAN	100472	7	355	Serine/threonine-protein phosphatase 4 regulatory subunit 4 PPP4R4	1	3.595	2.389	4
sp|P50990|TCPQ_HUMAN	60153	4	188	T-complex protein 1 subunit theta CCT8	1	3.581	0.443	7
sp|Q5QNW6|H2B2F_HUMAN	13912	2	120	Histone H2B type 2-F HIST2H2BF	1	3.465	0.641	13
sp|P04844|RPN2_HUMAN	69355	3	157	Dolichyl-diphosphooligosaccharide--protein glycosyltransferase subunit 2 RPN2	1	3.306	1.406	7

sp|Q71DI3|H32_HUMAN	15436	5	171	Histone H3.2 HIST2H3A	1	3.107	0.708	14
sp|Q99623|PHB2_HUMAN	33276	13	793	Prohibitin-2 PHB2	1	3.095	3.024	12
sp|P62195|PRS8_HUMAN	45768	2	114	26S protease regulatory subunit 8 PSMC5	1	3.095	1.733	10
sp|P25705|ATPA_HUMAN	59828	12	789	ATP synthase subunit alpha, mitochondrial ATP5A1	1	3.069	1.401	8
sp|O14579|COPE_HUMAN	34688	5	257	Coatomer subunit epsilon COPE	1	2.947	1.882	12
sp|Q13625|ASPP2_HUMAN	126222	15	669	Apoptosis-stimulating of p53 protein 2 TP53BP2	1	2.942	3.193	2
sp|P21796|VDAC1_HUMAN	30868	9	456	Voltage-dependent anion-selective channel protein 1 VDAC1	1	2.901	0.884	12
sp|Q13185|CBX3_HUMAN	20969	4	157	Chromobox protein homolog 3 CBX3	1	2.89	0.312	14
sp|P16615|AT2A2_HUMAN	116336	7	285	Sarcoplasmic/endoplasmic reticulum calcium ATPase 2 ATP2A2	1	2.88	2.178	4
sp|P41252|SYIC_HUMAN	145718	12	549	Isoleucyl-tRNA synthetase, cytoplasmic IARS	1	2.859	2.17	2
sp|Q8NB46|ANR52_HUMAN	116829	18	1039	Serine/threonine-protein phosphatase 6 regulatory ankyrin repeat subunit C ANKRD52	1	2.749	4.326	3
sp|O96008|TOM40_HUMAN	38211	2	149	Mitochondrial import receptor subunit TOM40 homolog TOMM40	1	2.732	1.396	11
sp|Q9P2J5|SYLC_HUMAN	135577	8	327	Leucyl-tRNA synthetase, cytoplasmic LARS	1	2.724	2.07	2
sp|P08865|RSSA_HUMAN	32947	3	222	40S ribosomal protein SA RPSA	1	2.71	1.847	12
sp|P15927|RFA2_HUMAN	29342	2	104	Replication protein A 32 kDa subunit RPA2	1	2.634	1.908	13
sp|P06748|NPM_HUMAN	32726	3	98	Nucleophosmin NPM1	1	2.583	0.993	12
sp|Q08945|SSRP1_HUMAN	81367	4	155	FACT complex subunit SSRP1 SSRP1	1	2.574	0.303	5
sp|Q9BQE3|TBA1C_HUMAN	50548	5	290	Tubulin alpha-1C chain TUBA1C	1	2.568	0.709	8
sp|P35637|FUS_HUMAN	53622	9	420	RNA-binding protein FUS FUS	1	2.488	2.827	6
sp|P55060|XPO2_HUMAN	111145	9	469	Exportin-2 CSE1L	1	2.441	2.822	4
sp|P45880|VDAC2_HUMAN	32060	8	428	Voltage-dependent anion-selective channel protein 2 VDAC2	1	2.429	0.808	12
sp|Q14697|GANAB_HUMAN	107263	4	134	Neutral alpha-glucosidase AB GANAB	1	2.34	1.749	3
sp|P53621|COPA_HUMAN	139797	11	559	Coatomer subunit alpha COPA	1	2.31	2.5	2
sp|O43175|SERA_HUMAN	57356	13	825	D-3-phosphoglycerate dehydrogenase PHGDH	1	2.26	1.507	8
sp|Q99460|PSMD1_HUMAN	106795	6	364	26S proteasome non-ATPase regulatory subunit 1 PSMD1	1	2.231	0.997	3
sp|P62136|PP1A_HUMAN	38229	16	992	Serine/threonine-protein phosphatase PP1-alpha catalytic subunit PPP1CA	1	2.221	1.811	12
sp|Q12904|AIMP1_HUMAN	34616	4	224	Aminoacyl tRNA synthase complex-interacting multifunctional protein 1 AIMP1	1	2.212	0.765	11
sp|P20340|RAB6A_HUMAN	23692	3	166	Ras-related protein Rab-6A RAB6A	1	2.207	1.243	14
sp|P40227|TCPZ_HUMAN	58444	6	280	T-complex protein 1 subunit zeta CCT6A	1	2.159	0.545	7
sp|P36957|ODO2_HUMAN	49041	2	85	Dihydrolipoyllysine-residue succinyltransferase component of 2-oxoglutarate dehydrogenase complex, mitochondrial DLST	1	2.146	1.019	9
sp|Q9Y375|CIA30_HUMAN	37797	2	122	Complex I intermediate-associated protein 30, mitochondrial NDUFAF1	1	2.114	0.861	12

sp|O94826|TOM70_HUMAN	68096	3	125	Mitochondrial import receptor subunit TOM70 TOMM70A	1	2.109	1.399	6
sp|Q96A33|CCD47_HUMAN	56123	2	84	Coiled-coil domain-containing protein 47 CCDC47	1	2.097	0.52	7
sp|P10515|ODP2_HUMAN	69466	3	133	Dihydrolipoyllysine-residue acetyltransferase component of pyruvate dehydrogenase complex, mitochondrial DLAT	1	2.095	1.051	6
sp|P05023|AT1A1_HUMAN	114135	7	387	Sodium/potassium-transporting ATPase subunit alpha-1 ATP1A1	1	2.07	1.66	4
sp|O15084|ANR28_HUMAN	118237	20	1248	Serine/threonine-protein phosphatase 6 regulatory ankyrin repeat subunit A ANKRD28	1	2.052	0.744	3
sp|Q8N766|K0090_HUMAN	112145	3	158	Uncharacterized protein KIAA0090 KIAA0090	1	2.03	1.318	3
sp|P62140|PP1B_HUMAN	37961	6	315	Serine/threonine-protein phosphatase PP1-beta catalytic subunit PPP1CB	1	2.028	1.824	12
sp|P20700|LMNB1_HUMAN	66653	10	437	Lamin-B1 LMNB1	1	1.983	2.441	6
sp|P67775|PP2AA_HUMAN	36142	14	924	Serine/threonine-protein phosphatase 2A catalytic subunit alpha isoform PPP2CA	1	1.972	4.391	12
sp|P35606|COPB2_HUMAN	103278	9	320	Coatomer subunit beta' COPB2	1	1.962	2.275	4
sp|Q8TF05|PP4R1_HUMAN	108361	27	1394	Serine/threonine-protein phosphatase 4 regulatory subunit 1 PPP4R1	1	1.961	3.109	3
sp|O00743|PPP6_HUMAN	35806	12	715	Serine/threonine-protein phosphatase 6 catalytic subunit PPP6C	1	1.951	2.048	12
sp|Q86VP6|CAND1_HUMAN	137999	14	524	Cullin-associated NEDD8-dissociated protein 1 CAND1	1	1.935	1.708	2
sp|P60510|PP4C_HUMAN	35628	13	743	Serine/threonine-protein phosphatase 4 catalytic subunit PPP4C	1	1.926	2.066	12
sp|P63151|2ABA_HUMAN	52173	6	274	Serine/threonine-protein phosphatase 2A 55 kDa regulatory subunit B alpha isoform PPP2R2A	1	1.91	1.784	8
sp|O00410|IPO5_HUMAN	125032	8	425	Importin-5 IPO5	1	1.89	1.379	3
sp|P00403|COX2_HUMAN	25719	3	161	Cytochrome c oxidase subunit 2 MT-CO2	1	1.89	0.599	14
sp|O14980|XPO1_HUMAN	124447	7	212	Exportin-1 XPO1	1	1.824	1.053	3
sp|O95816|BAG2_HUMAN	23928	2	78	BAG family molecular chaperone regulator 2 BAG2	1	1.813	0.328	14
sp|P35998|PRS7_HUMAN	49002	5	261	26S protease regulatory subunit 7 PSMC2	1	1.798	1.742	9
sp|Q13151|ROA0_HUMAN	30993	2	134	Heterogeneous nuclear ribonucleoprotein A0 HNRNPA0	1	1.79	0.338	12
sp|Q9H9B4|SFXN1_HUMAN	35881	9	521	Sideroflexin-1 SFXN1	1	1.737	1.967	12
sp|Q13200|PSMD2_HUMAN	100877	13	695	26S proteasome non-ATPase regulatory subunit 2 PSMD2	1	1.714	1.538	4
sp|P01891|1A68_HUMAN	41168	2	157	HLA class I histocompatibility antigen, A-68 alpha chain HLA-A	1	1.661	0.885	11
sp|O95373|IPO7_HUMAN	120751	5	267	Importin-7 IPO7	1	1.651	1.345	3
sp|P07437|TBB5_HUMAN	50095	3	280	Tubulin beta chain TUBB	1	1.636	0.591	9
sp|Q9NS69|TOM22_HUMAN	15512	2	133	Mitochondrial import receptor subunit TOM22 homolog TOMM22	1	1.628	0.531	14
sp|Q14257|RCN2_HUMAN	36911	3	178	Reticulocalbin-2 RCN2	1	1.602	0.411	11
sp|Q15393|SF3B3_HUMAN	136575	15	722	Splicing factor 3B subunit 3 SF3B3	1	1.588	0.979	2
sp|P55786|PSA_HUMAN	103895	6	305	Puromycin-sensitive aminopeptidase NPEPPS	1	1.574	0.941	4

sp|P62851|RS25_HUMAN	13791	4	159	40S ribosomal protein S25 RPS25	1	1.567	2.705	14
sp|Q07955|SFRS1_HUMAN	27842	2	140	Splicing factor, arginine/serine-rich 1 SFRS1	1	1.562	0.318	12
sp|Q92769|HDAC2_HUMAN	55899	2	65	Histone deacetylase 2 HDAC2	1	1.543	1.32	7
sp|Q9UKM9|RALY_HUMAN	32501	2	68	RNA-binding protein Raly RALY	1	1.514	0.458	12
sp|P61106|RAB14_HUMAN	24110	6	247	Ras-related protein Rab-14 RAB14	1	1.513	1.881	14
sp|P54136|SYRC_HUMAN	76129	6	279	Arginyl-tRNA synthetase, cytoplasmic RARS	1	1.5	1.45	6
sp|Q9BPX3|CND3_HUMAN	115345	5	216	Condensin complex subunit 3 NCAPG	1	1.497	1.153	3
sp|P29692|EF1D_HUMAN	31217	4	241	Elongation factor 1-delta EEF1D	1	1.49	0.761	12
sp|Q96AG4|LRC59_HUMAN	35308	3	124	Leucine-rich repeat-containing protein 59 LRRC59	1	1.485	1.325	12
sp|P04843|RPN1_HUMAN	68641	16	741	Dolichyl-diphosphooligosaccharide--protein glycosyltransferase subunit 1 RPN1	1	1.482	2.779	6
sp|A6NKD9|CC85C_HUMAN	45467	2	89	Coiled-coil domain-containing protein 85C CCDC85C	1	1.481	1.787	9
sp|Q8N8A2|ANR44_HUMAN	109360	15	632	Serine/threonine-protein phosphatase 6 regulatory ankyrin repeat subunit B ANKRD44	1	1.479	0.711	3
sp|Q09028|RBBP4_HUMAN	47911	5	217	Histone-binding protein RBBP4 RBBP4	1	1.472	0.347	9
sp|P63244|GBLP_HUMAN	35511	2	101	Guanine nucleotide-binding protein subunit beta-2-like 1 GNB2L1	1	1.458	1.127	12
sp|Q9NVI7|ATD3A_HUMAN	71610	3	97	ATPase family AAA domain-containing protein 3A ATAD3A	1	1.446	9.107	6
sp|P56192|SYMC_HUMAN	102249	5	186	Methionyl-tRNA synthetase, cytoplasmic MARS	1	1.442	1.213	4
sp|P53618|COPB_HUMAN	108214	3	97	Coatomer subunit beta COPB1	1	1.435	1.599	4
sp|Q02833|RASF7_HUMAN	40548	3	264	Ras association domain-containing protein 7 RASSF7	1	1.427	1.081	11
sp|P51149|RAB7A_HUMAN	23760	7	445	Ras-related protein Rab-7a RAB7A	1	1.408	0.92	14
sp|O96000|NDUBA_HUMAN	21048	2	81	NADH dehydrogenase [ubiquinone] 1 beta subcomplex subunit 10 NDUFB10	1	1.393	0.499	14
sp|P26641|EF1G_HUMAN	50429	6	284	Elongation factor 1-gamma EEF1G	1	1.391	4.717	9
sp|Q9NRG9|AAAS_HUMAN	60392	2	75	Aladin AAAS	1	1.388	1.133	8
sp|O43242|PSMD3_HUMAN	61054	2	120	26S proteasome non-ATPase regulatory subunit 3 PSMD3	1	1.366	0.662	7
sp|Q9BVC6|TM109_HUMAN	26194	2	109	Transmembrane protein 109 TMEM109	1	1.355	0.946	14
sp|P36873|PP1G_HUMAN	37701	8	446	Serine/threonine-protein phosphatase PP1-gamma catalytic subunit PPP1CC	1	1.348	1.999	13
sp|P49821|NDUV1_HUMAN	51469	4	167	NADH dehydrogenase [ubiquinone] flavoprotein 1, mitochondrial NDUFV1	1	1.333	0.794	9
sp|Q9BXL8|CDCA4_HUMAN	26553	2	98	Cell division cycle-associated protein 4 CDCA4	1	1.326	0.818	13
sp|Q9UBN7|HDAC6_HUMAN	132932	11	523	Histone deacetylase 6 HDAC6	1	1.319	3.487	2
sp|Q9H3U1|UN45A_HUMAN	104266	4	174	Protein unc-45 homolog A UNC45A	1	1.315	1.104	4
sp|Q14738|2A5D_HUMAN	70289	6	285	Serine/threonine-protein phosphatase 2A 56 kDa regulatory subunit delta isoform PPP2R5D	1	1.311	0.687	6
sp|Q9GZL7|WDR12_HUMAN	48191	2	77	Ribosome biogenesis protein WDR12 WDR12	1	1.309	0.255	9

sp|P27694|RFA1_HUMAN	68723	13	573	Replication protein A 70 kDa DNA-binding subunit RPA1	1	1.305	0.957	6
sp|P68363|TBA1B_HUMAN	50804	14	955	Tubulin alpha-1B chain TUBA1B	1	1.276	0.785	9
sp|P61026|RAB10_HUMAN	22755	3	93	Ras-related protein Rab-10 RAB10	1	1.275	2.113	14
sp|P17980|PRS6A_HUMAN	49458	5	180	26S protease regulatory subunit 6A PSMC3	1	1.273	1.172	9
sp|P46777|RL5_HUMAN	34569	5	207	60S ribosomal protein L5 RPL5	1	1.269	1.502	12
sp|P52907|CAZA1_HUMAN	33073	5	359	F-actin-capping protein subunit alpha-1 CAPZA1	1	1.268	0.451	12
sp|P29966|MARCS_HUMAN	31707	6	284	Myristoylated alanine-rich C-kinase substrate MARCKS	1	1.26	1.613	6
sp|Q15006|TTC35_HUMAN	34982	2	101	Tetratricopeptide repeat protein 35 TTC35	1	1.252	1.054	12
sp|Q9BYD6|RM01_HUMAN	37113	2	84	39S ribosomal protein L1, mitochondrial MRPL1	1	1.249	0.828	12
sp|O95292|VAPB_HUMAN	27439	2	89	Vesicle-associated membrane protein-associated protein B/C VAPB	1	1.237	0.819	13
sp|P49368|TCPG_HUMAN	61066	14	675	T-complex protein 1 subunit gamma CCT3	1	1.214	1.579	7
sp|Q15029|U5S1_HUMAN	110336	5	278	116 kDa U5 small nuclear ribonucleoprotein component EFTUD2	1	1.209	0.444	3
sp|P23284|PPIB_HUMAN	23785	2	92	Peptidyl-prolyl cis-trans isomerase B PPIB	1	1.195	0.344	14
sp|Q99873|ANM1_HUMAN	42059	3	155	Protein arginine N-methyltransferase 1 PRMT1	1	1.189	0.529	11
sp|Q99832|TCPH_HUMAN	59842	5	234	T-complex protein 1 subunit eta CCT7	1	1.185	2.483	7
sp|P51114|FXR1_HUMAN	70020	2	68	Fragile X mental retardation syndrome-related protein 1 FXR1	1	1.18	0.471	6
sp|P61586|RHOA_HUMAN	22096	4	208	Transforming protein RhoA RHOA	1	1.176	0.83	14
sp|Q8TEX9|IPO4_HUMAN	120179	2	73	Importin-4 IPO4	1	1.175	1.16	3
sp|Q14498|RBM39_HUMAN	59628	2	89	RNA-binding protein 39 RBM39	1	1.17	0.684	6
sp|P46782|RS5_HUMAN	23033	4	256	40S ribosomal protein S5 RPS5	1	1.166	1.906	14
sp|O75306|NDUS2_HUMAN	52911	4	208	NADH dehydrogenase [ubiquinone] iron-sulfur protein 2, mitochondrial NDUFS2	1	1.159	0.437	10
sp|P14868|SYDC_HUMAN	57499	11	512	Aspartyl-tRNA synthetase, cytoplasmic DARS	1	1.158	0.839	8
sp|Q9UNX3|RL26L_HUMAN	17246	2	75	60S ribosomal protein L26-like 1 RPL26L1	1	1.147	4.446	14
sp|P62266|RS23_HUMAN	15969	3	137	40S ribosomal protein S23 RPS23	1	1.144	1.9	14
sp|P31040|DHSA_HUMAN	73672	4	222	Succinate dehydrogenase [ubiquinone] flavoprotein subunit, mitochondrial SDHA	1	1.143	1.959	6
sp|Q13257|MD2L1_HUMAN	23666	4	125	Mitotic spindle assembly checkpoint protein MAD2A MAD2L1	1	1.138	1.245	14
sp|O75396|SC22B_HUMAN	24896	4	164	Vesicle-trafficking protein SEC22b SEC22B	1	1.133	0.916	14
sp|P09651|ROA1_HUMAN	38837	7	362	Heterogeneous nuclear ribonucleoprotein A1 HNRNPA1	1	1.121	0.228	12
sp|Q15019|SEPT2_HUMAN	41689	3	160	Septin-2 SEPT2	1	1.12	0.546	11
sp|P12956|XRCC6_HUMAN	70084	3	191	X-ray repair cross-complementing protein 6 XRCC6	1	1.115	0.345	6
sp|Q9Y6G9|DC1L1_HUMAN	56829	4	189	Cytoplasmic dynein 1 light intermediate chain 1 DYNC1LI1	1	1.112	0.514	7
sp|O00264|PGRC1_HUMAN	21772	6	385	Membrane-associated progesterone receptor component 1 PGRMC1	1	1.108	1.174	14

sp|P83731|RL24_HUMAN	17882	2	119	60S ribosomal protein L24 RPL24	1	1.097	1.177	14
sp|P00387|NB5R3_HUMAN	34441	2	100	NADH-cytochrome b5 reductase 3 CYB5R3	1	1.084	0.55	12
sp|O43809|CPSF5_HUMAN	26268	2	75	Cleavage and polyadenylation specificity factor subunit 5 NUDT21	1	1.068	0.663	13
sp|Q07812|BAX_HUMAN	21285	2	105	Apoptosis regulator BAX BAX	1	1.055	0.957	14
sp|P48047|ATPO_HUMAN	23377	4	215	ATP synthase subunit O, mitochondrial ATP5O	1	1.054	1.004	14
sp|Q13310|PABP4_HUMAN	71080	5	212	Polyadenylate-binding protein 4 PABPC4	1	1.05	0.61	6
sp|P61006|RAB8A_HUMAN	23824	3	111	Ras-related protein Rab-8A RAB8A	1	1.047	1.152	14
sp|P10398|ARAF_HUMAN	68341	3	96	Serine/threonine-protein kinase A-Raf ARAF	1	1.046	1.692	6
sp|P09012|SNRPA_HUMAN	31259	3	128	U1 small nuclear ribonucleoprotein A SNRPA	1	1.045	0.33	12
sp|Q16531|DDB1_HUMAN	128142	5	257	DNA damage-binding protein 1 DDB1	1	1.043	0.759	3
sp|P46779|RL28_HUMAN	15795	3	123	60S ribosomal protein L28 RPL28	1	1.039	2.635	14
sp|P11142|HSP7C_HUMAN	71082	23	1204	Heat shock cognate 71 kDa protein HSPA8	1	1.038	2.669	6
sp|Q9NYK5|RM39_HUMAN	39200	2	71	39S ribosomal protein L39, mitochondrial MRPL39	1	1.035	0.562	12
sp|P14314|GLU2B_HUMAN	60357	4	234	Glucosidase 2 subunit beta PRKCSH	1	1.033	1.661	6
sp|P16949|STMN1_HUMAN	17292	2	143	Stathmin STMN1	1	1.032	0.514	14
sp|P17812|PYRG1_HUMAN	67332	2	100	CTP synthase 1 CTPS	1	1.023	0.929	6
sp|P68371|TBB2C_HUMAN	50255	14	926	Tubulin beta-2C chain TUBB2C	1	1.023	0.674	9
sp|P10809|CH60_HUMAN	61187	17	1214	60 kDa heat shock protein, mitochondrial HSPD1	1	1.02	0.881	7
sp|P31942|HNRH3_HUMAN	36960	4	169	Heterogeneous nuclear ribonucleoprotein H3 HNRNPH3	1	1.017	0.511	12
sp|Q9Y265|RUVB1_HUMAN	50538	10	561	RuvB-like 1 RUVBL1	1	1.012	0.66	9
sp|Q15046|SYK_HUMAN	68461	9	317	Lysyl-tRNA synthetase KARS	1	1.008	1.5	6
sp|Q66LE6|2ABD_HUMAN	52580	2	68	Serine/threonine-protein phosphatase 2A 55 kDa regulatory subunit B delta isoform PPP2R2D	1	1.005	1.534	9
sp|P43307|SSRA_HUMAN	32215	2	81	Translocon-associated protein subunit alpha SSR1	1	1.005	0.908	12
sp|Q12972|PP1R8_HUMAN	38626	22	1195	Nuclear inhibitor of protein phosphatase 1 PPP1R8	1	1.005	0.827	11
sp|P62333|PRS10_HUMAN	44430	4	170	26S protease regulatory subunit 10B PSMC6	1	0.999	0.961	11
sp|Q9H788|SH24A_HUMAN	52922	9	459	SH2 domain-containing protein 4A SH2D4A	1	0.997	1.021	9
sp|P49755|TMEDA_HUMAN	25131	4	139	Transmembrane emp24 domain-containing protein 10 TMED10	1	0.994	1.576	14
sp|Q9HCE1|MOV10_HUMAN	114512	5	194	Putative helicase MOV-10 MOV10	1	0.984	0.51	3
sp|O14974|MYPT1_HUMAN	115610	3	90	Protein phosphatase 1 regulatory subunit 12A PPP1R12A	1	0.983	4.205	3
sp|Q02978|M2OM_HUMAN	34211	5	193	Mitochondrial 2-oxoglutarate/malate carrier protein SLC25A11	1	0.977	0.626	13
sp|Q9H0U4|RAB1B_HUMAN	22328	8	439	Ras-related protein Rab-1B RAB1B	1	0.975	0.895	14

sp|P51970|NDUA8_HUMAN	20548	2	85	NADH dehydrogenase [ubiquinone] 1 alpha subcomplex subunit 8 NDUFA8	1	0.968	0.71	14
sp|P54920|SNAA_HUMAN	33667	5	159	Alpha-soluble NSF attachment protein NAPA	1	0.966	0.765	12
sp|P38646|GRP75_HUMAN	73920	12	708	Stress-70 protein, mitochondrial HSPA9	1	0.964	1.776	6
sp|Q86V81|THOC4_HUMAN	26872	2	184	THO complex subunit 4 THOC4	1	0.956	0.733	13
sp|P22626|ROA2_HUMAN	37464	8	460	Heterogeneous nuclear ribonucleoproteins A2/B1 HNRNPA2B1	1	0.943	0.159	12
sp|P30153|2AAA_HUMAN	66065	30	1838	Serine/threonine-protein phosphatase 2A 65 kDa regulatory subunit A alpha isoform PPP2R1A	1	0.941	3.534	7
sp|P62829|RL23_HUMAN	14970	4	175	60S ribosomal protein L23 RPL23	1	0.931	1.17	14
sp|O75832|PSD10_HUMAN	24697	2	91	26S proteasome non-ATPase regulatory subunit 10 PSMD10	1	0.927	0.322	14
sp|P50914|RL14_HUMAN	23531	3	156	60S ribosomal protein L14 RPL14	1	0.922	0.728	13
sp|P31943|HNRH1_HUMAN	49484	7	319	Heterogeneous nuclear ribonucleoprotein H HNRNPH1	1	0.921	0.461	9
sp|P55735|SEC13_HUMAN	36031	3	212	Protein SEC13 homolog SEC13	1	0.92	0.867	12
sp|Q15291|RBBP5_HUMAN	59800	2	71	Retinoblastoma-binding protein 5 RBBP5	1	0.919	0.967	6
sp|P48739|PIPNB_HUMAN	31805	3	148	Phosphatidylinositol transfer protein beta isoform PITPNB	1	0.913	0.959	12
sp|P62277|RS13_HUMAN	17212	3	165	40S ribosomal protein S13 RPS13	1	0.908	1.223	14
sp|P53041|PPP5_HUMAN	57412	31	1748	Serine/threonine-protein phosphatase 5 PPP5C	1	0.907	2.029	8
sp|Q9UHG3|PCYOX_HUMAN	57003	3	100	Prenylcysteine oxidase 1 PCYOX1	1	0.906	0.85	8
sp|P62820|RAB1A_HUMAN	22891	2	97	Ras-related protein Rab-1A RAB1A	1	0.906	0.69	14
sp|P08107|HSP71_HUMAN	70294	29	1612	Heat shock 70 kDa protein 1A/1B HSPA1A	1	0.905	5.473	6
sp|P35232|PHB_HUMAN	29843	13	716	Prohibitin PHB	1	0.904	0.74	13
sp|Q96HS1|PGAM5_HUMAN	32213	4	201	Serine/threonine-protein phosphatase PGAM5, mitochondrial PGAM5	1	0.902	0.54	12
sp|P06576|ATPB_HUMAN	56525	17	1147	ATP synthase subunit beta, mitochondrial ATP5B	1	0.9	0.565	9
sp|P62701|RS4X_HUMAN	29807	4	238	40S ribosomal protein S4, X isoform RPS4X	1	0.892	0.738	13
sp|P35613|BASI_HUMAN	42573	6	238	Basigin BSG	1	0.892	0.418	11
sp|O14744|ANM5_HUMAN	73322	2	88	Protein arginine N-methyltransferase 5 PRMT5	1	0.888	0.822	6
sp|Q9P032|NDUF4_HUMAN	20311	2	66	NADH dehydrogenase [ubiquinone] 1 alpha subcomplex assembly factor 4 NDUFAF4	1	0.876	0.776	14
sp|Q9BVA1|TBB2B_HUMAN	50377	2	119	Tubulin beta-2B chain TUBB2B	1	0.872	0.645	9
sp|P08195|4F2_HUMAN	68180	2	129	4F2 cell-surface antigen heavy chain SLC3A2	1	0.859	1.11	6
sp|Q53H12|AGK_HUMAN	47564	2	89	Acylglycerol kinase, mitochondrial AGK	1	0.858	0.46	10
sp|O75489|NDUS3_HUMAN	30337	5	344	NADH dehydrogenase [ubiquinone] iron-sulfur protein 3, mitochondrial NDUFS3	1	0.856	0.369	13
sp|P39019|RS19_HUMAN	16051	3	127	40S ribosomal protein S19 RPS19	1	0.847	2.645	14
sp|O60506|HNRPQ_HUMAN	69788	8	352	Heterogeneous nuclear ribonucleoprotein Q SYNCRIP	1	0.845	0.376	6

sp|P24534|EF1B_HUMAN	24919	3	263	Elongation factor 1-beta EEF1B2	1	0.842	0.481	13
sp|P61009|SPCS3_HUMAN	20358	2	98	Signal peptidase complex subunit 3 SPCS3	1	0.836	0.955	14
sp|Q13765|NACA_HUMAN	23370	2	220	Nascent polypeptide-associated complex subunit alpha NACA	1	0.835	0.591	12
sp|P18621|RL17_HUMAN	21611	3	98	60S ribosomal protein L17 RPL17	1	0.817	0.472	14
sp|P18124|RL7_HUMAN	29264	3	123	60S ribosomal protein L7 RPL7	1	0.812	0.41	13
sp|P31930|QCR1_HUMAN	53297	3	177	Cytochrome b-c1 complex subunit 1, mitochondrial UQCRC1	1	0.808	0.309	10
sp|P61019|RAB2A_HUMAN	23702	5	329	Ras-related protein Rab-2A RAB2A	1	0.806	0.635	14
sp|Q07020|RL18_HUMAN	21735	2	107	60S ribosomal protein L18 RPL18	1	0.793	0.686	14
sp|Q9Y230|RUVB2_HUMAN	51296	12	652	RuvB-like 2 RUVBL2	1	0.789	0.671	9
sp|P62241|RS8_HUMAN	24475	7	270	40S ribosomal protein S8 RPS8	1	0.785	0.814	13
sp|P11021|GRP78_HUMAN	72402	12	762	78 kDa glucose-regulated protein HSPA5	1	0.783	1.267	6
sp|Q96CS3|FAF2_HUMAN	52933	2	93	FAS-associated factor 2 FAF2	1	0.781	0.647	9
sp|P06493|CDC2_HUMAN	34117	4	171	Cell division control protein 2 homolog CDC2	1	0.779	1.068	12
sp|Q13283|G3BP1_HUMAN	52189	3	177	Ras GTPase-activating protein-binding protein 1 G3BP1	1	0.778	0.35	7
sp|Q13347|EIF3I_HUMAN	36878	3	122	Eukaryotic translation initiation factor 3 subunit I EIF3I	1	0.777	0.718	12
sp|P27824|CALX_HUMAN	67982	2	70	Calnexin CANX	1	0.77	1.742	6
sp|P30050|RL12_HUMAN	17979	5	338	60S ribosomal protein L12 RPL12	1	0.769	0.735	14
sp|Q14232|EI2BA_HUMAN	33976	4	203	Translation initiation factor eIF-2B subunit alpha EIF2B1	1	0.764	0.323	12
sp|P62269|RS18_HUMAN	17708	5	263	40S ribosomal protein S18 RPS18	1	0.755	0.788	14
sp|P46060|RAGP1_HUMAN	63958	4	231	Ran GTPase-activating protein 1 RANGAP1	1	0.755	0.78	6
sp|O95831|AIFM1_HUMAN	67144	2	74	Apoptosis-inducing factor 1, mitochondrial AIFM1	1	0.754	0.668	6
sp|P51991|ROA3_HUMAN	39799	5	192	Heterogeneous nuclear ribonucleoprotein A3 HNRNPA3	1	0.754	0.12	11
sp|Q15366|PCBP2_HUMAN	38955	5	243	Poly(rC)-binding protein 2 PCBP2	1	0.753	0.307	12
sp|O00148|DDX39_HUMAN	49611	4	225	ATP-dependent RNA helicase DDX39 DDX39	1	0.742	0.276	9
sp|Q99497|PARK7_HUMAN	20050	7	298	Protein DJ-1 PARK7	1	0.738	0.521	14
sp|P07197|NFM_HUMAN	102468	9	361	Neurofilament medium polypeptide NEFM	1	0.737	1.014	3
sp|P38919|IF4A3_HUMAN	47126	2	73	Eukaryotic initiation factor 4A-III EIF4A3	1	0.733	0.259	10
sp|Q9Y266|NUDC_HUMAN	38276	11	556	Nuclear migration protein nudC NUDC	1	0.732	0.271	11
sp|P46459|NSF_HUMAN	83055	3	132	Vesicle-fusing ATPase NSF	1	0.725	0.634	5
sp|Q16775|GLO2_HUMAN	34240	3	129	Hydroxyacylglutathione hydrolase, mitochondrial HAGH	1	0.722	0.485	13
sp|P0C7M2|RA1L3_HUMAN	34373	2	112	Putative heterogeneous nuclear ribonucleoprotein A1-like 3 HNRPA1L3	1	0.721	0.149	11
sp|Q9BY41|HDAC8_HUMAN	42301	3	225	Histone deacetylase 8 HDAC8	1	0.719	0.385	11

sp|Q9H845|ACAD9_HUMAN	69344	3	93	Acyl-CoA dehydrogenase family member 9, mitochondrial ACAD9	1	0.718	0.567	7
sp|Q9UPN7|SAPS1_HUMAN	97291	2	92	Serine/threonine-protein phosphatase 6 regulatory subunit 1 SAPS1	1	0.715	0.937	6
sp|P19404|NDUV2_HUMAN	27659	4	235	NADH dehydrogenase [ubiquinone] flavoprotein 2, mitochondrial NDUFV2	1	0.712	0.16	14
sp|P53999|TCP4_HUMAN	14386	3	181	Activated RNA polymerase II transcriptional coactivator p15 SUB1	1	0.702	0.827	14
sp|Q13362|2A5G_HUMAN	61421	3	117	Serine/threonine-protein phosphatase 2A 56 kDa regulatory subunit gamma isoform PPP2R5C	1	0.699	0.872	8
sp|P17987|TCPA_HUMAN	60819	6	231	T-complex protein 1 subunit alpha TCP1	1	0.696	0.888	7
sp|Q15645|TRP13_HUMAN	48863	4	183	Thyroid receptor-interacting protein 13 TRIP13	1	0.696	0.477	10
sp|P62263|RS14_HUMAN	16434	5	221	40S ribosomal protein S14 RPS14	1	0.692	1.353	14
sp|P61978|HNRPK_HUMAN	51230	6	319	Heterogeneous nuclear ribonucleoprotein K HNRNPK	1	0.684	0.414	8
sp|P17844|DDX5_HUMAN	69618	6	242	Probable ATP-dependent RNA helicase DDX5 DDX5	1	0.683	1.173	6
sp|P35221|CTNA1_HUMAN	100693	2	128	Catenin alpha-1 CTNNA1	1	0.678	0.583	4
sp|O75947|ATP5H_HUMAN	18537	3	122	ATP synthase subunit d, mitochondrial ATP5H	1	0.677	0.853	14
sp|P24666|PPAC_HUMAN	18487	10	699	Low molecular weight phosphotyrosine protein phosphatase ACP1	1	0.677	0.633	14
sp|P60709|ACTB_HUMAN	42052	15	959	Actin, cytoplasmic 1 ACTB	1	0.676	0.347	11
sp|P07910|HNRPC_HUMAN	33707	8	469	Heterogeneous nuclear ribonucleoproteins C1/C2 HNRNPC	1	0.676	0.067	11
sp|Q16740|CLPP_HUMAN	30446	2	121	Putative ATP-dependent Clp protease proteolytic subunit, mitochondrial CLPP	1	0.673	0.396	13
sp|P08708|RS17_HUMAN	15597	3	144	40S ribosomal protein S17 RPS17	1	0.672	0.924	14
sp|O14818|PSA7_HUMAN	28041	5	303	Proteasome subunit alpha type-7 PSMA7	1	0.672	0.437	13
sp|Q9Y3I0|CV028_HUMAN	55688	2	62	UPF0027 protein C22orf28 C22orf28	1	0.672	0.433	8
sp|O60664|PLIN3_HUMAN	47189	2	105	Perilipin-3 PLIN3	1	0.658	0.715	10
sp|Q07021|C1QBP_HUMAN	31742	3	218	Complement component 1 Q subcomponent-binding protein, mitochondrial C1QBP	1	0.649	0.308	13
sp|Q8IVD9|NUDC3_HUMAN	40854	2	110	NudC domain-containing protein 3 NUDCD3	1	0.644	0.574	10
sp|Q99614|TTC1_HUMAN	33961	2	74	Tetratricopeptide repeat protein 1 TTC1	1	0.641	0.754	11
sp|Q13405|RM49_HUMAN	19243	4	202	39S ribosomal protein L49, mitochondrial MRPL49	1	0.636	0.538	14
sp|P52597|HNRPF_HUMAN	45985	4	214	Heterogeneous nuclear ribonucleoprotein F HNRNPF	1	0.632	2.483	10
sp|P62750|RL23A_HUMAN	17684	3	168	60S ribosomal protein L23a RPL23A	1	0.631	1.665	14
sp|P61353|RL27_HUMAN	15788	2	78	60S ribosomal protein L27 RPL27	1	0.626	1.037	14
sp|Q9UJV9|DDX41_HUMAN	70477	4	193	Probable ATP-dependent RNA helicase DDX41 DDX41	1	0.624	1.164	6
sp|P15880|RS2_HUMAN	31590	7	340	40S ribosomal protein S2 RPS2	1	0.623	0.284	12
sp|Q15717|ELAV1_HUMAN	36240	8	422	ELAV-like protein 1 ELAVL1	1	0.613	0.244	12
sp|P62280|RS11_HUMAN	18590	7	263	40S ribosomal protein S11 RPS11	1	0.61	1.038	14

sp|P08238|HS90B_HUMAN	83554	52	2711	Heat shock protein HSP 90-beta HSP90AB1	1	0.606	2.608	5
sp|Q9HDC9|APMAP_HUMAN	46622	3	122	Adipocyte plasma membrane-associated protein APMAP	1	0.599	0.509	10
sp|P62913|RL11_HUMAN	20468	2	135	60S ribosomal protein L11 RPL11	1	0.594	0.622	14
sp|P18085|ARF4_HUMAN	20612	3	101	ADP-ribosylation factor 4 ARF4	1	0.594	0.612	14
sp|Q5T1J5|CHCH9_HUMAN	15708	2	158	Coiled-coil-helix-coiled-coil-helix domain-containing protein 9, mitochondrial CHCHD9	1	0.592	0.755	14
sp|P38159|HNRPG_HUMAN	42306	4	223	Heterogeneous nuclear ribonucleoprotein G RBMX	1	0.591	0.131	11
sp|Q9Y3F4|STRAP_HUMAN	38756	3	160	Serine-threonine kinase receptor-associated protein STRAP	1	0.59	0.317	11
sp|Q8WVM8|SCFD1_HUMAN	72676	6	320	Sec1 family domain-containing protein 1 SCFD1	1	0.583	0.583	6
sp|P23396|RS3_HUMAN	26842	12	625	40S ribosomal protein S3 RPS3	1	0.582	0.398	13
sp|P05388|RLA0_HUMAN	34423	10	541	60S acidic ribosomal protein P0 RPLP0	1	0.582	0.286	12
sp|P62906|RL10A_HUMAN	24987	5	274	60S ribosomal protein L10a RPL10A	1	0.574	0.37	13
sp|Q13561|DCTN2_HUMAN	44318	3	252	Dynactin subunit 2 DCTN2	1	0.573	0.288	10
sp|O43399|TPD54_HUMAN	22281	4	294	Tumor protein D54 TPD52L2	1	0.572	0.504	13
sp|P42704|LPPRC_HUMAN	159003	29	1333	Leucine-rich PPR motif-containing protein, mitochondrial LRPPRC	1	0.564	0.662	2
sp|P50990|TCPQ_HUMAN	60153	5	182	T-complex protein 1 subunit theta CCT8	1	0.56	0.665	8
sp|P51571|SSRD_HUMAN	19158	2	146	Translocon-associated protein subunit delta SSR4	1	0.559	1.127	14
sp|P07195|LDHB_HUMAN	36900	4	188	L-lactate dehydrogenase B chain LDHB	1	0.555	0.377	12
sp|P62873|GBB1_HUMAN	38151	4	162	Guanine nucleotide-binding protein G(I)/G(S)/G(T) subunit beta-1 GNB1	1	0.548	0.646	12
sp|Q92900|RENT1_HUMAN	125578	2	76	Regulator of nonsense transcripts 1 UPF1	1	0.546	0.338	2
sp|P62826|RAN_HUMAN	24579	4	229	GTP-binding nuclear protein Ran RAN	1	0.543	0.428	13
sp|Q9Y3A3|MOBL3_HUMAN	26529	5	245	Mps one binder kinase activator-like 3 MOBKL3	1	0.54	0.393	13
sp|Q00577|PURA_HUMAN	35003	4	185	Transcriptional activator protein Pur-alpha PURA	1	0.536	0.169	11
sp|P48643|TCPE_HUMAN	60089	5	177	T-complex protein 1 subunit epsilon CCT5	1	0.532	0.438	7
sp|Q9UBB4|ATX10_HUMAN	54196	5	260	Ataxin-10 ATXN10	1	0.531	0.666	9
sp|P46781|RS9_HUMAN	22635	3	93	40S ribosomal protein S9 RPS9	1	0.529	0.888	14
sp|Q5VTE0|EF1A3_HUMAN	50495	4	133	Putative elongation factor 1-alpha-like 3 EEF1AL3	1	0.524	0.535	10
sp|O76071|CIAO1_HUMAN	38842	5	243	Probable cytosolic iron-sulfur protein assembly protein CIAO1 CIAO1	1	0.521	0.266	11
sp|P15153|RAC2_HUMAN	21814	2	76	Ras-related C3 botulinum toxin substrate 2 RAC2	1	0.518	0.868	14
sp|P52815|RM12_HUMAN	21563	3	141	39S ribosomal protein L12, mitochondrial MRPL12	1	0.517	0.34	14
sp|Q9Y224|CN166_HUMAN	28165	4	260	UPF0568 protein C14orf166 C14orf166	1	0.516	0.203	13
sp|Q92600|RCD1_HUMAN	33952	3	156	Cell differentiation protein RCD1 homolog RQCD1	1	0.513	0.33	13

sp|Q16537|2A5E_HUMAN	55064	6	313	Serine/threonine-protein phosphatase 2A 56 kDa regulatory subunit epsilon isoform PPP2R5E	1	0.509	0.693	9
sp|P62917|RL8_HUMAN	28235	2	86	60S ribosomal protein L8 RPL8	1	0.508	0.671	13
sp|Q15365|PCBP1_HUMAN	37987	3	155	Poly(rC)-binding protein 1 PCBP1	1	0.507	0.115	11
sp|Q9H3G5|CPVL_HUMAN	54414	2	84	Probable serine carboxypeptidase CPVL CPVL	1	0.498	0.483	9
sp|Q9Y3B3|TMED7_HUMAN	25498	3	145	Transmembrane emp24 domain-containing protein 7 TMED7	1	0.493	0.561	13
sp|Q99536|VAT1_HUMAN	42122	7	365	Synaptic vesicle membrane protein VAT-1 homolog VAT1	1	0.492	0.492	11
sp|P55036|PSMD4_HUMAN	40939	2	113	26S proteasome non-ATPase regulatory subunit 4 PSMD4	1	0.488	0.217	10
sp|P27348|1433T_HUMAN	28032	4	216	14-3-3 protein theta YWHAQ	1	0.482	0.318	13
sp|O75821|EIF3G_HUMAN	35874	3	124	Eukaryotic translation initiation factor 3 subunit G EIF3G	1	0.47	0.515	11
sp|P63104|1433Z_HUMAN	27899	8	598	14-3-3 protein zeta/delta YWHAZ	1	0.456	0.29	13
sp|Q9Y3D0|FA96B_HUMAN	17766	2	112	Protein FAM96B FAM96B	1	0.454	0.459	14
sp|P62258|1433E_HUMAN	29326	6	298	14-3-3 protein epsilon YWHAE	1	0.448	0.381	13
sp|Q9BU61|NDUF3_HUMAN	20566	2	80	NADH dehydrogenase [ubiquinone] 1 alpha subcomplex assembly factor 3 NDUFAF3	1	0.439	0.565	14
sp|P60900|PSA6_HUMAN	27838	2	89	Proteasome subunit alpha type-6 PSMA6	1	0.439	0.411	13
sp|Q14103|HNRPD_HUMAN	38581	4	260	Heterogeneous nuclear ribonucleoprotein D0 HNRNPD	1	0.437	0.083	11
sp|Q9Y5K5|UCHL5_HUMAN	37868	3	90	Ubiquitin carboxyl-terminal hydrolase isozyme L5 UCHL5	1	0.436	0.364	11
sp|P02768|ALBU_HUMAN	71317	6	203	Serum albumin ALB	1	0.436	0.359	6
sp|P19338|NUCL_HUMAN	76625	9	333	Nucleolin NCL	1	0.427	0.637	6
sp|P49770|EI2BB_HUMAN	39193	5	160	Translation initiation factor eIF-2B subunit beta EIF2B2	1	0.425	0.176	11
sp|P14866|HNRPL_HUMAN	64720	6	317	Heterogeneous nuclear ribonucleoprotein L HNRNPL	1	0.421	0.09	6
sp|P30049|ATPD_HUMAN	17479	3	174	ATP synthase subunit delta, mitochondrial ATP5D	1	0.42	0.939	14
sp|Q9NWS0|PIHD1_HUMAN	32513	3	134	PIH1 domain-containing protein 1 PIH1D1	1	0.416	0.613	12
sp|P07900|HS90A_HUMAN	85006	28	1429	Heat shock protein HSP 90-alpha HSP90AA1	1	0.406	2.055	5
sp|P50148|GNAQ_HUMAN	42400	2	88	Guanine nucleotide-binding protein G(q) subunit alpha GNAQ	1	0.404	0.396	11
sp|P22392|NDKB_HUMAN	17401	5	195	Nucleoside diphosphate kinase B NME2	1	0.397	0.337	14
sp|P43487|RANG_HUMAN	23467	4	183	Ran-specific GTPase-activating protein RANBP1	1	0.386	0.407	13
sp|P11940|PABP1_HUMAN	70854	15	873	Polyadenylate-binding protein 1 PABPC1	1	0.385	0.229	6
sp|O43324|MCA3_HUMAN	19855	2	85	Eukaryotic translation elongation factor 1 epsilon-1 EEF1E1	1	0.378	0.319	14
sp|P09661|RU2A_HUMAN	28512	3	195	U2 small nuclear ribonucleoprotein A' SNRPA1	1	0.377	0.381	13
sp|P62249|RS16_HUMAN	16549	5	212	40S ribosomal protein S16 RPS16	1	0.367	0.489	14
sp|O00425|IF2B3_HUMAN	64008	8	323	Insulin-like growth factor 2 mRNA-binding protein 3 IGF2BP3	1	0.36	0.738	6

sp|P47756|CAPZB_HUMAN	31616	2	106	F-actin-capping protein subunit beta CAPZB	1	0.357	0.314	12
sp|P61224|RAP1B_HUMAN	21040	3	132	Ras-related protein Rap-1b RAP1B	1	0.355	0.994	14
sp|P08754|GNAI3_HUMAN	41076	2	96	Guanine nucleotide-binding protein G(k) subunit alpha GNAI3	1	0.351	0.242	11
sp|Q9NZI8|IF2B1_HUMAN	63783	15	762	Insulin-like growth factor 2 mRNA-binding protein 1 IGF2BP1	1	0.347	0.477	6
sp|Q15293|RCN1_HUMAN	38866	4	193	Reticulocalbin-1 RCN1	1	0.345	0.196	11
sp|Q16543|CDC37_HUMAN	44953	9	624	Hsp90 co-chaperone Cdc37 CDC37	1	0.343	0.424	10
sp|Q9Y5S9|RBM8A_HUMAN	19934	2	117	RNA-binding protein 8A RBM8A	1	0.341	0.111	14
sp|Q9Y2Z0|SUGT1_HUMAN	41284	18	951	Suppressor of G2 allele of SKP1 homolog SUGT1	1	0.338	0.17	11
sp|P61289|PSME3_HUMAN	29602	2	132	Proteasome activator complex subunit 3 PSME3	1	0.331	0.154	12
sp|Q9HB71|CYBP_HUMAN	26308	2	72	Calcyclin-binding protein CACYBP	1	0.323	0.244	13
sp|P12273|PIP_HUMAN	16847	2	135	Prolactin-inducible protein PIP	1	0.32	0.229	14
sp|O14950|ML12B_HUMAN	19824	5	253	Myosin regulatory light chain 12B MYL12B	1	0.307	0.355	14
sp|P60174|TPIS_HUMAN	26938	2	82	Triosephosphate isomerase TPI1	1	0.307	0.208	13
sp|P28072|PSB6_HUMAN	25570	2	106	Proteasome subunit beta type-6 PSMB6	1	0.297	0.352	14
sp|P31025|LCN1_HUMAN	19409	2	134	Lipocalin-1 LCN1	1	0.296	0.17	14
sp|Q12905|ILF2_HUMAN	43263	9	517	Interleukin enhancer-binding factor 2 ILF2	1	0.29	0.085	11
sp|P63208|SKP1_HUMAN	18817	2	125	S-phase kinase-associated protein 1 SKP1	1	0.287	0.281	14
sp|Q96DG6|CMBL_HUMAN	28372	8	374	Carboxymethylenebutenolidase homolog CMBL	1	0.284	0.269	13
sp|O95433|AHSA1_HUMAN	38421	4	165	Activator of 90 kDa heat shock protein ATPase homolog 1 AHSA1	1	0.279	0.231	11
sp|P00492|HPRT_HUMAN	24792	2	105	Hypoxanthine-guanine phosphoribosyltransferase HPRT1	1	0.261	0.268	13
sp|Q9UBQ5|EIF3K_HUMAN	25329	2	128	Eukaryotic translation initiation factor 3 subunit K EIF3K	1	0.257	0.357	14
sp|Q5H9R7|SAPS3_HUMAN	98577	7	308	Serine/threonine-protein phosphatase 6 regulatory subunit 3 SAPS3	1	0.255	0.236	5
sp|Q06830|PRDX1_HUMAN	22324	6	301	Peroxiredoxin-1 PRDX1	1	0.246	0.302	14
sp|P32119|PRDX2_HUMAN	22049	2	76	Peroxiredoxin-2 PRDX2	1	0.246	0.231	14
sp|P12277|KCRB_HUMAN	42902	3	175	Creatine kinase B-type CKB	1	0.236	0.163	11
sp|P61421|VA0D1_HUMAN	40759	3	112	V-type proton ATPase subunit d 1 ATP6V0D1	1	0.234	25.931	11
sp|Q15185|TEBP_HUMAN	18971	3	133	Prostaglandin E synthase 3 PTGES3	1	0.227	0.294	14
sp|P12814|ACTN1_HUMAN	103563	4	189	Alpha-actinin-1 ACTN1	1	0.222	0.296	4
sp|P62899|RL31_HUMAN	14454	3	130	60S ribosomal protein L31 RPL31	1	0.218	0.907	14
sp|P09211|GSTP1_HUMAN	23569	2	82	Glutathione S-transferase P GSTP1	1	0.215	0.293	14
sp|P62424|RL7A_HUMAN	30148	3	123	60S ribosomal protein L7a RPL7A	1	0.211	0.128	12
sp|P35268|RL22_HUMAN	14835	3	214	60S ribosomal protein L22 RPL22	1	0.208	0.187	14

sp|P06733|ENOA_HUMAN	47481	3	257	Alpha-enolase ENO1	1	0.204	0.251	10
sp|P26378|ELAV4_HUMAN	42028	3	160	ELAV-like protein 4 ELAVL4	1	0.203	0.44	11
sp|Q5MIZ7|P4R3B_HUMAN	98181	2	113	Serine/threonine-protein phosphatase 4 regulatory subunit 3B SMEK2	1	0.2	0.406	5
sp|P67809|YBOX1_HUMAN	35903	3	302	Nuclease-sensitive element-binding protein 1 YBX1	1	0.199	0.093	11
sp|Q3MHD2|LSM12_HUMAN	21972	2	123	Protein LSM12 homolog LSM12	1	0.197	0.164	13
sp|P06753|TPM3_HUMAN	32856	2	90	Tropomyosin alpha-3 chain TPM3	1	0.192	0.096	13
sp|Q9Y6M1|IF2B2_HUMAN	66195	3	114	Insulin-like growth factor 2 mRNA-binding protein 2 IGF2BP2	1	0.191	0.128	6
sp|P13073|COX41_HUMAN	19621	3	119	Cytochrome c oxidase subunit 4 isoform 1, mitochondrial COX4I1	1	0.185	0.435	14
sp|Q96A72|MGN2_HUMAN	17322	2	90	Protein mago nashi homolog 2 MAGOHB	1	0.164	0.072	14
sp|Q15907|RB11B_HUMAN	24588	3	110	Ras-related protein Rab-11B RAB11B	1	0.157	1.171	13
sp|P61247|RS3A_HUMAN	30154	4	166	40S ribosomal protein S3a RPS3A	1	0.155	0.088	12
sp|P30154|2AAB_HUMAN	66799	2	49	Serine/threonine-protein phosphatase 2A 65 kDa regulatory subunit A beta isoform PPP2R1B	1	0.133	0.523	7
sp|Q15370|ELOB_HUMAN	13239	3	102	Transcription elongation factor B polypeptide 2 TCEB2	1	0.126	0.127	14
sp|P60660|MYL6_HUMAN	17090	6	339	Myosin light polypeptide 6 MYL6	1	0.106	0.143	14
sp|Q9NY27|PP4R2_HUMAN	47268	20	1184	Serine/threonine-protein phosphatase 4 regulatory subunit 2 PPP4R2	1	0.105	1.399	8
sp|O75170|SAPS2_HUMAN	106358	18	865	Serine/threonine-protein phosphatase 6 regulatory subunit 2 SAPS2	1	0.096	0.537	4
sp|Q6IN85|P4R3A_HUMAN	95935	21	1127	Serine/threonine-protein phosphatase 4 regulatory subunit 3A SMEK1	1	0.089	0.49	5
sp|P12004|PCNA_HUMAN	29092	5	192	Proliferating cell nuclear antigen PCNA	1	0.047	0.034	12
sp|P05141|ADT2_HUMAN	33102	11	543	ADP/ATP translocase 2 SLC25A5	1	0.038	0.027	12

Appendix II

Proteins were purified using GFP-Trap® beads from lysates of cells stably expressing GFP-TAP-PP1β, which were stimulated with forskolin or not, and in the presence or absence of H-89. Peptides were digested from the SDS gel (**Figure 3.5**) and identified from the SwissProt database (accession number; description) and their Mascot score (score) determined. The corresponding gel band (band) in which they were identified is given below. Peptides were quantitatively measured using the MS Quant software following the dimethyl labelling. The ratios of the different treatment conditions are listed in the table below (SS-serum starved, Fsk-forskolin, H-89+ Fsk-H-89 and forskolin).

Accession number	SPROT_description	Score	mass	SS/SS	Fsk/SS	H-89+ Fsk/SS	band
sp|P08865|RSSA_HUMAN	40S ribosomal protein SA RPSA	61	32947	1	1.425	0.663	7
sp|P10809|CH60_HUMAN	60 kDa heat shock protein, mitochondrial HSPD1	1038	61187	1	0.72	1.288	5
sp|P05388|RLA0_HUMAN	60S acidic ribosomal protein P0 RPLP0	303	34423	1	2.527	1.348	7
sp|P39023|RL3_HUMAN	60S ribosomal protein L3 RPL3	63	46365	1	2.833	1.251	7
sp|P36578|RL4_HUMAN	60S ribosomal protein L4 RPL4	340	47953	1	3.282	1.636	7
sp|P46777|RL5_HUMAN	60S ribosomal protein L5 RPL5	61	34569	1	2.954	1.672	7
sp|Q02878|RL6_HUMAN	60S ribosomal protein L6 RPL6	114	32765	1	2.908	2.021	7
sp|P11021|GRP78_HUMAN	78 kDa glucose-regulated protein HSPA5	1835	72402	1	0.715	0.715	4
sp|P60709|ACTB_HUMAN	Actin, cytoplasmic 1 ACTB	269	42052	1	2.147	1.128	7
sp|Q9P0K7|RAI14_HUMAN	Ankycorbin RAI14	820	110601	1	1.105	1.215	2
sp|Q96KQ4|ASPP1_HUMAN	Apoptosis-stimulating of p53 protein 1 PPP1R13B	376	120062	1	1.004	0.418	2
sp|Q13625|ASPP2_HUMAN	Apoptosis-stimulating of p53 protein 2 TP53BP2	2274	126222	1	3.297	1.943	1
sp|P25705|ATPA_HUMAN	ATP synthase subunit alpha, mitochondrial ATP5A1	908	59828	1	0.995	0.569	6
sp|P06576|ATPB_HUMAN	ATP synthase subunit beta, mitochondrial ATP5B	417	56525	1	0.79	0.684	6
sp|Q9NVI7|ATD3A_HUMAN	ATPase family AAA domain-containing protein 3A ATAD3A	379	71610	1	0.888	0.479	4
sp|P07814|SYEP_HUMAN	Bifunctional aminoacyl-tRNA synthetase EPRS	104	172080	1	1.026	0.927	1
sp|P27708|PYR1_HUMAN	CAD protein CAD	724	245167	1	1.508	0.803	1
sp|P27824|CALX_HUMAN	Calnexin CANX	61	67982	1	1.137	0.678	3
sp|Q00610|CLH1_HUMAN	Clathrin heavy chain 1 CLTC	56	193260	1	0.783	0.838	1
sp|A6NKD9|CC85C_HUMAN	Coiled-coil domain-containing protein 85C CCDC85C	1124	45467	1	0.901	0.618	6
sp|Q69YQ0|CYTSA_HUMAN	Cytospin-A CYTSA	168	124915	1	0.984	0.443	2
sp|O43175|SERA_HUMAN	D-3-phosphoglycerate dehydrogenase PHGDH	561	57356	1	0.866	0.803	5
sp|Q16531|DDB1_HUMAN	DNA damage-binding protein 1 DDB1	972	128142	1	0.882	0.987	2
sp|P78527|PRKDC_HUMAN	DNA-dependent protein kinase catalytic subunit PRKDC	1222	473749	1	0.695	0.194	1
sp|O14802|RPC1_HUMAN	DNA-directed RNA polymerase III subunit RPC1 POLR3A	75	157537	1	1.267	1.572	1

sp|P31689|DNJA1_HUMAN	DnaJ homolog subfamily A member 1 DNAJA1	347	45581	1	1.782	0.711	7
sp|O60884|DNJA2_HUMAN	DnaJ homolog subfamily A member 2 DNAJA2	239	46344	1	2.232	1.314	7
sp|O95793|STAU1_HUMAN	Double-stranded RNA-binding protein Staufen homolog 1 STAU1	207	63428	1	1.161	1.872	5
sp|Q8IUD2|RB6I2_HUMAN	ELKS/Rab6-interacting/CAST family member 1 ERC1	66	128236	1	1.506	1.232	2
sp|P26641|EF1G_HUMAN	Elongation factor 1-gamma EEF1G	74	50429	1	1.089	0.877	7
sp|P13639|EF2_HUMAN	Elongation factor 2 EEF2	101	96246	1	0.723	2.788	2
sp|P14625|ENPL_HUMAN	Endoplasmin HSP90B1	65	92696	1	0.732	0.776	2
sp|O94905|ERLN2_HUMAN	Erlin-2 ERLIN2	146	38044	1	3.107	1.489	7
sp|Q8WVX9|FACR1_HUMAN	Fatty acyl-CoA reductase 1 FAR1	296	59661	1	0.792	0.593	6
sp|P04075|ALDOA_HUMAN	Fructose-bisphosphate aldolase A ALDOA	89	39851	1	1.505	1.824	7
sp|P49448|DHE4_HUMAN	Glutamate dehydrogenase 2, mitochondrial GLUD2	49	61738	1	0.871	0.547	5
sp|Q9BQ67|GRWD1_HUMAN	Glutamate-rich WD repeat-containing protein 1 GRWD1	43	49787	1	0.946	0.534	6
sp|P13807|GYS1_HUMAN	Glycogen [starch] synthase, muscle GYS1	217	84531	1	2.361	18.633	3
sp|P46976|GLYG_HUMAN	Glycogenin-1 GYG1	70	39701	1	2.674	15.442	7
sp|Q9HAV0|GBB4_HUMAN	Guanine nucleotide-binding protein subunit beta-4 GNB4	44	38284	1	1.312	0.369	7
sp|O00165|HAX1_HUMAN	HCLS1-associated protein X-1 HAX1	63	31601	1	1.25	0.533	7
sp|P08107|HSP71_HUMAN	Heat shock 70 kDa protein 1A/1B HSPA1A	2481	70294	1	1.314	1.082	4
sp|P11142|HSP7C_HUMAN	Heat shock cognate 71 kDa protein HSPA8	2708	71082	1	1.273	1.122	4
sp|P07900|HS90A_HUMAN	Heat shock protein HSP 90-alpha HSP90AA1	574	85006	1	1.795	0.656	2
sp|P08238|HS90B_HUMAN	Heat shock protein HSP 90-beta HSP90AB1	1034	83554	1	1.183	0.717	3
sp|P54652|HSP72_HUMAN	Heat shock-related 70 kDa protein 2 HSPA2	102	70263	1	2.817	1.704	3
sp|Q13151|ROA0_HUMAN	Heterogeneous nuclear ribonucleoprotein A0 HNRNPA0	52	30993	1	0.764	0.438	7
sp|Q14103|HNRPD_HUMAN	Heterogeneous nuclear ribonucleoprotein D0 HNRNPD	82	38581	1	1.111	0.861	7
sp|P52597|HNRPF_HUMAN	Heterogeneous nuclear ribonucleoprotein F HNRNPF	83	45985	1	0.677	0.511	7
sp|P31943|HNRH1_HUMAN	Heterogeneous nuclear ribonucleoprotein H HNRNPH1	303	49484	1	1.643	0.747	6
sp|P52272|HNRPM_HUMAN	Heterogeneous nuclear ribonucleoprotein M HNRNPM	49	77749	1	1.078	1.483	3
sp|Q00839|HNRPU_HUMAN	Heterogeneous nuclear ribonucleoprotein U HNRNPU	85	91269	1	0.865	1.007	2
sp|Q9BUJ2|HNRL1_HUMAN	Heterogeneous nuclear ribonucleoprotein U-like protein 1 HNRNPUL1	521	96250	1	1.07	1.122	2
sp|P22626|ROA2_HUMAN	Heterogeneous nuclear ribonucleoproteins A2/B1 HNRNPA2B1	189	37464	1	1.131	0.574	7
sp|Q86X55|CARM1_HUMAN	Histone-arginine methyltransferase CARM1 CARM1	81	63989	1	0.758	1.96	5
sp|O14654|IRS4_HUMAN	Insulin receptor substrate 4 IRS4	739	134711	1	2.956	1.435	1
sp|Q53GT1|KLH22_HUMAN	Kelch-like protein 22 KLHL22	57	72648	1	1.238	1.525	4
sp|Q8NI77|KI18A_HUMAN	Kinesin-like protein KIF18A KIF18A	63	103414	1	1.517	1.423	2
sp|Q9BTT6|LRRC1_HUMAN	Leucine-rich repeat-containing protein 1 LRRC1	161	59946	1	1.294	2.164	5
sp|P07195|LDHB_HUMAN	L-lactate dehydrogenase B chain LDHB	63	36900	1	1.001	0.703	7
sp|Q3ZCQ8|TIM50_HUMAN	Mitochondrial import inner membrane translocase subunit TIM50 TIMM50	256	39850	1	1.563	0.648	7

sp|O94842|TOX4_HUMAN	Myosin light chain kinase 2, skeletal/cardiac muscle MYLK2	374	65214	1	1.106	1.86	3
sp|Q12972|PP1R8_HUMAN	Nuclear inhibitor of protein phosphatase 1 PPP1R8	663	38626	1	2.831	1.664	7
sp|P67809|YBOX1_HUMAN	Nuclease-sensitive element-binding protein 1 YBX1	139	35903	1	2.237	1.3	7
sp|Q14318|FKBP8_HUMAN	Peptidyl-prolyl cis-trans isomerase FKBP8 FKBP8	77	44990	1	0.934	0.557	6
sp|Q00325|MPCP_HUMAN	Phosphate carrier protein, mitochondrial SLC25A3	60	40525	1	1.068	0.651	7
sp|Q9NWS0|PIHD1_HUMAN	PIH1 domain-containing protein 1 PIH1D1	302	32513	1	1.716	2.572	7
sp|Q15365|PCBP1_HUMAN	Poly(rC)-binding protein 1 PCBP1	56	37987	1	0.822	0.503	7
sp|Q15366|PCBP2_HUMAN	Poly(rC)-binding protein 2 PCBP2	55	38955	1	1.653	1.118	7
sp|P11940|PABP1_HUMAN	Polyadenylate-binding protein 1 PABPC1	228	70854	1	1.086	0.607	4
sp|Q99623|PHB2_HUMAN	Prohibitin-2 PHB2	201	33276	1	2.26	1.644	7
sp|Q8NG31|CASC5_HUMAN	Protein CASC5 CASC5	161	268190	1	1.057	1.24	1
sp|Q96SW2|CRBN_HUMAN	Protein cereblon CRBN	470	51425	1	0.834	0.63	6
sp|Q96RT1|LAP2_HUMAN	Protein LAP2 ERBB2IP	58	158941	1	0.91	0.626	1
sp|Q7Z3U7|MON2_HUMAN	Protein MON2 homolog MON2	44	192475	1	1.25	0.532	1
sp|O60927|PP1RB_HUMAN	Protein phosphatase 1 regulatory subunit 11 PPP1R11	43	14229	1	1.104	1.1	8
sp|O14974|MYPT1_HUMAN	Protein phosphatase 1 regulatory subunit 12A PPP1R12A	4550	115610	1	1.143	0.784	2
sp|O60237|MYPT2_HUMAN	Protein phosphatase 1 regulatory subunit 12B PPP1R12B	733	110793	1	1.098	0.739	2
sp|Q9BZL4|PP12C_HUMAN	Protein phosphatase 1 regulatory subunit 12C PPP1R12C	2040	85286	1	1.158	1.163	2
sp|Q86XI6|PPR3B_HUMAN	Protein phosphatase 1 regulatory subunit 3B PPP1R3B	195	33073	1	2.283	2.457	7
sp|O95685|PPR3D_HUMAN	Protein phosphatase 1 regulatory subunit 3D PPP1R3D	228	33280	1	5.325	23.153	7
sp|Q15435|PP1R7_HUMAN	Protein phosphatase 1 regulatory subunit 7 PPP1R7	1644	41653	1	3.02	1.687	7
sp|Q14160|SCRIB_HUMAN	Protein scribble homolog SCRIB	119	175748	1	1.584	1.555	1
sp|Q92734|TFG_HUMAN	Protein TFG TFG	77	43478	1	1.016	0.797	6
sp|O15027|SC16A_HUMAN	Protein transport protein Sec16A SEC16A	153	234855	1	1.101	0.953	1
sp|P61619|S61A1_HUMAN	Protein transport protein Sec61 subunit alpha isoform 1 SEC61A1	46	52687	1	2.06	1.017	7
sp|Q9P035|PTAD1_HUMAN	Protein tyrosine phosphatase-like protein PTPLAD1 PTPLAD1	110	43360	1	2.698	1.088	7
sp|P41236|IPP2_HUMAN	Putative protein phosphatase inhibitor 2-like protein 3 PPP1R2P3	101	23091	1	0.246	0.706	8
sp|P31751|AKT2_HUMAN	RAC-alpha serine/threonine-protein kinase AKT1	72	56050	0	0	0	3
sp|Q02833|RASF7_HUMAN	Ras association domain-containing protein 7 RASSF7	175	40548	1	1.689	1.001	7
sp|Q8NHQ8|RASF8_HUMAN	Ras association domain-containing protein 8 RASSF8	296	48526	1	0.86	0.512	6
sp|Q8WUF5|IASPP_HUMAN	RelA-associated inhibitor PPP1R13L	767	89378	1	1.383	1.28	2
sp|Q15293|RCN1_HUMAN	Reticulocalbin-1 RCN1	41	38866	1	2.243	1.215	7
sp|O94822|RN160_HUMAN	RING finger protein 160 RNF160	126	203077	1	1.008	1.012	1
sp|Q9H6T3|RPAP3_HUMAN	RNA polymerase II-associated protein 3 RPAP3	333	75957	1	0.758	1.418	3
sp|Q01844|EWS_HUMAN	RNA-binding protein EWS EWSR1	268	68721	1	1.077	1	3
sp|Q9Y265|RUVB1_HUMAN	RuvB-like 1 RUVBL1	778	50538	1	0.579	0.93	6

sp|Q9Y230|RUVB2_HUMAN	RuvB-like 2 RUVBL2	2520	51296	1	0.776	1.036	6
sp|P16615|AT2A2_HUMAN	Sarcoplasmic/endoplasmic reticulum calcium ATPase 2 ATP2A2	391	116336	1	0.97	0.671	2
sp|Q96QC0|PP1RA_HUMAN	Serine/threonine-protein phosphatase 1 regulatory subunit 10 PPP1R10	730	99338	1	1.299	1.481	2
sp|Q08209|PP2BA_HUMAN	Serine/threonine-protein phosphatase 2B catalytic subunit alpha isoform PPP3CA	46	59335	1	1.002	1.262	3
sp|Q96HS1|PGAM5_HUMAN	Serine/threonine-protein phosphatase PGAM5, mitochondrial PGAM5	158	32213	1	2.669	1.382	7
sp|P62136|PP1A_HUMAN	Serine/threonine-protein phosphatase PP1-alpha catalytic subunit PPP1CA	63	38229	1	1.477	1.483	7
sp|P62140|PP1B_HUMAN	Serine/threonine-protein phosphatase PP1-beta catalytic subunit PPP1CB	4176	37961	1	1.152	0.866	3
sp|P36873|PP1G_HUMAN	Serine/threonine-protein phosphatase PP1-gamma catalytic subunit PPP1CC	79	37701	1	1.32	1.079	7
sp|Q9H788|SH24A_HUMAN	SH2 domain-containing protein 4A SH2D4A	1359	52922	1	0.846	0.45	6
sp|P05023|AT1A1_HUMAN	Sodium/potassium-transporting ATPase subunit alpha-1 ATP1A1	282	114135	1	0.87	0.617	2
sp|P38646|GRP75_HUMAN	Stress-70 protein, mitochondrial HSPA9	2554	73920	1	0.946	1.113	4
sp|P17987|TCPA_HUMAN	T-complex protein 1 subunit alpha TCP1	1942	60819	1	0.902	0.8	5
sp|P78371|TCPB_HUMAN	T-complex protein 1 subunit beta CCT2	2379	57794	1	0.946	0.797	5
sp|P50991|TCPD_HUMAN	T-complex protein 1 subunit delta CCT4	1786	58401	1	0.889	0.838	5
sp|P48643|TCPE_HUMAN	T-complex protein 1 subunit epsilon CCT5	1093	60089	1	0.939	0.849	5
sp|Q99832|TCPH_HUMAN	T-complex protein 1 subunit eta CCT7	2615	59842	1	1.08	0.91	5
sp|P49368|TCPG_HUMAN	T-complex protein 1 subunit gamma CCT3	1609	61066	1	0.994	0.91	5
sp|P50990|TCPQ_HUMAN	T-complex protein 1 subunit theta CCT8	3197	60153	1	0.978	0.937	5
sp|P40227|TCPZ_HUMAN	T-complex protein 1 subunit zeta CCT6A	1058	58444	1	1.097	1.256	5
sp|Q92526|TCPW_HUMAN	T-complex protein 1 subunit zeta-2 CCT6B	392	58299	1	0.396	0.24	5
sp|Q13263|TIF1B_HUMAN	Transcription intermediary factor 1-beta TRIM28	44	90261	1	0.821	0.652	2
sp|P55072|TERA_HUMAN	Transitional endoplasmic reticulum ATPase VCP	196	89950	1	0.73	0.785	2
sp|Q92616|GCN1L_HUMAN	Translational activator GCN1 GCN1L1	223	294967	1	0.766	0.488	1
sp|P43307|SSRA_HUMAN	Translocon-associated protein subunit alpha SSR1	109	32215	1	4.159	0.954	7
sp|Q9UPQ9|TNR6B_HUMAN	Trinucleotide repeat-containing gene 6B protein TNRC6B	39	194739	1	1.331	1.479	1
sp|P68363|TBA1B_HUMAN	Tubulin alpha-1B chain TUBA1B	2221	50804	1	0.823	0.383	6
sp|P07437|TBB5_HUMAN	Tubulin beta chain TUBB	3358	50095	1	0.781	0.472	6
sp|Q13885|TBB2A_HUMAN	Tubulin beta-2A chain TUBB2A	2737	50274	1	0.837	0.301	6
sp|Q9BVA1|TBB2B_HUMAN	Tubulin beta-2B chain TUBB2B	2787	50377	1	0.711	0.353	6
sp|P68371|TBB2C_HUMAN	Tubulin beta-2C chain TUBB2C	3707	50255	1	0.816	0.373	6
sp|Q9BUF5|TBB6_HUMAN	Tubulin beta-6 chain TUBB6	631	50281	1	0.452	0.154	6
sp|Q9BZF9|UACA_HUMAN	Uveal autoantigen with coiled-coil domains and ankyrin repeats UACA	711	163545	1	1.965	1.416	1
sp|P08670|VIME_HUMAN	Vimentin VIM	94	53676	1	0.955	0.413	6
sp|P21796|VDAC1_HUMAN	Voltage-dependent anion-selective channel protein 1 VDAC1	45	30868	1	1.838	0.909	7
sp|P45880|VDAC2_HUMAN	Voltage-dependent anion-selective channel protein 2 VDAC2	50	32060	1	1.549	0.897	7

sp|Q6UXN9|WDR82_HUMAN	WD repeat-containing protein 82 WDR82	78	35456	1	6.186	3.984	7
sp|Q96MX6|WDR92_HUMAN	WD repeat-containing protein 92 WDR92	267	40171	1	1.468	2.636	7
sp|P49750|YLPM1_HUMAN	YLP motif-containing protein 1 YLPM1	140	220077	1	1.208	1.101	1
sp|O95405|ZFYV9_HUMAN	Zinc finger FYVE domain-containing protein 9 ZFYVE9	344	158926	1	2.544	1.948	1
sp|O95229|ZWINT_HUMAN	ZW10 interactor ZWINT	52	31331	1	1.878	1.621	7

Appendix III

Proteins were purified using GFP-Trap® beads from lysates of cells stably expressing GFP-TAP-PP1α, GFP-TAP-PP1β and GFP-TAP-PP1γ. Peptides were extracted from the SDS gel (**Figure 3.10**) and identified from the UniProt database (UniProt; description). Peptides were quantitatively measured using the MS Quant software following the dimethyl labelling. For each protein, the sum of the raw intensity values obtained from the three preparations is also given.

Uniprot	Protein Descriptions	Peps	MW (kDa)	Intensity	Intensity PP1 alpha	Intensity PP1 beta	Intensity PP1 gamma
O00264	PGRC1_HUMAN Membrane-associated progesterone receptor component 1 PGRMC1	2	21.67	1990000	263480	1096300	630230
O00303	EIF3F_HUMAN Eukaryotic translation initiation factor 3 subunit F EIF3F	2	37.56	3264300	125970	2823400	314850
O14818	PSA7_HUMAN Proteasome subunit alpha type-7 PSMA7	2	27.89	3589700	479160	1416500	1694000
Q5SRD1	TI23B_HUMAN Putative mitochondrial import inner membrane translocase subunit Tim23B TIMM23B	2	28.05	2398600	796530	826910	775120
O43143	DHX15_HUMAN Putative pre-mRNA-splicing factor ATP-dependent RNA helicase DHX15 DHX15	2	90.93	21254000	14210000	6197000	847050
O43813	LANC1_HUMAN LanC-like protein 1 LANCL1	2	45.28	2282200	184690	1009000	1088500
P15531	NDKA_HUMAN Nucleoside diphosphate kinase A NME1	2	17.15	2886500	378820	1611500	896180
O60812	HNRCL_HUMAN Heterogeneous nuclear ribonucleoprotein C-like 1 HNRNPCL1	2	32.14	3129700	412270	1762800	954610
O60814	H2B1K_HUMAN Histone H2B type 1-K HIST1H2BK	2	13.89	9794300	749420	4518700	4526200
O75190	DNJB6_HUMAN DnaJ homolog subfamily B member 6 DNAJB6	2	36.09	1677200	496290	593720	587230
O75489	NDUS3_HUMAN NADH dehydrogenase [ubiquinone] iron-sulfur protein 3, mitochondrial NDUFS3	2	30.24	1404800	329960	697310	377540
O75533	SF3B1_HUMAN Splicing factor 3B subunit 1 SF3B1	2	145.83	2313400	725960	514670	1072800
O95347	SMC2_HUMAN Structural maintenance of chromosomes protein 2 SMC2	2	135.65	2030000	576850	1212200	240920
O95831	AIFM1_HUMAN Apoptosis-inducing factor 1, mitochondrial AIFM1	2	66.90	2039300	1368400	419100	251790

P01111	RASN_HUMAN GTPase NRas NRAS	2	21.23	5760800	382930	768000	4609900
P05198	IF2A_HUMAN Eukaryotic translation initiation factor 2 subunit 1 EIF2S1	2	36.11	1444100	166140	676610	601320
P05387	RLA2_HUMAN 60S acidic ribosomal protein P2 RPLP2	2	11.67	5034900	634660	2213500	2186700
P07737	PROF1_HUMAN Profilin-1 PFN1	2	15.05	2262300	344090	1189000	729160
P09104	ENOG_HUMAN Gamma-enolase ENO2	2	47.27	9967200	839770	5900200	3227300
P10606	COX5B_HUMAN Cytochrome c oxidase subunit 5B, mitochondrial COX5B	2	13.70	2282300	455550	639760	1187000
P14866	HNRPL_HUMAN Heterogeneous nuclear ribonucleoprotein L HNRNPL	2	64.13	858750	173630	393910	291210
P22087	FBRL_HUMAN rRNA 2-O-methyltransferase fibrillarin FBL	2	33.78	40577000	5016600	31394000	4166600
P23526	SAHH_HUMAN Adenosylhomocysteinase AHCY	2	47.72	1961700	407430	609620	944690
P23528	COF1_HUMAN Cofilin-1 CFL1	2	18.50	13612000	1514900	8331400	3765200
P24666	PPAC_HUMAN Low molecular weight phosphotyrosine protein phosphatase ACP1	2	18.04	4297500	478830	645330	3173300
P25789	PSA4_HUMAN Proteasome subunit alpha type-4 PSMA4	2	29.48	3905600	739220	2421600	744770
P26640	SYVC_HUMAN Valine--tRNA ligase VARS	2	140.47	2212500	406990	306010	1499500
P27348	1433T_HUMAN 14-3-3 protein theta YWHAQ	2	27.76	648960	40230	342010	266720
P27694	RFA1_HUMAN Replication protein A 70 kDa DNA-binding subunit RPA1	2	68.14	7397900	473520	6394200	530150
P27797	CALR_HUMAN Calreticulin CALR	2	48.14	1464700	365930	811890	286860
P28066	PSA5_HUMAN Proteasome subunit alpha type-5 PSMA5	2	26.41	2125000	361190	1168700	595050
P29692	EF1D_HUMAN Elongation factor 1-delta EEF1D	2	31.12	4433300	454080	1926100	2053100
P32119	PRDX2_HUMAN Peroxiredoxin-2 PRDX2	2	21.89	4494300	1577800	738240	2178200
P32969	RL9_HUMAN 60S ribosomal protein L9 RPL9	2	21.86	2154900	253280	832140	1069500
P34932	HSP74_HUMAN Heat shock 70 kDa protein 4 HSPA4	2	94.33	6605500	1401300	802060	4402100
P38919	IF4A3_HUMAN Eukaryotic initiation factor 4A-III EIF4A3	2	46.87	2352000	388410	835620	1128000
P39019	RS19_HUMAN 40S ribosomal protein S19 RPS19	2	16.06	11593000	1443600	5407700	4741900
P42677	RS27_HUMAN 40S ribosomal protein S27 RPS27	2	9.46	9171700	1806500	4357100	3008100
P42766	RL35_HUMAN 60S ribosomal protein L35 RPL35	2	14.55	2791400	174330	1618500	998580
P46782	RS5_HUMAN 40S ribosomal protein S5 RPS5	2	22.88	22718000	2649500	15808000	4260400
Q9NQ39	RS10L_HUMAN Putative 40S ribosomal protein S10-like RPS10P5 PE=5 SV=1	2	20.12	10766000	1206600	5876800	3682700

P49411	EFTU_HUMAN Elongation factor Tu, mitochondrial TUFM	2	49.54	3642400	602590	2310400	729430
P50914	RL14_HUMAN 60S ribosomal protein L14 RPL14	2	23.43	6871200	728500	3347200	2795500
P52907	CAZA1_HUMAN F-actin-capping protein subunit alpha-1 CAPZA1	2	32.92	3255100	380310	1777300	1097500
P53985	MOT1_HUMAN Monocarboxylate transporter 1 SLC16A1	2	53.94	1228400	267820	485880	474750
P54136	SYRC_HUMAN Arginine--tRNA ligase, cytoplasmic RARS	2	75.38	5290600	787540	3158200	1344800
P55209	NP1L1_HUMAN Nucleosome assembly protein 1-like 1 NAP1L1	2	45.37	3893200	271770	3026600	594750
P59190	RAB15_HUMAN Ras-related protein Rab-15 RAB15	2	24.39	154600000	151080000	1176500	2350100
P60174	TPIS_HUMAN Triosephosphate isomerase TPI1	2	30.79	4588100	736860	736060	3115200
P61224	RAP1B_HUMAN Ras-related protein Rap-1b RAP1B	2	20.83	2808700	158570	1969700	680340
P62081	RS7_HUMAN 40S ribosomal protein S7 RPS7	2	22.13	15305000	593460	5657800	9054100
P62244	RS15A_HUMAN 40S ribosomal protein S15a RPS15A	2	14.84	25609000	298970	1086000	24224000
P62318	SMD3_HUMAN Small nuclear ribonucleoprotein Sm D3 SNRPD3	2	13.92	4045400	648790	1453600	1943000
Q15907	RB11B_HUMAN Ras-related protein Rab-11B RAB11B	2	24.49	4034500	1007100	493560	2533900
P62805	H4_HUMAN Histone H4 HIST1H4A	2	11.37	7477000	542080	1798800	5136100
P62826	RAN_HUMAN GTP-binding nuclear protein Ran RAN	2	24.42	4236500	387240	2425600	1423700
P62851	RS25_HUMAN 40S ribosomal protein S25 RPS25	2	13.74	12283000	954930	6086400	5241900
P62854	RS26_HUMAN 40S ribosomal protein S26 RPS26	2	13.02	8586900	493800	5784600	2308500
P62899	RL31_HUMAN 60S ribosomal protein L31 RPL31	2	14.46	6470800	231030	2308700	3931100
P62995	TRA2B_HUMAN Transformer-2 protein homolog beta TRA2B	2	33.67	7097100	1455100	2805500	2836500
P63151	2ABA_HUMAN Serine/threonine-protein phosphatase 2A 55 kDa regulatory subunit B alpha isoform PPP2R2A	2	51.69	1319700	226370	518920	574360
P82933	RT09_HUMAN 28S ribosomal protein S9, mitochondrial MRPS9	2	45.83	1205600	151170	782290	272180
P84098	RL19_HUMAN 60S ribosomal protein L19 RPL19	2	23.47	4276600	563490	2492500	1220600
P84103	SRSF3_HUMAN Serine/arginine-rich splicing factor 3 SRSF3	2	19.33	4213200	559360	2731200	922640
Q01844	EWS_HUMAN RNA-binding protein EWS EWSR1	2	68.48	17205000	349120	8625000	8231100
Q04837	SSBP_HUMAN Single-stranded DNA-binding protein, mitochondrial SSBP1	2	17.26	17296000	702510	14403000	2191100
Q06787	FMR1_HUMAN Fragile X mental retardation protein 1 FMR1	2	71.17	7639900	1093300	1514100	5032400
Q07955	SRSF1_HUMAN Serine/arginine-rich splicing factor 1 SRSF1	2	27.74	3188300	1296100	699090	1193100

Q13148	TADBP_HUMAN TAR DNA-binding protein 43 TARDBP	2	44.74	1247700	118650	516580	612470
Q13243	SRSF5_HUMAN Serine/arginine-rich splicing factor 5 SRSF5	2	31.26	1824400	231240	636760	956440
Q13257	MD2L1_HUMAN Mitotic spindle assembly checkpoint protein MAD2A MAD2L1	2	23.51	2613000	574230	1496600	542230
Q13409	DC1I2_HUMAN Cytoplasmic dynein 1 intermediate chain 2 DYNC1I2	2	71.46	862990	288160	172640	402190
Q13765	NACA_HUMAN Nascent polypeptide-associated complex subunit alpha NACA	2	23.38	2272100	317940	714430	1239700
Q14257	RCN2_HUMAN Reticulocalbin-2 RCN2	2	36.88	4916100	669760	1755800	2490600
Q14978	NOLC1_HUMAN Nucleolar and coiled-body phosphoprotein 1 NOLC1	2	73.60	5793700	238000	1227200	4328500
Q15084	PDIA6_HUMAN Protein disulfide-isomerase A6 PDIA6	2	48.12	2281000	323710	578510	1378800
Q15717	ELAV1_HUMAN ELAV-like protein 1 ELAVL1	2	36.09	4779800	1732200	1424400	1623200
Q16576	RBBP7_HUMAN Histone-binding protein RBBP7 RBBP7	2	47.82	1526900	487150	330380	709320
Q16629	SRSF7_HUMAN Serine/arginine-rich splicing factor 7 SRSF7	2	27.37	3258800	443050	824020	1991800
Q53GT1	KLH22_HUMAN Kelch-like protein 22 KLHL22	2	71.67	5119700	732380	3328800	1058500
Q8N7X1	RMXL3_HUMAN RNA-binding motif protein, X-linked-like-3 RBMXL3	2	114.94	6639300	1131600	1774300	3733400
Q8NC51	PAIRB_HUMAN Plasminogen activator inhibitor 1 RNA-binding protein SERBP1	2	44.97	1882200	100690	496890	1284600
Q8WVX9	FACR1_HUMAN Fatty acyl-CoA reductase 1 FAR1	2	59.36	1703100	357360	598970	746780
Q8WXF1	PSPC1_HUMAN Paraspeckle component 1 PSPC1	2	58.74	1909500	587610	863980	457890
Q92878	RAD50_HUMAN DNA repair protein RAD50 RAD50	2	153.89	1539600	187270	385730	966560
Q92945	FUBP2_HUMAN Far upstream element-binding protein 2 KHSRP	2	73.11	9840900	567590	5810000	3463200
Q99873	ANM1_HUMAN Protein arginine N-methyltransferase 1 PRMT1	2	41.52	7592400	961990	3117800	3512700
Q9BTT6	LRRC1_HUMAN Leucine-rich repeat-containing protein 1 LRRC1	2	59.24	15743000	4937400	7378500	3427500
Q9GZN8	CT027_HUMAN UPF0687 protein C20orf27 C20orf27	2	19.29	10142000	4393900	615050	5133000
Q9H1R3	MYLK2_HUMAN Myosin light chain kinase 2, skeletal/cardiac muscle MYLK2	2	64.68	2.952E+09	796940000	130650000	2023900000
Q9NTJ3	SMC4_HUMAN Structural maintenance of chromosomes protein 4 SMC4	2	147.18	837800	136060	384990	316750
Q9NUG6	PDRG1_HUMAN p53 and DNA damage-regulated protein 1 PDRG1	2	15.51	3657000	953070	478960	2225000
Q9NX63	CHCH3_HUMAN Coiled-coil-helix-coiled-coil-helix domain-containing protein 3, mitochondrial CHCHD3	2	26.15	1487000	274160	681590	531210
Q9P035	HACD3_HUMAN 3-hydroxyacyl-CoA dehydratase 3 PTPLAD1	2	43.16	1597700	290050	523240	784400
Q9UQE7	SMC3_HUMAN Structural maintenance of chromosomes protein 3 SMC3	2	141.54	1240500	656560	281790	302190

Q9Y277	VDAC3_HUMAN Voltage-dependent anion-selective channel protein 3 VDAC3	2	30.66	1303200	196260	163110	943860
Q9Y3U8	RL36_HUMAN 60S ribosomal protein L36 RPL36	2	12.25	8922800	706030	3914300	4302500
Q13838	DX39B_HUMAN Spliceosome RNA helicase DDX39B DDX39B	3	48.99	34811000	9896700	21179000	3735300
O14979	HNRDL_HUMAN Heterogeneous nuclear ribonucleoprotein D-like HNRPDL	3	46.44	2778000	470450	367770	1939800
O43707	ACTN4_HUMAN Alpha-actinin-4 ACTN4	3	104.85	12136000	516760	5829600	5789600
O60506	HNRPQ_HUMAN Heterogeneous nuclear ribonucleoprotein Q SYNCRIP	3	69.60	4749200	1092700	934270	2722300
O60884	DNJA2_HUMAN DnaJ homolog subfamily A member 2 DNAJA2	3	45.75	4561000	821350	2510900	1228800
O95685	PPR3D_HUMAN Protein phosphatase 1 regulatory subunit 3D PPP1R3D	3	32.56	14941000	2732800	2307200	9900900
P00403	COX2_HUMAN Cytochrome c oxidase subunit 2 MT-CO2	3	25.57	8678800	1346900	3237300	4094500
P07910	HNRPC_HUMAN Heterogeneous nuclear ribonucleoproteins C1/C2 HNRNPC	3	33.67	24661000	2082700	11812000	10766000
P0CG48	UBC_HUMAN Polyubiquitin-C UBC	3	77.03	79493000	10503000	33640000	35349000
P13807	GYS1_HUMAN Glycogen [starch] synthase, muscle GYS1	3	83.79	3232200	191840	1289000	1751300
P18621	RL17_HUMAN 60S ribosomal protein L17 RPL17	3	21.40	4430300	597980	1844400	1988000
P27635	RL10_HUMAN 60S ribosomal protein L10 RPL10	3	24.60	5519100	548670	1946700	3023700
P30050	RL12_HUMAN 60S ribosomal protein L12 RPL12	3	17.82	21342000	1478800	11324000	8538900
P31946	1433B_HUMAN 14-3-3 protein beta/alpha YWHAB	3	28.08	2153300	175700	1715700	261920
P35268	RL22_HUMAN 60S ribosomal protein L22 RPL22	3	14.79	18567000	2833800	8795100	6938000
P35637	FUS_HUMAN RNA-binding protein FUS FUS	3	53.43	7841300	1476000	4606400	1758900
P36542	ATPG_HUMAN ATP synthase subunit gamma, mitochondrial ATP5C1	3	33.00	5059400	637700	1536300	2885300
P38159	RBMX_HUMAN RNA-binding motif protein, X chromosome RBMX	3	42.33	21727000	1540700	10519000	9666600
P43307	SSRA_HUMAN Translocon-associated protein subunit alpha SSR1	3	32.24	20870000	1416900	3106500	16347000
P48047	ATPO_HUMAN ATP synthase subunit O, mitochondrial ATP5O	3	23.28	5251500	806650	850990	3593900
P49006	MRP_HUMAN MARCKS-related protein MARCKSL1	3	19.53	16923000	416260	12817000	3689900
P52292	IMA2_HUMAN Importin subunit alpha-2 KPNA2	3	57.86	1889500	226550	649580	1013300
P53007	TXTP_HUMAN Tricarboxylate transport protein, mitochondrial SLC25A1	3	34.01	4825100	798940	1045400	2980800
P61353	RL27_HUMAN 60S ribosomal protein L27 RPL27	3	15.80	13586000	1049300	4671000	7866100
P61981	1433G_HUMAN 14-3-3 protein gamma YWHAG	3	28.30	1465800	203730	744870	517170

P62241	RS8_HUMAN 40S ribosomal protein S8 RPS8	3	24.21	13150000	1756800	4612500	6780400
P62277	RS13_HUMAN 40S ribosomal protein S13 RPS13	3	17.22	7431300	610340	4028900	2792100
P62750	RL23A_HUMAN 60S ribosomal protein L23a RPL23A	3	17.70	13076000	1959000	5511800	5604800
P62917	RL8_HUMAN 60S ribosomal protein L8 RPL8	3	28.02	11688000	757020	4750700	6179900
Q01130	SRSF2_HUMAN Serine/arginine-rich splicing factor 2 SRSF2	3	25.48	5880900	2602000	1319300	1959700
Q08380	LG3BP_HUMAN Galectin-3-binding protein LGALS3BP	3	65.33	29865000	2243500	23216000	4406000
Q12904	AIMP1_HUMAN Aminoacyl tRNA synthase complex-interacting multifunctional protein 1 AIMP1	3	34.35	2048000	258430	685320	1104300
Q12905	ILF2_HUMAN Interleukin enhancer-binding factor 2 ILF2	3	43.06	23912000	2637300	10946000	10328000
Q13151	ROA0_HUMAN Heterogeneous nuclear ribonucleoprotein A0 HNRNPA0	3	30.84	12151000	1325500	3068600	7756600
Q14103	HNRPD_HUMAN Heterogeneous nuclear ribonucleoprotein D0 HNRNPD	3	38.43	19049000	3571900	7791700	7685800
Q15029	U5S1_HUMAN 116 kDa U5 small nuclear ribonucleoprotein component EFTUD2	3	109.43	604190	133450	13412	457320
Q3ZCQ8	TIM50_HUMAN Mitochondrial import inner membrane translocase subunit TIM50 TIMM50	3	39.65	8671900	1947200	3065900	3658800
Q5T9A4	ATD3B_HUMAN ATPase family AAA domain-containing protein 3B ATAD3B	3	72.57	178410	33735	94447	50231
Q7Z417	NUFP2_HUMAN Nuclear fragile X mental retardation-interacting protein 2 NUFIP2	3	76.12	1393900	311300	639440	443130
Q92616	GCN1L_HUMAN Translational activator GCN1 GCN1L1	3	292.75	3723600	354490	1466000	1903000
Q92896	GSLG1_HUMAN Golgi apparatus protein 1 GLG1	3	134.55	1780400	752960	719890	307550
Q96HS1	PGAM5_HUMAN Serine/threonine-protein phosphatase PGAM5, mitochondrial PGAM5	3	32.00	36851000	9299300	7583700	19968000
Q96P70	IPO9_HUMAN Importin-9 IPO9	3	115.96	2589000	1023000	990260	575660
Q9P2K8	E2AK4_HUMAN Eukaryotic translation initiation factor 2-alpha kinase 4 EIF2AK4	3	186.91	3091400	1956200	489810	645340
Q9UHV9	PFD2_HUMAN Prefoldin subunit 2 PFDN2	3	16.65	8630700	1514100	1505800	5610800
Q9UMS4	PRP19_HUMAN Pre-mRNA-processing factor 19 PRPF19	3	55.18	5798500	600410	3184500	2013600
Q9Y262	EIF3L_HUMAN Eukaryotic translation initiation factor 3 subunit L EIF3L	3	66.73	1143900	290940	458490	394520
Q9Y2W1	TR150_HUMAN Thyroid hormone receptor-associated protein 3 THRAP3	3	108.66	1376300	288860	899860	187530
Q9Y3I0	RTCB_HUMAN tRNA-splicing ligase RtcB homolog C22orf28	3	55.21	7051600	2668000	1952100	2431400
O00567	NOP56_HUMAN Nucleolar protein 56 NOP56	4	66.05	3844700	725130	1442400	1677200
O43175	SERA_HUMAN D-3-phosphoglycerate dehydrogenase PHGDH	4	56.65	2812700	1063500	587310	1161900

O43390	HNRPR_HUMAN Heterogeneous nuclear ribonucleoprotein R HNRNPR	4	70.94	19185000	4093700	10187000	4904100
O60927	PP1RB_HUMAN Protein phosphatase 1 regulatory subunit 11 PPP1R11	4	13.95	31278000	3144400	5067400	23066000
O75643	U520_HUMAN U5 small nuclear ribonucleoprotein 200 kDa helicase SNRNP200	4	244.50	4884400	1051600	2815600	1017200
O75955	FLOT1_HUMAN Flotillin-1 FLOT1	4	47.36	16479000	2695300	5471600	8312100
O95793	STAU1_HUMAN Double-stranded RNA-binding protein Staufen homolog 1 STAU1	4	63.18	4189600	887130	908360	2394100
P00338	LDHA_HUMAN L-lactate dehydrogenase A chain LDHA	4	36.69	4398600	1419900	1941800	1036900
P04843	RPN1_HUMAN Dolichyl-diphosphooligosaccharide--protein glycosyltransferase subunit 1 RPN1	4	68.57	5990200	704570	3618500	1667200
P08865	RSSA_HUMAN 40S ribosomal protein SA RPSA	4	32.85	84344000	1393400	9429200	73522000
P12004	PCNA_HUMAN Proliferating cell nuclear antigen PCNA	4	28.77	8144400	934610	4264000	2945900
P14618	KPYM_HUMAN Pyruvate kinase isozymes M1/M2 PKM2	4	57.94	8200200	1620800	4929800	1649700
P19388	RPAB1_HUMAN DNA-directed RNA polymerases I, II, and III subunit RPABC1 POLR2E	4	24.55	20270000	12202000	1510400	6557400
P26196	DDX6_HUMAN Probable ATP-dependent RNA helicase DDX6 DDX6	4	54.42	5334500	1304000	1392200	2638200
P26641	EF1G_HUMAN Elongation factor 1-gamma EEF1G	4	50.12	12291000	1240200	3253900	7796800
P39656	OST48_HUMAN Dolichyl-diphosphooligosaccharide--protein glycosyltransferase 48 kDa subunit DDOST	4	50.80	5376200	1623900	1899900	1852400
P40429	RL13A_HUMAN 60S ribosomal protein L13a RPL13A	4	23.58	7398600	652570	2641500	4104500
P55060	XPO2_HUMAN Exportin-2 CSE1L	4	110.42	4546700	598940	966550	2981200
P62249	RS16_HUMAN 40S ribosomal protein S16 RPS16	4	16.45	8659800	693370	4676700	3289600
P62263	RS14_HUMAN 40S ribosomal protein S14 RPS14	4	16.27	5783300	583920	2412900	2786500
P62269	RS18_HUMAN 40S ribosomal protein S18 RPS18	4	17.72	8144100	699430	3425700	4018900
P62280	RS11_HUMAN 40S ribosomal protein S11 RPS11	4	18.43	6699200	518970	3711600	2468600
P62701	RS4X_HUMAN 40S ribosomal protein S4, X isoform RPS4X	4	29.60	7920200	742830	3171900	4005400
P62753	RS6_HUMAN 40S ribosomal protein S6 RPS6	4	28.68	11571000	1924500	4014700	5632300
P62829	RL23_HUMAN 60S ribosomal protein L23 RPL23	4	14.87	12238000	1221700	7380200	3636400
P62873	GBB1_HUMAN Guanine nucleotide-binding protein G(I)/G(S)/G(T) subunit beta-1 GNB1	4	37.38	1814800	242610	492420	1079800
P62879	GBB2_HUMAN Guanine nucleotide-binding protein G(I)/G(S)/G(T) subunit beta-2 GNB2	4	37.33	125320000	7736500	52181000	65406000
P62888	RL30_HUMAN 60S ribosomal protein L30 RPL30	4	12.78	6240700	673250	3312200	2255300

P62913	RL11_HUMAN 60S ribosomal protein L11 RPL11	4	20.25	763990000	7840700	729310000	26839000
P62937	PPIA_HUMAN Peptidyl-prolyl cis-trans isomerase A PPIA	4	18.01	4969900	329520	2323500	2316900
P63244	GBLP_HUMAN Guanine nucleotide-binding protein subunit beta-2-like 1 GNB2L1	4	35.08	7881800	1780000	2201000	3900800
P78347	GTF2I_HUMAN General transcription factor II-I GTF2I	4	112.42	1463000	133290	746200	583480
P83731	RL24_HUMAN 60S ribosomal protein L24 RPL24	4	17.78	18035000	3191900	7170000	7672600
Q07020	RL18_HUMAN 60S ribosomal protein L18 RPL18	4	21.63	24352000	3298300	10727000	10327000
Q14254	FLOT2_HUMAN Flotillin-2 FLOT2	4	47.06	26213000	7577300	9139900	9495600
Q14444	CAPR1_HUMAN Caprin-1 CAPRIN1	4	78.37	57751000	2756000	27280000	27715000
Q15834	CC85B_HUMAN Coiled-coil domain-containing protein 85B CCDC85B	4	22.09	23413000	4635500	15351000	3426600
Q7KZF4	SND1_HUMAN Staphylococcal nuclease domain-containing protein 1 SND1	4	102.00	7409500	327980	3049900	4031600
Q9HCE1	MOV10_HUMAN Putative helicase MOV-10 MOV10	4	113.67	4371600	101460	2299100	1971100
Q9NYF8	BCLF1_HUMAN Bcl-2-associated transcription factor 1 BCLAF1	4	106.12	1721400	231270	925010	565070
Q9Y3F4	STRAP_HUMAN Serine-threonine kinase receptor-associated protein STRAP	4	38.44	11021000	1601600	4603000	4816000
Q9Y6M1	IF2B2_HUMAN Insulin-like growth factor 2 mRNA-binding protein 2 IGF2BP2	4	66.12	11499000	2929600	7311300	1257600
O14802	RPC1_HUMAN DNA-directed RNA polymerase III subunit RPC1 POLR3A	5	155.64	12770000	1731200	7277000	3762000
O94905	ERLN2_HUMAN Erlin-2 ERLIN2	5	37.84	6854000	558360	4415000	1880600
O95373	IPO7_HUMAN Importin-7 IPO7	5	119.52	4916100	1042000	797540	3076500
P12956	XRCC6_HUMAN X-ray repair cross-complementing protein 6 XRCC6	5	69.84	13270000	1690500	7963000	3616500
P16989	DBPA_HUMAN DNA-binding protein A CSDA	5	40.09	5487500	1946100	2120700	1420800
P35579	MYH9_HUMAN Myosin-9 MYH9	5	226.53	21627000	1906200	8891800	10829000
P42285	SK2L2_HUMAN Superkiller viralicidic activity 2-like 2 SKIV2L2	5	117.80	3093300	517520	1364000	1211800
P45880	VDAC2_HUMAN Voltage-dependent anion-selective channel protein 2 VDAC2	5	31.57	35949000	12778000	5137900	18033000
P51991	ROA3_HUMAN Heterogeneous nuclear ribonucleoprotein A3 HNRNPA3	5	39.59	15436000	1091700	11513000	2831000
P53621	COPA_HUMAN Coatomer subunit alpha COPA	5	138.34	6808200	2634900	1594900	2578500
P61247	RS3A_HUMAN 40S ribosomal protein S3a RPS3A	5	29.95	36701000	2252700	13038000	21410000
P61978	HNRPK_HUMAN Heterogeneous nuclear ribonucleoprotein K HNRNPK	5	50.98	7495300	1945300	1640200	3909800
Q5JWF2	GNAS1_HUMAN Guanine nucleotide-binding protein G(s) subunit alpha isoforms XLas GNAS	5	111.02	25273000	3999900	11990000	9283400

P63104	1433Z_HUMAN 14-3-3 protein zeta/delta YWHAZ	5	27.75	3338100	506360	1522500	1309200
P80723	BASP1_HUMAN Brain acid soluble protein 1 BASP1	5	22.69	3709600	295420	2102100	1312100
Q01085	TIAR_HUMAN Nucleolysin TIAR TIAL1	5	41.59	27330000	2466400	13966000	10898000
Q03252	LMNB2_HUMAN Lamin-B2 LMNB2	5	67.69	19727000	1225300	10685000	7816100
Q04637	IF4G1_HUMAN Eukaryotic translation initiation factor 4 gamma 1 EIF4G1	5	175.49	10792000	2585400	6772200	1434100
Q06830	PRDX1_HUMAN Peroxiredoxin-1 PRDX1	5	22.11	21566000	3236300	11558000	6771300
Q14152	EIF3A_HUMAN Eukaryotic translation initiation factor 3 subunit A EIF3A	5	166.57	14559000	2096200	8478200	3984700
Q15365	PCBP1_HUMAN Poly(rC)-binding protein 1 PCBP1	5	37.50	58145000	41147000	8447400	8550400
Q58FF6	H90B4_HUMAN Putative heat shock protein HSP 90-beta 4 HSP90AB4P PE=5 SV=1	5	58.26	4582200	137030	3288000	1157200
Q6P2Q9	PRP8_HUMAN Pre-mRNA-processing-splicing factor 8 PRPF8	5	273.60	9307600	3305500	3238400	2763700
Q8TEX9	IPO4_HUMAN Importin-4 IPO4	5	118.71	1251900	128750	234620	888570
Q96PK6	RBM14_HUMAN RNA-binding protein 14 RBM14	5	69.49	11823000	1309000	3381800	7132000
Q9NVI7	ATD3A_HUMAN ATPase family AAA domain-containing protein 3A ATAD3A	5	71.37	8251900	3318400	3085600	1847900
O43795	MYO1B_HUMAN Myosin-Ib MYO1B	6	131.98	7081200	1926100	3501000	1654100
P04075	ALDOA_HUMAN Fructose-bisphosphate aldolase A ALDOA	6	39.42	16297000	2763000	5719000	7815400
P16402	H13_HUMAN Histone H1.3 HIST1H1D	6	22.35	89197000	11480000	18964000	58752000
P14625	ENPL_HUMAN Endoplasmin HSP90B1	6	92.47	13692000	915580	2619400	10157000
P31689	DNJA1_HUMAN DnaJ homolog subfamily A member 1 DNAJA1	6	44.87	12012000	2620100	4608700	4783200
P31942	HNRH3_HUMAN Heterogeneous nuclear ribonucleoprotein H3 HNRNPH3	6	36.93	18907000	3755900	4984300	10167000
P46777	RL5_HUMAN 60S ribosomal protein L5 RPL5	6	34.36	23495000	2370100	2989600	18135000
P46781	RS9_HUMAN 40S ribosomal protein S9 RPS9	6	22.59	27557000	3055300	10843000	13659000
P50402	EMD_HUMAN Emerin EMD	6	28.99	18527000	3925300	6556200	8045900
P55072	TERA_HUMAN Transitional endoplasmic reticulum ATPase VCP	6	89.32	39064000	3538700	20219000	15306000
P60842	IF4A1_HUMAN Eukaryotic initiation factor 4A-I EIF4A1	6	46.15	14135000	1691400	7623600	4820000
P62258	1433E_HUMAN 14-3-3 protein epsilon YWHAE	6	29.17	29131000	4386500	15313000	9431800
P63096	GNAI1_HUMAN Guanine nucleotide-binding protein G(i) subunit alpha-1 GNAI1	6	40.36	26108000	9304500	9200300	7602800
P68871	HBB_HUMAN Hemoglobin subunit beta HBB	6	16.00	26747000	2954700	19903000	3889000

Q13263	TIF1B_HUMAN Transcription intermediary factor 1-beta TRIM28	6	88.55	26105000	5627800	11113000	9364600
Q14126	DSG2_HUMAN Desmoglein-2 DSG2	6	122.29	21621000	3221900	11282000	7117100
Q14318	FKBP8_HUMAN Peptidyl-prolyl cis-trans isomerase FKBP8 FKBP8	6	44.56	8171700	1748200	3132600	3290900
Q15366	PCBP2_HUMAN Poly(rC)-binding protein 2 PCBP2	6	38.58	13664000	2295200	5239200	6130000
Q16891	IMMT_HUMAN Mitochondrial inner membrane protein IMMT	6	83.68	8803800	2428700	2034700	4340400
Q86VP6	CAND1_HUMAN Cullin-associated NEDD8-dissociated protein 1 CAND1	6	136.37	9338000	861870	2618100	5858000
Q9BQG0	MBB1A_HUMAN Myb-binding protein 1A MYBBP1A	6	148.85	8791600	5742100	1913300	1136200
Q9P2J5	SYLC_HUMAN Leucine--tRNA ligase, cytoplasmic LARS	6	134.46	10328000	8045400	1719800	563130
Q9UPQ9	TNR6B_HUMAN Trinucleotide repeat-containing gene 6B protein TNRC6B	6	194.00	10030000	1151900	5710000	3168600
Q9UQ80	PA2G4_HUMAN Proliferation-associated protein 2G4 PA2G4	6	43.79	17764000	1746100	4825400	11193000
O75864	PPR37_HUMAN Protein phosphatase 1 regulatory subunit 37 PPP1R37	7	74.78	9231000	3818400	4383800	1028800
P04899	GNAI2_HUMAN Guanine nucleotide-binding protein G(i) subunit alpha-2 GNAI2	7	40.45	6694300	438220	3092900	3163200
P05023	AT1A1_HUMAN Sodium/potassium-transporting ATPase subunit alpha-1 ATP1A1	7	112.89	33949000	2060100	15826000	16063000
P07195	LDHB_HUMAN L-lactate dehydrogenase B chain LDHB	7	36.64	13562000	2479400	3794700	7287800
P08754	GNAI3_HUMAN Guanine nucleotide-binding protein G(k) subunit alpha GNAI3	7	40.53	36964000	2051800	27419000	7492600
P09651	ROA1_HUMAN Heterogeneous nuclear ribonucleoprotein A1 HNRNPA1	7	38.75	34626000	3500500	7779900	23346000
P15880	RS2_HUMAN 40S ribosomal protein S2 RPS2	7	31.32	189760000	3938700	68566000	117250000
P41252	SYIC_HUMAN Isoleucine--tRNA ligase, cytoplasmic IARS	7	144.50	8517000	2548100	2611800	3357100
P62424	RL7A_HUMAN 60S ribosomal protein L7a RPL7A	7	30.00	46533000	2625600	14920000	28987000
P62906	RL10A_HUMAN 60S ribosomal protein L10a RPL10A	7	24.83	22114000	1587500	7845200	12681000
Q02878	RL6_HUMAN 60S ribosomal protein L6 RPL6	7	32.73	25714000	1743300	3844300	20126000
Q13283	G3BP1_HUMAN Ras GTPase-activating protein-binding protein 1 G3BP1	7	52.16	16786000	8864400	4954000	2968100
Q14974	IMB1_HUMAN Importin subunit beta-1 KPNB1	7	97.17	53491000	2456400	32760000	18275000
Q6PKG0	LARP1_HUMAN La-related protein 1 LARP1	7	123.51	18934000	6940800	6467900	5525400
Q6S8J3	POTEE_HUMAN POTE ankyrin domain family member E POTEE	7	121.36	13860000	2706900	10424000	728840
Q92734	TFG_HUMAN Protein TFG TFG	7	43.45	31245000	2853400	11101000	17291000
Q96SW2	CRBN_HUMAN Protein cereblon CRBN	7	50.55	29271000	5474300	16737000	7059900

Q9NWS0	PIHD1_HUMAN PIH1 domain-containing protein 1 PIH1D1	7	32.36	182380000	28545000	14796000	139040000
P06748	NPM_HUMAN Nucleophosmin NPM1	8	32.58	97545000	7093900	23016000	67436000
P12235	ADT1_HUMAN ADP/ATP translocase 1 SLC25A4	8	33.06	2799100	233370	2502300	63400
P12277	KCRB_HUMAN Creatine kinase B-type CKB	8	42.64	29750000	2328900	15637000	11784000
P18124	RL7_HUMAN 60S ribosomal protein L7 RPL7	8	29.23	56785000	8049700	18525000	30210000
P21796	VDAC1_HUMAN Voltage-dependent anion-selective channel protein 1 VDAC1	8	30.77	15767000	2902400	4690800	8173800
P22626	ROA2_HUMAN Heterogeneous nuclear ribonucleoproteins A2/B1 HNRNPA2B1	8	37.43	31874000	3355200	10576000	17943000
P26373	RL13_HUMAN 60S ribosomal protein L13 RPL13	8	24.26	33963000	2809600	16913000	14240000
P35232	PHB_HUMAN Prohibitin PHB	8	29.80	44942000	2826200	23486000	18630000
P41236	IPP2_HUMAN Protein phosphatase inhibitor 2 PPP1R2	8	23.02	296360000	46228000	91122000	159010000
P42704	LPPRC_HUMAN Leucine-rich PPR motif-containing protein, mitochondrial LRPPRC	8	157.90	6314500	2352500	1488700	2473300
P43243	MATR3_HUMAN Matrin-3 MATR3	8	94.62	13135000	525810	3612000	8997300
P67809	YBOX1_HUMAN Nuclease-sensitive element-binding protein 1 YBX1	8	35.92	30067000	3627000	14775000	11664000
P68104	EF1A1_HUMAN Elongation factor 1-alpha 1 EEF1A1	8	50.14	71923000	6712600	31996000	33215000
Q00325	MPCP_HUMAN Phosphate carrier protein, mitochondrial SLC25A3	8	40.09	89217000	16203000	29655000	43359000
Q02833	RASF7_HUMAN Ras association domain-containing protein 7 RASSF7	8	39.95	13485000	2041900	6671400	4771300
Q12906	ILF3_HUMAN Interleukin enhancer-binding factor 3 ILF3	8	95.34	42053000	5702900	8952500	27397000
Q14157	UBP2L_HUMAN Ubiquitin-associated protein 2-like UBAP2L	8	114.53	17791000	2327300	7032500	8430900
Q8IWU2	LMTK2_HUMAN Serine/threonine-protein kinase LMTK2 LMTK2	8	164.90	3785600	801930	826250	2157400
Q96SB3	NEB2_HUMAN Neurabin-2 PPP1R9B	8	89.19	10582000	1548900	1344200	7689300
O00425	IF2B3_HUMAN Insulin-like growth factor 2 mRNA-binding protein 3 IGF2BP3	9	63.70	15672000	2686700	3752900	9232700
O94763	RMP_HUMAN Unconventional prefoldin RPB5 interactor RMP	9	59.83	65470000	14398000	8132300	42940000
P06576	ATPB_HUMAN ATP synthase subunit beta, mitochondrial ATP5B	9	56.56	105420000	7315100	81466000	16637000
P07814	SYEP_HUMAN Bifunctional glutamate/proline--tRNA ligase EPRS	9	170.59	15491000	2977800	5533500	6980000
P31943	HNRH1_HUMAN Heterogeneous nuclear ribonucleoprotein H HNRNPH1	9	49.23	63073000	5132000	29287000	28654000
P35580	MYH10_HUMAN Myosin-10 MYH10	9	229.00	21643000	3766200	9608000	8268800
P39023	RL3_HUMAN 60S ribosomal protein L3 RPL3	9	46.11	52947000	4114700	27939000	20894000

Q16543	CDC37_HUMAN Hsp90 co-chaperone Cdc37 CDC37	9	44.47	36004000	8904800	5753000	21347000
Q92900	RENT1_HUMAN Regulator of nonsense transcripts 1 UPF1	9	124.34	13509000	5418700	3183300	4907000
Q99623	PHB2_HUMAN Prohibitin-2 PHB2	9	33.30	20655000	2779000	5057600	12818000
Q9H361	PABP3_HUMAN Polyadenylate-binding protein 3 PABPC3	9	70.03	5166400	661990	933590	3570800
Q9P0K7	RAI14_HUMAN Ankycorbin RAI14	9	110.04	14483000	1586400	12177000	719520
P36578	RL4_HUMAN 60S ribosomal protein L4 RPL4	10	47.70	31305000	1929000	11390000	17986000
P49327	FAS_HUMAN Fatty acid synthase FASN	10	273.42	23804000	3825600	12317000	7660900
P49790	NU153_HUMAN Nuclear pore complex protein Nup153 NUP153	10	153.94	23563000	2175800	9387900	11999000
P62736	ACTA_HUMAN Actin, aortic smooth muscle ACTA2	10	42.01	28233000	3129800	11733000	13371000
Q00839	HNRPU_HUMAN Heterogeneous nuclear ribonucleoprotein U HNRNPU	10	90.58	221170000	8636300	125080000	87453000
Q15233	NONO_HUMAN Non-POU domain-containing octamer-binding protein NONO	10	54.23	55880000	8163300	17364000	30352000
Q15393	SF3B3_HUMAN Splicing factor 3B subunit 3 SF3B3	10	135.58	15825000	11167000	2545700	2112400
Q8NHQ8	RASF8_HUMAN Ras association domain-containing protein 8 RASSF8	10	48.33	74753000	7522200	44559000	22672000
Q96MX6	WDR92_HUMAN WD repeat-containing protein 92 WDR92	10	39.74	21642000	6567700	4312900	10762000
O00571	DDX3X_HUMAN ATP-dependent RNA helicase DDX3X DDX3X	11	73.24	17744000	2146900	5582400	10015000
P04406	G3P_HUMAN Glyceraldehyde-3-phosphate dehydrogenase GAPDH	11	36.05	120710000	8332200	39470000	72908000
P09874	PARP1_HUMAN Poly [ADP-ribose] polymerase 1 PARP1	11	113.08	22023000	1292400	7626100	13105000
P12236	ADT3_HUMAN ADP/ATP translocase 3 SLC25A6	11	32.87	33358000	7572800	8888100	16897000
P16615	AT2A2_HUMAN Sarcoplasmic/endoplasmic reticulum calcium ATPase 2 ATP2A2	11	114.76	39729000	2469400	20326000	16933000
P48643	TCPE_HUMAN T-complex protein 1 subunit epsilon CCT5	11	59.67	50736000	22757000	18504000	9474600
P52597	HNRPF_HUMAN Heterogeneous nuclear ribonucleoprotein F HNRNPF	11	45.67	59438000	7330400	23658000	28450000
P53396	ACLY_HUMAN ATP-citrate synthase ACLY	11	120.84	14572000	5445700	4200400	4926100
Q69YQ0	CYTSA_HUMAN Cytospin-A SPECC1L	11	124.60	4338200	74481	3889200	374590
Q6UXN9	WDR82_HUMAN WD repeat-containing protein 82 WDR82	11	35.08	86352000	13604000	23296000	49453000
Q9UJS0	CMC2_HUMAN Calcium-binding mitochondrial carrier protein Aralar2 SLC25A13	11	74.18	22168000	5913000	5574700	10680000
O94842	TOX4_HUMAN TOX high mobility group box family member 4 TOX4	12	66.19	225450000	4647100	83840000	136960000
P05141	ADT2_HUMAN ADP/ATP translocase 2 SLC25A5	12	32.85	384090000	94845000	109980000	179270000

P05388	RLA0_HUMAN 60S acidic ribosomal protein P0 RPLP0	12	34.27	205060000	13137000	46938000	144980000
P13639	EF2_HUMAN Elongation factor 2 EEF2	12	95.34	64426000	4096000	18704000	41626000
P25705	ATPA_HUMAN ATP synthase subunit alpha, mitochondrial ATP5A1	12	59.75	59651000	18939000	19126000	21585000
P46013	KI67_HUMAN Antigen KI-67 MKI67	12	358.69	8760900	1262400	3842000	3656500
P49368	TCPG_HUMAN T-complex protein 1 subunit gamma CCT3	12	60.53	139850000	69877000	58257000	11718000
P49750	YLPM1_HUMAN YLP motif-containing protein 1 YLPM1	12	219.98	15827000	2865500	5123500	7837600
Q13310	PABP4_HUMAN Polyadenylate-binding protein 4 PABPC4	12	70.78	68315000	18139000	19039000	31136000
Q14160	SCRIB_HUMAN Protein scribble homolog SCRIB	12	174.88	15572000	5196700	2639700	7735600
Q9BUF5	TBB6_HUMAN Tubulin beta-6 chain TUBB6	12	49.86	14362000	3119500	6878100	4365000
Q9H2D6	TARA_HUMAN TRIO and F-actin-binding protein TRIOBP	12	261.37	52842000	20552000	22459000	9830500
Q9H788	SH24A_HUMAN SH2 domain-containing protein 4A SH2D4A	12	52.73	150010000	15695000	70797000	63515000
Q9NR30	DDX21_HUMAN Nucleolar RNA helicase 2 DDX21	12	87.34	74994000	6323900	31990000	36679000
O95405	ZFYV9_HUMAN Zinc finger FYVE domain-containing protein 9 ZFYVE9	13	156.40	44636000	4070900	16880000	23685000
P06733	ENOA_HUMAN Alpha-enolase ENO1	13	47.17	80436000	9199500	42030000	29206000
P10809	CH60_HUMAN 60 kDa heat shock protein, mitochondrial HSPD1	13	61.05	56889000	35593000	13678000	7618900
P40227	TCPZ_HUMAN T-complex protein 1 subunit zeta CCT6A	13	58.02	200690000	57429000	125690000	17566000
Q13509	TBB3_HUMAN Tubulin beta-3 chain TUBB3	13	50.43	10885000	2888400	6504800	1491400
Q7L2E3	DHX30_HUMAN Putative ATP-dependent RNA helicase DHX30 DHX30	13	133.94	7116000	1372600	2105100	3638300
A6NKD9	CC85C_HUMAN Coiled-coil domain-containing protein 85C CCDC85C	14	45.21	116920000	29474000	48234000	39216000
O60237	MYPT2_HUMAN Protein phosphatase 1 regulatory subunit 12B PPP1R12B	14	110.40	12428000	3778000	7871500	778240
O94822	LTN1_HUMAN E3 ubiquitin-protein ligase listerin LTN1	14	200.55	19826000	4348300	9261200	6216600
P17844	DDX5_HUMAN Probable ATP-dependent RNA helicase DDX5 DDX5	14	69.15	42169000	5785200	21385000	14998000
P17987	TCPA_HUMAN T-complex protein 1 subunit alpha TCP1	14	60.34	226680000	64749000	118940000	42985000
P23246	SFPQ_HUMAN Splicing factor, proline- and glutamine-rich SFPQ	14	76.15	221020000	10572000	112970000	97486000
P36873	PP1G_HUMAN Serine/threonine-protein phosphatase PP1-gamma catalytic subunit PPP1CC	14	36.98	224200000	92292000	9411500	122500000
P52272	HNRPM_HUMAN Heterogeneous nuclear ribonucleoprotein M HNRNPM	14	77.52	56544000	6118000	15031000	35395000
P68366	TBA4A_HUMAN Tubulin alpha-4A chain TUBA4A	14	49.92	924930	192250	624910	107780

Q12972	PP1R8_HUMAN Nuclear inhibitor of protein phosphatase 1 PPP1R8	14	38.48	286390000	45088000	108790000	132510000
Q8WWM7	ATX2L_HUMAN Ataxin-2-like protein ATXN2L	14	113.37	22939000	5936600	5667800	11335000
Q92841	DDX17_HUMAN Probable ATP-dependent RNA helicase DDX17 DDX17	14	72.37	332070000	155530000	78280000	98264000
Q99832	TCPH_HUMAN T-complex protein 1 subunit eta CCT7	14	59.37	103890000	28451000	68798000	6636600
Q9BUJ2	HNRL1_HUMAN Heterogeneous nuclear ribonucleoprotein U-like protein 1 HNRNPUL1	14	95.74	290450000	7288100	163350000	119820000
P20700	LMNB1_HUMAN Lamin-B1 LMNB1	15	66.41	168260000	21171000	84476000	62617000
P78371	TCPB_HUMAN T-complex protein 1 subunit beta CCT2	15	57.49	52999000	19272000	19024000	14704000
Q9H6T3	RPAP3_HUMAN RNA polymerase II-associated protein 3 RPAP3	15	75.72	45453000	15330000	6374800	23748000
Q9Y265	RUVB1_HUMAN RuvB-like 1 RUVBL1	15	50.23	159890000	27094000	13279000	119510000
P19338	NUCL_HUMAN Nucleolin NCL	16	76.61	374260000	35806000	212090000	126370000
P23396	RS3_HUMAN 40S ribosomal protein S3 RPS3	16	26.69	157510000	32821000	54290000	70399000
Q08211	DHX9_HUMAN ATP-dependent RNA helicase A DHX9	16	140.96	91019000	7686800	66548000	16785000
Q9NZI8	IF2B1_HUMAN Insulin-like growth factor 2 mRNA-binding protein 1 IGF2BP1	16	63.48	70209000	9547400	19554000	41108000
Q9Y230	RUVB2_HUMAN RuvB-like 2 RUVBL2	16	51.16	588780000	98278000	136760000	353740000
P62136	PP1A_HUMAN Serine/threonine-protein phosphatase PP1-alpha catalytic subunit PPP1CA	17	37.51	497390000	327950000	21760000	147670000
Q00610	CLH1_HUMAN Clathrin heavy chain 1 CLTC	17	191.61	47550000	4108700	25655000	17786000
Q9BQE3	TBA1C_HUMAN Tubulin alpha-1C chain TUBA1C	17	49.90	8163900	1773900	3075100	3314900
P50991	TCPD_HUMAN T-complex protein 1 subunit delta CCT4	18	57.92	137880000	21195000	88758000	27930000
P62140	PP1B_HUMAN Serine/threonine-protein phosphatase PP1-beta catalytic subunit PPP1CB	18	37.19	711640000	96634000	331810000	283190000
Q13885	TBB2A_HUMAN Tubulin beta-2A chain TUBB2A	18	49.91	16005000	3084700	6564400	6355600
Q96QC0	PP1RA_HUMAN Serine/threonine-protein phosphatase 1 regulatory subunit 10 PPP1R10	18	99.06	606260000	11377000	302290000	292580000
Q9BZF9	UACA_HUMAN Uveal autoantigen with coiled-coil domains and ankyrin repeats UACA	18	162.50	10290000	1866800	6873900	1548900
P11940	PABP1_HUMAN Polyadenylate-binding protein 1 PABPC1	19	70.67	236150000	51258000	81154000	103740000
P68363	TBA1B_HUMAN Tubulin alpha-1B chain TUBA1B	19	50.15	1.383E+09	337150000	594730000	450830000
P08670	VIME_HUMAN Vimentin VIM	20	53.65	88437000	26200000	34993000	27244000
P50990	TCPQ_HUMAN T-complex protein 1 subunit theta CCT8	20	59.62	119180000	42524000	41808000	34848000

P68371	TBB4B_HUMAN Tubulin beta-4B chain TUBB4B	20	49.83	1.139E+09	176430000	593400000	369550000
P07437	TBB5_HUMAN Tubulin beta chain TUBB	21	49.67	1.26E+09	250280000	494290000	514900000
Q8WUF5	IASPP_HUMAN RelA-associated inhibitor PPP1R13L	21	89.09	85900000	22728000	39471000	23700000
P11021	GRP78_HUMAN 78 kDa glucose-regulated protein HSPA5	22	72.33	314740000	74026000	136070000	104640000
Q13625	ASPP2_HUMAN Apoptosis-stimulating of p53 protein 2 TP53BP2	22	125.61	384000000	197590000	126860000	59545000
Q9BZL4	PP12C_HUMAN Protein phosphatase 1 regulatory subunit 12C PPP1R12C	22	84.88	81083000	4875800	68310000	7897600
Q96KQ4	ASPP1_HUMAN Apoptosis-stimulating of p53 protein 1 PPP1R13B	23	119.56	102470000	12636000	50107000	39723000
Q96RT1	LAP2_HUMAN Protein LAP2 ERBB2IP	23	158.30	201850000	51190000	13762000	136890000
O14654	IRS4_HUMAN Insulin receptor substrate 4 IRS4	24	133.77	97303000	44358000	34832000	18112000
Q15435	PP1R7_HUMAN Protein phosphatase 1 regulatory subunit 7 PPP1R7	24	41.56	1.639E+09	181660000	476830000	980200000
Q9H792	PEAK1_HUMAN Pseudopodium-enriched atypical kinase 1 PEAK1	24	193.10	41215000	17337000	8885100	14992000
P08107	HSP71_HUMAN Heat shock 70 kDa protein 1A/1B HSPA1A	26	70.05	2.626E+09	679140000	866750000	1079700000
P07900	HS90A_HUMAN Heat shock protein HSP 90-alpha HSP90AA1	27	84.66	645930000	94535000	161090000	390310000
P11142	HSP7C_HUMAN Heat shock cognate 71 kDa protein HSPA8	27	70.90	848120000	137370000	262330000	448420000
P08238	HS90B_HUMAN Heat shock protein HSP 90-beta HSP90AB1	28	83.26	2.355E+09	112550000	680150000	1562200000
P38646	GRP75_HUMAN Stress-70 protein, mitochondrial HSPA9	28	73.68	1.017E+09	249330000	332490000	434880000
Q14684	RRP1B_HUMAN Ribosomal RNA processing protein 1 homolog B RRP1B	29	84.43	971910000	35669000	314730000	621510000
P27708	PYR1_HUMAN CAD protein CAD	30	242.98	115290000	25552000	52310000	37424000
Q16531	DDB1_HUMAN DNA damage-binding protein 1 DDB1	37	126.97	203100000	24195000	55835000	123070000
O14974	MYPT1_HUMAN Protein phosphatase 1 regulatory subunit 12A PPP1R12A	45	115.28	268120000	9522900	246310000	12295000

Appendix IVa

Proteins listed in **Appendix III** were used to determine the ratio of the different isoform preferences from the raw intensity values. The raw intensity values of each isoform was divided as follows: alpha/beta (A/B); alpha/gamma (A/G); beta/alpha (B/A); beta/gamma (B/G); gamma/alpha (G/A); gamma/beta (G/B). Values were then converted to log 2 and are listed below.

Uniprot	Uniprot description	Log 2 A/B	Log 2 A/G	Log 2 B/A	Log 2 B/G	Log 2 G/A	Log 2 G/B
A6NKD9	CC85C Coiled-coil domain-containing protein 85C CCDC85C	0.680	1.082	1.898	0.352	-0.901	-0.352
O00264	PGRC1 Membrane-associated progesterone receptor component 1 PGRMC1	-0.666	0.236	0.414	0.852	-0.372	-0.852
O00303	EIF3F Eukaryotic translation initiation factor 3 subunit F EIF3F	-3.096	0.172	0.481	3.218	-0.133	-3.218
O00425	IF2B3 Insulin-like growth factor 2 mRNA-binding protein 3 IGF2BP3	0.908	-0.287	1.698	-1.245	1.252	1.245
O00567	NOP56 Nucleolar protein 56 NOP56	0.398	0.284	0.198	-0.164	-0.106	0.164
O00571	DDX3X ATP-dependent RNA helicase DDX3X DDX3X	0.012	-0.728	-0.193	-0.789	-0.134	0.789
O14654	IRS4 Insulin receptor substrate 4 IRS4	1.739	2.786	-1.764	0.997	-1.622	-0.997
O14802	RPC1 DNA-directed RNA polymerase III subunit RPC1 POLR3A	-0.681	0.374	0.517	1.006	0.618	-1.006
O14818	PSA7 Proteasome subunit alpha type-7 PSMA7	-0.173	-0.328	2.106	-0.204	2.009	0.204
O14974	MYPT1 Protein phosphatase 1 regulatory subunit 12A PPP1R12A	-3.303	1.125	2.033	4.378	-3.357	-4.378
O14979	HNRDL Heterogeneous nuclear ribonucleoprotein D-like HNRPDL	1.746	-0.550	-1.176	-2.345	-0.558	2.345
O43143	DHX15 Putative pre-mRNA-splicing factor ATP-dependent RNA helicase DHX15	2.588	5.562	-1.159	2.925	-0.319	-2.925
O43175	SERA D-3-phosphoglycerate dehydrogenase PHGDH	2.247	1.366	-3.097	-0.931	-3.919	0.931
O43390	HNRPR Heterogeneous nuclear ribonucleoprotein R HNRNPR	0.075	1.233	0.017	1.108	0.618	-1.108
O43707	ACTN4 Alpha-actinin-4 ACTN4	-2.105	-1.992	-0.340	0.064	0.023	-0.064
O43795	MYO1B Myosin-Ib MYO1B	0.528	1.713	0.307	1.136	0.392	-1.136
O43813	LANC1 LanC-like protein 1 LANCL1	-1.059	-1.065	0.598	-0.056	0.176	0.056
O60237	MYPT2 Protein phosphatase 1 regulatory subunit 12B PPP1R12B	0.331	3.773	-2.029	3.392	-3.207	-3.392
O60506	HNRPQ Heterogeneous nuclear ribonucleoprotein Q SYNCRIP	1.616	0.177	1.552	-1.489	1.486	1.489
O60812	HNRCL Heterogeneous nuclear ribonucleoprotein C-like 1 HNRNPCL1	-0.706	0.282	1.651	0.939	1.301	-0.939
O60814	H2B1K Histone H2B type 1-K HIST1H2BK	-1.202	-1.101	-1.495	0.051	-2.321	-0.051

O60884	DNJA2 DnaJ homolog subfamily A member 2 DNAJA2	-0.222	0.913	0.095	1.085	-0.903	-1.085
O60927	PP1RB Protein phosphatase 1 regulatory subunit 11 PPP1R11	0.702	-1.381	-1.376	-2.133	-1.288	2.133
O75190	DNJB6 DnaJ homolog subfamily B member 6 DNAJB6	1.132	1.251	2.087	0.070	-0.291	-0.070
O75489	NDUS3 NADH dehydrogenase [ubiquinone] iron-sulfur protein 3, mitochondrial	0.311	1.299	-0.121	0.939	0.701	-0.939
O75533	SF3B1 Splicing factor 3B subunit 1 SF3B1	1.887	0.930	-1.313	-1.006	0.679	1.006
O75643	U520 U5 small nuclear ribonucleoprotein 200 kDa helicase SNRNP200	-0.030	1.542	-1.457	1.523	-0.544	-1.523
O75864	PPR37 Protein phosphatase 1 regulatory subunit 37 PPP1R37	1.191	3.386	1.441	2.145	0.674	-2.145
O75955	FLOT1 Flotillin-1 FLOT1	0.369	-0.131	0.610	-0.549	-0.188	0.549
O94763	RMP Unconventional prefoldin RPB5 interactor RMP	2.215	-0.083	-0.240	-2.347	-1.828	2.347
O94822	LTN1 E3 ubiquitin-protein ligase listerin LTN1	0.300	0.978	0.213	0.629	1.288	-0.629
O94842	TOX4 TOX high mobility group box family member 4 TOX4	-2.783	-3.388	1.917	-0.654	1.853	0.654
O94905	ERLN2 Erlin-2 ERLIN2	-1.593	-0.258	0.835	1.285	0.052	-1.285
O95347	SMC2 Structural maintenance of chromosomes protein 2 SMC2	0.319	2.753	0.338	2.385	-1.913	-2.385
O95373	IPO7 Importin-7 IPO7	1.776	-0.068	-0.679	-1.894	-1.065	1.894
O95405	ZFYV9 Zinc finger FYVE domain-containing protein 9 ZFYVE9	-0.661	-1.047	-2.020	-0.435	-0.216	0.435
O95685	PPR3D Protein phosphatase 1 regulatory subunit 3D PPP1R3D	1.635	-0.363	-2.770	-2.048	-3.701	2.048
O95793	STAU1 Double-stranded RNA-binding protein Staufen homolog 1 STAU1	1.356	0.061	-0.076	-1.344	-0.523	1.344
O95831	AIFM1 Apoptosis-inducing factor 1, mitochondrial AIFM1	3.098	3.936	1.253	0.789	0.637	-0.789
P00338	LDHA L-lactate dehydrogenase A chain LDHA	0.939	1.947	-1.475	0.959	-0.624	-0.959
P00403	COX2 Cytochrome c oxidase subunit 2 MT-CO2	0.125	-0.110	1.070	-0.285	-0.163	0.285
P01111	RASN GTPase NRas NRAS	0.386	-2.096	-2.114	-2.532	-1.508	2.532
P04075	ALDOA Fructose-bisphosphate aldolase A ALDOA	0.341	-0.006	-0.125	-0.397	0.127	0.397
P04406	G3P Glyceraldehyde-3-phosphate dehydrogenase GAPDH	-0.854	-1.636	-0.900	-0.832	-0.095	0.832
P04843	RPN1 Dolichyl-diphosphooligosaccharide-protein glycosyltransferase subunit	-0.970	0.251	0.222	1.172	-1.110	-1.172
P04899	GNAI2 Guanine nucleotide-binding protein G(i) subunit alpha-2 GNAI2	-1.429	-1.358	-4.227	0.021	-1.253	-0.021
P05023	AT1A1 Sodium/potassium-transporting ATPase subunit alpha-1 ATP1A1	-1.551	-1.469	4.317	0.032	0.853	-0.032
P05141	ADT2 ADP/ATP translocase 2 SLC25A5	1.177	0.575	-1.266	-0.651	-1.931	0.651

P05198	IF2A Eukaryotic translation initiation factor 2 subunit 1 EIF2S1	-0.636	-0.362	-2.129	0.224	-0.996	-0.224
P05387	RLA2 60S acidic ribosomal protein P2 RPLP2	-0.412	-0.291	-0.183	0.071	0.870	-0.071
P05388	RLA0 60S acidic ribosomal protein P0 RPLP0	-0.447	-1.970	-2.380	-1.573	-2.139	1.573
P06576	ATPB ATP synthase subunit beta, mitochondrial ATP5B	-2.087	0.308	0.949	2.346	1.059	-2.346
P06733	ENOA Alpha-enolase ENO1	-0.801	-0.173	-0.011	0.579	0.745	-0.579
P06748	NPM Nucleophosmin NPM1	-0.308	-1.755	0.496	-1.497	-0.103	1.497
P07195	LDHB L-lactate dehydrogenase B chain LDHB	0.776	-0.062	-1.295	-0.888	-0.460	0.888
P07437	TBB5 Tubulin beta chain TUBB	0.409	0.453	-2.587	-0.005	-5.545	0.005
P07737	PROF1 Profilin-1 PFN1	-0.398	0.410	-0.773	0.759	-0.071	-0.759
P07814	SYEP Bifunctional glutamate/proline--tRNA ligase EPRS	0.496	0.265	1.724	-0.281	-0.350	0.281
P07900	HS90A Heat shock protein HSP 90-alpha HSP90AA1	0.621	-0.552	-0.575	-1.223	-0.609	1.223
P07910	HNRPC Heterogeneous nuclear ribonucleoproteins C1/C2 HNRNPC	-1.113	-0.876	0.222	0.188	-0.896	-0.188
P08107	HSP71 Heat shock 70 kDa protein 1A/1B HSPA1A	1.039	0.825	-1.131	-0.263	-1.234	0.263
P08238	HS90B Heat shock protein HSP 90-beta HSP90AB1	-1.205	-2.301	0.418	-1.146	-0.334	1.146
P08670	VIME Vimentin VIM	0.973	1.437	-0.292	0.415	-2.883	-0.415
P08754	GNAI3 Guanine nucleotide-binding protein G(k) subunit alpha GNAI3	-2.350	-0.375	-3.388	1.925	-3.077	-1.925
P08865	RSSA 40S ribosomal protein SA RPSA	-1.368	-4.228	0.863	-2.909	0.830	2.909
P09104	ENOG Gamma-enolase ENO2	-1.422	-0.449	0.695	0.924	0.700	-0.924
P09651	ROA1 Heterogeneous nuclear ribonucleoprotein A1 HNRNPA1	0.238	-1.244	0.002	-1.532	1.175	1.532
P09874	PARP1 Poly [ADP-ribose] polymerase 1 PARP1	-1.170	-1.848	0.801	-0.727	1.868	0.727
P0CG48	UBC Polyubiquitin-C UBC ;>spP0CG47UBB Polyubiquitin-B UBB	-0.289	-0.257	0.549	-0.018	-1.201	0.018
P10606	COX5B Cytochrome c oxidase subunit 5B, mitochondrial COX5B	0.900	0.112	0.626	-0.838	-0.550	0.838
P10809	CH60 60 kDa heat shock protein, mitochondrial HSPD1	2.770	3.718	3.096	0.898	-0.155	-0.898
P11021	GRP78 78 kDa glucose-regulated protein HSPA5	0.512	0.994	-0.734	0.433	-1.038	-0.433
P11142	HSP7C Heat shock cognate 71 kDa protein HSPA8	0.457	-0.213	-1.672	-0.720	-1.571	0.720
P11940	PABP1 Polyadenylate-binding protein 1 PABPC1	0.728	0.477	-0.650	-0.300	-0.441	0.300
P12004	PCNA Proliferating cell nuclear antigen PCNA	-0.799	-0.163	0.802	0.587	0.190	-0.587

P12235	ADT1 ADP/ATP translocase 1 SLC25A4	-2.032	3.374	1.423	5.356	0.465	-5.356
P12236	ADT3 ADP/ATP translocase 3 SLC25A6	1.159	0.336	0.127	-0.873	1.995	0.873
P12277	KCRB Creatine kinase B-type CKB	-1.357	-0.845	1.593	0.462	0.275	-0.462
P12956	XRCC6 X-ray repair cross-complementing protein 6 XRCC6	-0.845	0.397	3.237	1.192	3.082	-1.192
P13639	EF2 Elongation factor 2 EEF2	-0.801	-1.851	-0.645	-1.100	-0.414	1.100
P13807	GYS1 Glycogen [starch] synthase, muscle GYS1	-1.358	-1.697	0.297	-0.388	-0.475	0.388
P14618	KPYM Pyruvate kinase isozymes M1/M2 PKM2	-0.214	1.468	1.256	1.633	-1.745	-1.633
P14625	ENPL Endoplasmin HSP90B1	-0.126	-1.978	-0.548	-1.901	-0.564	1.901
P14866	HNRPL Heterogeneous nuclear ribonucleoprotein L HNRNPL	0.209	0.748	-0.368	0.490	0.148	-0.490
P15531	NDKA Nucleoside diphosphate kinase A NME1	-0.698	0.251	-1.119	0.900	-1.151	-0.900
P15880	RS2 40S ribosomal protein S2 RPS2	-2.731	-3.402	-0.920	-0.720	0.726	0.720
P16402	H13 Histone H1.3 HIST1H1D	0.666	-0.862	1.966	-1.578	1.132	1.578
P16615	AT2A2 Sarcoplasmic/endoplasmic reticulum calcium ATPase 2 ATP2A2	-1.651	-1.284	0.252	0.317	-1.224	-0.317
P16989	DBPA DNA-binding protein A CSDA	1.266	1.948	-2.229	0.632	-3.055	-0.632
P17844	DDX5 Probable ATP-dependent RNA helicase DDX5 DDX5	-0.496	0.119	0.854	0.566	1.652	-0.566
P17987	TCPA T-complex protein 1 subunit alpha TCP1	0.513	2.085	-0.369	1.522	0.677	-1.522
P18124	RL7 60S ribosomal protein L7 RPL7	0.188	-0.414	1.364	-0.652	1.603	0.652
P18621	RL17 60S ribosomal protein L17 RPL17	-0.235	-0.239	-1.084	-0.054	-0.345	0.054
P19338	NUCL Nucleolin NCL	-1.176	-0.326	0.658	0.801	0.948	-0.801
P19388	RPAB1 DNA-directed RNA polymerases I, II, and III subunit RPABC1 POLR2E	4.405	2.390	-1.406	-2.064	-1.768	2.064
P20700	LMNB1 Lamin-B1 LMNB1	-0.606	-0.071	1.429	0.486	1.375	-0.486
P21796	VDAC1 Voltage-dependent anion-selective channel protein 1 VDAC1	0.698	0.000	2.350	-0.747	0.392	0.747
P22087	FBRL rRNA 2-O-methyltransferase fibrillarin FBL	-1.255	1.762	0.194	2.967	-0.262	-2.967
P22626	ROA2 Heterogeneous nuclear ribonucleoproteins A2/B1 HNRNPA2B1	-0.266	-0.925	-0.975	-0.709	-0.674	0.709
P23246	SFPQ Splicing factor, proline- and glutamine-rich SFPQ	-2.027	-1.711	-0.512	0.266	-0.978	-0.266
P23396	RS3 40S ribosomal protein S3 RPS3	0.664	0.393	-1.455	-0.321	-2.769	0.321
P23526	SAHH Adenosylhomocysteinase AHCY	0.809	0.280	1.095	-0.578	0.653	0.578

P23528	COF1 Cofilin-1 CFL1 ;>spQ9Y281COF2 Cofilin-2 CFL2	-1.069	0.180	1.358	1.200	1.714	-1.200
P24666	PPAC Low molecular weight phosphotyrosine protein phosphatase ACP1	0.960	-1.235	-0.666	-2.244	0.879	2.244
P25705	ATPA ATP synthase subunit alpha, mitochondrial ATP5A1	1.376	1.305	1.202	-0.121	1.118	0.121
P25789	PSA4 Proteasome subunit alpha type-4 PSMA4	-0.321	1.483	0.341	1.755	1.767	-1.755
P26196	DDX6 Probable ATP-dependent RNA helicase DDX6 DDX6	1.296	0.477	3.195	-0.868	1.601	0.868
P26373	RL13 60S ribosomal protein L13 RPL13	-1.199	-0.848	-0.539	0.302	-0.042	-0.302
P26640	SYVC Valine--tRNA ligase VARS	1.802	-0.388	1.362	-2.239	-1.081	2.239
P26641	EF1G Elongation factor 1-gamma EEF1G	-0.001	-1.159	0.706	-1.207	-0.266	1.207
P27348	1433T 14-3-3 protein theta YWHAQ	-1.697	-1.235	-1.745	0.412	0.567	-0.412
P27635	RL10 60S ribosomal protein L10 RPL10	-0.437	-0.969	1.123	-0.582	1.004	0.582
P27694	RFA1 Replication protein A 70 kDa DNA-binding subunit RPA1	-2.365	1.331	-0.982	3.646	-0.040	-3.646
P27708	PYR1 CAD protein CAD	0.357	0.943	3.096	0.537	2.562	-0.537
P27797	CALR Calreticulin CALR	0.241	1.845	1.114	1.555	0.893	-1.555
P28066	PSA5 Proteasome subunit alpha type-5 PSMA5	-0.304	0.774	-0.265	1.028	-0.371	-1.028
P29692	EF1D Elongation factor 1-delta EEF1D	-0.694	-0.683	0.301	-0.038	0.480	0.038
P30050	RL12 60S ribosomal protein L12 RPL12	-1.546	-1.036	-1.636	0.461	-0.470	-0.461
P31689	DNJA1 DnaJ homolog subfamily A member 1 DNAJA1	0.576	0.625	-0.208	0.000	-0.731	0.000
P31942	HNRH3 Heterogeneous nuclear ribonucleoprotein H3 HNRNPH3	0.982	0.057	-0.093	-0.975	1.056	0.975
P31943	HNRH1 Heterogeneous nuclear ribonucleoprotein H HNRNPH1	-1.122	-0.987	-1.616	0.085	-0.160	-0.085
P31946	1433B 14-3-3 protein beta/alpha YWHAB	-1.897	0.918	-0.075	2.765	-1.216	-2.765
P32119	PRDX2 Peroxiredoxin-2 PRDX2	2.486	1.029	2.466	-1.507	1.863	1.507
P32969	RL9 60S ribosomal protein L9 RPL9	-0.326	-0.584	-0.621	-0.308	0.569	0.308
P34932	HSP74 Heat shock 70 kDa protein 4 HSPA4	2.195	-0.158	1.205	-2.403	2.318	2.403
P35232	PHB Prohibitin PHB	-1.664	-1.227	-1.038	0.388	-0.808	-0.388
P35268	RL22 60S ribosomal protein L22 RPL22	-0.244	0.202	-2.195	0.396	0.175	-0.396
P35579	MYH9 Myosin-9 MYH9	-0.831	-1.012	-0.457	-0.231	0.230	0.231
P35580	MYH10 Myosin-10 MYH10	0.039	0.359	-0.594	0.270	-1.416	-0.270

P35637	FUS RNA-binding protein FUS FUS	-0.252	1.241	0.636	1.443	0.379	-1.443
P36542	ATPG ATP synthase subunit gamma, mitochondrial ATP5C1	0.122	-0.684	-0.356	-0.855	0.629	0.855
P36578	RL4 60S ribosomal protein L4 RPL4	-1.171	-1.727	-0.070	-0.605	-2.697	0.605
P36873	PP1G Serine/threonine-protein phosphatase PP1-gamma catalytic subunit PPP1	4.684	1.085	-0.908	-3.648	0.304	3.648
P38159	RBMX RNA-binding motif protein, X chromosome RBMX	-1.381	-1.156	0.782	0.176	0.034	-0.176
P38646	GRP75 Stress-70 protein, mitochondrial HSPA9	0.975	0.691	-0.285	-0.334	0.061	0.334
P38919	IF4A3 Eukaryotic initiation factor 4A-III EIF4A3	0.285	-0.044	-0.001	-0.379	-2.327	0.379
P39019	RS19 40S ribosomal protein S19 RPS19	-0.515	-0.222	0.663	0.243	0.493	-0.243
P39023	RL3 60S ribosomal protein L3 RPL3	-1.373	-0.850	-0.739	0.473	0.787	-0.473
P39656	OST48 Dolichyl-diphosphooligosaccharide--protein glycosyltransferase 48 kD	1.164	1.304	0.130	0.090	0.684	-0.090
P40227	TCPZ T-complex protein 1 subunit zeta CCT6A	0.260	3.203	2.347	2.893	1.418	-2.893
P40429	RL13A 60S ribosomal protein L13a RPL13A	-0.627	-1.159	-1.645	-0.582	-0.639	0.582
P41236	IPP2 Protein phosphatase inhibitor 2 PPP1R2	0.411	-0.289	-0.524	-0.749	1.310	0.749
P41252	SYIC Isoleucine--tRNA ligase, cytoplasmic IARS	1.355	1.096	-1.776	-0.308	0.085	0.308
P42285	SK2L2 Superkiller viralicidic activity 2-like 2 SKIV2L2	-0.008	0.266	-1.437	0.224	-2.306	-0.224
P42677	RS27 40S ribosomal protein S27 RPS27	0.120	0.758	-0.411	0.588	0.305	-0.588
P42704	LPPRC Leucine-rich PPR motif-containing protein, mitochondrial LRPPRC	2.051	1.422	-1.739	-0.679	-2.769	0.679
P42766	RL35 60S ribosomal protein L35 RPL35	-1.824	-1.024	1.357	0.750	0.862	-0.750
P43243	MATR3 Matrin-3 MATR3	-1.390	-2.603	0.216	-1.263	0.057	1.263
P43307	SSRA Translocon-associated protein subunit alpha SSR1	0.258	-2.034	0.795	-2.342	-0.946	2.342
P45880	VDAC2 Voltage-dependent anion-selective channel protein 2 VDAC2	2.705	0.997	0.215	-1.758	-1.451	1.758
P46013	KI67 Antigen KI-67 MKI67	-0.215	-0.041	1.060	0.125	1.082	-0.125
P46777	RL5 60S ribosomal protein L5 RPL5	1.055	-1.442	-3.285	-2.547	-0.058	2.547
P46781	RS9 40S ribosomal protein S9 RPS9	-0.437	-0.667	-1.492	-0.279	-1.806	0.279
P46782	RS5 40S ribosomal protein S5 RPS5	-1.186	0.808	-0.938	1.945	-1.930	-1.945
P48047	ATPO ATP synthase subunit O, mitochondrial ATP5O	1.313	-0.662	-0.776	-2.025	0.079	2.025
P48643	TCPE T-complex protein 1 subunit epsilon CCT5	1.689	2.758	1.981	1.019	-0.503	-1.019

P49006	MRP MARCKS-related protein MARCKSL1	-3.554	-1.654	0.607	1.850	0.088	-1.850
P49327	FAS Fatty acid synthase FASN	-0.296	0.492	1.735	0.739	1.196	-0.739
P49368	TCPG T-complex protein 1 subunit gamma CCT3	1.653	4.070	-1.347	2.367	-0.049	-2.367
P49411	EFTU Elongation factor Tu, mitochondrial TUFM	-0.548	1.218	-2.050	1.717	-1.405	-1.717
P49750	YLPM1 YLP motif-containing protein 1 YLPM1	0.552	0.042	-0.810	-0.560	-2.003	0.560
P49790	NU153 Nuclear pore complex protein Nup153 NUP153	-0.719	-0.970	-0.299	-0.300	-0.961	0.300
P50402	EMD Emerin EMD	0.650	0.458	1.390	-0.242	2.620	0.242
P50914	RL14 60S ribosomal protein L14 RPL14	-0.810	-0.446	-2.975	0.314	-3.814	-0.314
P50990	TCPQ T-complex protein 1 subunit theta CCT8	1.415	1.781	-0.008	0.316	-1.560	-0.316
P50991	TCPD T-complex protein 1 subunit delta CCT4	-0.676	1.096	-0.530	1.722	-0.651	-1.722
P51991	ROA3 Heterogeneous nuclear ribonucleoprotein A3 HNRNPA3	-2.008	0.119	3.112	2.078	2.803	-2.078
P52272	HNRPM Heterogeneous nuclear ribonucleoprotein M HNRNPM	0.094	-1.039	-0.518	-1.182	-0.057	1.182
P52292	IMA2 Importin subunit alpha-2 KPNA2	-0.129	-0.667	3.555	-0.588	1.671	0.588
P52597	HNRPF Heterogeneous nuclear ribonucleoprotein F HNRNPF	-0.300	-0.463	-0.039	-0.212	-0.342	0.212
P52907	CAZA1 F-actin-capping protein subunit alpha-1 CAPZA1	-0.834	-0.035	0.832	0.749	1.029	-0.749
P53007	TXTP Tricarboxylate transport protein, mitochondrial SLC25A1	1.003	-0.406	-3.999	-1.458	-0.132	1.458
P53396	ACLY ATP-citrate synthase ACLY	1.765	1.638	-0.528	-0.176	-1.697	0.176
P53621	COPA Coatomer subunit alpha COPA	2.115	1.525	3.303	-0.639	-1.108	0.639
P53985	MOT1 Monocarboxylate transporter 1 SLC16A1	0.531	0.668	-0.331	0.087	-3.756	-0.087
P54136	SYRC Arginine--tRNA ligase, cytoplasmic RARS	-0.613	0.722	-0.222	1.285	0.486	-1.285
P55060	XPO2 Exportin-2 CSE1L	0.700	-0.822	0.699	-1.571	-0.235	1.571
P55072	TERA Transitional endoplasmic reticulum ATPase VCP	-1.124	-0.619	-0.310	0.455	-1.283	-0.455
P55209	NP1L1 Nucleosome assembly protein 1-like 1 NAP1L1	-2.087	0.364	-1.594	2.401	0.835	-2.401
P59190	RAB15 Ras-related protein Rab-15 RAB15	8.395	7.500	0.977	-0.944	2.708	0.944
P60174	TPIS Triosephosphate isomerase TPI1	1.392	-0.586	-0.301	-2.028	0.418	2.028
P60842	IF4A1 Eukaryotic initiation factor 4A-I EIF4A1	-0.782	-0.017	-0.398	0.715	-0.267	-0.715
P61224	RAP1B Ras-related protein Rap-1b RAP1B	-2.244	-0.607	2.087	1.587	-0.347	-1.587

P61247	RS3A 40S ribosomal protein S3a RPS3A	-1.143	-1.755	0.308	-0.662	1.772	0.662
P61353	RL27 60S ribosomal protein L27 RPL27	-0.764	-1.412	0.719	-0.698	0.986	0.698
P61978	HNRPK Heterogeneous nuclear ribonucleoprotein K HNRNPK	1.637	0.487	1.177	-1.199	0.342	1.199
P61981	1433G 14-3-3 protein gamma YWHAG	-0.480	0.150	-0.351	0.580	-0.967	-0.580
P62081	RS7 40S ribosomal protein S7 RPS7	-1.863	-2.438	-1.163	-0.625	-1.287	0.625
P62136	PP1A Serine/threonine-protein phosphatase PP1-alpha catalytic subunit PPP1	5.304	2.645	0.077	-2.709	1.203	2.709
P62140	PP1B Serine/threonine-protein phosphatase PP1-beta catalytic subunit PPP1C	-0.389	-0.057	-0.727	0.282	-0.460	-0.282
P62241	RS8 40S ribosomal protein S8 RPS8	-0.002	-0.455	-0.894	-0.502	0.954	0.502
P62244	RS15A 40S ribosomal protein S15a RPS15A	-0.471	-4.847	-1.320	-4.426	-0.697	4.426
P62249	RS16 40S ribosomal protein S16 RPS16	-1.363	-0.752	0.913	0.561	2.196	-0.561
P62258	1433E 14-3-3 protein epsilon YWHAE	-0.413	0.389	1.171	0.753	1.865	-0.753
P62263	RS14 40S ribosomal protein S14 RPS14	-0.657	-0.761	-3.674	-0.154	-3.744	0.154
P62269	RS18 40S ribosomal protein S18 RPS18	-0.902	-1.029	-0.199	-0.177	-0.060	0.177
P62277	RS13 40S ribosomal protein S13 RPS13	-1.332	-0.700	0.800	0.583	0.179	-0.583
P62280	RS11 40S ribosomal protein S11 RPS11	-1.448	-0.756	-0.552	0.642	0.614	-0.642
P62318	SMD3 Small nuclear ribonucleoprotein Sm D3 SNRPD3	0.227	-0.089	-2.383	-0.365	-0.254	0.365
P62424	RL7A 60S ribosomal protein L7a RPL7A	-1.116	-1.971	-2.354	-0.904	-1.687	0.904
P62701	RS4X 40S ribosomal protein S4, X isoform RPS4X	-0.704	-0.937	-1.398	-0.283	0.413	0.283
P62736	ACTA Actin, aortic smooth muscle ACTA2	-0.516	-0.601	-1.684	-0.135	-0.374	0.135
P62750	RL23A 60S ribosomal protein L23a RPL23A	-0.102	-0.023	0.667	0.030	-0.219	-0.030
P62753	RS6 40S ribosomal protein S6 RPS6	0.330	-0.055	1.665	-0.435	1.244	0.435
P62805	H4 Histone H4 HIST1H4A	-0.340	-1.750	-0.526	-1.460	0.729	1.460
P62826	RAN GTP-binding nuclear protein Ran RAN	-1.257	-0.385	-2.338	0.822	0.807	-0.822
P62829	RL23 60S ribosomal protein L23 RPL23	-1.204	-0.080	0.555	1.075	-3.370	-1.075
P62851	RS25 40S ribosomal protein S25 RPS25	-1.282	-0.963	2.419	0.269	-0.781	-0.269
P62854	RS26 40S ribosomal protein S26 RPS26	-2.160	-0.731	-5.304	1.379	-2.628	-1.379
P62873	GBB1 Guanine nucleotide-binding protein G(I)/G(S)/G(T) subunit beta-1 GNB1	0.369	-0.660	0.390	-1.079	0.074	1.079

P62879	GBB2 Guanine nucleotide-binding protein G(I)/G(S)/G(T) subunit beta-2 GNB2	-1.363	-1.586	-4.684	-0.272	-1.068	0.272
P62888	RL30 60S ribosomal protein L30 RPL30	-0.908	-0.250	0.002	0.608	0.955	-0.608
P62899	RL31 60S ribosomal protein L31 RPL31	-1.931	-2.595	-0.119	-0.714	0.078	0.714
P62906	RL10A 60S ribosomal protein L10a RPL10A	-0.915	-1.504	3.342	-0.639	3.208	0.639
P62913	RL11 60S ribosomal protein L11 RPL11	-5.149	-0.282	-0.701	4.818	1.398	-4.818
P62917	RL8 60S ribosomal protein L8 RPL8	-1.259	-1.535	-0.959	-0.326	1.252	0.326
P62937	PPIA Peptidyl-prolyl cis-trans isomerase A PPIA	-1.427	-1.320	1.428	0.058	1.337	-0.058
P62995	TRA2B Transformer-2 protein homolog beta TRA2B	0.443	0.531	-1.191	0.038	-3.369	-0.038
P63096	GNAI1 Guanine nucleotide-binding protein G(i) subunit alpha-1 GNAI1	1.407	1.785	-1.634	0.329	0.380	-0.329
P63104	1433Z 14-3-3 protein zeta/delta YWHAZ	-0.198	0.123	0.447	0.272	-0.412	-0.272
P63151	2ABA Serine/threonine-protein phosphatase 2A 55 kDa regulatory subunit B	0.194	0.150	-2.486	-0.093	-1.012	0.093
P63244	GBLP Guanine nucleotide-binding protein subunit beta-2-like 1 GNB2L1	1.084	0.362	0.399	-0.772	-0.393	0.772
P67809	YBOX1 Nuclease-sensitive element-binding protein 1 YBX1	-0.636	-0.191	1.017	0.395	0.269	-0.395
P68104	EF1A1 Elongation factor 1-alpha 1 EEF1A1	-0.863	-0.813	-1.419	0.000	-1.735	0.000
P68363	TBA1B Tubulin alpha-1B chain TUBA1B	0.572	1.075	0.322	0.453	-1.466	-0.453
P68366	TBA4A Tubulin alpha-4A chain TUBA4A	-0.310	2.329	0.304	2.589	-0.757	-2.589
P68371	TBB4B Tubulin beta-4B chain TUBB4B	-0.359	0.427	0.174	0.737	0.345	-0.737
P68871	HBB Hemoglobin subunit beta HBB	-1.361	1.097	-0.834	2.409	-1.837	-2.409
P78347	GTF2I General transcription factor II-I GTF2I	-1.095	-0.636	-0.356	0.409	-0.926	-0.409
P78371	TCPB T-complex protein 1 subunit beta CCT2	1.409	1.884	-8.394	0.425	-7.483	-0.425
P80723	BASP1 Brain acid soluble protein 1 BASP1	-1.441	-0.657	-0.347	0.734	0.891	-0.734
P82933	RT09 28S ribosomal protein S9, mitochondrial MRPS9	-0.981	0.645	1.551	1.577	-2.618	-1.577
P83731	RL24 60S ribosomal protein L24 RPL24	0.223	0.228	1.257	-0.044	0.401	0.044
P84098	RL19 60S ribosomal protein L19 RPL19	-0.755	0.379	2.245	1.084	0.624	-1.084
P84103	SRSF3 Serine/arginine-rich splicing factor 3 SRSF3	-0.897	0.772	0.318	1.619	-0.252	-1.619
Q00325	MPCP Phosphate carrier protein, mitochondrial SLC25A3	0.518	0.074	1.177	-0.494	0.115	0.494
Q00610	CLH1 Clathrin heavy chain 1 CLTC	-1.252	-0.620	-0.386	0.582	2.113	-0.582

Q00839	HNRPU Heterogeneous nuclear ribonucleoprotein U HNRNPU	-2.466	-1.846	-2.419	0.570	-0.146	-0.570
Q01085	TIAR Nucleolysin TIAR TIAL1	-1.111	-0.650	-1.950	0.412	-0.935	-0.412
Q01130	SRSF2 Serine/arginine-rich splicing factor 2 SRSF2	2.370	1.903	-0.020	-0.517	0.969	0.517
Q01844	EWS RNA-binding protein EWS EWSR1	-3.236	-3.066	1.382	0.121	1.173	-0.121
Q02833	RASF7 Ras association domain-containing protein 7 RASSF7	-0.318	0.269	0.001	0.537	0.418	-0.537
Q02878	RL6 60S ribosomal protein L6 RPL6	0.250	-2.035	-2.157	-2.334	-1.620	2.334
Q03252	LMNB2 Lamin-B2 LMNB2	-1.734	-1.180	2.365	0.505	-1.314	-0.505
Q04637	IF4G1 Eukaryotic translation initiation factor 4 gamma 1 EIF4G1	0.001	2.344	0.437	2.293	0.985	-2.293
Q04837	SSBP Single-stranded DNA-binding protein, mitochondrial SSBP1	-2.967	-0.147	0.915	2.770	1.521	-2.770
Q06787	FMR1 Fragile X mental retardation protein 1 FMR1	0.921	-0.709	5.150	-1.679	0.298	1.679
Q06830	PRDX1 Peroxiredoxin-1 PRDX1	-0.446	0.429	1.547	0.825	1.053	-0.825
Q07020	RL18 60S ribosomal protein L18 RPL18	-0.311	-0.153	1.200	0.109	0.865	-0.109
Q07955	SRSF1 Serine/arginine-rich splicing factor 1 SRSF1	2.281	1.613	0.627	-0.717	1.176	0.717
Q08211	DHX9 ATP-dependent RNA helicase A DHX9	-1.724	0.367	0.810	2.041	0.463	-2.041
Q08380	LG3BP Galectin-3-binding protein LGALS3BP	-1.981	0.520	0.235	2.451	0.256	-2.451
Q12904	AIMP1 Aminoacyl tRNA synthase complex-interacting multifunctional protein	-0.017	-0.602	0.312	-0.635	0.170	0.635
Q12905	ILF2 Interleukin enhancer-binding factor 2 ILF2	-0.663	-0.476	0.755	0.138	-0.362	-0.138
Q12906	ILF3 Interleukin enhancer-binding factor 3 ILF3	0.740	-0.770	0.244	-1.560	-0.185	1.560
Q12972	PP1R8 Nuclear inhibitor of protein phosphatase 1 PPP1R8	0.120	-0.062	1.205	-0.231	0.097	0.231
Q13148	TADBP TAR DNA-binding protein 43 TARDBP	-0.732	-0.874	0.103	-0.192	0.040	0.192
Q13151	ROA0 Heterogeneous nuclear ribonucleoprotein A0 HNRNPA0	0.179	-1.055	-0.222	-1.284	-0.212	1.284
Q13243	SRSF5 Serine/arginine-rich splicing factor 5 SRSF5	-0.071	-0.555	0.764	-0.533	1.429	0.533
Q13257	MD2L1 Mitotic spindle assembly checkpoint protein MAD2A MAD2L1	0.008	1.576	1.374	1.518	0.867	-1.518
Q13263	TIF1B Transcription intermediary factor 1-beta TRIM28	0.409	0.759	0.909	0.301	0.267	-0.301
Q13283	G3BP1 Ras GTPase-activating protein-binding protein 1 G3BP1	2.230	3.072	1.931	0.793	2.612	-0.793
Q13310	PABP4 Polyadenylate-binding protein 4 PABPC4	1.321	0.714	1.825	-0.656	1.041	0.656
Q13409	DC1I2 Cytoplasmic dynein 1 intermediate chain 2 DYNC1I2	2.130	1.013	1.081	-1.166	1.130	1.166

Q13509	TBB3 Tubulin beta-3 chain TUBB3	0.219	2.447	1.172	2.179	1.744	-2.179
Q13625	ASPP2 Apoptosis-stimulating of p53 protein 2 TP53BP2	2.030	3.224	-1.055	1.145	1.459	-1.145
Q13765	NACA Nascent polypeptide-associated complex subunit alpha NACA	0.222	-0.469	-0.249	-0.741	2.052	0.741
Q13838	DX39B Spliceosome RNA helicase DDX39B DDX39B	0.293	2.899	-0.187	2.557	0.431	-2.557
Q13885	TBB2A Tubulin beta-2A chain TUBB2A	0.301	0.451	1.117	0.100	1.988	-0.100
Q14103	HNRPD Heterogeneous nuclear ribonucleoprotein D0 HNRNPD	0.265	0.388	1.260	0.074	1.552	-0.074
Q14126	DSG2 Desmoglein-2 DSG2	-0.418	0.350	0.326	0.718	0.601	-0.718
Q14152	EIF3A Eukaryotic translation initiation factor 3 subunit A EIF3A	-0.626	0.567	0.447	1.143	1.987	-1.143
Q14157	UBP2L Ubiquitin-associated protein 2-like UBAP2L	-0.205	-0.363	0.412	-0.208	0.308	0.208
Q14160	SCRIB Protein scribble homolog SCRIB	2.368	0.920	-2.214	-1.497	0.100	1.497
Q14254	FLOT2 Flotillin-2 FLOT2	1.120	1.168	-0.741	-0.001	0.245	0.001
Q14257	RCN2 Reticulocalbin-2 RCN2	0.000	-0.401	-0.179	-0.451	1.072	0.451
Q14318	FKBP8 Peptidyl-prolyl cis-trans isomerase FKBP8 FKBP8	0.549	0.581	-0.238	-0.017	1.261	0.017
Q14444	CAPR1 Caprin-1 CAPRIN1	-1.917	-1.836	0.266	0.031	0.942	-0.031
Q14684	RRP1B Ribosomal RNA processing protein 1 homolog B RRP1B	-1.751	-2.629	2.009	-0.928	-0.102	0.928
Q14974	IMB1 Importin subunit beta-1 KPNB1	-2.347	-1.401	-4.404	0.896	-2.373	-0.896
Q14978	NOLC1 Nucleolar and coiled-body phosphoprotein 1 NOLC1	-0.976	-2.691	-2.656	-1.765	-0.845	1.765
Q15029	U5S1 116 kDa U5 small nuclear ribonucleoprotein component EFTUD2	4.705	-0.283	0.682	-5.038	-0.357	5.038
Q15084	PDIA6 Protein disulfide-isomerase A6 PDIA6	0.553	-0.597	0.971	-1.199	-0.234	1.199
Q15233	NONO Non-POU domain-containing octamer-binding protein NONO	0.302	-0.401	1.752	-0.752	2.646	0.752
Q15365	PCBP1 Poly(rC)-binding protein 1 PCBP1	3.675	3.760	0.894	0.036	0.133	-0.036
Q15366	PCBP2 Poly(rC)-binding protein 2 PCBP2	0.200	0.076	1.448	-0.173	0.773	0.173
Q15393	SF3B3 Splicing factor 3B subunit 3 SF3B3	3.524	3.896	1.333	0.323	0.717	-0.323
Q15435	PP1R7 Protein phosphatase 1 regulatory subunit 7 PPP1R7	-0.002	-0.938	0.657	-0.986	0.778	0.986
Q15717	ELAV1 ELAV-like protein 1 ELAVL1	1.673	1.588	0.471	-0.135	4.863	0.135
Q15834	CC85B Coiled-coil domain-containing protein 85B CCDC85B	-0.337	1.930	1.364	2.217	0.769	-2.217
Q15907	RB11B Ras-related protein Rab-11B RAB11B	2.419	0.163	0.902	-2.306	1.046	2.306

Q16531	DDB1 DNA damage-binding protein 1 DDB1	0.184	-0.853	0.516	-1.086	0.239	1.086
Q16543	CDC37 Hsp90 co-chaperone Cdc37 CDC37	2.021	0.232	2.732	-1.838	3.419	1.838
Q16576	RBBP7 Histone-binding protein RBBP7 RBBP7	1.951	0.952	1.282	-1.049	0.980	1.049
Q16629	SRSF7 Serine/arginine-rich splicing factor 7 SRSF7	0.495	-0.675	2.160	-1.220	0.748	1.220
Q16891	IMMT Mitochondrial inner membrane protein IMMT	1.646	0.656	-0.120	-1.039	-0.741	1.039
Q3ZCQ8	TIM50 Mitochondrial import inner membrane translocase subunit TIM50 TIMM50	0.736	0.584	-0.664	-0.201	-0.376	0.201
Q53GT1	KLH22 Kelch-like protein 22 KLHL22	-0.794	0.962	1.143	1.707	1.772	-1.707
Q58FF6	H90B4 Putative heat shock protein HSP 90-beta 4 HSP90AB4P	-3.194	-1.584	0.704	1.560	0.954	-1.560
Q5JWF2	GNAS1 Guanine nucleotide-binding protein G(s) subunit alpha isoforms XLas	-0.193	0.279	1.187	0.423	-0.792	-0.423
Q5SRD1	TI23B Putative mitochondrial import inner membrane translocase subunit Tim	1.336	1.533	-0.329	0.147	0.072	-0.147
Q5T9A4	ATD3B ATPase family AAA domain-containing protein 3B ATAD3B	-0.095	0.919	1.863	0.965	2.454	-0.965
Q69YQ0	CYTSA Cytospin-A SPECC1L	-4.316	-0.837	0.003	3.430	0.472	-3.430
Q6P2Q9	PRP8 Pre-mRNA-processing-splicing factor 8 PRPF8	1.420	1.752	0.438	0.282	0.684	-0.282
Q6PKG0	LARP1 La-related protein 1 LARP1	1.492	1.823	1.369	0.281	4.245	-0.281
Q6S8J3	POTEE POTE ankyrin domain family member E POTEE	-0.555	3.387	0.982	3.892	-0.629	-3.892
Q6UXN9	WDR82 WD repeat-containing protein 82 WDR82	0.614	-0.368	-1.841	-1.032	-1.611	1.032
Q7KZF4	SND1 Staphylococcal nuclease domain-containing protein 1 SND1	-1.827	-2.126	-2.419	-0.349	0.664	0.349
Q7L2E3	DHX30 Putative ATP-dependent RNA helicase DHX30 DHX30	0.773	0.087	-0.913	-0.736	0.371	0.736
Q7Z417	NUFP2 Nuclear fragile X mental retardation-interacting protein 2 NUFIP2	0.352	0.984	-0.808	0.583	-0.264	-0.583
Q86VP6	CAND1 Cullin-associated NEDD8-dissociated protein 1 CAND1	-0.213	-1.271	-2.367	-1.108	-0.903	1.108
Q8IWU2	LMTK2 Serine/threonine-protein kinase LMTK2 LMTK2	1.347	0.066	-2.246	-1.331	-1.349	1.331
Q8N7X1	RMXL3 RNA-binding motif protein, X-linked-like-3 RBMXL3	0.742	-0.228	-1.886	-1.019	-0.913	1.019
Q8NC51	PAIRB Plasminogen activator inhibitor 1 RNA-binding protein SERBP1	-0.913	-2.180	-3.523	-1.317	-3.879	1.317
Q8NHQ8	RASF8 Ras association domain-containing protein 8 RASSF8	-1.176	-0.098	2.028	1.029	1.728	-1.029
Q8TEX9	IPO4 Importin-4 IPO4	0.525	-1.293	0.784	-1.867	0.540	1.867
Q8WUF5	IASPP RelA-associated inhibitor PPP1R13L	0.594	1.433	0.008	0.790	-0.249	-0.790
Q8WVX9	FACR1 Fatty acyl-CoA reductase 1 FAR1	0.645	0.430	-0.318	-0.264	-2.737	0.264

Q8WWM7	ATX2L Ataxin-2-like protein ATXN2L	1.457	0.561	-2.610	-0.946	-2.596	0.946
Q8WXF1	PSPC1 Paraspeckle component 1 PSPC1	0.834	1.854	0.111	0.970	-0.258	-0.970
Q92616	GCN1L Translational activator GCN1 GCN1L1	-0.658	-0.931	-0.226	-0.323	0.106	0.323
Q92734	TFG Protein TFG TFG	-0.570	-1.106	1.827	-0.586	2.143	0.586
Q92841	DDX17 Probable ATP-dependent RNA helicase DDX17 DDX17	2.381	2.156	-2.280	-0.274	-1.596	0.274
Q92878	RAD50 DNA repair protein RAD50 RAD50	0.348	-0.874	-2.370	-1.271	-1.886	1.271
Q92896	GSLG1 Golgi apparatus protein 1 GLG1	1.455	2.786	0.898	1.281	-0.755	-1.281
Q92900	RENT1 Regulator of nonsense transcripts 1 UPF1	2.158	1.637	0.072	-0.571	0.571	0.571
Q92945	FUBP2 Far upstream element-binding protein 2 KHSRP	-1.965	-1.115	-0.495	0.800	0.692	-0.800
Q96HS1	PGAM5 Serine/threonine-protein phosphatase PGAM5, mitochondrial PGAM5	1.685	0.391	2.968	-1.343	0.164	1.343
Q96KQ4	ASPP1 Apoptosis-stimulating of p53 protein 1 PPP1R13B	-0.597	-0.159	-0.257	0.389	2.051	-0.389
Q96MX6	WDR92 WD repeat-containing protein 92 WDR92	1.997	0.781	-1.356	-1.265	-0.045	1.265
Q96P70	IPO9 Importin-9 IPO9	1.437	2.323	0.133	0.836	0.111	-0.836
Q96PK6	RBM14 RNA-binding protein 14 RBM14	0.021	-0.952	-0.496	-1.023	-0.248	1.023
Q96QC0	PP1RA Serine/threonine-protein phosphatase 1 regulatory subunit 10 PPP1R10	-3.341	-3.191	-1.354	0.101	-1.079	-0.101
Q96RT1	LAP2 Protein LAP2 ERBB2IP	3.286	0.075	-3.616	-3.260	-5.314	3.260
Q96SB3	NEB2 Neurabin-2 PPP1R9B	1.595	-0.818	0.614	-2.462	-0.705	2.462
Q96SW2	CRBN Protein cereblon CRBN	-0.222	1.127	-1.801	1.299	0.405	-1.299
Q99623	PHB2 Prohibitin-2 PHB2	0.527	-0.712	0.732	-1.288	0.891	1.288
Q99832	TCPH T-complex protein 1 subunit eta CCT7	0.117	3.594	-1.262	3.428	-2.541	-3.428
Q99873	ANM1 Protein arginine N-methyltransferase 1 PRMT1	-0.306	-0.375	-0.571	-0.118	-1.058	0.118
Q9BQE3	TBA1C Tubulin alpha-1C chain TUBA1C	0.597	0.592	-0.596	-0.055	-0.575	0.055
Q9BQG0	MBB1A Myb-binding protein 1A MYBBP1A	2.976	3.831	0.311	0.806	-2.312	-0.806
Q9BTT6	LRRC1 Leucine-rich repeat-containing protein 1 LRRC1	0.811	2.020	-0.300	1.160	-0.434	-1.160
Q9BUF5	TBB6 Tubulin beta-6 chain TUBB6	0.250	1.009	-0.219	0.710	-2.430	-0.710
Q9BUJ2	HNRL1 Heterogeneous nuclear ribonucleoprotein U-like protein 1 HNRNPUL1	-3.096	-2.545	0.360	0.501	-0.410	-0.501
Q9BZF9	UACA Uveal autoantigen with coiled-coil domains and ankyrin repeats UACA	-0.490	1.763	-0.408	2.204	-0.436	-2.204

Q9BZL4	PP12C Protein phosphatase 1 regulatory subunit 12C PPP1R12C	-2.418	0.798	-0.249	3.166	-0.992	-3.166
Q9GZN8	CT027 UPF0687 protein C20orf27 C20orf27	4.227	1.269	-0.513	-3.007	-2.068	3.007
Q9H1R3	MYLK2 Myosin light chain kinase 2, skeletal/cardiac muscle MYLK2	3.999	0.149	-1.409	-3.900	-1.867	3.900
Q9H2D6	TARA TRIO and F-actin-binding protein TRIOBP	1.262	2.558	0.676	1.246	-1.079	-1.246
Q9H361	PABP3 Polyadenylate-binding protein 3 PABPC3	0.894	-0.938	-1.688	-1.882	-2.741	1.882
Q9H6T3	RPAP3 RNA polymerase II-associated protein 3 RPAP3	2.656	0.862	-1.652	-1.844	-4.053	1.844
Q9H788	SH24A SH2 domain-containing protein 4A SH2D4A	-0.783	-0.523	-0.116	0.210	-3.577	-0.210
Q9H792	PEAK1 Pseudopodium-enriched atypical kinase 1 PEAK1	2.355	1.703	-1.414	-0.701	-1.764	0.701
Q9HCE1	MOV10 Putative helicase MOV-10 MOV10	-3.112	-2.786	-0.260	0.276	-3.186	-0.276
Q9NQ39	RS10L Putative 40S ribosomal protein S10-like RPS10P5	-0.894	-0.116	1.125	0.728	0.636	-0.728
Q9NR30	DDX21 Nucleolar RNA helicase 2 DDX21	-0.948	-1.042	0.570	-0.144	1.122	0.144
Q9NTJ3	SMC4 Structural maintenance of chromosomes protein 4 SMC4	-0.110	0.275	-1.336	0.335	-1.516	-0.335
Q9NUG6	PDRG1 p53 and DNA damage-regulated protein 1 PDRG1	2.383	0.271	1.112	-2.162	0.667	2.162
Q9NVI7	ATD3A ATPase family AAA domain-containing protein 3A ATAD3A	1.495	2.338	-0.408	0.793	-0.742	-0.793
Q9NWS0	PIHD1 PIH1 domain-containing protein 1 PIH1D1	2.338	-0.790	-0.735	-3.178	-0.567	3.178
Q9NX63	CHCH3 Coiled-coil-helix-coiled-coil-helix domain-containing protein 3	0.077	0.539	0.920	0.413	-0.017	-0.413
Q9NYF8	BCLF1 Bcl-2-associated transcription factor 1 BCLAF1	-0.609	0.205	2.783	0.765	3.404	-0.765
Q9NZI8	IF2B1 Insulin-like growth factor 2 mRNA-binding protein 1 IGF2BP1	0.356	-0.612	-1.391	-1.018	0.603	1.018
Q9P035	HACD3 3-hydroxyacyl-CoA dehydratase 3 PTPLAD1	0.539	0.058	0.250	-0.530	-2.100	0.530
Q9P0K7	RAI14 Ankycorbin RAI14	-1.550	2.634	-0.443	4.135	-0.514	-4.135
Q9P2J5	SYLC Leucine--tRNA ligase, cytoplasmic LARS	3.616	5.330	-1.002	1.664	0.423	-1.664
Q9P2K8	E2AK4 Eukaryotic translation initiation factor 2-alpha kinase 4 EIF2AK4	3.388	3.094	0.031	-0.344	-1.525	0.344
Q9UHV9	PFD2 Prefoldin subunit 2 PFDN2	1.398	-0.396	-4.705	-1.844	0.300	1.844
Q9UJS0	CMC2 Calcium-binding mitochondrial carrier protein Aralar2 SLC25A13	1.475	0.641	0.491	-0.884	-1.746	0.884
Q9UMS4	PRP19 Pre-mRNA-processing factor 19 PRPF19	-1.017	-0.252	0.290	0.715	0.274	-0.715
Q9UPQ9	TNR6B Trinucleotide repeat-containing gene 6B protein TNRC6B	-0.919	0.034	0.206	0.903	0.380	-0.903
Q9UQ80	PA2G4 Proliferation-associated protein 2G4 PA2G4	-0.076	-1.187	-0.697	-1.160	0.017	1.160

Q9UQE7	SMC3 Structural maintenance of chromosomes protein 3 SMC3	2.611	2.613	-2.704	-0.047	-0.980	0.047
Q9Y230	RUVB2 RuvB-like 2 RUVBL2	0.914	-0.354	-1.657	-1.317	0.789	1.317
Q9Y262	EIF3L Eukaryotic translation initiation factor 3 subunit L EIF3L	0.734	1.054	-0.972	0.271	-1.421	-0.271
Q9Y265	RUVB1 RuvB-like 1 RUVBL1	2.419	-0.647	-0.614	-3.116	0.385	3.116
Q9Y277	VDAC3 Voltage-dependent anion-selective channel protein 3 VDAC3	1.657	-0.772	-1.997	-2.479	-0.764	2.479
Q9Y2W1	TR150 Thyroid hormone receptor-associated protein 3 THRAP3	-0.249	2.117	-0.699	2.316	0.839	-2.316
Q9Y3F4	STRAP Serine-threonine kinase receptor-associated protein STRAP	-0.133	-0.095	0.846	-0.011	-0.380	0.011
Q9Y3I0	RTCB tRNA-splicing ligase RtcB homolog C22orf28	1.841	1.628	0.636	-0.263	0.208	0.263
Q9Y3U8	RL36 60S ribosomal protein L36 RPL36	-1.081	-1.114	-0.551	-0.083	-0.025	0.083
Q9Y6M1	IF2B2 Insulin-like growth factor 2 mRNA-binding protein 2 IGF2BP2	0.071	2.714	0.662	2.593	1.064	-2.593

Appendix IVb

Proteins listed in **Appendix III** were used to determine the ratio of the PP1 isoform preferences of each protein from the raw intensity values. The raw intensity values of were divided as follows: PP1 alpha/beta; alpha/gamma; beta/alpha; beta/gamma; gamma/alpha; gamma/beta. Values were converted to log 2 and plotted on the graphs shown below.

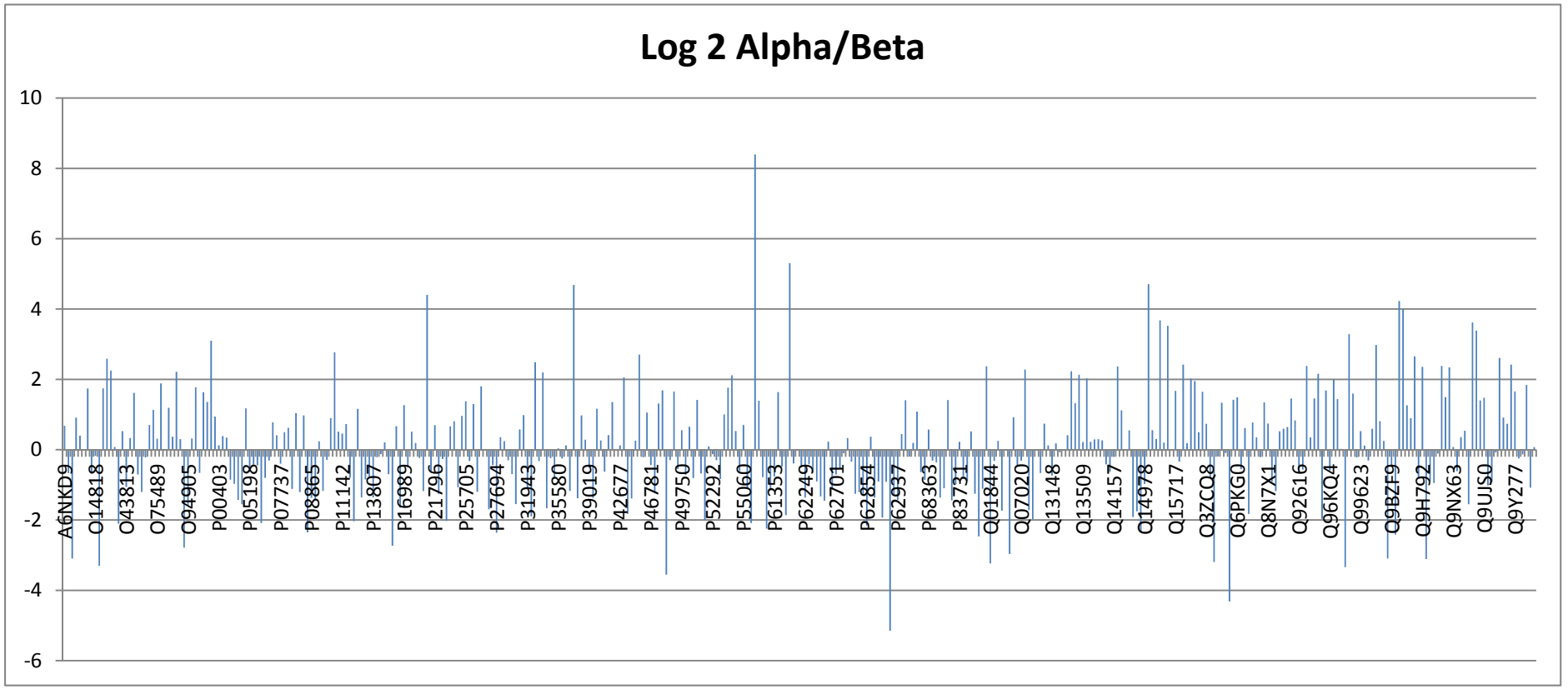

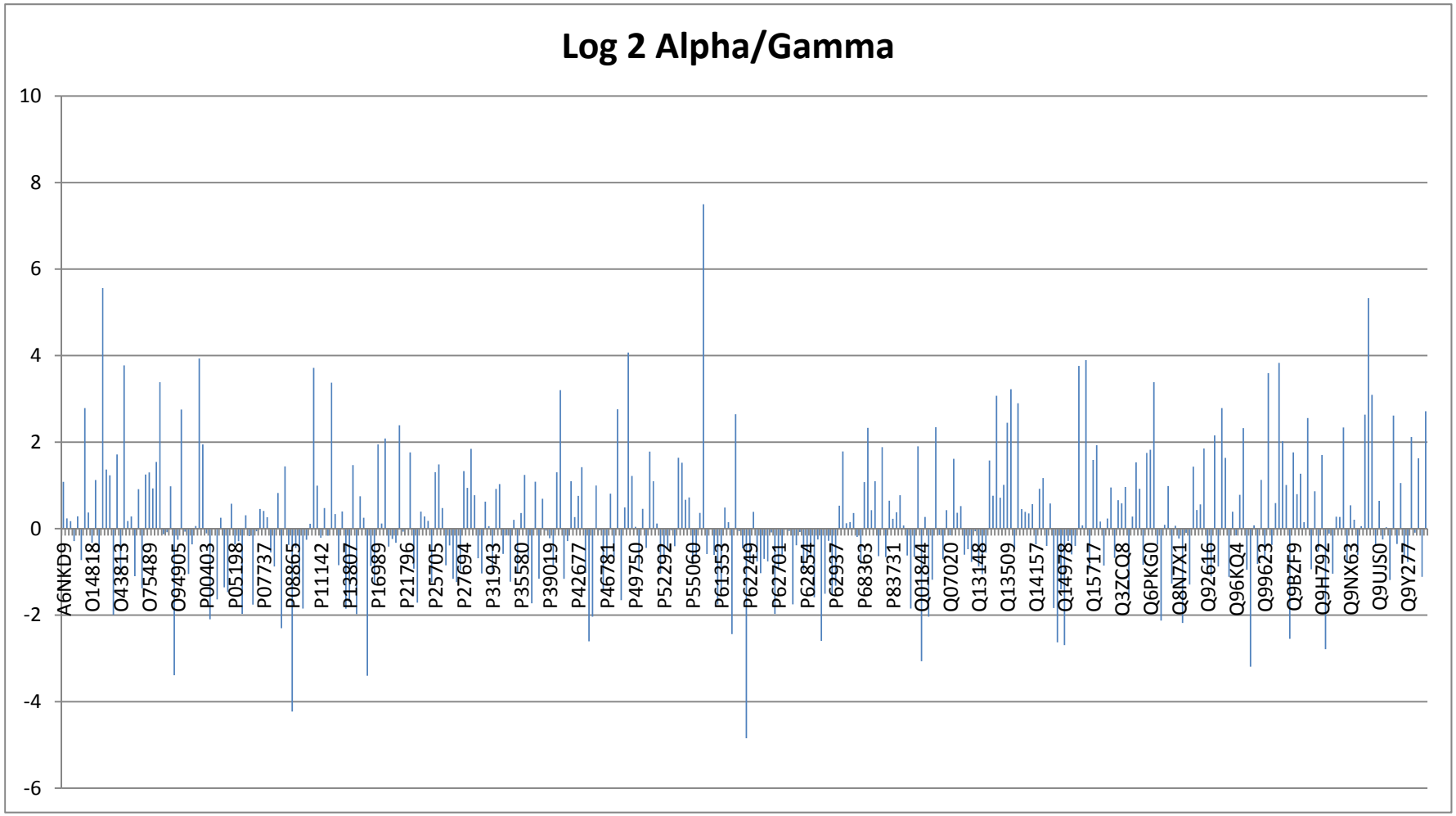
Log 2 Alpha/Gamma
10
8
6
4
2
0
-2
-4
-6
A6NKD9
O14818
O43813
O75489
O94905
P00403
P05198
P07737
P08865
P11142
P13807
P16989
P21796
P25705
P27694
P31943
P35580
P39019
P42677
P46781
P49750
P52292
P55060
P61353
P62249
P62701
P62854
P62937
P68363
P83731
Q01844
Q07020
Q13148
Q13509
Q14157
Q14978
Q15717
Q3ZCQ8
Q6PKG0
Q8N7X1
Q92616
Q96KQ4
Q99623
Q9BZF9
Q9H792
Q9NX63
Q9UJS0
Q9Y277

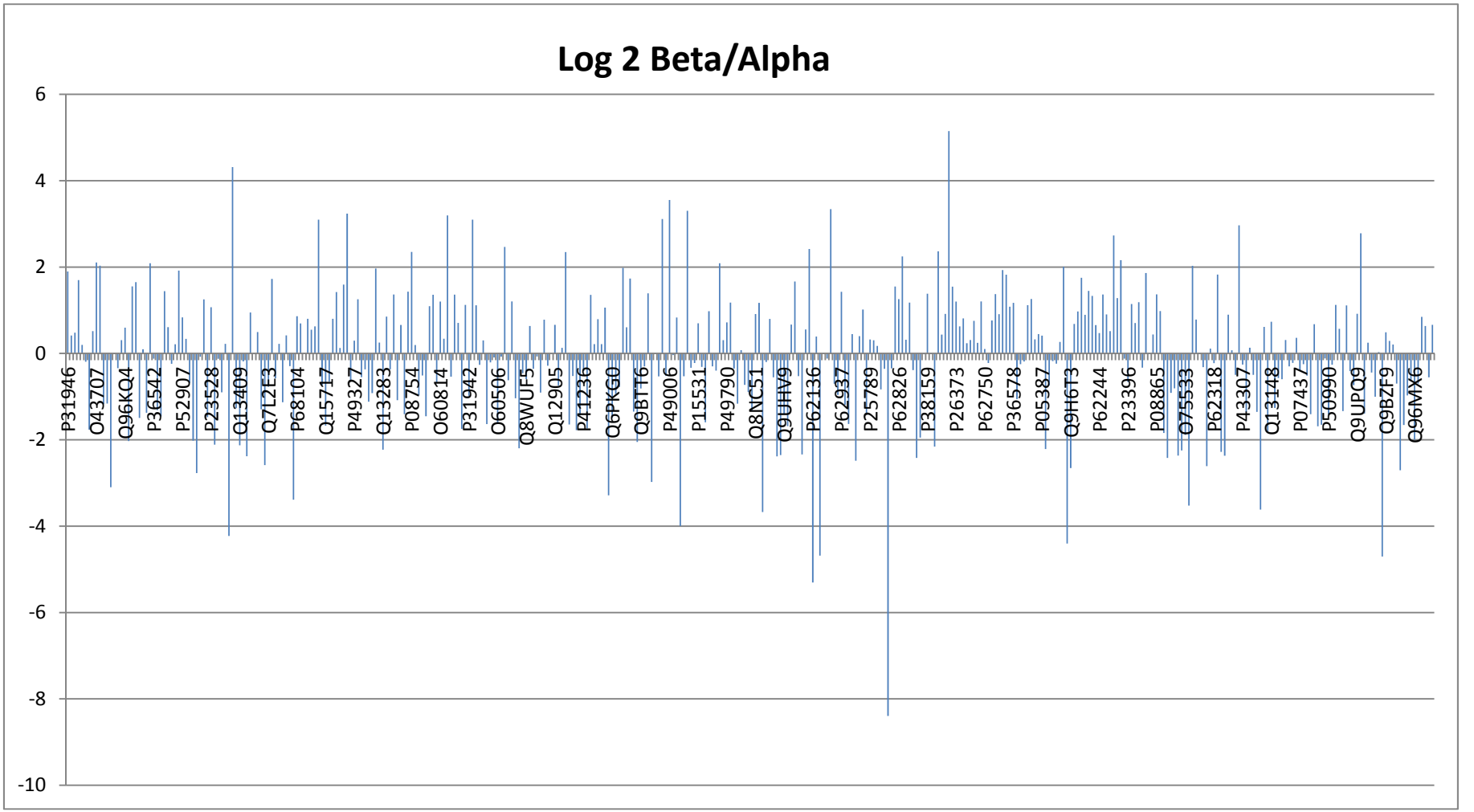
Log 2 Beta/Alpha
6
4
2
0
-2
-4
-6
-8
-10
P31946
O43707
Q96KQ4
P36542
P52907
P23528
Q13409
Q7L2E3
P68104
Q15717
P49327
Q13283
P08754
O60814
P31942
O60506
Q8WUF5
Q12905
P41236
Q6PKG0
Q9BTT6
P49006
P15531
P49790
Q8NC51
Q9UHV9
P62136
P62937
P25789
P62826
P38159
P26373
P62750
P36578
P05387
Q9H6T3
P62244
P23396
P08865
O75533
P62318
P43307
Q13148
P07437
P50990
Q9UPQ9
Q9BZF9
Q96MX6

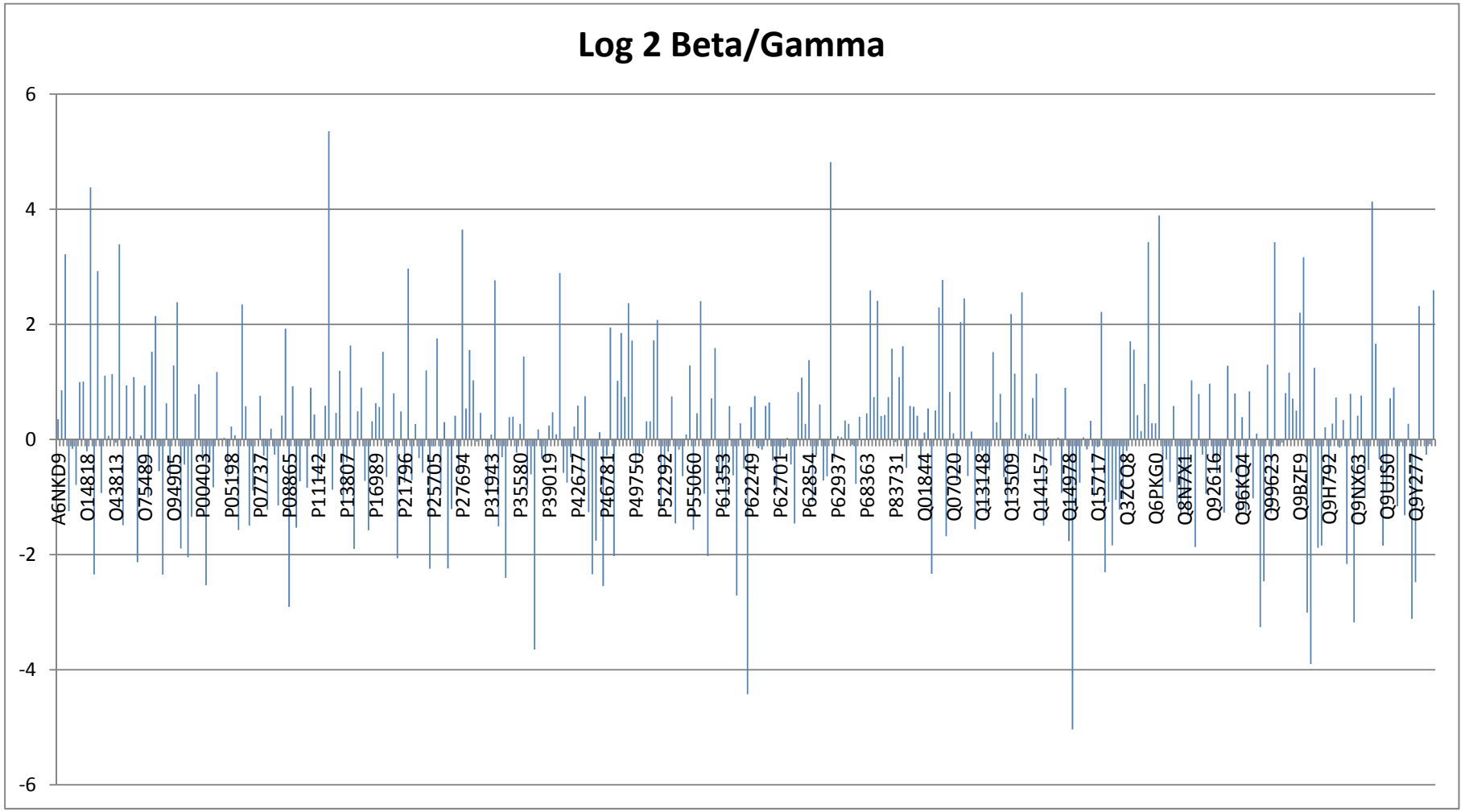
Log 2 Beta/Gamma
6
4
2
0
-2
-4
-6
A6NKD9
O14818
O43813
O75489
O94905
P00403
P05198
P07737
P08865
P11142
P13807
P16989
P21796
P25705
P27694
P31943
P35580
P39019
P42677
P46781
P49750
P52292
P55060
P61353
P62249
P62701
P62854
P62937
P68363
P83731
Q01844
Q07020
Q13148
Q13509
Q14157
Q14978
Q15717
Q3ZCQ8
Q6PKG0
Q8N7X1
Q92616
Q96KQ4
Q99623
Q9BZF9
Q9H792
Q9NX63
Q9UJ50
Q9Y277

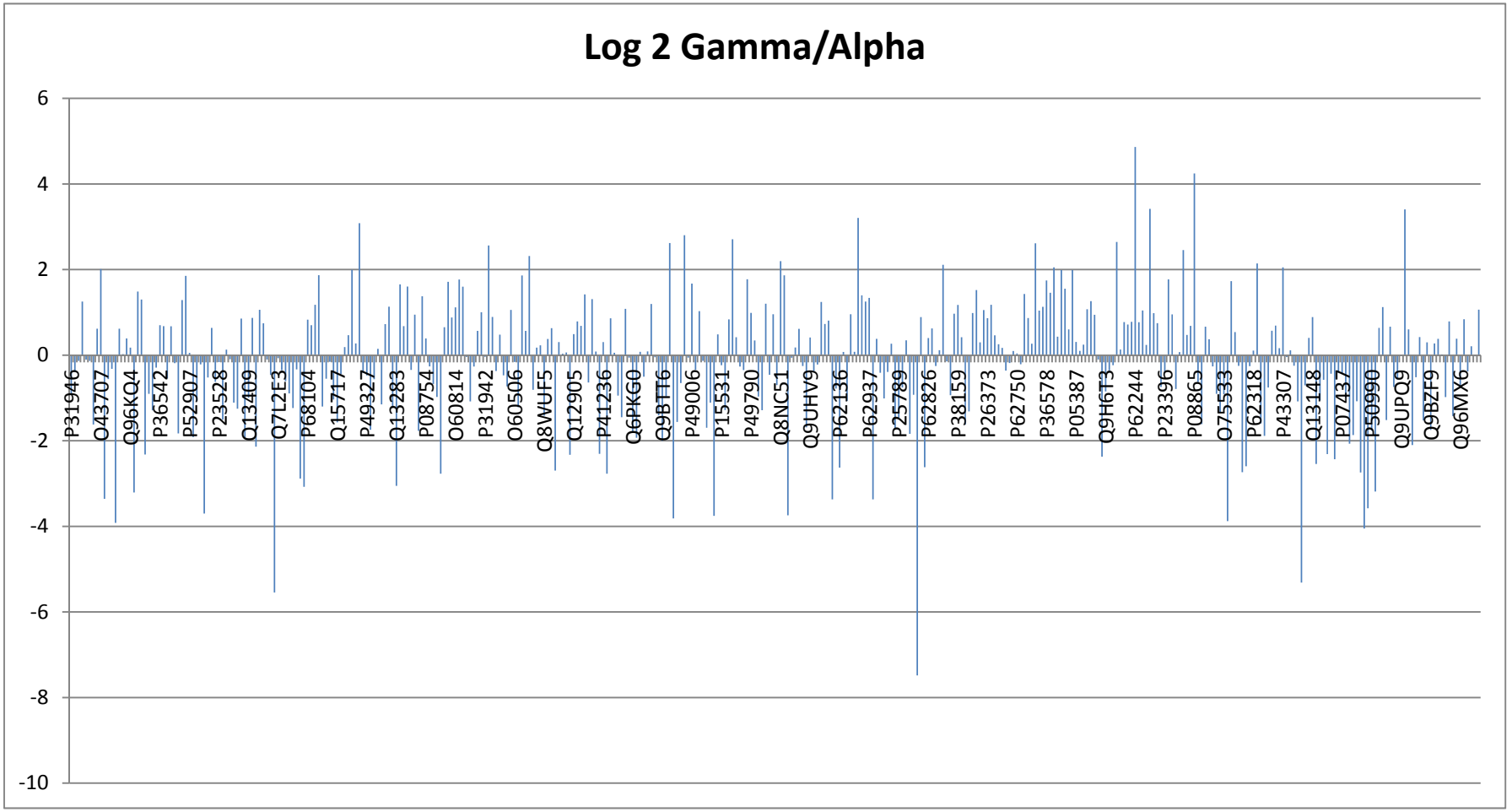
Log 2 Gamma/Alpha
6
4
2
0
-2
-4
-6
-8
-10
P31946
O43707
Q96KQ4
P36542
P52907
P23528
Q13409
Q7L2E3
P68104
Q15717
P49327
Q13283
P08754
O60814
P31942
O60506
Q8WUF5
Q12905
P41236
Q6PKG0
Q9BTT6
P49006
P15531
P49790
Q8NC51
Q9UHV9
P62136
P62937
P25789
P62826
P38159
P26373
P62750
P36578
P05387
Q9H6T3
P62244
P23396
P08865
O75533
P62318
P43307
Q13148
P07437
P50990
Q9UPQ9
Q9BZF9
Q96MX6

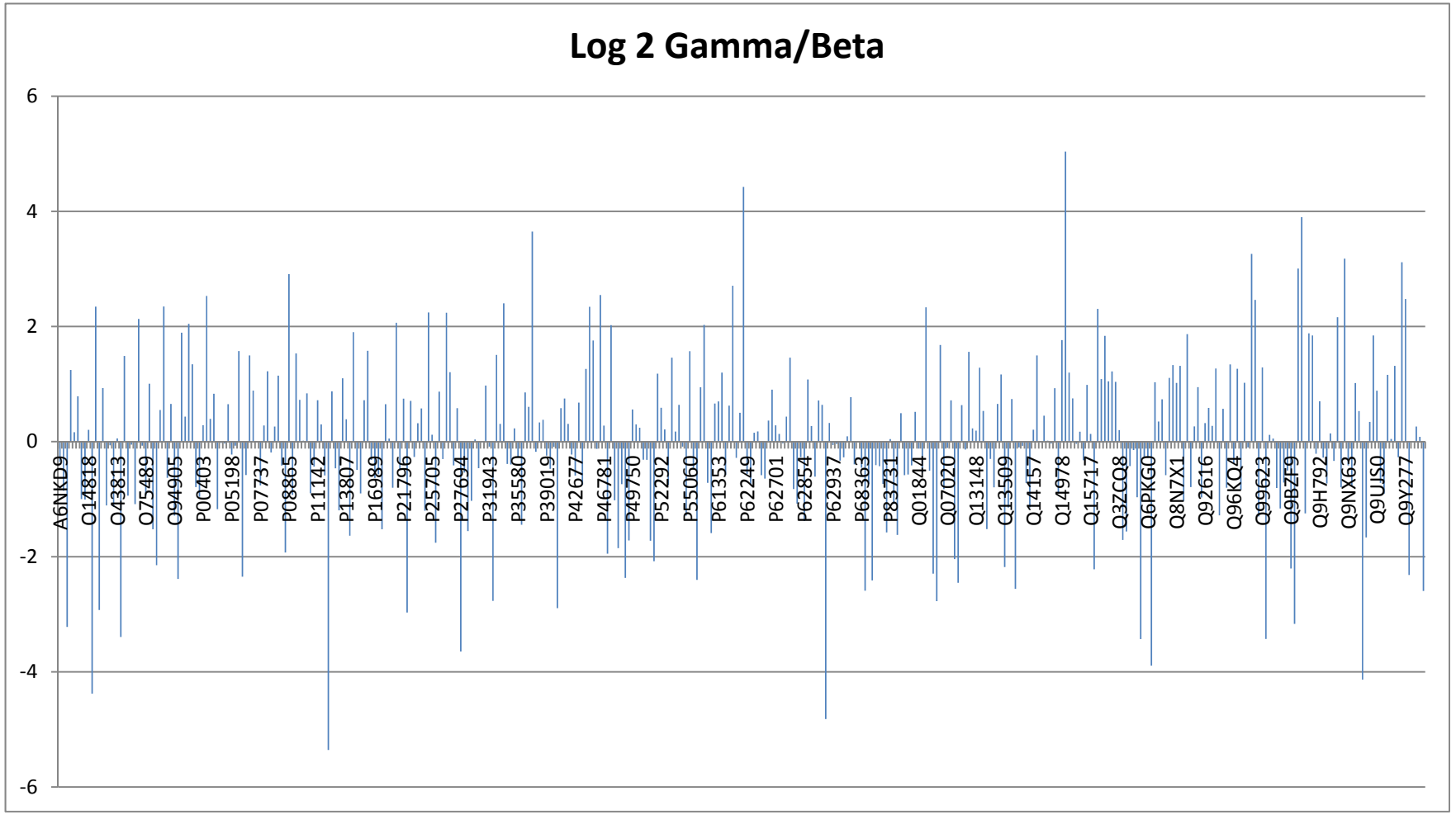
Log 2 Gamma/Beta
6
4
2
0
-2
-4
-6
A6NKD9
O14818
O43813
O75489
O94905
P00403
P05198
P07737
P08865
P11142
P13807
P16989
P21796
P25705
P27694
P31943
P35580
P39019
P42677
P46781
P49750
P52292
P55060
P61353
P62249
P62701
P62854
P62937
P68363
P83731
Q01844
Q07020
Q13148
Q13509
Q14157
Q14978
Q15717
Q3ZCQ8
Q6PKG0
Q8NZX1
Q92616
Q96KQ4
Q99623
Q9BZF9
Q9H792
Q9NX63
Q9UJS0
Q9Y277

Appendix V

Proteins that were captured on 14-3-3-Sepharose in lysates of HEK293 cells stimulated with forskolin or not, and in the presence or absence of H-89. Peptides were extracted from the SDS gel (**Figure 4.1**) and identified from the UniProt database (320 proteins were identified) (Uniprot; description). Peptides were quantitatively measured using the MS Quant software following the dimethyl labelling. The ratios of the peptide enrichment following the different treatment conditions are listed in the table below (SS-serum starved, Fsk-forskolin, H-89+ Fsk-H-89 and forskolin). (**N.B.:** The last lane refers to the ratio of H-89+FsK/SS: Fsk/SS).

Uniprot	Protein Descriptions	Fsk/SS	H-89 + Fsk/SS	H-89 + Fsk/Fsk
P31946	1433B_HUMAN 14-3-3 protein beta/alpha YWHAB	0.54	-0.54	-0.95
P62258	1433E_HUMAN 14-3-3 protein epsilon YWHAE	0.40	1.46	1.20
Q04917	1433F_HUMAN 14-3-3 protein eta YWHAH	-1.56	1.83	3.52
P27348	1433T_HUMAN 14-3-3 protein theta YWHAQ	0.20	-0.64	-0.70
P63104	1433Z_HUMAN 14-3-3 protein zeta/delta YWHAZ	0.36	-1.45	-1.68
P30153	2AAA_HUMAN Serine/threonine-protein phosphatase 2A 65 kDa regulatory subunit A alpha isoform PPP2R1A	0.50	0.36	-0.01
Q7L8J4	3BP5L_HUMAN SH3 domain-binding protein 5-like SH3BP5L	-0.22	0.00	0.35
Q8IZP0	ABI1_HUMAN Abl interactor 1 ABI1	-1.84	2.72	4.69
Q9NYB9	ABI2_HUMAN Abl interactor 2 ABI2	0.09	0.83	0.87
P00519	ABL1_HUMAN Tyrosine-protein kinase ABL1 ABL1	0.37	4.11	3.88
O14639	ABLM1_HUMAN Actin-binding LIM protein 1 ABLIM1	-0.76	2.35	3.24
P05141	ADT2_HUMAN ADP/ATP translocase 2 SLC25A5	0.77	0.07	-0.57
P55196	AFAD_HUMAN Afadin MLLT4	-1.16	-1.93	-0.63
Q09666	AHNK_HUMAN Neuroblast differentiation-associated protein AHNAK AHNAK	-1.33	2.52	3.98
Q12802	AKP13_HUMAN A-kinase anchor protein 13 AKAP13	-0.45	2.24	2.82
Q96B36	AKTS1_HUMAN Proline-rich AKT1 substrate 1 AKT1S1	-0.35	-3.34	-2.86
Q96Q42	ALS2_HUMAN Alsin ALS2	0.12	0.61	0.63
Q92625	ANS1A_HUMAN Ankyrin repeat and SAM domain-containing protein 1A ANKS1A	-0.27	1.27	1.67
Q92974	ARHG2_HUMAN Rho guanine nucleotide exchange factor 2 ARHGEF2	-0.58	-3.79	-3.07
Q14155	ARHG7_HUMAN Rho guanine nucleotide exchange factor 7 ARHGEF7	0.01	-1.13	-1.01
Q5VV41	ARHGG_HUMAN Rho guanine nucleotide exchange factor 16 ARHGEF16	-0.62	-1.02	-0.27
Q7Z3C6	ATG9A_HUMAN Autophagy-related protein 9A ATG9A	4.83	2.62	-2.08
Q9BSB4	ATGA1_HUMAN Autophagy-related protein 101 ATG101	0.03	2.36	2.46

P25705	ATPA_HUMAN ATP synthase subunit alpha, mitochondrial ATP5A1	0.65	1.01	0.49
P06576	ATPB_HUMAN ATP synthase subunit beta, mitochondrial ATP5B	-1.52	-0.73	0.92
P36542	ATPG_HUMAN ATP synthase subunit gamma, mitochondrial ATP5C1	-0.06	0.08	0.28
P48047	ATPO_HUMAN ATP synthase subunit O, mitochondrial ATP5O	1.84	0.70	-1.01
O95816	BAG2_HUMAN BAG family molecular chaperone regulator 2 BAG2	1.20	0.07	-0.99
Q9UQB8	BAIP2_HUMAN Brain-specific angiogenesis inhibitor 1-associated protein 2 BAIAP2	-0.75	0.70	1.58
P35613	BASI_HUMAN Basigin BSG	1.12	0.19	-0.80
P11274	BCR_HUMAN Breakpoint cluster region protein BCR	-0.22	0.22	0.57
Q14457	BECN1_HUMAN Beclin-1 BECN1	0.20	0.10	0.04
Q9UHR4	BI2L1_HUMAN Brain-specific angiogenesis inhibitor 1-associated protein 2-like protein 1 BAIAP2L1	0.91	3.34	2.57
P78537	BL1S1_HUMAN Biogenesis of lysosome-related organelles complex 1 subunit 1 BLOC1S1	4.56	2.83	-1.59
Q6QNY1	BL1S2_HUMAN Biogenesis of lysosome-related organelles complex 1 subunit 2 BLOC1S2	7.59	2.04	-5.41
P62158	CALM_HUMAN Calmodulin CALM1	3.83	0.52	-3.18
P27824	CALX_HUMAN Calnexin CANX	-1.44	-0.22	1.36
Q08AD1	CAMP2_HUMAN Calmodulin-regulated spectrin-associated protein 2 CAMSAP1L1	1.34	-0.41	-1.62
Q9P1Y5	CAMP3_HUMAN Calmodulin-regulated spectrin-associated protein 3 KIAA1543	-2.38	-0.56	1.95
P47756	CAPZB_HUMAN F-actin-capping protein subunit beta CAPZB	-2.20	-1.18	1.16
P52907	CAZA1_HUMAN F-actin-capping protein subunit alpha-1 CAPZA1	-0.24	-1.67	-1.29
Q16204	CCDC6_HUMAN Coiled-coil domain-containing protein 6 CCDC6	1.84	-0.12	-1.83
Q8ND76	CCNY_HUMAN Cyclin-Y CCNY	-1.39	-0.77	0.75
Q8N7R7	CCYL1_HUMAN Cyclin-Y-like protein 1 CCNYL1	0.14	1.81	1.80
Q16543	CDC37_HUMAN Hsp90 co-chaperone Cdc37 CDC37	0.51	0.42	0.05
O94921	CDK14_HUMAN Cell division protein kinase 14 CDK14	2.01	2.65	0.77
Q00536	CDK16_HUMAN Cell division protein kinase 16 CDK16	0.97	1.35	0.51
Q00537	CDK17_HUMAN Cell division protein kinase 17 CDK17	0.52	0.37	-0.01
Q07002	CDK18_HUMAN Cell division protein kinase 18 CDK18	1.50	1.10	-0.26
Q01850	CDR2_HUMAN Cerebellar degeneration-related protein 2 CDR2	-0.51	0.99	1.64
Q86X02	CDR2L_HUMAN Cerebellar degeneration-related protein 2-like CDR2L	-0.10	1.08	1.32
Q5SW79	CE170_HUMAN Centrosomal protein of 170 kDa CEP170	-1.40	-0.28	1.25
P10809	CH60_HUMAN 60 kDa heat shock protein, mitochondrial HSPD1	-0.03	0.13	0.30
O14757	CHK1_HUMAN Serine/threonine-protein kinase Chk1 CHEK1	1.19	2.95	1.89
Q9P2M7	CING_HUMAN Cingulin CGN	-1.72	-1.33	0.52

O75390	CISY_HUMAN Citrate synthase, mitochondrial CS	-2.03	0.16	2.33
Q14008	CKAP5_HUMAN Cytoskeleton-associated protein 5 CKAP5	0.98	-0.27	-1.11
Q7Z460	CLAP1_HUMAN CLIP-associating protein 1 CLASP1	-1.74	-0.14	1.73
O75122	CLAP2_HUMAN CLIP-associating protein 2 CLASP2	-1.16	0.64	1.93
Q00610	CLH1_HUMAN Clathrin heavy chain 1 CLTC	0.27	-0.12	-0.26
Q96DG6	CMBL_HUMAN Carboxymethylenebutenolidase homolog CMBL	-0.13	-1.13	-0.87
A5YKK6	CNOT1_HUMAN CCR4-NOT transcription complex subunit 1 CNOT1	1.13	-1.61	-2.60
Q9H3G5	CPVL_HUMAN Probable serine carboxypeptidase CPVL CPVL	-1.88	-0.78	1.23
Q96GS4	CQ059_HUMAN Uncharacterized protein C17orf59 C17orf59	2.75	0.21	-2.41
P46109	CRKL_HUMAN Crk-like protein CRKL	0.65	-0.16	-0.67
Q6UUV9	CRTC1_HUMAN CREB-regulated transcription coactivator 1 CRTC1	-2.36	-0.44	2.05
Q53ET0	CRTC2_HUMAN CREB-regulated transcription coactivator 2 CRTC2	-3.61	-0.06	3.68
Q9BQD3	CS050_HUMAN UPF0459 protein C19orf50 C19orf50	4.19	0.53	-3.53
O60716	CTND1_HUMAN Catenin delta-1 CTNND1	-2.08	-2.17	0.05
Q6ICG6	CV009_HUMAN Uncharacterized protein C22orf9 C22orf9	0.31	1.89	1.72
Q9Y3I0	CV028_HUMAN UPF0027 protein C22orf28 C22orf28	1.72	2.13	0.54
Q7L576	CYFP1_HUMAN Cytoplasmic FMR1-interacting protein 1 CYFIP1	-0.45	-0.50	0.08
Q96F07	CYFP2_HUMAN Cytoplasmic FMR1-interacting protein 2 CYFIP2	0.27	0.13	-0.01
Q69YQ0	CYTSA_HUMAN Cytospin-A CYTSA	3.70	1.83	-1.74
Q9NR28	DBLOH_HUMAN Diablo homolog, mitochondrial DIABLO	0.36	0.10	-0.13
Q9UJU6	DBNL_HUMAN Drebrin-like protein DBNL	1.73	0.19	-1.41
P61962	DCAF7_HUMAN DDB1- and CUL4-associated factor 7 DCAF7	-2.44	-2.12	0.46
Q9NPI6	DCP1A_HUMAN mRNA-decapping enzyme 1A DCP1A	0.30	-1.82	-1.98
Q8IZD4	DCP1B_HUMAN mRNA-decapping enzyme 1B DCP1B	1.10	-0.26	-1.23
Q92499	DDX1_HUMAN ATP-dependent RNA helicase DDX1 DDX1	-0.02	0.63	0.79
O75064	DEN4B_HUMAN DENN domain-containing protein 4B DENND4B	1.82	4.14	2.45
Q5VZ89	DEN4C_HUMAN DENN domain-containing protein 4C DENND4C	2.55	-0.93	-3.34
O75140	DEPD5_HUMAN DEP domain-containing protein 5 DEPDC5	-0.52	0.69	1.34
P15924	DESP_HUMAN Desmoplakin DSP	1.11	1.28	0.31
P21912	DHSB_HUMAN Succinate dehydrogenase [ubiquinone] iron-sulfur subunit, mitochondrial SDHB	0.07	1.04	1.10
Q9UBS4	DJB11_HUMAN DnaJ homolog subfamily B member 11 DNAJB11	-0.46	-0.74	-0.14
Q09019	DMWD_HUMAN Dystrophia myotonica WD repeat-containing protein DMWD	-1.72	0.74	2.59

Q5JSL3	DOC11_HUMAN Dedicator of cytokinesis protein 11 DOCK11	-0.36	0.32	0.81
Q9H7D0	DOCK5_HUMAN Dedicator of cytokinesis protein 5 DOCK5	-0.38	-2.31	-1.79
Q96HP0	DOCK6_HUMAN Dedicator of cytokinesis protein 6 DOCK6	-0.23	0.79	1.15
Q96N67	DOCK7_HUMAN Dedicator of cytokinesis protein 7 DOCK7	-0.43	-1.12	-0.56
Q9BZ29	DOCK9_HUMAN Dedicator of cytokinesis protein 9 DOCK9	-0.84	0.43	1.40
Q9NRW4	DUS22_HUMAN Dual specificity protein phosphatase 22 DUSP22	-1.47	0.14	1.75
P33316	DUT_HUMAN Deoxyuridine 5'-triphosphate nucleotidohydrolase, mitochondrial DUT	-0.98	-0.85	0.27
Q14204	DYHC1_HUMAN Cytoplasmic dynein 1 heavy chain 1 DYNC1H1	-0.51	0.28	0.92
Q9Y2J2	E41L3_HUMAN Band 4.1-like protein 3 EPB41L3	2.82	0.12	-2.56
Q5VYK3	ECM29_HUMAN Proteasome-associated protein ECM29 homolog ECM29	-2.45	-0.59	2.00
Q96F86	EDC3_HUMAN Enhancer of mRNA-decapping protein 3 EDC3	0.44	-0.59	-0.90
P68104	EF1A1_HUMAN Elongation factor 1-alpha 1 EEF1A1	-0.32	-0.19	0.26
P26641	EF1G_HUMAN Elongation factor 1-gamma EEF1G	-0.97	-0.69	0.42
Q15370	ELOB_HUMAN Transcription elongation factor B polypeptide 2 TCEB2	2.94	-0.80	-3.60
Q32P44	EMAL3_HUMAN Echinoderm microtubule-associated protein-like 3 EML3	0.75	-3.27	-3.88
P06733	ENOA_HUMAN Alpha-enolase ENO1	0.00	0.36	0.50
O95208	EPN2_HUMAN Epsin-2 EPN2	-1.25	-2.38	-0.99
Q9UI08	EVL_HUMAN Ena/VASP-like protein EVL	-4.67	-2.23	2.57
Q96E09	F122A_HUMAN Protein FAM122A FAM122A	1.85	3.76	2.05
Q7Z309	F122B_HUMAN Protein FAM122B FAM122B	-0.02	2.62	2.77
O60825	F262_HUMAN 6-phosphofructo-2-kinase/fructose-2,6-biphosphatase 2 PFKFB2	1.66	0.49	-1.05
Q16877	F264_HUMAN 6-phosphofructo-2-kinase/fructose-2,6-biphosphatase 4 PFKFB4	2.10	0.63	-1.34
Q52LJ0	FA98B_HUMAN Protein FAM98B FAM98B	-5.29	-0.73	4.69
Q9UK99	FBX3_HUMAN F-box only protein 3 FBXO3	-1.51	-1.43	0.22
Q15007	FL2D_HUMAN Pre-mRNA-splicing regulator WTAP WTAP	-0.51	-0.25	0.39
P21333	FLNA_HUMAN Filamin-A FLNA	1.16	-0.64	-1.67
O75044	FNBP2_HUMAN SLIT-ROBO Rho GTPase-activating protein 2 SRGAP2	0.46	1.00	0.68
P85037	FOXK1_HUMAN Forkhead box protein K1 FOXK1	0.17	-2.03	-2.07
O43524	FOXO3_HUMAN Forkhead box protein O3 FOXO3	1.35	-1.85	-3.07
O94915	FRYL_HUMAN Protein furry homolog-like FRYL	0.19	0.57	0.51
Q92538	GBF1_HUMAN Golgi-specific brefeldin A-resistance guanine nucleotide exchange factor 1 GBF1	1.43	0.25	-1.05
Q9Y2X7	GIT1_HUMAN ARF GTPase-activating protein GIT1 GIT1	0.03	-0.64	-0.53

Q3V6T2	GRDN_HUMAN Girdin CCDC88A	-0.42	-1.32	-0.77
P38646	GRP75_HUMAN Stress-70 protein, mitochondrial HSPA9	0.66	0.34	-0.19
P11021	GRP78_HUMAN 78 kDa glucose-regulated protein HSPA5	-0.26	0.01	0.41
P56524	HDAC4_HUMAN Histone deacetylase 4 HDAC4	-2.95	-3.05	0.03
Q9UQL6	HDAC5_HUMAN Histone deacetylase 5 HDAC5	-1.90	-1.91	0.12
Q9ULT8	HECD1_HUMAN E3 ubiquitin-protein ligase HECTD1 HECTD1	-3.56	-1.65	2.05
Q9P2P5	HECW2_HUMAN E3 ubiquitin-protein ligase HECW2 HECW2	1.56	-0.58	-2.01
P07900	HS90A_HUMAN Heat shock protein HSP 90-alpha HSP90AA1	-1.17	-1.42	-0.12
P08238	HS90B_HUMAN Heat shock protein HSP 90-beta HSP90AB1	-1.72	-4.03	-2.17
P08107	HSP71_HUMAN Heat shock 70 kDa protein 1A/1B HSPA1A	-0.75	-0.46	0.43
P11142	HSP7C_HUMAN Heat shock cognate 71 kDa protein HSPA8	-0.54	-0.70	-0.02
O60573	IF4E2_HUMAN Eukaryotic translation initiation factor 4E type 2 EIF4E2	0.69	0.02	-0.53
P08069	IGF1R_HUMAN Insulin-like growth factor 1 receptor IGF1R	-0.36	-0.10	0.39
Q9NRR6	INP5E_HUMAN 72 kDa inositol polyphosphate 5-phosphatase INPP5E	-1.50	-1.22	0.41
Q9Y4H2	IRS2_HUMAN Insulin receptor substrate 2 IRS2	-0.49	1.70	2.32
Q9NZM3	ITSN2_HUMAN Intersectin-2 ITSN2	-7.15	-4.29	3.00
Q9Y4D8	K0614_HUMAN Probable E3 ubiquitin-protein ligase C12orf51 C12orf51	0.36	2.75	2.53
P10644	KAP0_HUMAN cAMP-dependent protein kinase type I-alpha regulatory subunit PRKAR1A	2.20	0.36	-1.71
P13861	KAP2_HUMAN cAMP-dependent protein kinase type II-alpha regulatory subunit PRKAR2A	-1.07	-0.04	1.16
Q9NYR9	KBRS2_HUMAN NF-kappa-B inhibitor-interacting Ras-like protein 2 NKIRAS2	-2.38	-3.89	-1.38
P12277	KCRB_HUMAN Creatine kinase B-type CKB	1.68	-1.07	-2.62
Q9NQT8	KI13B_HUMAN Kinesin-like protein KIF13B KIF13B	-0.88	-3.56	-2.54
O43896	KIF1C_HUMAN Kinesin-like protein KIF1C KIF1C	-0.36	0.60	1.09
O60282	KIF5C_HUMAN Kinesin heavy chain isoform 5C KIF5C	-1.39	-3.14	-1.61
P33176	KINH_HUMAN Kinesin-1 heavy chain KIF5B	-0.33	-3.75	-3.29
Q8N5S9	KKCC1_HUMAN Calcium/calmodulin-dependent protein kinase kinase 1 CAMKK1	2.73	0.67	-1.93
Q07866	KLC1_HUMAN Kinesin light chain 1 KLC1	-0.50	-0.41	0.23
Q9H0B6	KLC2_HUMAN Kinesin light chain 2 KLC2	0.00	-0.39	-0.26
Q6P597	KLC3_HUMAN Kinesin light chain 3 KLC3	-0.44	0.02	0.60
Q9NSK0	KLC4_HUMAN Kinesin light chain 4 KLC4	-0.10	-0.84	-0.60
Q969J3	L12R1_HUMAN Loss of heterozygosity 12 chromosomal region 1 protein LOH12CR1	4.66	2.02	-2.51
Q6PKG0	LARP1_HUMAN La-related protein 1 LARP1	-1.90	-1.53	0.50

Q14739	LBR_HUMAN Lamin-B receptor LBR	0.92	2.31	1.53
Q13136	LIPA1_HUMAN Liprin-alpha-1 PPFIA1	-1.41	-0.02	1.52
Q9HAR2	LPHN3_HUMAN Latrophilin-3 LPHN3	0.48	0.18	-0.17
Q5VUJ6	LRCH2_HUMAN Leucine-rich repeat and calponin homology domain-containing protein 2 LRCH2	-1.34	-3.13	-1.66
Q96II8	LRCH3_HUMAN Leucine-rich repeat and calponin homology domain-containing protein 3 LRCH3	-0.89	-1.58	-0.55
Q6PJG9	LRFN4_HUMAN Leucine-rich repeat and fibronectin type-III domain-containing protein 4 LRFN4	0.91	0.77	-0.01
Q9Y2U5	M3K2_HUMAN Mitogen-activated protein kinase kinase kinase 2 MAP3K2	-1.41	-4.53	-2.98
O95382	M3K6_HUMAN Mitogen-activated protein kinase kinase kinase 6 MAP3K6	1.46	-0.01	-1.34
Q96PK2	MACF4_HUMAN Microtubule-actin cross-linking factor 1, isoform 4 MACF1	-1.23	1.29	2.65
O60307	MAST3_HUMAN Microtubule-associated serine/threonine-protein kinase 3 MAST3	1.30	3.32	2.15
Q8N4C8	MINK1_HUMAN Misshapen-like kinase 1 MINK1	0.02	2.65	2.76
Q7L9L4	MOL1A_HUMAN Mps one binder kinase activator-like 1A MOBKL1A	0.04	-3.18	-3.09
Q02750	MP2K1_HUMAN Dual specificity mitogen-activated protein kinase kinase 1 MAP2K1	-0.80	0.50	1.43
P36507	MP2K2_HUMAN Dual specificity mitogen-activated protein kinase kinase 2 MAP2K2	-3.86	-1.02	2.97
P30307	MPIP3_HUMAN M-phase inducer phosphatase 3 CDC25C	0.08	1.87	1.93
Q6WCQ1	MPRIP_HUMAN Myosin phosphatase Rho-interacting protein MPRIP	-0.55	-0.42	0.27
Q13496	MTM1_HUMAN Myotubularin MTM1	-0.56	0.93	1.63
Q9NXD2	MTMRA_HUMAN Myotubularin-related protein 10 MTMR10	-1.29	-2.55	-1.12
Q765P7	MTSSL_HUMAN MTSS1-like protein MTSS1L	2.26	0.19	-1.94
Q7Z401	MYCPP_HUMAN C-myc promoter-binding protein DENND4A	2.17	-1.58	-3.62
P60660	MYL6_HUMAN Myosin light polypeptide 6 MYL6	1.10	1.22	0.25
O14974	MYPT1_HUMAN Protein phosphatase 1 regulatory subunit 12A PPP1R12A	0.73	-1.68	-2.28
O95544	NADK_HUMAN NAD kinase NADK	-2.22	-1.17	1.18
Q6ZNJ1	NBEL2_HUMAN Neurobeachin-like protein 2 NBEAL2	0.05	-0.39	-0.31
Q9Y2A7	NCKP1_HUMAN Nck-associated protein 1 NCKAP1	-0.59	-2.25	-1.52
P15531	NDKA_HUMAN Nucleoside diphosphate kinase A NME1	-0.06	-1.36	-1.16
O75489	NDUS3_HUMAN NADH dehydrogenase [ubiquinone] iron-sulfur protein 3, mitochondrial NDUFS3	-0.70	0.03	0.86
Q96PU5	NED4L_HUMAN E3 ubiquitin-protein ligase NEDD4-like NEDD4L	3.13	-0.90	-3.90
P21359	NF1_HUMAN Neurofibromin NF1	2.66	-0.13	-2.65
P07197	NFM_HUMAN Neurofilament medium polypeptide NEFM	-0.56	-0.17	0.52
Q9UJF2	NGAP_HUMAN Ras GTPase-activating protein nGAP RASAL2	0.03	-1.09	-0.99
Q8WTW4	NPRL2_HUMAN Nitrogen permease regulator 2-like protein NPRL2	-0.13	-2.49	-2.23

Q12980	NPRL3_HUMAN Nitrogen permease regulator 3-like protein NPRL3	-0.76	0.99	1.88
P49757	NUMB_HUMAN Protein numb homolog NUMB	-0.33	-1.91	-1.45
Q9Y6R0	NUMBL_HUMAN Numb-like protein NUMBL	-1.05	-1.65	-0.47
P04181	OAT_HUMAN Ornithine aminotransferase, mitochondrial OAT	0.37	-0.57	-0.80
P36957	ODO2_HUMAN Dihydrolipoyllysine-residue succinyltransferase component of 2-oxoglutarate dehydrogenase complex, mitochondrial DLST	0.05	0.08	0.17
O15294	OGT1_HUMAN UDP-N-acetylglucosamine--peptide N-acetylglucosaminyltransferase 110 kDa subunit OGT	0.01	-4.72	-4.60
Q9H4L5	OSBL3_HUMAN Oxysterol-binding protein-related protein 3 OSBPL3	-0.93	-4.10	-3.03
Q9BZF3	OSBL6_HUMAN Oxysterol-binding protein-related protein 6 OSBPL6	-1.61	-3.22	-1.47
P39656	OST48_HUMAN Dolichyl-diphosphooligosaccharide--protein glycosyltransferase 48 kDa subunit DDOST	-3.00	-0.58	2.55
Q8IYS1	P20D2_HUMAN Peptidase M20 domain-containing protein 2 PM20D2	-2.89	-1.00	2.03
O00443	P3C2A_HUMAN Phosphatidylinositol-4-phosphate 3-kinase C2 domain-containing subunit alpha PIK3C2A	0.02	0.84	0.95
Q86VP3	PACS2_HUMAN Phosphofurin acidic cluster sorting protein 2 PACS2	1.30	0.77	-0.40
O96013	PAK4_HUMAN Serine/threonine-protein kinase PAK 4 PAK4	-1.90	-1.26	0.77
Q9BZ23	PANK2_HUMAN Pantothenate kinase 2, mitochondrial PANK2	1.02	0.79	-0.10
Q8TEW0	PARD3_HUMAN Partitioning defective 3 homolog PARD3	-0.82	-0.28	0.67
Q99497	PARK7_HUMAN Protein DJ-1 PARK7	-0.02	-0.22	-0.06
P30101	PDIA3_HUMAN Protein disulfide-isomerase A3 PDIA3	1.58	0.19	-1.26
Q9Y2S7	PDIP2_HUMAN Polymerase delta-interacting protein 2 POLDIP2	-0.07	0.36	0.56
Q5EBL8	PDZ11_HUMAN PDZ domain-containing protein 11 PDZD11	-1.23	-2.27	-0.90
Q6Y7W6	PERQ2_HUMAN PERQ amino acid-rich with GYF domain-containing protein 2 GIGYF2	1.77	2.22	0.59
Q96HS1	PGAM5_HUMAN Serine/threonine-protein phosphatase PGAM5, mitochondrial PGAM5	-0.17	1.37	1.67
O00264	PGRC1_HUMAN Membrane-associated progesterone receptor component 1 PGRMC1	0.49	0.16	-0.20
P35232	PHB_HUMAN Prohibitin PHB	-0.05	0.23	0.42
Q99623	PHB2_HUMAN Prohibitin-2 PHB2	-0.37	1.37	1.87
Q99570	PI3R4_HUMAN Phosphoinositide 3-kinase regulatory subunit 4 PIK3R4	0.63	-0.15	-0.64
Q9UBF8	PI4KB_HUMAN Phosphatidylinositol 4-kinase beta PI4KB	-0.63	-2.84	-2.07
P22061	PIMT_HUMAN Protein-L-isoaspartate(D-aspartate) O-methyltransferase PCMT1	-0.04	-0.81	-0.64
Q8NEB9	PK3C3_HUMAN Phosphatidylinositol 3-kinase catalytic subunit type 3 PIK3C3	0.29	-4.29	-4.44
Q15149	PLEC_HUMAN Plectin PLEC	2.44	1.31	-0.99
O00444	PLK4_HUMAN Serine/threonine-protein kinase PLK4 PLK4	-2.03	0.34	2.50
Q9BZL4	PP12C_HUMAN Protein phosphatase 1 regulatory subunit 12C PPP1R12C	-0.86	-3.80	-2.80

P62140	PP1B_HUMAN Serine/threonine-protein phosphatase PP1-beta catalytic subunit PPP1CB	-0.13	-1.06	-0.80
P24666	PPAC_HUMAN Low molecular weight phosphotyrosine protein phosphatase ACP1	1.20	-0.37	-1.44
P62937	PPIA_HUMAN Peptidyl-prolyl cis-trans isomerase A PPIA	1.60	-0.01	-1.48
Q9ULR3	PPM1H_HUMAN Protein phosphatase 1H PPM1H	2.09	1.16	-0.80
O95685	PPR3D_HUMAN Protein phosphatase 1 regulatory subunit 3D PPP1R3D	-0.90	-0.04	1.00
Q06830	PRDX1_HUMAN Peroxiredoxin-1 PRDX1	0.36	0.31	0.08
P32119	PRDX2_HUMAN Peroxiredoxin-2 PRDX2	0.69	0.50	-0.06
P78527	PRKDC_HUMAN DNA-dependent protein kinase catalytic subunit PRKDC	-0.09	0.90	1.12
P28066	PSA5_HUMAN Proteasome subunit alpha type-5 PSMA5	-0.04	-0.94	-0.77
P60900	PSA6_HUMAN Proteasome subunit alpha type-6 PSMA6	-1.27	-2.96	-1.55
Q8TAA3	PSA7L_HUMAN Proteasome subunit alpha type-7-like PSMA8	-3.17	-1.34	1.96
P28072	PSB6_HUMAN Proteasome subunit beta type-6 PSMB6	1.08	0.03	-0.92
O00231	PSD11_HUMAN 26S proteasome non-ATPase regulatory subunit 11 PSMD11	-1.78	-0.68	1.23
Q9UNM6	PSD13_HUMAN 26S proteasome non-ATPase regulatory subunit 13 PSMD13	0.25	-0.28	-0.40
O00487	PSDE_HUMAN 26S proteasome non-ATPase regulatory subunit 14 PSMD14	0.72	0.59	0.01
Q15008	PSMD6_HUMAN 26S proteasome non-ATPase regulatory subunit 6 PSMD6	-2.89	-1.74	1.29
Q12923	PTN13_HUMAN Tyrosine-protein phosphatase non-receptor type 13 PTPN13	-0.11	0.03	0.28
P27708	PYR1_HUMAN CAD protein CAD	0.76	-1.51	-2.14
Q96QF0	RAB3I_HUMAN Rab-3A-interacting protein RAB3IP	0.77	1.38	0.74
P20340	RAB6A_HUMAN Ras-related protein Rab-6A RAB6A	0.87	0.59	-0.14
P51149	RAB7A_HUMAN Ras-related protein Rab-7a RAB7A	0.28	-0.11	-0.26
Q15276	RABE1_HUMAN Rab GTPase-binding effector protein 1 RABEP1	0.28	-2.82	-2.97
Q9UJ41	RABX5_HUMAN Rab5 GDP/GTP exchange factor RABGEF1	-0.54	0.29	0.96
P04049	RAF1_HUMAN RAF proto-oncogene serine/threonine-protein kinase RAF1	0.66	-0.03	-0.56
Q9P0K7	RAI14_HUMAN Ankycorbin RAI14	-1.21	-3.26	-1.91
P62826	RAN_HUMAN GTP-binding nuclear protein Ran RAN	-0.74	-1.75	-0.87
P43487	RANG_HUMAN Ran-specific GTPase-activating protein RANBP1	-0.20	-0.81	-0.47
Q15907	RB11B_HUMAN Ras-related protein Rab-11B RAB11B	-0.33	-0.20	0.26
Q8IUD2	RB6I2_HUMAN ELKS/Rab6-interacting/CAST family member 1 ERC1	-1.59	-1.40	0.32
Q92600	RCD1_HUMAN Cell differentiation protein RCD1 homolog RQCD1	-0.01	-3.67	-3.52
Q6NUK4	REEP3_HUMAN Receptor expression-enhancing protein 3 REEP3	0.28	2.45	2.30
Q9H6H4	REEP4_HUMAN Receptor expression-enhancing protein 4 REEP4	0.38	0.66	0.41

Q6WKZ4	RFIP1_HUMAN Rab11 family-interacting protein 1 RAB11FIP1	-1.82	-0.42	1.54
Q9BXF6	RFIP5_HUMAN Rab11 family-interacting protein 5 RAB11FIP5	0.23	0.69	0.59
O15211	RGL2_HUMAN Ral guanine nucleotide dissociation stimulator-like 2 RGL2	-0.99	-3.48	-2.36
Q8IWW6	RHG12_HUMAN Rho GTPase-activating protein 12 ARHGAP12	-1.42	-4.18	-2.62
Q9Y4G8	RPGF2_HUMAN Rap guanine nucleotide exchange factor 2 RAPGEF2	-0.04	3.31	3.48
Q8N122	RPTOR_HUMAN Regulatory-associated protein of mTOR RPTOR	-1.63	0.16	1.93
P62269	RS18_HUMAN 40S ribosomal protein S18 RPS18	2.55	0.00	-2.41
Q9Y6M7	S4A7_HUMAN Sodium bicarbonate cotransporter 3 SLC4A7	0.07	2.73	2.79
O94885	SASH1_HUMAN SAM and SH3 domain-containing protein 1 SASH1	0.36	2.12	1.90
Q9P0V9	SEP10_HUMAN Septin-10 SEPT10	4.47	2.60	-1.74
Q9NVA2	SEP11_HUMAN Septin-11 SEPT11	4.15	2.35	-1.66
Q15019	SEPT2_HUMAN Septin-2 SEPT2	5.28	4.15	-1.00
Q16181	SEPT7_HUMAN Septin-7 SEPT7	5.05	2.81	-2.10
O43175	SERA_HUMAN D-3-phosphoglycerate dehydrogenase PHGDH	2.33	2.19	-0.01
Q5HYK7	SH319_HUMAN SH3 domain-containing protein 19 SH3D19	-0.07	1.90	2.10
Q9H0K1	SIK2_HUMAN Serine/threonine-protein kinase SIK2 SIK2	0.37	-2.44	-2.67
Q9GZT3	SLIRP_HUMAN SRA stem-loop-interacting RNA-binding protein, mitochondrial SLIRP	0.93	0.78	-0.02
Q9NQG6	SMC7L_HUMAN Smith-Magenis syndrome chromosomal region candidate gene 7 protein-like SMCR7L	-1.44	-0.48	1.09
O95295	SNAPN_HUMAN SNARE-associated protein Snapin SNAPIN	3.46	1.35	-1.97
Q13813	SPTA2_HUMAN Spectrin alpha chain, brain SPTAN1	-0.13	0.54	0.81
Q01082	SPTB2_HUMAN Spectrin beta chain, brain 1 SPTBN1	-0.14	1.11	1.38
O15020	SPTN2_HUMAN Spectrin beta chain, brain 2 SPTBN2	-0.09	1.28	1.50
Q7Z6B7	SRGP1_HUMAN SLIT-ROBO Rho GTPase-activating protein 1 SRGAP1	-1.33	-0.39	1.07
Q9UQ35	SRRM2_HUMAN Serine/arginine repetitive matrix protein 2 SRRM2	0.20	3.73	3.67
Q76I76	SSH2_HUMAN Protein phosphatase Slingshot homolog 2 SSH2	-3.59	-0.07	3.65
P51571	SSRD_HUMAN Translocon-associated protein subunit delta SSR4	1.35	0.04	-1.17
Q9UMX1	SUFU_HUMAN Suppressor of fused homolog SUFU	3.37	1.89	-1.35
O15056	SYNJ2_HUMAN Synaptojanin-2 SYNJ2	1.69	1.51	-0.05
Q5T011	SZT2_HUMAN Protein SZT2 SZT2	0.45	2.65	2.34
Q15750	TAB1_HUMAN TGF-beta-activated kinase 1 and MAP3K7-binding protein 1 TAB1	0.95	3.19	2.38
Q9NYJ8	TAB2_HUMAN TGF-beta-activated kinase 1 and MAP3K7-binding protein 2 TAB2	0.13	4.15	4.15
Q4KMP7	TB10B_HUMAN TBC1 domain family member 10B TBC1D10B	1.31	-2.02	-3.19

Q9NU19	TB22B_HUMAN TBC1 domain family member 22B TBC1D22B	2.55	4.51	2.09
P68371	TBB2C_HUMAN Tubulin beta-2C chain TUBB2C	0.16	0.89	0.86
P07437	TBB5_HUMAN Tubulin beta chain TUBB	0.42	0.79	0.50
Q3MII6	TBC25_HUMAN TBC1 domain family member 25 TBC1D25	-0.67	-0.96	-0.15
Q86TI0	TBCD1_HUMAN TBC1 domain family member 1 TBC1D1	0.78	0.76	0.11
O60343	TBCD4_HUMAN TBC1 domain family member 4 TBC1D4	0.65	-1.11	-1.62
Q92609	TBCD5_HUMAN TBC1 domain family member 5 TBC1D5	1.99	-2.14	-3.99
Q9P0N9	TBCD7_HUMAN TBC1 domain family member 7 TBC1D7	-0.13	-0.67	-0.41
P49368	TCPG_HUMAN T-complex protein 1 subunit gamma CCT3	0.68	0.78	0.24
P10599	THIO_HUMAN Thioredoxin TXN	1.50	-2.50	-3.87
Q13009	TIAM1_HUMAN T-lymphoma invasion and metastasis-inducing protein 1 TIAM1	-1.21	-2.57	-1.22
Q8N9M5	TM102_HUMAN Transmembrane protein 102 TMEM102	0.92	1.32	0.53
Q13049	TRI32_HUMAN E3 ubiquitin-protein ligase TRIM32 TRIM32	3.50	1.34	-2.02
Q92574	TSC1_HUMAN Hamartin TSC1	0.28	1.10	0.96
P49815	TSC2_HUMAN Tuberin TSC2	-0.16	-0.98	-0.69
Q96AY4	TTC28_HUMAN Tetratricopeptide repeat protein 28 TTC28	2.21	2.55	0.47
O95881	TXD12_HUMAN Thioredoxin domain-containing protein 12 TXNDC12	1.69	-0.08	-1.64
Q8NBS9	TXND5_HUMAN Thioredoxin domain-containing protein 5 TXNDC5	-1.91	-2.05	-0.01
Q96FH0	U402_HUMAN UPF0402 protein	4.72	3.25	-1.33
P0CG48	UBC_HUMAN Polyubiquitin-C UBC	0.43	-0.04	-0.33
P62068	UBP46_HUMAN Ubiquitin carboxyl-terminal hydrolase 46 USP46	-0.46	0.35	0.94
P40818	UBP8_HUMAN Ubiquitin carboxyl-terminal hydrolase 8 USP8	-0.46	1.46	2.05
A0JNW5	UH1BL_HUMAN UHRF1-binding protein 1-like UHRF1BP1L	2.96	-1.50	-4.33
Q9P0L0	VAPA_HUMAN Vesicle-associated membrane protein-associated protein A VAPA	0.50	-0.61	-0.98
P50552	VASP_HUMAN Vasodilator-stimulated phosphoprotein VASP	-2.26	-0.95	1.44
P21796	VDAC1_HUMAN Voltage-dependent anion-selective channel protein 1 VDAC1	-0.25	0.22	0.60
P45880	VDAC2_HUMAN Voltage-dependent anion-selective channel protein 2 VDAC2	0.37	0.14	-0.09
P08670	VIME_HUMAN Vimentin VIM	-0.30	0.43	0.86
Q9H9C1	VIPAR_HUMAN VPS33B-interacting protein VIPAR	0.86	3.79	3.06
Q69YN4	VIR_HUMAN Protein virilizer homolog KIAA1429	-0.44	-3.96	-3.38
Q9H267	VP33B_HUMAN Vacuolar protein sorting-associated protein 33B VPS33B	0.05	3.10	3.18
Q92558	WASF1_HUMAN Wiskott-Aldrich syndrome protein family member 1 WASF1	-0.78	0.93	1.84

Q9Y6W5	WASF2_HUMAN Wiskott-Aldrich syndrome protein family member 2 WASF2	-1.10	0.59	1.83
Q9Y2I8	WDR37_HUMAN WD repeat-containing protein 37 WDR37	1.87	1.47	-0.26
Q8TAF3	WDR48_HUMAN WD repeat-containing protein 48 WDR48	-1.39	-0.66	0.86
O43379	WDR62_HUMAN WD repeat-containing protein 62 WDR62	-0.55	0.63	1.31
P30291	WEE1_HUMAN Wee1-like protein kinase WEE1	0.04	-0.99	-0.89
Q9H4A3	WNK1_HUMAN Serine/threonine-protein kinase WNK1 WNK1	2.41	1.70	-0.58
Q9ULE0	WWC3_HUMAN Protein WWC3 WWC3	0.13	-0.22	-0.22
P46937	YAP1_HUMAN Yorkie homolog YAP1	-0.25	0.16	0.54
Q8NHG8	ZNRF2_HUMAN E3 ubiquitin-protein ligase ZNRF2 ZNRF2	1.52	-0.35	-1.73
Q9C0D3	ZY11B_HUMAN Protein zyg-11 homolog B ZYG11B	-0.06	-0.42	-0.22

Appendix VI

Proteins were captured on 14-3-3-Sepharose in lysates of HEK293 cells stimulated with forskolin or not, and in the presence or absence of H-89. Peptides were extracted from the SDS gel (**Figure 4.1**) and phosphopeptides from the forskolin treated samples were enriched using titanium dioxide beads in C-8-Empore disks. The phosphopeptides identified from the forskolin treated samples are listed below. The phosphorylated residues identified in this screen are underlined in each peptide. In cases where the 14-3-3 binding sites were also identified in either the literature (SK) or in the MacKintosh group (S(CM)), a Y is listed next to that residue in the relevant column; in cases where sites are known but were not identified in this screen, those sites are listed in parentheses where relevant (e.g. Y(642)). For predicted sites, a P next to the relevant residues denotes a potential candidate residue based either on sequence comparison with amphioxus (SP) or based on the mode I and II consensus sequences (PC). SP ID: SwissProt ID; Prot id: SwissProt protein Id; pS/T: phosphorylated serine/threonine residue; pS/T Pos: phosphorylated serine/threonine position in the protein; Score: peptide score; p-value: peptide p-value; SK: site known-published 14-3-3-binding sites with their references; S(CM): sites identified by the MacKintosh group (unpublished); SP: sites predicted by comparing with the amphioxus sequence; PC: potential 14-3-3-binding candidate based on mode I and mode II consensus motifs.

SP Id	Prot id	Digestion product	pS/T	pS/T pos	Score	p-value	Mass	SK	S(CM)	SP	PC	References
Q7L8J4	3BP5L	GL<u>S</u>DHV<u>S</u>LDGQELGTR	S	358	51.0	0.00056	588.6				P	
			S	362	66.3	1.80E-05	882.4			P		
		ETPQGELRPEVVEDEVPR<u>S</u>PVAEEPGGGGSSSSEAK	S	30	53.4	0.00085	1258.2					
Q8IZP0	ABI1	NTPYK<u>T</u>LEPVKPPTVPNDYM<u>T</u>SPAR	T	200	43.2	0.0077	998.1					
			T	215	38.0	0.025	998.1					
O14639	ABLM1	RS<u>S</u>GREEDDEELLR	S	587	46.1	0.0017	590.9					
		GV<u>S</u>MPNMLEPK	S	706	44.8	0.0012	657.8				P	
		TA<u>S</u>LPGYGR	S	655	28.8	0.036	501.2			P	P	
P55196	AFAD	ADHR<u>S</u>SPNVANQPP<u>S</u>PGGK	S	1172	55.9	0.00019	692.6					
			S	1182	55.9	0.00019	692.6					
		S<u>S</u>PNVANQPPSPGGK	S	1173	47.5	0.001	758.8					
		SQDAD<u>S</u>PGSSGAPENLTFK	S	1779	85.8	1.70E-07	994.4					
		<u>S</u>QEELREDK	S	1275	36.0	0.0081	607.3					
Q96B36	AKTS1	AATAARPPAPPPAPQPP<u>S</u>P<u>T</u>P<u>S</u>PPRP<u>T</u>LAR	S	88	94.6	3.70E-08	1042.2					

			T	90	61.5	7.80E-05	1042.2					
			S	92	86.2	2.60E-07	1042.2					
			T	97	94.6	3.70E-08	1042.2					Kovacina et al., 2003; Nascimento et al., 2010
		SLPVSVPVWGFK	S	183	52.6	0.0003	698.4	Y				
		RTEARSSDEENGPPSSPDLDR	T	198	35.5	0.023	825.7					
			S	202	57.3	0.00015	825.7					
		SSDEENGPPSSPDLDR	S	203	70.2	2.30E-06	931.3					
			S	211	78.1	6.60E-07	891.3					
			S	212	84.1	1.70E-07	891.3					
		LNTSDFQK	T	246	51.1	0.00021	516.7	Y				
Q96Q42	ALS2	SSSLVDIREEETEGGSR	S	466	38.4	0.011	965.9			P		
		RLSLPGLLSQVSPR	S	492	52.0	0.00041	841.9					
			S	483	52.0	0.00041	841.9			P	P	
Q92625	ANS1A	SLSKSDSDLLTCSPTEDATMGSR	S	626	43.7	0.0047	852.0					
			S	628	66.5	2.40E-05	852.0					
		SPSFASEWDEIEK	S	661	58.1	6.70E-05	802.8					
			S	663	63.6	1.90E-05	802.8					
			S	666	37.8	0.0047	842.8					
		SESLSNCSIGK	S	647	39.7	0.0032	631.3				P	
Q92974	ARHG2	ILSQSTDSLNMR	S	174	53.2	0.00026	722.8					
		LSPPHSPR	S	956	27.4	0.042	525.7					
			S	960	27.4	0.042	525.7					
		QELGSPEER	S	932	34.6	0.008	562.7					
		SESLESPR	S	645	42.8	0.001	492.7					
		SLPAGDALYLSFNPPQPSR	S	886	53.8	0.00039	1055.5				P	
Q15052	ARHG6	MSGFIYQGK	S	488	51.5	0.00019	555.7					
Q14155	ARHG7	MSGFIYQGK	S	518	51.5	0.00019	555.7					

		KPSDEEFASR	S	694	40.2	0.0031	623.3					
Q7Z3C6	ATG9A	RESDESGESAPDEGGEGAR	S	735	82.6	2.30E-07	1007.9					
			S	738	47.8	0.00019	1087.9					
			S	741	47.8	0.00019	1087.9					
		LEASYSDSPPGEEDLLVHVAEGSK	S	18	43.3	0.006	870.4					
		HPEPVPEEGSEDELPPQVHKV	S	828	34.0	0.047	810.4					
Q9UQB8	BAIP2	SSSTGNLLDKDDLAIPPPDYGAASR	S	452	35	0.043	880.7	Y(360)				Robens et al., 2003
			S	454	60.4	0.00012	1320.6					
			T	455	46.7	0.0029	880.7					
		SSSMAAGLER	S	366	61.5	1.70E-05	552.7					
		SLSPPQSQSK	S	325	32.6	0.019	569.8					
		LSDSYSNTLPVR	T	340	34.7	0.018	716.3	Y		P		
Q9H3Q1	BORG4	NAMSLPQLNEK	S	118	33.6	0.018	670.8			P		
P15056	BRAF	RDSSDDWEIPDGQITVGQR	S	446	55.7	0.00028	1127.5					
Q08AD1	CAMP2	SISNEGLTLNNSHVSK	S	464	51.5	0.00054	890.4			P		
Q16204	CCDC6	LDQPVSAPPSPR	S	240	31.6	0.028	712.3					
			S	244	31.6	0.028	712.3		Y	P		
Q8ND76	CCNY	SASADNLTLPR	S	326	72.5	2.40E-06	612.8			P		
P06493	CDK1	IGEGTYGVVYK	T	14	32.2	0.019	673.3					
O94921	CDK14	RHSSPSSPTSPK	S	120	48.6	0.0007	449.9					
Q00536	CDK16	KISTEDINK	S	110	41.9	0.0029	564.3					
Q00537	CDK17	RASLSEIGFGK	S	180	60.9	3.90E-05	622.8			P		
Q07002	CDK18	RASLSDIGFGK	S	130	46.7	0.001	615.8			P		
P24941	CDK2	IGEGTYGVVYK	T	14	32.2	0.019	673.3					
Q00526	CDK3	IGEGTYGVVYK	T	14	32.2	0.019	673.3					
Q01850	CDR2	SSSETILSSLAGSDIVK	S	311	59.9	7.40E-05	887.4			P		
Q7Z7L8	CK096	STQSLSLQR	T	407	52.7	0.00021	550.3					

			S	406	45.2	0.0012	550.3					
		LRNSLDSSDSDSAL	S	425	46.0	0.0012	780.3					
Q7Z460	CLAP1	RQSSGSATNVASTPDNR	S	646	85.5	0.00000021	914.4					
			S	647	49.2	0.00069	954.4					
			S	649	46.7	0.0016	914.4					
			T	651	36.7	0.016	914.4					
		SRSDIDVNAAAGAK	S	598	33.2	0.025	742.8			P		
			S	600	90.1	5.30E-08	727.8					
O75122	CLAP2	SRSDIDVNAAAGAK	S	368	38.2	0.0082	727.8					
			S	370	90.1	5.30E-08	727.8			P		
Q96GS4	CQ059	RATISSPLELEGTVSR	T	196	39.7	0.0076	599.3					
			S	199	49.6	0.00077	599.3					
		SLDGLSEACGGAGSSGSAESGAGGGR	S	168	88.1	1.20E-07	1167.5			P		
		LQDSRSLDGLSEACGGAGSSGSAESGAGGGR	S	166	86.5	3.00E-07	978.4					
O60716	CTND1	VGGSSVDLHR	S	268	76.8	8.40E-07	553.8					
		GSLASLDSLR	S	346	30	0.034	589.7					
			S	349	31.8	0.022	589.7					
			S	352	31.8	0.022	589.7					
Q69YQ0	CYTSA	KGSSGNASEVSVACLTER	S	384	73.9	3.40E-06	966.4					
			S	385	37.5	0.015	966.4					
			S	389	33.1	0.041	644.6					
		RSSTSSEPTPTVK	S	832	53.6	0.00025	728.8					
Q9UJU6	DBNL	AMSTTSISSPQPGK	T	270	61.8	3.40E-05	744.3					
Q9BUQ8	DDX23	RSSLSPGR	S	109	48.1	0.0003	510.2					
			S	107	48.1	0.0003	510.2					
Q09019	DMWD	AEEAATAAGADGERSGEEEEEEPEAAGTGSAGGAPLSPLPK	S	397	89.3	2.30E-07	1325.9					
		YHSLGNISR	S	545	40.9	0.003	563.8			P		

		SNSLPHPAGGGK	S	495	34.4	0.015	601.3			P		
Q96N67	DOCK7	KGSWSER	S	432	38.4	0.003	465.2			P		
		RNSSIVGR	S	439	69.1	4.70E-06	484.7					
		SMSIDDTPR	S	182	35.1	0.0053	551.2					
		SLSNSNPDISGTPTSPDDEVR	S	896	52.0	0.00046	1174.5					
			S	900	111.7	6.20E-10	1134.5					
			S	910	52.0	0.00046	1174.5					
		SPSGSAFGSQENLR	S	1438	41.9	0.0031	758.8					
Q9Y2J2	E41L3	GISQTNLITTVTPEKK	S	460	36.4	0.02	945.5					
			T	469	36.4	0.02	945.5					
Q96F86	EDC3	SQDVAVSPQQQQCSK	S	131	66.2	1.60E-05	885.4					
		RHNSWSSSSR	S	161	42.5	0.0019	642.3	Y		P		
Q32P44	EMAL3	AISSANLLVR	S	176	77.8	7.60E-07	562.3		Y (127, 147)			
O95208	EPN2	GSSQPNLSTSHSEQEYGK	S	173	59.4	6.30E-05	1048.4					
			S	178	45.3	0.0022	1008.4					
			S	182	59.4	6.30E-05	1048.4					
Q96E09	F122A	SNSAPLIHGLSDTSPVFQAEAPSAR	S	45	40.7	0.011	878.1		Y(37)			
		RNSTTFPSR	S	62	53.2	0.0002	573.3		Y			
		RIDFIPVSPAPSPTR	S	143	88.4	1.10E-07	906.9					
			S	147	88.4	1.10E-07	906.9					
			T	149	78.5	1.10E-06	906.9					
Q7Z309	F122B	RNSTTIMSR	S	50	42.9	0.002	573.3					
			T	51	29.8	0.039	573.3					
		LYSPK	S	105	28.1	0.022	344.2					
		RIDFTPVSPAPSPTRGFGK	T	112	33.5	0.047	730.7					
		RIDFTPVSPAPSPTR	S	115	85.5	2.20E-07	900.9					

			S	119	85.5	2.20E-07	900.9					
			T	121	49.8	0.00081	600.9					
		MFVSSSGLPPSPVPSPR	S	137	69.1	9.50E-06	959.4					
			S	141	69.1	9.50E-06	959.4					
Q14153	FA53B	SSSFSLPSR	S	167	46.5	0.00063	524.2					
Q9H019	FA54B	NASVPNLR	S	103	32.2	0.018	475.7					
P85037	FOXK1	QSPGPALAR	S	101	62.3	2.00E-05	488.7					
		SAPASPTHPGLMSPR	S	416	78.6	6.70E-07	833.3			P		
			S	420	78.6	6.70E-07	833.3					
			T	422	46.2	0.0012	841.3					
			S	428	43.3	0.0014	881.3					
		SGGLQTPECLSREGSPIPHDPEFGSK	T	436	40.3	0.013	981.4					
			S	441	42.8	0.0074	981.4					
			S	445	42.8	0.0074	981.4					
		YSQSAPGSPVSAQPVIMAVPPRPSSLVAK	S	468	47.9	0.0022	1033.2			P	P	
			S	472	47.9	0.0022	1033.2					
Q96NE9	FRMD6	GQSTDSLPQTICR	T	523	45.0	0.0011	811.8				P	
			S	525	45.0	0.0011	811.8			P	P	
		HSLSLDDIR	S	544	39.8	0.0036	568.3			P		
Q9Y2X7	GIT1	SLSSPTDNLELSLR	S	362	55.9	0.00018	806.4					
		SQSDLDDQHDYDSVASDEDTDQEPLR	S	385	42.7	0.0036	1047.7					
			S	388	61.5	4.60E-05	1047.4					
Q14161	GIT2	TINNQHSVESQDNDQPDYDSVASDEDTDLETTASK	S	394	49.7	0.0013	1343.5					
			S	397	49.7	0.0013	1343.5					
Q3V6T2	GRDN	SSSQENLLDEVMK	S	1701	60.0	5.00E-05	788.3					
Q58FF8	H90B2	IEDVGSDEEDDSGKDK	S	177	60.2	3.40E-05	909.3					
		IEDVGSDEEDDSGKDKK	S	183	49.2	0.00079	973.4					

Q9P2P5	HECW2	AN<u>S</u>DTDLVTSESR	S	48	62.5	2.40E-05	737.8			P		
		SH<u>S</u>AGEVGEDSR	S	1042	51.5	0.00018	655.8					
P08238	HS90B	IEDVG<u>S</u>DEEDDSGKDK	S	255	60.2	3.40E-05	909.3					
		IEDVGSDEEDD<u>S</u>GKDKK	S	261	49.2	0.00079	973.4					
P08069	IGF1R	A<u>S</u>FDER	S	1339	27.7	0.015	402.6					
Q9Y4H2	IRS2	TA<u>S</u>EGDGGAAAGAAAAGAR	S	365	79.2	6.00E-07	806.3	Y(573)				Neukamm et al., 2012
		PVSVAG<u>S</u>PL<u>S</u>PGPVR	S	388	43.5	0.0028	790.4					
			S	391	43.5	0.0028	790.4					
		RV<u>S</u>GDAAQDLDR	S	560	59.7	5.00E-05	691.8			P		
		KS<u>S</u>EGGVGVGPGGGDEPPTSPR	S	1186	59.8	0.0001	702.0					
Q6ICG6	K0930	VSTGDT<u>S</u>PCGTEEDSSPASPMHER	S	267	32.7	0.034	877.3					
		VTSF<u>S</u>TPP<u>T</u>PER	S	289	48.7	0.00051	739.8					
			T	293	48.7	0.00051	739.8					
		SR<u>S</u>L<u>S</u>GTGR	S	351	30.1	0.02	540.7				P	
			S	353	30.1	0.02	540.7				P	
Q9NQT8	KI13B	SI<u>S</u>SPNVNR	S	1381	38.4	0.0043	527.2				P	
Q8N5S9	KKCC1	AA<u>S</u>VIPGSTSR	S	52	61.2	3.20E-05	563.3			P	P	
		KL<u>S</u>LQERPAG<u>S</u>YLEAQAGPYA<u>T</u>GPASHISPR	S	74	60.5	0.00011	833.9	Y				
			S	82	39.1	0.015	833.9					
			T	93	43.2	0.008	1138.2					
		RPTIE<u>S</u>HHVAISDAEDCVQLNQYK	S	111	43.2	0.0071	964.1					
		<u>S</u>FGNPFEPQAR	S	458	62.8	2.10E-05	665.3					
		SM<u>S</u>APGNLLVK	S	475	60.7	3.80E-05	606.8			P	P	
		EGFGEGGK<u>S</u>PELPGVQEDEAAS	S	492	56.8	0.00019	1135.5					
Q07866	KLC1	<u>S</u>RE<u>S</u>LNVDVVK	S	521	55.7	0.00015	663.3					Johnson et al., 2011
			S	524	42.5	0.0031	663.3			P		
Q9H0B6	KLC2	KLDEDA<u>S</u>PNEEK	S	151	50.3	0.00042	727.8					

		RSSRDMAGGAGPR	S	508	59.9	4.80E-05	466.5					Johnson et al., 2011
		RSSEMLVK	S	557	45.4	0.00094	515.2					
		ASSLNFLNK	S	582	38.8	0.0051	537.3	Y				
		TLSSSSMDLSR	S	608	45.0	0.00067	672.3					
			S	610	56.7	7.00E-05	632.3					
			S	611	51.4	0.00026	632.3					
			S	615	47.1	0.00041	672.3					
Q6P597	KLC3	QYDPPAESQQSESPPRRDSLASLFPSEEEER	S	167	43.0	0.0094	931.1					Johnson et al., 2011
		RDSLASLFPSEEEER	S	173	78.4	1.10E-06	922.9					
		AMSLNTLNVDAPR	S	466	83.0	2.90E-07	749.3	Y		P		
		TLSASTQDLSPH	T	498	41.4	0.0032	668.8					
Q9NSK0	KLC4	TSQEGPGDSVK	T	518	34.3	0.011	592.7					Johnson et al., 2011
		RTSQEGPGDSVK	S	519	47.2	0.0008	670.8					
		SSELLVR	S	565	46.8	0.00077	442.2					
			S	566	50.6	0.00032	442.2					
		AASLNYLNQPSAAPLQVSR	S	590	56.6	0.00019	1040.5	Y		P		
		GLSASTMDLSSSS	S	611	85.2	8.40E-08	661.8					
			T	612	34.2	0.011	669.8					
Q15139	KPCD1	RLSNVSLTGVSTIR	S	205	33.7	0.031	831.9					
			T	210	33.7	0.031	831.9					
Q6PKG0	LARP1	SLPTTVPESPNYR	S	766	32.0	0.031	810.8			P		
			S	774	32.0	0.031	810.8					
Q14739	LBR	SASASHQADIK	S	99	37.6	0.0064	597.8				P	
Q86X29	LSR	SRSRDDLYDQDDSRDFPR	S	530	38.0	0.015	581.7				P	
Q9Y2U5	M3K2	RLSIIGPTSR	S	153	35.1	0.013	590.3					
		DRSSPPPGYIPDELHQVAR	S	163	39.8	0.011	738.7				P	
		AQSYPDNHQEFSDYDNPIFEK	S	239	44.0	0.0039	875.4			P	P	

		RRGSDIDNPTLTVMDISPPSR	S	331	53.4	0.00055	808.4			P	P	
			S	344	41.2	0.0093	835.0					
O43318	M3K7	SIQDLTVTGTEPGQVSSR	S	439	80.3	8.00E-07	978.0					
Q6P0Q8	MAST2	SRSLSPGR	S	299	35.9	0.0051	510.2			P	P	
			S	301	35.9	0.0051	510.2					
O60307	MAST3	RLSADIR	S	747	31.5	0.021	455.7				P	
O15021	MAST4	SRSLSPGR	S	358	35.9	0.0051	510.2			P	P	
		RGSLGGALTGR	S	166	55.6	0.00012	562.8				P	
Q8N4C8	MINK1	SQSLQDQPTR	S	601	41.9	0.0024	620.3			P	P	
		KGSVVNVNPTNTR	S	993	51.5	0.0004	733.4				P	
Q6WCQ1	MPRIP	AEEQQLPPPLSPPSPSTPNHR	S	289	37.2	0.022	813.7					
			S	292	37.2	0.022	813.7					
Q7Z401	MYCPP	HKSDNETNLQQQVVWGNR	S	1015	42.7	0.0055	745.0			P	P	
		SISTSGPLDKEDTGR	S	1587	68.8	7.80E-06	821.9				P	
			S	1589	65.1	2.00E-05	821.9				P	
O14974	MYPT1	DKKSPLIESTANMDNNQSQK	S	299	42.6	0.0063	782.0	Y(472)		P	P	Koga and Ikebe, 2008; Zagorska et al., 2010
		ISPKEEER	S	422	31.6	0.022	534.2					
		TGSYGALAEITASK	T	443	92.4	3.20E-08	724.8					
			S	445	106.4	1.30E-09	724.8					
		RSTQGVTLTDLQEAEK	S	695	71.9	5.50E-06	928.4					
			T	696	73.2	4.00E-06	928.4				P	
			T	700	53.2	0.0004	619.3					
		STGVSFWTQDSDENEQEQQSDTEEGSNK	S	862	85.0	2.30E-07	1108.1					
			S	871	85.0	2.30E-07	1108.1					
			T	873	58.6	0.00014	1081.4					
		SGSYSYLEER	S	910	52.4	0.00017	635.8				P	
O60237	MYPT2	RSTQGVTLTDLQEAEK	T	650	53.2	0.0004	619.3			P		

Q96PU5	NED4L	SLSSPTVTLSAPLEGAK	S	446	62.9	3.40E-05	869.4					
			S	448	79.4	7.80E-07	869.4	Y		P		
P18615	NELFE	SISADDDLQESSR	S	115	30.3	0.034	751.8			P		
P21359	NF1	SMSLDMGQPSQANTK	S	2521	30.8	0.035	853.8			P		
			S	2523	50.9	0.00035	853.8					
P07197	NFM	PKSPVEEKGKSPV	S	620	35.5	0.017	771.4					
			S	628	35.5	0.017	771.4					
		AKSPVPKSPVEEAK	S	685	37.6	0.012	813.9					
Q9UJF2	NGAP	SISGTSTSEKPNSMDTANTSPFK	S	16	40.9	0.0097	828.4					
		QNSTGQAQIR	S	864	46.6	0.00077	591.8					
Q14978	NOLC1	IKLQTPNTFPK	T	607	36.1	0.014	723.8					
			T	610	36.1	0.014	723.8			P		
Q9H4L5	OSBL3	QDSWEVVEGLR	S	34	40.2	0.0044	699.3					
		TYSAPAINAIQGGSFESPK	T	249	83.9	3.80E-07	1009.5					
			S	251	88.5	1.30E-07	1009.5					
		LHSSNPNLSTLDFGEEK	S	304	82.8	4.80E-07	984.4					
Q9BZF3	OSBL6	TASSSTEPSVSR	S	44	35.2	0.0094	644.8					
Q86VP3	PACS2	ANSLDNER	S	453	38.1	0.0028	499.7	Y(487)				
O96013	PAK4	LAAGRPFNTYPR	T	207	40.3	0.0056	721.9					
		DKRPLSGPDVGTPQPAGLASGAK	S	181	46.7	0.0018	767.1					
Q8TEW0	PARD3	RSSDPALIGLSTSVSDSNFSSEEPSR	S	144	55.0	0.00047	935.8			P		
			S	154	45.1	0.0046	935.8					
		SSLSASHPMVGK	S	223	34.6	0.015	648.8					
		RISHSLYSGIEGLDESPSR	S	715	41.2	0.0078	728.3			P		
			S	720	35.4	0.031	728.3					
Q6Y7W6	PERQ2	WRPHSPDGPR	S	236	29.9	0.042	642.8					
Q9UBF8	PI4KB	SKSDATASISLSSNLK	S	275	98.6	1.10E-08	844.9	Y(294)				

			S	277	89.3	9.10E-08	844.9			P		
		STRSVENLPECGITHEQR	T	426	36.6	0.022	731.7					
		SVENLPECGITHEQR	S	428	79.6	8.10E-07	924.9					
		RLSEQLAHTPTAFK	S	511	52.1	0.00043	560.3					
Q9HB20	PKHA3	SVSHPGSCSSER	S	211	33.7	0.012	685.3			P		
Q9BZL4	PP12C	TGSSGALGPPER	S	427	58.2	5.70E-05	604.8			P		
		SASSSWLEGTSTQAK	S	452	70.6	4.90E-06	810.4					
		RSTQGVTLTDLQEAEK	T	560	73.2	4.00E-06	928.4					
Q12923	PTN13	AISTGSLASSTLNK	S	908	47.6	0.001	755.3					
			T	909	41.8	0.0037	755.3					
			S	911	47.6	0.001	755.3					
Q15276	RABE1	GSVHSLDAGLLLPSGDPFSK	S	374	67.2	1.80E-05	1079.0			P		
			S	377	67.2	1.80E-05	1079.0					
		AQSTDSLGTSGSLQSK	S	407	129.6	6.80E-12	823.9					
		RAQSTDSLGTSGSLQSK	T	408	88.3	9.50E-08	941.9					
			S	410	88.3	9.50E-08	941.9					
			T	413	46.2	0.0018	901.9					
Q9UJ41	RABX5	QTSIETDR	S	310	44.6	0.00075	515.2					
		LDAQSLNLSQEDFDRYMSGQTSPR	S	607	70.7	1.30E-05	952.1					
P04049	RAF1	RASDDGKLTDPSK	S	43	33.8	0.021	490.6					
Q6NUK4	REEP3	SFSMHDLTTIQGDEPVGQRPYQPLPEAK	S	150	47.1	0.0031	1079.8					Tinti et al., 2012
			S	152	49.6	0.0017	1079.8	Y		P		
Q9H6H4	REEP4	SFSMQDLR	S	152	37.0	0.0046	532.2	Y		P		Tinti et al., 2012
Q9BXF6	RFIP5	TYSDEANQMR	S	307	32.6	0.0097	655.7					
		SNSSSEAVLGQEELSAQAK	S	397	36.1	0.022	1008.0					
			S	395	77.8	1.50E-06	1008.0					
Q86X27	RGPS2	SVAAEGALLPQTPPSPR	S	315	50.3	0.00075	925.9					

			S	329	50.3	0.00075	925.9					
Q8IWW6	RHG12	ATTPPNQGRPDSPVYANLQELK	T	230	37.3	0.025	852.7					
			T	231	41.5	0.0093	852.7					
			S	240	41.5	0.0093	852.7					
Q15019	SEPT2	IYHLPDAESDEDEDFKEQTR	S	218	43.4	0.0049	839.7					
Q9BRG2	SH23A	SFSEDTLMDGPAR	S	125	58.7	5.30E-05	761.3			P		
Q9H0K1	SIK2	SSFPVEQR	S	342	32.5	0.015	515.2					
			S	343	35.1	0.0077	515.2					
Q01082	SPTB2	RPPSPEPSTK	S	2102	30.0	0.044	588.3					
Q9UMX1	SUFU	RLSGKDTEQIR	S	301	35.7	0.015	691.8					
Q4KMP7	TB10B	ALAAGADSPKTEEARPSPAPGPGTPTGTPTR	S	132	43.9	0.0063	1040.1			P		
		TEEARPSPAPGPGTPTGTPTR	T	148	45.9	0.0025	746.3					
			T	150	46.3	0.0023	746.3					
			T	152	46.3	0.0023	746.3					
		ALAAGADSPKTEEARPSPAPGPGTPTGTPTR	T	154	43.9	0.0063	1040.1					
		QQPPLGPSSSLLSLPGLK	S	656	33.8	0.034	990.0					
			S	657	57.2	0.00015	990.0					
			S	658	60.0	8.10E-05	990.0					
			S	661	60.0	8.10E-05	990.0					
		AAGGAPSPPPPVR	S	678	53.8	0.0002	627.3					
		RASAGPAPGPVVTAEGLHPSLPSPTGNSTPLGSSK	S	687	41.0	0.0086	1125.6					
			T	697	36.1	0.029	844.4					
		KLSLR	S	780	30.9	0.024	348.7					
Q3MII6	TBC25	QASLDGLQQLR	S	506	38.7	0.0058	654.8			P	P	
O60343	TBCD4	HASAPSHVQPSDSEK	S	341	52.7	0.00032	828.9	Y		P		Geraghty et al., 2007
			S	344	55.1	0.00018	828.9	Y(642)				
		LGSVDSFER	S	588	66.4	6.60E-06	545.2					

			S	591	44.4	0.00063	585.2					
		DYSPGDSPPGTPPASPPSSAWQTFPEEDSDSPQFR	T	613	49.6	0.0019	1271.9					
		TSSTCSNESLSVGGTSVTPR	S	750	39.2	0.0054	1133.9					
			S	751	56.0	0.00017	1093.9					
			T	752	56.0	0.00017	1093.9					
			S	754	67.1	1.30E-05	1093.9					
			S	757	67.1	1.30E-05	1093.9					
Q92609	TBCD5	RTSSTLDSEGTFNSYR	S	43	41.6	0.0059	950.9					
		SESMPVQLNK	S	522	55.6	0.0001	614.8					
		NISSSPSVESLPGGR	S	539	31.8	0.036	823.8					
			S	541	44.0	0.0022	823.8					
			S	544	44.0	0.0022	823.8					
		EFTGSPPSSATK	S	554	28.6	0.048	644.8					
Q13009	TIAM1	ANSLGDLYAQK	S	231	54.2	0.00018	630.3			P		
P49815	TSC2	SQSGTLDGESAAWSASGEDSR	S	1420	85.8	1.60E-07	1089.4	Y (939, 1462)				
			T	1422	75.4	1.80E-06	1089.4					
		SPSGLRPR	S	1452	27.9	0.047	475.2					
P40818	UBP8	SYSSPDITQAIQEEEK	S	718	71.4	5.70E-06	952.9			P		
Q9H4A3	WNK1	DVDDGSGSPHSPHQLSSK	S	2027	50.8	0.0004	1005.4					
			S	2029	50.8	0.0004	1005.4					
			S	2032	32.7	0.025	1005.4					
		RGSKGHMNYEGPGMAR	S	2270	44.6	0.0022	620.6				P	
P46937	YAP1	GDSETDLEALFNAVMNPK	S	61	87.7	1.40E-07	1023.9				P	Zhao et al., 2007; Schlegelmilch et al., 2011
			T	63	102.6	4.60E-09	1023.9					
		SHSRQASTDAGTAGALTPQHVR	S	103	59.0	0.00014	803.4					
			S	105	50.2	0.001	803.4					
			T	110	59.0	0.00014	803.4				P	

		QASTDAGTAGALTPQHVR	S	109	47.8	0.0013	621.0					
			T	114	37.4	0.015	930.9			P		
		AHSSPASLQLGAVSPGTLTPTGVVSGPAATPTAQHLR	S	127	83.8	3.50E-07	1205.6	Y		P		
			S	128	68.9	1.10E-05	904.5					
			S	131	67.2	1.60E-05	904.5					
			S	138	48.7	0.0019	924.5					
			T	156	39.1	0.017	924.5					
Q8NHG8	ZNRF2	AYSGSDLPSSSSGGANGTAGGGGGAR	S	19	57.9	0.00012	1140.0	Y		P		Hoxhaj et al., 2012
			S	21	40.0	0.0077	1140.0					
			S	27	33.4	0.035	1140.0					
		SLGGAVGSVASGAR	S	82	88.7	6.70E-08	634.8	Y		P		
		AAQSPFSIPNSSSGPYGSQDSVHSSPEDGGGGR	S	113	64.3	3.60E-05	1153.8					
			S	116	64.3	3.60E-05	1153.8					
			S	119	81.2	7.30E-07	1153.8					
			S	120	81.2	7.30E-07	1153.8					
		DRPVGGSPGGPR	S	135	55.3	0.00012	616.3					

Appendix VII

Proteins were purified from lysates of cells stably expressing GFP-ATG9A using GFP-Trap® beads. Peptides were digested from the SDS gel (**Figure 4.20**) and identified from the SwissProt database (SPROT_ID; description) and their Mascot score (score) determined. The corresponding gel band (band) in which each protein was identified is given, together with the molecular weight (Mass).

SPROT_ID	SPROT_description	Score	Mass	Band
sp|P78527|PRKDC_HUMAN	DNA-dependent protein kinase catalytic subunit PRKDC	5952	473749	1
sp|Q92616|GCN1L_HUMAN	Translational activator GCN1 GCN1L1	5168	294967	1
sp|Q00610|CLH1_HUMAN	Clathrin heavy chain 1 CLTC	1209	193260	1
sp|P42345|MTOR_HUMAN	Serine/threonine-protein kinase mTOR MTOR	572	290759	1
sp|P49327|FAS_HUMAN	Fatty acid synthase FASN	513	275877	1
sp|Q9NVI1|FANCI_HUMAN	Fanconi anemia group I protein FANCI	456	150769	1
sp|P20020|AT2B1_HUMAN	Plasma membrane calcium-transporting ATPase 1 ATP2B1	439	139637	1
sp|Q9BQG0|MBB1A_HUMAN	Myb-binding protein 1A MYBBP1A	406	149731	1
sp|O75976|CBPD_HUMAN	Carboxypeptidase D CPD	302	153919	1
sp|Q13308|PTK7_HUMAN	Inactive tyrosine-protein kinase 7 PTK7	279	119799	1
sp|Q92621|NU205_HUMAN	Nuclear pore complex protein Nup205 NUP205	272	230171	1
sp|P07814|SYEP_HUMAN	Bifunctional glutamate/proline--tRNA ligase EPRS	261	172080	1
sp|P27708|PYR1_HUMAN	CAD protein CAD	209	245167	1
sp|P55011|S12A2_HUMAN	Solute carrier family 12 member 2 SLC12A2	198	132048	1
sp|Q5VYK3|ECM29_HUMAN	Proteasome-associated protein ECM29 homolog ECM29	161	205985	1
sp|P21333|FLNA_HUMAN	Filamin-A FLNA	157	283301	1
sp|O15439|MRP4_HUMAN	Multidrug resistance-associated protein 4 ABCC4	134	150344	1
sp|Q9UIQ6|LCAP_HUMAN	Leucyl-cystinyl aminopeptidase LNPEP	122	117787	1
sp|P35579|MYH9_HUMAN	Myosin-9 MYH9	115	227646	1
sp|P53621|COPA_HUMAN	Coatomer subunit alpha COPA	102	139797	1
sp|O15118|NPC1_HUMAN	Niemann-Pick C1 protein NPC1	101	144868	1

sp|P11717|MPRI_HUMAN	Cation-independent mannose-6-phosphate receptor IGF2R	100	281155	1
sp|Q7Z3C6|ATG9A_HUMAN	Autophagy-related protein 9A ATG9A	6086	95356	2
sp|Q15155|NOMO1_HUMAN	Nodal modulator 1 NOMO1	1143	135209	2
sp|P05556|ITB1_HUMAN	Integrin beta-1 ITGB1	786	91664	2
sp|Q9BSJ8|ESYT1_HUMAN	Extended synaptotagmin-1 ESYT1	527	123293	2
sp|Q9HAV4|XPO5_HUMAN	Exportin-5 XPO5	458	138332	2
sp|Q86VP6|CAND1_HUMAN	Cullin-associated NEDD8-dissociated protein 1 CAND1	295	137999	2
sp|P23634|AT2B4_HUMAN	Plasma membrane calcium-transporting ATPase 4 ATP2B4	288	139030	2
sp|P08648|ITA5_HUMAN	Integrin alpha-5 ITGA5	176	115605	2
sp|P22413|ENPP1_HUMAN	Ectonucleotide pyrophosphatase/phosphodiesterase family member 1 ENPP1	140	107024	2
sp|O14980|XPO1_HUMAN	Exportin-1 XPO1	2247	124447	3
sp|P55060|XPO2_HUMAN	Exportin-2 CSE1L	1734	111145	3
sp|Q8N766|EMC1_HUMAN	ER membrane protein complex subunit 1 EMC1	1454	112145	3
sp|Q13423|NNTM_HUMAN	NAD(P) transhydrogenase, mitochondrial NNT	720	114564	3
sp|Q9UIA9|XPO7_HUMAN	Exportin-7 XPO7	699	125196	3
sp|O95373|IPO7_HUMAN	Importin-7 IPO7	416	120751	3
sp|Q13263|TIF1B_HUMAN	Transcription intermediary factor 1-beta TRIM28	330	90261	3
sp|Q9P2B2|FPRP_HUMAN	Prostaglandin F2 receptor negative regulator PTGFRN	266	99464	3
sp|Q86XL3|ANKL2_HUMAN	Ankyrin repeat and LEM domain-containing protein 2 ANKLE2	254	104905	3
sp|P11279|LAMP1_HUMAN	Lysosome-associated membrane glycoprotein 1 LAMP1	249	45367	3
sp|O00410|IPO5_HUMAN	Importin-5 IPO5	232	125032	3
sp|Q92542|NICA_HUMAN	Nicastrin NCSTN	227	79103	3
sp|Q5JPE7|NOMO2_HUMAN	Nodal modulator 2 NOMO2	213	140435	3
sp|Q4KMQ2|ANO6_HUMAN	Anoctamin-6 ANO6	209	107180	3
sp|P22314|UBA1_HUMAN	Ubiquitin-like modifier-activating enzyme 1 UBA1	190	118858	3
sp|O15397|IPO8_HUMAN	Importin-8 IPO8	173	120945	3
sp|Q99460|PSMD1_HUMAN	26S proteasome non-ATPase regulatory subunit 1 PSMD1	163	106795	3

sp|Q9Y2U8|MAN1_HUMAN	Inner nuclear membrane protein Man1 LEMD3	136	100790	3
sp|Q14697|GANAB_HUMAN	Neutral alpha-glucosidase AB GANAB	124	107263	3
sp|O00461|GOLI4_HUMAN	Golgi integral membrane protein 4 GOLIM4	121	81888	3
sp|P05023|AT1A1_HUMAN	Sodium/potassium-transporting ATPase subunit alpha-1 ATP1A1	2991	114135	4
sp|P02786|TFR1_HUMAN	Transferrin receptor protein 1 TFRC	1571	85274	4
sp|P46459|NSF_HUMAN	Vesicle-fusing ATPase NSF	1356	83055	4
sp|P27824|CALX_HUMAN	Calnexin CANX	1340	67982	4
sp|Q9UGP8|SEC63_HUMAN	Translocation protein SEC63 homolog SEC63	1255	88341	4
sp|P16615|AT2A2_HUMAN	Sarcoplasmic/endoplasmic reticulum calcium ATPase 2 ATP2A2	1079	116336	4
sp|Q14974|IMB1_HUMAN	Importin subunit beta-1 KPNB1	999	98420	4
sp|P08238|HS90B_HUMAN	Heat shock protein HSP 90-beta HSP90AB1	934	83554	4
sp|P07900|HS90A_HUMAN	Heat shock protein HSP 90-alpha HSP90AA1	893	85006	4
sp|P13639|EF2_HUMAN	Elongation factor 2 EEF2	568	96246	4
sp|O96005|CLPT1_HUMAN	Cleft lip and palate transmembrane protein 1 CLPTM1	526	76277	4
sp|O94874|UFL1_HUMAN	E3 UFM1-protein ligase 1 UFL1	447	89996	4
sp|Q9Y4R8|TELO2_HUMAN	Telomere length regulation protein TEL2 homolog TELO2	427	92430	4
sp|Q6ZXV5|TMTC3_HUMAN	Transmembrane and TPR repeat-containing protein 3 TMTC3	408	104854	4
sp|Q9Y5L0|TNPO3_HUMAN	Transportin-3 TNPO3	394	105961	4
sp|Q92973|TNPO1_HUMAN	Transportin-1 TNPO1	299	103771	4
sp|Q13724|MOGS_HUMAN	Mannosyl-oligosaccharide glucosidase MOGS	269	92032	4
sp|Q9UBF2|COPG2_HUMAN	Coatomer subunit gamma-2 COPG2	266	98700	4
sp|P55072|TERA_HUMAN	Transitional endoplasmic reticulum ATPase VCP	254	89950	4
sp|A0FGR8|ESYT2_HUMAN	Extended synaptotagmin-2 ESYT2	241	102807	4
sp|O14967|CLGN_HUMAN	Calmegin CLGN	181	70451	4
sp|Q9Y4W6|AFG32_HUMAN	AFG3-like protein 2 AFG3L2	180	88984	4
sp|Q5ZPR3|CD276_HUMAN	CD276 antigen CD276	173	57941	4
sp|Q9BUJ2|HNRL1_HUMAN	Heterogeneous nuclear ribonucleoprotein U-like protein 1 HNRNPUL1	173	96250	4

sp|P47897|SYQ_HUMAN	Glutamine--tRNA ligase QARS	172	88655	4
sp|Q13740|CD166_HUMAN	CD166 antigen ALCAM	148	65745	4
sp|O95202|LETM1_HUMAN	LETM1 and EF-hand domain-containing protein 1, mitochondrial LETM1	147	83986	4
sp|P14625|ENPL_HUMAN	Endoplasmin HSP90B1	146	92696	4
sp|Q86Y56|HEAT2_HUMAN	HEAT repeat-containing protein 2 HEATR2	141	94774	4
sp|P19338|NUCL_HUMAN	Nucleolin NCL	131	76625	4
sp|P12814|ACTN1_HUMAN	Alpha-actinin-1 ACTN1	121	103563	4
sp|Q96J02|ITCH_HUMAN	E3 ubiquitin-protein ligase Itchy homolog ITCH	118	103593	4
sp|Q6ZRP7|QSOX2_HUMAN	Sulfhydryl oxidase 2 QSOX2	113	78221	4
sp|Q9UH99|SUN2_HUMAN	SUN domain-containing protein 2 SUN2	110	80490	4
sp|P30825|CTR1_HUMAN	High affinity cationic amino acid transporter 1 SLC7A1	107	68449	4
sp|Q01813|K6PP_HUMAN	6-phosphofructokinase type C PFKP	101	86454	4
sp|P08107|HSP71_HUMAN	Heat shock 70 kDa protein 1A/1B HSPA1A	2721	70294	5
sp|P11142|HSP7C_HUMAN	Heat shock cognate 71 kDa protein HSPA8	2154	71082	5
sp|P04843|RPN1_HUMAN	Dolichyl-diphosphooligosaccharide-protein glycosyltransferase subunit 1 RPN1	1754	68641	5
sp|O95573|ACSL3_HUMAN	Long-chain-fatty-acid--CoA ligase 3 ACSL3	1552	81338	5
sp|P31040|DHSA_HUMAN	Succinate dehydrogenase [ubiquinone] flavoprotein subunit, mitochondrial SDHA	1227	73672	5
sp|P38646|GRP75_HUMAN	Stress-70 protein, mitochondrial HSPA9	1107	73920	5
sp|Q9NVI7|ATD3A_HUMAN	ATPase family AAA domain-containing protein 3A ATAD3A	1065	71610	5
sp|Q07065|CKAP4_HUMAN	Cytoskeleton-associated protein 4 CKAP4	1036	66097	5
sp|Q15758|AAAT_HUMAN	Neutral amino acid transporter B(0) SLC1A5	1029	57018	5
sp|P16435|NCPR_HUMAN	NADPH--cytochrome P450 reductase POR	874	77097	5
sp|Q5T9A4|ATD3B_HUMAN	ATPase family AAA domain-containing protein 3B ATAD3B	771	73098	5
sp|Q8WVM8|SCFD1_HUMAN	Sec1 family domain-containing protein 1 SCFD1	737	72676	5
sp|O94826|TOM70_HUMAN	Mitochondrial import receptor subunit TOM70 TOMM70A	728	68096	5
sp|A1L0T0|ILVBL_HUMAN	Acetolactate synthase-like protein ILVBL	597	68452	5
sp|P11021|GRP78_HUMAN	78 kDa glucose-regulated protein HSPA5	533	72402	5

sp|P28288|ABCD3_HUMAN	ATP-binding cassette sub-family D member 3 ABCD3	521	75941	5
sp|Q9BU23|LMF2_HUMAN	Lipase maturation factor 2 LMF2	452	79933	5
sp|Q96S52|PIGS_HUMAN	GPI transamidase component PIG-S PIGS	450	61731	5
sp|Q8WTV0|SCRB1_HUMAN	Scavenger receptor class B member 1 SCARB1	404	61636	5
sp|Q14108|SCRB2_HUMAN	Lysosome membrane protein 2 SCARB2	397	54712	5
sp|Q8IXI1|MIRO2_HUMAN	Mitochondrial Rho GTPase 2 RHOT2	384	69101	5
sp|P49748|ACADV_HUMAN	Very long-chain specific acyl-CoA dehydrogenase, mitochondrial ACADVL	327	70745	5
sp|Q8IYS2|K2013_HUMAN	Uncharacterized protein KIAA2013 KIAA2013	323	69684	5
sp|P29966|MARCS_HUMAN	Myristoylated alanine-rich C-kinase substrate MARCKS	306	31707	5
sp|Q9NRW7|VPS45_HUMAN	Vacuolar protein sorting-associated protein 45 VPS45	277	65435	5
sp|Q9UJS0|CMC2_HUMAN	Calcium-binding mitochondrial carrier protein Aralar2 SLC25A13	270	74528	5
sp|Q969N2|PIGT_HUMAN	GPI transamidase component PIG-T PIGT	270	66228	5
sp|Q03519|TAP2_HUMAN	Antigen peptide transporter 2 TAP2	246	76186	5
sp|O00116|ADAS_HUMAN	Alkyldihydroxyacetonephosphate synthase, peroxisomal AGPS	240	73664	5
sp|Q03518|TAP1_HUMAN	Antigen peptide transporter 1 TAP1	234	87733	5
sp|Q96QD8|S38A2_HUMAN	Sodium-coupled neutral amino acid transporter 2 SLC38A2	234	56332	5
sp|O00186|STXB3_HUMAN	Syntaxin-binding protein 3 STXBP3	233	68633	5
sp|O75027|ABCB7_HUMAN	ATP-binding cassette sub-family B member 7, mitochondrial ABCB7	225	82874	5
sp|Q7Z434|MAVS_HUMAN	Mitochondrial antiviral-signaling protein MAVS	218	57063	5
sp|P17812|PYRG1_HUMAN	CTP synthase 1 CTPS1	201	67332	5
sp|P08195|4F2_HUMAN	4F2 cell-surface antigen heavy chain SLC3A2	186	68180	5
sp|Q9NVH0|EXD2_HUMAN	Exonuclease 3~-5~ domain-containing protein 2 EXD2	183	57165	5
sp|Q4ZIN3|MBRL_HUMAN	Membralin C19orf6	172	68130	5
sp|O14975|S27A2_HUMAN	Very long-chain acyl-CoA synthetase SLC27A2	165	71066	5
sp|Q9Y639|NPTN_HUMAN	Neuroplastin NPTN	155	44702	5
sp|P52272|HNRPM_HUMAN	Heterogeneous nuclear ribonucleoprotein M HNRNPM	153	77749	5
sp|Q9UKV5|AMFR2_HUMAN	E3 ubiquitin-protein ligase AMFR AMFR	144	73747	5

sp|P28331|NDUS1_HUMAN	NADH-ubiquinone oxidoreductase 75 kDa subunit, mitochondrial NDUFS1	142	80443	5
sp|Q8TCJ2|STT3B_HUMAN	Dolichyl-diphosphooligosaccharide--protein glycosyltransferase subunit STT3B	134	94241	5
sp|P43003|EAA1_HUMAN	Excitatory amino acid transporter 1 SLC1A3	132	59705	5
sp|P02768|ALBU_HUMAN	Serum albumin ALB	129	71317	5
sp|Q13641|TPBG_HUMAN	Trophoblast glycoprotein TPBG	127	46573	5
sp|Q92575|UBXN4_HUMAN	UBX domain-containing protein 4 UBXN4	120	57028	5
sp|P11940|PABP1_HUMAN	Polyadenylate-binding protein 1 PABPC1	111	70854	5
sp|Q7Z2K6|ERMP1_HUMAN	Endoplasmic reticulum metallopeptidase 1 ERMP1	106	101023	5
sp|P06576|ATPB_HUMAN	ATP synthase subunit beta, mitochondrial ATP5B	4458	56525	6
sp|P25705|ATPA_HUMAN	ATP synthase subunit alpha, mitochondrial ATP5A1	3234	59828	6
sp|P07437|TBB5_HUMAN	Tubulin beta chain TUBB	2751	50095	6
sp|P68371|TBB4B_HUMAN	Tubulin beta-4B chain TUBB4B	2574	50255	6
sp|Q9BVA1|TBB2B_HUMAN	Tubulin beta-2B chain TUBB2B	2018	50377	6
sp|P04350|TBB4A_HUMAN	Tubulin beta-4A chain TUBB4A	2014	50010	6
sp|P68363|TBA1B_HUMAN	Tubulin alpha-1B chain TUBA1B	1812	50804	6
sp|Q71U36|TBA1A_HUMAN	Tubulin alpha-1A chain TUBA1A	1571	50788	6
sp|Q9BQE3|TBA1C_HUMAN	Tubulin alpha-1C chain TUBA1C	1497	50548	6
sp|P04844|RPN2_HUMAN	Dolichyl-diphosphooligosaccharide--protein glycosyltransferase subunit 2 RPN2	1377	69355	6
sp|P10809|CH60_HUMAN	60 kDa heat shock protein, mitochondrial HSPD1	990	61187	6
sp|P42167|LAP2B_HUMAN	Lamina-associated polypeptide 2, isoforms beta/gamma TMPO	810	50696	6
sp|Q9NTJ5|SAC1_HUMAN	Phosphatidylinositide phosphatase SAC1 SACM1L	736	67437	6
sp|Q9BUF5|TBB6_HUMAN	Tubulin beta-6 chain TUBB6	708	50281	6
sp|P18031|PTN1_HUMAN	Tyrosine-protein phosphatase non-receptor type 1 PTPN1	678	50505	6
sp|Q9NRG9|AAAS_HUMAN	Aladin AAAS	669	60392	6
sp|Q8NF37|PCAT1_HUMAN	Lysophosphatidylcholine acyltransferase 1 LPCAT1	541	59741	6
sp|Q969V3|NCLN_HUMAN	Nicalin NCLN	491	63106	6
sp|Q8WVX9|FACR1_HUMAN	Fatty acyl-CoA reductase 1 FAR1	418	59661	6

sp|P48643|TCPE_HUMAN	T-complex protein 1 subunit epsilon CCT5	407	60089	6
sp|Q14318|FKBP8_HUMAN	Peptidyl-prolyl cis-trans isomerase FKBP8	393	44990	6
sp|P49257|LMAN1_HUMAN	Protein ERGIC-53 LMAN1	389	57798	6
sp|P35613|BASI_HUMAN	Basigin BSG	377	42573	6
sp|P46977|STT3A_HUMAN	Dolichyl-diphosphooligosaccharide--protein glycosyltransferase subunit STT3A	356	81104	6
sp|Q10471|GALT2_HUMAN	Polypeptide N-acetylgalactosaminyltransferase 2 GALNT2	344	65433	6
sp|P78371|TCPB_HUMAN	T-complex protein 1 subunit beta CCT2	334	57794	6
sp|P50991|TCPD_HUMAN	T-complex protein 1 subunit delta CCT4	331	58401	6
sp|Q9NRK6|ABCBA_HUMAN	ATP-binding cassette sub-family B member 10, mitochondrial ABCB10	303	79497	6
sp|P14618|KPYM_HUMAN	Pyruvate kinase isozymes M1/M2 PKM2	276	58470	6
sp|Q96A33|CCD47_HUMAN	Coiled-coil domain-containing protein 47 CCDC47	271	56123	6
sp|Q16850|CP51A_HUMAN	Lanosterol 14-alpha demethylase CYP51A1	235	57169	6
sp|P50990|TCPQ_HUMAN	T-complex protein 1 subunit theta CCT8	234	60153	6
sp|Q99832|TCPH_HUMAN	T-complex protein 1 subunit eta CCT7	229	59842	6
sp|Q5JTV8|TOIP1_HUMAN	Torsin-1A-interacting protein 1 TOR1AIP1	205	66379	6
sp|Q15392|DHC24_HUMAN	Delta(24)-sterol reductase DHCR24	195	60803	6
sp|O43175|SERA_HUMAN	D-3-phosphoglycerate dehydrogenase PHGDH	194	57356	6
sp|Q14739|LBR_HUMAN	Lamin-B receptor LBR	187	71057	6
sp|P08670|VIME_HUMAN	Vimentin VIM	182	53676	6
sp|Q15904|VAS1_HUMAN	V-type proton ATPase subunit S1 ATP6AP1	180	52164	6
sp|P49368|TCPG_HUMAN	T-complex protein 1 subunit gamma CCT3	178	61066	6
sp|Q9C0E8|LNP_HUMAN	Protein lunapark LNP	171	48052	6
sp|Q96S66|CLCC1_HUMAN	Chloride channel CLIC-like protein 1 CLCC1	166	62667	6
sp|P06744|G6PI_HUMAN	Glucose-6-phosphate isomerase GPI	165	63335	6
sp|Q5VTE0|EF1A3_HUMAN	Putative elongation factor 1-alpha-like 3 EEF1A1P5	163	50495	6
sp|Q96CS3|FAF2_HUMAN	FAS-associated factor 2 FAF2	151	52933	6
sp|P17987|TCPA_HUMAN	T-complex protein 1 subunit alpha TCP1	150	60819	6

sp|P80723|BASP1_HUMAN	Brain acid soluble protein 1 BASP1	146	22680	6
sp|P52429|DGKE_HUMAN	Diacylglycerol kinase epsilon DGKE	133	65482	6
sp|Q96KA5|CLP1L_HUMAN	Cleft lip and palate transmembrane protein 1-like protein CLPTM1L	131	62531	6
sp|P40227|TCPZ_HUMAN	T-complex protein 1 subunit zeta CCT6A	127	58444	6
sp|Q9H845|ACAD9_HUMAN	Acyl-CoA dehydrogenase family member 9, mitochondrial ACAD9	120	69344	6
sp|O95470|SGPL1_HUMAN	Sphingosine-1-phosphate lyase 1 SGPL1	104	64053	6
sp|P39656|OST48_HUMAN	Dolichyl-diphosphooligosaccharide--protein glycosyltransferase 48 kDa subunit DDOST	1223	50940	7
sp|P68104|EF1A1_HUMAN	Elongation factor 1-alpha 1 EEF1A1	1091	50451	7
sp|P22695|QCR2_HUMAN	Cytochrome b-c1 complex subunit 2, mitochondrial UQCRC2	1047	48584	7
sp|P06733|ENOA_HUMAN	Alpha-enolase ENO1	927	47481	7
sp|P04439|1A03_HUMAN	HLA class I histocompatibility antigen, A-3 alpha chain HLA-A	913	41100	7
sp|P60709|ACTB_HUMAN	Actin, cytoplasmic 1 ACTB	902	42052	7
sp|P12277|KCRB_HUMAN	Creatine kinase B-type CKB	765	42902	7
sp|P31930|QCR1_HUMAN	Cytochrome b-c1 complex subunit 1, mitochondrial UQCRC1	719	53297	7
sp|O60664|PLIN3_HUMAN	Perilipin-3 PLIN3	643	47217	7
sp|P67809|YBOX1_HUMAN	Nuclease-sensitive element-binding protein 1 YBX1	595	35903	7
sp|P07099|HYEP_HUMAN	Epoxide hydrolase 1 EPHX1	568	53143	7
sp|O75844|FACE1_HUMAN	CAAX prenyl protease 1 homolog ZMPSTE24	561	55063	7
sp|P37268|FDFT_HUMAN	Squalene synthase FDFT1	516	48597	7
sp|Q96HY6|DDRGK_HUMAN	DDRGK domain-containing protein 1 DDRGK1	459	35589	7
sp|P49585|PCY1A_HUMAN	Choline-phosphate cytidylyltransferase A PCYT1A	447	42047	7
sp|P01893|HLAH_HUMAN	Putative HLA class I histocompatibility antigen, alpha chain H HLA-H	421	41094	7
sp|Q9UBM7|DHCR7_HUMAN	7-dehydrocholesterol reductase DHCR7	420	55195	7
sp|P20645|MPRD_HUMAN	Cation-dependent mannose-6-phosphate receptor M6PR	419	31487	7
sp|Q8TCT9|HM13_HUMAN	Minor histocompatibility antigen H13 HM13	415	41747	7
sp|P26641|EF1G_HUMAN	Elongation factor 1-gamma EEF1G	411	50429	7
sp|Q3ZCQ8|TIM50_HUMAN	Mitochondrial import inner membrane translocase subunit TIM50 TIMM50	410	39850	7

sp|Q29960|1C16_HUMAN	HLA class I histocompatibility antigen, Cw-16 alpha chain HLA-C	395	41240	7
sp|P54709|AT1B3_HUMAN	Sodium/potassium-transporting ATPase subunit beta-3 ATP1B3	394	31834	7
sp|Q99536|VAT1_HUMAN	Synaptic vesicle membrane protein VAT-1 homolog VAT1	388	42122	7
sp|Q9NX62|IMPA3_HUMAN	Inositol monophosphatase 3 IMPAD1	383	38828	7
sp|P18465|1B57_HUMAN	HLA class I histocompatibility antigen, B-57 alpha chain HLA-B	379	40541	7
sp|Q92643|GPI8_HUMAN	GPI-anchor transamidase PIGK	378	45508	7
sp|O94905|ERLN2_HUMAN	Erlin-2 ERLIN2	371	38044	7
sp|P16422|EPCAM_HUMAN	Epithelial cell adhesion molecule EPCAM	370	35594	7
sp|P53985|MOT1_HUMAN	Monocarboxylate transporter 1 SLC16A1	360	54593	7
sp|O96008|TOM40_HUMAN	Mitochondrial import receptor subunit TOM40 homolog TOMM40	300	38211	7
sp|Q9Y282|ERGI3_HUMAN	Endoplasmic reticulum-Golgi intermediate compartment protein 3 ERGIC3	299	43765	7
sp|Q9HCU5|PREB_HUMAN	Prolactin regulatory element-binding protein PREB	292	46010	7
sp|Q9NQC3|RTN4_HUMAN	Reticulon-4 RTN4	289	130250	7
sp|P61619|S61A1_HUMAN	Protein transport protein Sec61 subunit alpha isoform 1 SEC61A1	281	52687	7
sp|Q99805|TM9S2_HUMAN	Transmembrane 9 superfamily member 2 TM9SF2	281	76809	7
sp|Q9BTV4|TMM43_HUMAN	Transmembrane protein 43 TMEM43	259	44904	7
sp|Q9HD45|TM9S3_HUMAN	Transmembrane 9 superfamily member 3 TM9SF3	257	68584	7
sp|Q8N2K0|ABD12_HUMAN	Monoacylglycerol lipase ABHD12 ABHD12	251	45524	7
sp|Q92604|LGAT1_HUMAN	Acyl-CoA:lysophosphatidylglycerol acyltransferase 1 LPGAT1	212	43289	7
sp|P04075|ALDOA_HUMAN	Fructose-bisphosphate aldolase A ALDOA	194	39851	7
sp|Q15645|PCH2_HUMAN	Pachytene checkpoint protein 2 homolog TRIP13	185	48863	7
sp|Q53EU6|GPAT3_HUMAN	Glycerol-3-phosphate acyltransferase 3 AGPAT9	181	49187	7
sp|Q9BT22|ALG1_HUMAN	Chitobiosyldiphosphodolichol beta-mannosyltransferase ALG1	178	53282	7
sp|O75695|XRP2_HUMAN	Protein XRP2 RP2	168	40471	7
sp|Q8NBX0|SCPDL_HUMAN	Saccharopine dehydrogenase-like oxidoreductase SCCPDH	157	47464	7
sp|Q96EY1|DNJA3_HUMAN	DnaJ homolog subfamily A member 3, mitochondrial DNAJA3	155	53083	7
sp|P08962|CD63_HUMAN	CD63 antigen CD63	152	26474	7

sp|O75306|NDUS2_HUMAN	NADH dehydrogenase [ubiquinone] iron-sulfur protein 2, mitochondrial NDUFS2	149	52911	7
sp|Q9NRX5|SERC1_HUMAN	Serine incorporator 1 SERINC1	148	51488	7
sp|O95674|CDS2_HUMAN	Phosphatidate cytidylyltransferase 2 CDS2	146	51954	7
sp|Q9HDC9|APMAP_HUMAN	Adipocyte plasma membrane-associated protein APMAP	145	46622	7
sp|Q7Z7N9|T179B_HUMAN	Transmembrane protein 179B TMEM179B	145	24048	7
sp|Q16563|SYPL1_HUMAN	Synaptophysin-like protein 1 SYPL1	141	28889	7
sp|P49006|MRP_HUMAN	MARCKS-related protein MARCKSL1	138	19574	7
sp|P08865|RSSA_HUMAN	40S ribosomal protein SA RPSA	136	32947	7
sp|Q70UQ0|IKIP_HUMAN	Inhibitor of nuclear factor kappa-B kinase-interacting protein IKBIP	134	39399	7
sp|Q99808|S29A1_HUMAN	Equilibrative nucleoside transporter 1 SLC29A1	131	50757	7
sp|Q9Y679|AUP1_HUMAN	Ancient ubiquitous protein 1 AUP1	131	53508	7
sp|P52597|HNRPF_HUMAN	Heterogeneous nuclear ribonucleoprotein F HNRNPF	130	45985	7
sp|Q96GC9|VMP1_HUMAN	Vacuole membrane protein 1 VMP1	128	46607	7
sp|P22234|PUR6_HUMAN	Multifunctional protein ADE2 PAICS	124	47790	7
sp|Q9P2W9|STX18_HUMAN	Syntaxin-18 STX18	122	38821	7
sp|O60884|DNJA2_HUMAN	DnaJ homolog subfamily A member 2 DNAJA2	120	46344	7
sp|P60842|IF4A1_HUMAN	Eukaryotic initiation factor 4A-I EIF4A1	120	46353	7
sp|Q9UJZ1|STML2_HUMAN	Stomatin-like protein 2 STOML2	114	38624	7
sp|Q6NUK1|SCMC1_HUMAN	Calcium-binding mitochondrial carrier protein SCaMC-1 SLC25A24	109	53548	7
sp|P09543|CN37_HUMAN	2~,3~-cyclic-nucleotide 3~-phosphodiesterase CNP	108	47948	7
sp|P36578|RL4_HUMAN	60S ribosomal protein L4 RPL4	108	47953	7
sp|Q99747|SNAG_HUMAN	Gamma-soluble NSF attachment protein NAPG	107	35066	7
sp|Q8NBU5|ATAD1_HUMAN	ATPase family AAA domain-containing protein 1 ATAD1	107	41060	7
sp|O94766|B3GA3_HUMAN	Galactosylgalactosylxylosylprotein 3-beta-glucuronosyltransferase 3 B3GAT3	106	37270	7
sp|Q5T1Q4|S35F1_HUMAN	Solute carrier family 35 member F1 SLC35F1	102	45659	7
sp|P43686|PRS6B_HUMAN	26S protease regulatory subunit 6B PSMC4	100	47451	7
sp|P00387|NB5R3_HUMAN	NADH-cytochrome b5 reductase 3 CYB5R3	1624	34441	8

sp|P35232|PHB_HUMAN	Prohibitin PHB	1424	29843	8
sp|Q99623|PHB2_HUMAN	Prohibitin-2 PHB2	1251	33276	8
sp|P54920|SNAA_HUMAN	Alpha-soluble NSF attachment protein NAPA	976	33667	8
sp|P21796|VDAC1_HUMAN	Voltage-dependent anion-selective channel protein 1 VDAC1	945	30868	8
sp|Q00325|MPCP_HUMAN	Phosphate carrier protein, mitochondrial SLC25A3	859	40525	8
sp|P12236|ADT3_HUMAN	ADP/ATP translocase 3 SLC25A6	783	33073	8
sp|Q9H9B4|SFXN1_HUMAN	Sideroflexin-1 SFXN1	771	35881	8
sp|Q02978|M2OM_HUMAN	Mitochondrial 2-oxoglutarate/malate carrier protein SLC25A11	743	34211	8
sp|Q53GQ0|DHB12_HUMAN	Estradiol 17-beta-dehydrogenase 12 HSD17B12	721	34416	8
sp|P36542|ATPG_HUMAN	ATP synthase subunit gamma, mitochondrial ATP5C1	704	33032	8
sp|O15400|STX7_HUMAN	Syntaxin-7 STX7	689	29911	8
sp|O14828|SCAM3_HUMAN	Secretory carrier-associated membrane protein 3 SCAMP3	652	38661	8
sp|P05141|ADT2_HUMAN	ADP/ATP translocase 2 SLC25A5	648	33059	8
sp|P12235|ADT1_HUMAN	ADP/ATP translocase 1 SLC25A4	643	33271	8
sp|P45880|VDAC2_HUMAN	Voltage-dependent anion-selective channel protein 2 VDAC2	583	32060	8
sp|Q12907|LMAN2_HUMAN	Vesicular integral-membrane protein VIP36 LMAN2	573	40545	8
sp|P30519|HMOX2_HUMAN	Heme oxygenase 2 HMOX2	570	36181	8
sp|P04406|G3P_HUMAN	Glyceraldehyde-3-phosphate dehydrogenase GAPDH	564	36201	8
sp|Q14165|MLEC_HUMAN	Malectin MLEC	531	32385	8
sp|P50402|EMD_HUMAN	Emerin EMD	528	29033	8
sp|Q86Y82|STX12_HUMAN	Syntaxin-12 STX12	522	31736	8
sp|P62873|GBB1_HUMAN	Guanine nucleotide-binding protein G(I)/G(S)/G(T) subunit beta-1 GNB1	514	38151	8
sp|Q9P0L0|VAPA_HUMAN	Vesicle-associated membrane protein-associated protein A VAPA	478	28103	8
sp|Q9P035|HACD3_HUMAN	3-hydroxyacyl-CoA dehydratase 3 PTPLAD1	446	43360	8
sp|Q9Y277|VDAC3_HUMAN	Voltage-dependent anion-selective channel protein 3 VDAC3	444	30981	8
sp|O15126|SCAM1_HUMAN	Secretory carrier-associated membrane protein 1 SCAMP1	431	38295	8
sp|P43307|SSRA_HUMAN	Translocon-associated protein subunit alpha SSR1	325	32215	8

sp|Q5VT66|MOSC1_HUMAN	MOSC domain-containing protein 1, mitochondrial MARC1	320	37989	8
sp|P07195|LDHB_HUMAN	L-lactate dehydrogenase B chain LDHB	310	36900	8
sp|Q15006|EMC2_HUMAN	ER membrane protein complex subunit 2 EMC2	306	34982	8
sp|Q8TC12|RDH11_HUMAN	Retinol dehydrogenase 11 RDH11	301	35763	8
sp|P53007|TXTP_HUMAN	Tricarboxylate transport protein, mitochondrial SLC25A1	281	34333	8
sp|Q96G23|CERS2_HUMAN	Ceramide synthase 2 CERS2	280	44961	8
sp|P62258|1433E_HUMAN	14-3-3 protein epsilon YWHAE	279	29326	8
sp|Q9HBH5|RDH14_HUMAN	Retinol dehydrogenase 14 RDH14	270	37184	8
sp|Q9NZ01|TECR_HUMAN	Trans-2,3-enoyl-CoA reductase TECR	269	36410	8
sp|Q9Y673|ALG5_HUMAN	Dolichyl-phosphate beta-glucosyltransferase ALG5	264	37150	8
sp|Q6UWP7|LCLT1_HUMAN	Lysocardiolipin acyltransferase 1 LCLAT1	258	49344	8
sp|Q96AG4|LRC59_HUMAN	Leucine-rich repeat-containing protein 59 LRRC59	255	35308	8
sp|P62879|GBB2_HUMAN	Guanine nucleotide-binding protein G(I)/G(S)/G(T) subunit beta-2 GNB2	252	38048	8
sp|O15127|SCAM2_HUMAN	Secretory carrier-associated membrane protein 2 SCAMP2	233	37082	8
sp|O14662|STX16_HUMAN	Syntaxin-16 STX16	233	37179	8
sp|Q969X5|ERGI1_HUMAN	Endoplasmic reticulum-Golgi intermediate compartment protein 1 ERGIC1	232	32971	8
sp|Q9P0I2|EMC3_HUMAN	ER membrane protein complex subunit 3 EMC3	218	29932	8
sp|O75787|RENR_HUMAN	Renin receptor ATP6AP2	210	38983	8
sp|Q07021|C1QBP_HUMAN	Complement component 1 Q subcomponent-binding protein, mitochondrial C1QBP	209	31742	8
sp|P00338|LDHA_HUMAN	L-lactate dehydrogenase A chain LDHA	201	36950	8
sp|P29692|EF1D_HUMAN	Elongation factor 1-delta EEF1D	194	31217	8
sp|P84157|MXRA7_HUMAN	Matrix-remodeling-associated protein 7 MXRA7	182	21509	8
sp|P24534|EF1B_HUMAN	Elongation factor 1-beta EEF1B2	180	24919	8
sp|P21912|DHSB_HUMAN	Succinate dehydrogenase [ubiquinone] iron-sulfur subunit, mitochondrial SDHB	180	32407	8
sp|Q12846|STX4_HUMAN	Syntaxin-4 STX4	178	34273	8
sp|Q8NHW5|RLA0L_HUMAN	60S acidic ribosomal protein P0-like RPLP0P6	177	34514	8
sp|Q9H0V9|LMA2L_HUMAN	VIP36-like protein LMAN2L	177	39913	8

sp|O43808|PM34_HUMAN	Peroxisomal membrane protein PMP34 SLC25A17	172	34659	8
sp|Q9H490|PIGU_HUMAN	Phosphatidylinositol glycan anchor biosynthesis class U protein PIGU	164	50361	8
sp|O15121|DEGS1_HUMAN	Sphingolipid delta(4)-desaturase DES1 DEGS1	163	38012	8
sp|P08574|CY1_HUMAN	Cytochrome c1, heme protein, mitochondrial CYC1	160	35741	8
sp|P23396|RS3_HUMAN	40S ribosomal protein S3 RPS3	154	26842	8
sp|Q8NBQ5|DHB11_HUMAN	Estradiol 17-beta-dehydrogenase 11 HSD17B11	150	33257	8
sp|Q8NEW0|ZNT7_HUMAN	Zinc transporter 7 SLC30A7	149	41941	8
sp|O60499|STX10_HUMAN	Syntaxin-10 STX10	143	28210	8
sp|Q6IAN0|DRS7B_HUMAN	Dehydrogenase/reductase SDR family member 7B DHRS7B	143	35382	8
sp|P63104|1433Z_HUMAN	14-3-3 protein zeta/delta YWHAZ	141	27899	8
sp|P40926|MDHM_HUMAN	Malate dehydrogenase, mitochondrial MDH2	137	35937	8
sp|Q9H3N1|TMX1_HUMAN	Thioredoxin-related transmembrane protein 1 TMX1	134	32170	8
sp|Q9UBX3|DIC_HUMAN	Mitochondrial dicarboxylate carrier SLC25A10	133	31718	8
sp|Q8TB61|S35B2_HUMAN	Adenosine 3~-phospho 5~-phosphosulfate transporter 1 SLC35B2	129	48054	8
sp|Q9Y3E0|GOT1B_HUMAN	Vesicle transport protein GOT1B GOLT1B	126	15415	8
sp|Q9BUM1|G6PC3_HUMAN	Glucose-6-phosphatase 3 G6PC3	125	39108	8
sp|O00767|ACOD_HUMAN	Acyl-CoA desaturase SCD	122	41667	8
sp|Q96FZ7|CHMP6_HUMAN	Charged multivesicular body protein 6 CHMP6	116	23527	8
sp|P0CG08|GPHRB_HUMAN	Golgi pH regulator B GPR89B	114	53167	8
sp|Q9Y6C9|MTCH2_HUMAN	Mitochondrial carrier homolog 2 MTCH2	114	33936	8
sp|Q01650|LAT1_HUMAN	Large neutral amino acids transporter small subunit 1 SLC7A5	107	55659	8
sp|Q5BJH7|YIF1B_HUMAN	Protein YIF1B YIF1B	107	34527	8
sp|O14579|COPE_HUMAN	Coatomer subunit epsilon COPE	105	34688	8
sp|P51149|RAB7A_HUMAN	Ras-related protein Rab-7a RAB7A	1284	23760	09rerun
sp|O75396|SC22B_HUMAN	Vesicle-trafficking protein SEC22b	1265	24806	09rerun
sp|Q9H0U4|RAB1B_HUMAN	Ras-related protein Rab-1B RAB1B	972	22328	09rerun
sp|P61224|RAP1B_HUMAN	Ras-related protein Rap-1b RAP1B	892	21040	09rerun

sp|P48047|ATPO_HUMAN	ATP synthase subunit O, mitochondrial ATP5O	882	23377	09rerun
sp|P62820|RAB1A_HUMAN	Ras-related protein Rab-1A RAB1A	877	22891	09rerun
sp|P51572|BAP31_HUMAN	B-cell receptor-associated protein 31 BCAP31	842	28031	09rerun
sp|P51148|RAB5C_HUMAN	Ras-related protein Rab-5C RAB5C	815	23696	09rerun
sp|P49755|TMEDA_HUMAN	Transmembrane emp24 domain-containing protein 10 TMED10	786	25131	09rerun
sp|O75947|ATP5H_HUMAN	ATP synthase subunit d, mitochondrial ATP5H	723	18537	09rerun
sp|P24539|AT5F1_HUMAN	ATP synthase subunit b, mitochondrial ATP5F1	707	28947	09rerun
sp|P62834|RAP1A_HUMAN	Ras-related protein Rap-1A RAP1A	648	21316	09rerun
sp|O00264|PGRC1_HUMAN	Membrane-associated progesterone receptor component 1 PGRMC1	641	21772	09rerun
sp|Q9BVK6|TMED9_HUMAN	Transmembrane emp24 domain-containing protein 9 TMED9	640	27374	09rerun
sp|Q7Z7H5|TMED4_HUMAN	Transmembrane emp24 domain-containing protein 4 TMED4	578	26097	09rerun
sp|O60762|DPM1_HUMAN	Dolichol-phosphate mannosyltransferase DPM1	552	29673	09rerun
sp|Q15907|RB11B_HUMAN	Ras-related protein Rab-11B RAB11B	535	24588	09rerun
sp|P61026|RAB10_HUMAN	Ras-related protein Rab-10 RAB10	512	22755	09rerun
sp|Q92520|FAM3C_HUMAN	Protein FAM3C FAM3C	511	24950	09rerun
sp|O15260|SURF4_HUMAN	Surfeit locus protein 4 SURF4	508	30602	09rerun
sp|P61006|RAB8A_HUMAN	Ras-related protein Rab-8A RAB8A	474	23824	09rerun
sp|Q15286|RAB35_HUMAN	Ras-related protein Rab-35 RAB35	471	23296	09rerun
sp|P20340|RAB6A_HUMAN	Ras-related protein Rab-6A RAB6A	469	23692	09rerun
sp|Q15363|TMED2_HUMAN	Transmembrane emp24 domain-containing protein 2 TMED2	467	22860	09rerun
sp|P00403|COX2_HUMAN	Cytochrome c oxidase subunit 2 MT-CO2	422	25719	09rerun
sp|P51809|VAMP7_HUMAN	Vesicle-associated membrane protein 7 VAMP7	395	25261	09rerun
sp|Q9NP72|RAB18_HUMAN	Ras-related protein Rab-18 RAB18	382	23248	09rerun
sp|O95292|VAPB_HUMAN	Vesicle-associated membrane protein-associated protein B/C VAPB	364	27439	09rerun
sp|O43819|SCO2_HUMAN	Protein SCO2 homolog, mitochondrial SCO2	359	29962	09rerun
sp|Q9NRW1|RAB6B_HUMAN	Ras-related protein Rab-6B RAB6B	357	23561	09rerun
sp|Q92930|RAB8B_HUMAN	Ras-related protein Rab-8B RAB8B	351	23740	09rerun

sp|O43169|CYB5B_HUMAN	Cytochrome b5 type B CYB5B	351	16436	09rerun
sp|Q99653|CHP1_HUMAN	Calcium-binding protein p22 CHP	335	22442	09rerun
sp|P61106|RAB14_HUMAN	Ras-related protein Rab-14 RAB14	328	24110	09rerun
sp|P47985|UCRI_HUMAN	Cytochrome b-c1 complex subunit Rieske, mitochondrial UQCRFS1	322	29934	09rerun
sp|O15173|PGRC2_HUMAN	Membrane-associated progesterone receptor component 2 PGRMC2	312	23861	09rerun
sp|P60033|CD81_HUMAN	CD81 antigen CD81	310	26476	09rerun
sp|P51153|RAB13_HUMAN	Ras-related protein Rab-13 RAB13	300	22988	09rerun
sp|P61586|RHOA_HUMAN	Transforming protein RhoA RHOA	298	22096	09rerun
sp|Q8WUY1|THEM6_HUMAN	UPF0670 protein THEM6 THEM6	293	24135	09rerun
sp|Q9UL25|RAB21_HUMAN	Ras-related protein Rab-21 RAB21	293	24731	09rerun
sp|Q9Y3E5|PTH2_HUMAN	Peptidyl-tRNA hydrolase 2, mitochondrial PTRH2	293	19466	09rerun
sp|P57088|TMM33_HUMAN	Transmembrane protein 33 TMEM33	281	28302	09rerun
sp|P61020|RAB5B_HUMAN	Ras-related protein Rab-5B RAB5B	270	23920	09rerun
sp|P20339|RAB5A_HUMAN	Ras-related protein Rab-5A RAB5A	266	23872	09rerun
sp|P46782|RS5_HUMAN	40S ribosomal protein S5 RPS5	264	23033	09rerun
sp|Q99720|SGMR1_HUMAN	Sigma non-opioid intracellular receptor 1 SIGMAR1	258	25169	09rerun
sp|Q99943|PLCA_HUMAN	1-acyl-sn-glycerol-3-phosphate acyltransferase alpha AGPAT1	249	32038	09rerun
sp|Q9UM00|TMCO1_HUMAN	Transmembrane and coiled-coil domain-containing protein 1 TMCO1	242	21389	09rerun
sp|P51151|RAB9A_HUMAN	Ras-related protein Rab-9A RAB9A	235	23108	09rerun
sp|Q9UNK0|STX8_HUMAN	Syntaxin-8 STX8	234	27004	09rerun
sp|P60953|CDC42_HUMAN	Cell division control protein 42 homolog CDC42	230	21587	09rerun
sp|Q15005|SPCS2_HUMAN	Signal peptidase complex subunit 2 SPCS2	230	25272	09rerun
sp|P84095|RHOG_HUMAN	Rho-related GTP-binding protein RhoG RHOG	228	21751	09rerun
sp|O43760|SNG2_HUMAN	Synaptogyrin-2 SYNGR2	228	25079	09rerun
sp|Q9NX47|MARH5_HUMAN	E3 ubiquitin-protein ligase MARCH5	225	31781	09rerun
sp|P61019|RAB2A_HUMAN	Ras-related protein Rab-2A RAB2A	201	23702	09rerun
sp|Q8N183|MIMIT_HUMAN	Mimitin, mitochondrial NDUFAF2	181	19844	09rerun

sp|P32119|PRDX2_HUMAN	Peroxiredoxin-2 PRDX2	177	22049	09rerun
sp|Q9NYL4|FKB11_HUMAN	Peptidyl-prolyl cis-trans isomerase FKBP11	170	22337	09rerun
sp|O75489|NDUS3_HUMAN	NADH dehydrogenase [ubiquinone] iron-sulfur protein 3, mitochondrial NDUFS3	163	30337	09rerun
sp|O15258|RER1_HUMAN	Protein RER1 RER1	161	23057	09rerun
sp|Q06830|PRDX1_HUMAN	Peroxiredoxin-1 PRDX1	160	22324	09rerun
sp|P26373|RL13_HUMAN	60S ribosomal protein L13 RPL13	151	24304	09rerun
sp|O75352|MPU1_HUMAN	Mannose-P-dolichol utilization defect 1 protein MPDU1	150	26906	09rerun
sp|O95816|BAG2_HUMAN	BAG family molecular chaperone regulator 2 BAG2	150	23928	09rerun
sp|P63000|RAC1_HUMAN	Ras-related C3 botulinum toxin substrate 1 RAC1	144	21835	09rerun
sp|Q9Y5M8|SRPRB_HUMAN	Signal recognition particle receptor subunit beta SRPRB	142	29912	09rerun
sp|P61009|SPCS3_HUMAN	Signal peptidase complex subunit 3 SPCS3	141	20358	09rerun
sp|Q9H3K2|GHITM_HUMAN	Growth hormone-inducible transmembrane protein GHITM	139	37352	09rerun
sp|Q04760|LGUL_HUMAN	Lactoylglutathione lyase GLO1	132	20992	09rerun
sp|O96011|PX11B_HUMAN	Peroxisomal membrane protein 11B PEX11B	129	28869	09rerun
sp|Q07020|RL18_HUMAN	60S ribosomal protein L18 RPL18	126	21735	09rerun
sp|P60174|TPIS_HUMAN	Triosephosphate isomerase TPI1	123	31057	09rerun
sp|Q9BRX8|F213A_HUMAN	Redox-regulatory protein FAM213A FAM213A	122	25861	09rerun
sp|P24390|ERD21_HUMAN	ER lumen protein retaining receptor 1 KDELR1	116	24754	09rerun
sp|Q9BRK0|REEP2_HUMAN	Receptor expression-enhancing protein 2 REEP2	114	28243	09rerun
sp|P11233|RALA_HUMAN	Ras-related protein Ral-A RALA	113	23723	09rerun
sp|P19404|NDUV2_HUMAN	NADH dehydrogenase [ubiquinone] flavoprotein 2, mitochondrial NDUFV2	113	27659	09rerun
sp|P21926|CD9_HUMAN	CD9 antigen CD9	112	25969	09rerun
sp|Q9Y3A6|TMED5_HUMAN	Transmembrane emp24 domain-containing protein 5 TMED5	111	26102	09rerun
sp|P21964|COMT_HUMAN	Catechol O-methyltransferase COMT	110	30474	09rerun
sp|Q5SRD1|TI23B_HUMAN	Putative mitochondrial import inner membrane translocase subunit Tim23B TIMM23B	102	28315	09rerun
sp|Q86YN1|DOPP1_HUMAN	Dolichyldiphosphatase 1 DOLPP1	101	27127	09rerun
sp|P31946|1433B_HUMAN	14-3-3 protein beta/alpha YWHAB	100	28179	09rerun

sp|Q9NWW5|CLN6_HUMAN	Ceroid-lipofuscinosis neuronal protein 6 CLN6	100	36010	09rerun
sp|P27348|1433T_HUMAN	14-3-3 protein theta YWHAQ	59	28032	09rerun
sp|Q15836|VAMP3_HUMAN	Vesicle-associated membrane protein 3 VAMP3	717	11359	10
sp|P63027|VAMP2_HUMAN	Vesicle-associated membrane protein 2 VAMP2	523	12712	10
sp|P05386|RLA1_HUMAN	60S acidic ribosomal protein P1 RPLP1	504	11621	10
sp|P62937|PPIA_HUMAN	Peptidyl-prolyl cis-trans isomerase A PPIA	471	18229	10
sp|O60831|PRAF2_HUMAN	PRA1 family protein 2 PRAF2	466	19588	10
sp|Q8N5K1|CISD2_HUMAN	CDGSH iron-sulfur domain-containing protein 2 CISD2	449	15497	10
sp|Q5QNW6|H2B2F_HUMAN	Histone H2B type 2-F HIST2H2BF	425	13912	10
sp|Q9NS69|TOM22_HUMAN	Mitochondrial import receptor subunit TOM22 homolog TOMM22	372	15512	10
sp|P18859|ATP5J_HUMAN	ATP synthase-coupling factor 6, mitochondrial ATP5J	358	12580	10
sp|P13073|COX41_HUMAN	Cytochrome c oxidase subunit 4 isoform 1, mitochondrial COX4I1	342	19621	10
sp|P51571|SSRD_HUMAN	Translocon-associated protein subunit delta SSR4	332	19158	10
sp|P62158|CALM_HUMAN	Calmodulin CALM1	332	16827	10
sp|P30049|ATPD_HUMAN	ATP synthase subunit delta, mitochondrial ATP5D	318	17479	10
sp|P0C0S8|H2A1_HUMAN	Histone H2A type 1 HIST1H2AG	312	14083	10
sp|Q15388|TOM20_HUMAN	Mitochondrial import receptor subunit TOM20 homolog TOMM20	311	16459	10
sp|Q8WY22|BRI3B_HUMAN	BRI3-binding protein BRI3BP	307	27932	10
sp|P62829|RL23_HUMAN	60S ribosomal protein L23 RPL23	291	14970	10
sp|O75964|ATP5L_HUMAN	ATP synthase subunit g, mitochondrial ATP5L	269	11421	10
sp|P20674|COX5A_HUMAN	Cytochrome c oxidase subunit 5A, mitochondrial COX5A	242	16923	10
sp|Q8N5M9|JAGN1_HUMAN	Protein jagunal homolog 1 JAGN1	227	21111	10
sp|P0CW22|RS17L_HUMAN	40S ribosomal protein S17-like RPS17L	227	15597	10
sp|P10620|MGST1_HUMAN	Microsomal glutathione S-transferase 1 MGST1	222	17644	10
sp|P60468|SC61B_HUMAN	Protein transport protein Sec61 subunit beta SEC61B	219	10025	10
sp|P15954|COX7C_HUMAN	Cytochrome c oxidase subunit 7C, mitochondrial COX7C	209	7298	10
sp|Q96IX5|USMG5_HUMAN	Up-regulated during skeletal muscle growth protein 5 USMG5	206	6510	10

sp|P14174|MIF_HUMAN	Macrophage migration inhibitory factor MIF	205	12639	10
sp|Q9NR77|PXMP2_HUMAN	Peroxisomal membrane protein 2 PXMP2	204	22238	10
sp|P56134|ATPK_HUMAN	ATP synthase subunit f, mitochondrial ATP5J2	204	11025	10
sp|O15155|BET1_HUMAN	BET1 homolog BET1	198	13395	10
sp|P67812|SC11A_HUMAN	Signal peptidase complex catalytic subunit SEC11A	196	20612	10
sp|Q3ZAQ7|VMA21_HUMAN	Vacuolar ATPase assembly integral membrane protein VMA21	194	11347	10
sp|Q04837|SSBP_HUMAN	Single-stranded DNA-binding protein, mitochondrial SSBP1	185	17249	10
sp|Q96QV6|H2A1A_HUMAN	Histone H2A type 1-A HIST1H2AA	185	14225	10
sp|P56385|ATP5I_HUMAN	ATP synthase subunit e, mitochondrial ATP5I	183	7928	10
sp|Q04941|PLP2_HUMAN	Proteolipid protein 2 PLP2	182	17022	10
sp|Q9Y3D6|FIS1_HUMAN	Mitochondrial fission 1 protein FIS1	180	16984	10
sp|P07737|PROF1_HUMAN	Profilin-1 PFN1	179	15216	10
sp|P62888|RL30_HUMAN	60S ribosomal protein L30 RPL30	179	12947	10
sp|P24666|PPAC_HUMAN	Low molecular weight phosphotyrosine protein phosphatase ACP1	177	18487	10
sp|P61803|DAD1_HUMAN	Dolichyl-diphosphooligosaccharide--protein glycosyltransferase subunit DAD1	174	12660	10
sp|Q9BV40|VAMP8_HUMAN	Vesicle-associated membrane protein 8 VAMP8	173	11488	10
sp|O00483|NDUA4_HUMAN	NADH dehydrogenase [ubiquinone] 1 alpha subcomplex subunit 4 NDUFA4	172	9421	10
sp|O95406|CNIH_HUMAN	Protein cornichon homolog CNIH	171	17029	10
sp|Q5J8M3|EMC4_HUMAN	ER membrane protein complex subunit 4 EMC4	168	20244	10
sp|Q9Y5U9|IR3IP_HUMAN	Immediate early response 3-interacting protein 1 IER3IP1	166	9020	10
sp|P60604|UB2G2_HUMAN	Ubiquitin-conjugating enzyme E2 G2 UBE2G2	163	18725	10
sp|P05387|RLA2_HUMAN	60S acidic ribosomal protein P2 RPLP2	162	11658	10
sp|P60602|ROMO1_HUMAN	Reactive oxygen species modulator 1 ROMO1	158	8405	10
sp|P14927|QCR7_HUMAN	Cytochrome b-c1 complex subunit 7 UQCRB	155	13522	10
sp|P62805|H4_HUMAN	Histone H4 HIST1H4A	155	11360	10
sp|P46783|RS10_HUMAN	40S ribosomal protein S10 RPS10	154	18886	10
sp|P27449|VATL_HUMAN	V-type proton ATPase 16 kDa proteolipid subunit ATP6V0C	149	15725	10

sp|P14406|CX7A2_HUMAN	Cytochrome c oxidase subunit 7A2, mitochondrial COX7A2	146	9390	10
sp|P30050|RL12_HUMAN	60S ribosomal protein L12 RPL12	144	17979	10
sp|Q9BQB6|VKOR1_HUMAN	Vitamin K epoxide reductase complex subunit 1 VKORC1	142	18622	10
sp|Q8N4V1|MMGT1_HUMAN	Membrane magnesium transporter 1 MMGT1	139	14734	10
sp|O43759|SNG1_HUMAN	Synaptogyrin-1 SYNGR1	139	25667	10
sp|Q9Y2R0|CCD56_HUMAN	Coiled-coil domain-containing protein 56 CCDC56	134	11724	10
sp|P39210|MPV17_HUMAN	Protein Mpv17 MPV17	132	19948	10
sp|P39019|RS19_HUMAN	40S ribosomal protein S19 RPS19	131	16051	10
sp|Q9BVK8|TM147_HUMAN	Transmembrane protein 147 TMEM147	129	25586	10
sp|Q9P2X0|DPM3_HUMAN	Dolichol-phosphate mannosyltransferase subunit 3 DPM3	112	10258	10
sp|Q5BJF2|TMM97_HUMAN	Transmembrane protein 97 TMEM97	112	21005	10
sp|Q9BUR5|APOO_HUMAN	Apolipoprotein O APOO	111	22385	10
sp|Q9P0S9|TM14C_HUMAN	Transmembrane protein 14C TMEM14C	111	11557	10
sp|P62269|RS18_HUMAN	40S ribosomal protein S18 RPS18	110	17708	10
sp|Q6NXT2|H3C_HUMAN	Histone H3.3C H3F3C	109	15318	10
sp|P63173|RL38_HUMAN	60S ribosomal protein L38 RPL38	109	8270	10
sp|Q8N0U8|VKORL_HUMAN	Vitamin K epoxide reductase complex subunit 1-like protein 1 VKORC1L1	108	20108	10
sp|O95562|SFT2B_HUMAN	Vesicle transport protein SFT2B SFT2D2	108	18167	10
sp|P63241|IF5A1_HUMAN	Eukaryotic translation initiation factor 5A-1 EIF5A	106	17049	10
sp|P62277|RS13_HUMAN	40S ribosomal protein S13 RPS13	106	17212	10
sp|Q9Y3D7|TIM16_HUMAN	Mitochondrial import inner membrane translocase subunit TIM16 PAM16	105	13816	10
sp|P60660|MYL6_HUMAN	Myosin light polypeptide 6 MYL6	105	17090	10
sp|Q71UM5|RS27L_HUMAN	40S ribosomal protein S27-like RPS27L	105	9813	10